Systematics, ecology, and evolution of hydrothermal vent endemic peltospirids (Mollusca: Gastropoda) from the Indian and Southern oceans

by

Chong Chen

Merton College

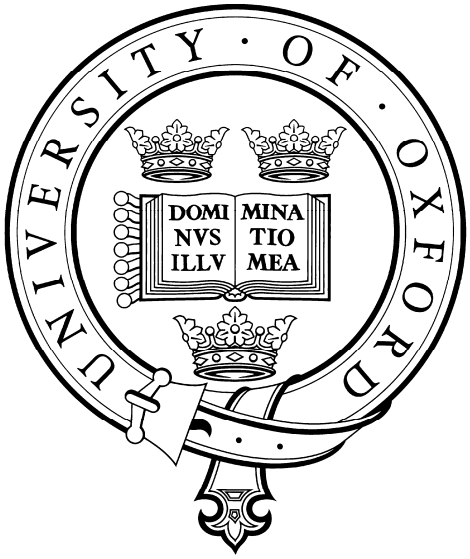

Thesis submitted for partial fulfilment of the requirements for the degree of

Doctor of Philosophy

University of Oxford

Department of Zoology

Hilary 2015

OSS Student No. 400014

This work is dedicated to

My beloved family, friends, and colleagues.

"It is perhaps a more fortunate destiny to have a taste for collecting shells than to be born a millionaire."

Robert Louis Stevenson

"I was like a boy playing on the sea-shore, and diverting myself now and then finding a smoother pebble or a prettier shell than ordinary, whilst the great ocean of truth lay all undiscovered before me."

Sir Issac Newton

"Man cannot discover new oceans unless he has the courage to lose sight, for a very long time, of the shore."

André Gide

"To go places and do things that have never been done before – that's what living is all about."

Michael Collins

Table of Contents

ACKNOWLEDGEMENTS

First and foremost, I would like to express my great gratitude to my primary supervisor Prof Alex D. Rogers and my co-supervisors Dr Jonathan T. Copley and Dr Katrin Linse. I thank Alex for accepting my application to start my studies towards the degree of Doctor of Philosophy, taking on the role of primary supervisor, securing essential research funding for the projects, and providing me a berth on the RRS *James Cook* Expeditions JC66/67 and JC80 which transformed my life and opened up fantastic opportunities beyond my wildest dreams. Jon allowed me to work on the hydrothermal vent gastropod material from his cruise JC67, particularly the 'scaly-foot gastropod', and kindly accepted being a co-supervisor of my project for which I am ever so grateful. I am deeply indebted to Katrin for her support on-board JC80 and afterwards, for granting permission for me to work on the East Scotia Ridge peltospirid, for her indispensable mentorship in molluscan systematics, and for accepting me as her student. I thank all three supervisors for their unceasing support and encouragement not only in the scientific aspect but also in personal life throughout my studies.

I owe a great deal to Dr Julia D. Sigwart, who took me under her wings when I needed much support and encouragement for the anatomy work. Julia has supervised much of the internal and external anatomy work in this thesis, and has given much help in dealing with taxonomy and nomenclature. Julia kindly invited me to her laboratory in Portaferry, Northern Ireland several times where she spent much of her valuable time teaching me molluscan anatomy and state-of-the-art techniques such as 3D tomographic reconstruction, without which my 'scaly-foot gastropod' anatomy project would never have realised. I also owe Julia for inspiring me to start the molluscan scleritome evolution project and for helping me gain confidence in staying in the field of scientific research. Julia has also taken very good care of me during my several visits for which I am deeply grateful.

Dr Hiromi Watanabe and Dr Ken Takai deserve special mention and recognition for their continued patronage in the 'scaly-foot gastropod' work, which would have been much narrower in scope had they not kindly allowed access to the Central Indian Ridge material and data collected in JAMSTEC (Japan Agency for Marine-Earth Sciences and Technology) cruises. Hiromi especially has been an invaluable mentor in vent population genetics and biogeography, and provided generous and instrumental support during my visits to JAMSTEC and my participation in JAMSTEC cruises KY14-01 and KY14-02.

Supportive words from Hiromi and Ken have been crucial in inspiring me to take on a path in deep-sea research in Japan, for which words cannot describe my gratitude.

I would also like to thank here my scientific advisors. Dr Sammy De Grave, who provided me with key support in taxonomy, as well as lasting patronage and encouragement in dealing with the difficulties of scientific publishing. Dr Martin Speight, who not only assisted me in the application and planning of this DPhil but was also my personal tutor during my undergraduate years in St Anne's College, University of Oxford. Martin's encouragement and reassurance has been key in me successfully completing my Bachelor's degree, without which I would not have had the chance to take up this DPhil project. I am also indebted to my college advisor and head of department Prof Peter Holland, who allowed me access to essential equipment in his laboratory and provided provision of my work.

Throughout my DPhil studies I have been fortunate enough to carry out many collaboration projects with a wide range and variety of scientists around the world, many of which has already resulted in a number of co-author publications. Firstly I would like to give my special thanks to Dr Anders Warén for seeing the chance in me and allowing me to proceed with the formal description of the 'scaly-foot gastropod', which is an important basis of my DPhil thesis. I would like to mention Dr Ryota Nakajima, Dr Masako Nakamura, Dr Satoshi Mitarai, Dr Shinsuke Kawagucci, Dr Tatsuo Nozaki, Dr Katsunori Fujikura, and Dr Hiroyuki Yamamoto for the Okinawa Trough work and especially Nozaki-san and Kawagucci-san for allowing me to join the KY14-02 cruise; Dr Jin Sun, Ting Xu, and Dr Jian-Wen Qiu for permitting me to work on the cold seep gastropods of South China Sea collected by the DSV *Jiaolong* ; Roland Houart and Christopher Owen Moe for our collaboration in the revision of the Indo-Pacific muricid genus *Chicomurex*. I would also like to thank Dr Dhugal Lindsay, Dr Takenori Sasaki, Prof Takashi Okutani, Dr Yasunori Kano, Takuya Yahagi, Archer Wong, Prof Gray A. Williams, Prof Kenneth M.Y. Leung, and Dr Moriaki Yasuhara for allowing me to visit their laboratory and for valuable contributions to discussions. In addition, I am grateful for Prof Paul Tyler's support of my work in the ChEsSO project and for being a huge inspiration during the difficult cruise of JC80.

Vast majority of the materials that I have been working with during my DPhil were collected from the most inaccessible great depths of the oceans, and I would like to pay my tribute to the captains and crews of the RRS *James Cook* and R/V *KAIYO*, as well as

the technical crews of ROV *Isis*, ROV *KIEL 6000*, and ROV *Hyper-Dolphin* who strived to secure these specimens in the most difficult and challenging conditions and seas.

The following grants from the Natural Environment Research Council, United Kingdom has been instrumental for the research cruises which secured the study materials used in this thesis:

NE/DO1249X/1 : The ChEsSO (Chemosynthetic Ecosystems of the Southern Oceans) Consortium
NE/F005504/1 : Benthic Biodiversity of Seamounts in the Southwest Indian Ocean
NE/H012087/1 : Biogeography and Ecology of the First Known Deep-Sea Hydrothermal Vent Site on the Ultraslow-Spreading Southwest Indian Ridge

Furthermore, I thank the following institutions, societies, and organisations for awarding me research, travel, or support grants without which my cruise participations and DPhil project would have been much limited: the Malacological Society of London, the Conchological Society of Great Britain and Ireland, InterRidge, Unitas Malacologica, Merton College (University of Oxford), and Department of Zoology (University of Oxford).

I must thank my colleagues and friends around the globe, especially Oxford, Cambridge, London, Southampton, Belfast, Yokosuka, Okinawa, and Hong Kong, for everything they have done for me during the course of my DPhil project. Dr Christopher Nicolai Roterman, Dr Michelle Taylor, Lauren Sumner-Looney, Dr Philippe Boersch-Supan, Anni Djurhuus, and Jennifer Freer deserve particular mention for the help they provided in the shaping of this thesis. Last but not least, I would like to express my deepest gratitude to my parents Prof Ziguang Chen and Xin Lin for their endless love and encouragement, for providing support mentally and financially during my studies, and for reminding me that there is always a home to return to.

DECLARATION AND STATEMENT OF AUTHORSHIP

I hereby declare that the work presented within this thesis was conducted by myself under the supervision of Prof Alex D. Rogers (University of Oxford), Dr Jonathan T. Copley (National Oceanography Centre, Southampton), and Dr Katrin Linse (British Antarctic Survey, Cambridge); except those instances where the contribution of others has been specifically acknowledged. Any material and information, including figures, charts, tables, or graphs quoted, paraphrased, or referenced from other sources has been clearly indicated and their origins has been properly cited.

All data chapters (i.e., chapters 2, 3, 4, 5, 6) are original scientific research papers lead authored by me currently under revision, in press, or published by the international journal indicated in the chapter introduction of each chapter. I confirm that in each case I have written the original manuscripts myself and majority of the work is directly attributable to me. For all publications I am acting or have acted as the corresponding author. I have been granted permission to submit the thesis as a collection of papers by the Director of Graduate Studies and the MPLS Division Graduate School. A summary of author contributions is provided below.

As primary supervisor Alex Rogers supervised the development of my work for all data chapters, and Jonathan Copley as well as Katrin Linse did the same as co-supervisors. For all chapters the supervisors were responsible for securing the funding for sample collection, data collection, and data analyses through NERC grants NE/DO1249X/1 (East Scotia Ridge work), NE/F005504/1 and NE/H012087/1 (Southwest Indian Ridge work). All supervisors contributed to the ideas, planning, and methodology of chapters 2, 3, and 6 in discussion with me. Chapters 4 and 5 were carried out in the laboratory of Dr Julia D. Sigwart (Queen's University Belfast); for these two chapters Julia Sigwart conceived the ideas with me prior to the project and provided necessary equipment and methodology for data collection and data analyses. Alex Rogers, Jonathan Copley and I collected the Southwest Indian Ridge specimens used in this project (on-board RRS *James Cook* Cruise 67); while specimens from the East Scotia Ridge were collected by Katrin Linse, Alex Rogers, Jonathan Copley, and I (on-board RRS *James Cook* Cruises 42 and 80). Julia Sigwart secured polyplacophoran materials for chapter 5.

For all chapters I carried out data collection, for chapters 4 and 5 this was done together with Julia Sigwart and for chapter 6 with Katrin Linse. Dr Christopher N. Roterman

(University of Oxford) provided sequences for the East Scotia Ridge specimens for Chapter 6. For all chapters I performed all the data analyses myself; except together for chapters 4 and 5 where this was done with Julia Sigwart. For all chapters I wrote the original manuscripts myself. All co-authors in each data chapter evaluated the results and their implications, and edited the manuscript for improvement prior to final submission to the concerned international journal.

I hereby confirm that this thesis has not been submitted for any other qualification or degree at this university or any other institution.

Chong Chen
February 2015 (*Hilary Term*)

OSS Student No. 400014

Disclaimer

All nomenclaturally relevant information and acts in this thesis publication are disclaimed for purposes of zoological nomenclatural according to Article 8.2 of the International Code of Zoological Nomenclature (Fourth Edition, incorporating amendments).

> **ICZN (International Commission on Zoological Nomenclature). 1999.** *International Code of Zoological Nomenclature, Fourth Edition*. London, UK: The International Trust for Zoological Nomenclature. 306 pp.

THESIS ABSTRACT

This thesis centres around two genera of large peltospirid gastropods (Mollusca: Neomphalina: Peltospiridae) endemic to hydrothermal vent ecosystems. One is the 'scaly-foot gastropod', an emblematic species of the Indian Ocean vents with unique dermal sclerites covering the foot like roof tiles. The other was recently discovered from expeditions to the Southern and Indian oceans, lacks sclerites and possesses large opercula. As both genera and their assigned species remained undescribed, they were formally described herein which forms a basis to understanding their biology.

The 'scaly-foot gastropod' from both the Central Indian Ridge (CIR) and the Southwest Indian Ridge (SWIR) were confirmed to represent a single species and is formally named as *Chrysomallon squamiferum*. Through molecular genetic analyses using the COI gene, genetic differentiation between SWIR and CIR populations was detected for the 'scaly-foot gastropod'. In contrast, the peltospirids with large opercula from the East Scotia Ridge (ESR) and the SWIR proved to be two distinct species within an undescribed genus. The ESR species was formally described as *Gigantopelta chessoia* and the SWIR species as *G. aegis*. The molecular genetic analyses of the COI gene, confirmed the genetic isolation of the two and consolidated their status as separate species.

A 3D tomographic model of *Chrysomallon squamiferum* was generated to characterise the soft anatomy and morphology as well as to understand its internal anatomy and adaptation which remained little-studied. Further to the enlarged esophageal gland already known to house chemosynthetic endosymbionts, *C. squamiferum* was discovered to have a hypertrophied circulatory system with a gigantic, muscular heart and large ctenidium to adapt to life in a hypoxic environment and to supply the endosymbionts with necessary chemicals. Histological examinations of the sclerites and operculum showed that it was unlikely that the sclerites originated from operculum duplication. Comparisons with polyplacophoran scales revealed starkly different secretion mechanisms despite the superficial similarity, which has implications on the placement of sclerite-bearing Cambrian taxa.

Overall, the results from this thesis ascertained the systematic positions of these large-sized, enigmatic peltospirids, and led to improved understanding of their ecology and evolution. The important role of larval dispersal in maintaining metapopulations across the distribution of a vent-endemic taxa is highlighted. The adaptations of vent-endemic taxa remains little-known even in well-studied species, warranting future studies on these and other species.

Chapter 1

General introduction to hydrothermal vent ecosystems and peltospirid gastropods

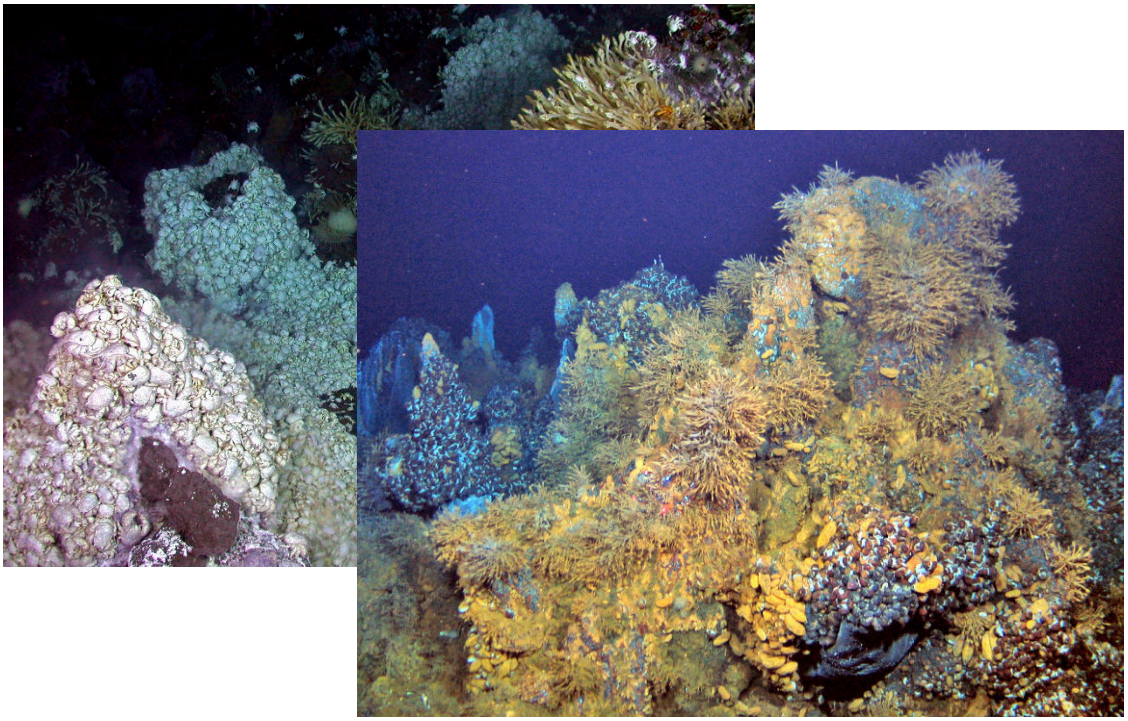

Hydrothermal Vents

With 70% of the Earth's surface covered by the sea, the oceans are the largest ecosystems on this planet. The average depth of the oceans is 3.8 km, and 88% of the oceans are more than 1 km deep. At great depths lies perhaps one of the greatest discoveries of biology in the last Century – hydrothermal vents. Discovered in 1977 (Lonsdale, 1977; Corliss & Ballard, 1977; Corliss *et al.*, 1979) off the Galapagos Islands on the Galapagos Rift, this was the first encounter with chemosynthetic communities, which are now known to manifest in a variety of ways and settings (such as cold seeps, whale falls, wood falls, and oxygen minimum zones) and are widespread (Baker *et al.*, 2010).

Hydrothermal vents are essentially hot springs in the sea and occur when cold seawater seeps into the ocean's crust mainly along mid-ocean ridges but also in other settings (Figure 1). Traditionally it was considered seawater recharge occurred only along off-axis faults, but it can also occur on the axis through rocks made permeable by tectonic fracturing (Tolstoy *et al.*, 2008). Cold water contacts, and is heated by, hot rocks deep inside the crust, which is in turn heated by the molten lava below. Oxygen and magnesium are lost and in turn water becomes rich in hydrogen sulfide, methane, and metals such as iron, zinc, copper (Van Dover, 2000). This is known as the end-member fluid (Van Dover, 2000). The hot water becomes buoyant and rushes up back into the sea and is expelled vigorously into the surrounding cold seawater. End-member fluid precipitates to form dark coloured metal sulfides, hence the name 'black smokers' (Van Dover, 2000). The temperature of exiting fluid may reach

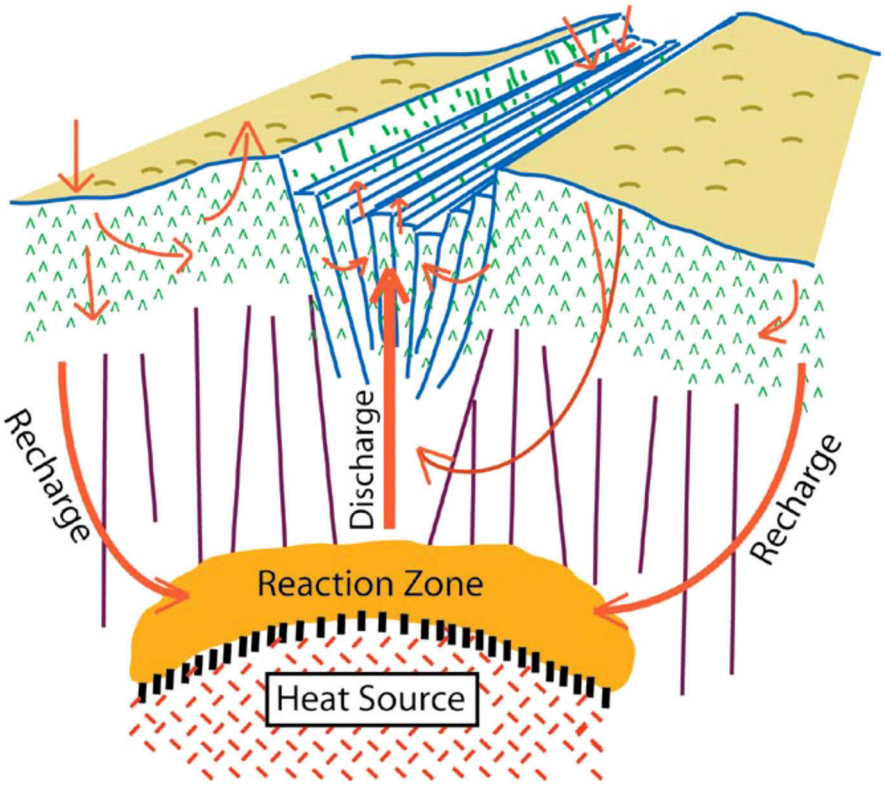

Figure 1. Schematic of hydrothermal circulation on mid-ocean ridges leading to formation of hydrothermal vents (from German & Von Damm, 2004; Ramirez-Llodra *et al*., 2007).

more than 400℃ (Connelly *et al*., 2012). Dynamic mixing of the end-member fluid and ambient seawater lead to the metal and sulfur reacting with oxygen spontaneously to form oxidised forms such as elemental sulfur and sulphate (Fisher, Takai & Le Bris, 2007). In some vents hot and cold water mixes before being expelled from the crust as lower temperature white smokers comprising a high concentration of silica and anhydrite. Low temperature fluids (<0.2 to 100℃, due to mixture of ambient seawater and end-member fluid before reaching seafloor surface) also slowly discharge through sulfide mounds or seafloor fractures in vent fields, and a significant portion of vent communities occur on these 'diffuse flow' sites (Baker *et al*., 2010; Bemis, Lowell & Farough, 2012). Over time the minerals in the hot water precipitate to form chimneys (Figure 2A, B). The composition of vent fluid varies greatly in different vent fields and

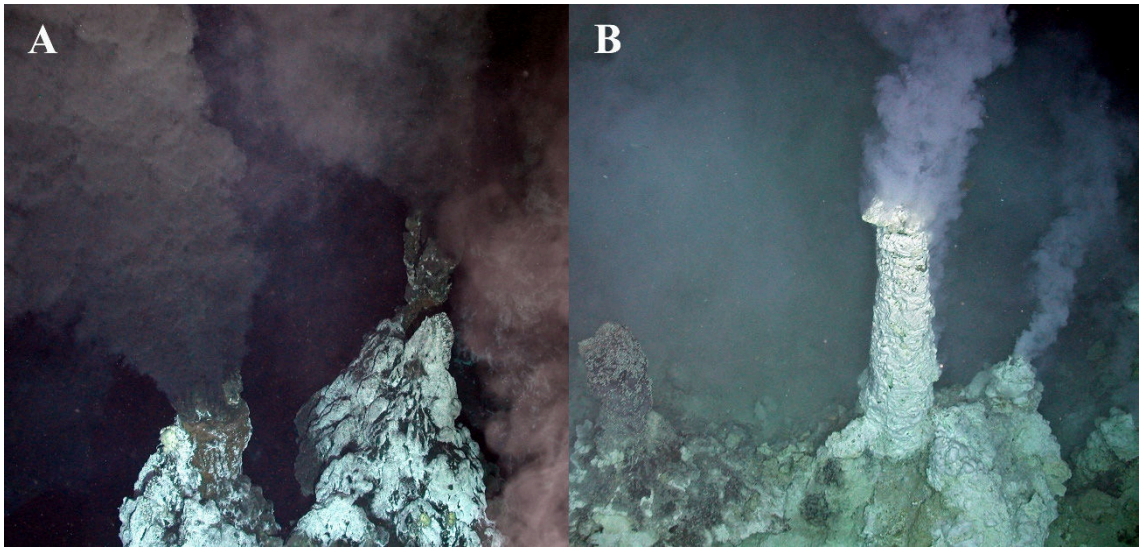

Figure 2. Typical hydrothermal vent chimneys. **A**: Black smoker chimneys, 'Dog's Head' Site, Segment E2, East Scotia Ridge; **B:** White smoker chimneys, 'Winter Palace' Site, Kemp Caldera, East Scotia Ridge. Photos courtesy of the ChEsSO Consortium, Cruise JC42.

depends on the underlying geology, the degree of sub-surface mixing with seawater and whether the vent field is rock or sediment hosted (Tivet, 2007).

Since the initial discovery, more hydrothermal vents have been rapidly found around the globe (Figure 3). The InterRidge Vents Database v2.1 lists a total of 646 vents in total including active, inactive, and inferred sites; removing inferred sites gives a number of 327 confirmed sites (InterRidge, 2010; Hoagland *et al*., 2010; Hannington *et al*., 2012). The majority of the hydrothermal vent systems are distributed on the Earth's mid-ocean ridges which form chains of volcanoes around the planet; others are known from back-arc basins, and on-axis seamounts (with some exceptions such as the off-axis alkaline vent Lost City, Kelley *et al.*, 2001; Figure 3). Systematic exploration of the global ridge system for active vents is still limited to date, however (Baker & German, 2004; Hoagland *et al*., 2010), and our knowledge of hydrothermal vent biogeography is far from complete (Ramirez-Llodra *et al.*, 2007; Rogers *et al*., 2012).

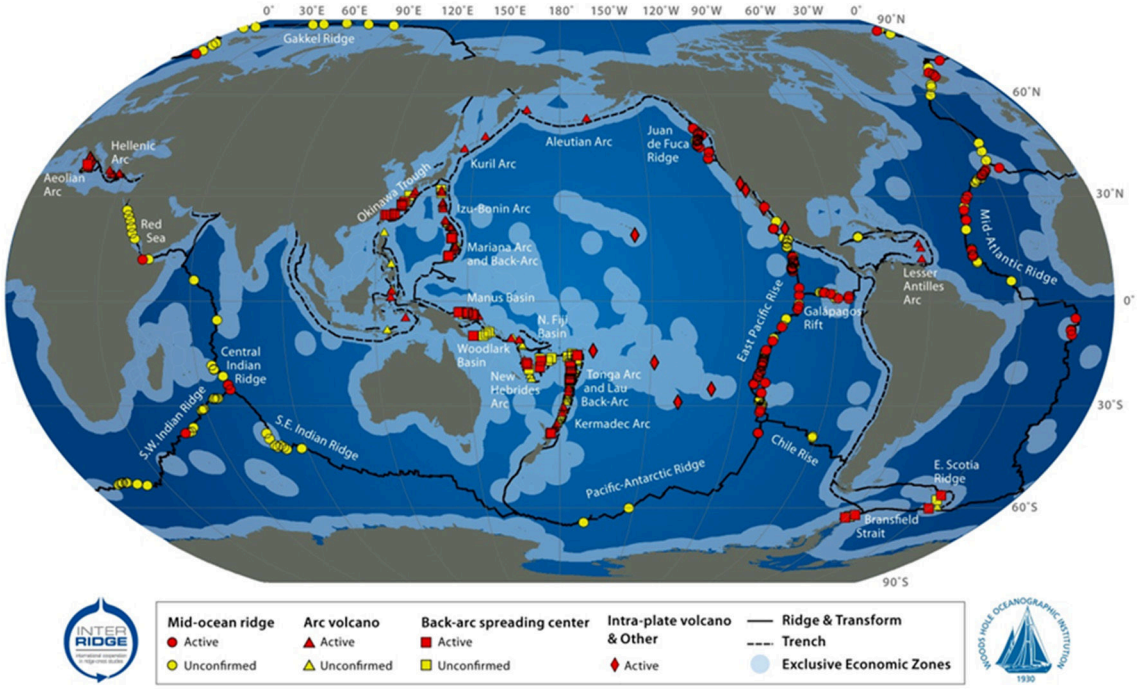

Figure 3. Distributions of hydrothermal vent fields around the globe, both confirmed and unconfirmed. Map produced for InterRidge by the Woods Hole Oceanographic Institute (based on InterRidge, 2010).

Vent Ecosystems

At the time the first photographs of hydrothermal vents were taken by the towed system Deep Tow in 1976 (Lonsdale, 1977), it was not expected that these would host extensive ecosystems because the only method of primary production known at the time was photosynthesis. Hydrothermal vents are located in the deep-sea (>1000m depth), beyond the reach of photosynthetically available light (PAR). The deep-sea is generally considered a food-limited environment because the biological communities it hosts are reliant on surface primary production which is mostly used up in the upper few hundred meters of the ocean (Gage & Tyler, 1991). Indeed, the studies which led to the discovery of vents were entirely geology based, aimed at understanding heat flux from the Earth's

mantle (Grassle, 1989). Therefore, it came as a great surprise when the enormous biomass comprising various seemingly alien organisms aggregating around vents was first sighted from the submersible *Alvin* (Grassle *et al.*, 1979). Two-metre long giant siboglinid tube worms *Riftia pachyptila* Jones, 1981, large bivalves including the vesicomyid clam *Calyptogena magnifica* Boss & Turner, 1980 and *Bathymodiolus thermophilus* Kenk & Wilson, 1985, and the large alvinellid polychaete *Alvinella pompejana* Desbruyéres & Laubier, 1980, among others, populated the site (Figure 5A).

In vast majority of the deep sea, habitats can be characterised by very high species diversity, but generally low biomass and population density (Lutz & Kennish, 1993). The general trend is for the biomass of organisms to show a pattern of exponential decrease along the environmental gradient from shallow to deep water (Rex *et al.,* 2006; Wei *et al.,* 2010). Hydrothermal vents do not conform to the norm. Vent ecosystems exhibit very high biomass (up to 70 kg/m^2, Gebruk *et al*., 2000) and population density, while the species diversity is considered low, with fields normally dominated by a few species (Van Dover *et al.*, 2002).

For a while it was a puzzle as to how these organisms extracted sufficient energy to maintain such high biomasses. They could not be sustained by organic matter falling from the epipelagic zone as much of this material is consumed as it sinks. It was soon discovered, through studying the giant tube worm *Riftia pachyptila*, that these ecosystems relied on a completely new type of primary production, termed chemosynthesis (Cavanaugh *et al.*, 1981; Felbeck, 1981). Chemosynthesis is the process by which microbes biologically synthesise organic carbon compounds from CO_2 in

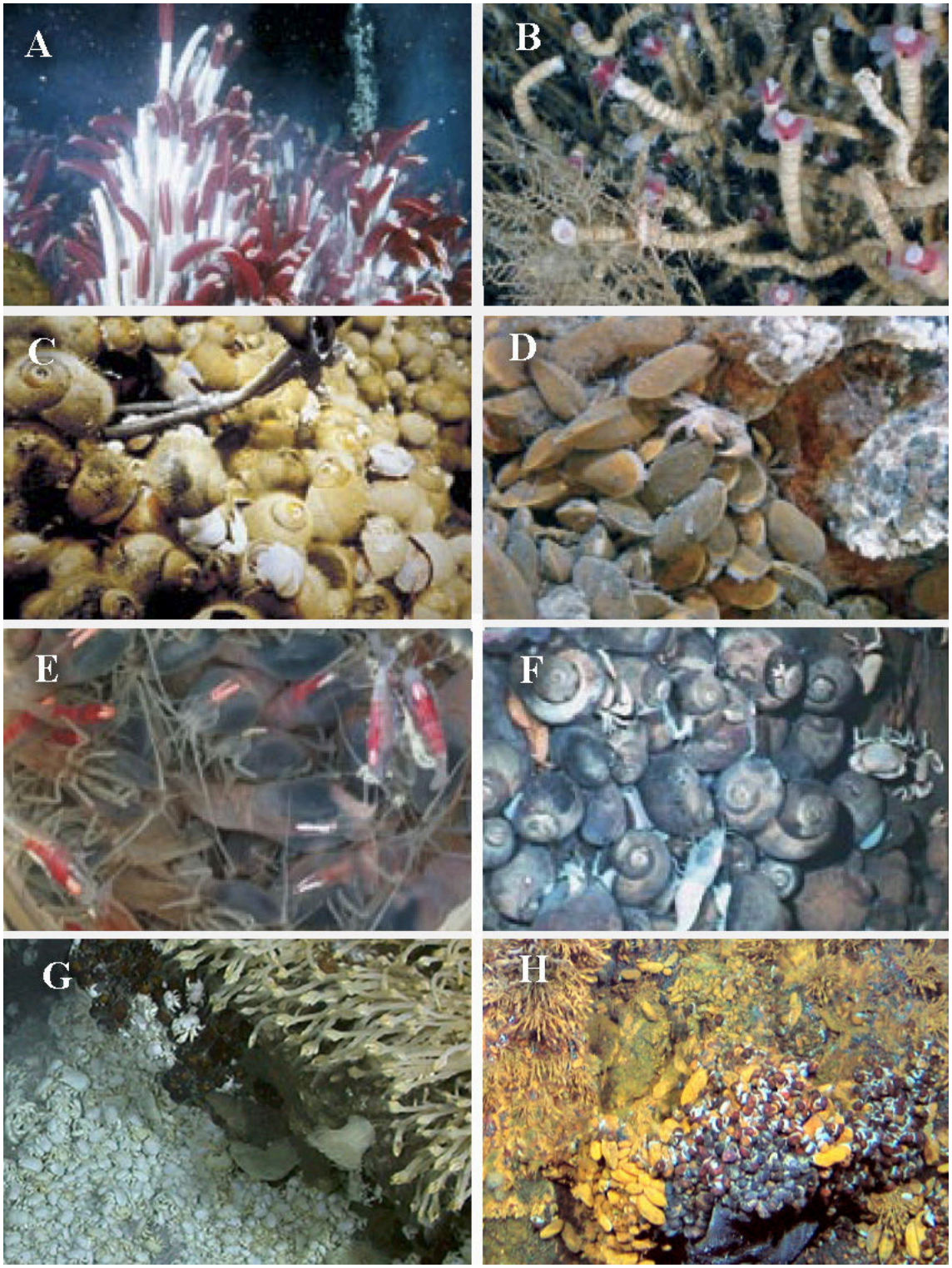

Figure 4. Photographs of representative faunal assemblage at vents found at different parts of the world. **A**: Eastern Pacific; **B**: Northeast Pacific; **C**: Western Pacific; **D**: Shallower Atlantic; **E**: Deeper Atalantic; **F:** Central Indian Ridge, Indian Ocean; **G**: Southwest Indian Ridge, Indian Ocean; **G**: Southern Ocean (adapted from Ramirez-Llodra *et al.*, 2007; Rogers *et al.,* 2012; Copley, 2012).

seawater or other C1 compounds such as CO or CH_4; using energy produced by oxidising various reduced inorganic chemicals (Karl, 1995; De Busserolles *et al.*, 2009). Such reduced inorganic chemicals are abundant in hydrothermal vent fluids, the most commonly used in chemosynthesis is hydrogen sulfide H_2S, followed by methane CH_4. Chemosynthesis is, however, in most cases not entirely independent from sunlight because the oxygen used in the oxidation reaction is taken from surrounding seawater, which is recharged by photosynthesis occurring in the surface water layers. The chemical formula for the oxidation of hydrogen sulfide is shown below as an example:

$$CO_{2\,(aq)} + H_2S_{\,(aq)} + H_2O + O_{2\,(aq)} \rightarrow [CH_2O] + HSO^{-4} + H^+$$

Microbes grow in vast amounts near hydrothermal vents, energised by chemosynthesis, and they form the base of food webs at chemosynthetic ecosystems. It is now known that cold seeps, whale falls, and wood falls also host chemosynthetic ecosystems (De Busserolles *et al.*, 2009); and these are often argued to be evolutionary (i.e., animals evolve and adapt to live in seeps or food-falls before colonising vents) and dispersal (i.e., vent species complete life cycles in food-falls to disperse to distant vents which are normally unreachable) stepping stones for vent organisms (Smith *et al*., 1989; Smith & Baco, 2003; Fujiwara & Kawato, 2010). It has most recently been recognised that subsurface microbial communities living at depths of up to 1800 m below the seabed are also reliant on chemosynthesis (Santelli *et al*., 2008; Lever *et al*., 2013).

Adaptation to Life in Vents

With a high concentration of toxic chemicals such as hydrogen sulfide and heavy metals, high temperatures, hypoxia or even anoxia, and high pressure, hydrothermal vents are hostile environments but are teeming with life. A new species description from these ecosystems has been published on average every two weeks, and this rate has been nearly constant since discovery of vents (Van Dover *et al.*, 2002). Wolff (2005) surveyed known species recorded from hydrothermal vents, and, stunningly, out of 712 recorded species, 71% were endemic to vents. Such a high endemism was considered to possibly reflect a long history of evolution in adapting to the extreme environmental conditions of vents, but as recent evidence suggests most vent groups are only within tens of millions of years old (Vrijenhoek, 2013) it seems more likely to be a result of the extreme environment.

Indeed, many animal species have unique adaptations to survive and prosper at vents. Primary consumers at chemosynthetic ecosystems mainly consume chemoautotrophic microbes either by filter feeding or grazing. However, many fauna have intricate ectosymbiotic and/or endosymbiotic relationships with chemoautotrophic bacteria. For example, the galatheid squat lobster *Shinkaia crosnieri* Baba & Williams, 1998 'farms' ectosymbionts on the underside of its carapace and feeds off them (Watsuji *et al.*, 2014); and the vent shrimp *Rimicaris exoculata* Williams & Rona, 1986 hosts both sulfur-oxidizing and methanotrophic bacteria inside the gill chamber (Petersen *et al.*, 2010). Holobionts with endosymbionts often rely entirely on the symbionts for nutrition. For example, the giant tube worm *Riftia pachyptila* is known to host sulfur-oxidizing

endosymbionts in a specialised organ, the trophosome; and has only a vestigial digestive system lacking mouth or anus (Cavanaugh *et al.*, 1981). Similarly vesicomyid clams house endosymbionts in the gill and also has much reduced digestive tract (Kim *et al*., 1995). Some species are able to combine multiple feeding strategies to suit a variety of environments; *Bathymodiolus thermophilus*, for example, is capable of filter-feeding while also hosting endosymbionts in the gill (Page *et al*., 1991).

To increase the chances of settling on a suitable vent site, hydrothermal vent animals benefit from being able to recognize active vents and distinguish them from other sites. A number of proposed cues are likely to be important, though different species appear to be using different cues. Renninger *et al.* (1995) proposed that chemosensory signals characteristic of vent fluids, especially sulfides, act as settlement cues for vent invertebrates. Jinks *et al.* (2002) gave indications that in addition to chemosensory and thermal signals from vents, some organisms may be able to use visual cues to locate active vents. The vent crab *Bythograea thermydron* has eyes suited for detecting vent illumination (blue light) at the zoëa larval stage, though this ability is lost as they metamorphose towards the adult stage. In addition, biogenic cues are likely to have some importance, especially in late successional species to assess habitat suitability. For example, Mullineaux *et al.* (2000) suggested that tube worm *Tevnia jerichonana* likely releases a biogenic chemical cue which induces settlement of other species such as *Riftia pachyptila*. The alvinocaridid vent shrimps, for example *Rimicaris exoculata*, not only has antennae sensitive to chemicals from vent bacteria and sulfides (Renninger *et al.*, 1995) but also evolved a hypertrophied dorsal ‘eye’ (Figure 5). The dorsal ‘eye’ is located underneath the carapace and contains a high concentration of the photoreceptor

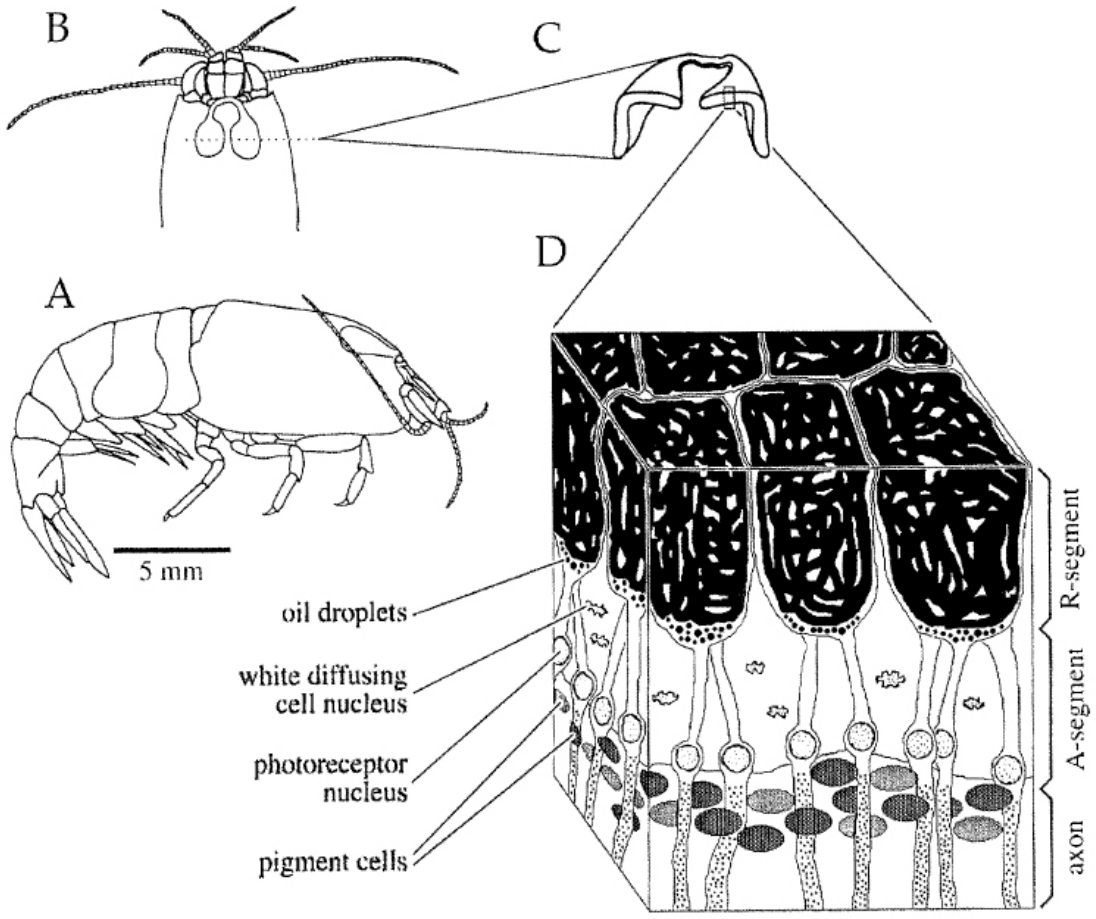

Figure 5. 'Dorsal eye' of alvinocaridid shrimps. **A**. Lateral view of *Rimicaris*; **B.** Dorsal view showing positions of the dorsal 'eye'; **C**. Cutaway sketch of the dorsal 'eye'; **D**. Retinal organisation within the dorsal 'eye' showing major cell types (from Nuckley *et al*., 2006).

rhodopsin (Pelli & Chamberlain, 1989). Although unable to form images, the dorsal 'eye' is hypothesised to be able to detect faint black-body radiation given off by the hot vents (Pelli & Chamberlain, 1989; Chamberlain, 2000).

To survive in vent environments, especially close to effluents, animals must be adapted to tolerate the high temperature and toxicity. For instance, alvinellid worms such as *Alvinella pompejana* are among the most physicochemical-tolerant animals of all, living directly on black smoker walls and tolerating up to 55ºC with a thermal optimum

beyond 42ºC (Chevaldonné *et al*., 2000; Ravaux *et al*., 2013). It also has a series of defences against the toxic and redox environment such as high anti-oxidative stress capacities (Genard *et al*., 2013) and detoxification capabilities (Le Bris & Gaill, 2007). The extreme tolerance ability has been attributed to a number of physiological and structural properties such as elevated levels of heat shock proteins and upregulation of antioxidant glutathione when temperature is raised; these polychaetes also show high stability at transcriptomic and proteomic level (Toulmond *et al*., 1990; Shin *et al*., 2009; Dilly *et al*., 2012; Holder *et al*., 2013). Furthermore, brains of these alvinellids are surrounded by multiple layers of protective membranes, hypothesised to be protecting fragile neurons from oxidative stress (Shigeno *et al*., 2014). Similar adaptations are seen in other vent invertebrates.

Global Biogeography of Hydrothermal Vents

Hydrothermal vents in different regions of the world are characterised by different species composition and dominant taxa (Figure 5), forming so called biogeographic provinces of hydrothermal vents (Ramirez-Llodra *et al.*, 2007). On the eastern Pacific, where vents were first discovered, the clearly dominant fauna is the giant tube worm *Riftia pachyptila*. Other members include *Calyptogena* large vent clams, *Bathymodiolus* vent mussels, and *Alvinella* polychaetes. In the northeast Pacific, vents are dominated by much smaller tubeworms *Ridgeia piscesae* Jones, 1985. In the western Pacific, the dominant taxa are two genera of large gastropods *Alviniconcha* spp. (Johnson *et al*., 2014) and *Ifremeria nautilei* Bouchet & Warén, 1991, accompanied by numerous *Lepitodrilus* limpets as well as *Bathymodiolus* mussels. In the Atlantic Ocean, vents

typically differ in composition greatly by depth. In shallow vents, the most dominant group is several species of *Bathymodiolus* mussels, while the deep vents are dominated by visually stunning swarms of *Rimicaris exoculata* shrimps. In the Indian Ocean, the Central Indian Ridge (CIR) is characterised by swarms of *Rimicaris kairei* shrimps, *Bathymodiolus* mussels, as well as 'scaly-foot gastropods' and *Alviniconcha marisindica* hairy gastropods (Van Dover *et al*., 2001); whereas on the Southwest Indian Ridge (SWIR) the 'scaly-foot gastropod' and another large peltospirid gastropod dominate, with eolepadid stalked barnacle and *Bathymodiolus* mussels (Copley, 2011). The dominant taxa on the East Scotia Ridge (ESR) vents in the Southern Ocean is an undescribed species of *Kiwa* yeti crab, accompanied by large peltospirids, and the stalked barnacle *Vulcanolepis scotiaensis* Buckeridge, Linse & Jackson, 2013, as well as an undescribed *Lepetodrilus* species.

Bachraty *et al.* (2009) conducted a statistical modelling of vent biogeographic provinces using data from 63 hydrothermal fields using multivariate regression trees (MRT), and concluded that there are six biogeographic provinces. Rogers *et al.* (2012), however, raised concerns about the methods used in Bachraty *et al.* (2009), most notably their use of latitude and longitude as constraining factors. Rogers *et al.* (2012) carried out an improved analyses with cross-validation, with new data from ESR vents. The result was an 11-province model shown in Figure 6. Furthermore, they noted that the current presence/absence data used for analyses does not provide enough resolution, hence a low stability in the output. There is also the caveat of unequal sampling of vents, for example East Pacific Rise (EPR) and northern Mid-Atlantic Ridge (MAR) has been regularly revisited and therefore much more data is available than other vents; and

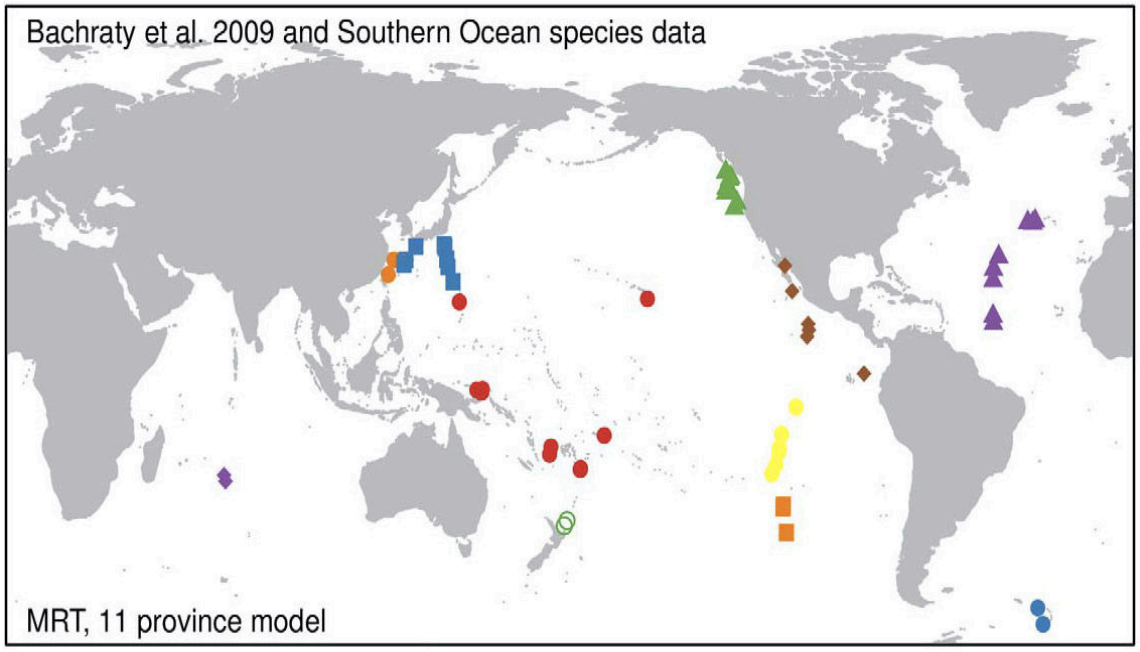

Figure 6. 11-provinces model of global vent biogeography using constrained clustering of multivariate regression trees (from Rogers *et al.*, 2012). Vent provinces recognised are as follows: blue diamonds, Central Indian Ridge; orange circles, southern Okinawa Trough; blue squares, northern Okinawa Trough/Izu-Bonin-Ogasawara Arc; red circles, Mariana-Fiji-Lau; open circles, Kermadec Arc; green triangles, northernmost East Pacific Rise; red diamonds, central East Pacific Rise; yellow circles, southern East Pacific Rise (north of the Easter Microplate); green squares, southernmost East Pacific Rise (south of the Easter Microplate); blue triangles, Mid-Atlantic Ridge; blue circles, East Scotia Ridge.

cryptic species often remain undetected in less surveyed vents. Species abundance or at least ranked abundance is likely to provide a much better resolution, when it becomes available in the future.

Dispersal and Connectivity

Endemism of many vent taxa to this unique ecosystem means they are unable to colonise the vast majority of the deep-sea floor. It was evident from early investigations of dead clam fields (e.g., *Calyptogena magnifica* bed in Clam Bake, Galapagos; Corliss & Ballard, 1977) that cessation of vent fluid leads to death of the vent community (Van Dover, 2000). Given the highly endemic nature of the species inhabiting hydrothermal

vents (Van Dover *et al.*, 2002), they must disperse between vents before individual sites lose productivity or are destroyed by volcanic eruption (e.g., Shank *et al.,* 1997), especially in fast spreading mid-ocean ridges. Many hydrothermal vent endemics, such as the mussel *Bathymodiolus septemdierum*, are known to occur in different vent systems over a very long distance (Kyuno *et al*., 2009; Fujikura *et al*., 2012). Many groups such as siboglinid tube worms have immobile adult stages and most vent invertebrates are unable to travel between vent fields, but their larvae are capable of dispersing across a long distance in non-vent environments. Factors that are considered to be important in determining connectivity include hydrodynamic transportation (Adams & Mullineaux, 2008), seafloor topology and physical barriers (Vrijenhoek, 2010), extent of buoyant plume (Mullineaux *et al*., 1995), frequency of available vents, larval type and longevity (Marsh *et al.*, 2001) and larval distribution in water column (Mullineaux *et al.*, 2005).

Different types of dispersal mechanisms and strategies are used by different vent species and movement during dispersal can be either passive or active. *Riftia pachyptila*, for example, disperses during its passive larval stage, its lecithotrophic larva carries yolk or lipid and relies on it for energy and simply follows ocean currents. The mussel *Bathymodiolus thermophilus*, on the other hand, has an active free-swimming planktotrophic larva stage and feeds on plankton during dispersal. Similarly, the vent shrimp *Rimicaris exoculata* has planktotrophic larvae which feed on phytodetritus during dispersal (Tyler & Young, 2003). In general species with planktotrophic larvae have higher dispersal potential as the larvae can sustain themselves by feeding, compared to lecithotrophy where the dispersal duration is limited by the yolk supply

(Vrijenhoek, 2010). Within a vent field and across short distances, dispersal can also occur at the adult stage, for example in vent crabs (Tyler & Young, 2003). To study the dispersal of vent species a variety of approaches are available including the use of genetic techniques to determine relatedness and gene flow between discrete populations, *in situ* studies through tracking dispersal and random net or pump sampling, or by recreating deep water environment in labs.

There are considerable difficulties in *in situ* studies of vent dispersal due to difficulty in tracking (Adams *et al.*, 2010; Mullineaux & Manahan, 1998). There are examples where this is done, however, for example Herring & Dixon (1998) sampled *Rimicaris exoculata* in the Atlantics and found their larvae travelled up to 100 km away from the origin. Marsh *et al.* (2001) recreated the dispersal condition of 2°C and 250 atm pressure to study the dispersal of *Riftia pachyptila* larvae, and found that they are able to survive an average of 38 days and travel more than 100 km if favoured by currents. The chance of settling on a new vent was, however, low and implies vent species must send out a large number of individuals to have a reasonable chance of settling on a new vent. Genetic methods are more straightforward and effective in studying dispersal and connectivity due to the inaccessibility of the vent habitat. Much of the current knowledge on genetic connectivity and dispersal between hydrothermal vents (reviewed in Vrijenhoek, 2010) is based on genetic studies of the well-studied vent systems in the Pacific and Atlantic oceans such as EPR and MAR.

Connectivity between vents at either fine scales or across biogeographic regions has been assessed by population genetic techniques. A common practice is to use F-statistics

(F_{ST}; Wright, 1950) to compare genetic diversity among subpopulations to diversity within subpopulations. For example, Craddock *et al.* (1995) carried out a study to examine dispersal between discrete *Bathymodiolus thermophilus* populations in the East Pacific Rise and Galapagos Rift Ridge using allozyme loci and mitochondrial restriction length polymorphisms. They found no significant dispersal barriers, and across 2,300 km, these populations showed no genetic subdivision indicating high connectivity. Teixeira *et al.* (2012) studied connectivity of *Rimicaris exoculata* along approximately 7,000 km of the Mid-Atlantic Ridge using population genetics approach with 710bp of cytochrome *c* oxidase subunit I (COI) sequence and found very high connectivity which in turn indicates high dispersal capability; agreeing with previous results (Creasey,

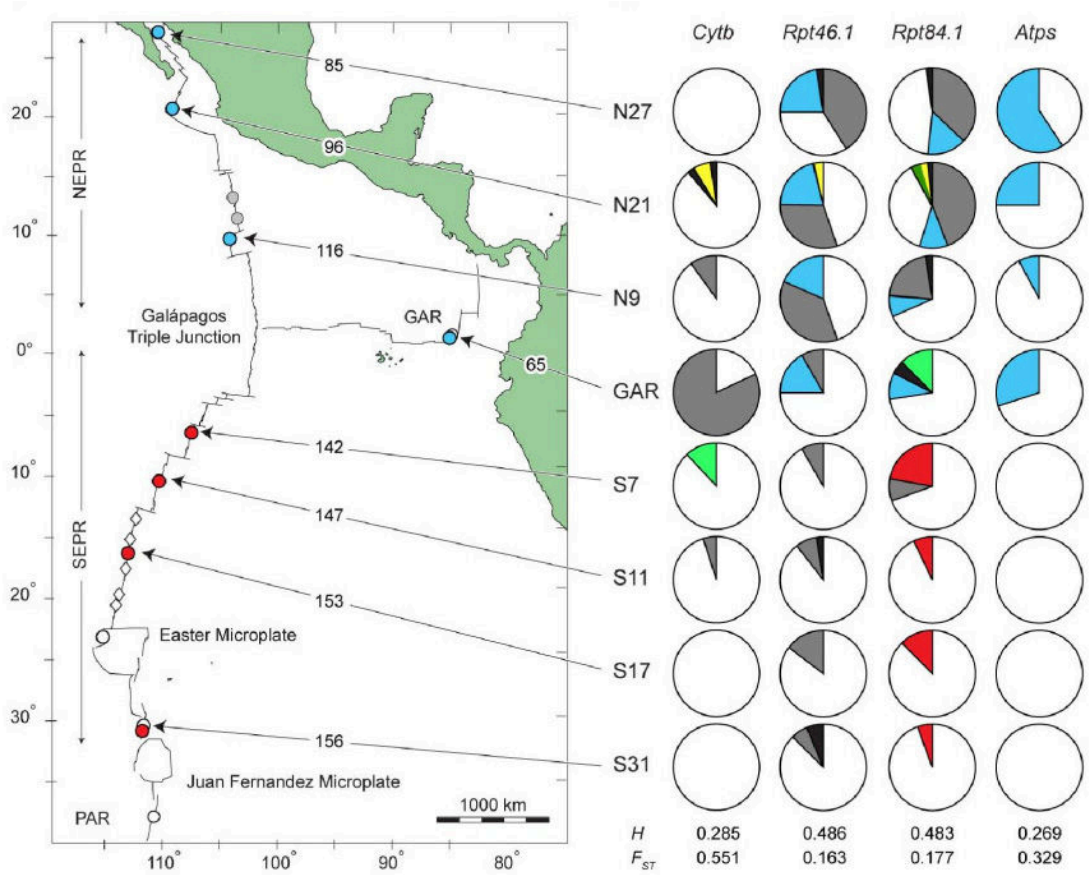

Figure 7. Frequency of *Riftia pachyptila* haplotypes in eight vent fields, for four genes (from Coykendall *et al.*, 2011).

Rogers & Tyler, 1996). In contrast with these two species with planktotrophic larvae, *Riftia pachyptila* with a lecithotrophic larvae showed clear evidence of genetic subdivision along 7,000 km of the EPR (Figure 7), indicating isolation by distance (Coykendall *et al*., 2011).

Various genetic markers are used, from single genes to microsatellite loci; and recently more high-resolution genomic approaches such as using single-nucleotide polymorphism markers across the genome detected with Restriction site Associated DNA sequencing (RAD-seq; Etter *et al*., 2011) are starting to be used (e.g., Herrera *et al*., 2015). Lack of genetic differentiation is likely attributable to panmixia (i.e., individuals are able to randomly mate across populations) but may also represent recent range expansion where differentiation is difficult to detect.

Testing genetic diversities of populations of vent-endemic invertebrates using statistics such as Tajima's *D* (Tajima, 1989), Fu's F_S (Fu, 1997), and mismatch distributions for deviations from genetic neutrality often reveal significant deviations consistent with a scenario of a recent population bottleneck followed by demographic expansion. This is supplemented with the fact that the mitochondrial DNA haplotype network of vent species investigated generally show a 'star-burst pattern' with an excess of rare haplotypes surrounding few dominant haplotypes, also consistent with the same scenario of recent demographic expansion (Hurtado *et al.,* 2004; Plouviez *et al*., 2009; Teixeira *et al*., 2010; Nakamura *et al*., 2012; Beedessee *et al*., 2013). This likely reflects the ephemerality and instability of vent populations, meaning endemic species must maintain viable metapopulation networks across many vent fields (Vrijenhoek, 1997;

Vrijenhoek, 2010).

Vrijenhoek (2010) provides an exhaustive review of the current knowledge of connectivity between vents, and recognises that although barriers to dispersal such as vents in differing depths, deep currents, and transform faults often subdivide populations, many patterns observed are species-specific because of different life histories and behaviours exhibited by different vent species. Pioneer species, for example, usually have much higher dispersal ability and as a result observed connectivity is usually high. Also, although it is true that results from most studies (e.g., Johnson *et al.*, 2006; Young *et al.*, 2008) conform to the prediction that dispersal of taxa occurs along mid-ocean ridges, some dispersal may not follow this pattern as a result of distribution of deep currents or stepping stones of non-vent chemosynthetic ecosystems (Rogers *et al.*, 2012).

Study Area Background

Central Indian Ridge and Southwest Indian Ridge

Although since 1977 many hydrothermal vents have been discovered in the Pacific and Atlantic Oceans, discovery of a vent field in the Indian Ocean had to wait until the 21st Century, when a vent field was discovered by Japanese scientists from Japan Agency for Marine-Earth Science and Technology (JAMSTEC) in August 2000 (Hashimoto *et al.,* 2001). The first Indian Ocean vent was discovered on the Central Indian Ridge (CIR) near Rodriguez Triple Junction. The field was named the Kairei field (25°19.23'S,

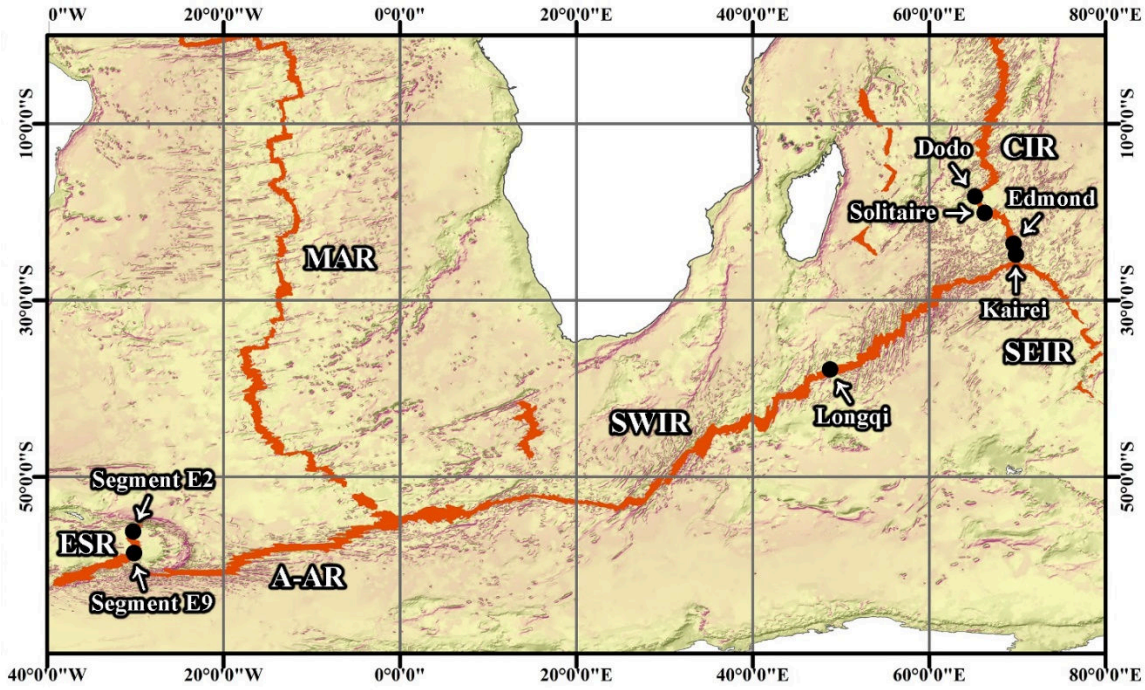

Figure 8. Map of surveyed and confirmed hydrothermal vent fields of Central Indian Ridge, Southwest Indian Ridge, and East Scotia Ridge. Solid red indicates spreading mid-ocean ridges. Abbreviations. A-AR: American-Antarctic Ridge; CIR: Central Indian Ridge; ESR: East Scotia Ridge; MAR: Mid-Atlantic Ridge; SEIR: Southeast Indian Ridge; SWIR: Southwest Indian Ridge. Map created using Esri ArcMap 10.1 (ESRI 2012) and General Bathymetric Chart of the Oceans (GEBCO) Grid Display Ver.2.13 (BODC 2010). Data source: Bathymetry, GEBCO; continents data. ArcWorld Supplement; oceanic ridges, United States Geologic Service (USGS).

70°02.42'E), and was sampled extensively in 2001 (Van Dover *et al.*, 2001). The expedition reported that most organisms found at Kairei had an affinity with the Pacific vent fauna, and one species, *Rimicaris kairei* Watabe & Hashimoto, 2002, had Atlantic affinity. The dominant taxon was *R. kairei* which swarms like *R. exoculata* in vents in Mid-Atlantic Ridge. Other notable taxa included the hairy snail *Alviniconcha marisindica* Okutani, 2014, sea anemones from the genus *Marianactis*, and the vent mussel *Bathymodiolus septemdierum* Hashimoto & Okutani, 1994. Some novel taxa were also discovered, including the 'scaly-foot gastropod' which uniquely carries dermal sclerites mineralised with iron sulfides (Suzuki *et al.*, 2006). Since then, three more vent fields have been discovered on CIR (Figure 8), including Edmond field

(23°52.68'S, 69°35.80'E), also near the Rodriguez Triple Junction (Van Dover *et al.*, 2001), and the Dodo field (18°20.10'S, 65°17.90'E) and Solitaire field (19°33.41'S, 65°50.89'E), about 700 km further north (Nakamura *et al*., 2012).

In 2010, a Chinese cruise confirmed the first visual sighting of a hydrothermal vent field on Southwest Indian Ridge (Tao *et al.*, 2012; Figure 8). The SWIR vent field was later named Longqi field (37°47' S 49°39' E; Tao *et al*., 2014), and was first surveyed by a team from United Kingdom on board *RRS James Cook* Cruise JC67 (PI: JT Copley; Copley, 2011). Before it was formally given a name, it was tentatively referred to as 'Dragon field' (Copley, 2011; Roterman *et al*., 2013). Longqi field is of particular interest because SWIR is an ultraslow spreading ridge (14-16 mm $year^{-1}$), where hydrothermal vents are expected to remain active for a very long time, possibly centuries or more. Ultraslow spreading ridges have only very recently become targets in the search for hydrothermal vents, as it was long believed that the low level of tectonic activity on these ridges was unable to support many vents. The SWIR, for example, was thought to have distance of 200-300 km between vents (Baker *et al.*, 1996). The only other two ultraslow spreading ridges that have been surveyed for hydrothermal vents are the Cayman Trough, where the world's deepest vents have been found (Connelly *et al.*, 2012), and Gakkel Ridge (Pedersen *et al.*, 2010).

The community structure of Longqi was notably different from known CIR vents (Copley, 2011). Although a number of seemingly shared taxa such as the *Marianactis* anemone, *Bathymodiolus* mussels and *Rimicaris* shrimps were found; the abundance was different as very few shrimps were present vividly contrasting with CIR's huge

swarms of *Rimicaris kairei.* A number of characteristic species of CIR were missing, for example *Alvinoconcha marisindica* Okutani in Jones *et al*., 2014, the hairy snail, and *Austinograea rodriguezensis* Tsuchida & Hashimoto, 2002. Instead there was clear affinity to the East Scotia Ridge vents (Rogers *et al*., 2012), with a similar operculated large peltospirid ("Peltospiroid n. sp., ESR" sensu Rogers *et al*., 2012) and *Kiwa* yeti

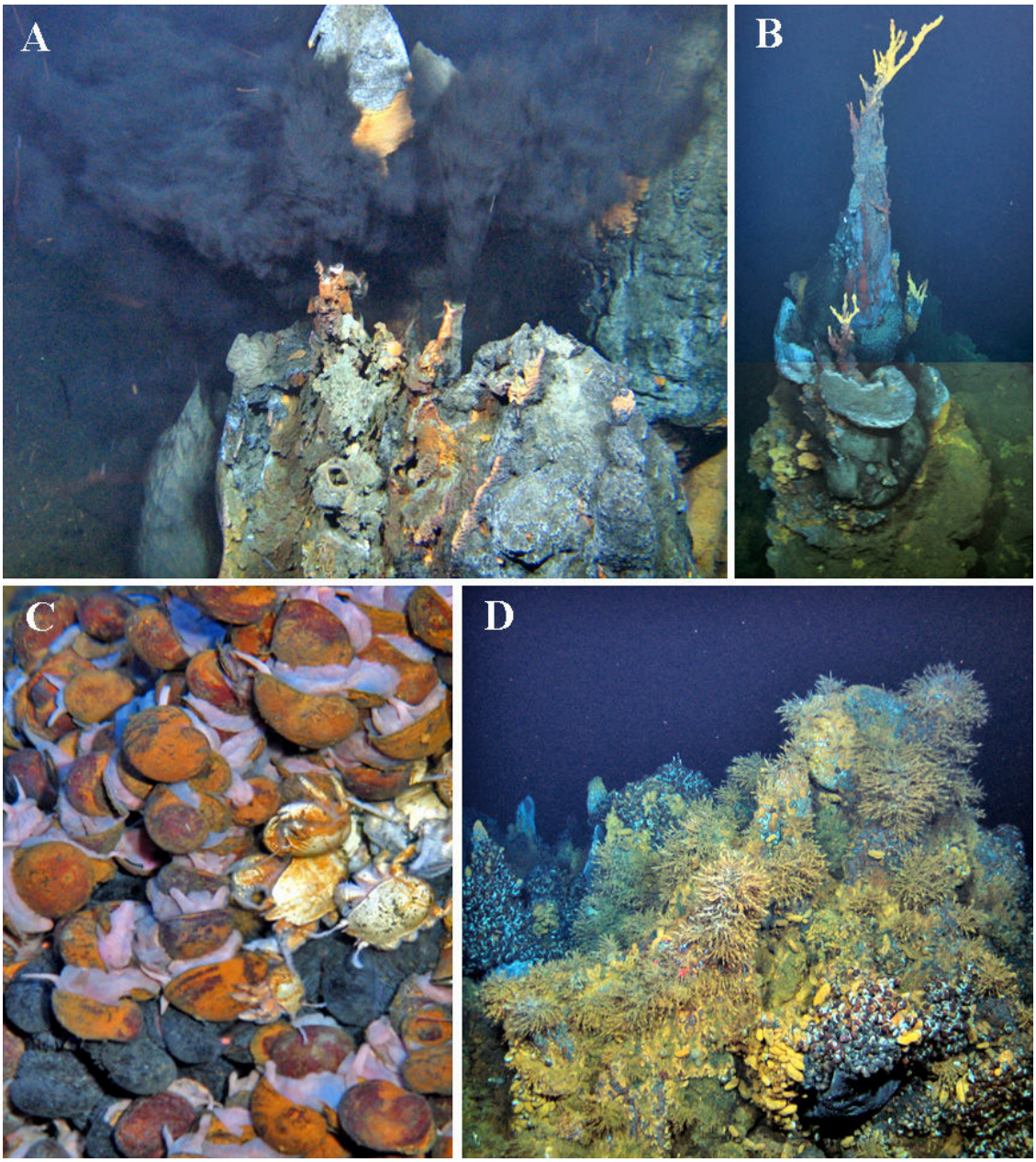

Figure 9. Longqi Field, Southwest Indian Ridge. **A**. Black smoker; **B**. Chimney, about 20m tall; **C.** Aggregation of the two peltospirid species and some *Kiwa* sp.; **D.** Aggregation of fauna on diffuse flow site 'Tiamat'. Photos from RRS *James Cook* cruise JC67.

crabs. Notably a new population of the 'scaly-foot gastropod' was found to inhabit Longqi, and it was one of the most dominant species there (Figure 9). There are relatively few population genetic studies concerning the hydrothermal vents of the Indian Ocean, with only two studies to date (Nakamura *et al.*, 2012; Beedessee *et al*., 2013) and none across two ridge systems. Longqi is approximately 2,300 km away from Kairei and 2,500 km away from Solitaire; the discovery of shared taxa such as the 'scaly-foot gastropod' between SWIR and CIR provides an opportunity to study genetic connectivity between the ridges.

East Scotia Ridge

Hydrothermal vents in the East Scotia Ridge (ESR), Southern Ocean were until recently known only from plume signals (e.g., German *et al.*, 2010; Pedersen *et al.*, 2010; Edmonds *et al.*, 2003), partly because of the difficult weather and sea conditions at high latitudes (Vrijenhoek, 2010). In 2010, hydrothermal vents on ESR (also the first Antarctic vents) were surveyed for the first time by the Chemosynthetic Ecosystems of the Southern Oceans (ChEsSO) Consortium (Rogers *et al.*, 2012). It was hypothesised that Drake Passage in Southern Ocean may be an important gateway connecting the hydrothermal vent fauna of different oceans, and therefore vents at the ESR would perhaps host a collection of fauna seen in other vents across various different oceans.

The discovered vents at segments E2 (56°05.31'S 30°19.10'W) and E9 (60°03.00'S 29°58.60'W), however, show a completely different faunal composition from any previously known vents (Figure 10). The vent was dominated by an undescribed species

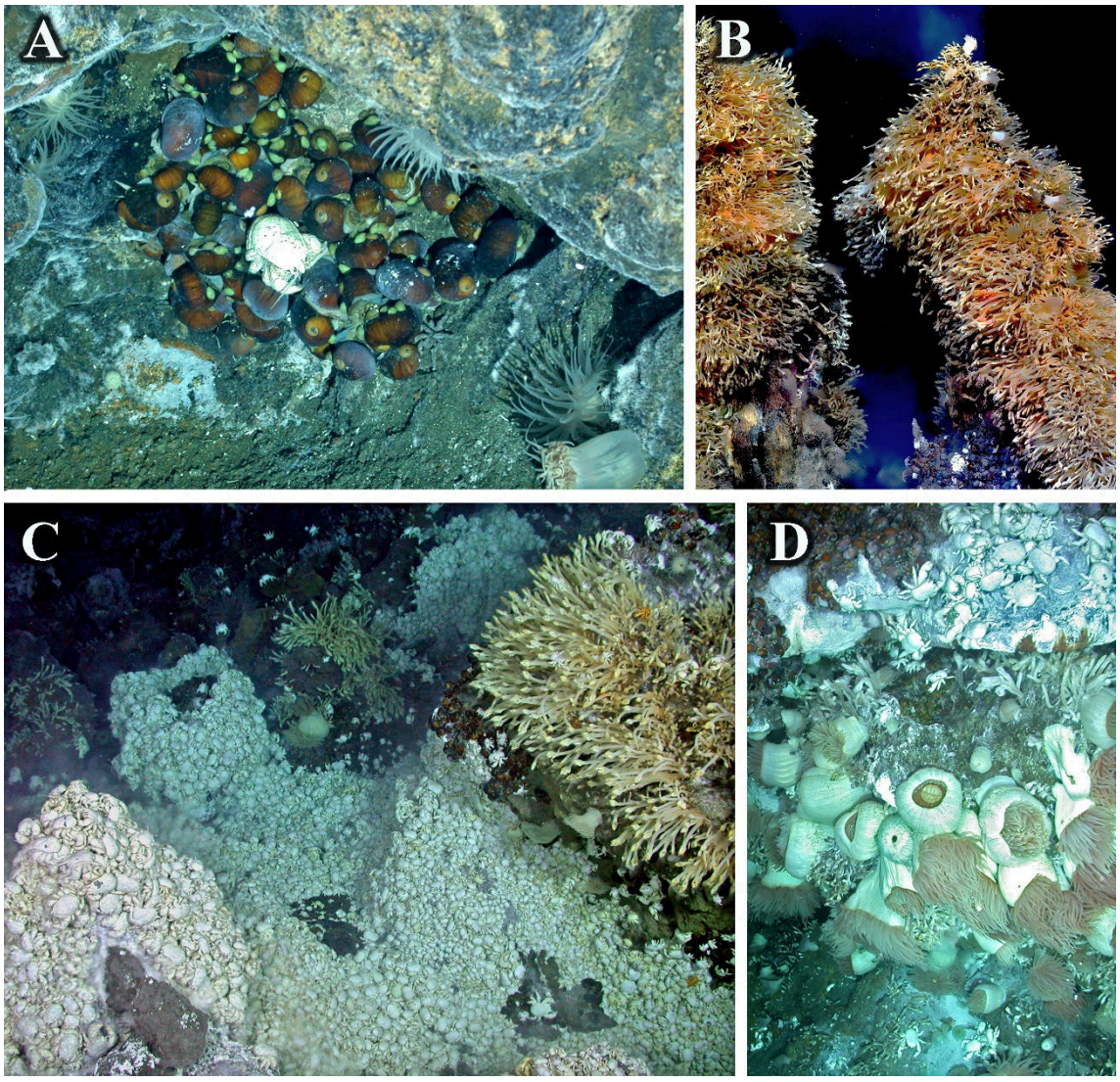

Figure 10. Hydrothermal vents on the East Scotia Ridge. **A**. Aggregation of 'Peltospirid n. sp., ESR'; **B**. The 'Carwash' chimney, E9; **C.** Dense aggregations of *Kiwa* sp. surrounded by 'Peltospirid n. sp. ESR' and *Vulcanolepis scotiaensis*; **D.** Aggregation of large actinostolid sea anemone. Photos from ChEsSO Consortium, RRS *James Cook* cruise JC42 (Rogers *et al*., 2012; Marsh *et al*., 2012).

of the yeti crab *Kiwa* which form huge clusters near the vent fluid, of up to 4000 individuals per square metre (Marsh *et al.*, 2012). Other dominant taxa included stalked barnacles *Vulcanolepis scotiaensis*, actinostolid sea anemones, an undescribed species of vent limpet *Lepetodrilus*, and an undescribed large peltospirid gastropod named "Peltospiroid n. sp. ESR" (Rogers *et al.,* 2012). Many taxa abundant in other vent provinces such as tubeworms, bathymodiolid mussels, and alvinocaridid shrimps were

absent (Rogers *et al*., 2012). The ESR was identified as a new vent biogeographic province in its own right (Figure 6; Rogers *et al*., 2012).

Clade Neomphalina and Family Peltospiridae

The diverse molluscan class Gastropoda is an important component in the faunal composition of hydrothermal vents, and often characterise vent biogeographic provinces (e.g., *Alviniconcha hessleri* and *Ifremeria nautilei* that dominate west Pacific vents; 'scaly-foot gastropod' and *Alviniconcha marisindica* in Indian Ocean; *Lepetodrilus* limpets in most vents around the globe). The vast majority of vent gastropods are endemic to vent ecosystems. Sasaki *et al*. (2010) provides a review of the current knowledge and lists 145 species known from vents, of which 138 are only known from vents (>95% endemism).

Neomphalina is a chemosynthetic environment endemic clade (unranked but roughly equivalent to order) of gastropods comprising of three families including Peltospiridae, Neomphalidae, and Melanodrymiidae; totalling about 45 described species but many undescribed (Sasaki *et al.*, 2010). The relationship of Neomphalina with other groups of gastropods has been enigmatic and is much debated (Figures 11). Neomphalines used to be placed within the clade Vetigastropoda, but in light of recent phylogenetic work it was deemed as a separate clade in its own right, sister to Cocculinoidea (Figure 12; McArthur & Harasewych, 2003; Aktipis *et al*., 2008; Heß *et al*., 2008; Kano, 2008; Williams *et al.*, 2008; Aktipis & Giribet, 2012). Although shell pores have once been suggested as a key character of the group (e.g., Batten, 1984; Heß *et al*., 2008) it is now

known that not all neomphalines have shell pores (Sasaki *et al*., 2010). The internal relationship of genera within Neomphalina is also enigmatic, partly because neomphalines are extremely morphologically diverse (Figure 13).

The current assignment of genera to the three families is based on genetic evidence (Heß *et al*., 2008). There are genera with uncertain familial assignment, such as *Retiskenea*. The anatomy is known in detail for several genera through either dissection (e.g., Fretter, 1989) or reconstruction of three-dimensional computer models from stacking semi-thin sections digitally (e.g., Heß *et al*., 2008; methods in Ruthensteiner, 2000), in Peltospiridae mainly *Rhynchopelta*, *Peltospira* (Fretter, 1981; also includes brief overview of *Nodopelta, Echinopelta,* and *Hirtopelta*), as well as *Pachydermia* (Israelsson, 1998); in Neomphalidae *Neomphalus* (Fretter *et al*., 1981) and *Symmetromphalus* (Beck, 1992); in Melanodrymiidae *Melanodrymia* (Haszprunar, 1989) *Leptogyra,* and *Leptogyropsis* (Heß *et al*., 2008; also mentions *Xyleptogyra*).

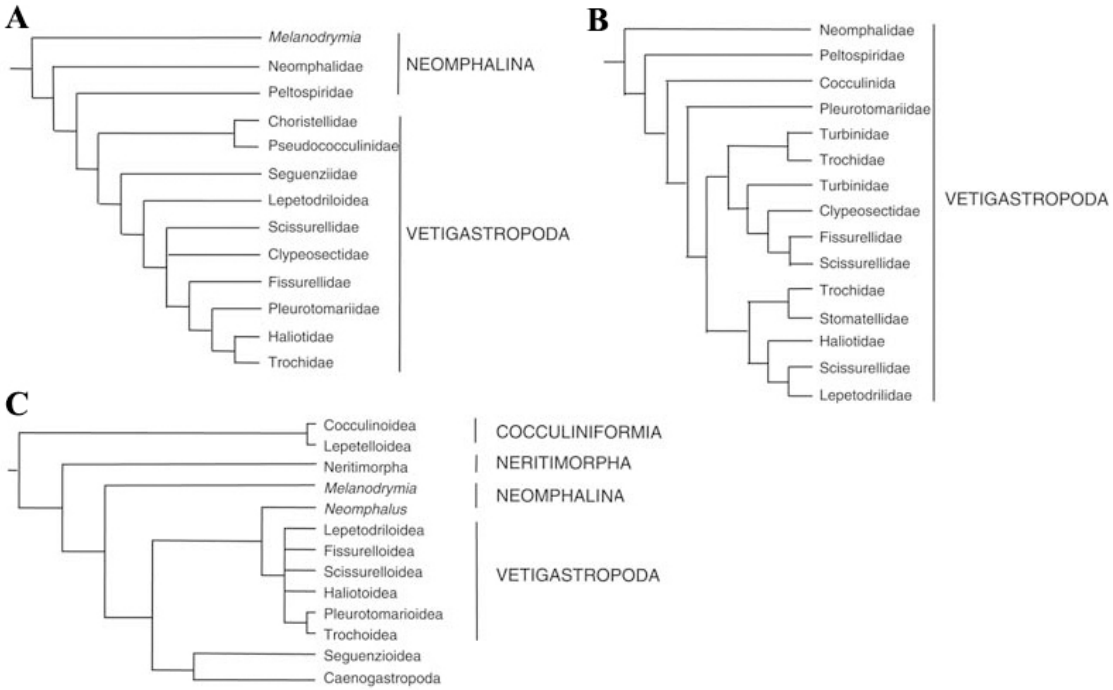

Figure 11. Some previously suggested relationships of Neomphalina to other closely related gastropod clades. **A**. Ponder & Lindberg, 1997; **B**. Geiger & Thacker, 2005; **C.** Haszprunar, 1988. From Aktipis & Giribet, 2012.

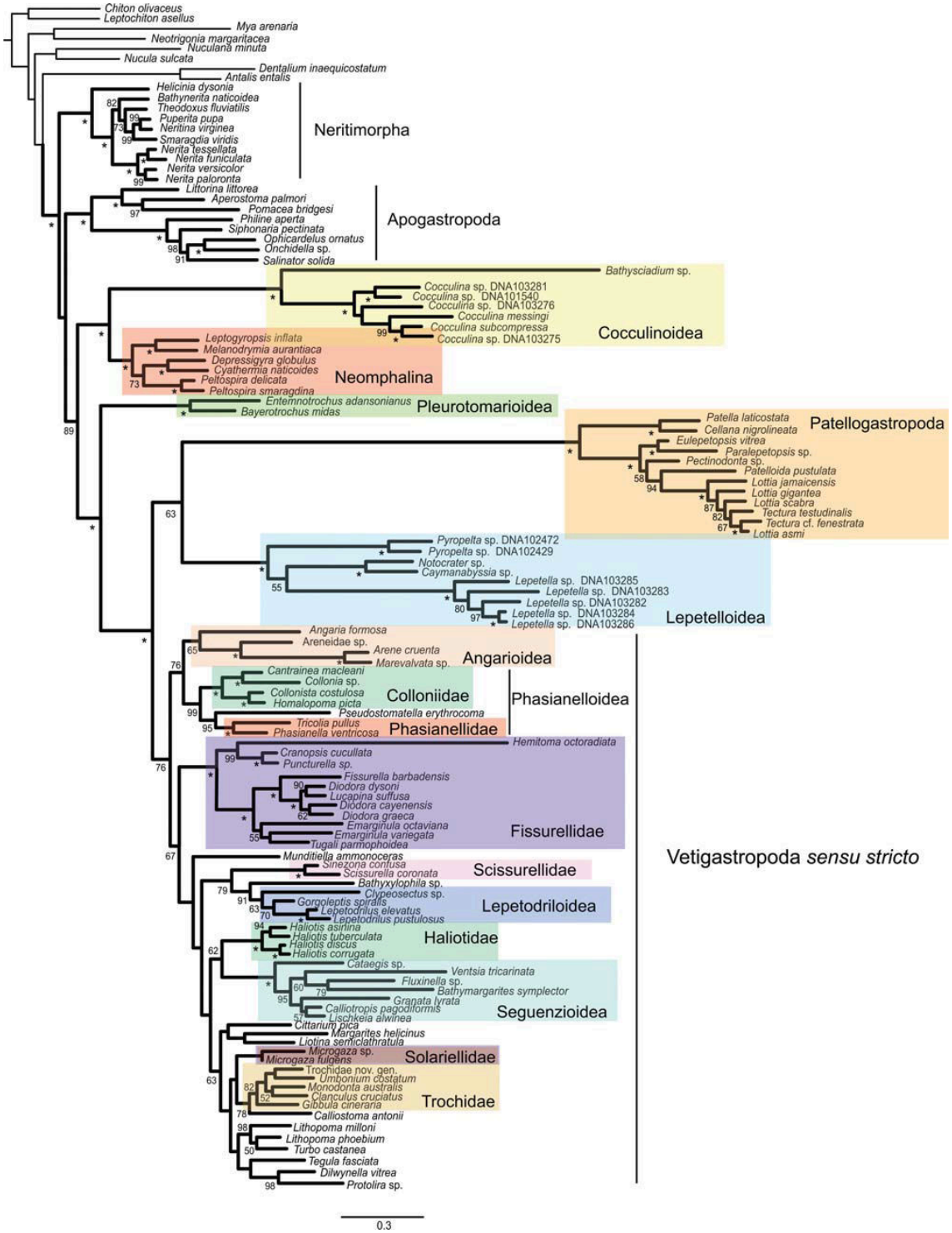

Figure 12. Maximum-likelihood tree based on five-genes (18S, 28S, H3, 16S, COI) from the most recent extensive phylogenetic study of Neomphalina and related gastropod clades showing a monophyletic Neomphalina sister to Cocculinoidea (Aktipis & Giribet, 2012).

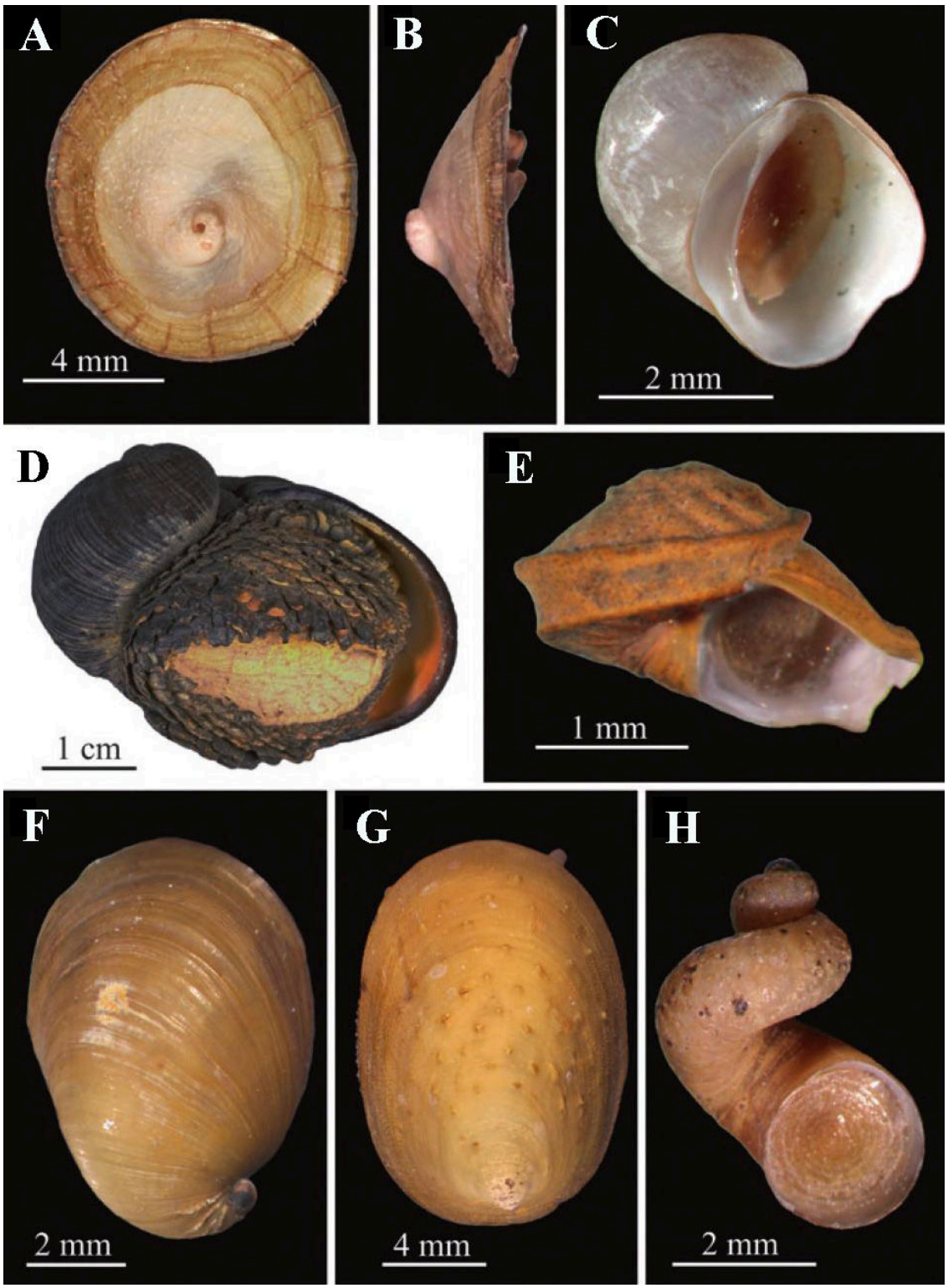

Figure 13. Neomphaline gastropods. **A-B.** *Neomphalus fretterae* McLean, 1981 (Neomphalidae); **C.** *Cyathermia naticoides* Warén & Bouchet, 1989 (Neomphalidae); **D.** The 'scaly-foot gastropod' (Peltospiridae; Warén *et al*., 2003); **E.** *Melanodrymia aurantiaca* Hickman, 1984 (Melanodrymiidae); **F**. *Peltospira operculata* McLean, 1989 (Peltospiridae); **G.** *Nodopelta heminoda* McLean, 1989 (Peltospiridae); **H.** *Pachydermia laevis* Warén & Bouchet, 1989 (Peltospiridae). From Sasaki *et al*., 2010.

The primary morphological characteristic distinguishing the three families is the copulatory organ. All investigated neomphalines are internally fertilised. Members of the family Neomphalidae have separate sexes with the left tentacle of males modified into a penis. In Melanodrymiidae both hermaphrodites (*Leptogyra*) and males (all other genera) have an array of species-specific copulatory organs on the head, which are not simple modifications of the left cephalic tentacle (Heß *et al*., 2008). Peltospirids however, do not have specialised copulatory organs of any sort and although all species investigated so far have separate sexes none exhibit significant sexual dimorphism (Fretter, 1989; Sasaki *et al*., 2010). Use of spermatophores is known from Peltospiridae (Warén *et al*., 2003) and Melanodrymiidae (Haszprunar, 1989).

The feeding mechanisms vary greatly between species. For example: melanodrymiids are detritivores (Heß *et al*., 2008); *Cyathermia naticoides* (Neomphalidae) is a filter-feeder but also grazes on siboglinid tubes; *Hirtopelta tufari* Beck, 2002 (Peltospiridae) hosts endosymbiotic bacteria in the gill (Beck, 2002); and the 'scaly-foot gastropod' hosts endosymbiotic bacteria in an enlarged esophageal gland (Goffredi *et al*., 2004; Nakagawa *et al*., 2014).

The dispersal mode in known species is lecithotropic with a planktonic dispersal stage (Warén *et al.*, 2006; Mills *et al*., 2007). Two pausispiral protoconch types occur, one with irregular net-like sculpture and the other with strong ridges (McLean, 1981; McLean, 1989; Warén & Bouchet, 1989; Warén & Bouchet, 1993). The protoconch sculpture was once used to separate Neomphalidae (net-like sculpture) and Peltospiridae (ridge sculpture), but the current placement based on molecular phylogeny defy this

separation as some peltospirid genera have net-like sculptures on the protoconch, for example *Depressigyra* and *Pachydermia*.

The vast majority of species are small (less than 15mm in shell length) but a couple oddities in Peltospiridae, exceeding 45 mm, have been discovered, including the 'scaly-foot gastropod' from CIR (Warén *et al*., 2003) and the yet-to-be-described "Peltospiroid n. sp." from ESR (Rogers *et al*., 2012).

The 'Scaly-foot Gastropod'

Each hydrothermal vent ecosystem, of every region, has a widely recognised emblematic species or two that are restricted to the region, for examples *Riftia pachyptila* of the EPR, *Rimicaris exoculata* of the MAR, *Alviniconcha hessleri* of the Mariana Trough (Johnson *et al*., 2014), etc. For the Indian Ocean this is certainly the 'scaly-foot gastropod' (Figure 11D). First discovered at Kairei Field, CIR (Van Dover *et al*, 2001) it attracted great interest because instead of having a regular operculum seen in most gastropod species, it had thousands of black sclerites covering its foot. Detailed morphological description and preliminary genetic phylogenetic results were released by Warén *et al.* (2003) after its discovery, although this did not consist of an official species description, as no name was given and no type specimen was designated. This species was placed in Peltospiridae using evidence from both molecular data and morphology, but remains undescribed to this date.

The sclerites were reported to be made of conchiolin and covered with pyrite (FeS_2) and

greigite (Fe_3S_4), two forms of iron sulfide (Warén *et al.*, 2003). It was suggested that the sclerites could have originated from an operculum duplication event. Yao *et al.* (2010) reported that its shell is also covered with a layer of iron sulfide, and that the [calcium carbonate – periostracum – iron sulfide] layering provided great flexibility to the shell while also adding to strength, especially against attempts to crack the shell. Currently, the scaly-foot gastropod remains the only known metazoan species to utilise iron in part of its skeleton. Furthermore, the scaly-foot gastropod was the first gastropod ever known to host symbiotic bacteria in an enlarged esophageal gland (Goffredi *et al.*, 2004). All other chemosymbiotic gastropods host their symbionts in the gills, and it is not clear why the scaly-foot gastropod does it differently.

Warén *et al*. (2003) and Suzuki *et al*. (2006) suggested that iron sulfide is actively biomineralised and the gastropod has some degree of control over the process. The conchiolin layer of sclerite contains some sulfide granules, the iron sulfide purity being high and without contamination, and the isotopic analyses indicating that the origin of sulfur and iron is from vent fluids and not bacteria. Suzuki *et al*. (2006) found that the sclerites are not optimised for magnetoreception and the purpose of sclerites is most likely a defence against predators or have some role in detoxification. Warén *et al*. (2003) identified the predatory gastropod *Phymorhynchus* which possesses dart-like radular teeth functioning to inject poison to their prey, as a potential predator and suggested the sclerites provide effective defence against this. Iron isotopic data suggest that unless iron uptake is extremely efficient, the iron in the sclerites is probably directly deposited from vent fluids, but the animal may have control over the reduced sulfur concentration (Suzuki *et al*., 2006). To prevent poisoning and to control symbiotic

bacteria, the concentration of reduced sulfur compounds must be strictly regulated. The sclerites may have first evolved as a method of disposing toxic sulfur compounds from the body and only became a defence mechanism as a by-product.

More recently another population of the 'scaly-foot gastropod' has been discovered in the Solitaire vent field, which has white sclerites and a brown shell in contrast with Kairei population's black shell and sclerites (Figure 14; Nakamura *et al*., 2012). The sclerites and shell lacked an iron sulfide layer but are yet mechanically stronger than those from Kairei vent field (Nakamura *et al*., 2012). The COI and 18S rRNA parsimonious networks suggests high genetic connectivity between Kairei and Solitaire, as the two populations share many haplotypes in both genes. It can be inferred from this that the two sites likely regularly exchange larvae and are well connected. This is a notable example in hydrothermal vents where the appearance of a species can change greatly according to composition of chemicals in the local vent fluid. Similarly a number of vent gastropods (e.g., *Lirapex*, *Pachydermia*, *Melanodrymia*) have been reported to have rusty deposits (likely deposited by bacteria) or lack them depending on

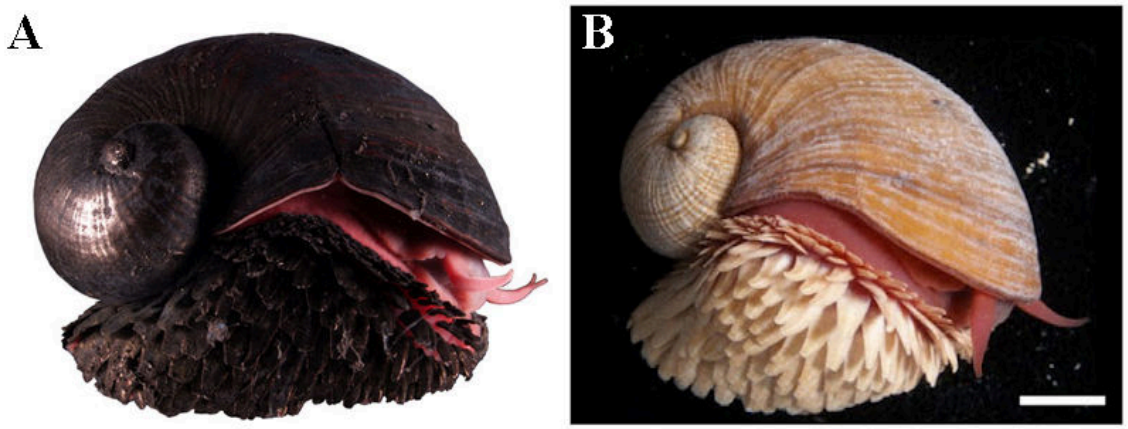

Figure 14. The 'scaly-foot gastropod' from CIR vents. **A.** Kairei field; **B**. Solitaire field. Scale bar (applies to both **A** and **B**) = 1cm (from Nakamura *et al*., 2012).

the vent field (Warén & Bouchet, 2003). Also, notably, a true operculum was reported from some specimens of the Solitaire population, which had never been reported from the Kairei population before.

Endosymbionts housed in the esophageal glands of Kairei specimens are known to comprise of a single phylotype related to thioautotrophic gammaproteobacterial endosymbionts of other molluscs (Goffredi *et al.*, 2004). It is known from Kairei specimens that there are no endosymbiotic bacteria found in the gill (Goffredi *et al*., 2004). Chemoautotrophy of the endosymbionts was confirmed using stable carbon isotope (^{13}C) labelling, and the symbionts were reported to have extreme genetic homogeneity with only two synonymous mutations across 13,810 positions in 32 host individuals sampled from Kairei (Nakagawa *et al*., 2014). This suggests the 'scaly-foot gastropod' likely carry out very strict selection of the symbionts. Furthermore, the symbiont genome is reported to have all genes necessary for aerobic respiration, and may switch between aerobic and anaerobic respiration depending on oxygen availability (Nakagawa *et al*., 2014).

The newly discovered and undescribed large peltospirids discovered from ESR ('Peltospiroid n. sp. ESR', Rogers *et al.*, 2012) as well as SWIR (Copley, 2011) closely resemble the 'scaly-foot gastropod' in shell morphology. These species are also very large for the family and exceed 40 mm in shell length, but have a large operculum and lack sclerites. Its phylogenetic affinity within Peltospiridae and relationship to the 'scaly-foot gastropod' is, as yet, unclear.

Project Aims and Contribution

The research presented in this thesis is the product of recent discoveries and explorations of hydrothermal vents on the SWIR (Copley, 2011) and the ESR (Rogers *et al*., 2012). New materials from these previously unexplored vent fields, in particular numerous specimens of the 'scaly-foot gastropod' from SWIR and the operculated giant peltospirids from both SWIR and ESR, allowed detailed examination of their taxonomy, phylogenetics, population genetics, anatomy, and adaptations to the vent environment.

Upon discovery of the 'scaly-foot gastropod' from Longqi field, SWIR (Copley, 2011; Tao *et al*., 2012), an immediate question was if this population belonged to the same species as the previously known 'scaly-foot gastropod' from Kairei and Solitaire fields of CIR (Warén *et al*., 2003; Nakamura *et al*., 2014). Chapter 2 is dedicated to characterising the SWIR 'scaly-foot gastropod' morphologically and genetically to confirm that it is the same species as the CIR populations, and to formally name the species and genus in accordance to the International Code of Zoological Nomenclature (ICZN, 1999) which is long overdue. Another aim of this chapter is to investigate the systematic position of the 'scaly-foot gastropod' using a five-gene dataset, as there has never been a comprehensive multi-gene phylogeny confirming its initial placement in Peltospiridae or Neomphalina by Warén *et al*. (2003; where only a small 16S single gene tree was presented).

The new Longqi, SWIR population of the 'scaly-foot gastropod' represents a considerable range extension as this site is 1,700 km away from the nearest known

population (Kairei field, CIR) and is on a separate mid-ocean ridge. The 'scaly-foot gastropod' is assumed to have lecithotrophic larvae like other neomphalines (Warén *et al*., 2006) and its eggs are known to have negative buoyancy (under atmospheric pressure, Beedessee *et al*., 2013), so its dispersal ability may be rather low. It is therefore interesting to investigate the genetic connectivity across the three populations, which is the aim of Chapter 3. This will be done using the mitochondrial COI gene. Understanding the gene flow between SWIR and CIR is important for environmental assessment in the light of upcoming mining activity in Longqi, SWIR; for which results from Chapter 3 provides the first piece of information.

Although the intriguing sclerites of the 'scaly-foot gastropod' have attracted much attention, its internal anatomy remains poorly known with most information coming from the short supplementary materials presented by Warén *et al*. (2003). The only feature explored is the enlarged esophageal gland due to investigations of the endosymbiotic bacteria housed there (Goffredi *et al*., 2004). A detailed anatomical characterisation is therefore still lacking and Chapter 4 aims to bridge this gap. Another important aim is to see if the 'scaly-foot gastropod' has any novel, previously undocumented anatomical adaptation to survive in the extreme vent environment. The methods include traditional dissection and histology, as well as tomographic reconstruction of a state-of-the-art 3D anatomical model of the major systems using a serially sectioned specimen.

Following the description of the internal anatomy, Chapter 5 focuses on the histological investigations of the sclerites to assess a widely quoted hypothesis that sclerites

originate from multiplication of the operculum (Warén *et al*., 2003). A further aim is to compare and contrast the 'scaly-foot gastropod' sclerites and superficially similar structures in other molluscs ('Aculifera', including classes Caudofoveata, Solenogastres, and Polyplacophora; Scheltema, 1993; Sigwart & Sutton, 2007) as well as scale-bearing Cambrian taxa such as Halwaxiida for which similarity in scleritomes has been central in the argument for their placement in Mollusca (Vinther & Nielsen, 2005; Vinther, 2009).

Finally, Chapter 6 endeavours to describe and characterise the two newly discovered operculated giant peltospirids from ESR and SWIR (Copley, 2011; Rogers *et al*., 2012) both morphologically and genetically. Key aims are to understand how the two populations are related to each other, to ascertain their systematic position, and to give them formal name(s) based on the results. Furthermore, population genetic methods using the COI gene allow investigations into the genetic connectivity as well as population demographics. A five-gene phylogenetic reconstruction (COI, H3, 16S, 18S, 28S) warrants assessment of their phylogenetic relationship with the superficially similar 'scaly-foot gastropod'.

It is hoped therefore that this body of work will contribute significantly to the systematics, ecology, and evolution of the two enigmatic giant vent-endemic gastropods; as well as to hydrothermal vent ecology and biogeography as a whole by providing novel information on dispersal and connectivity as well as autecology.

References

Adams D, Mills S, Shank T, Mullineaux L. 2010. Expanding dispersal studies at hydrothermal vents through species identification of cryptic larval forms. *Marine Biology* **157:** 1049-1062.

Aktipis SW, Giribet G. 2010. A phylogeny of Vetigastropoda and other "archaeogastropods": re-organizing old gastropod clades. *Invertebrate Biology* **129:** 220-240.

Aktipis SW, Giribet G. 2011. Testing relationships among the vetigastropod taxa: a molecular approach. *Journal of Molluscan Studies***:** eyr023.

Aktipis SW, Giribet G, Lindberg DR, Ponder WF. 2008. Gastropod phylogeny: an overview and analysis. In: Lindberg DR and Ponder WF, eds. *Phylogeny and evolution of the Mollusca*. Berkeley, California: University of California Press. 201-237.

Bachraty C, Legendre P, Desbruyères D. 2009. Biogeographic relationships among deep-sea hydrothermal vent faunas at global scale. *Deep Sea Research Part I: Oceanographic Research Papers* **56:** 1371-1378.

Baker ET, Chen YJ, Phipps Morgan J. 1996. The relationship between near-axis hydrothermal cooling and the spreading rate of mid-ocean ridges. *Earth and Planetary Science Letters* **142:** 137-145.

Baker ET, Edmonds HN, Michael PJ, Bach W, Dick HJB, Snow JE, Walker SL, Banerjee NR, Langmuir CH. 2004. Hydrothermal venting in magma deserts: The ultraslow-spreading Gakkel and Southwest Indian Ridges. *Geochem. Geophys. Geosyst.* **5:** Q08002.

Baker ET, German CR. 2004. On the Global Distribution of Hydrothermal Vent Fields *Mid-Ocean Ridges*: American Geophysical Union. 245-266.

Baker MC, Ramirez-Llodra EZ, Tyler PA, German CR, Boetius A, Cordes EE, Dubilier N, Fisher CR, Levin LA, Metaxas A. 2010. Biogeography, ecology and vulnerability of chemosynthetic ecosystems in the deep sea. In: McIntyre A, ed. *Life in the World's Oceans: Diversity, Distribution, and Abundance*: Wiley-Blackwell. 161-183.

Batten RL. 1984. Shell structure of the Galapagos Rift limpet *Neomphalus fretterae* McLean 1981, with notes on muscle scars and insertions. American Museum novitates; no. 2776.

Beck LA. 1989. *Symmetromphalus hageni* sp. n., a new neomphalid gastropod (Prosobranchia: Neomphalidae) from hydrothermal vents at the Manus Back-Arc Basin (Bismarck Sea, Papua New Guinea). *Annalen des Naturhistorischen Museums in Wien. Serie B für Botanik und Zoologie***:** 243-257.

Beck LA. 2002. *Hirtopelta tufari* sp. n., a new gastropod species from hot vents at the East Pacific Rise (21° S) harbouring endocytosymbiotic bacteria in its gill (Gastropoda: Rhipidoglossa:

Peltospiridae). *Arch Molluskenkd* **130:** 249-257.

Beedessee G, Watanabe H, Ogura T, Nemoto S, Yahagi T, Nakagawa S, Nakamura K, Takai K, Koonjul M, Marie DEP. 2013. High Connectivity of Animal Populations in Deep-Sea Hydrothermal Vent Fields in the Central Indian Ridge Relevant to Its Geological Setting. *PLoS ONE* **8:** e81570.

Bemis K, Lowell RP, Farough A. 2012. Diffuse flow on and around hydrothermal vents at mid-ocean ridges. *Oceanography* **25:** 182-191.

BODC (British Oceanographic Data Centre). 2010. GEBCO Grid Display. *Available at: https://www.bodc.ac.uk/products/software_products/gebco_grid_display/*.

Cavanaugh CM, Gardiner SL, Jones ML, Jannasch HW, Waterbury JB. 1981. Prokaryotic cells in the hydrothermal vent tube worm *Riftia pachyptila* Jones: possible chemoautotrophic symbionts. *Science* **213:** 340-342.

Chamberlain SC. 2000. Vision in hydrothermal vent shrimp. *Philosophical Transactions of the Royal Society of London. Series B: Biological Sciences* **355:** 1151-1154.

Chevaldonné P, Fisher C, Childress J, Desbruyères D, Jollivet D, Zal F, Toulmond A. 2000. Thermotolerance and the 'Pompeii worms'. *Marine Ecology Progress Series* **208:** 293-295.

Connelly DP, Copley JT, Murton BJ, Stansfield K, Tyler PA, German CR, Van Dover CL, Amon D, Furlong M, Grindlay N, Hayman N, Huhnerbach V, Judge M, Le Bas T, McPhail S, Meier A, Nakamura K-i, Nye V, Pebody M, Pedersen RB, Plouviez S, Sands C, Searle RC, Stevenson P, Taws S, Wilcox S. 2012. Hydrothermal vent fields and chemosynthetic biota on the world's deepest seafloor spreading centre. *Nature Communications* **3:** 620.

Copley JT. 2011. Research cruise JC67, Dragon vent field, SW Indian Ocean, 27-30 November 2011 *RRS James Cook cruise report*: British Oceanographic Data Centre. Available from http://www.bodc.ac.uk/data/information_and_inventories/cruise_inventory/report/10593/.

Corliss JB, Ballard RD. 1977. Oases of life in the cold abyss. *National Geographic Magazine* **152: 441-453**.

Corliss JB, Dymond J, Gordon LI, Edmond JM, von Herzen RP, Ballard RD, Green K, Williams D, Bainbridge A, Crane K, van Andel TH. 1979. Submarine thermal sprirngs on the Galapagos Rift. *Science* **203:** 1073-1083.

Coykendall DK, Johnson S, Karl S, Lutz R, Vrijenhoek R. 2011. Genetic diversity and demographic instability in *Riftia pachyptila* tubeworms from eastern Pacific hydrothermal vents. *BMC Evolutionary Biology* **11:** 96.

Craddock C, Hoeh WR, Lutz RA, Vrijenhoek RC. 1995. Extensive gene flow among mytilid (*Bathymodiolus thermophilus*) populations from hydrothermal vents of the eastern Pacific. *Marine Biology* **124:** 137-146.

Creasey S, Rogers AD, Tyler PA. 1996. Genetic comparison of two populations of the deep-sea vent shrimp *Rimicaris exoculata* (Decapoda: Bresiliidae) from the Mid-Atlantic Ridge. *Marine Biology* **125:** 473-482.

De Busserolles F, Sarrazin J, Gauthier O, Gélinas Y, Fabri MC, Sarradin PM, Desbruyères D. 2009. Are spatial variations in the diets of hydrothermal fauna linked to local environmental conditions? *Deep Sea Research Part II: Topical Studies in Oceanography* **56:** 1649-1664.

Dilly GF, Young CR, Lane WS, Pangilinan J, Girguis PR. 2012. *Exploring the limit of metazoan thermal tolerance via comparative proteomics: thermally induced changes in protein abundance by two hydrothermal vent polychaetes*.

Esri. 2012. *ArcGIS Desktop: Release 10.1*. Environmental Systems Research Institute: Redlands, CA.

Etter PD, Bassham S, Hohenlohe PA, Johnson EA, Cresko WA. 2011. SNP discovery and genotyping for evolutionary genetics using RAD sequencing *Molecular methods for evolutionary genetics*: Springer. 157-178.

Felbeck H. 1981. Chemoautotrophic potential of the hydrothermal vent tube worm, *Riftia pachyptila* Jones (Vestimentifera). *Science* **213:** 336-338.

Fisher CR, Takai K, Le Bris N. 2007. Hydrothermal vent ecosystems. *Oceanography* **20:** 14-23.

Fretter V. 1989. The anatomy of some new archaeogastropod limpets (Superfamily Peltospiracea) from hydrothermal vents. *J Zool* **218:** 123-169.

Fretter V, Graham A, McLean J. 1981. The anatomy of the galapagos rift limpet, Neomphalus fretterae. *Malacologia* **21:** 337-361.

Fu YX. 1997. Statistical Tests of Neutrality of Mutations against Population Growth, Hitchhiking and Background Selection. *Genetics* **147:** 915-925.

Fujikura K, Okutani T, Maruyama T. 2012. *Deep-sea Life - Biological observations using reseearch submersibles*. Tokai University Press: Tokyo, Japan.

Fujiwara Y, Kawato M. 2010. Whale-Fall Ecosystems and Two “Stepping Stone” Hypotheses. *The Review of High Pressure Science and Technology* **20:** 315-320.

Gage JD, Tyler PA. 1991. *Deep-sea Biology: A Natural History of Organisms at the Deep-sea Floor*. Cambridge University Press: Cambridge, UK.

Gebruk AV, Chevaldonné P, Shank T, Lutz RA, Vrijenhoek RC. 2000. Deep-sea hydrothermal vent communities of the Logatchev area (14°45′N, Mid-Atlantic Ridge): diverse biotopes and high biomass. *Journal of the Marine Biological Association of the United Kingdom* **80:** 383-393.

Geiger DL, Thacker CE. 2005. Molecular phylogeny of Vetigastropoda reveals non-monophyletic Scissurellidae, Trochoidea, and Fissurelloidea. *Molluscan Research* **25**: 47–55.

Genard B, Marie B, Loumaye E, Knoops B, Legendre P, Zal F, Rees J. 2013. Living in a hot

redox soup: antioxidant defences of the hydrothermal worm Alvinella pompejana. *Aquatic Biology* **18:** 217-228.

German CR, Von Damm KL. 2004. Hydrothermal processes: Treatise on geochemistry. In: Turekian KK and Holland HD, eds. *The Oceans and Marine Geochemistry* Oxford: Elsevier. 181-222.

Goffredi SK, Warén A, Orphan VJ, Van Dover CL, Vrijenhoek RC. 2004. Novel forms of structural integration between microbes and a hydrothermal vent gastropod from the Indian Ocean. *Applied and Environmental Microbiology* **70:** 3082-3090.

Grassle JF. 1989. Species diversity in deep-sea communities. *Trends in ecology & evolution (Personal edition)* **4:** 12-15.

Grassle JF, Patil GP, Smith WK, Taille C. 1979. Galapagos '79: Initial findings of a biology quest. *Oceanus* **22:** 2-10.

Hannington M, Jamieson J, Monecke T, Petersen S, Beaulieu S. 2011. The abundance of seafloor massive sulfide deposits. *Geology* **39:** 1155-1158.

Hashimoto J, Ohta S, Gamo T, Chiba H, Yamaguchi T, Tsuchida S, Okudaira T, Watabe H, Yamanaka T, Kitazawa M. 2001. First hydrothermal vent communities from the Indian Ocean discovered. *Zoological Science* **18:** 717-721.

Haszprunar G. 1988. A preliminary phylogenetic analysis of streptoneurous Gastropoda. *Malacological Review, Supplement* **4**: 7–16.

Haszprunar G. 1989. The anatomy of *Melanodrymia aurantiaca* Hickman, a coiled Archaeogastropod from the East Pacific hydrothermal vents (Mollusca, Gastropoda). *Acta Zool* **70:** 175-186.

Herrera S, Watanabe H, Shank TM. 2015. Evolutionary and biogeographical patterns of barnacles from deep-sea hydrothermal vents. *Molecular Ecology* **24:** 673-689.

Herring PJ, Dixon DR. 1998. Extensive deep-sea dispersal of postlarval shrimp from a hydrothermal vent. *Deep Sea Research Part I: Oceanographic Research Papers* **45:** 2105-2118.

Heß M, Beck F, Gensler H, Kano Y, Kiel S, Haszprunar G. 2008. Microanatomy, shell structre and molecular phylogeny of *Leptogyra*, *Xyleptogyra* and *Leptogyropsis* (Gastropoda: Neomphalida: Melanodrymiidae) from sunken wood. *Journal of Molluscan Studies* **74:** 383-401.

Hoagland P, Beaulieu S, Tivey MA, Eggert RG, German C, Glowka L, Lin J. 2010. Deep-sea mining of seafloor massive sulfides. *Marine Policy* **34:** 728-732.

Holder T, Basquin C, Ebert J, Randel N, Jollivet D, Conti E, Jekely G, Bono F. 2013. Deep transcriptome-sequencing and proteome analysis of the hydrothermal vent annelid Alvinella pompejana identifies the CvP-bias as a robust measure of eukaryotic thermostability.

Biology Direct **8:** 2.

Hurtado LA, Lutz RA, Vrijenhoek RC. 2004. Distinct patterns of genetic differentiation among annelids of eastern Pacific hydrothermal vents. *Molecular Ecology* **13:** 2603-2615.

ICZN (International Commission on Zoological Nomenclature). 1999. *International Code of Zoological Nomenclature, Fourth Edition*. The International Trust for Zoological Nomenclature: London, UK.

InterRidge. 2010. InterRidge Vents Database Ver. 2.1. *Available at: http://vents-data.interridge.org/maps*.

Israelsson O. 1998. The anatomy of *Pachydermia laevis* (Archaeogastropoda: 'Peltospiridae'). *J Moll Stud* **64:** 93-109.

Jinks RN, Markley TL, Taylor EE, Perovich G, Dittel AI, Epifanio CE, Cronin TW. 2002. Adaptive visual metamorphosis in a deep-sea hydrothermal vent crab. *Nature* **420:** 68-70.

Johnson SB, Warén A, Tunnicliffe V, Dover CV, Wheat CG, Schultz TF, Vrijenhoek RC. 2014. Molecular taxonomy and naming of five cryptic species of *Alviniconcha* snails (Gastropoda: Abyssochrysoidea) from hydrothermal vents. *Systematics and Biodiversity***:** 1-18.

Johnson SB, Warén A, Vrijenhoek RC. 2008. DNA Barcoding of Lepetodrilus Limpets Reveals Cryptic Species. *Journal of Shellfish Research* **27:** 43-51.

Kano Y. 2008. Vetigastropod phylogeny and a new concept of Seguenzioidea: independent evolution of copulatory organs in the deep‐sea habitats. *Zoologica Scripta* **37:** 1-21.

Kelley DS, Karson JA, Blackman DK, Fruh-Green GL, Butterfield DA, Lilley MD, Olson EJ, Schrenk MO, Roe KK, Lebon GT, Rivizzigno P. 2001. An off-axis hydrothermal vent field near the Mid-Atlantic Ridge at 30 degrees N. *Nature* **412:** 145-149.

Kim YW, Yasuda M, Yamagishi A, Oshima T, Ohta S. 1995. Characterization of the endosymbiont of a deep-sea bivalve, *Calyptogena soyoae*. *Applied and Environmental Microbiology* **61:** 823-827.

Kyuno A, Shintaku M, Fujita Y, Matsumoto H, Utsumi M, Watanabe H, Fujiwara Y, Miyazaki J-I. 2009. Dispersal and differentiation of deep-sea mussels of the genus *Bathymodiolus* (Mytilidae, Bathymodiolinae). *Journal of Marine Biology* **2009**.

Le Bris N, Gaill F. 2007. How does the annelid *Alvinella pompejana* deal with an extreme hydrothermal environment? *Reviews in Environmental Science and Bio/Technology* **6:** 197-221.

Lever MA, Rouxel O, Alt JC, Shimizu N, Ono S, Coggon RM, Shanks WC, Lapham L, Elvert M, Prieto-Mollar X, Hinrichs K-U, Inagaki F, Teske A. 2013. Evidence for microbial carbon and sulfur cycling in deeply buried ridge flank basalt. *Science* **339:** 1305-1308.

Lonsdale P. 1977. Structural geomorphology of a fast-spreading rise crest: The East Pacific Rise near 3°25′S. *Marine Geophysical Research* **3:** 251-293.

Lutz RA, Kennish MJ. 1993. Ecology of deep-sea hydrothermal vent communities: A review. *Reviews of Geophysics* **31:** 211-242.

Marsh AG, Mullineaux LS, Young CM, Manahan DT. 2001. Larval dispersal potential of the tubeworm *Riftia pachyptila* at deep-sea hydrothermal vents. *Nature* **411:** 77-80.

Marsh L, Copley JT, Huvenne VAI, Linse K, Reid WDK, Rogers AD, Sweeting CJ, Tyler PA. 2012. Microdistribution of faunal assemblages at deep-sea hydrothermal vents in the Southern Ocean. *PLoS ONE* **7:** e48348.

McArthur A, Harasewych M. 2003. Molecular systematics of the major lineages of the Gastropoda. In: Lydeard C, Lindberg DR, ed. *Molecular Systematics and Phylogeography of Mollusks*: Smithsonian Books, Washington. 140-160.

McLean J. 1981. The galapagos rift limpet *Neomphalus* - relevance to understanding the evolution of a major paleozoic-mesozoic radiation. *Malacologia* **21:** 291-336.

McLean JH. 1989. New archaeogastropod limpets from hydrothermal vents: new family Peltospiridae, new superfamily Peltospiracea. *Zoologica Scripta* **18:** 49-66.

Mills SW, Mullineaux LS, Tyler PA. 2007. Habitat associations in gastropod species at East Pacific Rise hydrothermal vents (9 50′ N). *The Biological Bulletin* **212:** 185-194.

Mullineaux LS, Fisher CR, Peterson CH, Schaeffer SW. 2000. Tubeworm succession at hydrothermal vents: use of biogenic cues to reduce habitat selection error? *Oecologia* **123:** 275-284.

Mullineaux LS, Manahan D. 1998. Deep-sea diaspora: the LARVAE project explores how species migrate from vent to vent. *Oceanus* **41:** 6-9.

Mullineaux LS, Mills SW, Sweetman AK, Beaudreau AH, A. Metaxas HLH. 2005. Vertical, lateral and temporal structure in larval distributions at hydrothermal vents. *Marine Ecology Progress Series* **293:** 1-16.

Nakagawa S, Shimamura S, Takaki Y, Suzuki Y, Murakami S-i, Watanabe T, Fujiyoshi S, Mino S, Sawabe T, Maeda T, Makita H, Nemoto S, Nishimura S-I, Watanabe H, Watsuji T-o, Takai K. 2014. Allying with armored snails: the complete genome of gammaproteobacterial endosymbiont. *The ISME Journal* **8:** 40-51.

Nakamura K, Watanabe H, Miyazaki J, Takai K, Kawagucci S, Noguchi T, Nemoto S, Watsuji T-o, Matsuzaki T, Shibuya T, Okamura K, Mochizuki M, Orihashi Y, Ura T, Asada A, Marie D, Koonjul M, Singh M, Beedessee G, Bhikajee M, Tamaki K. 2012. Discovery of new hydrothermal activity and chemosynthetic fauna on the Central Indian Ridge at 18°–20°S. *PLoS ONE* **7:** e32965.

Nuckley DJ, Jinks RN, Battelle B-A, Herzog ED, Kass L, Renninger GH, Chamberlain SC. 1996. Retinal anatomy of a new species of bresiliid shrimp from a hydrothermal vent field on the Mid-Atlantic Ridge. *Biological Bulletin* **190:** 98-110.

O'Neill PJ, Jinks RN, Herzog ED, Battelle BA, Kass L, Renninger GH, Chamberlain SC. 1995. The morphology of the dorsal eye of the hydrothermal vent shrimp, *Rimicaris exoculata*. *Vis Neurosci* **12:** 861-875.

Page HM, Fiala-Medioni A, Fisher CR, Childress JJ. 1991. Experimental evidence for filter-feeding by the hydrothermal vent mussel, *Bathymodiolus thermophilus*. *Deep Sea Research Part A. Oceanographic Research Papers* **38:** 1455-1461.

Pedersen RB, Rapp HT, Thorseth IH, Lilley MD, Barriga FJAS, Baumberger T, Flesland K, Fonseca R, Fruh-Green GL, Jorgensen SL. 2010. Discovery of a black smoker vent field and vent fauna at the Arctic Mid-Ocean Ridge. *Nature Communications* **1:** 126.

Pelli DG, Chamberlain SC. 1989. The visibility of 350 °C black-body radiation by the shrimp *Rimicaris exoculata* and man. *Nature* **337:** 460-461.

Petersen JM, Ramette A, Lott C, Cambon-Bonavita M-A, Zbinden M, Dubilier N. 2010. Dual symbiosis of the vent shrimp *Rimicaris exoculata* with filamentous gamma- and epsilonproteobacteria at four Mid-Atlantic Ridge hydrothermal vent fields. *Environmental Microbiology* **12:** 2204-2218.

Phipps Morgan J, Ghen YJ. 1993. Dependence of ridge-axis morphology on magma supply and spreading rate. *Nature* **364:** 706-708.

Plouviez S, Shank TM, Faure B, Daguin-Thiebaut C, Viard F, Lallier FH, Jollivet D. 2009. Comparative phylogeography among hydrothermal vent species along the East Pacific Rise reveals vicariant processes and population expansion in the South. *Molecular Ecology* **18:** 3903-3917.

Ponder WF, Lindberg DR. 1997. Towards a phylogeny of gastropod molluscs: an analysis using morphological characters. *Zoological Journal of the Linnean Society* **119**: 83–265.

Powell MA, Somero GN. 1986. Adaptations to sulfide by hydrothermal vent animals: sites and mechanisms of detoxification and metabolism. *The Biological Bulletin* **171:** 274-290.

Ramirez-Llodra E, Shank TM, German CR. 2007. Biodiversity and biogeography of hydrothermal vent species: thirty years of discovery and investigations. *Oceanography* **20:** 30-41.

Ravaux J, Hamel G, Zbinden M, Tasiemski AA, Boutet I, Léger N, Tanguy A, Jollivet D, Shillito B. 2013. Thermal limit for metazoan life in question: *in vivo* heat tolerance of the Pompeii worm. *PLoS ONE* **8:** e64074.

Renninger G, Kass L, Gleeson R, Van Dover C, Battelle B, Jinks R, Herzog E, Chamberlain S. 1995. Sulfide as a chemical stimulus for deep-sea hydrothermal vent shrimp. *The Biological Bulletin* **189:** 69-76.

Rex MA, Etter RJ, Morris JS, Crouse J, McClain CR, Johnson NA, Stuart CT, Deming JW, Thies R, Avery R. 2006. Global bathymetric patterns of standing stock and body size in the

deep-sea benthos. *Marine Ecology Progress Series* **317:** 1-8.

Rogers AD, Tyler PA, Connelly DP, Copley JT, James R, Larter RD, Linse K, Mills RA, Garabato AN, Pancost RD, Pearce DA, Polunin NVC, German CR, Shank T, Boersch-Supan PH, Alker BJ, Aquilina A, Bennett SA, Clarke A, Dinley RJJ, Graham AGC, Green DRH, Hawkes JA, Hepburn L, Hilario A, Huvenne VAI, Marsh L, Ramirez-Llodra E, Reid WDK, Roterman CN, Sweeting CJ, Thatje S, Zwirglmaier K. 2012. the discovery of new deep-sea hydrothermal vent communities in the Southern Ocean and implications for biogeography. *PLoS Biology* **10:** e1001234.

Rowe GT. 1983. Biomass and production of the deep-sea macrobenthos. In: Rowe GT, ed. *The Sea vol. 8, Deep-Sea Biology*. New York: John Wiley. **97-121**.

Ruthensteiner B. 2008. Soft Part 3D visualization by serial sectioning and computer reconstruction. *2008* **1:** 38.

Santelli CM, Orcutt BN, Banning E, Bach W, Moyer CL, Sogin ML, Staudigel H, Edwards KJ. 2008. Abundance and diversity of microbial life in ocean crust. *Nature* **453:** 653-656.

Sasaki T, Warén A, Kano Y, Okutani T, Fujikura K, Kiel S. 2010. Gastropods from recent hot vents and cold seeps: systematics, diversity and life strategies. In: Kiel S, ed. *Topics in Geobiology 33: The Vent and Seep Biota*. Netherlands: Springer 169-254.

Shank TM, Fornari DJ, Von Damm KL, Lilley MD, Haymon RM, Lutz RA. 1998. Temporal and spatial patterns of biological community development at nascent deep-sea hydrothermal vents (9°50′N, East Pacific Rise). *Deep Sea Research Part II: Topical Studies in Oceanography* **45:** 465-515.

Shigeno S, Ogura A, Mori T, Toyohara H, Yoshida T, Tsuchida S, Fujikura K. 2014. Sensing deep extreme environments: the receptor cell types, brain centers, and multi-layer neural packaging of hydrothermal vent endemic worms. *Frontiers in Zoology* **11:** 82.

Shin DS, DiDonato M, Barondeau DP, Hura GL, Hitomi C, Berglund JA, Getzoff ED, Cary SC, Tainer JA. 2009. Superoxide dismutase from the eukaryotic thermophile *Alvinella pompejana*: structures, stability, mechanism, and insights into amyotrophic lateral sclerosis. *Journal of Molecular Biology* **385:** 1534-1555.

Smith CR, Baco AR. 2003. Ecology of whale falls at the deep-sea floor. *Oceanography and Marine Biology* **41:** 311-354.

Smith CR, Mullineaux LS, Levin LA. 1998. Deep-sea biodiversity: a compilation of recent advances in honor of Robert R. Hessler. *Deep-Sea Research II* **45:** 1-12.

Stein JL, Cary SC, Hessler RR, Ohta S, Vetter RD, Childress JJ, Felbeck H. 1988. Chemoautotrophic symbiosis in a hydrothermal vent gastropod. *Biological Bulletin* **174:** 373-378.

Suzuki Y, Kopp RE, Kogure T, Suga A, Takai K, Tsuchida S, Ozaki N, Endo K, Hashimoto J,

Kato Y, Mizota C, Hirata T, Chiba H, Nealson KH, Horikoshi K, Kirschvink JL. 2006. Sclerite formation in the hydrothermal-vent 'scaly-foot gastropod' —possible control of iron sulfide biomineralization by the animal. *Earth and Planetary Science Letters* **242:** 39-50.

Tajima F. 1989. Statistical method for testing the neutral mutation hypothesis by DNA polymorphism. *Genetics* **123:** 585-595.

Tao C, Li H, Jin X, Zhou J, Wu T, He Y, Deng X, Gu C, Zhang G, Liu W. 2014. Seafloor hydrothermal activity and polymetallic sulfide exploration on the Southwest Indian ridge. *Chinese Science Bulletin***:** 1-11.

Tao C, Lin J, Guo S, Chen YJ, Wu G, Han X, German CR, Yoerger DR, Zhou N, Li H, Su X, Zhu J, DY115-19 at, Parties D-S. 2012. First active hydrothermal vents on an ultraslow-spreading center: Southwest Indian Ridge. *Geology* **40:** 47-50.

Teixeira S, Serrão EA, Arnaud-Haond S. 2012. Panmixia in a fragmented and unstable environment: The hydrothermal shrimp *Rimicaris exoculata* disperses extensively along the Mid-Atlantic Ridge. *PLoS ONE* **7:** e38521.

Tivey MK. 2007. Generation of seafloor hydrothermal vent fluids and associated mineral deposits. *Oceanography* **20:** 50-65.

Tolstoy M, Waldhauser F, Bohnenstiehl DR, Weekly RT, Kim WY. 2008. Seismic identification of along-axis hydrothermal flow on the East Pacific Rise. *Nature* **451:** 181-184.

Toulmond A, Slitine FEI, Frescheville JD, Jouin C. 1990. Extracellular hemoglobins of hydrothermal vent annelids: structural and functional characteristics in three alvinellid species. *Biological Bulletin* **179:** 366-373.

Tyler PA, Young CM. 2003. Dispersal at hydrothermal vents: a summary of recent progress. *Hydrobiologia* **503:** 9-19.

Van Dover CL. 1990. Biogeography of hydrothermal vent communities along seafloor spreading centers. *Trends in Ecology & Evolution* **5:** 242-246.

Van Dover CL. 2000. *The Ecology of Deep-Sea Hydrothermal Vents*. Princeton University Press: Princeton.

Van Dover CL, German CR, Speer KG, Parson LM, Vrijenhoek RC. 2002. Evolution and biogeography of deep-sea vent and seep invertebrates. *Science* **295:** 1253-1257.

Van Dover CL, Humphris SE, Fornari D, Cavanaugh CM, Collier R, Goffredi SK, Hashimoto J, Lilley MD, Reysenbach AL, Shank TM, Von Damm KL, Banta A, Gallant RM, Gテカtz D, Green D, Hall J, Harmer TL, Hurtado LA, Johnson P, McKiness ZP, Meredith C, Olson E, Pan IL, Turnipseed M, Won Y, Young CR, Vrijenhoek RC. 2001. Biogeography and ecological setting of Indian Ocean hydrothermal vents. *Science* **294:** 818-823.

Vrijenhoek R. 1997. Gene flow and genetic diversity in naturally fragmented metapopulations of

deep-sea hydrothermal vent animals. *Journal of Heredity* **88:** 285-293.

Vrijenhoek RC. 2010. Genetic diversity and connectivity of deep-sea hydrothermal vent metapopulations. *Molecular Ecology* **19:** 4391-4411.

Waren A. 2001. Gastropoda and Monoplacophora from hydrothermal vents and seeps; new taxa and records. *The Veliger* **44:** 116-231.

Warén A, Bengtson S, Goffredi SK, Van Dover CL. 2003. A hot-vent gastropod with iron sulfide dermal sclerites. *Science* **302:** 1007-1007.

Waren A, Bouchet P. 1989. New gastropods from East Pacific hydrothermal vents. *Zoologica Scripta* **18:** 67-102.

Waren A, Bouchet P. 1993. New records, species, genera, and a new family of gastropods from hydrothermal vents and hydrocarbon seeps. *Zoologica Scripta* **22:** 1-90.

Warén A, Bouchet P, Cosel RV. 2006. Mollusca, Gastropoda. In: Desbruyères D, Segonzac M and Bright M, eds. *Denisia*. 2 ed. Zurich, Switzerland: Swiss National Museum. 82-137.

Watsuji T-o, Yamamoto A, Motoki K, Ueda K, Hada E, Takaki Y, Kawagucci S, Takai K. 2014. Molecular evidence of digestion and absorption of epibiotic bacterial community by deep-sea crab Shinkaia crosnieri. *The ISME Journal* **9**: 821-831.

Wei C, Rowe G, Hubbard G, Scheltema A, Wilson G, Petrescu I, Foster J, Wicksten M, Chen M, Davenport R, Soliman Y, Wang Y. 2010. Bathymetric zonation of deep-sea macrofauna in relation to export of surface phytoplankton production. *Marine Ecology Progress Series* **399:** 1-14.

Williams ST, Karube S, Ozawa T. 2008. Molecular systematics of Vetigastropoda: Trochidae, turbinidae and trochoidea redefined. *Zoologica Scripta* **37:** 483-506.

Wolff T. 2005. Composition and endemism of the deep-sea hydrothermal vent fauna. *Cahiers de Biologie Marine* **46:** 97-104.

Wright S. 1950. Genetical structure of populations. *Nature* **166:** 247-249.

Yao H, Dao M, Imholt T, Huang J, Wheeler K, Bonilla A, Suresh S, Ortiz C. 2010. Protection mechanisms of the iron-plated armor of a deep-sea hydrothermal vent gastropod. *Proceedings of the National Academy of Sciences* **107:** 987-992.

Young CR, Fujio S, Vrijenhoek RC. 2008. Directional dispersal between mid-ocean ridges: deep-ocean circulation and gene flow in Ridgeia piscesae. *Molecular Ecology* **17:** 1718-1731.

Chapter 2

The ‘scaly-foot gastropod’: a new genus and species of hydrothermal vent endemic gastropod (Neomphalina: Peltospiridae) from the Indian Ocean

(*Journal of Molluscan Studies,* In press)

CHAPTER INTRODUCTION

Although discovered as early as 2001 (Van Dover *et al*., 2001) from the Central Indian Ridge (CIR), the 'scaly-foot gastropod' has not been formally named to date. Warén *et al*. (2003) presented a detailed account of its morphology and some genetic information, but did not give a name and did not designate any type specimens. The name '*Chrysomallon squamiferum*' appeared on the 16S sequence submission in GenBank, but this is a *nomen nudum* and not valid according to the International Code for Zoological Nomenclature (ICZN, 1999).

When the population of 'scaly-foot gastropod' in Longqi vent field, Southwest Indian Ridge (SWIR) was discovered, a key question was whether it belonged to the same species as the CIR populations or not. This chapter presents evidences that they indeed are. Dr Anders Warén (Swedish Museum of Natural History) very kindly allowed me to describe this enigmatic species. This chapter forms a formal description of the 'scaly-foot gastropod', as a basis for other chapters to follow. In the description we keep the original manuscript name *Chrysomallon squamiferum* Dr Warén gave to it.

Disclaimer:

All nomenclatural relevant acts in this chapter are disclaimed for nomenclatural purposes according to Article 8.2-8.3 of the International Code of Zoological Nomenclature (Fourth Edition, incorporating amendments).

ICZN (International Commission on Zoological Nomenclature). 1999. *International Code of Zoological Nomenclature, Fourth Edition*. London, UK: The International Trust for Zoological Nomenclature. 306 pp.

STATEMENT OF AUTHOR CONTRIBUTIONS

The main body of this chapter takes the form of a manuscript formatted as a Research Article for *Journal of Molluscan Studies* (ID JMS 2013053). It has been accepted for publication on March 8th, 2015 and is currently in press. The authors (in this order) are Chong Chen (corresponding author), Jonathan T. Copley, Katrin Linse, and Alex D. Rogers; the detailed author contributions are as follows.

The original idea for the project was conceived from discussion among all authors. JTC and ADR provided funding for both sample collection on-board *RRS* James Cook research cruises JC66/67 as well as laboratory work afterwards. On-board the cruises CC, JTC, and ADR participated in sample collection and tissue fixation of the specimens used in this study. CC was responsible for all laboratory work, data collection, data analyses, and wrote the original manuscript. ADR illustrated the detailed anatomical drawing. All authors discussed the results and implications of the study in detail and edited the manuscript for improvement. ADR, JTC, and KL supervised the work of CC during the length of this study.

The supplementary material included here was not part of the submitted manuscript but included here for additional insights and discussion.

The 'scaly-foot gastropod': a new genus and species of hydrothermal vent-endemic gastropod (Neomphalina: Peltospiridae) from the Indian Ocean

Chong Chen[1*], Katrin Linse[2], Jonathan T. Copley[3], Alex D. Rogers[1]

[1] *Department of Zoology, University of Oxford, Oxford, United Kingdom;* [2] *British Antarctic Survey, High Cross, Cambridge, United Kingdom; and* [3] *Ocean and Earth Science, National Oceanography Centre, University of Southampton, Southampton, United Kingdom*

SHORT RUNNING HEAD

THE 'SCALY-FOOT GASTROPOD'

[*] Corresponding author: Chong Chen, e-mail: chong.chen@zoo.ox.ac.uk

ABSTRACT

The ‘scaly-foot gastropod’ is widely recognised as the iconic species of the deep-sea hydrothermal vent ecosystems of the Indian Ocean. The species, uniquely among gastropods, carries hundreds of dermal sclerites on the foot. These can be covered in iron sulphide which also covers its shell, making it the only known extant metazoan to utilise iron sulphide as part of its skeleton. It was not formally named despite generating great attention from both scientists and the general public alike, although a manuscript name has occasionally shown up in various sources. The RRS *James Cook* JC67 expedition in 2011 surveyed the biota of the Longqi vent field (37°47.027’S 49°38.963’E), South West Indian Ridge, for the first time, revealing a previously unknown population of the ‘scaly-foot gastropod’. The present study gives a formal name to the ‘scaly-foot gastropod’, *Chrysomallon squamiferum* gen. et sp. nov., Longqi vent field serves as the type locality. The erection of a new monotypic genus *Chrysomallon* gen. nov. is supported by both morphological and molecular characterisation resulting in sufficient differences with existing genera of the family Peltospiridae. The analysis of cytochrome *c* oxidase subunit I gene resulted in 24-26% pairwise distance between *Chrysomallon* and five other genera in Peltospiridae, while the range among those five genera was 14-25%. The new genus is placed in the family Peltospiridae based on morphological characteristics consistent with other members of the family, including lack of sexual dimorphism with no copulation organ, the distal end of marginal teeth being subdivided into many denticles, and the ventral margin of the gill leaflets carrying a series of bulges. A five-genes Bayesian phylogenetic reconstruction agrees with the placement within Peltospiridae.

INTRODUCTION

The first hydrothermal vent field located in the Indian Ocean, the Kairei vent field (25°19.23'S, 70°02.42'E; Figure 1) on the Central Indian Ridge (CIR), was discovered by the RV *Kairei* KR00-05 cruise in 2000 (Hashimoto *et al*., 2001) and subsequently surveyed by the RV *Knorr* 162-13 expedition in 2001 (Van Dover *et al*., 2001). This survey yielded perhaps the most peculiar deep-sea hydrothermal vent-endemic gastropod known to date, tentatively named the 'scaly-foot gastropod' (Warén *et al*., 2003). The species attracted attention because it had hundreds of black metallic sclerites covering its foot. The soft tissue core of each sclerite was covered in conchiolin, which was in turn covered with pyrite (FeS_2) and greigite (Fe_3S_4), two forms of iron sulphide (Warén *et al*., 2003). Its shell was also covered in the same material, making it the only known metazoan to use iron in its skeleton (Yao *et al*., 2010). Recently, Nakamura *et al.* (2012) reported a white variety of the scaly-foot gastropod, which lacks the iron sulphide layer, from the newly discovered CIR Solitaire vent field (19°33.41'S, 65°50.89'E; Figure 1) even though genetic analyses revealed that they are the same species as the Kairei scaly-foot gastropod.

An extensive description of this species with anatomical details and preliminary molecular phylogenetic results based on 16S rRNA was published by Warén *et al.* (2003), placing it in the neomphaline family Peltospiridae; this work is sufficient for the recognition of the species and to distinguish it from all other known gastropods. Unfortunately this did not meet the requirement of the ICZN code as no name was given and no type specimen was designated. There was, however, a manuscript name,

Chrysomallon squamiferum, which was released with the 16S sequence data filed on GenBank; despite it being a *nomen nudum* it has been extensively quoted in various literature (e.g., Yao *et al*., 2010; Nakagawa *et al*., 2014).

In 2011 the RRS *James Cook* expedition JC67 surveyed the first confirmed deep-sea hydrothermal vent field on the Southwest Indian Ridge (SWIR), the Longqi vent field (37°47.027'S 49°38.963'E; Figure 1; Tao *et al*., 2012; Tao *et al*., 2014), using the remotely operated vehicle (ROV) *Kiel 6000* (Copley, 2012). This survey yielded a third population of the 'scaly-foot gastropod'. This is the fifth known vent field in the Indian Ocean and the first one outside of the CIR. Specimens from Longqi closely resemble those from Kairei. At Longqi, the 'scaly-foot gastropod' was a visually dominant species, forming numerous dense aggregations both on black smoker chimneys and around diffuse flow in contrast to both the Kairei or Solitaire vent fields, where they occurred at a lower abundance (Van Dover, 2001; JAMSTEC, 2009; Nakamura *et al*., 2012). The distance between Longqi and Kairei is approximately 2,300 km, and Solitaire is 700 km further north of Kairei (Nakamura *et al*., 2012).

The family Peltospiridae is nested within the superfamily Neomphaloidea, the only superfamily in the clade Neomphalina, which also contains two other families Neomphalidae and Melanodrymiidae (Sasaki *et al*., 2010). This clade includes about 50 species and is well supported as monophyletic by molecular studies (e.g., Heβ *et al.,* 2008; Kano, 2008; Atkipis & Giribet, 2012), although its relationship with other gastropod clades has been enigmatic. Most recent molecular phylogenies place Neomphalina basal to Vetigastropoda, with Cocculinoidea as the sister clade (Aktipis & Giribet, 2012). The

systematic positioning of genera within Neomphalina is problematic as morphology is extremely diverse. The current placement of genera in the families is based on molecular studies by Heβ *et al.* (2008), but some studies do not support this scheme (e.g., Aktipis & Giribet, 2012).

Morphological and genetic comparisons of the Longqi specimens with Kairei and Solitaire specimens lead to the conclusion that the populations at the three vent fields represent one single species belonging to the family Peltospiridae. The purpose of this study is to name the 'scaly-foot gastropod', in order to normalise and rectify the confusion of names used to refer to this charismatic species in past years. As it cannot be assigned to any described genera in the family, a new genus *Chrysomallon* gen. nov. is erected to house this unusual species, named here as *Chrysomallon squamiferum* sp. nov. This species was studied extensively by Dr Anders Warén (Swedish Museum of Natural History) since its initial discovery. The present paper draws heavily from the initial work by Warén *et al*. (2003) and to which we owe a great debt of gratitude. In recognition of the work by Warén *et al*. (2003) and to avoid further confusion in literature, here we keep their manuscript name for the formal description. Its status within the clade Neomphalina is investigated using the specimens collected from Longqi vent field as the holotype and paratypes but also taking into account published information from the other two known populations.

112 MATERIALS & METHODS

113

114 *Materials*

115

116 The Longqi vent field (37°47.027'S 49°38.963'E, approximately 2780m deep; Tao *et al.*,
117 2014; Fig. 1) was detected by the RV *Da Yang Yi Hao* expeditions DY115-19 and DY115-
118 20 from 2007 to 2009 (Tao *et al.,* 2012) and is the first visually-confirmed hydrothermal
119 vent field on the SWIR. This site was first surveyed and sampled during the RRS *James*
120 *Cook* expedition JC67 in 2011 (Copley, 2012). Specimens of the 'scaly-foot gastropod'
121 were collected from the 'Tiamat Chimney' using the suction sampler of the ROV *Kiel*
122 *6000* and fixed in 4% buffered formalin for morphological examination and in 99%
123 ethanol for genetic studies.

124

125 *Morphology*

126

127 Investigation of external morphology was carried out under a Leica 10x dissection
128 microscope. The radula was dissected from specimens preserved in 99% ethanol and
129 treated with 10% KOH solution upon extraction overnight to dissolve tissue. The area
130 containing the protoconch was cut out in the case of adult specimens in attempts to
131 observe the protoconch. Both radula and protoconch specimens for Scanning Electron
132 Microscopy (SEM) underwent a hydration series in 75%-60%-40%-20%-0% ethanol
133 solution and were rinsed in distilled water. The specimens underwent sonication and then
134 a reverse dehydration series. Specimens were dried completely using
135 hexamethyldisilazane, SEM micrographs were taken with a Jeol JSM-5510 SEM

(Department of Plant Sciences, University of Oxford). Shell morphometric measurements were carried out with digital vernier callipers.

Genetics

Partial sequences of the mitochondrial cytochrome *c* oxidase subunit I (COI) gene were used to assess the genetic homogeneity of the Longqi population to Kairei and Solitaire, with other peltospirid species represented on GenBank. To investigate the relatedness of the new peltospiroid species to other known species of Neomphalina, five genes were used for a phylogenetic reconstruction. The genes chosen include COI, H3, 16S rRNA, 18S rRNA, and 28S rRNA. Non-neomphaline gastropods were selected from Vetigastropoda, Cocculiniformia, Caenogastropoda, and Patellogastropoda. Selection of taxa was limited to those with all five genes available on GenBank. A recent five-gene phylogenetic reconstruction by Aktipis & Giribet (2012) placed Cocculinoidea as the sister clade to Neomphalina, and thus *Cocculina messingi* was used as an outgroup in the COI tree. Sequences used in the present study were obtained from NCBI GenBank except for the Longqi 'scaly-foot gastropod' which was newly sequenced. For the COI tree, five haplotypes from each of the Kairei, Solitaire and Longqi vent fields were randomly chosen and used for the analyses.

Genomic DNA was extracted using QIAGEN DNeasy Blood and Tissue Kit following the manufacturer's instructions (Crawley, United Kingdom). Primer pairs used are listed in Table 1. The polymerase chain reaction (PCR) was carried out in 12 µl reactions, including 2 µl DNA template (100-200 ng/µl), 8 µl QIAGEN Master Mix, 0.4 µl double-

160 distilled water, 1.6 µl primer mix containing 0.8 µl each of forward and reverse primers
161 at concentration of 4 pmol/µl. PCR was performed with the following protocol: 95 °C for
162 15 mins followed by 40 cycles of [94°C, 45 s; primer-specific annealing temperature, 60
163 s, 72°C, 60 s], ending with 72°C for 5 mins. The annealing temperatures used for 16S,
164 18S, and 28S were 47°C; for COI was 45°C; and for H3 was 43°C. Amplification of the
165 desired region was confirmed with 1 % agarose gel electrophoresis visualised using
166 ethidium bromide staining. Successful PCR products were purified using QIAGEN
167 QIAquick PCR purification kit using standard protocols. Cycle sequencing reactions were
168 carried out with the protocol: 96 °C for 1 min followed by 25 cycles of [96°C, 10 s; 50°C,
169 5 s; 60°C, 4 mins], ending with 60°C, 4 mins. Sequenced products were precipitated using
170 an EDTA/ethanol method (Zeugin & Hartley, 1985). Sequences were resolved from
171 precipitated products using an Applied Biosystems 3100 DNA sequencer (Department of
172 Zoology, University of Oxford).
173
174 Alignment and editing of genetic sequences were carried out in Geneious 5.6 (Drummond
175 *et al*., 2011), and reads were manually quality-checked and corrected by eye. Only
176 sequences with both good quality matching forward and reverse readings were used in
177 downstream analyses. Pairwise distances of COI were calculated with software MEGA
178 5.05 (Tamura *et al*., 2011). Poorly aligned sites were identified in ribosomal RNAs using
179 the software Gblocks (Castresana, 2000) and removed from downstream analyses. Prior
180 to analyses, the most suitable evolutionary model was tested using program
181 PartitionFinder v1.0.1 (Lanfear *et al*. 2012), using scores for the Akaike Information
182 Criterion. The models selected are as follows: H3, COI (first and second codons), 16S,
183 28S = GTR+I+G; COI (third codon) = HKY+I+G; 18S = K80+G. The total sequence

184 length used was 2753-bp for the five-gene tree and 457-bp for the COI tree.

185

186 Phylogenetic reconstruction was carried out with Bayesian inference using MrBayes 3.2
187 (Ronquist *et al*., 2012). In both COI and five-gene analyses, Metropolis-coupled Monte
188 Carlo Markov Chains were run for five million generations. Convergence Topologies
189 were sampled every 100 generations, and the first 25% were discarded as burn-in to
190 ensure chains sampled a stationary position. The software Tracer v1.6 (Rambaut, Suchard
191 & Drummond, 2013) was used to check for convergence, and calculate adequate burn-in
192 values.

193

194 Table 2 shows GenBank accession numbers of sequences used in the COI tree and Table
195 3 shows the same for the five-gene phylogeny. New sequences generated from this study
196 are deposited in GenBank under accession numbers XXYYYYYY-XXYYYYYY.

197

198 *Type Repositories*

199

200 The holotype specimen is deposited in the invertebrate collection at the Natural History
201 Museum, London (NHMUK), paratypes are deposited in global museums with significant
202 malacological collections. Repositories and abbreviations used are listed as follows:

203

204 AMS: Australian Museum, Sydney, Australia
205 ANSP: Academy of Natural Sciences of Drexel University, Philadelphia, USA
206 FMNH: Field Museum of Natural History, Chicago, USA
207 MNHN: Museum national d'Histoire naturelle, Paris, France

208 NHMUK: Natural History Museum, London, UK

209 NHMW: Collection Mollusca, Museum of Natural History Vienna, Austria

210 NMINH: National Museum of Ireland – Natural History, Dublin, Ireland

211 NMNZ: Museum of New Zealand Te Papa Tongarewa, Wellington, New Zealand

212 NMSA: KwaZulu-Natal Museum, Pietermaritzburg, South Africa

213 NMW: National Museum of Wales, Cardiff, UK

214 OUMNH.ZC: Zoological Collection, Oxford University Museum of Natural History,
215 Oxford, UK

216 RBINS: Royal Belgian Institute of Natural Sciences, Brussels, Belgium

217 ROMZ: Invertebrate Zoology Section, Department of Natural History, Royal Ontario
218 Museum, Toronto, Canada

219 SIO-BIC: Scripps Institution of Oceanography Benthic Invertebrate Collection, San
220 Diego, California, USA

221 SMNH: Swedish Museum of Natural History, Stockholm, Sweden

222 UCMP: University of California Museum of Paleontology, Berkeley, California, USA

223 UMUT: The University Museum, The University of Tokyo, Tokyo, Japan

224 UMZ: University Museum of Zoology, University of Cambridge, Cambridge, UK

225 USNM: Smithsonian Institution, National Museum of Natural History, Washington DC,
226 USA

227 ZISP: Zoological Institute of Russian Academy of Sciences, St. Petersburg, Russia

228 ZMB: Museum für Naturkunde, Berlin, Germany

229 ZSM: Zoologische Staatssammlung München, Munich, Germany

230

231

232

233 SYSTEMATIC DESCRIPTIONS

234

235 **Clade NEOMPHALINA McLean, 1990**

236 **Superfamily NEOMPHALOIDEA McLean, 1981**

237 **Family PELTOSPIRIDAE McLean, 1989**

238 ***Chrysomallon* gen. nov.**

239

240 *Chrysomallon* – Warén ms. (Warén *et al*., 2003)

241

242 *Type species*: *Chrysomallon squamiferum* sp. nov., by monotypy and original designation.

243

244 *Etymology*: Chrysomallon (Greek), golden haired. The name is given in reference to the
245 metal coating often found on the gastropod's shell and sclerites, which includes the metal
246 pyrite commonly known as fool's gold. The gender of genus is neuter.

247

248 *Diagnosis*: Very large for Peltospiridae, up to 45.5 mm in maximum shell diameter.
249 Coiled shell with three whorls. Spire compressed, aperture elliptic. Periostracum thick.
250 Foot large. Epipodium lacking in epipodial tentacles but instead covered by hundreds of
251 hard dermal sclerites. Anterior pedal gland lacking. Esophageal gland hypertrophied. Rest
252 of the digestive system reduced with short intestines forming simple loop. Cephalic
253 tentacles thick at base, elongate, tapering towards tip. Ctenidium bipectinate, very large.
254 No sexual dimorphism. Radula rhipidoglossate, formula ~ 50 + 4 + 1 + 4 + ~ 50. Central
255 tooth solid, strong with smooth cusps. Lateral teeth strong with finely serrated cusps.

Marginal teeth long and slender, truncated, and comb-like to the distal end.

Remarks: As already discussed by Warén *et al*. (2003), within Neomphalina, the morphological information places *Chrysomallon* gen. nov. in Peltospiridae. Morphologically the primary distinguishing characteristic between the three neomphaline family is the copulatory appendages (Heß *et al*., 2008). Known species in Neomphalidae all have separate sexes and exhibit sexual dimorphism where the left tentacle in males is modified and serves as a penis (Fretter, Graham & McLean, 1981; Beck, 1992; Heß *et al*., 2008). Melanodrymiidae species also have specialised copulatory organs in males (both tentacles in *Melanodrymia* males, Hazprunar, 1989; a large and ciliated swelling between cephalic tentacles in *Leptogyropsis* males, Heβ *et al.*, 2008) or simultaneous hermaphrodites (additional copulatory appendages innervated by left cerebral ganglion; Heβ *et al.*, 2008). In Peltospiridae this is not the case and species do not have distinct copulatory organs or modifications of the cephalic tentacles (Fretter, 1989; Israelsson, 1998). *Chrysomallon* also does not exhibit external sexual dimorphism and does not have copulatory appendages, which is consistent with Peltospiridae. *Chrysomallon* also has a truncated comb-like ending to the marginal teeth, which is present in only the Peltospiridae and Melanodrymiidae. A series of bulges along ventral margin of the gill leaflets is a key characteristic separating Peltospiridae from other groups and is also present in *Chrysomallon*, as reported by Warén *et al*. (2003, fig. S2D).

Chrysomallon gen. nov. can be easily distinguished from all other described gastropod genera by having hundreds of dermal sclerites covering the foot, which is a unique characteristic (Warén *et al*., 2003) of the new genus. For Neomphalina epipodial structure

is an important characteristic in identification and no species has such hard sclerites except *Chrysomallon*. Within Peltospiridae, it can be easily distinguished from the limpet-form genera *Echinopelta* McLean, 1989*, Nodopelta* McLean, 1989, and *Rhynchopelta* McLean, 1989, as it has a distinctly coiled shell with approximately three whorls. *Chrysomallon* has much more depressed spire, larger aperture and inflated form than *Pachydermia* Warén & Bouchet, 1989, *Depressigyra* Warén & Bouchet, 1989 and *Lirapex* Warén & Bouchet, 1989. The teleoconch surface of *Chrysomallon* lacks tubercles characteristic of *Ctenopelta* Warén & Bouchet, 1993, and periostracum lacks folds characteristic of *Hirtopelta* McLean, 1989. The shell roughly resembles *Peltospira* McLean, 1989 in shape, but the initial whorl is depressed and the shell has no strong lamellae sculpture which is present in all species of *Peltospira*. The adult attains a large size and has an enlarged esophageal gland (Warén *et al*., 2003; Goffredi *et al*., 2004). The anatomy of many peltospirid genera has been investigated, including *Rhynchopelta*, *Peltospira*, *Nodopelta, Echinopelta, Hirtopelta* (Fretter, 1981) as well as *Pachydermia* (Israelsson, 1998); none of these have a hypertrophied esophageal gland.

***Chrysomallon squamiferum* sp. nov.**

Chrysomallon squamiferum – Warén *et al*. MS, GenBank AY163398 (*nomen nudum*)

Crysomallon squamiferum – Warén *et al*. MS (miss-spelt, Anders Warén personal communication), GenBank AY163398 (*nomen nudum*)

"Scaly-foot" gastropods – Van Dover *et al*., 2001: 820.

The scaly-footed gastropod – Warén *et al*., 2003: 1007

The scaly snail – Goffredi *et al*., 2004: 3082

The "scaly-foot" gastropod – Suzuki *et al*., 2006: 39

Crysomallon squamiferum – Yao *et al*., 2010: 987 (*nomen nudum*)

Scaly footed gastropods – Tao *et al*., 2012: 49

'Scaly-foot' gastropod – Nakamura *et al*., 2012: 1

Scaly-foot gastropods – Beedessee *et al*., 2013: 1

Scaly-foot gastropod – Watanabe & Beedessee, 2015: 207

Crysomallon squamiferum – Nakagawa *et al*., 2014: 40 (*nomen nudum*)

The 'scaly-foot gastropod' – Chen *et al*., 2015

Type material:

Holotype (shell diameter 32.03 mm, 99% ethanol). Longqi vent field, Southwest Indian Ridge, 37°47.03'S 49°38.97'E ('Tiamat Chimney'), 2785 m deep, RRS *James Cook* expedition JC67, ROV *Kiel 6000* Dive 142, 29.11.2011, leg. J. T. Copley (NHMUK 2015.XX).

Paratypes. One dissected specimen, shell diameter 36.03mm, 99% ethanol (NHMUK 2015.XX); growth series of five specimens, 99% ethanol (NHMUK 2015.XX); growth series of five specimens, 99% ethanol (OUMNH.ZC 2013.02.001); growth series of five specimens, 99% ethanol (SMNH Type Collection 8449); two specimens, 99% ethanol (AMS C.483502); two specimens, 99% ethanol (ANSP A23851); two specimens, 99% ethanol (FMNH 344546); two specimens, 99% ethanol (MNHN IM-2000-30072); two specimens, 99% ethanol (Mollusca NHMW 110415); five specimens, 99% ethanol (NMINH:2015.1.1-5); two specimens, 99% ethanol (NMNZ NMNZ M.317895); two

328 specimens, 99% ethanol (NMSA L9729/T4023); two specimens, 99% ethanol (NMW
329 Z.2015.005.00001-00002); two specimens, 99% ethanol (RBINS IG XXXX MT XXXX);
330 two specimens, 99% ethanol (ROMIZ M11286); two specimens, 99% ethanol (SIO-BIC
331 XXXX); two specimens 99% ethanol (UMUT RM31814); 10 specimens, 99% ethanol
332 (UCMP XXXX); two specimens, 99% ethanol (UMZ XXXX); two specimens, 99%
333 ethanol (USNM XXXXXXX); two specimens, 99% ethanol (ZISP 62033); two
334 specimens, 99% ethanol (ZMB XXXX); two specimens, 99% ethanol (ZSM
335 2015XXXX): collection data identical to the holotype. Five specimens, 10% buffered
336 formalin (NHMUK 2015.XX); 10 specimens, 4% buffered formalin (UCMP XXXX); one
337 specimen, fixed in 4% buffered formalin, serially sectioned into 1.5 µm semi-thin section
338 series (ZSM 20151000): Longqi vent field, Southwest Indian Ridge, 37°47.03'S
339 49°38.96'E ('Tiamat Chimney'), 2783m deep, RRS *James Cook* expedition JC67, ROV
340 *Kiel 6000* Dive 140, 27.11.2011, leg. J. T. Copley.
341
342 *Non-type material examined*: Approximately 100 specimens, same collection data as the
343 holotype.
344
345 *Etymology*: From the Latin, *squamiferum*, meaning scale-bearing referring to the
346 numerous hard sclerites covering the foot. Used as an adjective.
347
348 *Description*: Shell. Three whorls, globose with a depressed spire, tightly coiled. Milky
349 white and thin. Aperture elliptic, very large. Shell shape in-between neritiform and
350 limpet-form. Surface sculptured with subtle ribs in close proximity to one another. Fine
351 growth lines present. Periostracum thick, brown. Exterior often coated by a black layer

352 of iron sulphide. Periostracum envelopes shell edge. Columellar region covered by thin
353 callus. Average shell diameter 32 mm for adults (100 specimens), maximum shell
354 diameter 45.5 mm. Protoconchs investigated too corroded to be of taxonomic value.
355
356 External anatomy (Figure 2A-B, E-G). Cephalic tentacles elongate, thick at base, tapering
357 to a fine point at the distal tip. Eyes lacking in visible pigmented retina. Snout tapered,
358 thick. Foot large, unable to contract entirely into the shell, red when alive. Sole of foot
359 surrounded by pedal flange. Epipodium without epipodial tentacles, covered by hundreds
360 of hard sclerites. As discussed in Warén *et al*. (2003), shell muscle large and horse-shoe
361 shaped with two anterior parts on each side connected by a narrow connective posteriorly.
362
363 Operculum. Present in metapodium buried under layers of sclerites (Chen *et al*., 2015,
364 Fig. 2A). Multispiral, concentric in juveniles. Shifts to a curved, bent shape as animal
365 grows to adult (Chen *et al*., 2015, Fig. 2C).
366
367 Sclerite. Curved and elongate, not calcareous but proteinaceous. Approximately 1 mm x
368 5 mm in size in adult specimens (Figure 3). White to metallic black depending on extent
369 of iron sulphide coating, newly grown sclerites milky white. Ferrimagnetic when coated
370 with iron sulphide.
371
372 Internal anatomy (Figure 4). As discussed in Warén *et al*. (2003): Ctenidium bipectinate,
373 very large (Figure 4). Leaflet ventral margin carries series of bulges (Warén *et al*., 2003:
374 fig. S2D). Vascular system hypertrophied. Heart monotocardian with discrete auricle and
375 ventricle. Oesophageal gland hypertrophied. Rest of digestive system relatively small

(Figure 4). Rectum exits to mantle cavity on the right. Gonads displaced anteriorly to head-foot region, occupying ventral face of visceral mass. 'Spermatophore packaging organ' present, spermatophores known and described by Warén *et al*. (2003: fig. S2M). Genital slit simple, opening to mantle cavity on the right ventral of rectum. No sexual dimorphism observed. Digestive gland occupies dorsal face of visceral mass into apex. Interconnected pedal nerves large, conspicuous under oesophageal gland. Anterior pedal gland absent.

Radula. Rhipidoglossate (Figure 5). Ribbon approximately 0.5 mm wide and 4 mm long in adults. No difference between anterior and posterior rows in radula investigated, showing no signs of wear. General appearance of radula typical of the family, with a formula of ~ 50 + 4 + 1 + 4 + ~ 50. Cusp of central tooth blunt-ended, not crenulated. Laterals solid with reinforced bases, cusps blunt ended, inner and outer side very finely crenulated. Marginal teeth elongate with a truncated distal end dividing into about 20 slender denticles.

Distribution: Known from the following three hydrothermal vent fields in the Indian Ocean, found on active black smokers as well as on diffuse flow sites. Longqi vent field (37°47.027'S 49°38.963'E), SWIR, around 2780 m depth; Kairei vent field (25°19.239S, 70°02.429E), Central Indian Ridge, depth 2415 to 2460 m (Van Dover *et al*., 2001); and Solitaire vent field (19°33.413S, 65°50.888E), Central Indian Ridge, depth 2606 m (Nakamura *et al*., 2012).

399 *Remarks*: The shell parameters and proportions are summarised in Table 4. The
400 relationships between the five parameters measured (height, width, depth, aperture height,
401 aperture width) were investigated, and they were all linear across all life stages. Figure 6
402 shows a scatterplot of shell diameter against shell height across life stages (shell diameter
403 range 9.80-40.02 mm), the regression shows a significantly linear relationship (R^2 =
404 0.9868, $p < 0.001$). The protoconchs investigated were extremely brittle and appear to
405 have been severely corroded outside-in and have lost the surface layer.
406
407 The above description is based on specimens from the designated type locality: Longqi
408 vent field, SWIR. This locality is chosen for type locality due to the large amount of
409 specimens available. Warén *et al*. (2003) published many relevant observations made
410 from specimens collected from the Kairei vent field, CIR, which clearly belong to the
411 same species from the present study primarily from genetic support (see section below)
412 but also the morphology. From literature figures, specimens from Kairei and Solitaire
413 vent fields in CIR appear to have broader sclerites than those from the Longqi (Fig. 2E;
414 Warén *et al*., 2003, fig. S2E; Nakamura *et al*., 2012, fig. 5) but are otherwise
415 indistinguishable from Longqi. The specimens from the Solitaire vent field are not
416 covered in iron sulphide and thus have white sclerites and a light brown shell resulting
417 from the exposed periostracum (Nakamura *et al*., 2012, fig. 5B). Examined specimens
418 from SWIR reached a maximum size of 40 mm in shell diameter, whereas from Kairei,
419 CIR they are known to reach a maximum of 45.5 mm (Anders Warén, personal
420 communication). The operculum is known from all populations (Chen *et al*., 2015).
421
422

Genetic Support

The COI consensus tree constructed with five randomly selected haplotypes from each of the three populations of *Chrysomallon squamiferum* sp. nov. is shown in Figure 7. *C. squamiferum* represents a discrete lineage within Peltospiridae, the three populations are genetically homogeneous and indistinguishable providing evidence that they represent the same species. It has been previously indicated that the COI gene does not provide enough resolution to clarify the internal relationships of the Neomphalina (Atkipis & Giribet, 2012), hence to avoid confusion only peltospirid species were included in this tree except the outgroup.

The consensus tree from the five-genes combined Bayesian phylogenetic analyses is shown in Figure 8. *Chrysomallon squamiferum* sp. nov. fell within a well-supported Peltospiridae clade (Posterior Probability, PP = 98%), with Peltospiridae falling sister to *Cyanthermia naticoides* (i.e., Neomphalidae). The clade Neomphalina was recovered with full support (PP = 100%). This supports the placement of *C. squamiferum* sp. nov. within the family Peltospiridae.

A maximum-likelihood distance matrix constructed from COI sequences of six Peltospiridae genera including *Chrysomallon* gen. nov. is shown in Table 5. All species used are the type species of their representative genera, except *Nodopelta* where COI sequences of the type species *N. heminoda* McLean, 1989 were not available and therefore *N. subnoda* McLean, 1989 was used instead. The pairwise COI divergence between representatives of the five described peltospirid genera averages 20.81% (range 13.65%-24.68%), while their divergence from *Chrysomallon* (Longqi vent field)

447 averaged 25.34% (range 24.20%-26.41%). This supports the generic status of
448 *Chrysomallon*. The divergence of Longqi specimen from Kairei (average of five
449 specimens 0.74%, range 0.35-0.98%) and Solitaire specimens (average of five specimens
450 0.86%, range 0.39-1.38%) averaged at 0.80%, while the divergence between Kairei and
451 Solitaire specimens was 0.88% (average of five specimens, range 0.19-1.58%). This
452 difference is small (the difference between separate species is usually approximated 4%;
453 Meyer & Paulay, 2005) and together with the COI tree, supports the contention that the
454 three populations represent a single species, *C. squamiferum*.
455
456 DISCUSSION
457
458 *The scientific name*
459
460 Since its discovery, the eccentric biology of *Chrysomallon squamiferum* sp. nov., even
461 among deep-sea animals and its position as the representative endemic species of Indian
462 Ocean hydrothermal vents has attracted great interest in the scientific community as well
463 as the public. Numerous papers have been published on various aspects of the biology
464 and ecology of this species (e.g., sclerites and anatomy, Warén *et al*., 2003;
465 endosymbionts, Goffredi *et al*., 2004; sclerite biomineralisation, Suzuki *et al*., 2006; shell
466 biomineralisation, Yao *et al*., 2010). However, in the absence of a formal name, each
467 publication has used a slightly different version of the 'scaly-foot gastropod' to address
468 the species. Yao *et al*. (2010) used a misspelt manuscript name '*Crysomallon*
469 *squamiferum*' (Anders Warén, personal communication), which has gained popularity as
470 the binomial name of the 'scaly-foot gastropod' (e.g., Nakagawa *et al*., 2014), although it

471 has no validity. The name put forward here, *Chrysomallon squamiferum*, is the same as
472 the original manuscript name submitted with the 16S sequence of an individual from the
473 Kairei vent field by Warén *et al*. (2003, AY163398), and this name is retained to prevent
474 further confusion.
475
476 *Distribution across two mid-ocean ridges*
477
478 Both morphology and genetic results are consistent with the conclusion that the
479 population newly discovered in Longqi vent field, SWIR represents the same species as
480 the previously known populations in Kairei and Solitaire fields, CIR. This extends the
481 distribution of *Chrysomallon squamiferum* sp. nov. to across 2,500 km distance from
482 Longqi to Solitaire. The Longqi population has black sclerites and shell like the Kairei
483 population, although the sclerite is more elongate; while the Solitaire population has
484 white sclerites and brown shell because of a lack of iron sulphide (Nakamura *et al*., 2012).
485 This is likely to result from the lack of iron in the vent fluid of Solitaire (Nakamura *et al*.,
486 2012). Similarly a number of neomphalines (e.g., *Lirapex*, *Pachydermia*, *Melanodrymia*)
487 have been reported to have rusty deposits (likely deposited by bacteria) or lack them
488 depending on the environment (Warén & Bouchet, 2003).
489
490 Although the SWIR and CIR populations are revealed to be genetically homogeneous the
491 question as to whether or not high connectivity is maintained over this vast distance needs
492 further investigation. Two studies (Nakamura *et al.,* 2012; Beedessee *et al*., 2013) have
493 shown that connectivity is very high between two populations of scaly-foot gastropods
494 on CIR in the Kairei and Solitaire vent fields approximately 700 km apart from each other.

Although 2,500 km is not a particularly long distance for vent species to maintain connectivity (e.g., *Rimicaris exoculata* Williams & Rona, 1986 vent shrimps with planktotrophic larvae have been shown to maintain high connectivity over 7,000 km of Mid-Atlantic Ridge; Teixeira *et al*., 2012) the dispersal ability of *Chrysomallon squamiferum* sp. nov. may be low as it most likely has lecithotrophic development (presumably with a planktonic dispersal stage like all other known peltospirids; Warén, Bouchet & Cosel, 2006) and negatively buoyant eggs (Beedessee *et al*., 2013). Across the East Pacific Rise the vent limpet *Lepetodrilus elevatus* McLean, 1988, also with lecithotrophic development, was shown to exhibit significant genetic differentiation (Plouviez et al., 2009). The new population at Longqi provides ideal opportunity for a future study of connectivity between hydrothermal vents across different mid-ocean ridges, for which there is currently no knowledge from within the Indian Ocean. Interestingly a number of active vents have been inferred in between Longqi and Kairei (e.g., SWIR 63.9° E, Tao *et al.*, 2009; SWIR 58.9°E, German *et al.*, 1998), and it is likely that these and further undiscovered fields act as stepping stones between Longqi and CIR vent fields to maintain connectivity.

ACKNOWLEDGEMENTS

We would like to express our greatest gratitude to Dr Anders Warén of the Swedish Museum of Natural History for kindly allowing us to name this fascinating species, and for suggesting to keep the name he originally assigned to it. Dr Julia Sigwart (Queen's University Belfast, Marine Laboratory) deserves special mention and recognition for her key aid in taxonomic discussion and great support of the project. We owe a great deal to

519 Dr Sammy De Grave (Oxford University Museum of Natural History) for providing
520 taxonomic opinions; as well as Dr Hiromi Watanabe (Japan Agency for Marine-Earth
521 Science and Technology) for making COI sequences from Kairei and Solitaire vent fields
522 available on the DNA Data Bank of Japan. We thank David Shale and Pete Bucktrout
523 (British Antarctic Survey) for specimen photography. This work was funded by NERC
524 Small Research Grant NE/H012087/1, Biogeography and ecology of the first known
525 deep-sea hydrothermal vent site on the ultraslow-spreading Southwest Indian Ridge, to
526 J.T.C. The funder had no role in research design, data analysis, publication decisions or
527 preparation of the manuscript. The authors would like to thank the Master and crew of
528 the RRS *James Cook* expedition JC67 for their great support of scientific activity during
529 the cruise. The pilots and technical teams of ROV *Kiel 6000* are thanked for their
530 sampling efforts. The authors also express gratitude to staff of the UK National Marine
531 Facilities at the National Oceanography Centre for logistic and shipboard support. Finally,
532 we also thank two anonymous reviewers who helped improve this paper.
533
534
535
536

REFERENCES

AKTIPIS, S.W. & GIRIBET, G. 2010. A phylogeny of Vetigastropoda and other "archaeogastropods": re-organizing old gastropod clades. *Invertebrate Biology*, **129**: 220-240.

AKTIPIS, S.W. & GIRIBET, G. 2012. Testing relationships among the vetigastropod taxa: a molecular approach. *Journal of Molluscan Studies*, **78**: 12-27.

AKTIPIS, S.W., GIRIBET, G., LINDBERG, D.R. & PONDER, W.F. 2008. Gastropod phylogeny: an overview and analysis. In: *Phylogeny and evolution of the Mollusca* (Lindberg, D.R. and Ponder, W.F., eds), pp. 201-237. University of California Press, Berkeley, California.

BECK, L. 1992. *Symmetromphalus hageni* sp. n., a new neomphalid gastropod (Prosobranchia: Neomphalidae) from hydrothermal vents at the Manus Back-Arc Basin (Bismark Sea, Papua New Guinea). *Annalen des Naturhistorischen Museums in Wien*, **93**: 243-257.

BEEDESSEE, G., WATANABE, H., OGURA, T., NEMOTO, S., YAHAGI, T., NAKAGAWA, S., NAKAMURA, K., TAKAI, K., KOONJUL, M. & MARIE, D.E.P. 2013. High connectivity of animal populations in deep-sea hydrothermal vent fields in the Central Indian Ridge relevant to its geological setting. *PLoS ONE*, **8**: e81570.

BODC (BRITISH OCEANOGRAPHIC DATA CENTRE). 2010. GEBCO grid display. *Available from https://www.bodc.ac.uk/products/software_products/gebco_grid_display/*.

BOUCHET, P. & ROCROI, J.P. 2005. Classification and nomenclator of gastropod families. *Malacologia*, **47**: 1-397.

CASTRESANA, J. 2000. Selection of conserved blocks from multiple alignments for their use in phylogenetic analysis. *Molecular Biology and Evolution*, **17**: 540-552.

CHEN, C., COPLEY, J.T., LINSE, K., ROGERS, A.D. & SIGWART, J. 2015. How the mollusc got its scales: convergent evolution of the molluscan scleritome. *Biological Journal of the Linnean Society*: http://dx.doi.org/10.1111/bij.12462.

COPLEY, J.T. 2012. RRS James Cook research cruise JC67 cruise report. *Available from http://www.bodc.ac.uk/data/information_and_inventories/cruise_inventory/report/10593/*.

DRUMMOND, A., ASHTON, B., CHEUNG, M., HELED, J., KEARSE, M., MOIR, R., STONES-HAVAS, S., THIERER, T. & WILSON, A. 2011. Geneious v5.6. *Available from http://www.geneious.com*.

ESRI. 2012 *ArcGIS Desktop: Release 10.1*. Environmental Systems Research Institute, Redlands, CA.

FOLMER, O., BLACK, M., HOEH, W., LUTZ, R. & VRIJENHOEK, R. 1994. DNA primers for amplification of mitochondrial cytochrome *c* oxidase subunit I from diverse metazoan invertebrates. *Molecular Marine Biology and Biotechnology*, **3**: 294-299.

FRETTER, V. 1989. The anatomy of some new archaeogastropod limpets (superfamily Peltospiracea) from hydrothermal vents. *Journal of Zoology*, **218**: 123-169.

573 FRETTER, V., GRAHAM, A. & MCLEAN, J. 1981. The anatomy of the Galapagos rift limpet.
574 *Neomphalus fretterae*. *Malacologia*, **21**: 337-361.
575 GERMAN, C.R., BAKER, E.T., MEVEL, C., TAMAKI, K. & THE FUJI SCIENCE TEAM. 1998.
576 Hydrothermal activity along the Southwest Indian Ridge. *Nature*, **395**: 490-493.
577 GOFFREDI, S.K., WARÉN, A., ORPHAN, V.J., VAN DOVER, C.L. & VRIJENHOEK, R.C. 2004.
578 Novel forms of structural integration between microbes and a hydrothermal vent gastropod from
579 the Indian Ocean. *Applied and Environmental Microbiology*, **70**: 3082-3090.
580 HASEGAWA, K. 1997. Sunken wood-associated gastropods collected from Suruga Bay, Pacific side
581 of the Central Honshu, Japan, with descriptions of 12 new species. *National Science Museum*
582 *Monographs*, **12**: 59-123.
583 HASHIMOTO, J., OHTA, S., GAMO, T., CHIBA, H., YAMAGUCHI, T., TSUCHIDA, S.,
584 OKUDAIRA, T., WATABE, H., YAMANAKA, T. & KITAZAWA, M. 2001. First
585 hydrothermal vent communities from the Indian Ocean discovered. *Zoological Science*, **18**: 717-
586 721.
587 HASZPRUNAR, G. 1989. The anatomy of *Melanodrymia aurantiaca* Hickman, a coiled
588 Archaeogastropod from the East Pacific hydrothermal vents (Mollusca, Gastropoda). *Acta*
589 *Zoologica*, **70**: 175-186.
590 HEB, M., BECK, F., GENSLER, H., KANO, Y., KIEL, S. & HASZPRUNAR, G. 2008.
591 Microanatomy, shell structure and molecular phylogeny of *Leptogrya*, *Xyleptogyra* and
592 *Leptogyropsis* (Gastropoda: Neomphalida: Melanodrymiidae) from sunken wood. *Journal of*
593 *Molluscan Studies*, **74**: 383-402.
594 HICKMAN, C.S. 1984. A new Archaeogastropod (Rhipidoglossa, Trochacea) from hydrothermal
595 vents on the East Pacific Rise. *Zoologica Scripta*, **13**: 19-25.
596 ISRAELSSON, O. 1998. The anatomy of *Pachydermia laevis* (Archaeogastropoda: 'Peltospiridae').
597 *Journal of Molluscan Studies*, **64**: 93-109.
598 JAMSTEC (JAPAN AGENCY FOR MARINE-EARCH SCIENCE AND TECHNOLOGY). 2009.
599 Extensive population of a "rare" scaly-foot gastropod discovered. *JAMSTEC Press Releases,*
600 *Available from: http://www.jamstec.go.jp/e/about/press_release/20091130/.*
601 KANO, Y. 2008. Vetigastropod phylogeny and a new concept of Seguenzioidea: independent
602 evolution of copulatory organs in the deep-sea habitats. *Zoologica Scripta*, **37**: 1-21.
603 KIM, K.-S., MACEY, D.J., WEBB, J. & MANN, S. 1989. Iron mineralization in the radula teeth of
604 the chiton *Acanthopleura hirtosa*. *Proceedings of the Royal Society of London. B. Biological*
605 *Sciences*, **237**: 335-346.
606 LANFEAR, R., CALCOTT, B., HO, S.Y.W. & GUINDON, S. 2012. PartitionFinder: combined
607 selection of partitioning schemes and substitution models for phylogenetic analyses. *Molecular*
608 *Biology and Evolution*, **29**: 1695-1701.

609 MCLEAN, J.H. 1989. New Archaeogastropod limpets from hydrothermal vents: new family
610 Peltospiridae, new superfamily Peltospiracea. *Zoologica Scripta*, **18**: 49-66.
611 MCLEAN, J.H. 1990. A new genus and species of neomphalid limpet from the Mariana vents: with a
612 review of current understanding of relationships among Neomphalacea and Peltospiracea.
613 *Nautilus*, **104**: 77-86.
614 MCLEAN, J.H. 1995. Review of western Atlantic species of Cocculinid and Pseudococculinid limpets,
615 with descriptions of new species (Gastropoda : Cocculiniformia). In: *Contributions in science*
616 *(Los Angeles, CA)* (Harasewych, M.G., ed). Natural History Museum of Los Angeles County,
617 Los Angeles, CA.
618 MEYER, C.P. & PAULAY, G. 2005. DNA Barcoding: Error Rates Based on Comprehensive
619 Sampling. *PLoS Biology*, **3**: e422.
620 NAKAGAWA, S., SHIMAMURA, S., TAKAKI, Y., SUZUKI, Y., MURAKAMI, S.-I.,
621 WATANABE, T., FUJIYOSHI, S., MINO, S., SAWABE, T., MAEDA, T., MAKITA, H.,
622 NEMOTO, S., NISHIMURA, S.-I., WATANABE, H., WATSUJI, T.-O. & TAKAI, K. 2014.
623 Allying with armored snails: the complete genome of gammaproteobacterial endosymbiont. *The*
624 *ISME Journal*, **8**: 40-51.
625 NAKAMURA, K., WATANABE, H., MIYAZAKI, J., TAKAI, K., KAWAGUCCI, S., NOGUCHI,
626 T., NEMOTO, S., WATSUJI, T.-O., MATSUZAKI, T., SHIBUYA, T., OKAMURA, K.,
627 MOCHIZUKI, M., ORIHASHI, Y., URA, T., ASADA, A., MARIE, D., KOONJUL, M.,
628 SINGH, M., BEEDESSEE, G., BHIKAJEE, M. & TAMAKI, K. 2012. Discovery of new
629 hydrothermal activity and chemosynthetic fauna on the Central Indian Ridge at 18°–20°S. *PLoS*
630 *ONE*, **7**: e32965.
631 RAMBAUT, A., SUCHARD, M. & DRUMMOND, A. 2013. Tracer v1.6. *Available from*
632 *http://tree.bio.ed.ac.uk/software/tracer/*.
633 RONQUIST, F., TESLENKO, M., VAN DER MARK, P., AYRES, D.L., DARLING, A., H HNA, S.,
634 LARGET, B., LIU, L., SUCHARD, M.A. & HUELSENBECK, J.P. 2012. MrBayes 3.2:
635 Efficient bayesian phylogenetic inference and model choice across a large model space.
636 *Systematic Biology*, **61**: 539-542.
637 ROZEN, S. & SKALETSKY, H.J. 2000. Primer3 on the WWW for general users and for biologist
638 programmers. In: *Bioinformatics Methods and Protocols: Methods in Molecular Biology*:
639 (Krawetz, S. and Misener, S., eds), pp. 365-386. Humana Press, Totowa.
640 SASAKI, T., WARÉN, A., KANO, Y., OKUTANI, T., FUJIKURA, K. & KIEL, S. 2010. Gastropods
641 from recent hot vents and cold seeps: systematics, diversity and life strategies the vent and seep
642 biota. *Topics in Geobiology*, **33**: 169-254.
643 ST PIERRE, T.G., MANN, S., WEBB, J., DICKSON, D.P.E., RUNHAM, N.W. & WILLIAMS, R.J.P.
644 1986. Iron oxide biomineralization in the radula teeth of the limpet *Patella vulgata*: Mossbauer

spectroscopy and high resolution transmission electron microscopy studies. *Proceedings of the Royal Society of London. Series B. Biological Sciences*, **228**: 31-42.

SUZUKI, Y., KOPP, R.E., KOGURE, T., SUGA, A., TAKAI, K., TSUCHIDA, S., OZAKI, N., ENDO, K., HASHIMOTO, J., KATO, Y., MIZOTA, C., HIRATA, T., CHIBA, H., NEALSON, K.H., HORIKOSHI, K. & KIRSCHVINK, J.L. 2006. Sclerite formation in the hydrothermal-vent 'scaly-foot gastropod': possible control of iron sulfide biomineralization by the animal. *Earth and Planetary Science Letters*, **242**: 39-50.

TALAVERA, G. & CASTRESANA, J. 2007. Improvement of phylogenies after removing divergent and ambiguously aligned blocks from protein sequence alignments. *Systematic Biology*, **56**: 564-577.

TAMURA, K., NEI, M. & KUMAR, S. 2004. Prospects for inferring very large phylogenies by using the neighbor-joining method. *Proceedings of the National Academy of Sciences of the United States of America*, **101**: 11030-11035.

TAMURA, K., PETERSON, D., PETERSON, N., STECHER, G., NEI, M. & KUMAR, S. 2011. MEGA5: molecular evolutionary genetics analysis using maximum likelihood, evolutionary distance, and maximum parsimony methods. *Molecular Biology and Evolution*, **28**: 2731-2739.

TAO, C., LI, H., JIN, X., ZHOU, J., WU, T., HE, Y., DENG, X., GU, C., ZHANG, G. & LIU, W. 2014. Seafloor hydrothermal activity and polymetallic sulfide exploration on the southwest Indian ridge. *Chinese Science Bulletin*: 1-11.

TAO, C., LIN, J., GUO, S., CHEN, Y.J., WU, G., HAN, X., GERMAN, C.R., YOERGER, D.R., ZHOU, N., LI, H., SU, X., ZHU, J., DY115-19, A.T. & PARTIES, D.-S. 2012. First active hydrothermal vents on an ultraslow-spreading center: Southwest Indian Ridge. *Geology*, **40**: 47-50.

TAO, C., WU, G., NI, J., ZHAO, H., SU, X., ZHOU, N., LI, J., CHEN, Y.J., CUI, R., DENG, X., EGOROV, I., DOBRETSOVA, I.G., SUN, G., QIU, Z., DENG, X., ZHOU, J., GU, C., LI, J., YANG, J., ZHANG, K., WU, X., CHEN, Z., LEI, J., HUANG, W., ZHOU, P., DING, T., JIN, W., LI, H. & LIN, J. 2009. New hydrothermal fields found along the SWIR during the Legs 5-7 of the Chinese DY115-20 Expedition (Abstract #OS21A-1150). In: *American Geophysical Union, Fall Meeting 2009*). American Geophysical Union, San Francisco, California, USA.

TEIXEIRA, S., SERR O, E.A. & ARNAUD-HAOND, S. 2012. Panmixia in a fragmented and unstable environment: the hydrothermal shrimp *Rimicaris exoculata* disperses extensively along the Mid-Atlantic Ridge. *PLoS ONE*, **7**: e38521.

TIVEY, M.K. 2007. Generation of seafloor hydrothermal vent fluids and associated mineral deposits. *Oceanography*, **20**: 50-65.

VAN DOVER, C.L., HUMPHRIS, S.E., FORNARI, D., CAVANAUGH, C.M., COLLIER, R., GOFFREDI, S.K., HASHIMOTO, J., LILLEY, M.D., REYSENBACH, A.L., SHANK, T.M.,

681 VON DAMM, K.L., BANTA, A., GALLANT, R.M., G TZ, D., GREEN, D., HALL, J.,
682 HARMER, T.L., HURTADO, L.A., JOHNSON, P., MCKINESS, Z.P., MEREDITH, C.,
683 OLSON, E., PAN, I.L., TURNIPSEED, M., WON, Y., YOUNG, C.R. & VRIJENHOEK, R.C.
684 2001. Biogeography and ecological setting of Indian Ocean hydrothermal vents. *Science*, **294**:
685 818-823.
686 WARÉN, A., BENGTSON, S., GOFFREDI, S.K. & VAN DOVER, C.L. 2003. A hot-vent gastropod
687 with iron sulfide dermal sclerites. *Science*, **302**: 1007.
688 WARÉN, A. & BOUCHET, P. 1989. New gastropods from East Pacific hydrothermal vents.
689 *Zoologica Scripta*, **18**: 67-102.
690 WARÉN, A. & BOUCHET, P. 1993. New records, species, genera, and a new family of gastropods
691 from hydrothermal vents and hydrocarbon seeps. *Zoologica Scripta*, **22**: 1-90.
692 WARÉN, A. & BOUCHET, P. 2001. Gastropoda and Monoplacophora from hydrothermal vents and
693 seeps; new taxa and records. *Veliger*, **44**: 116-231.
694 WARÉN, A., BOUCHET, P. & COSEL, R.V. 2006. Mollusca, Gastropoda. In: *Denisia*, Vol. 18:
695 *Handbook of deep-sea hydrothermal vent fauna (2nd edition)* (Desbruyères, D., Segonzac, M.
696 and Bright, M., eds), pp. 82-137. Swiss National Museum, Zurich, Switzerland.
697 WATANABE, H. & BEEDESSEE, G. 2015. Vent Fauna on the Central Indian Ridge. In:
698 *Subseafloor Biosphere Linked to Hydrothermal Systems*: *Earth System Sciences* (Ishibashi, J.-i.,
699 Okino, K. and Sunamura, M., eds), pp. 205-212. Springer.
700 YAO, H., DAO, M., IMHOLT, T., HUANG, J., WHEELER, K., BONILLA, A., SURESH, S. &
701 ORTIZ, C. 2010. Protection mechanisms of the iron-plated armor of a deep-sea hydrothermal
702 vent gastropod. *Proceedings of the National Academy of Sciences*, **107**: 987-992.
703 ZENGUIN, J.A., HARTLEY, J.L. 1985. Ethanol Precipitation of DNA. *Focus*, **7**(4): 1-2.
704

705 FIGURES

706

707 **Figure 1.** Map of deep-sea hydrothermal vent fields where *Chrysomallon squamiferum*
708 sp. nov. is known to occur. Abbreviations used are as follows: SWIR = South West Indian
709 Ridge, CIR = Central Indian Ridge, SEIR = South East Indian Ridge, A-AR = American-
710 Antarctic Ridge and MAR = Mid Atlantic Ridge. This map was created using Esri
711 ArcMap 10.1 (ESRI, 2012) and General Bathymetric Chart of the Oceans (GEBCO) Grid
712 Display Ver.2.13 (BODC, 2010). Data source: Bathymetry, GEBCO; continents data.
713 ArcWorld Supplement; oceanic ridges, United States Geologic Service (USGS).

714

715

716

717

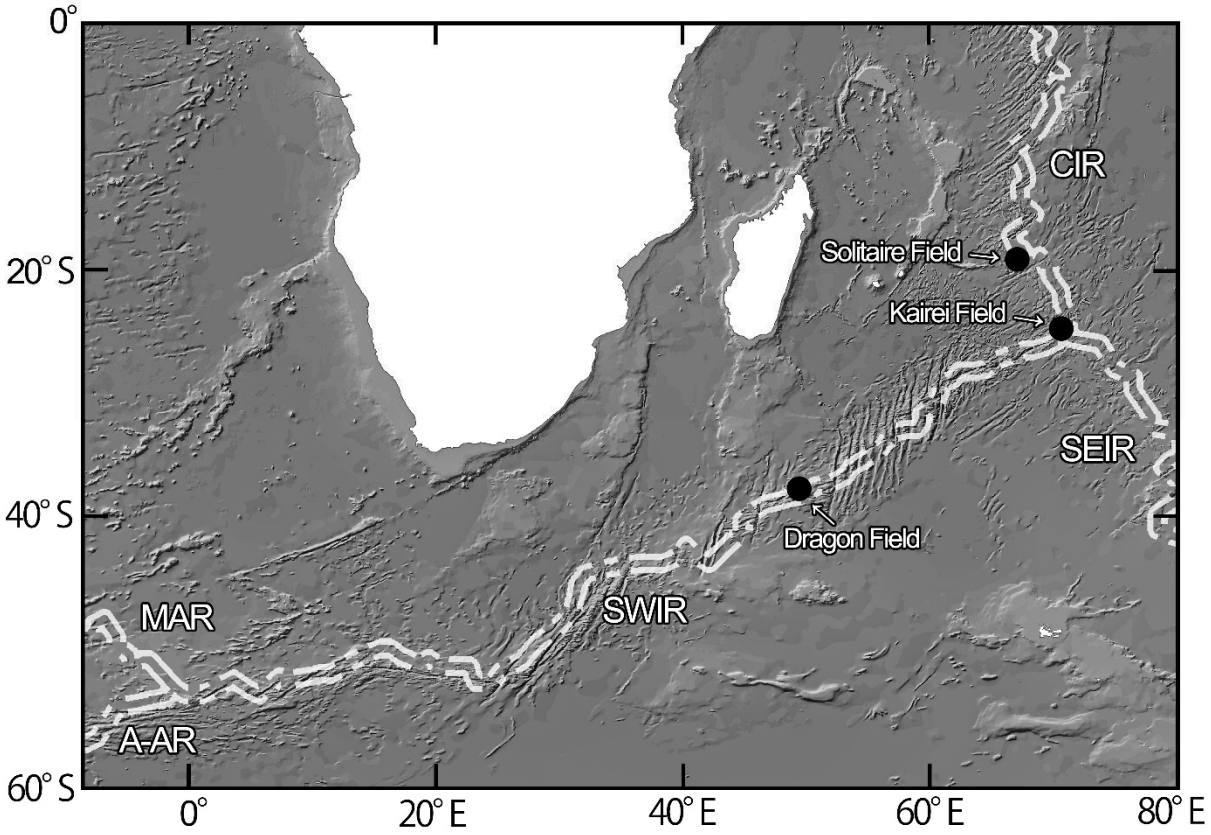

718 **Figure 2.** *Chrysomallon squamiferum* sp. nov. **A, B.** Live specimen from Longqi vent
719 field, Southwest Indian Ridge (SWIR). **C, D.** Paratype shell (NHMUK 2015-XX). **E, F.**
720 Holotype (NHMUK 2015-XX). **G.** Close-up of sclerites. **H.** *In-situ* photograph, Longqi
721 vent field, SWIR, arrow indicate *C. squamiferum* aggregation. Scale bars. **A, B, G** = 1
722 cm; **C-F** = 5 mm; **H** = 5 cm. Photographs credit: **A, B** by David Shale; **C-F** by Pete
723 Bucktrout (British Antarctic Survey).
724

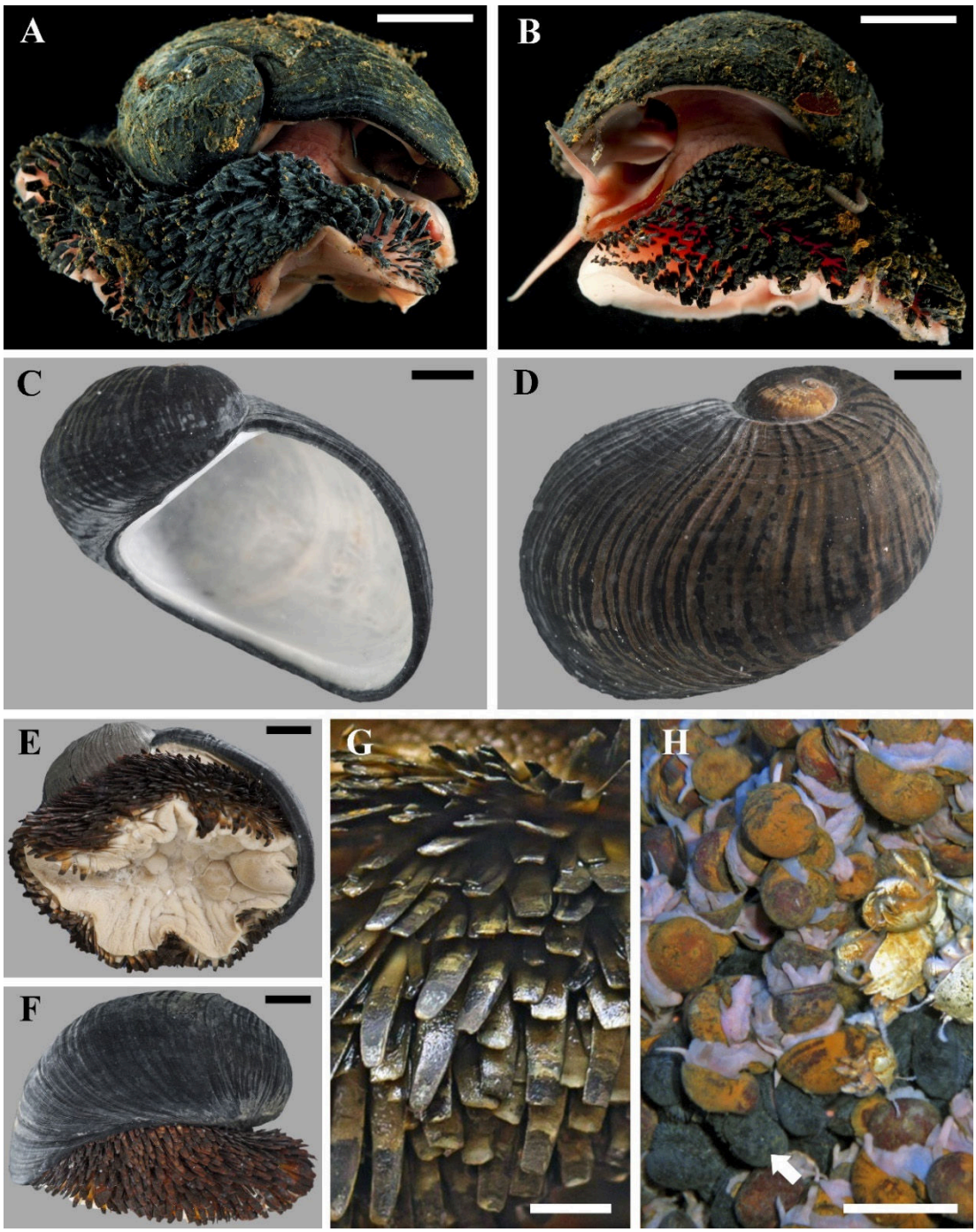

725

726 **Figure 3**. Scanning electron microscopy images of a single sclerite of *Chrysomallon*
727 *squamiferum* sp. nov. from Longqi, SWIR. **A.** Overview. **B.** Surface texture of the organic
728 layer. **C.** Surface of the iron sulfide layer. **D.** Sulfide deposits commonly seen near tip of
729 sclerites. Scale bars. **A** = 400 μm; **B** = 20 μm; **C, D** = 10 μm.

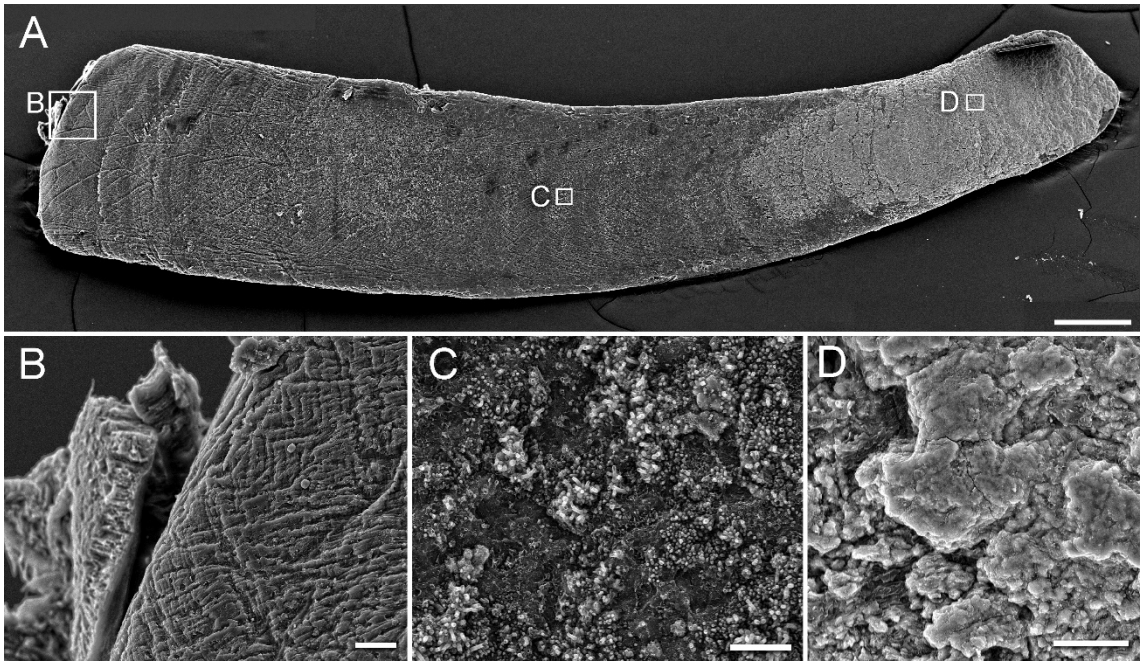

730
731

Figure 4. Internal anatomy of *Chrysomallon squamiferum* sp. nov. drawn with shell and mantle, and part of the ctenidium removed. The oesophageal gland and gonad are partly dissected to show structures underneath or within. Abbreviations: Au = Auricle, Ct = Ctenidium, Dg = Digestive gland, Go = Gonad, Gs = Genital slit, In = Intestine, Mo = Mouth, Ne = Nephridium, Oe = Oesophagus, Og = Oesophageal gland, Re = Rectum, Sc = Sclerite, Sp = 'Sperm packaging organ', Ve = Ventricle. Scale bar = 1 cm.

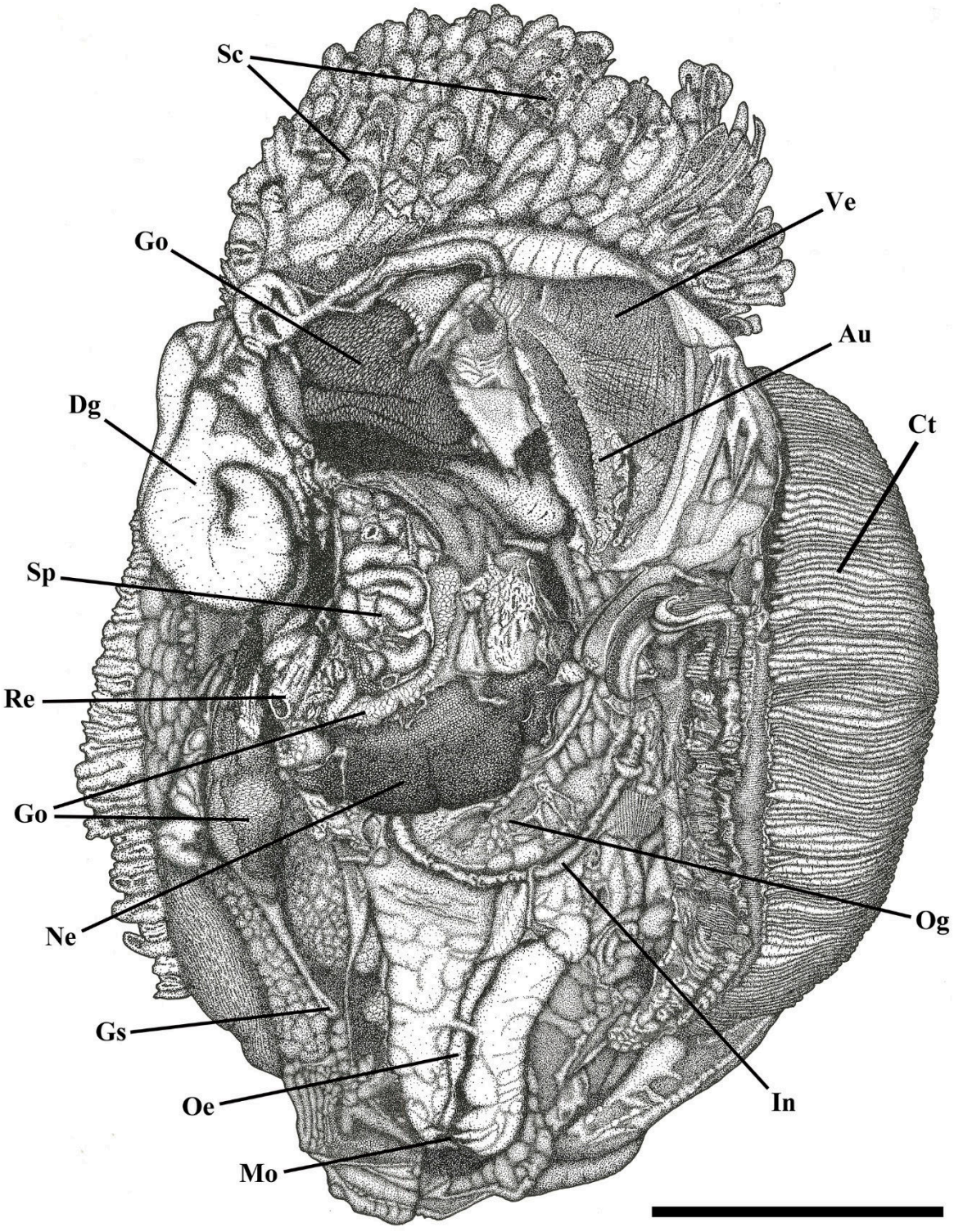

740 **Figure 5.** Scanning electron microscopy images of the radula of *Chrysomallon*
741 *squamiferum* sp. nov. **A.** Radula ribbon. **B.** Close-up of central and lateral teeth. **C.** Details
742 of central and lateral teeth. **D.** Marginal teeth. **E.** Marginal teeth overview. Scale bars. **A**
743 = 100 μm; **B**, **C** = 20 μm; **D** = 10 μm; **E** = 50μm.
744

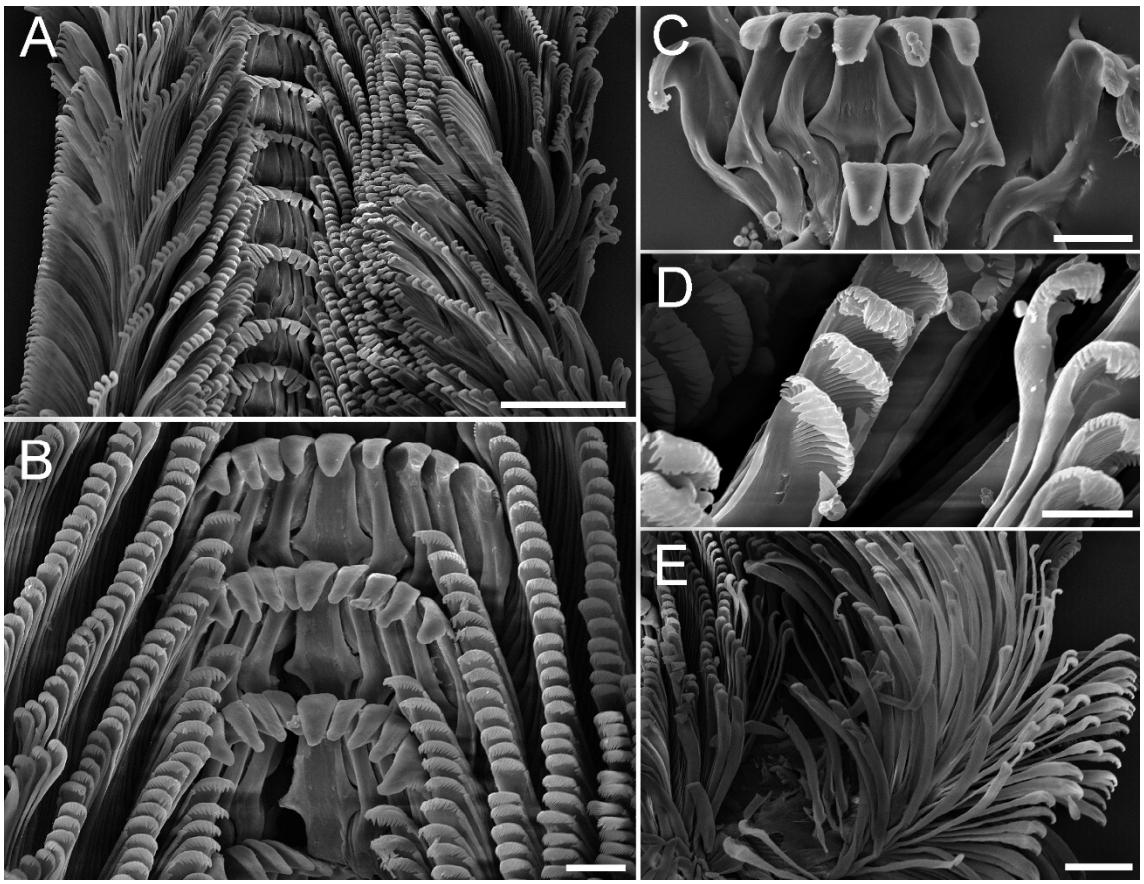

745
746

747 **Figure 6.** Scatterplot of shell diameter vs shell height of 50 specimens of *Chrysomallon*
748 *squamiferum* sp. nov. across a size range. Line of best fit formula y=0.7657x+0.2069;
749 R^2=0.9868, $p < 0.001$.
750

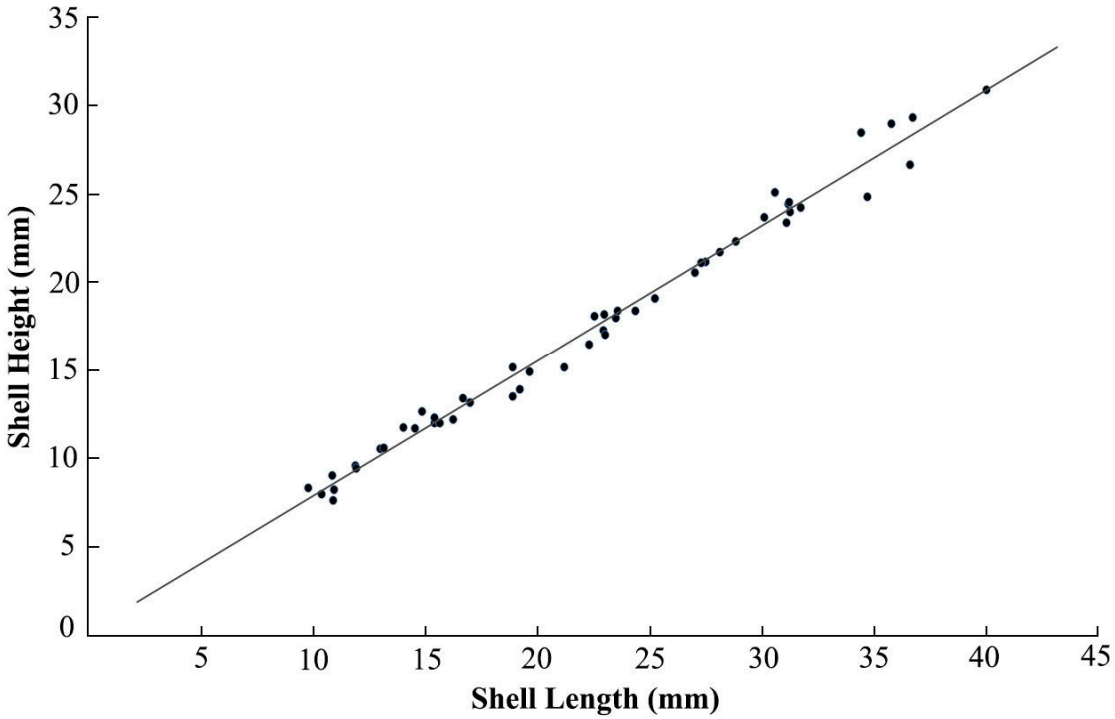

751
752
753

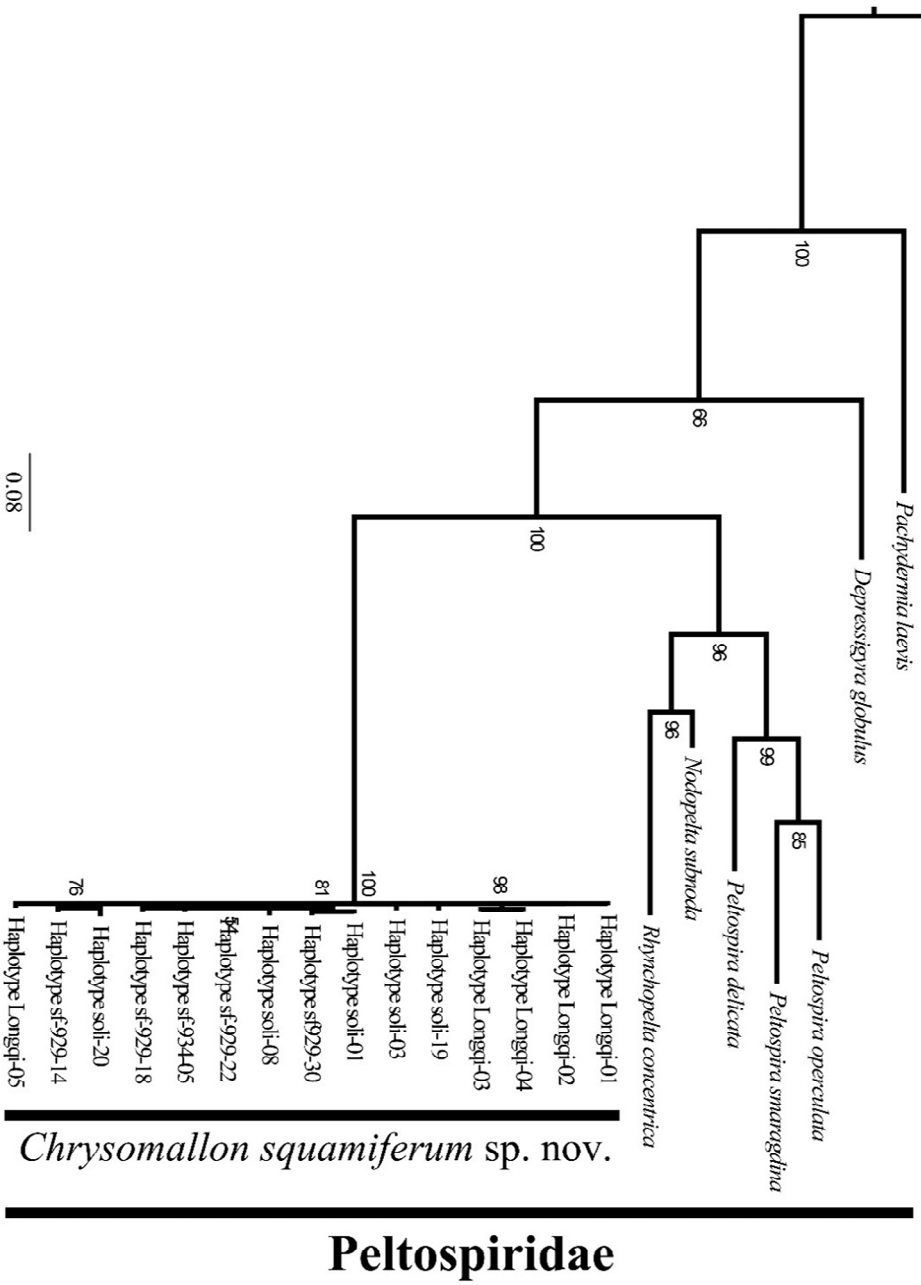

Figure 7. Consensus tree reconstructed from a codon-partitioned 457-bp fragment of COI gene using Bayesian inference. In the analysis Metropolis-coupled Monte Carlo Markov Chains was run for five million generations, sampled every 100 generations with first 25% discarded as:"burnin". Node values represent Bayesian posterior probability.

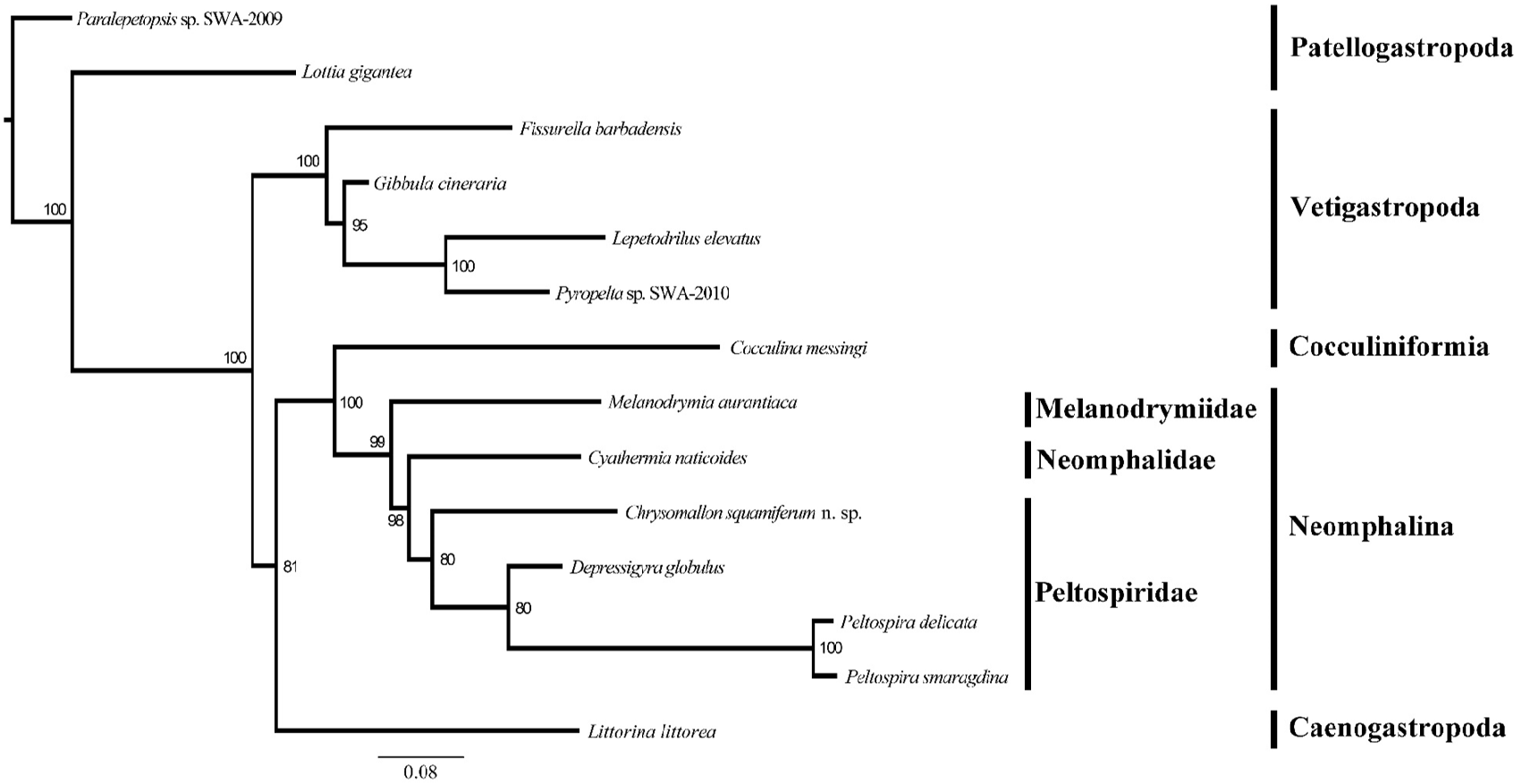

Figure 8. Consensus tree reconstructed from a combined five-genes (H3, COI, 16S, 18S, 28S) 2753-bp dataset using Bayesian inference. In the analysis Metropolis-coupled Monte Carlo Markov Chains was run for five million generations, sampled every 100 generations with first 25% discarded as "burnin". Node values represent Bayesian posterior probability.

761 TABLES

762

763 **Table 1.** List of PCR primers used in obtaining sequences of *Chrysomallon squamiferum*
764 sp. nov. from the Longqi population specimens.

Gene	Direction	Name	Sequence 5'-3'	Citation
H3	Forward	H3aF	ATG GCT CGT ACC AAG CAG ACV GC	Colgan *et al.*, 1998
	Reverse	H3aR	ATA TCC TTR GGC ATR ATR GTG AC	
COI	Forward	LCO1490	GGT CAA CAA ATC ATA AAG ATA TTG G	Folmer *et al.*, 1994
	Reverse	HCO2198	TTA ACT TCA GGG TGA CCA AAA AAT CA	
COI	Forward	SF1F	GAT CTG GTC TTT TAG GAA CAG GAT TCA	Newly designed, specific to the 'scaly-foot'
	Reverse	SF1R	TGT GAG ATA CCA TTC CAA ATC CAG G	
16S	Forward	16Sa	CGC CTG TTT ATC AAA AAC AT	Palumbi et al., 1991
	Reverse	16Sb	CCG GTC TGA ACT CAG ATC ACG T	
18S Part 1	Forward	18Sa2.0	ATG GTT GCA AAG CTG AAA C	Whiting *et al.*, 1997
	Reverse	18S9R	GAT CCT TCC GCA GGT TCA CCT AC	
18S Part 2	Forward	18S1F	TAC CTG GTT GAT CCT GCC AGT AG	Giribet *et al.*, 1996
	Reverse	18S5R	CTT GGC AAA TGC TTT CGC	
18S Part 3	Forward	18S3F	GTT CGA TTC CGG AGA GGG A	Whiting *et al.*, 1997
	Reverse	18Sbi	GAG TCT CGT TCG TTA TCG GA	
28S	Forward	28SSFF	AGT AAC GGC GAG TGA AGC GGG	Newly designed, specific to the 'scaly-foot'
	Reverse	28SSFR	CGG TTT CAC GTA CTC TTG AAC TCT CTC	

765 **Table 2.** List of species used in analyses with GenBank accession numbers for COI tree.
766

Species	COI
Nodopelta subnoda McLean, 1989	GU984280
Rhynchopelta concentrica McLean, 1989	GU984282
Depressigyra globulus Warén & Bouchet, 1989	DQ093519
Pachydermia laevis Warén & Bouchet, 1989	AB429222
Peltospira delicata McLean, 1989	FJ977764
Peltospira operculata McLean, 1989	GU984278
Peltospira smaragdina Warén & Bouchet, 2001	GQ160764
Chrysomallon squamiferum sp. nov.	
Lonqgi haplotype: longqi-01	*To be deposited*
Lonqgi haplotype: longqi-02	
Lonqgi haplotype: longqi-03	
Lonqgi haplotype: longqi-04	
Lonqgi haplotype: longqi-05	
Kairei haplotype: sf929-14	AB540635
Kairei haplotype: sf929-18	AB540638
Kairei haplotype: sf929-22	AB540629
Kairei haplotype: sf929-30	AB540645
Kairei haplotype: sf934-5	AB540631
Solitaire haplotype: soli-1	AB634505
Solitaire haplotype: soli-3	AB634507
Solitaire haplotype: soli-8	AB634508
Solitaire haplotype: soli-19	AB634512
Solitaire haplotype: soli-20	AB634513
Cocculina messingi McLean & Harasewych, 1995	AY923910

767

768
769
770

Table 3. List of clade, family, species, and genes used in the five-gene phylogenetic reconstruction with GenBank accession numbers

Clade	Family	Taxa	COI	H3	16S	18S	28S
Patellogastropoda	Lottidae	*Lottia gigantea* Gray in Sowerby I, 1834	FJ977750	FJ977725	FJ977696	FJ977632	AB282783
	Neolepetopsidae	*Paralepetopsis* sp. SWA-2009 (from Aktipis & Giribet, 2012)	FJ977752	FJ977728	FJ977699	FJ977635	FJ977665
Vetigastropoda	Fissurellidae	*Fissurella barbadensis* (Gmelin, 1791)	HM771628	HM771595	HM771551	HM771467	HM771511
	Lepetodrilidae	*Lepetodrilus elevatus* McLean, 1988	U56846	AY923959	EF549688	AY145381	AY145413
	Trochidae	*Gibbula cineraria* (Linnaeus, 1758)	AM049339	FJ977737	AY163410	AY340430	FJ977676
	Pyropeltidae	*Pyropelta* sp. SWA-2010 (from Aktipis & Giribet, 2012)	GQ160750	GQ160719	GQ160680	GQ160785	GQ160633
Cocculiniformia	Cocculinidae	*Coccalina messingi* McLean & Harasewych, 1995	AY923910	AY923945	AY377624	AF120508	AY377696
Neomphalina	Melanodrymiidae	*Melanodrymia aurantiaca* Hickman, 1984	GQ160763	GQ160740	GQ160700	GQ160805	GQ160656
	Neomphalidae	*Cyathermia naticoides* Warén & Bouchet, 1989	DQ093518	DQ093498	DQ093472	DQ093430	FJ977685
	Peltospiridae	*Chrysomallon squamiferum* sp. nov. (Longqi field, SWIR)	To be deposited				
		Depressigyra globulus Warén & Bouchet, 1989	DQ093519	AY923969	AY163400	DQ093431	DQ279978
		Peltospira delicata McLean, 1989	FJ977764	FJ977745	FJ977716	FJ977653	FJ977684
		Peltospira smaragdina Warén & Bouchet, 2001	GQ160764	GQ160741	GQ160701	GQ160806	GQ160657
Caenogastropoda	Littorinidae	*Littorina littorea* (Linnaeus, 1758)	DQ093525	DQ093507	DQ093481	DQ093437	FJ977692

771
772
773

Table 4. Shell parameters of *Chrysomallon squamiferum* sp. nov. Range and proportion to shell diameter calculated from 50 specimens across a size range.

	Shell Parameters (mm)			**Aperture Parameters (mm)**	
	Length	***Height***	***Dorsal-Ventral***	***Length***	***Height***
Holotype (NHM 2015-XX)	32.03	24.84	20.24	26.65	22.84
Paratype (NHM 2015-XX)	36.03	28.19	22.96	27.55	25.11
Range	9.80 ~ 40.02	7.65 ~ 30.87	5.39 ~ 27.92	7.26 ~ 32.52	6.38 ~ 27.29
Proportion to Shell Length	1	0.778	0.660	0.773	0.667
SD of Proportion	-	0.035	0.053	0.040	0.036

774

Table 5. Maximum-likelihood distance matrix of seven Peltospiridae genera constructed from 457bp fragment of COI gene. Analyses were conducted using the Maximum Composite Likelihood model (Tamura, Nei & Kumar, 2004). *Chrysomallon squamiferum* sp. nov. sequences represent one single specimen.

		1	2	3	4	5	6	7	8
1	*Chrysomallon squamiferum* sp. nov. (Longqi, SWIR)								
2	*Chrysomallon squamiferum* sp. nov. (Kairei, CIR)	0.66%							
3	*Chrysomallon squamiferum* sp. nov. (Solitaire, CIR)	0.66%	0.88%						
4	*Depressigyra globulus*	26.41%	26.15%	26.41%					
5	*Nodopelta subnoda*	24.46%	23.83%	24.16%	17.73%				
6	*Pachydermia laevis*	25.48%	25.74%	25.49%	24.05%	21.29%			
7	*Peltospira operculata*	24.20%	24.24%	24.49%	23.31%	17.10%	24.08%		
8	*Rhynchopelta concentrica*	26.14%	26.10%	26.14%	22.94%	13.65%	24.68%	19.32%	

Supplementary Material: Energy Dispersive X-ray Spectrometry Results

Objective & Methods

To ascertain the existence of iron sulphide mineralisation on the sclerites and shell of the 'scaly-foot gastropod' from Longqi hydrothermal field, Southwest Indian Ridge, scanning electron microscopy with energy dispersive X-ray spectrometry (SEM-EDS) analyses was undertaken using a Hitachi S-2400 SEM-EDS (University of Tokyo) to examine their elemental composition. Sclerites and shell of the 'scaly-foot gastropod' from Kairei and Solitaire fields, Central Indian Ridge was used for comparison. For sclerites a similar position near the tip was examined for all specimens, and for shell a section of the body whorl was used. Platinum (Pt) was used as a standard reference material, meaning a fixed amount was used for calibration across all observations allowing quantitative comparison across different observations.

Results and Discussion

Both sclerites (Figure S1) and shell (Figure S2) of the 'scaly-foot gastropod' from Longqi field showed clear peaks in the position of sulfur and iron, which was also seen in the specimens from Kairei field. The specimens from Solitaire field however lacks significant peak in iron, although a clear peak in sulfur was observed. These are consistent with the previous observations that the Kairei specimens have crystallised iron sulfides on both shell and sclerite (Suzuki *et al*., 2006), while Solitaire specimens lack iron and only has sulfur (Nakamura *et al*., 2012).

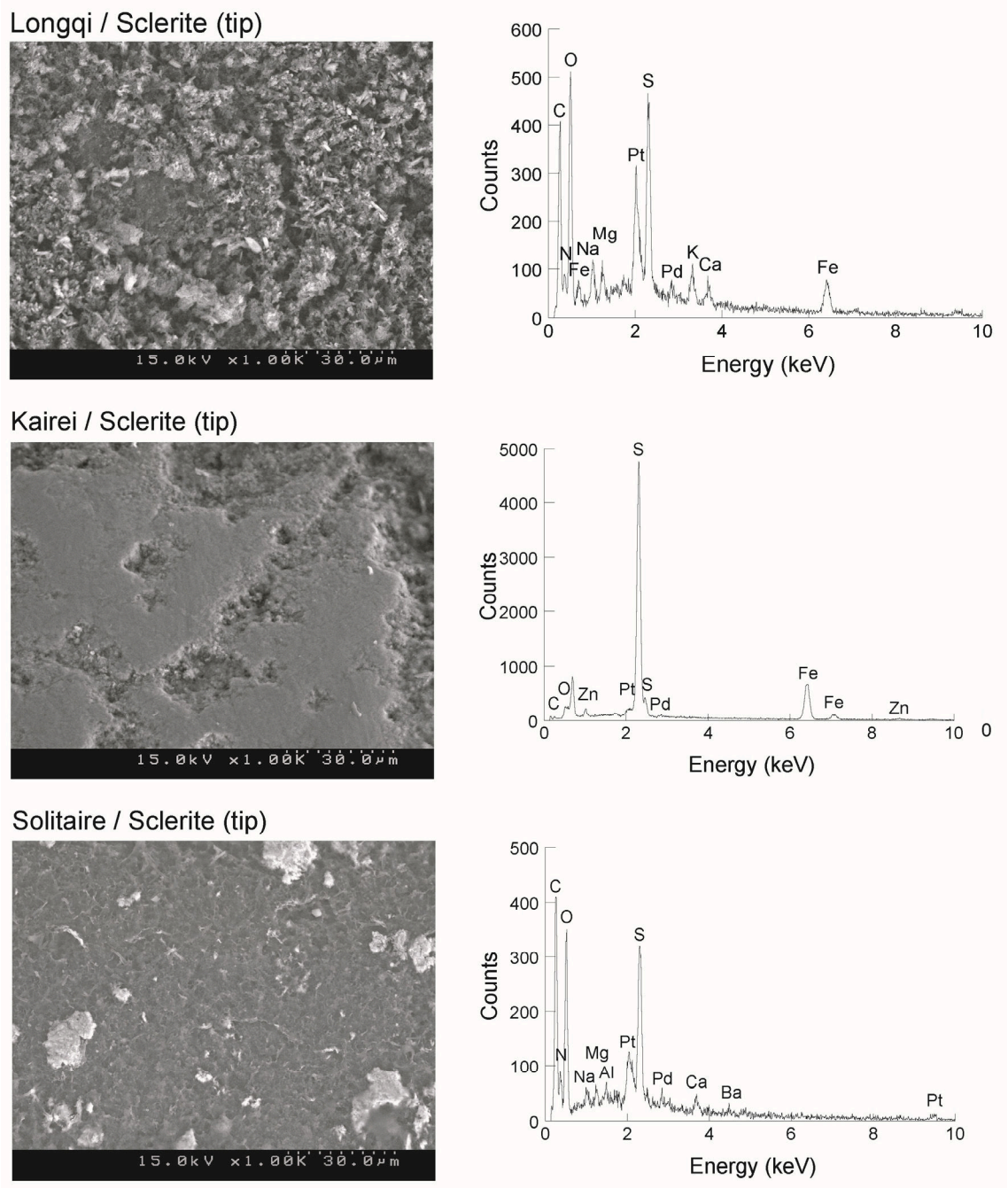

Figure S1. Micrographs and spectrums from SEM-EDS analyses of the sclerites of the 'scaly-foot gastropod' from Longqi, Kairei, and Solitaire vent fields, to investigate relative quantity of sulfur (S) and iron (Fe) across populations. Platinum (Pt) was used as a standard reference material in same quantity across all observations.

The amount of sulfur in Kairei specimens (sclerite around 4800 counts, shell around 750 counts) was much higher than Solitaire (sclerite around 330 counts, shell around 180

counts) or Longqi (sclerite around 480 counts, shell around 200 counts); and the amount of iron in Kairei specimens (sclerite around 900 counts, shell around 350 counts) was also much higher than in Longqi specimens (sclerite around 100 counts, shell around 50 counts) (also compare to the standard peak of platinum, Pt, Figure S1-2).

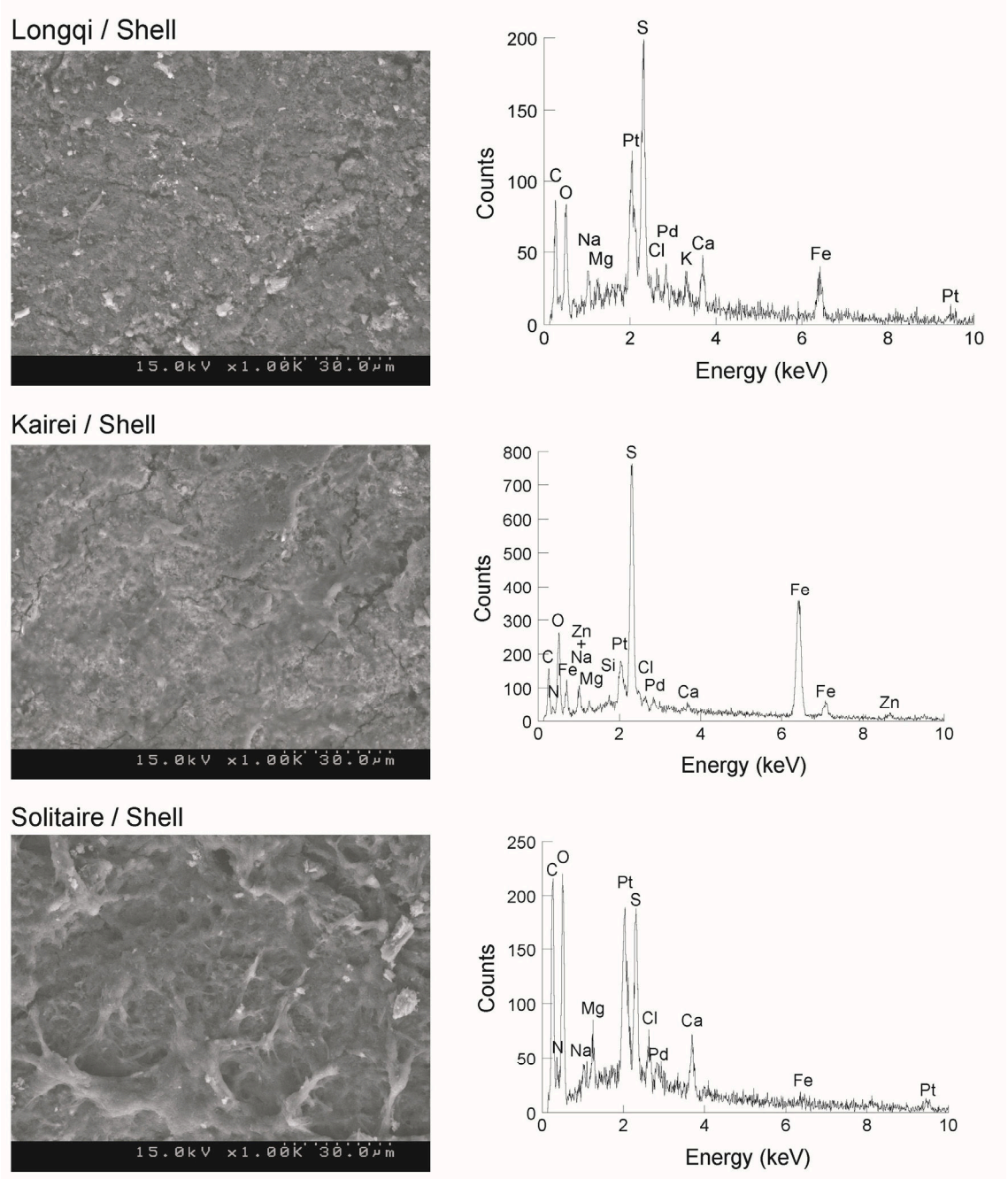

Figure S2. Micrographs and spectrum from SEM-EDS analyses of the shell (body whorl) of the 'scaly-foot gastropod' from Longqi, Kairei, and Solitaire vent fields, to investigate relative quantity of sulfur (S) and iron (Fe) across populations. Platinum (Pt) was used as a standard reference material in same quantity across all observations.

These results indicate that although the Longqi 'scaly-foot gastropods' exhibit a certain degree of iron sulfide mineralisation, the extent of this is much less than those from Kairei field. The differences are most likely due to compositions of vent fluids at the different sites (Nakamura *et al*., 2012). However as the fluid composition at Longqi field so far remains unknown (Copley, 2011) no conclusions can be made at present regarding whether the reduced level of iron sulfide in Longqi specimens compared to Kairei specimens is due to reduced availability of iron in the vent fluid.

Acknowledgements

Dr Yohey Suzuki (University of Tokyo) and Dr Katsuaki Watanabe (University of Tokyo) are gratefully acknowledged for allowing access to the required equipments and helping with data collection. Dr Hiromi Watanabe (Japan Agency for Marine-Earth Science and Technology) is thanked for providing Kairei field and Solitaire field specimens for comparison.

References

Copley JT. 2011. Research cruise JC67, Dragon vent field, SW Indian Ocean, 27-30 November 2011 *RRS James Cook cruise report*: British Oceanographic Data Centre. Available from http://www.bodc.ac.uk/data/information_and_inventories/cruise_inventory/report/10593/.

Nakamura K, Watanabe H, Miyazaki J, Takai K, Kawagucci S, Noguchi T, Nemoto S, Watsuji T-o, Matsuzaki T, Shibuya T, Okamura K, Mochizuki M, Orihashi Y, Ura T, Asada A, Marie D, Koonjul M, Singh M, Beedessee G, Bhikajee M, Tamaki K. 2012. Discovery of new hydrothermal activity and chemosynthetic fauna on the Central Indian Ridge at 18°–20°S. *PLoS ONE* **7:** e32965.

Suzuki Y, Kopp RE, Kogure T, Suga A, Takai K, Tsuchida S, Ozaki N, Endo K, Hashimoto J, Kato Y, Mizota C, Hirata T, Chiba H, Nealson KH, Horikoshi K, Kirschvink JL. 2006. Sclerite formation in the hydrothermal-vent 'scaly-foot gastropod': Possible control of iron sulfide biomineralization by the animal. *Earth Planet Sc Lett* **242:** 39-50.

Chapter 3

Low connectivity between 'scaly-foot gastropod' populations at hydrothermal vents of on the Southwest Indian Ridge and Central Indian Ridge

(*Journal of Biogeography*, Submitted)

CHAPTER INTRODUCTION

The results from the previous chapter proved that the population of *Chrysomallon squamiferum*, the 'scaly-foot gastropod', found in Longqi hydrothermal vent field, Southwest Indian Ridge (SWIR) in fact belongs to the same species as those found in Kairei and Solitaire hydrothermal vent fields, Central Indian Ridge (CIR). This means its distribution spans two mid-ocean ridges in the Indian Ocean, over distances exceeding 2,500 km. Although this is not particularly a great distance for vent organisms' range, as species with planktotrophic larvae such as *Rimicaris exoculata* Williams & Rona, 1986 ranges over more than 7,000 km stretch of Mid Atlantic Ridge (Teixeira *et al.*, 2012) and *Bathymodiolus septemdierum* Hashimoto & Okutani, 1994 maintains connectivity from southwest Pacific to CIR (Kyuno *et al*., 2009; Vrijenhoek, 2010; Fujikura *et al*., 2012), *C. squamiferum* presumably has a lecithotrophic larvae (Warén *et al.*, 2006). This is the norm in Peltospiridae (Warén *et al.*, 2006) and in addition they have eggs of negative buoyancy under atmospheric pressure (Beedessee *et al*., 2013). Taken together, *C. squamiferum* may have a rather low dispersal ability and seafloor features such as fracture zones or depressions are likely to become dispersal barriers. Therefore, it is of great interest to investigate how well the SWIR population is connected with the CIR sites in terms of gene flow; especially in the light of upcoming commercial mining activities in Longqi. In this chapter, this is investigated using the cytochrome *c* oxidase subunit I (COI) gene.

STATEMENT OF AUTHOR CONTRIBUTIONS

The main body of this chapter takes the form of a manuscript formatted for *Journal of Biogeography*. It has been submitted as a Research Article (January 2015; ID JBI-15-0084) and is currently under review. The authors (in this order) are Chong Chen (corresponding author), Jonathan T. Copley, Katrin Linse, and Alex D. Rogers; the detailed author contributions are as follows.

The original idea for the project was conceived between CC, JTC, and ADR; plan and methodology were initially by ADR and JTC, while refined by CC. JTC and ADR provided funding for both sample collection on-board *RRS* James Cook research cruises JC66/67 as well as laboratory work afterwards. On-board the cruises CC, JTC, and ADR participated in sample collection and tissue fixation of the specimens used in this study. CC was responsible for all laboratory work, data collection, data analyses, and wrote the original manuscript. All authors discussed the results and implications of the study in detail and edited the manuscript for improvement. ADR, JTC, and KL supervised the work of CC during the length of this study.

ORIGINAL ARTICLE

Low connectivity between 'scaly-foot gastropod' populations at hydrothermal vents of the Southwest Indian Ridge and Central Indian Ridge

Chong Chen[1*], Jonathan T. Copley[2], Katrin Linse[3], and Alex D. Rogers[1]

[1] Department of Zoology, University of Oxford, The Tinbergen Building, South Parks Road, Oxford, OX1 3PS, UK; [2] National Oceanography Centre, University of Southampton, European Way, Southampton, SO14 3ZH, UK; [3] British Antarctic Survey, High Cross, Madingley Road, Cambridge, CB3 0ET, UK

* Correspondence: Chong Chen,
Department of Zoology, University of Oxford, Oxford, OX1 3PS, UK.
E-mail: chong.chen@zoo.ox.ac.uk

Short running head: Low connectivity between SWIR and CIR hydrothermal vents

Word count: Abstract 279 words; main text 5240 words

ABSTRACT

Aim

Hydrothermal vents on mid-oceanic ridges are patchily distributed and host many taxa endemic to deep-sea chemosynthetic environments, whose dispersal may be constrained by geographical barriers. The aim of this study was to investigate the connectivity of three populations of "scaly-foot gastropod" (Mollusca: Peltospiridae), a species endemic to hydrothermal vents in the Indian Ocean, between two vent fields on the Central Indian Ridge (CIR) and the first sampled vent field on the Southwest Indian Ridge (SWIR).

Location

Longqi vent field (37°47'S 49°39'E), SWIR; Kairei (25°19.23'S, 70°02.42'E) and Solitaire (19°33.41'S, 65°50.89'E) vent fields, CIR.

Methods

Connectivity and population structure across the two mid-oceanic ridges, was investigated using a 489-bp fragment of the cytochrome oxidase *c* subunit I gene. Tools used include measures of genetic differentiation (F_{ST}), reconstruction of parsimony haplotype network, mismatch analyses, and neutrality tests. Relative migrants per generation was estimated between the fields.

Results

Significant differentiation was revealed between the vent field in SWIR and the two in CIR, while high connectivity was inferred between the two CIR fields. Signatures were detected indicating recent bottleneck events followed by demographic expansion in all populations. Estimates of relative number of migrants was much lower between the SWIR and CIR, compared with values between the CIR vent fields.

51

52 **Main conclusions**

53 The present study is the first to investigate connectivity between hydrothermal vents on
54 two mid-ocean ridges in the Indian Ocean. The phylogeography revealed for the 'scaly-
55 foot gastropod' indicates low connectivity between SWIR and CIR vent populations, with
56 implications for the future management of environmental impacts for seafloor mining at
57 hydrothermal vents in the region, as proposed for Longqi.

58

59 **Keywords**

60 Deep-sea, dispersal, hydrothermal vent, Indian Ocean, mitochondrial DNA, population
61 connectivity, scaly-foot gastropod

62

63

INTRODUCTION

Hydrothermal vents were first discovered in 1977 (Lonsdale, 1977) along the Galapagos Rift (GAR), and typically host rich benthic communities containing a large proportion of vent-endemic species. As a result of continued discovery and sampling it has become clear that hydrothermal vents in different regions of the world are characterised by different species compositions and different dominant taxa, forming distinct biogeographic provinces (Ramirez-Llodra *et al.*, 2007). Recent statistical modelling using multivariate regression trees (MRT) recognised 11 hydrothermal vent provinces world-wide (Bachraty *et al.*, 2009; Rogers *et al.*, 2012). Elucidating how vent-endemic species disperse and maintain connectivity between different hydrothermal vent fields is important in understanding their biogeography and speciation. As well as their unique fauna, hydrothermal vent fields also hold rich mineral resources in the form of seafloor mass sulphides (SMS) containing high grade polymetallic ores (Hannington *et al.*, 2011), and recently there has been a growing interest in their exploitation through deep-sea mining (e.g., Nautilus Minerals in Papua New Guinea and Bluewater Metals in Solomon Islands; Van Dover, 2011b).

Distances between active vents on mid-ocean ridges and stability of these vents largely depends on the spreading rate (Hannington *et al*., 2011). Fast-spreading ridges such as the East Pacific Rise (EPR) have short distances of tens of kilometres between vents and a longevity of decades or less, while slow-spreading ridges like the Mid-Atlantic Ridge (MAR) have vents separated by hundreds to thousands of kilometres with a longevity of centuries or more (Vrijenhoek, 2010). Connectivity between different vents and fields is maintained largely by larval dispersal (Van Dover, 1990), which is influenced by a number of factors such as dispersal capability, life-history traits, oceanic currents, ocean temperature, vent geology, vent fluid chemistry and the presence of physical barriers

(Vrijenhoek, 2010). Much of the current knowledge on genetic connectivity between hydrothermal vents (reviewed in Vrijenhoek, 2010) is based on the well-studied systems in the Pacific and Atlantic oceans such as EPR and MAR.

The Indian Ocean is the least studied of the three major oceans in terms of hydrothermal vents and other deep-sea ecosystems. The first vent field was not discovered until 2000 (Hashimoto *et al.,* 2001; Van Dover *et al.*, 2001): the Kairei field (25°19.23'S, 70°02.42'E), located on the Central Indian Ridge (CIR), which has an intermediate spreading rate of 50-60 mm $year^{-1}$, near the Rodriguez Triple Junction. Since then, three further vent fields have been discovered on the CIR: the Edmond (23°52.68'S, 69°35.80'E; Van Dover *et al.*, 2001); Dodo (18°20.10'S, 65°17.90'E); and Solitaire (19°33.41'S, 65°50.89'E) fields (Nakamura *et al.*, 2012). Kairei, Edmond and Solitaire are larger fields (area of hydrothermal emissions approx. 50 m by 50 m, Nakamura *et al*., 2014) with higher species richness, while Dodo is smaller (emission area approx. 10 m by 10 m, Nakamura *et al*., 2014) and only hosts a subset of the fauna found at the larger fields. The alvinocaridid shrimp *Rimicaris kairei* Watabe & Hashimoto, 2002 is one of the dominant species at these CIR vents, forming dense aggregations over black smoker chimney structures in Kairei, Edmond and Solitaire, and present in smaller patches on chimneys at Dodo. Other dominant fauna in Kairei include hairy snails (*Alviniconcha marisindica* Okutani, 2014), 'scaly-foot gastropods', mussels (*Bathymodiolus septemdierum* Hashimoto & Okutani, 1994, *B. marisindicus* Hashimoto, 2001 is a synonym; Vrijenhoek, 2010; Fujikura *et al*., 2012), *Lepetodrilus* limpets, brachyuran crabs (*Austinograea rodriguezensis* Tsuchida & Hashimoto, 2002), stalked barnacles (*Neolepas* sp.), and large anamones (*Marianactis* sp.). The faunal assemblage at the Edmond vent field is similar but lacks the two large snails and stalked barnacles (Van Dover *et al*., 2001), while Solitaire is similar to Kairei in composition of dominant fauna and also has alvinellid polychaetes (Nakamura *et al.*, 2012). At Dodo, the visually

dominant species are *R. kairei* and *A. rodriguezensis* although *Marianactis* sp. anemones and *Lepetodrilus* limpets are also present (Nakamura *et al*., 2012). Watanabe & Beedessee (2015) give a checklist of known species in the four CIR fields.

In 2007, the first vent field was visually confirmed on the ultra-slow spreading (14-16 mm $year^{-1}$; Tao *et al*., 2014) Southwest Indian Ridge (SWIR) by expedition DY115-20 of the D/V *Dayang Yihao*, and subsequently named the Longqi (also known as 'Dragon'; Roterman *et al*., 2013) vent field (37°47' S 49°39' E, Tao *et al.,* 2012; Tao *et al*., 2014; Fig. 1a). The Longqi field is more than 2,300 km away from Kairei, the closest neighbouring surveyed vent field, and more than 2,500 km away from Solitaire (Tao *et al.,* 2012), both lying beyond the intersection of the SWIR and CIR at the Rodriguez Triple Junction. The distance between Kairei and Solitaire is approximately 750 km along the CIR.

The recently discovered SWIR vent field provides the first opportunity to study across-ridge connectivity in the Indian Ocean. Tao *et al*. (2012) reported the presence of the 'scaly-foot gastropod' (Mollusca: Peltospiridae, Warén *et al*., 2003) at the Longqi field based on visual observation. In November 2011, the first faunal samples were collected from the vent field during expedition JC67 of the RRS *James Cook*, using the Remotely Operated Vehicle (ROV) *Kiel6000* (Copley *et al.*, 2012). The 'scaly-foot gastropod' is unique among gastropods in possessing numerous dermal sclerites which may be mineralised with iron sulphide (Warén *et al*., 2003; Chen *et al*., 2015; Fig. 1b). Also unusual among chemosymbiotic molluscs is that it is a holobiont which houses symbiotic bacteria not in the gills but in a much enlarged oesophageal gland (Goffredi *et al*., 2004; Nakagawa *et al*., 2014). First discovered at the Kairei field as a dark morphotype with dark shell and sclerites (Van Dover *et al*., 2001; Fig. 1b, middle), a light morphotype of this species is also known, with a yellowish shell and white sclerites from Solitaire in CIR

(Nakamura *et al*., 2012; Fig. 1b bottom), and now also a third morphotype with brown shell and dark sclerites from Longqi (Fig. 1b, top). This species has not been formally named and described to date.

Connectivity of four dominant vent-endemic species at the CIR vents, including the 'scaly-foot gastropod', was investigated by Beedessee *et al*. (2013), revealing no genetic differentiation across all four known CIR sites, consistent with either panmixia or a recent range expansion. The presence of the 'scaly-foot gastropod' on the SWIR now provides the opportunity to study the population structure of vent organisms in the Indian Ocean over a greater scale. This is important in terms of management of hydrothermal vent ecosystems as it provides a measure of the unique genetic identity and variation of individual populations, as well as their connectivity which may relate to likelihood of recolonisation following disturbance (Van Dover, 2011a). The China Ocean Mineral Resources Research and Development Association (COMRA) signed a contract in 2011 with the International Seabed Authority (ISA) to explore seafloor massive sulphides (SMS) deposits on the SWIR for 15 years (Tao *et al*., 2014), with the Longqi field within the contracted area while the population connectivity of its fauna to other known Indian Ocean vent fields has yet to be determined. This study therefore aims to investigate the connectivity of three populations of 'scaly-foot gastropod' between two vent fields on the Central Indian Ridge (CIR) and the first sampled vent field on the Southwest Indian Ridge (SWIR).

MATERIALS AND METHODS

Study Materials

Specimens of the 'scaly-foot gastropod' were collected from the Longqi hydrothermal vent field (Tao *et al*., 2014), Southwest Indian Ridge (37°47.03'S 49°38.97'E, 'Tiamat Chimney'), depth 2785 m, during the RRS *James Cook* cruise JC67 in November 2011 using the suction sampler of the ROV *Kiel 6000* (Copley *et al.*, 2012). Thirty-five specimens (sample code JC67-F-070/X) were fixed and stored in 99% ethanol for genetic investigations in the present study.

Genetics

Partial sequences of the mitochondrial cytochrome *c* oxidase subunit I (COI) gene were used for the population genetic analyses in the present study. Sequences of the 'scaly-foot gastropod' from the Longqi hydrothermal vent field, SWIR (Tao *et al*., 2014) were newly sequenced, while sequences from the Kairei and Solitaire fields, CIR were obtained from the DNA Databank of Japan (DDBJ) under the accession numbers of AB540629 to AB540646, AB543244 to AB543246, AB634505 to AB634513, and AB691090 to AB691129. The total COI dataset comprised individual sequences of 35 specimens from the Longqi Field, SWIR, 35 specimens from the Kairei Field and 23 specimens from Solitaire Field, CIR (Table 1). The CIR data were also used in two previous studies (Nakamura *et al*., 2012; Beedessee *et al*., 2013). The newly obtained SWIR data are deposited in GenBank under accession numbers XX000000 to XX000000.

Genomic DNA was extracted using QIAGEN DNeasy Blood and Tissue Kit following the manufacturer's instructions (QIAGEN, Crawley, West Sussex, United Kingdom), and

196 extractions were stored in -20^{o}C freezers. Quality checking of extractions was carried out
197 with a Nanodrop 2000 spectrophotometer. Initially the COI region of the 'scaly-foot
198 gastropod' was amplified with the primer pair LOC1490 and HCO2198 (Folmer *et al*.,
199 1994) but several specimens required a species-specific primer pair for successful
200 amplification designed using Primer3 (Rozen & Skaletsky, 2000) from sequences
201 successfully obtained using the Folmer *et al.* (1994) pair: *SF1F* (5'-
202 GATCTGGTCTTTTAGGAACAGGATTCA-3') and *SF1R* (5'-
203 TGTGAGATACCATTCCAAATCCAGG-3'). This latter set of primers amplified an
204 approximately 500-bp fragment of COI.
205
206 Polymerase chain reaction was carried out in 12 µl reactions, including 2 µl DNA
207 template (100-200 ng µl^{-1}), 8 µl QIAGEN Master Mix, 0.4 µl double-distilled water, 1.6
208 µl primer mix containing 0.8 µl each of forward and reverse primers at concentration of
209 4 pmol µl^{-1}. Thermo cycling was performed using a Bio-Rad C1000 Thermal Cycler, with
210 the following protocol: initial denaturation at 95^{o}C for 15 minutes followed by 40 cycles
211 of 94^{o}C for 45 seconds, 45^{o}C for 60 seconds, 72^{o}C for 60 seconds, ending with final
212 extension at 72^{o}C for 5 minutes. Amplification of desired region was confirmed using 1%
213 agarose gel electrophoresis stained with ethidium bromide (3 µl of 10 mg mL^{-1}). PCR
214 products were purified using QIAGEN QIAquick PCR purification kit (QIAGEN,
215 Crawley, UK) using the manufacturer's protocol. Cycle sequencing reactions were
216 carried out in 10µl volume, containing 0.5 µl BigDye Terminator v3.1 (Applied
217 Biosystems, Paisley, UK), 2.5 µl 5x buffer, 2.5 µl PCR product, 2.5 µl primer (0.8 pmol
218 µl^{-1}), 2 µl double-distilled water. The following protocol was used: initial denaturation at
219 96 ^{o}C for 1 minute followed by 25 cycles of 96 ^{o}C for 10 seconds, 50 ^{o}C for 5 seconds, 60
220 ^{o}C for 4 minutes, ending with final extension at 60 ^{o}C for 4 minutes. Products were
221 precipitated using the EDTA/ethanol method. Sequences were resolved from precipitated

products using Applied Biosystems 3100 DNA sequencer (Paisley, UK) in the Department of Zoology, University of Oxford, UK.

Forward and reverse readings were assembled into contigs in the software package Geneious 5.6 (Drummond *et al*., 2011), and reads were manually quality-checked and corrected by eye. Only sequences with both good quality matching forward and reverse readings were used in downstream analyses. Population genetic inferences were made from the sequences using the software Arlequin v3.5.1.3 (Excofficer & Lischer, 2010). Mismatch distribution analyses and departures from equilibrium as expected for neutral markers were tested statistically using Tajima's *D* test (Tajima, 1989) and Fu's F_S test (Fu, 1997) in the same program, using 10,000 permutations. The statistical parsimony network was constructed using the software TCS v1.21 with the connection probability set to 95% (Clement, Posada & Crandall, 2000). The program Migrate-n v3.6.6 (Beerli, 2009) was used to estimate relative migrants per generation with Bayesian inference. Length of COI fragments used for final population genetic inferences was 489-bp.

RESULTS & DISCUSSION

Significant genetic differentiation was confirmed across the populations of the 'scaly-foot gastropod'. In particular, pairwise F_{ST}s revealed significant genetic divergence between the Longqi, SWIR field and the two CIR fields (Table 2). Both Longqi-Kairei pair (F_{ST} = 0.292, $P < 0.001$) and Longqi-Solitaire pair ($F_{ST} = 0.280$, $P < 0.001$) displayed significant genetic differentiation. The Kairei-Solitaire CIR pair ($F_{ST} = 0.000$, $P = 0.576$), in contrast, showed very little genetic divergence and appear to be well-mixed. This agrees well with results reported previously by Nakamura *et al.* (2012) and Beedessee *et al*. (2013).

A haplotype network (Fig. 2a) was reconstructed from the partial 489 bp COI sequences. Haplotypes from Longqi, SWIR formed a discrete cluster from the CIR haplotypes, with one single shared haplotype between two individuals from Longqi and one individual from Solitaire. This haplotype appears to link the two ridge systems in the network, although this may be a result of homoplasy. There are two other haplotypes from SWIR nested within CIR that suggest further shared haplotypes are likely to exist but were not sampled. The dominant haplotype in the two CIR fields was the same, but distinct from the SWIR population haplotypes. The results clearly show that the population of the 'scaly-foot gastropod' from SWIR is genetically distinct from the population from CIR, and we infer a lack of dispersal and connectivity across the vents on the two ridges. The two CIR populations share many haplotypes, as has already been previously reported (Beedessee *et al*., 2013). Furthermore, results of Migrate-n analyses (Fig. 2b) estimated number of relative migrants per generation to be much lower between SWIR and CIR populations (112-221) than between the two CIR sites (520-582). The predominant direction of dispersal in CIR is inferred to be from the southern Kairei to the northern Solitaire (582), which agrees with previous study (Beedessee *et al*., 2013). Deep-ocean currents have strong influence on the predominant direction of dispersal in vent organisms as the larvae of many species are transported in them (Vrijenhoek, 2010). A net northward flow in the deep currents of the area resulting from circumpolar deep water entering northwards into the Indian Ocean (Talley *et al*., 2011) may explain the trend of dispersal seen on the CIR. This is supported by data from investigating the hydrothermal plume spread over Kairei which showed a north to northwest direction (Noguchi *et al*., 2015). The gene flow direction between SWIR and CIR is inferred to be predominantly from SWIR to CIR (221 vs 115 from CIR to SWIR). The prevailingly eastward Antarctic Circumpolar Current, Aghulas Current retroflection, and South Indian Current over SWIR (Talley *et al*., 2011) are likely to be the driving forces of this trend.

The generally star-shaped haplotype network with many private haplotypes from both SWIR sites, and the negative Fu's F_S (significant for Longqi and Kairei; Fu, 1997) and Tajima's *D* (significant for Solitaire; Tajima, 1989) statistics of neutrality tests (Table 3) are suggestive of departure from mutation-drift equilibrium (Table 3). Both haplotype and nucleotide diversities were lower in the SWIR population compared to the CIR population (Table 1). The mismatch analyses for all three fields revealed distributions without multiple peaks (Fig. 3) and did not differ from model predicted frequency significantly (sums of squared deviation (SSD) and raggedness index, Table 3). These results are consistent with a recent demographic expansion after a bottleneck, or a selective sweep. Such signatures seem to be the norm in the case of vent organisms. Previously reported results for the vent crab *Austinograea rodriguezensis* and shrimp *Rimicaris kairei* of CIR also indicated similar demographic history (Beedessee *et al*., 2013), and similar results have been reported by hydrothermal vent endemic animals of other oceans such as *Rimicaris exoculata* Williams & Rona, 1986 of Mid-Atlantic Ridge (Teixeira *et al*., 2011) and *Ifremeria nautilei* Bouchet & Warén, 1991 from the Manus Basin (Thaler *et al*., 2011). This reflects perhaps the demographic instability of vent metapopulations surviving across ephemeral patches (Vrijenhoek, 2010).

Vent organisms have a great diversity of dispersal strategies (Vrijenhoek, 2010) and may produce planktotrophic larvae that can rise up in the water column and feed to extend pre-settlement lifespan (e.g., *Bathymodiolus* mussels, *Rimicaris* shrimps) or lecithotrophic larvae which generally rely on yolk for nutrition (e.g., vesicomyid clams, neomphaline gastropods and vetigastropods, *Riftia* giant tube worms). Furthermore, some species brood their larvae (e.g., provannid gastropod *Ifremeria nautilei* Bouchet & Warén, 1991, amphipod *Ventiella sulfuris* Barnard & Ingram, 1990). In general, species with planktotrophic larvae have been shown to disperse further distances and maintain higher connectivity over long distances. *Rimicaris exoculata* populations have been shown to be

303 well connected over a ~7,000 km stretch of the MAR (Teixeira *et al*., 2012) and a similar
304 case has been reported in the *Bathymodiolus septemdierum* complex where the
305 populations are well connected across southwest Pacific to the CIR (Kyuno *et al*., 2009).
306 In contrast, populations of *Riftia pachyptila* Jones, 1980 with lecithotrophic larvae show
307 genetic differentiation over the EPR which increased with geographical distance
308 (Coykendall *et al*., 2011) and significant genetic differentiation was also shown for the
309 EPR vent limpet *Lepetodrilus elevatus* McLean, 1988, also with lecithotrophic
310 development (Plouviez *et al*., 2009). A number of potential dispersal barriers, such as
311 transform faults, topographic depressions, fracture zones, and current regimes have been
312 proposed (Vrijenhoek, 2010); although the extent to which these restrict gene flow
313 depends on a species' dispersal strategy.
314
315 The development of the 'scaly-foot gastropod' is assumed to be lecithotrophic with a
316 planktonic dispersal stage, which is the norm in Peltospiridae (Warén *et al.*, 2006);
317 although neither larvae nor intact protoconchs are yet known. Though lecithotrophic
318 larvae do not preclude the possibility of long-distance dispersal (Marsh *et al*., 2001;
319 Pradillon *et al*., 2001), the eggs of the 'scaly-foot gastropod' are known to have a negative
320 buoyancy under atmospheric pressure (Beedessee *et al*., 2013), suggesting a possible low
321 dispersal ability compared with other species. Features such as fracture zones or
322 depressions are likely to act as barriers of dispersal for this species (Creasey & Rogers,
323 1999; Vrijenhoek, 2010).
324
325 With only one site sampled it is not currently possible to explore the scaly-foot
326 gastropod's dispersal and connectivity among other vent fields on the SWIR, but other
327 active vent fields on the SWIR have been detected (e.g. 63.9°E, Tao *et al.*, 2009; 58.9°E,
328 German *et al.*, 1998; 53.25°E and 51.01°E; Tao et al., 2014). It may be the case, however,
329 that not all vent fields are suitable for scaly-foot gastropods, if their dependence on a

nearly clonal gammaproteobacterial endosymbiont (Goffredi *et al.,* 2004; Nakagawa *et al.,* 2014) restricts them to vent fields in particular geological settings (Nakamura & Takai, 2014). Future explorations of other SWIR vent fields will lead to discovery of how this gastropod is distributed, and provide further insights into its population connectivity and phylogeography on the SWIR.

The presented results strongly indicates that the 'scaly-foot gastropod' population at Longqi, SWIR, may represent a genetically unique population among currently known Indian Ocean vent fields. In addition to taxa shared with CIR vents such as the 'scaly-foot gastropod' and *Rimicaris kairei*, a number of taxa new to science were discovered at the Longqi field, for examples an undescribed species of *Kiwa* yeti crab (Roterman *et al*., 2013) and an undescribed large-sized peltospirid gastropod (Chen *et al.*, submitted) with affinities to vent communities at the East Scotia Ridge in Antarctica (Rogers *et al.*, 2012). With the potential for COMRA's exploitation of SMS in the SWIR vents planned for the very near future (Tao *et al*., 2014), these population genetic results may have implications for management of the Longqi site and possibly other sites on the SWIR (Van Dover *et al.,* 2013). What is clear is that SWIR vent communities are different to the CIR and the exact consequences of mineral extraction will remain unclear until further observations and sampling are undertaken for other vent sites between 46°E and 53°E. Such exploration is a prerequisite to the design of appropriate long-term environmental monitoring and management measures for deep-sea mining in this region.

ACKNOWLEDGEMENTS

The authors are greatly indebted to Dr Hiromi Watanabe and Dr Ken Takai (JAMSTEC) for their kind help with the data for 'scaly-foot gastropod' from the CIR vents, and for useful discussion. The authors would like to express their gratitude to the Master and crew of the RRS *James Cook* as well as pilots and technical teams of ROV *Kiel 6000* for their immense support of scientific activity during the cruise JC66/67 funded by NERC Small Research Grant NE/H012087/1 to J.T.C. and NERC Research Grant NE/F005504/1 to A.D.R. Staffs of the UK National Marine Facilities at the National Oceanography Centre are thanked for their logistics and shipboard support.

REFERENCES

Bach, W., Banerjee, N.R., Dick, H.J.B. & Baker, E.T. (2002) Discovery of ancient and active hydrothermal systems along the ultra-slow spreading Southwest Indian Ridge 10°–16°E. *Geochemistry, Geophysics, Geosystems*, **3**, 1-14.

Bachraty, C., Legendre, P. & Desbruyères, D. (2009) Biogeographic relationships among deep-sea hydrothermal vent faunas at global scale. *Deep Sea Research Part I: Oceanographic Research Papers*, **56**, 1371-1378.

Beedessee, G., Watanabe, H., Ogura, T., Nemoto, S., Yahagi, T., Nakagawa, S., Nakamura, K., Takai, K., Koonjul, M. & Marie, D.E.P. (2013) High connectivity of animal populations in deep-sea hydrothermal vent fields in the Central Indian Ridge relevant to its geological setting. *PLoS ONE*, **8**, e81570.

Beerli, P. (2009) How to use migrate or why are markov chain monte carlo programs difficult to use? *Population Genetics for Animal Conservation* (ed. by G. Bertorelle, M.W. Bruford, H.C. Haue, A. Rizzoli and C. Vernesi), pp. 42-79. Cambridge University Press, Cambridge, U.K.

BODC (British Oceanographic Data Centre) (2010) *GEBCO Grid Display*. British Oceanographic Data Centre (BODC). <*http://www.gebco.net/*>

Chen, C., Copley, J.T., Linse, K., Rogers, A.D. & Sigwart, J. (In press) How the mollusc got its scales: convergent evolution of the molluscan scleritome. *Biological Journal of the Linnean Society*,

Chen, C., Linse, K., Roterman, C.N., Copley, J.T., Rogers, A.D. (Submitted) A new genus of large hydrothermal vent-endemic gastropod (Neomphalina: Peltospiridae). *Zoological Journal of the Linnean Society*.

Clement, M., Posada, D. & Crandall, K. (2000) TCS: a computer program to estimate gene genealogies. *Molecular Ecology*, **9**, 1657-1660.

Copley, J.T. (2012) *RRS James Cook research cruise JC67 cruise report*. British Oceanographic Data Centre (BODC) <*http://www.bodc.ac.uk/data/information_and_inventories/cruise_inventory/report/10593/*>

Coykendall, D.K., Johnson, S., Karl, S., Lutz, R. & Vrijenhoek, R. (2011) Genetic diversity and demographic instability in Riftia pachyptila tubeworms from eastern Pacific hydrothermal vents. *BMC Evolutionary Biology*, **11**, 96.

Creasey, S. & Rogers, A. (1999) Population genetics of bathyal and abyssal organisms. *Advances in Marine Biology*, **35**, 1-151.

Douville, E., Charlou, J.L., Oelkers, E.H., Bienvenu, P., Colon, C.F.J., Donval, J.P., Fouquet, Y., Prieur, D. & Appriou, P. (2002) The rainbow vent fluids (36°14'N, MAR): the influence of

ultramafic rocks and phase separation on trace metal content in Mid-Atlantic Ridge hydrothermal fluids. *Chemical Geology*, **184**, 37-48.

Drummond, A.J., Ashton, B., Buxton, S., Cheung, M., Cooper, A., Duran, C., Field, M., Heled, J., Kearse, M., Markowitz, S., Moir, R., Stones-Havas, S., Sturrock, S., Thierer, T. & Wilson, A. (2011) Geneious v5.6. <*http://www.geneious.com*>,

Esri (2012) *ArcGIS Desktop: Release 10.1*. Environmental Systems Research Institute, Redlands, CA.

Excoffier, L. & Lischer, H.E.L. (2010) Arlequin suite ver 3.5: a new series of programs to perform population genetics analyses under Linux and Windows. *Molecular Ecology Resources*, **10**, 564-567.

Folmer, O., Black, M., Hoeh, W., Lutz, R. & Vrijenhoek, R. (1994) DNA primers for amplification of mitochondrial cytochrome c oxidase subunit I from diverse metazoan invertebrates. *Molecular Marine Biology and Biotechnology*, **3**, 294-9.

Fu, Y.X. (1997) Statistical tests of neutrality of mutations against population growth, hitchhiking and background selection. *Genetics*, **147**, 915-925.

Fujikura, K., Okutani, T. & Maruyama, T. (2012) *Deep-sea Life - Biological observations using reseearch submersibles*, 2nd edn. Tokai University Press, Tokyo, Japan.

German, C.R., Baker, E.T., Mevel, C., Tamaki, K. & the, F.S.T. (1998) Hydrothermal activity along the southwest Indian ridge. *Nature*, **395**, 490-493.

German, C.R., Bowen, A., Coleman, M.L., Honig, D.L., Huber, J.A., Jakuba, M.V., Kinsey, J.C., Kurz, M.D., Leroy, S., McDermott, J.M., de Lépinay, B.M., Nakamura, K., Seewald, J.S., Smith, J.L., Sylva, S.P., Van Dover, C.L., Whitcomb, L.L. & Yoerger, D.R. (2010) Diverse styles of submarine venting on the ultraslow spreading Mid-Cayman Rise. *Proceedings of the National Academy of Sciences*, **107**, 14020-14025.

Goffredi, S.K., Warén, A., Orphan, V.J., Van Dover, C.L. & Vrijenhoek, R.C. (2004) Novel forms of structural integration between microbes and a hydrothermal vent gastropod from the Indian Ocean. *Applied and Environmental Microbiology*, **70**, 3082-3090.

Hannington, M., Jamieson, J., Monecke, T., Petersen, S. & Beaulieu S. (2011) The abundance of seafloor massive sulphide deposits. *Geology* **39**, 1155-1158.

Hashimoto, J., Ohta, S., Gamo, T., Chiba, H., Yamaguchi, T., Tsuchida, S., Okudaira, T., Watabe, H., Yamanaka, T. & Kitazawa, M. (2001) First hydrothermal vent communities from the Indian Ocean discovered. *Zoological Science*, **18**, 717-721.

Kyuno, A., Shintaku, M., Fujita, Y., Matsumoto, H., Utsumi, M., Watanabe, H., Fujiwara, Y. & Miyazaki, J.-I. (2009) Dispersal and differentiation of deep-sea mussels of the genus *Bathymodiolus* (Mytilidae, Bathymodiolinae). *Journal of Marine Biology*, **2009**

433 Lonsdale, P. (1977) Structural geomorphology of a fast-spreading rise crest: The East Pacific Rise
434 near 3°25'S. *Marine Geophysical Research*, **3**, 251-293.
435 Marbler, H., Koschinsky, A., Pape, T., Seifert, R., Weber, S., Baker, E.T., de Carvalho, L.M. &
436 Schmidt, K. (2010) Geochemical and physical structure of the hydrothermal plume at the
437 ultramafic-hosted Logatchev hydrothermal field at 14°45'N on the Mid-Atlantic Ridge.
438 *Marine Geology*, **271**, 187-197.
439 Marsh, A.G., Mullineaux, L.S., Young, C.M. & Manahan, D.T. (2001) Larval dispersal potential of
440 the tubeworm *Riftia pachyptila* at deep-sea hydrothermal vents. *Nature*, **411**, 77-80.
441 Melchert, B., Devey, C.W., German, C.R., Lackschewitz, K.S., Seifert, R., Walter, M., Mertens, C.,
442 Yoerger, D.R., Baker, E.T., Paulick, H. & Nakamura, K. (2008) First evidence for high-
443 temperature off-axis venting of deep crustal/mantle heat: The Nibelungen hydrothermal
444 field, southern Mid-Atlantic Ridge. *Earth and Planetary Science Letters*, **275**, 61-69.
445 Nakagawa, S., Shimamura, S., Takaki, Y., Suzuki, Y., Murakami, S.-i., Watanabe, T., Fujiyoshi, S.,
446 Mino, S., Sawabe, T., Maeda, T., Makita, H., Nemoto, S., Nishimura, S.-I., Watanabe, H.,
447 Watsuji, T.-o. & Takai, K. (2014) Allying with armored snails: the complete genome of
448 gammaproteobacterial endosymbiont. *The ISME Journal*, **8**, 40-51.
449 Nakamura, K. & Takai, K. (2014) Theoretical constraints of physical and chemical properties of
450 hydrothermal fluids on variations in chemolithotrophic microbial communities in seafloor
451 hydrothermal systems. *Progress in Earth and Planetary Science*, **1**, 5.
452 Noguchi, T., Fukuba, T., Okamura, K., Ijiri, A., Yanagawa, K., Ishitani, Y., Fujii, T. & Sunamura,
453 M. (2015) Distribution and biogeochemical properties of hydrothermal plumes in the
454 Rodriguez Triple Junction. *Subseafloor Biosphere Linked to Hydrothermal Systems* (ed. by
455 J.-I. Ishibashi, K. Okino and M. Sunamura), pp. 195-204. Springer.
456 Perner, M., Hansen, M., Seifert, R., Strauss, H., Koschinsky, A. & Petersen, S. (2013) Linking
457 geology, fluid chemistry, and microbial activity of basalt- and ultramafic-hosted deep-sea
458 hydrothermal vent environments. *Geobiology*, **11**, 340-355.
459 Petersen, S., Kuhn, K., Kuhn, T., Augustin, N., Hékinian, R., Franz, L. & Borowski, C. (2009) The
460 geological setting of the ultramafic-hosted Logatchev hydrothermal field (14°45'N, Mid-
461 Atlantic Ridge) and its influence on massive sulfide formation. *Lithos*, **112**, 40-56.
462 Plouviez, S., Shank, T.M., Faure, B., Daguin-Thiebaut, C., Viard, F., Lallier, F.H. & Jollivet, D.
463 (2009) Comparative phylogeography among hydrothermal vent species along the East
464 Pacific Rise reveals vicariant processes and population expansion in the South. *Molecular*
465 *Ecology*, **18**, 3903-3917.
466 Pradillon, F., Shillito, B., Young, C.M. & Gaill, F. (2001) Deep-sea ecology: Developmental arrest
467 in vent worm embryos. *Nature*, **413**, 698-699.

Ramirez-Llodra, E., Shank, T.M. & German, C.R. (2007) Biodiversity and biogeography of hydrothermal vent species: thirty years of discovery and investigations. *Oceanography*, **20**, 30-41.

Rogers, A.D., Tyler, P.A., Connelly, D.P., Copley, J.T., James, R., Larter, R.D., Linse, K., Mills, R.A., Garabato, A.N., Pancost, R.D., Pearce, D.A., Polunin, N.V.C., German, C.R., Shank, T., Boersch-Supan, P.H., Alker, B.J., Aquilina, A., Bennett, S.A., Clarke, A., Dinley, R.J.J., Graham, A.G.C., Green, D.R.H., Hawkes, J.A., Hepburn, L., Hilario, A., Huvenne, V.A.I., Marsh, L., Ramirez-Llodra, E., Reid, W.D.K., Roterman, C.N., Sweeting, C.J., Thatje, S. & Zwirglmaier, K. (2012) The discovery of new deep-sea hydrothermal vent communities in the Southern Ocean and implications for biogeography. *PLoS Biology*, **10**, e1001234.

Roterman, C.N., Copley, J.T., Linse, K.T., Tyler, P.A. & Rogers, A.D. (2013) The biogeography of the yeti crabs (Kiwaidae) with notes on the phylogeny of the Chirostyloidea (Decapoda: Anomura). *Proceedings of the Royal Society of London B: Biological Sciences*, **280**: 20130718.

Sauter, D. & Cannat, M. (2013) The ultraslow spreading Southwest Indian Ridge. *Diversity Of Hydrothermal Systems On Slow Spreading Ocean Ridges* (ed. by P.A. Rona, C.W. Devey, J. Dyment and B.J. Murton), pp. 153-173. American Geophysical Union.

Tajima, F. (1989) Statistical method for testing the neutral mutation hypothesis by DNA polymorphism. *Genetics*, **123**, 585-595.

Tao, C., Li, H., Jin, X., Zhou, J., Wu, T., He, Y., Deng, X., Gu, C., Zhang, G. & Liu, W. (2014) Seafloor hydrothermal activity and polymetallic sulfide exploration on the southwest Indian ridge. *Chinese Science Bulletin*, 1-11.

Tao, C., Lin, J., Guo, S., Chen, Y.J., Wu, G., Han, X., German, C.R., Yoerger, D.R., Zhou, N., Li, H., Su, X., Zhu, J., DY115-19, a.t. & Parties, D.-S. (2012) First active hydrothermal vents on an ultraslow-spreading center: Southwest Indian Ridge. *Geology*, **40**, 47-50.

Tao, C., Wu, G., Ni, J., Zhao, H., Su, X., Zhou, N., Li, J., Chen, Y.J., Cui, R., Deng, X., Egorov, I., Dobretsova, I.G., Sun, G., Qiu, Z., Deng, X., Zhou, J., Gu, C., Li, J., Yang, J., Zhang, K., Wu, X., Chen, Z., Lei, J., Huang, W., Zhou, P., Ding, T., Jin, W., Li, H. & Lin, J. (2009) New hydrothermal fields found along the SWIR during the Legs 5-7 of the Chinese DY115-20 Expedition (Abstract #OS21A-1150). In: *American Geophysical Union, Fall Meeting 2009*. American Geophysical Union, San Francisco, California, USA.

Teixeira, S., Serrão, E.A. & Arnaud-Haond, S. (2012) Panmixia in a fragmented and unstable environment: the hydrothermal shrimp *Rimicaris exoculata* Disperses Extensively along the Mid-Atlantic Ridge. *PLoS ONE*, **7**, e38521.

Teixeira, S., Cambon−Bonavita, M.A., Serrão, E.A., Desbruyéres, D. & Arnaud−Haond, S. (2011) Recent population expansion and connectivity in the hydrothermal shrimp *Rimicaris exoculata* along the Mid−Atlantic Ridge. *Journal of Biogeography*, **38**, 564-574.

Thaler, A., Zelnio, K., Saleu, W., Schultz, T., Carlsson, J., Cunningham, C., Vrijenhoek, R. & Van Dover, C. (2011) The spatial scale of genetic subdivision in populations of *Ifremeria nautilei*, a hydrothermal-vent gastropod from the southwest Pacific. *BMC Evolutionary Biology*, **11**, 372.

Van Dover, C.L. (1990) Biogeography of hydrothermal vent communities along seafloor spreading centers. *Trends in Ecology & Evolution*, **5**, 242-246.

Van Dover, C.L. (2011a) Tighten regulations on deep-sea mining. *Nature*, **470**, 31-33.

Van Dover, C.L. (2011b) Mining seafloor massive sulphides and biodiversity: what is at risk? *ICES Journal of Marine Science: Journal du Conseil*, **68**, 341-348.

Van Dover, C.L. (2014) Impacts of anthropogenic disturbances at deep-sea hydrothermal vent ecosystems: A review. *Marine Environmental Research*, **102**, 59-72.

Van Dover, C.L., Aronson, J., Pendleton, L., Smith, S., Arnaud-Haond, S., Moreno-Mateos, D., Barbier, E., Billett, D., Bowers, K., Danovaro, R., Edwards, A., Kellert, S., Morato, T., Pollard, E., Rogers, A. & Warner, R. (2014) Ecological restoration in the deep sea: Desiderata. *Marine Policy*, **44**, 98-106.

Van Dover, C.L., Humphris, S.E., Fornari, D., Cavanaugh, C.M., Collier, R., Goffredi, S.K., Hashimoto, J., Lilley, M.D., Reysenbach, A.L., Shank, T.M., Von Damm, K.L., Banta, A., Gallant, R.M., Götz , D., Green, D., Hall, J., Harmer, T.L., Hurtado, L.A., Johnson, P., McKiness, Z.P., Meredith, C., Olson, E., Pan, I.L., Turnipseed, M., Won, Y., Young, C.R. & Vrijenhoek, R.C. (2001) Biogeography and ecological setting of Indian Ocean hydrothermal vents. *Science*, **294**, 818-823.

Vrijenhoek, R.C. (2010) Genetic diversity and connectivity of deep-sea hydrothermal vent metapopulations. *Molecular Ecology*, **19**, 4391-4411.

Warén, A., Bouchet, P. & Cosel, R.V. (2006) Mollusca, Gastropoda (Handbook of deep-sea hydrothermal vent fauna). *Denisia*, **18**, 82-137.

Warén, A., Bengtson, S., Goffredi, S.K. & Van Dover, C.L. (2003) A hot-vent gastropod with iron sulfide dermal sclerites. *Science*, **302**, 1007.

Watanabe, H. & Beedessee, G. (2015) Vent fauna on the Central Indian Ridge. *Subseafloor Biosphere Linked to Hydrothermal Systems* (ed. by J.-I. Ishibashi, K. Okino and M. Sunamura), pp. 205-212. Springer.

TABLES

Table 1 Statistical summary of the 'scaly-foot gastropod' COI gene data for the three localities; h = haplotype diversity, π = nucleotide diversity. Abbreviations: SWIR = Southwest Indian Ridge, CIR = Central Indian Ridge.

Population	*n*	Haplotypes	Polymorphic Loci	*h* ± SD	*π* ± SD
Longqi, SWIR	35	12	12	0.6689 ± 0.0877	0.0031 ± 0.0021
Kairei, CIR	35	18	18	0.8941 ± 0.0438	0.0058 ± 0.0035
Solitaire, CIR	23	12	22	0.8972 ± 0.0404	0.0064 ± 0.0038

545 **Table 2** Results of genetic structure analyses showing the fixation index (F_{ST}) with
546 significance levels indicated: * $P < .05$; ** $P < .01$; *** $P < .001$. Abbreviations: SWIR
547 = Southwest Indian Ridge, CIR = Central Indian Ridge.
548

Population	Longqi, SWIR	Kairei, CIR	Solitaire, CIR
		Pairwise FST	
Longqi, SWIR	0.00000	-	-
Kairei, CIR	0.29180 ***	0.00000	-
Solitaire, CIR	0.28010 ***	0.00000	0.00000

549
550
551

552 **Table 3** Neutrality test statistics (Fu's *Fs* and Tajima's *D*) and mismatch distribution
553 (SSD and raggedness index), with significance levels indicated: * $P < .05$; ** $P < .01$;
554 *** $P < .001$. Abbreviations: SWIR = Southwest Indian Ridge, CIR = Central Indian
555 Ridge, SSD = sum of squared deviations.
556

Population	Tajima's *D*	Fu's *FS*	SSD	Raggedness
Longqi, SWIR	-1.4909	-6.5709 ***	0.0110	0.0494
Kairei, CIR	-1.1854	-10.5875 ***	0.0012	0.0153
Solitaire, CIR	-1.6579 *	-3.0427	0.0131	0.0515

557
558

559 **FIGURES**

560

561 **Figure 1** (a) Map of western Indian Ocean vent fields with 'scaly-foot gastropod' records
562 (Mollweide projection), created using ArcMap 10.1 (Esri, 2012) with bathymetry data
563 from GEBCO (BODC, 2010); Abbreviations: SWIR = South West Indian Ridge, CIR =
564 Central Indian Ridge, SEIR = South East Indian Ridge. (b) Morphotypes of adult 'scaly-
565 foot gastropod' specimens from Longqi (top), Kairei (middle), and Solitaire (bottom).

566

567 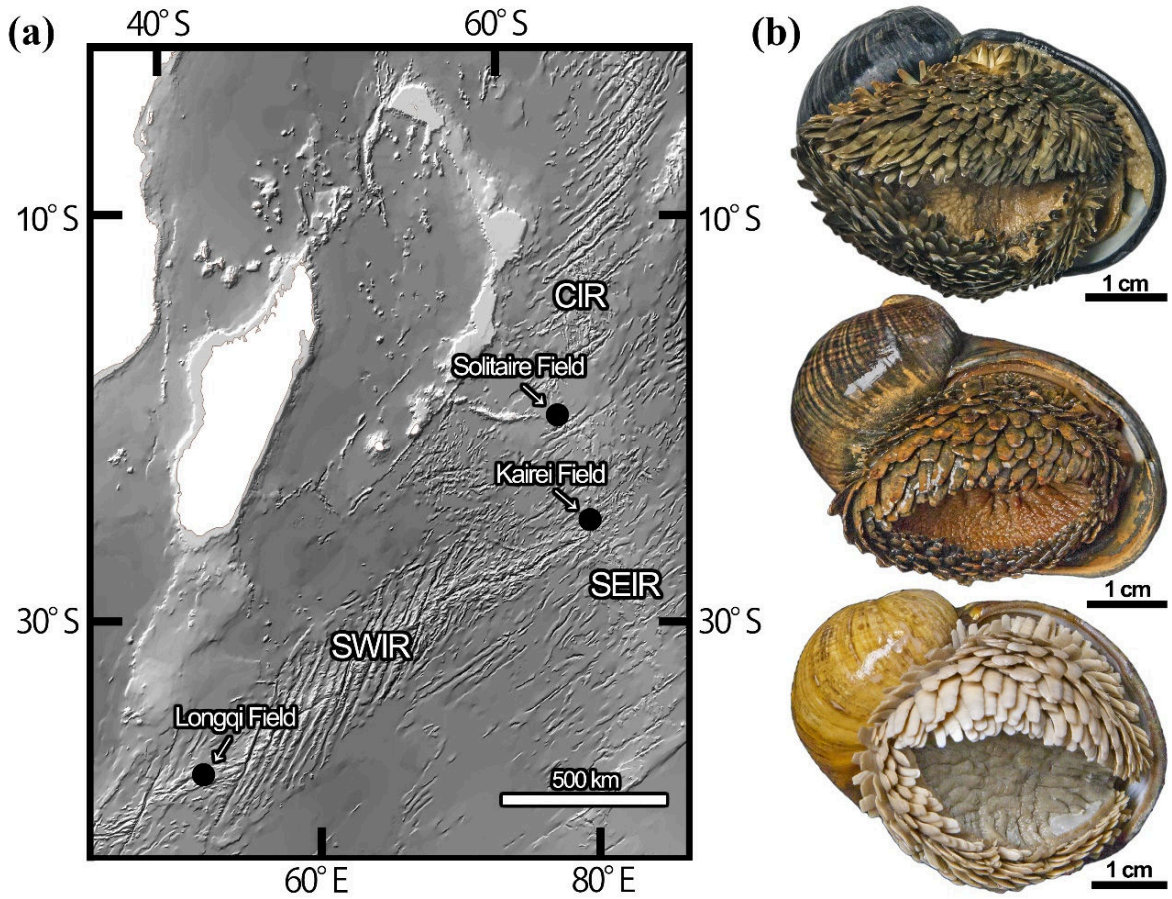

568

569

570 **Figure 2** (a) Parsimony haplotype network of the 'scaly-foot gastropod' based on 489bp
571 of the COI gene, colours of circles indicate locality: white = Longqi, black = Kairei, grey
572 = Solitaire, numbers indicate sampled frequency from each site; and (b) Results of
573 Migrate-n analyses showing relative migrants per generation shown in a schematic
574 drawing. Abbreviations: SWIR = Southwest Indian Ridge, CIR = Central Indian Ridge.

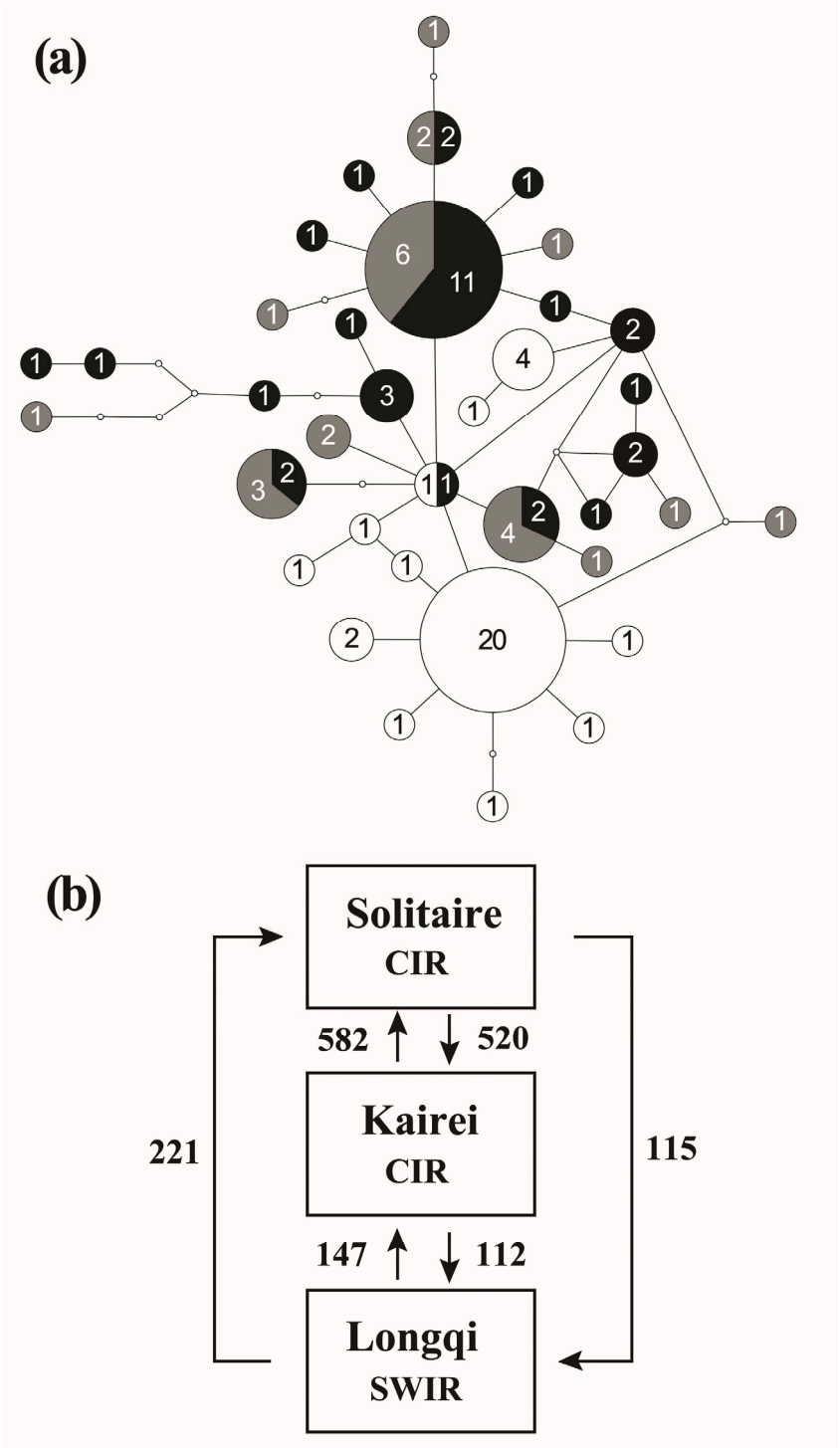

575

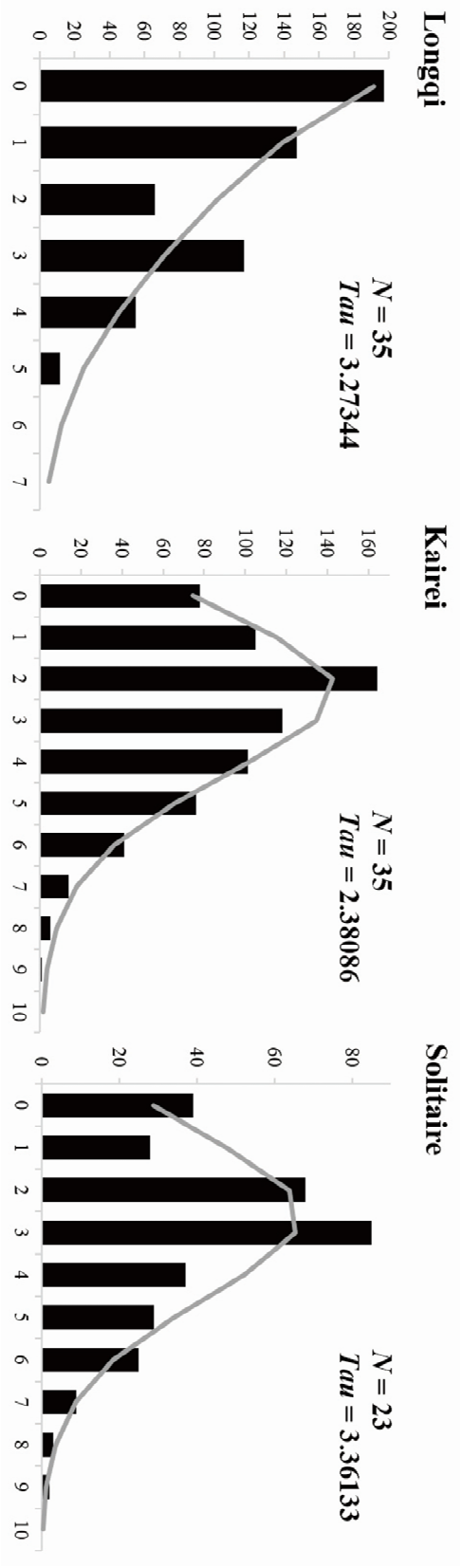

Figure 3 Mismatch distribution of the 'scaly-foot gastropod' in the three localities with grey line showing model distribution; x-axis = pairwise difference and y-axis = frequency.

581 **BIOSKETCH**

582

583 **Chong Chen** is a deep-sea biologist with a special interest in the molluscs of
584 chemosynthetic ecosystems. His current researches focus on the systematics, evolution,
585 and ecology of gastropods. He is based at the Alex Rogers Lab at the Department of
586 Zoology, University of Oxford and this study is part of his DPhil thesis.

587

588 Author contributions: C.C., J.T.C., and A.D.R. conceived the ideas; J.T.C. and A.D.R.
589 provided funding for the project; C.C., J.T.C., and A.D.R. collected the samples; C.C.
590 collected and analysed data and wrote the paper; A.D.R., J.T.C., K.L. supervised the
591 project; All authors discussed the results and implications of the study and edited the
592 manuscript for improvement.

593

594

Chapter 4

The heart of a dragon: 3D anatomical reconstruction of the 'scaly-foot gastropod' (Mollusca: Gastropoda: Neomphalina) reveals its extraordinary circulatory system

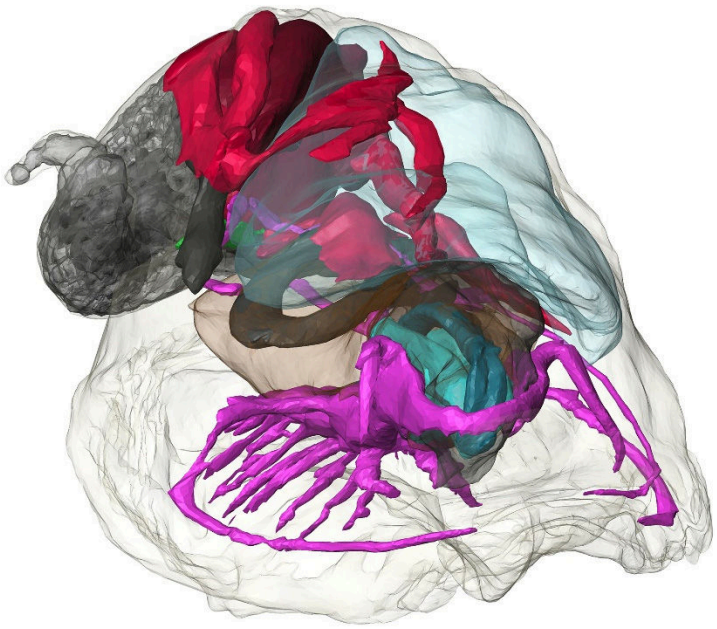

(*Frontiers in Zoology*, Submitted)

CHAPTER INTRODUCTION

Much investigation has gone into the biology of the 'scaly-foot gastropod' *Chrysomallon squamiferum* due to its biological uniqueness among gastropods in having dermal sclerites, but a general understanding of its internal anatomy is still overdue. Much of the knowledge about its anatomy comes from the supplementary materials of Warén *et al*. (2003), which provides the essential facts but is lacking in detail. Follow-up studies concentrated on the enlarged esophageal gland (the peculiarity of which was noted also by Warén *et al*., 2003) and revealed it to contain endosymbiont bacteria (Goffredi *et al*., 2004; Nakagawa *et al*., 2014); but not detailing other aspects of the anatomy such as circulatory system, nervous system, and reproductive system.

This chapter aims to fill this gap in knowledge of the anatomy of *Chrysomallon squamiferum*. Also, vent organisms often have many intriguing adaptations to survive and prosper in the extreme environment like the trochosome of siboglinid tubeworms (Cavanaugh *et al.,* 1981) or 'farming' epibiotic bacteria in the case of galatheid squat lobster *Shinkaia crosnieri* Baba & Williams, 1998 (Watsuji *et al*., 2014), and in-depth anatomical investigation may reveal previously overlooked anatomical adaptations in the 'scaly-foot gastropod' in addition to the esophageal gland.

For these purposes a complete 3D tomographic model reconstructed for three major systems of *Chrysomallon squamiferum*, including the digestive system, nervous system, and circulatory system. Due to size constraints on the specimens that can be used in the methods used (Ruthensteiner, 2000), a juvenile specimen was selected for the

reconstruction. This was aided by traditional dissection of adult specimens to form a comprehensive characterisation of the anatomy of *C. squamiferum* to cover a wide range of the post-settlement ontogeny.

The detailed histological methods used in this chapter are largely based on Ruthensteiner (2008) but with some modifications, the detailed protocol is attached as a supplement. The 3D tomographic model is also supplemented as a data disc appended to the printed thesis.

STATEMENT OF AUTHOR CONTRIBUTIONS

This chapter comprises a manuscript written and formatted for *Frontiers in Zoology*. It has been submitted as a Research Article (February 2015; Manuscript ID FINZ-S-15-00018) and is currently under review. The authors (in this order) are Chong Chen (corresponding author), Jonathan T. Copley, Katrin Linse, Alex D. Rogers, and Julia D. Sigwart; the detailed author contributions are as follows.

The original idea for the project was conceived between CC and JDS. Methodology and project plan were developed by JDS. JTC and ADR provided funding for both sample collection on-board *RRS* James Cook research cruises JC66/67. On-board the cruises CC, JTC, and ADR participated in sample collection and tissue fixation of the specimens used in this study. JS provided equipment, lab space, and reagents for the study. CC and JDS were responsible for all laboratory work, data collection, and data analyses including the construction of the 3D model. CC wrote the original manuscript draft. All authors discussed the results and implications of the study in detail and edited the manuscript for improvement. JS, ADR, JTC, and KL supervised the work of CC during the length of this study.

The heart of a dragon: 3D anatomical reconstruction of the 'scaly-foot gastropod' (Mollusca: Gastropoda: Neomphalina) reveals its extraordinary circulatory system

Chong Chen[1*], Jonathan T. Copley[2], Katrin Linse[3], Alex D. Rogers[1], and Julia D. Sigwart[4]

[1]Department of Zoology, University of Oxford, the Tinbergen Building, South Parks Road, Oxford, OX1 3PS, UK

[2]Ocean and Earth Science, University of Southampton, European Way, Southampton SO14 3ZH, UK

[3]British Antarctic Survey, High Cross, Cambridge CB3 0ET, UK

[4]Queen's University Belfast, Marine Laboratory, Portaferry BT22 1PF, Co. Down, Northern Ireland

* Corresponding author

Email addresses:

CC: chong.chen@zoo.ox.ac.uk

JTC: jtc@soton.ac.uk

KL: kl@bas.ac.uk

ADR: alex.rogers@zoo.ox.ac.uk

JDS: j.sigwart@qub.ac.uk

Abstract

Introduction

The 'scaly-foot gastropod' from deep-sea hydrothermal vent ecosystems of the Indian Ocean is an active mobile gastropod occurring in locally high densities, and it is distinctive for the dermal scales covering the exterior surface of its foot. These iron-sulphide coated sclerites, and its nutritional dependence on endosymbiotic bacteria, are both noted as specialist adaptations to the extreme environment in the flow of hydrogen sulfide. We present evidence for further adaptations of the 'scaly-foot gastropod' to life in an extreme environment, investigated through dissection and 3D tomographic reconstruction of the internal anatomy.

Results

Our anatomical investigations of juvenile and adult specimens reveal a large unganglionated nervous system, a simple and reduced digestive system, and that the animal is a simultaneous hermaphrodite. We show that 'scaly-foot gastropod' relies on endosymbiotic bacteria throughout post-larval life. Of particular interest is the circulatory system: the 'scaly-foot gastropod' has a very large ctenidium supported by extensive blood sinuses filled with haemocoel. The ctenidium provides oxygen for the host but the circulatory system is enlarged beyond the scope of other similar vent gastropods. At the posterior of the ctenidium is a remarkably large and well-developed heart. Based on the volume of the auricle and ventricle, the heart complex represents approximately 4% of the body volume. This proportinally giant heart primarily sucks blood through the ctenidium and supplies to the highly vascularised oesophageal gland. Thus we infer the

elaborate cardiovascular system most likely evolved to oxygenate the endosymbionts in an oxygen poor environment and/or to supply hydrogen sulfide to the endosymbionts.

Conclusions

This study exemplifies how understanding the autecology of an organism can be enhanced and even changed dramatically by detailed investigation of internal anatomy. This gastropod is a large and active species that is abundant in its hydrothermal vent ecosystem. Yet all of its remarkable specialist adaptations—protective dermal sclerites, circulatory system, high fecundity—can equally be viewed as beneficial to its endosymbiont microbes. As a result of specialisation to resolve energetic needs in an extreme chemosynthetic environment, this dramatic dragon-like species has become a carrying vessel for its bacteria.

Keywords

'scaly-foot gastropod', morphology, hydrothermal vents, anatomy, deep-sea, adaptation, Neomphalina

Introduction

Deep-sea hydrothermal vents represent a challenging environment where organisms face 'extreme' conditions such as hypoxia, very acidic water, and the presence of toxic materials such as hydrogen sulfide and heavy metals [1,2]. Despite this, hydrothermal vents host a high biomass, comparable to that of tropical coral reefs (Van Dover, 2000). Vent ecosystems are supported by chemosynthetic primary production carried out by bacteria that oxidise reduced compounds such as hydrogen sulfide and methane to produce energy for fixing carbon dioxide or other carbon compounds into organic matter [3].

Animals flourishing in vents often have specialised anatomical adaptations. Many species host epibiotic microbes that they feed on for nutrition, for instance the vent shrimp *Rimicaris exoculata* Williams & Rona, 1986 houses both sulfur-oxidizing and methanotrophic bacteria in the gill chamber [4] and the galatheid squat lobster *Shinkaia crosnieri* Baba & Williams, 1998 farms bacteria on dense setae on the ventral face of the carapace [5]. Some species further house chemosynthetic bacteria internally as endosymbionts. The giant tube worm *Riftia pachyptila* Jones, 1981 is known to host thioautotrophic (sulfur-oxidizing) endosymbionts in a specialised organ, the trophosome; and has a vestigial digestive system [6]. Similarly, vesicomyid clams house endosymbionts in the gill and also have a much reduced digestive tract [7]. Some species are able to combine multiple feeding strategies, for example *Bathymodiolus thermophilus* Kenk & Wilson, 1985 is capable of filter-feeding while also hosting endosymbionts in the gill [8]. Other anatomical adaptations to thrive in chemosynthetic environments are also

known. Many vent polychaetes have increased gill surface area to facilitate effective oxygen extraction, as well as high oxygen affinity haemoglobins and haemocyanins [9,10].

The 'scaly-foot gastropod' is distinctive among hydrothermal-vent molluscs for its numerous dermal sclerites, which are often mineralised with iron sulfide. This species inhabits the hydrothermal vent fields of the Indian Ocean, on the walls of black-smoker chimneys or directly on diffuse flow sites. First discovered in the Kairei hydrothermal vent field, Central Indian Ridge (CIR) [11], it has also been found in two more vent fields: Solitaire field, CIR (Nakamura *et al*., 2012) and Longqi field (also known as Dragon field, [12,13]), Southwest Indian Ridge (SWIR) [12,14,15]. Both morphological and genetic characters place the 'scaly-foot gastropod' in Peltospiridae, a family restricted to hydrothermal vent ecosystems in the clade Neomphalina [16]. The 'scaly-foot gastopod' reaches 45 mm in shell length, much larger than the other members of the family which are generally small (<15 mm in shell length).

The unusual external morphology of the 'scaly-foot' has been described by a number of studies [16-18] with the surface mineralogy investigated in detail [19,20], and a number of studies have concentrated on its unique way of housing endosymbionts in the oesophageal gland [21,22], instead of the gill, like other vent gastropods such as *Alviniconcha* spp. [23]. The internal anatomy of several peltospirid genera have been investigated previously (mainly *Rhynchopelta concentrica* McLean, 1989 but also *Peltospira, Nodopelta, Echinopelta* and *Hirtopelta* [24]; as well as *Pachydermia laevis* Warén & Bouchet, 1989 [25]), and the 'scaly-foot gastropod' is known to differ from

114 these, particularly in its acquisition of endosymbionts and gigantism [16,21]. The only
115 previous description of the internal anatomy of the 'scaly-foot gastropod' is a short
116 supplementary text [16]. The aim of the present study was to investigate this unusual
117 species to examine possible further anatomical adaptations to life in the vent environment.
118
119
120 **Results**
121
122 The overall anatomical plan of the 'scaly-foot gastropod' conforms to that of
123 Neomphalina (Figure 1, 2). This include non-papillate tentacles, single left bipectinate
124 ctenidium, single auricle, rhiphidoglossate radula with a single pair of radular cartilages,
125 a rectum that does not penetrate the heart but passes ventral to it, and statocyst with a
126 single statolith (Figure 3, 4; [26]). A number of histological characters can also be
127 compared to other members of Neomphalina (Figure 5). The basic organ anatomy in adult
128 specimens was previously described by Warén *et al.* [16] but our dissections expand
129 considerably on that report (Figure 6).
130
131 *External Morphology*
132
133 The 'scaly-foot gastropod' is a loosely coiled snail with the soft parts occupying
134 approximately two whorls (Figure 1, 3A). The snout is thick and taper distally to a blunt
135 end, the mouth is a circular ring of muscles when contracted and closed. Two smooth
136 cephalic tentacles are present, these are thick at base and gradually tapers to a fine point
137 at the distal tips (Figure 2). There are no eyes. Specialised copulatory appendages are

lacking in the anterior head-foot region. There is no pedal gland in the propodium. The epipodium does not carry any epipodial tentacles but is instead densely covered in hard sclerites, imbricating in a roof-tile manner. An operculum is present at the metapodium, exposed and well-sized in juveniles but the relative size decreases as individuals grow. In adults the operculum is elongate and clearly distinct but buried under layers of sclerites ([18]: fig. 2). The shell muscle is horse-shoe shaped and large, divided in two parts on the left and right, connected by a narrower attachment. The mantle edge is thick but simple without distinct features. The mantle cavity of the 'scaly-foot gastropod' is deep and reaches the posterior edge of the shell. The medial to left side of the cavity is dominated by a very large bipectinate ctenidium (Figure 1, 2, 3A). Ventral to the visceral mass the body cavity is occupied by a huge oesophageal gland extended to fill the ventral floor of the mantle cavity (Figure 3F).

Digestive and Excretory Systems

The mouth opening on the ventral side of the snout leads to a buccal cavity that contains a rhipidoglossate radula (Figure 4A). The epithelium of the inner lip is composed of a columnar epithelium with a thin cuticle (Figure 5A). There are no jaws. The radula ribbon is long, width to length ratio is approximately 1:10 in the serially sectioned specimen (Figure 3C, 4B; structural details shown by Warén *et al.* [16]: fig. S2A). A single pair of prominent radula cartilages support the anterior radula ribbon. The two cartilages are in contact at their anterior extent and become separate ventrally (Figure 4G). At the posterior end of the cartilage pair the radula ribbon folds under and emerges from the growing radular sac below the buccal mass. A part of the anterior oesophagus rapidly expands into

a huge hypertrophied blind-ended oesophageal gland (Figure 4A) which occupies much of the ventral face of the mantle cavity (estimated 9.3% body volume). The oesophageal gland has a uniform texture (Figure 5C) and is highly vascularised with fine blood vessels (Figure 6B).

The digestive system apart from the oesophageal gland is relatively small and forms a simple loop (Figure 4B). The midgut forms a clearly discernable stomach as a distinctly widened and enlarged region separating it from the foregut and hindgut (Figure 4B). The stomach has at least three ducts at its anterior right connecting to the digestive gland; the extensive and unconsolidated digestive gland extends to the posterior filling the shell apex (Figure 2D, 2F). The nephridium is central, tending to the right side of the body (Figure 1, 4B), as a thin dark layer of glandular tissue (Figure 6E). It is anterior and ventral of the digestive gland and in contact with the dorsal aspect of the foregut (Figure 4A).

The posterior aspect of the oesophagus passes directly above the oesophageal gland and ventral of the auricle to reach the ventral face of the visceral mass (Figure 4A). The digestive system runs directly from anterior to posterior in contact with the dorsal aspect of the oesophageal gland, and the nephridium (immediately posterior to the oesophageal gland); it widens into a distinct stomach embedded within the digestive gland. The posterior intestine emerges from the left anterior side of the stomach, runs anteriorly and curving to the right into the oesophageal gland and the next turn of the digestive tract is completely embedded within the oesophageal gland. It then returns out of the oesophageal gland to the left, crossing dorsally over the oesophagus, runs posteriorly to contact the digestive gland dorsal of the stomach, and then turns anteriorly down the right mantle

wall to exit the mantle cavity on the right, as the rectum (Figure 3A, 6G). The anus opening is also located on right side of animal, close to the transverse mid-line of the gastropod, above the genital slit (Figure 1).

The hindgut was typically filled with consolidated pellets of chalky unidentified material, present in stomach and posterior to it (but not in the foregut), and seen in specimens of all sizes (Figure 6B). These are possibly sulphur granules produced by the endosymbiont and represent a way for detoxing hydrogen sulphide.

Circulatory System

The single large ctenidium (Figure 1, 4E); occupying 15.5% of the body volume in the serially sectioned specimen) reaches the posterior end of the mantle cavity and further curls to enter the visceral mass. It is densely packed with thin gill filaments on both sides (Figure 2, 5C). There are two prominent semi-enclosed blood sinuses under the gill (0.7% body volume), which fill the concavity formed by the ventral aspect of the gill filaments (Figure 4E, 5E, 6C). To the posterior right of the ctenidium lies a hypertrophied auricle (Figure 4C, 5F). A ventricle of even larger size lies directly ventral of the auricle (Figure 6A). A simple pericardium is present (not illustrated) and encloses the heart with tissue connected to the dorsal mantle. The ventricle has thick muscular walls with many crossing muscle bundles (Figure 6D). The auricle and ventricle together occupy 4% of the body volume (Figure 4D, 5F). Diagonally above the right half of the auricle is a prominent blood sinus directly connected to the auricle (0.8% body volume), it begins anteriorly before the anterior end of the auricle and extends posteriorly to reach posterior end of the

ventricle (Figure 4C). Thick blood vessels are clear above and below the ctenidium (Figure 4E). In adult specimens several blood sinuses are located in the posterior half of the mantle cavity but the location and extent differed between individuals. Some of these blood sinuses are connected to the mantle tissue but other large areas of haemocoel, jellylike and with a pale blue-grey colour in preserved specimens, are found covering the gonad and throughout the body (Figure 1). The oesophageal gland is highly vascularised with smaller blood sinuses and a dense network of fine blood vessels (Figure 6B).

Nervous System and Sensory Structures

The nervous system is voluminous (Figure 4F, 4H; occupying approximately 5.7% of body volume in the serially sectioned juvenile specimen, although proportionately much smaller in adults). The brain lacks structure and there are no eyes or other cephalic sensory structures. Typically for gastropods, the nervous system is composed of an anterior oesophageal nerve ring and two pairs of longitudinal nerve cords, with the ventral pair innervating the foot and the dorsal pair forming a twist via streptoneury. The oesophageal nerve ring and pedal nerves are thickened and medullary in nature (Figure 5B). There is no clear structural evidence from juvenile or adult specimen for the identification of specific ganglia (*sensu* Richter *et al.* [27], *i.e.* nerve tissue in discrete units separated by an area containing no cell bodies), although the anterior region of the nervous system shows some lobe-like intergressions of cell bodies into the central neuropil, the neural masses appear to be wholly fused and without ganglionic structure.

The anterior commissure, or frontal aspect of the oesophageal nerve ring, is large,

connecting two lateral swellings (Figure 4H). Laterally from each of these swellings is a large, prominent tentacular nerve projecting into the cephalic tentacles. There are no eyes and no evidence of even a remnant optic nerve emerging from the oesophageal nerve ring. At the posterior margin of the oesophageal nerve ring is a pair of prominent pleural swellings. From each pleural swelling a long nerve goes anteriorly along the margin of the mantle around the head.

Both the lateral (visceral) and pedal nerves, as well as a pair of mantle nerves, emerge from the posterior aspect of the oesophageal nerve ring more or less co-located in a large junction (Figure 4F, 5B). The pedal nerves are fused in a large body and extend into two thick medullary cords, separating posteriorly into two clear cords (Figure 5C) but joined at several points by bridging commissures. The pedal nerves are not embedded within the foot musculature but sit on the dorsal aspect of the foot muscle block, below the oesophageal gland mass (Figure 6H). A number of branching nerves penetrate distally between muscle fibres into the muscle block of the foot, and the main pair of pedal nerves penetrate the ventral wall of the body cavity into the foot at the posterior (Figure 3B). A pair of statocysts are located medially, anterior of the pedal nerve cords, apparently innervated by them, more or less central in the animal body (Figure 4H). The statocysts are surrounded by the oesophageal gland; each statocyst contains a single statolith (Figure 5C).

The left lateral nerve cord is embedded within the oesophageal gland, passing underneath the intestinal loop and emerging at the right posterior, continuing to the nephridial tissue (Figure 3F). The right lateral nerve cord crosses through the oesophageal gland above the

left lateral nerve and emerges between the foregut and the hindgut underneath the gill. At this point a small nerve, positionally similar to the osphradial nerve in some other gastropods, splits from the main lateral nerve cord and runs anteriorly to the anterior mantle (Figure 3E, 4F). The right lateral nerve posterior of this point continues above the digestive tract and below the gill and runs posteriorly to meet the terminus of the left lateral nerve cord.

A small pigmented patch is present at the right side of the gill stem at the anterior of the ctenidium; we tentatively compare this to the osphradium of other gastropods. This area could not been identified in the tomographic reconstruction of the juvenile specimen, and the putative osphradial nerve could not be seen in adult specimens.

Reproductive System

The 'scaly-foot gastropod' is a simultaneous hermaphrodite. Adults possess both testis and ovary, although the level of development of the two varied in different individuals. The gonads are arranged as two discrete layers with the nephridial tissue between them, the testis to the ventral and the ovary dorsal (Figure 6E).

A large organ is present on the distal body cavity on the right side of the animal as a distinct complex twisted duct fused into a disc distal of the testis, and this is associated with the male gonoduct, (Figure 6G). We were not able to confirm spermatophores being packaged inside this organ (Figure 6E). A packaged spermatophore was confirmed to be discharged from the gonopore of one individual (Figure 6F), providing further evidence

for internal fertilisation through transfer of spermatophore packets. Gonoducts from the testis and ovary are initially separate but apparently fuse to a single duct and emerge as a single genital opening on the right of the mantle cavity, ventral and anterior of the rectum (Figure 1). This was also seen in the serially sectioned juvenile specimen (Figure 5D), although this could not be traced as there was no mature gonad present, only putative proto-gonad found associated with the digestive gland (Figure 5F). The genital opening in adults is simple, not associated with any specialised copulatory organs or appendages, and there is no penis modified from cephalic tentacles. In adults the gonads are displaced out of the shell apex into to the head-foot region at the right side (Figure 1).

Discussion

Members of the gastropod clade Neomphalina are endemic to reducing environments in the deep sea, primarily living on hydrothermal vents (all Peltospiridae) but with some species on natural deposits of sunken wood [28]. The comprehensive anatomical framework presented in the present study allows us to consider both evidence for the phylogenetic affinity of the 'scaly-foot gastropod' and also the nature of its particular anatomical characters.

The 'scaly-foot gastropod' represents an unusual animal with numerous apparently specialist adaptations associated to its habitat in the acidic flow of hydrothermal vent fluids. The anatomy of several other genera in Neomphalina has been described in detail through either dissection (e.g., [24]) or tomographic reconstruction [26]. The diversity of

306 taxa with well-characterised anatomy encompasses the 'scaly-foot gastropod' and
307 members of all three families currently recognised in Neomphalina: in Peltospiridae
308 mainly *Rhynchopelta*, *Peltospira* ([24]; also includes brief overview of *Nodopelta,*
309 *Echinopelta,* and *Hirtopelta*), as well as *Pachydermia* [25]; in Neomphalidae *Neomphalus*
310 [29] and *Symmetromphalus* [30]; in Melanodrymiidae *Melanodrymia* [31], *Leptogyra*,
311 and *Leptogyropsis* ([26], with mentions of *Xyleptogyra*). The present study is the first to
312 include both of these approaches to encompass comprehensive description across full
313 post-settlement ontogeny.
314
315 The gross anatomy of the 'scaly-foot gastropod' generally conforms to the neomphaline
316 plan [26]. Warén *et al*. ([16]: fig. S2C) showed sensory bursicles on the tip of the gill
317 filaments which are known to be present in most vetigastropods and present in some
318 neomphalines [26,31], though the majority of taxa lack them (e.g., *Pachyermia laevis*
319 [25]; *Lirapex* [32]). The lack of specialised copulatory organs in the 'scaly-foot gastropod'
320 conforms to Peltospiridae; members of the family Neomphalidae have the left cephalic
321 tentacle modified as a penis [24,30,33] and melanodrymiids have various special cephalic
322 copulatory modifications [26,31]. However, as a member of Peltospiridae, the 'scaly-foot
323 gastropod' is the only taxon in that family so far known to be a simultaneous
324 hermaphrodite.
325
326 *Comparative Anatomy*
327
328 The circulatory system of the 'scaly-foot gastropod' is notably enlarged compared to
329 other gastropods, as was briefly mentioned by Warén *et al*. [16]. On dissection, the blood

sinuses and lumps of haemocoel material are a prominent feature throughout the body cavity. A cephalopedal haemocoel lined by a net of lacunae reported by Warén *et al*. [16] could not be found, but the blood sinuses are large and apparently mobile as they differ in position among individuals. The bipectinate ctenidium extends far behind the heart into the upper shell whorls, which is much larger compared to *Peltospira* with a similar shell shape and general form as well as other peltospirids [24,25] or melanodrymiids [26,31]. It is similar, however, in proportional size to *Hirtopelta* which has the largest gill among peltospirid genera investigated anatomically so far [24,34]. An enlarged gill may be associated with filter-feeding (as is shown for neomphalid genera *Neomphalus* [29] and *Symmetromphalus* [30]), symbiotic bacteria on the gill (such as endosymbionts in *Hirtopelta tufari* Beck, 2002 [34] or *Alviniconcha* spp. provannids [35]), and/or high respiratory demand. There are no endosymbionts in the gill of the 'scaly-foot gastropod' [21].

Given that the 'scaly foot gastropods' host endosymbionts in the oesophageal gland, have no symbionts in or on the gill [21], and probably do not filter-feed, the most likely reason for enlargement of the gill is to fulfill raised respiratory needs. Nakagawa *et al.* [22] showed through whole-genome sequencing that the endosymbionts of the 'scaly-foot gastropod' are thioautotrophic gammaproteobacteria with a full set of genes required for aerobic respiration, and probably capable of switching between more efficient aerobic respiration and less efficient anaerobic respiration depending on oxygen availability. The host also requires oxygen for survival, and the enlargement of gill is also likely to facilitate extracting oxygen from low oxygen conditions.

354 The most exceptional part of the circulatory system is the extremely large monotocardian
355 heart, which has an especially well-developed ventricle with very thick muscular walls
356 reinforced by muscle bundles running across the lumen. A muscular ventricle is known
357 in Peltospiridae from *Rynchopelta concentrica* [24], but the proportional size of heart is
358 greater in the 'scaly-foot gastropod'. In neomphalids the heart is not markedly muscular
359 (*Neomphalus*, [29]). Unlike *Pachydermia laevis* where the auricle is larger than the
360 ventricle [25], the ventricle is even larger than the auricle in the 'scaly-foot gastropod'.
361 Large blood vessels dorsal and ventral to the ctenidium, together with numerous large
362 blood sinuses under the gill and in the mantle cavity and the fact that the oesophageal
363 gland is highly vascularised, indicate that the giant heart primarily serves the ctenidium
364 and the oesophageal gland (also briefly noted by Warén *et al*. [16]).
365
366 The heart is unusually large for a peltospirid (compare to [24]) or indeed any animal
367 proportionally. The 'scaly-foot' heart is estimated at 4% of the body volume; by contrast
368 the heart of a healthy human is averages at around 1.3% of the body volume (mean total
369 heart volume of adult humans 778 ml, taken from [36]; mean human body volume 61.05
370 L, average of both genders [37]). We interpret that the heart, and particularly the muscular
371 ventricle, functions to create suction that draws blood through the gill and thus pump
372 haeomocoel to the rest of the circulatory system.
373
374 An enlarged oesophageal gland is a common feature in so-called plesiomorphic gastropod
375 clades, including Patelloidea, Vetigastropoda, Cocculiniformia, Neritimorpha and
376 Neomphalina [38], but the extent of enlargement seen in the 'scaly-foot gastropod' is
377 orders of magnitude greater than any other gastropod anatomy described to date [16]. In

other peltospirids, the posterior portion of the oesophagus forms a pair of blind mid-oesophageal pouches or gutters extending only to the anterior end of the foot (*Rynchopelta*, *Peltospira*, *Nodopelta*, *Echinopelta*, [24]: fig. 12; *Pachydermia* [25]; also *Melanodrymia* [31]). The 'scaly-foot gatropod' oesophageal gland forms one single voluminous blind sac that extends much further posterior, to reach the heart. There are no other reports of oesophageal glands that are highly vascularized and containing blood sinuses as seen in the 'scaly-foot gastropod'. The oesophageal gland is known definitively to house one single strain of thioautotrophic endosymbiotic bacteria [21,22]. The dominance of the greatly enlarged oesophageal gland housing endosymbiotic bacteria is in contrast with rest of the digestive system which is relatively small, suggesting that the endosymbionts are the key nutrient source. We further infer the function of the enlarged circulatory system and extremely high blood volume is relevant to the metabolism of the bacterial endosymbionts.

Unlike other holobiont vent gastropods such as *Alviniconcha* and *Ifremeria* which house endosymbionts in the gill [35,39] where bacteria can readily contact vent fluid and water through circulation in the mantle cavity, in the 'scaly-foot gastropod' the endosymbionts are housed in oesophageal gland where they are isolated from the vent fluid. The host is thus likely to play a major role in supplying the endosymbionts with necessary chemicals leading to increased respiratory needs, similar to the scenario in the trophosome of *Riftia pachyptila*. To supply endosymbionts with sulfides, *R. pachyptila* takes in sulfides from the vent fluid through its plume and has a hydrogen sulfide specific binding site on the haemoglobin molecule in the blood that transports sulphides to the trophosome [40]. The same may be happening with the 'scaly-foot gastropod' and an elaborative cardiovascular

system with a powerful heart is likely to help circulate sufficient oxygen or hydrogen sulfide through the blood stream, for the needs of the host (oxygen) and its symbiotic bacteria (oxygen and sulfide). Detailed investigation of the 'scaly-foot gastropod' haemocoel will reveal further information regarding its oxygen carriers and if it has respiratory pigments that bind to sulphides or an alternative means of sulfide transport.

The stomach of the 'scaly-foot gastropod' is similar in form to other neomphalines including the tubes we observed in the juvenile specimen that connect the stomach directly to the digestive gland ([29]: fig. 6). The intestine however is reduced [16] and only has a single loop, unlike grazing peltospirids [24,25], most likely because of its nutritional reliance on endosymbiotic bacteria. *Hirtopelta* also has a reduced and narrow intestine [24], but members of that genus house endosymbionts on their enlarged gill filaments [34], and the intestinal reduction is likely to also be a result of convergence due to reliance on endosymbionts for nutrition. In filter-feeding neomphalids the intestine is also rather short (*Neomphalus* and *Symmetromphalus*); the gills of these are enlarged as well, but it is unknown if they house symbionts on the gill filaments. Melanodrimiids are detritivores and have longer intestines like grazing peltospirids [26,31]. There is a general trend associating short simple guts with reliance on endosymbiosis rather than external nutrition through grazing.

Gut contents from the scaly-foot specimens did not include any coarse inorganic particles such as those commonly found ingested together with food by grazing or deposit feeding peltospirids such as *Rhynchopelta concentrica* [24]. Warén *et al*. [16] reported finely granular sulphides from the gut of 'scaly-foot gastropod' and suggested that these likely

originated from the endosymbionts; we also confirmed these sulfides. The material nature of the predominant chalky material in the posterior region of the gut is still unclear. The chalky gut content may represent ingested endosymbionts or other food source (such as filter-feeding), it is currently unclear whether this species has other mechanisms of feeding.

The radula of the 'scaly-foot gastropod' is proportionately much larger in juveniles compared with adults. The animals could feed by grazing as juveniles; there is also a putative shift in diet reported from *Neomphalus* where juveniles feed by grazing and shift to exclusive filter-feeding in later life [29]. However the material in the gut of the serially-sectioned juvenile 'scaly-foot' contained similar material to the adult guts, the foregut of the juvenile was also empty and the oesophageal gland was proportionately as large in the juvenile as in adults. This suggests the 'scaly-foot gastropod' likely relies on endosymbionts for nutrition throughout its entire post-larval life. The endosymbionts are remarkably similar in their genome with only two synonymous changes in 19 genes and 13810 codon positions, across 32 host individuals [22]. Nakagawa *et al*. [22] suggested this is a result of stringent selection of horizontally transferred endosymbiont by the host.

No other neomphalines are known to have endosymbionts housed in the oesophageal gland, although *Hirtopelta tufari* is known to house endosymbionts in the ctenidium (Beck, 2002) in a similar association as found in provannid gastropod species in *Alviniconcha* and *Ifremeria* [28]. Another undescribed peltospirid from Antarctic vents at East Scotia Ridge of similar body size to the 'scaly-foot gastropod' ('Peltospiroid n. sp. ESR', [41]) has been shown through stable isotope analyses to possibly be reliant on

endosymbionts for nutrition [42].

The single nephridium in the 'scaly-foot' is displaced to the right of the body, similar to the structure seen in *Hirtopelta* ([24]: fig. 15). This may be attributable to the enlarged gill taking up the entire left side of mantle cavity, seen in both taxa. The left side of the body in the 'scaly-foot gastropod' has numerous voluminous blood sinuses that occupy all available space.

The arrangement of the nervous system in the 'scaly-foot gastropod' is reduced in complexity and enlarged in size compared to other neomphaline taxa. The lateral swellings of the oesophageal nerve ring, emitting the tentacular nerves, may represent a homologous region to cerebral ganglia in other gastropods; however, their forward placement relative to the origin of the lateral nerve cords confounds positional homology. The cerebral ganglia emit the lateral nerve cords in molluscan tetraneury [43] but in the 'scaly-foot gastropod' there is a large multi-way junction at the posterior margin of the oesophageal nerve ring that seems to represent a fusion of the typical molluscan ganglia. The medullary nature of the major nerve cords and the enlarged anterior commissure (incorporating the 'cerebral' lateral swellings) is reminiscent of the nervous system of Polyplacophora [44].

The single statolith in the pair of statocysts is the same condition as for all other reported instances in Neomphalina [26]. There is a distinct nerve extending to the anterior mantle, positionally equivalent to the nerve extending forward from the osphradial ganglion particularly in *Leptogyra* [26]. The 'osphradium' was described as located on the shell

474 muscle in *Rhychopelta* [24], but on the gill stem in *Pachydermia* [25] and in the 'scaly-
475 foot' gastropod. This level of variability is typical among molluscs and the function (if
476 any) of these structures is entirely speculative [45].
477
478 The simultaneous hermaphrodite condition in the 'scaly-foot gastropod' is so far unique
479 among Peltospiridae [24,28,46] and paralleled only among Neomphalina by *Leptogyra* in
480 Melanodrymiidae (known definitively for *L. constricta* Marshall, 1988 and *L. patula*
481 Marshall, 1988; [26]). Early observations suggesting separate males and females in the
482 'scaly-foot gastropod' [16] were probably a result of variation in the relative development
483 of the two gonads in different individuals. At the time of the first discovery and
484 description of the 'scaly-foot' all known neomphalines (*i.e.* then excluding *Leptogyra*)
485 had separate sexes.
486
487 The 'scaly-foot gastropod' also does not have any specialised copulatory organs on the
488 head, which is consistent with other peltospirids [24,25]. In Melanodrymiidae, *Leptogyra*
489 hermaphrodites have a penis and accessory penis extending from the base of the left
490 cephalic tentacle. All other three melanodrymiid genera have separate sexes and males
491 have copulatory organs [26,31,47]. All four genera in family Neomphalidae with
492 available information have separate sexes and the left cephalic tentacle in males is
493 modified into a penis (also *Retiskenea* but the familial placement of this genus is
494 uncertain) [26,32].
495
496 Both gonads in *Leptogyra* share a single gonoduct with the ovary positioned anterior of
497 the testis and the species maybe protandric [31]; by contrast the gonads in the 'scaly-foot'

498 are clearly simultaneously present in vertical stacking and two gonoducts appear to fuse
499 into a single genital opening. We have observed the structure previously reported as a
500 'spermatophore producing organ' [16]; however, we note that it is similar in position and
501 structure to the seminal receptical illustrated in *Leptogyra* [26]. Previously,
502 spermatophores in Neomphalina were known from other taxa in Peltospiridae
503 (*Pachydermia laevis*; [16]) and also Melanodrymiidae (*Melanodrymia*; [32]) but not from
504 Neomphalidae.
505
506 Convergent evolution to achieve a limpet-form from spirally coiled ancestors has
507 occurred repeatedly among Gastropoda [48,49]. Shifting from a coiled form to a limpet
508 form has impacts on the positions of organ systems, in particular the relative positions of
509 gonads and digestive gland [50]. In gastropods, the gonad can either be located to the
510 extreme posterior, near the shell apex (the norm for species with a coiled shell) or in an
511 opposite arrangement with the digestive glands at the apex and gonads anterior of it (the
512 norm for limpets) [50]. In the 'scaly-foot gastropod', the digestive gland occupies the
513 apex and gonads are displaced anteriorly, and this has previously been attributed to a
514 morphological shift toward the limpet form [16]. Among other Peltospiridae, the anterior
515 gonad is observed in the coiled *Peltospira* and the 'scaly-foot gastropod', as well as
516 limpet-formed species (*e.g.*, *Rhynchopelta*, *Echinopelta* [24]); but some, such as
517 *Hirtopelta*, have the opposite arrangement ([24]: fig. 15). Neomphalina as a clade is
518 extremely variable in shell forms ([28]: fig. 7.6). Hence another possible interpretation is
519 that the 'scaly-foot gastropod' may be a secondarily coiled derivation from a recent
520 limpet-form ancestor. Gonad position is, unfortunately, apparently not particularly
521 informative for phylogenetic inference.

Vent invertebrates exhibit a wide range of reproductive traits but tend to have high dispersal ability associated with rapid growth and continuous reproduction [51-53]. Individual hydrothermal vent fields are generally ephemeral and patchy in distribution and vent-endemic invertebrate species must maintain a viable metapopulation across many vent fields to persist and prosper [54,55]. The patchiness of many deep-sea habitats also means that the chances of larvae successfully colonising a suitable habitat may be low [55,56]. Displacing the gonads out of the coiled shell apex and into the body whorl provides a larger volume of space for gonads to develop; this may have advantages for the 'scaly-foot gastropod' in increasing fecundity and in turn increasing the chance of its larvae arriving at a different vent field. Additional inference of gonad index and reproductive quality and fecundity could be determined anatomically [57-60], although we have not attempted this within the present study. The 'scaly-foot gastropod' is presumed to have lecithotrophic larvae with a planktonic dispersal stage like other neomphalines [61], but further aspects of larval dispersal, behaviour, survivability, and metamorphosis are so far largely intractable in deep-sea ecosystems because of the inaccessibility of the living organisms.

Adaptive Significance

This study exemplifies how understanding and perception of an organism can be enhanced and changed dramatically by understanding the internal anatomy. The 'scaly-foot gastropod' differs distinctly from other deep-sea gastropods, even closely-related neomphalines. As a result of adaptation and specialisation to resolve energetic needs in a

546 chemosythetic environment, this dramatic ‘dragon-like’ animal has become a carrying
547 vessel for its bacterial endosymbionts. The adaptations with significantly altered anatomy
548 serve the host’s survival but can equally be seen to suit the needs of the endosymbionts,
549 housed in the greatly enlarged and vascularised oesophageal gland. The rest of the
550 digestive system is simple and reduced as nutrition is mainly provided by the
551 endosymbionts, and may be processing solid waste perhaps accidentally ingested. The
552 circulatory system has a huge blood volume and a muscular ‘dragon heart’ that draws
553 blood from the elaborate gill to supply the bacteria. It has no brain, the huge fused neural
554 mass is directly adjacent to and passes through the oesophageal gland where the bacteria
555 are housed. The reproductive system is displaced anteriorly, perhaps enabling greater
556 fecundity. The ‘scaly-foot gastropod’ lives adjacent to acidic and reducing vent fluid from
557 black smokers or diffuse venting, which contain the chemical and substrates required by
558 the chemoautotrophic bacteria [11,17,21]. The unique external armature of hard dermal
559 sclerites, which are often biomineralised with iron sulfide [18,19] , may help protect the
560 gastropod from the vent fluid, so that its bacteria can live close to the source of electron
561 donors for chemosynthesis.
562
563
564 **Materials and methods**
565
566 All specimens examined herein were collected from the Longqi vent field [15] (also
567 known as Dragon vent field [12,13]), Southwest Indian Ridge, 37°47.03'S 49°38.97'E
568 (‘Tiamat Chimney’), depth 2785 m, on-board RRS *James Cook* expedition JC67 using
569 the suction sampler of the remotely operated vehicle (ROV) *Kiel 6000* [12]. The ‘scaly-

570 foot gastropod' densely populated the areas immediately surrounding diffuse-flow
571 venting, seen visually as shimmering water. The specimens were fixed and stored in 4%
572 buffered formalin upon retrieval on-board the ship.
573
574 10 adult specimens were dissected with the aid of stereo microscopes (Olympus SZX9,
575 SZX16) and photographs were taken using a digital single lens reflex (DSLR) camera
576 (Olympus E-600) mounted to the microscope trinocular.
577
578 One specimen with shell and mantle removed was freeze-dried overnight and Scanning
579 Electron Microscopy (SEM) was undertaken using a Hitachi TM3000 table-top SEM
580 (British Antarctic Survey, Cambridge), to capture the structural details of head and
581 ctenidium. As the specimen was large 22 micrographs were stacked in the software Adobe
582 Photoshop CS4 to compose the final image.
583
584 One of the smallest 'scaly-foot gastropod' juvenile specimens ever collected (shell length
585 ca. 3mm) was selected for serial sectioning and 3D tomographic reconstruction. The
586 selected juvenile specimen was decalcified in 2% EDTA (pH 7.2) for 48 hours, followed
587 by subsequent acetone dehydration series, embedding, and tomographic model
588 reconstruction using the software AMIRA v.5.3.3 (FEI Visualisation Sciences Group) as
589 described by Ruthensteiner [62].
590
591 Prior to embedding, the specimen was stored in diluted Epon epoxy resin mixture (1:1
592 with 100% acetone) overnight at room temperature unlidded, allowing acetone to
593 evaporate. The specimen was then embedded in Epon with DPM-30 accelerator for a

further 24 hours at 60°C, according to the manufacturer's instructions (Sigma). Samples were serially sectioned at a thickness of 1.5 μm using an automated rotary microtome (Leica RM2255) fitted with a diamond knife (HistoJumbo 8 mm, DiATOME, Switzerland). Sections were stained using the high contrast monochromatic methylene blue-azure II stain [63] and cover-slipped using Araldite resin following manufacturer's instructions (Agar Scientific).

The serial semithin sections of the complete animal included 1700 sections; a subsample of every third section throughout the entire specimen was digitally captured using a DSLR camera (Olympus E-600) mounted to a compound microscope trinocular (Olympus BX41), at an appropriate magnification to maximise specimen visibility. The resulting images were processed in Adobe Photoshop CS4 for contrast enhancement, size reduction, and converted to greyscale. The processed images were imported into Amira v5.3.3 and aligned into a single stack. Materials of interest were highlighted digitally throughout the stack for 3D visualisation and the final tomographic model was produced by post-processing including surface rendering and smoothing. The resulting semithin sections are deposited in Zoologische Staatssammlung München (Munich, Germany), with catalogue number ZSM 20151000.

Availability of Supporting Data

The data sets supporting the results of this article are included within the article and its additional files.

618 **Competing Interests**

619

620 The authors declare that they have no competing interests.

621

622 **Author Contributions**

623

624 CC and JDS conceived the study, and conducted all laboratory work and analysis. JTC,
625 ADR, and CC contributed to collecting the original specimens. KL assisted with the
626 interpretation of data. CC drafted the manuscript, all authors contributed to and approved
627 the final manuscript.

628

629 **Acknowledgements**

630

631 Lauren Sumner-Looney (Queen's University Belfast) is gratefully acknowledged for her
632 great help in the laboratory work and 3D modelling, as well as stimulating discussions.
633 We also thank Dr John Grahame (University of Leeds) and many other colleagues who
634 contributed further valuable discussions to the project. This research was supported by a
635 Research Grant from the Malacological Society of London to CC. We owe a great deal to
636 the Master and crew of the RRS *James Cook*, as well as pilots and technical teams of
637 ROV *Kiel 6000* for their tremendous support of the scientific activities during the cruises
638 JC66/67 funded by NERC Small Research Grant NE/H012087/1 to JTC and NERC
639 Research Grant NE/F005504/1 to ADR. We are grateful for the logistics and shipboard
640 support provided by the staffs of the UK National Marine Facilities at the National
641 Oceanography Centre, Southampton.

642

643 **References**

644

645 1. Van Dover CL. *The Ecology of Deep-Sea Hydrothermal Vents*. Princeton: Princeton University
646 Press; 2000.
647 2. Hourdez S, Lallier F. Adaptations to hypoxia in hydrothermal-vent and cold-seep invertebrates. In:
648 Amils R, Ellis-Evans C, Hinghofer-Szalkay H, editors. *Life in Extreme Environments*. Springer
649 Netherlands; 2007:297-313.
650 3. Fisher CR. Ecophysiology of primary production at deep-sea vents and seeps. In: Uiblein F, Ott J,
651 Stachowtisch M, editors. *Deep-sea and Extreme Shallow-water Habitats: Affinities and*
652 *Adaptations*. Biosyst Ecol Ser, vol 11. 1996:313-36.
653 4. Petersen JM, Ramette A, Lott C, Cambon-Bonavita M-A, Zbinden M, Dubilier N. Dual symbiosis
654 of the vent shrimp *Rimicaris exoculata* with filamentous gamma- and epsilonproteobacteria at four
655 Mid-Atlantic Ridge hydrothermal vent fields. Environ Microbiol 2010, 12(8):2204-18.
656 5. Watsuji T-o, Yamamoto A, Motoki K, Ueda K, Hada E, Takaki Y et al. Molecular evidence of
657 digestion and absorption of epibiotic bacterial community by deep-sea crab *Shinkaia crosnieri*.
658 ISME J 2014.
659 6. Cavanaugh CM, Gardiner SL, Jones ML, Jannasch HW, Waterbury JB. Prokaryotic cells in the
660 hydrothermal vent tube worm *Riftia pachyptila* Jones: possible chemoautotrophic symbionts.
661 Science 1981, 213:340-2.
662 7. Kim YW, Yasuda M, Yamagishi A, Oshima T, Ohta S. Characterization of the endosymbiont of a
663 deep-sea bivalve, *Calyptogena soyoae*. Appl Environ Microb 1995, 61(2):823-7.
664 8. Page HM, Fiala-Medioni A, Fisher CR, Childress JJ. Experimental evidence for filter-feeding by
665 the hydrothermal vent mussel, *Bathymodiolus thermophilus*. Deep-Sea Res Pt A 1991,
666 38(12):1455-61.
667 9. Jouin C, Gaill F. Gills of hydrothermal vent annelids: structure, ultrastructure and functional
668 implications in two alvinellid species. Prog Oceanogr 1990, 24(1–4):59-69.
669 10. Andersen AC, Jolivet S, Claudinot S, Lallier FH. Biometry of the branchial plume in the
670 hydrothermal vent tubeworm *Riftia pachyptila* (Vestimentifera; Annelida). Can J Zoolog 2002,
671 80(2):320-32.
672 11. Van Dover CL, Humphris SE, Fornari D, Cavanaugh CM, Collier R, Goffredi SK et al.
673 Biogeography and ecological setting of Indian Ocean hydrothermal vents. Science 2001,
674 294(5543):818-23.
675 12. Copley JT. Research cruise JC67, Dragon vent field, SW Indian Ocean, 27-30 November 2011.
676 *RRS James Cook cruise report*. British Oceanographic Data Centre; 2011: Available from
677 http://www.bodc.ac.uk/data/information_and_inventories/cruise_inventory/report/10593/.
678 13. Roterman CN, Copley JT, Linse KT, Tyler PA, Rogers AD. The biogeography of the yeti crabs

679 (Kiwaidae) with notes on the phylogeny of the Chirostyloidea (Decapoda: Anomura). Proc R Soc
680 B 2013, 280(1764):20130718.
681 14. Tao C, Lin J, Guo S, Chen YJ, Wu G, Han X et al. First active hydrothermal vents on an ultraslow-
682 spreading center: Southwest Indian Ridge. Geology 2012, 40(1):47-50.
683 15. Tao C, Li H, Jin X, Zhou J, Wu T, He Y et al. Seafloor hydrothermal activity and polymetallic
684 sulfide exploration on the Southwest Indian Ridge. Chinese Sci Bull 2014:1-11.
685 16. Warén A, Bengtson S, Goffredi SK, Van Dover CL. A hot-vent gastropod with iron sulfide dermal
686 sclerites. Science 2003, 302(5647):1007-.
687 17. Nakamura K, Watanabe H, Miyazaki J, Takai K, Kawagucci S, Noguchi T et al. Discovery of new
688 hydrothermal activity and chemosynthetic fauna on the Central Indian Ridge at 18°–20°S. PLoS
689 ONE 2012, 7(3):e32965.
690 18. Chen C, Copley JT, Linse K, Rogers AD, Sigwart J. How the mollusc got its scales: convergent
691 evolution of the molluscan scleritome. Biol J Linn Soc 2015: doi: 10.1111/bij.12462.
692 19. Suzuki Y, Kopp RE, Kogure T, Suga A, Takai K, Tsuchida S et al. Sclerite formation in the
693 hydrothermal-vent 'scaly-foot gastropod': Possible control of iron sulfide biomineralization by the
694 animal. Earth Planet Sc Lett 2006, 242:39-50.
695 20. Yao H, Dao M, Imholt T, Huang J, Wheeler K, Bonilla A et al. Protection mechanisms of the iron-
696 plated armor of a deep-sea hydrothermal vent gastropod. P Natl Acad Sci USA 2010, 107(3):987-
697 92.
698 21. Goffredi SK, Warén A, Orphan VJ, Van Dover CL, Vrijenhoek RC. Novel forms of structural
699 integration between microbes and a hydrothermal vent gastropod from the Indian Ocean. Appl
700 Environ Microb 2004, 70(5):3082-90.
701 22. Nakagawa S, Shimamura S, Takaki Y, Suzuki Y, Murakami S-i, Watanabe T et al. Allying with
702 armored snails: the complete genome of gammaproteobacterial endosymbiont. ISME J 2014,
703 8(1):40-51.
704 23. Beinart RA, Sanders JG, Faure B, Sylva SP, Lee RW, Becker EL et al. Evidence for the role of
705 endosymbionts in regional-scale habitat partitioning by hydrothermal vent symbioses. P Natl Acad
706 Sci USA 2012, 109(47):E3241–E50.
707 24. Fretter V. The anatomy of some new archaeogastropod limpets (Superfamily Peltospiracea) from
708 hydrothermal vents. J Zool 1989, 218(1):123-69.
709 25. Israelsson O. The anatomy of *Pachydermia laevis* (Archaeogastropoda: 'Peltospiridae'). J Moll
710 Stud 1998, 64(1):93-109.
711 26. Heß M, Beck F, Gensler H, Kano Y, Kiel S, Haszprunar G. Microanatomy, shell structre and
712 molecular phylogeny of *Leptogyra, Xyleptogyra* and *Leptogyropsis* (Gastropoda: Neomphalida:
713 Melanodrymiidae) from sunken wood. J Moll Stud 2008, 74(4):383-401.
714 27. Richter S, Loesel R, Purschke G, Schmidt-Rhaesa A, Scholtz G, Stach T et al. Invertebrate

715 neurophylogeny: suggested terms and definitions for a neuroanatomical glossary. Front Zool 2010,
716 7(1):29.
717 28. Sasaki T, Warén A, Kano Y, Okutani T, Fujikura K, Kiel S. Gastropods from recent hot vents and
718 cold seeps: systematics, diversity and life strategies. In: Kiel S, editor. *The Vent and Seep Biota*.
719 Topics in Geobiology. Netherlands: Springer 2010:169-254.
720 29. Fretter V, Graham A, McLean J. The anatomy of the galapagos rift limpet, *Neomphalus fretterae*.
721 Malacologia 1981, 21(1-2):337-61.
722 30. Beck LA. *Symmetromphalus hageni* sp. n., a new neomphalid gastropod (Prosobranchia:
723 Neomphalidae) from hydrothermal vents at the Manus Back-Arc Basin (Bismarck Sea, Papua New
724 Guinea). Ann Nat Hist Mus Wien Ser B Bot Zool 1992, 92B:277-87.
725 31. Haszprunar G. The anatomy of *Melanodrymia aurantiaca* Hickman, a coiled Archaeogastropod
726 from the East Pacific hydrothermal vents (Mollusca, Gastropoda). Acta Zool 1989, 70(3):175-86.
727 32. Warén A, Bouchet P. Gastropoda and Monoplacophora from hydrothermal vents and seeps: New
728 taxa and records. The Veliger 2001, 44.
729 33. Warén A, Bouchet P. New gastropods from East Pacific hydrothermal vents. Zool Scr 1989,
730 18(1):67-102.
731 34. Beck LA. *Hirtopelta tufari* sp. n., a new gastropod species from hot vents at the East Pacific Rise
732 (21° S) harbouring endocytosymbiotic bacteria in its gill (Gastropoda: Rhipidoglossa:
733 Peltospiridae). Arch Molluskenkd 2002, 130:249-57.
734 35. Stein JL, Cary SC, Hessler RR, Ohta S, Vetter RD, Childress JJ et al. Chemoautotrophic symbiosis
735 in a hydrothermal vent gastropod. Biol Bull 1988, 174(3):373-8.
736 36. Carlsson M, Cain P, Holmqvist C, Stahlberg F, Lundback S, Arheden H. Total heart volume
737 variation throughout the cardiac cycle in humans. Am J Physiol Heart Circ Physiol 2004,
738 287(1):H243-H50.
739 37. Sendroy JJ, Collison HA. Determination of human body volume from height and weight. J Appl
740 Physiol 1965, 21(1):167-72.
741 38. Sasaki T. Comparative anatomy and phylogeny of the recent Archaeogastropoda (Mollusca:
742 Gastropoda). Univ Mus Tokyo Bull 1998, 38:1-224.
743 39. Suzuki Y, Sasaki T, Suzuki M, Nogi Y, Miwa T, Takai K et al. Novel chemoautotrophic
744 endosymbiosis between a member of the *Epsilonproteobacteria* and the hydrothermal-vent
745 gastropod *Alviniconcha* aff. *hessleri* (Gastropoda: Provannidae) from the Indian Ocean. Appl
746 Environ Microb 2005, 71(9):5440-50.
747 40. Arp AJ, Childress JJ, Vetter RD. The sulphide-binding protein in the blood of the vestimentiferan
748 tube-worm, *Riftia pachyptila*, is the extracellular haemoglobin. J Exp Biol 1987, 128(1):139-58.
749 41. Rogers AD, Tyler PA, Connelly DP, Copley JT, James R, Larter RD et al. The discovery of new
750 deep-sea hydrothermal vent communities in the Southern Ocean and implications for biogeography.

751 PLoS Biol 2012, 10(1):e1001234.
752 42. Reid WDK, Sweeting CJ, Wigham BD, Zwirglmaier K, Hawkes JA, McGill RAR et al. Spatial
753 differences in East Scotia Ridge hydrothermal vent food webs: influences of chemistry,
754 microbiology and predation on trophodynamics. PLoS ONE 2013, 8(6):e65553.
755 43. Sigwart JD, Sumner-Rooney LH. Mollusca: Caudofoveata, Monoplacophora, Polyplacophora,
756 Scaphopoda, Solenogastres. In: Schmidt-Rhaesa A, Harzsch S, Purschke G, editors. *Structure and*
757 *Evolution of Invertebrate Nervous Systems*. Oxford, UK: Oxford University Press; in press.
758 44. Sigwart JD, Sumner-Rooney LH, Schwabe E, Heß M, Brennan GP, Schrödl M. A new sensory
759 organ in "primitive" molluscs (Polyplacophora: Lepidopleurida), and its context in the nervous
760 system of chitons. Front Zool 2014, 11(1):7.
761 45. Lindberg DR, Sigwart JD. What is the molluscan osphradium? An evaluation of homology. Zool
762 Anz in press.
763 46. Tyler PA, Pendlebury S, Mills SW, Mullineaux L, Eckelbarger KJ, Baker M et al. Reproduction of
764 gastropods from vents on the East Pacific Rise and the Mid-Atlantic Ridge. J Shellfish Res 2008,
765 27(1):107-18.
766 47. Marshall BA. Skeneidae, Vitrinellidae and Orbitestellidae (Mollusca: Gastropoda) associated with
767 biogenic substrata from bathyal depth off New Zealand and New South Wales. J Nat Hist 1988,
768 22:949-1004.
769 48. Ponder WF, Lindberg DR. Towards a phylogeny of gastropod molluscs: an analysis using
770 morphological characters. Zool J Linn Soc 1997, 119(2):83-265.
771 49. Ponder WF, Lindberg DR. *Phylogeny and Evolution of the Mollusca*. Oakland, California, USA:
772 University of California Press; 2008.
773 50. Fretter V, Graham A. *British Prosobranch Molluscs: Their Functional Anatomy and Ecology*
774 *(Revised Edition)*. London, UK: Ray Society; 1994.
775 51. Desbruyères D, Laubier L. Primary consumers from hydrothermal vents animal communities. In:
776 Rona P, Boström K, Laubier L, Smith K, Jr., editors. *Hydrothermal Processes at Seafloor*
777 *Spreading Centers*. NATO Conference Series: Springer US; 1983:711-34.
778 52. Adams DK, Arellano SM, Govenar B. Larval dispersal: vent life in the water column.
779 Oceanography 2012, 25:256-68.
780 53. Nakamura M, Chen C, Mitarai S. Insights into life-history traits of *Munidopsis* spp. (Anomura:
781 Munidopsidae) from hydrothermal vent fields in the Okinawa Trough, in comparison with the
782 existing data. Deep-Sea Res Pt I in press.
783 54. Vrijenhoek R. Gene flow and genetic diversity in naturally fragmented metapopulations of deep-
784 sea hydrothermal vent animals. J Hered 1997, 88(4):285-93.
785 55. Vrijenhoek RC. Genetic diversity and connectivity of deep-sea hydrothermal vent metapopulations.
786 Mol Ecol 2010, 19(20):4391-411.

787 56. Yearsley JM, Sigwart JD. Larval transport modeling of deep-sea invertebrates can aid the search
788 for undiscovered populations. PLoS ONE 2011, 6(8):e23063.
789 57. Nakamura M, Watanabe H, Sasaki T, Ishibashi J, Fujikura K, Mitarai S. Life history traits of
790 *Lepetodrilus nux* in the Okinawa Trough, based upon gametogenesis, shell size, and genetic
791 variability. Mar Ecol Prog Ser 2014, 505:119-30.
792 58. Tyler P, Young C. Reproduction and dispersal at vents and cold seeps. J Mar Biol Assoc UK 1999,
793 79(2):193-208.
794 59. Young CM. Reproduction, development and life-history traits. In: Tyler PA, editor. *Ecosystems of*
795 *the World*. Rotterdam Elsevier; 2003:381-426.
796 60. Nye V, Copley JT, Tyler PA. Spatial variation in the population structure and reproductive biology
797 of *Rimicaris hybisae* (Caridea: Alvinocarididae) at hydrothermal vents on the Mid-Cayman
798 Spreading Centre. PLoS ONE 2013, 8(3):e60319.
799 61. Warén A, Bouchet P, Cosel RV. Mollusca, Gastropoda. In: Desbruyères D, Segonzac M, Bright M,
800 editors. *Denisia*. 2 ed. Handbook of Deep-Sea Hydrothermal Vent Fauna (2nd edition). Zurich,
801 Switzerland: Swiss National Museum; 2006:82-137.
802 62. Ruthensteiner B, Heß M. Embedding 3D models of biological specimens in PDF publications.
803 Microsc Res Techniq 2008, 71(11):778-86.
804 63. Richardson KC, Jarett L, Finke EH. Embedding in epoxy resins for ultrathin sectioning in electron
805 microscopy. Stain Technol 1960, 35:313-23.
806
807

Figures

Figure 1. The 'scaly-foot gastropod', mantle cavity overview (shell and mantle tissue removed). Scale bar: 1 cm.

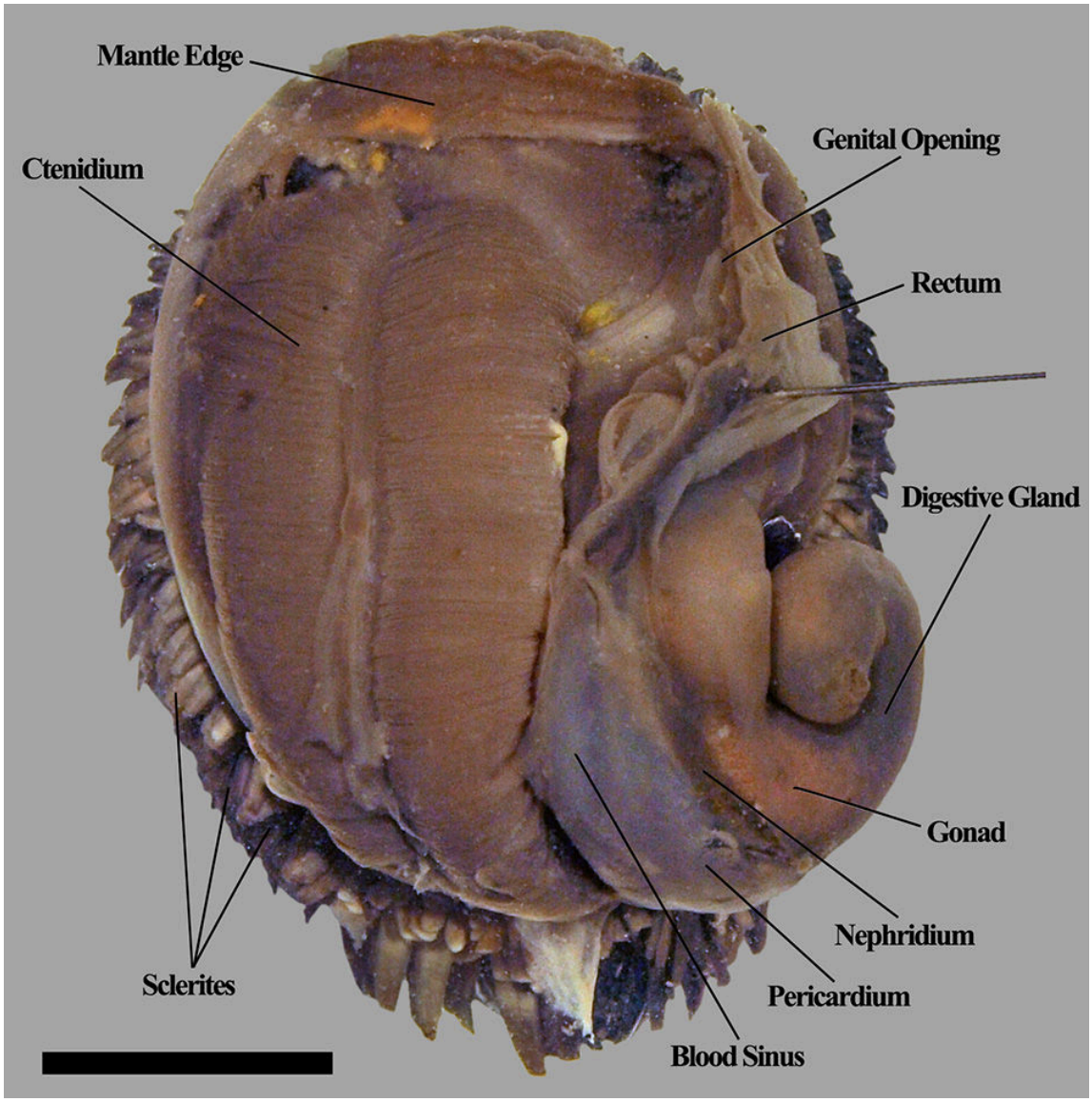

Figure 2. Structural details of the ‘scaly-foot gastropod’ head and ctenidium, composite of 22 scanning electron micrographs of a freeze-dried juvenile specimen. Abbreviations: ct, ctenidium; sn, snout; tt, cephalic tentacle. Scale bar: 2 mm.

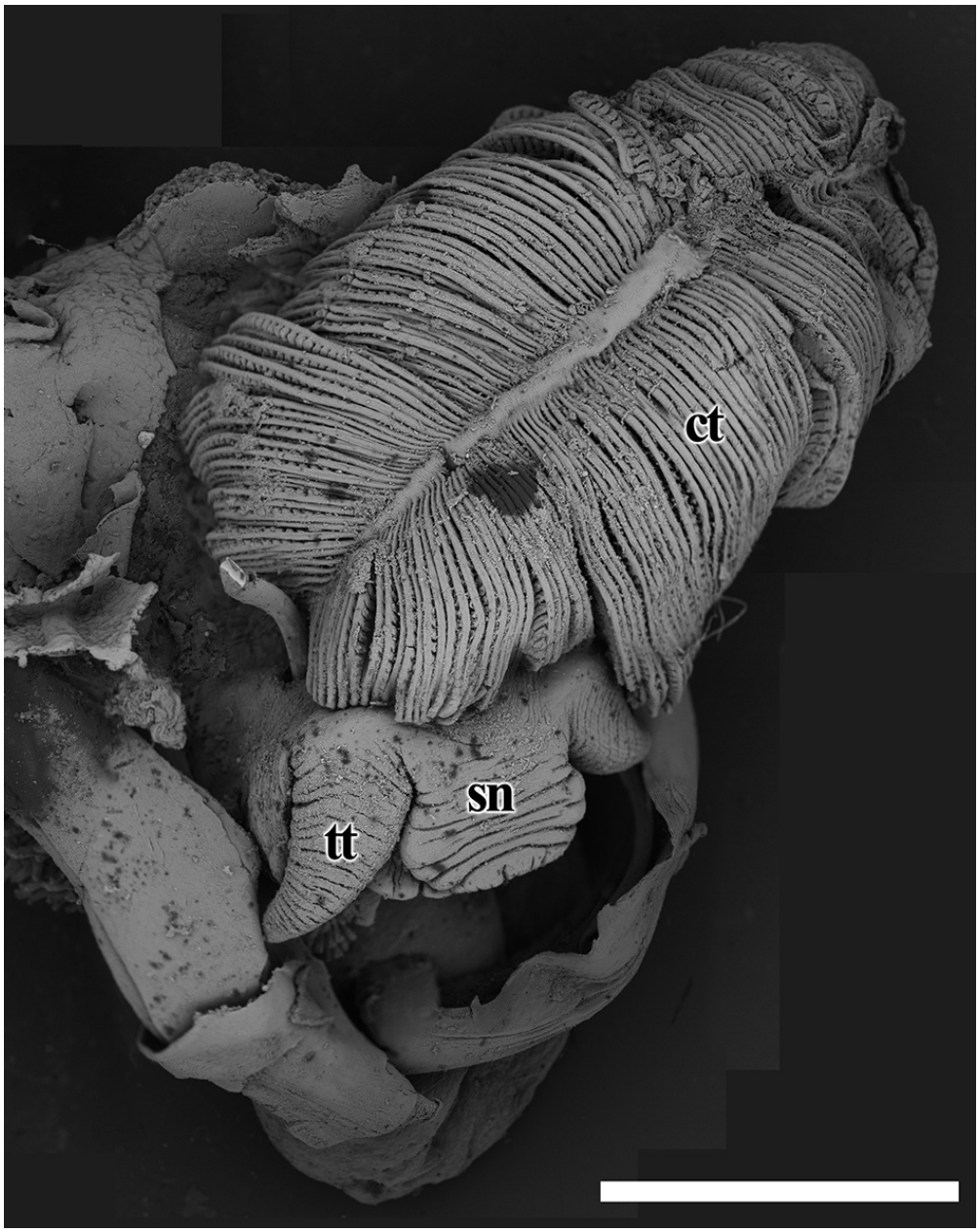

821 **Figure 3.** 3D tomographic reconstruction of the 'scaly-foot gastropod', the full
822 anatomical model in various views. Soft body outline (mantle and foot) shown in
823 transparency. Ctenidium, anterior oesophagus, oesophageal gland, and digestive gland are
824 rendered semi-transparent to show structures underneath. For all parts, the tomographic
825 model is shown to left and a second copy of the same view with labelled parts shown to
826 right. **A.** Dorsal view. **B.** Ventral view. **C.** Frontal view. **D.** Rear view. **E.** Left view. **G.**
827 Angled view. Each colour group corresponds to a specific anatomical system: grey/black,
828 digestive tract; green, oesophageal gland; translucent blue, ctenidium; red, circulatory
829 system (excluding ctenidium); fuchsia, nervous system. Abbreviations: a, auricle; ac,
830 anterior commissure; ct, ctenidium; dg, digestive gland; i, intestine; ln, lateral (visceral)
831 nerve; ls, lateral swelling; mn, mantle nerve; ne, nephridium; oe, oesophagus; og,
832 oesophageal gland; on, osphradial nerve; pn, pedal nerve; ps, pleural swelling; r, radula;
833 rc, radula cartilage; re, rectum; sd, duct connecting stomach to digestive gland; sg, blood
834 sinus under the ctenidium; si, blood sinus; ss, statocyst; st, stomach; tn, tentacular nerves;
835 v, ventricle; ve, blood vessel. Scale bars: 250 μm.
836
837

83
83

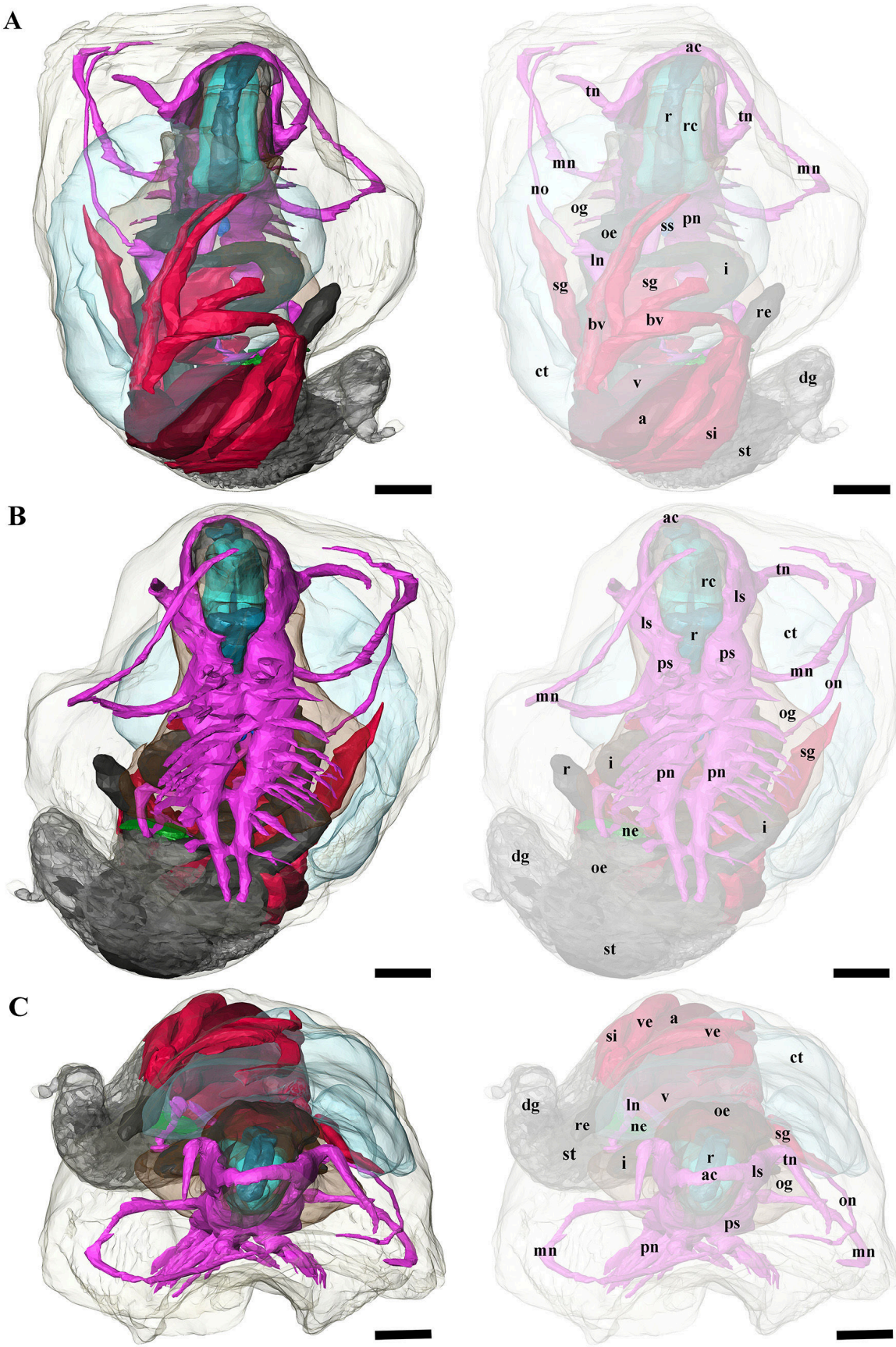
A
ac
tn
r
rc
tn
mn
mn
no
og
ss
pn
oe
ln
i
sg
sg
re
bv
bv
ct
v
dg
a
si
st
B
ac
tn
rc
ls
ls
r
ct
ps
ps
mn
mn
on
og
sg
r
i
pn
pn
ne
i
dg
oe
st
C
ve
a
si
ve
ct
dg
ln
v
oe
re
ne
sg
st
i
r
tn
ac
ls
og
on
ps
mn
pn
mn

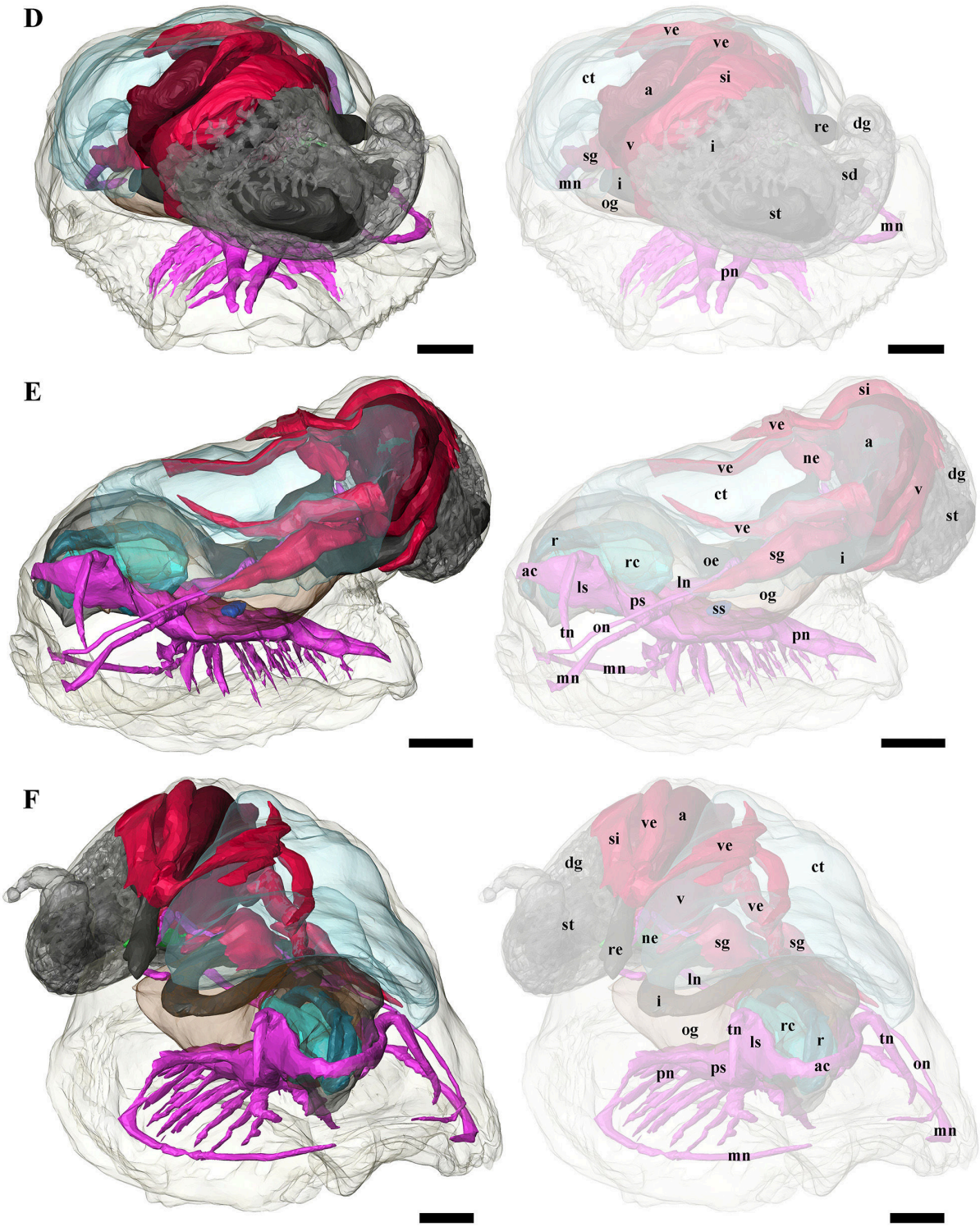
D
ve
ve
ct
a
si
re
dg
v
i
sg
sd
mn
i
og
st
mn
pn
E
si
ve
a
ne
ve
dg
ct
v
st
ve
r
rc
oe
sg
i
ac
ls
ln
ps
og
ss
tn
on
pn
mn
mn
F
ve
a
si
ve
dg
ct
v
ve
st
ne
sg
sg
re
ln
i
og
tn
rc
r
tn
ls
pn
ps
ac
on
mn
mn

841 **Figure 4.** 3D tomographic reconstruction of the 'scaly-foot gastropod'. Soft body outline
842 shown in transparency. Ctenidium, anterior oesophagus, oesophageal gland, and digestive
843 gland are rendered semi-transparent to show structures underneath. **A-B.** Digestive and
844 excretory systems. **C.** Heart. **D-E.** Circulatory system. **F.** Radula and radula cartilage. **G-**
845 **H.** Nervous system. Abbreviations: a, auricle; ac, anterior commissure; ct, ctenidium; dg,
846 digestive gland; i, intestine; ln, lateral (visceral) nerve; ls, lateral swelling; mn, mantle
847 nerve; ne, nephridium; oe, oesophagus; og, oesophageal gland; on, osphradial nerve; pn,
848 pedal nerve; ps, pleural swelling; r, radula; rc, radula cartilage; re, rectum; sd, duct
849 connecting stomach to digestive gland; sg, blood sinus under the ctenidium; si, blood
850 sinus; ss, statocyst; st, stomach; tn, tentacular nerves; v, ventricle; ve, blood vessel. Scale
851 bars: 250 μm.
852
853

85

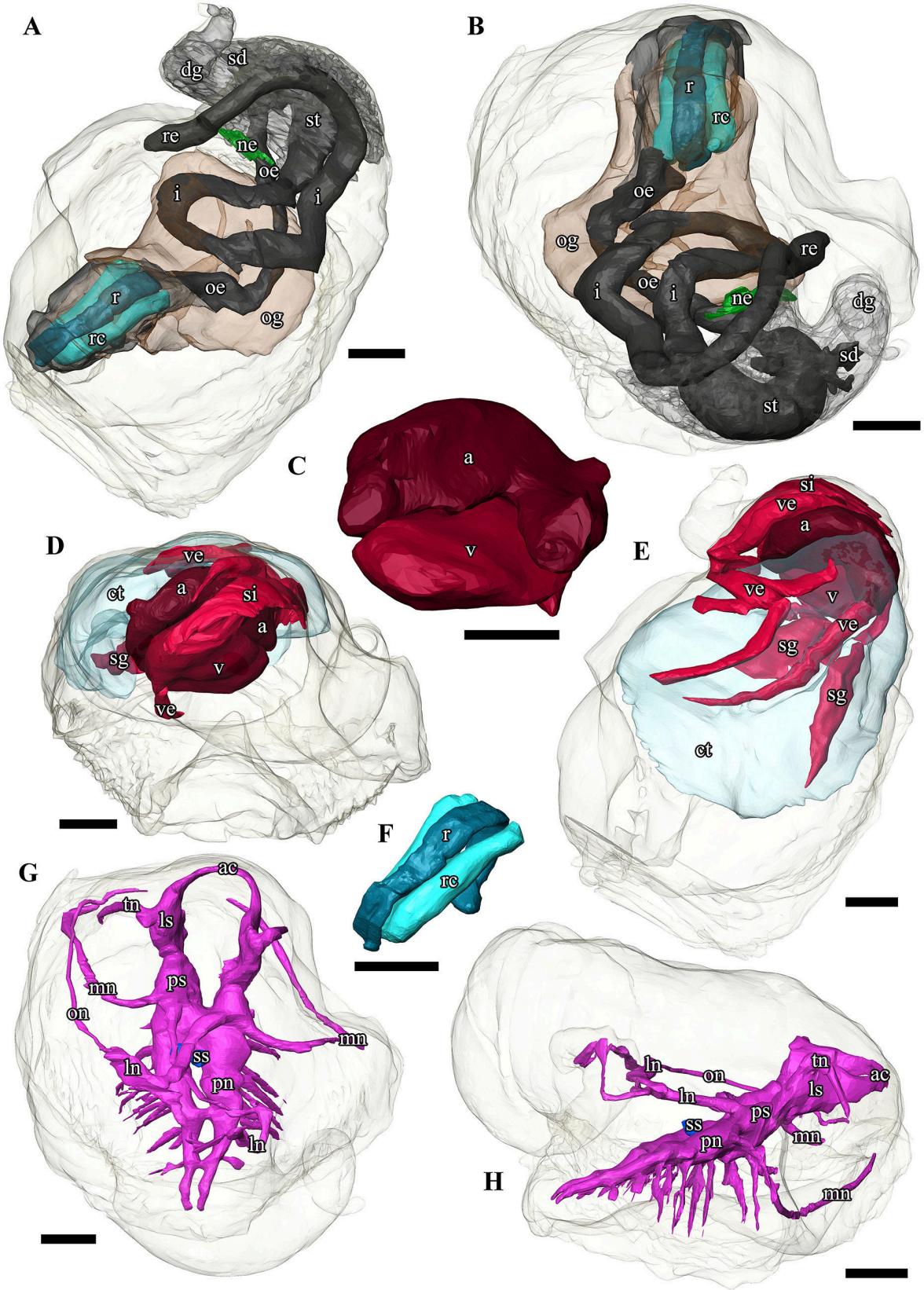
A
dg
sd
st
re
ne
oe
i
i
r
oe
rc
og
B
r
rc
oe
og
re
i
oe
i
ne
dg
sd
st
C
a
v
D
ve
ct
a
si
a
sg
v
ve
E
si
ve
a
ve
v
ve
sg
sg
ct
F
r
rc
G
ac
tn
ls
mn
ps
on
mn
ln
ss
pn
ln
H
ln
on
tn
ac
ln
ls
ps
ss
mn
pn
mn

855 **Figure 5.** Transverse semi-thin sections from the 'scaly-foot gastropod'. **A.** Mouth and
856 buccal mass showing the epithelium cuticle (black arrows). **B.** Posterior part of the head
857 showing the large fused neural mass. **C.** Mid-body section showing ctenidium,
858 oesophageal gland, pedal nerves, and statocysts. **D.** Anterior of the heart. **E.** Ctenidium
859 and associated blood vessels and sinuses. **F.** Posterior visceral mass. Abbreviations: a,
860 auricle; bc, buccal cavity; ct, ctenidium; dg, digestive gland; go, gonoduct; i, intestine;
861 mo, mouth; mt, mantle; ne, nephridium; oe, oesophagus; og, oesophageal gland; pg,
862 putative proto-gonad; pm, pedal musculature; pn, pedal nerve; ps, pleural swelling; r,
863 radula; rc, radula cartilage; re, rectum; sc, sclerites; sd, duct connecting stomach to
864 digestive gland; sg, blood sinus under the ctenidium; si, blood sinus; sl, statolith; ss,
865 statocyst; st, stomach; v, ventricle; ve, blood vessel. Scale bars: 100 μm.
866
867

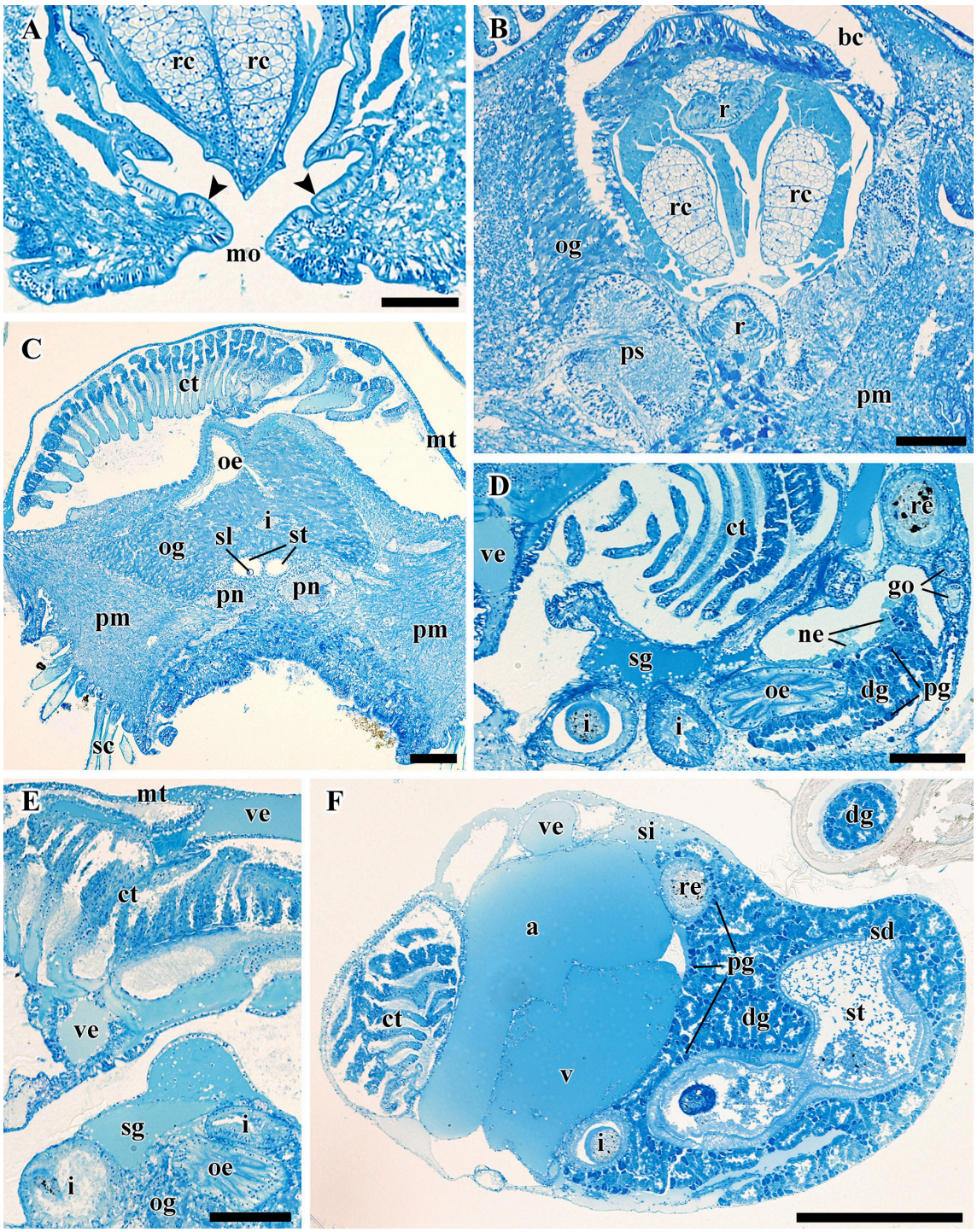
A
rc
rc
mo
B
bc
r
rc
rc
og
r
ps
pm
C
ct
mt
oe
i
sl
st
og
pn
pn
pm
pm
sc
D
re
ct
ve
go
ne
sg
oe
dg
pg
i
i
E
mt
ve
ct
ve
sg
i
oe
i
og
F
ve
si
dg
re
a
sd
pg
ct
dg
st
v
i

868
869

Figure 6. Photographs of the soft parts of adult 'scaly-foot gastropod'. **A**. Dorsal view with shell and part of mantle removed, showing the ctenidium, heart, and associated blood vessels. **B.** Sagittal section; white arrows indicate sections of the hindgut showing white, chalky material inside. **C.** Transverse section through the ctenidium showing a pair of blood sinus (white arrows). **D**. Sagittal section through ventricle showing muscle bundles. **E.** Transverse section of the visceral mass showing testis, ovary, and nephridium; white arrowhead indicates spermatophores inside the 'spermatophore producing organ'. **F.** Packaged spermatophore (white arrow). **G.** 'Spermatophore producing organ'. **H.** Pedal nerve cords, fused neural mass at anterior and numerous lateral offshoots distally into the foot. Abbreviations: a, auricle; ct, ctenidium; ne, nephridium; og, oesophageal gland; ov, ovary; re, rectum; sp, 'spermatophore producing organ'; te, testis; v, ventricle; ve, blood vessel. Scale bars: **A-C, E-F, H** = 5 mm, **D, G** = 2 mm.

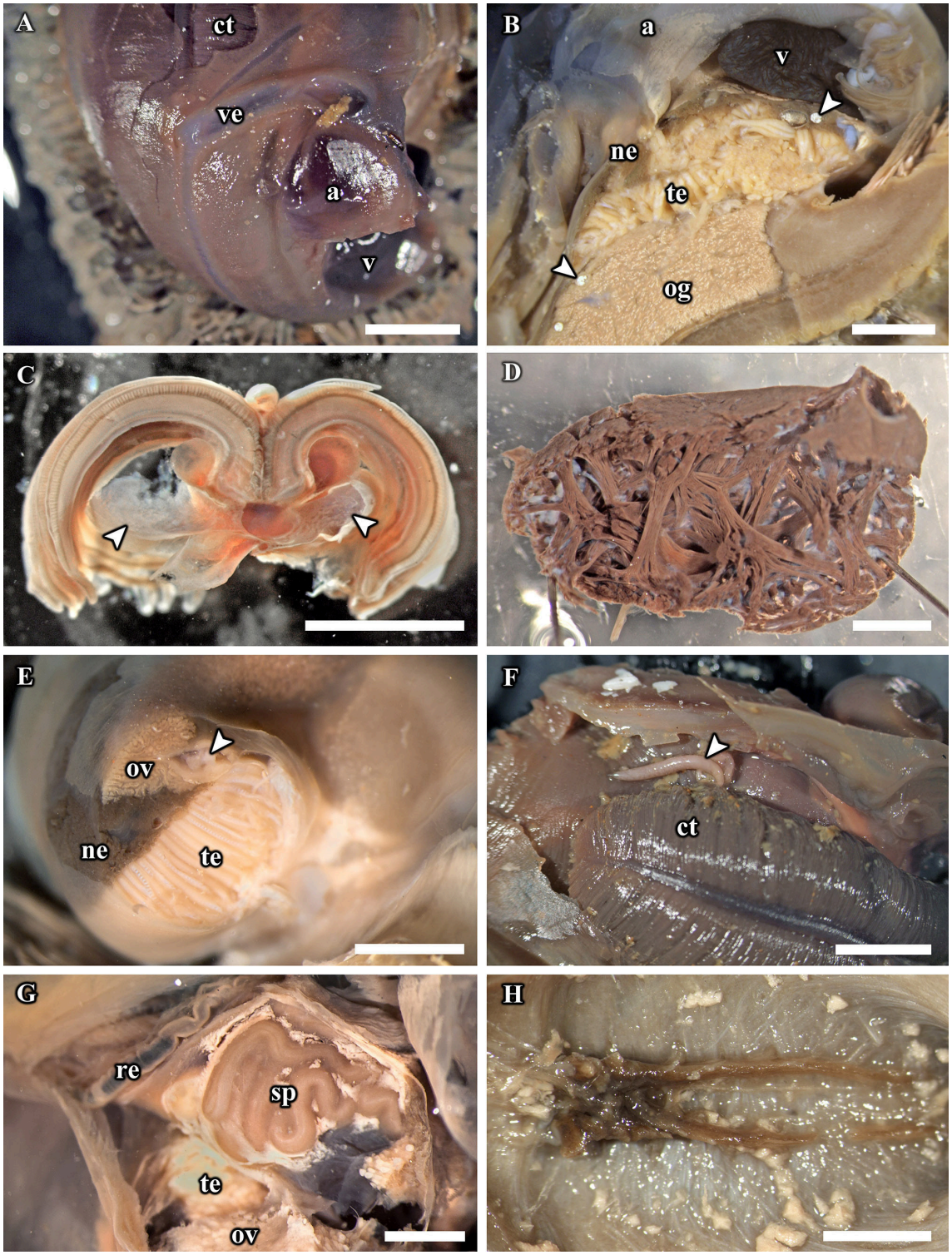

884

Supplementary Material 1: Detailed Histology Protocols

3D Reconstruction of Micromollusc Soft Parts
Ruthensteiner, 2008 Zoosymposia 1: 63-100.

The whole process occurs in the following steps:

1. Fixed specimen is decalcified
2. Decalcified specimens goes through acetone dilution series to replace water completely with acetone
3. Epoxy resin is made up
4. Specimen in acetone is embedded in resin
5. Resin-embedded specimen block is trimmed with blade
6. Trimmed specimen block is sliced to 1~1.5um thick slices using a microtome with diamond blade, which are mounted in series of ribbons on to slide glasses
7. The slides are stained with a dilute Richardson's Stain and a cover slip may be applied to improve photographic quality
8. Slides are visualised under light microscopes, and each slice of the specimen is photographed using a digital camera
9. The digital images are imported to computer and aligned
10. The aligned images are compiled and edited to form the final 3D model

Decalcification Protocol

Ruthensteiner, 2008 Zoosymposia 1: 63-100.

1. Make EDTA (2%) solution for decalcification.
   i. Measure 10g of EDTA powder and fill with distilled water to 100ml.
   ii. Place on hotplate and stir using a magnetic stirrer. The temperature should be around 80 degrees Celsius, MUST NOT BOIL. The result should be a clear fluid with no precipitation. If precipitation occurs, throw away and re-do.
   iii. With NaOH solution, adjust pH drop by drop to 7.2-7.4. The best is 7.2.
   iv. Top up to 400ml with distilled water.
   v. Check that pH is still 7.2. If not adjust with NaOH.
   vi. Finally top up to 500ml with distilled water. Store in glass container.
2. Place specimen in plastic or glass container, fill with EDTA (2%) solution. Label with name, contents, and time/date.
   i. The specimens should be fixed prior to decalcification in glutaldehyde, formalin, or other fixatives to prevent rotting.
3. Leave the specimen for 12-60 hours, depending on how much calcified contents the specimen contains. The EDTA (2%) solution should be replaced periodically.
4. Check periodically for softness, if sufficiently soft then process is complete.
5. Move specimen into 30% acetone solution for storage.

Specimen Dehydration Protocol

Ruthensteiner, 2008 Zoosymposia 1: 63-100.

1. Make up a dilution series of acetone by mixing acetone with distilled water.
   - 30%, 50%, 60%, 70%, 90%, 100% acetone solutions required. Store in glass container with tight sealed lid.
2. Move specimen that has completed the decalcification process to 30% acetone solution. The container should be relatively deep in comparison to the specimen size.
   - The container must be sealed or capped especially later in the dilution series because acetone can evaporate quite quickly and reduce the concentration in the solution.
3. Place the container with specimen on to a gently swaying stirring plate. Leave the specimen for 20 minutes or more (20 minutes is the minimum, does not hurt to be longer, even for long-term).
4. With a plastic pipette, carefully replace the solution with fresh 30% acetone solution.
   - Gently pipette, make sure not to suck up the specimen.
   - To prevent drying out, always leave a film of liquid around the specimen.
5. Repeat steps 3-4 again.
6. Now that the specimen has had two changes of 30% acetone, it is ready to move up the dilution series to 50% acetone solution. It stays in this solution for another 20 minutes + and then replaced with fresh 50% acetone solution, so on.
   - The specimens need to be in each dilution series for three fresh solutions, ie. 30% * 3, 50% * 3, 60% * 3, 70% * 3, 90% * 3, 100% * 3.
   - It is useful to have a piece of paper beside the specimen with all dilution series written down (ie. 30 30 30 50 50 50 etc.) and crossed out with progress. Also helpful to write time down when crossing out to know exactly how long specimens have been in each step.
7. Continue up the dilution series until 100% solution has gone through two changes. At this point, ALL water in the specimen should have been replaced with acetone.
   - Now the specimen is ready for embedding in resin, and the acetone in the tissue will then be replaced by resin.

Epoxy Resin Mixing Protocol

SIGMA 45359 Epoxy – Embedding Kit

- Must use glassware or silicone, as acetone ruins plastic
- Nothing touches any water during the process. This is because Epoxy resin is VERY hygroscopic and will not set if there is any water in the mixture.

1. Mix 5ml of Epoxy Embedding Medium with 8ml of DDSA anhydride curling agent in one glass tube. Label this MIXTURE A.
2. Mix 8ml of Epoxy Embedding Medium with 7ml of NMA anhydride curling agent in another glass tube. Label this MIXTURE B.
   - Mix has to be through, can be checked by colour (curling agents are yellowish whereas epoxy is transparent), and by seeing if 'lines' of uneven density is present.
   - Best to mix with glass stirrer, which can be cleaned afterwards using acetone as epoxy mixtures dissolve in acetone.
   - Transferring of fluids is best done with a disposable plastic pipette that can measure. Wait patiently for all drops to fall off because they are viscous.
3. Mix MIXTURE A and B together to make 28ml of FINAL EMBEDDING MEDIUM.
   - This will not set in room temperature. Best stored in freezer and can last several weeks. Check for thorough mixing as before.
   - Ratio of A to B will change hardness. Increased proportion of B will make it harder. For general use do not change the proportions as this is usually the best.
4. Add DPM-30 hardening accelerator before use. For 28ml of FINAL EMBEDDING MEDIUM, this will be approximately 16 drops (1.5~2.0%, or 0.45ml). Mix completely and thoroughly. The final colouration should look translucent yellow, slightly darker than before adding the accelerator. Label as FINAL EMBEDDING MEDIUM WITH ACCELERATOR.
   - This must be measured very carefully as overhardening (can be detected by mixture turning very dark) will make epoxy very brittle and unable to withstand sectioning with microtome.
   - This mixture can be kept in freezer for use of up to a couple of weeks.
   - Some FINAL EMBEDDING MEDIUM may be stored separately before mixing with accelerator to keep for longer. Label this FINAL EMBEDDING MEDIUM WITHOUT ACCELERATOR. In this case, carefully adjust accelerator volume to add to the rest.

Epoxy Resin Embedding Protocol

SIGMA 45359 Epoxy – Embedding Kit

✸ Nothing should touch water during the process — specimen must be completely dehydrated (i.e., water replaced by acetone completely) before the process begins. This is because Epoxy resin is VERY hygroscopic and will not set if there is any water in the mixture.

1. Prepare completely dry resin moulds made of silicone or other material.
2. Using a disposable pipette, fill the moulds to be used with FINAL EMBEDDING MEDIUM WITH ACCELERATOR but not completely full.
   - It is useful to have a couple of empty blocks made, just to check the quality and slicing texture of this batch of resin before sectioning the actual specimens.
3. Gently place specimen in the filled moulds. Position them so they are close to the front (ready for sectioning) and that they sit firmly on the bottom.
4. Top up the moulds full so the final block will have a flat top.
5. Draw in lab notebook how the specimens look and are positioned in each block.
6. Leave specimen to set in room temperature for 1-2 hours. This is for the air bubbles to come up from the block and they should be all gone by end of this step.
   - Make sure no fibre or dust is in the block. If there is, remove with forceps (can be cleaned with acetone later).
   - If some air bubbles are persisting on the top, pop them with forceps. This will be quite difficult due to the viscosity of the embedding medium.
7. Place the moulds into an oven at low temperature (60 degrees Celsius) for 18~36 hours. The best results can usually be achieved already at 20 hours.
8. Pop blocks off the moulds, check that there are no cracks or breaks.

Specimen Block Trimming Protocol

✸ Do not trim into the specimen or too close to it. The block can shatter. If whole specimen falls off this may be rescued by re-embedding or attaching to other pieces of plastic but if blade goes through the specimen it is definitely ruined.

1. The specimen block is applied to the microtome specimen mounting block, and placed under microscope, specimen-up.
   - A piece of wood / plastic / silicone is applied to the bottom of the mounting block to provide stability.
2. A blade is used to trim away extra resin of the specimen block where there is no tissue.
   - This is to reduce wear and chance of damage to the expensive diamond knife, so that minimum thickness goes through the knife.
   - It is best to first trim away a large block by going from top then chopping off from the side, and then as approach the specimen go at it in very thin slices.
3. The face which goes through the blade should be the side with less thickness. The face which goes through knife first and the face that the blade passes through last MUST be more or less parallel.
   - If not parallel the glue will not attach the slices and ribbons cannot form.
4. Usually, this means bottom and up faces are trimmed to parallel. These are best slightly sloped outwards so there is more mechanical strength to the block.
5. The right side should be the resin block bottom, which should be completely flat and specimen should sit at the edge of it, no need to trim this side.
6. The left side should be trimmed at a slope so the whole specimen block is a trapezoid, growing larger as the sectioning progresses. This helps to locate slice location if the slice is misaligned.
7. When trimming is complete, trim off the sides so they are clean and there is no plastic dust on the block. The specimen is now ready to proceed to the microtome.

Slideglass Cleaning Protocol

1. Place clean glasses in the soaking solution made up of 1:9 of 35% ammonia (NH_3) : 95% ethanol. Soak overnight at least.
2. Wash and scrub hard with washing liquid (any) and household sponge until foamy.
3. Wash off with tap water and rinse with distilled water thoroughly.
4. Store in glass container filled up with distilled water. This can be stored indefinitely for long-term.

Microtome Sectioning Protocol

LEICA RM2255 with DiATOME histo Jumbo diamond blade

- Three golden rules to make a perfect ribbon:
  1. Perfectly parallel trimming for lower & upper sides
  2. Layer of glue perfectly covers the lower side
  3. Blade trough filled up just right, tension on edge
- Above all, dust is the enemy.
- Nothing should touch the diamond knife blade except the specimen block.

1. Set specimen on the microtome using the specimen holder. Tighten down the screws of the holder. Do not touch other knobs around the holder as these will change the angle of specimen.
2. Gently apply a layer of glue (best glue: EVO-STIK TIMEBOND Multi-Purpose Adjustable Contact Adhesive, 65g tube) over the bottom side of the specimen block. This makes specimen slices ribbon.
   - The glue may be applied prior to mounting, under a microscope. The glue is the magic part of the process, yet it is also the most intricate. If ribbons do not form properly, re-apply the glue as an uneven glue layer is usually the cause.
3. Take the diamond knife out of case and place onto the microtome. Tighten down the screws.
4. Have the following ready beside the microtome:
   - Beaker half-full of distilled water, colour-coded and marked with CLEAN, and a glass pipette of the same colour code. This will be used to pipette clean water into the diamond knife trough. Must be glass pipettes as plastic introduce plastic

dust.

- Beaker empty, colour-coded and marked with WASTE, a glass pipette of the same colour code. This will be used to pipette off waste, dusty water from the diamond knife trough.
- Eyelash brushes for manipulating slices.
- Filter paper to wipe specimen off of excess water.
- "Pith", the heart of palm trees. This material is used to clean the diamond knife, by letting it gently cut through the pith.
- Forceps for picking fibre or dust out.
- A box of Kim-Wipe.
- A dark surface or tile.
- A hot plate switched on.

5. Pour water into the knife trough from CLEAN beaker, adjust with pipettes. With tip of pipette, bring a film of water (use surface tension) over top of knife. The surface tension of water needs to come up right to the knife edge.
   - Check the trough for over-filling. If water level is above the metal sides of the trough due to surface tension, pipette away until level using WASTE pipette. This is because if there is no drop in water level away from the blade edge, the slices will not automatically flow away to form ribbons.
6. Retract the specimen completely using the ⇈ button.
7. Check the settings on the microtome. The slice thickness should be 1.5um, the speed should be set to 1.4 (ie. black line) OR LESS (faster speeds will damage the diamond blade). The only two modes to be used are SINGLE and CONTINUOUS.
8. With hand on the microtome turner (palm-on preferred), bring the specimen close to the blade. Adjust the position of specimen using ⇊ and ↓ buttons so they are close to the blade.
   - Adjust lights so that the specimen surface reflect the diamond knife edge, this gives a better prediction of how close the specimen is to the blade.
   - Rock hand back and forwards above the blade to test the position. It is better to be generous and leave more space rather than haste and risk damaging the diamond blade.
   - The microtome should only go one way. Never manually back-turn the microtome for a full turn.
9. When satisfied with specimen position, set the cutting window (a space when the microtome slows down for precision slicing) for the specimen. Position the specimen one specimen height above the blade, press the ↕ button once. Pass the specimen

through the knife, and one specimen height below the knife, press the ↕ button again. This sets the cutting window.

- It is better to be generous than risking damage to the blade. It is easier to be generous above the blade than below because you can't really see the specimen when setting the lower end, so be even more generous. Smaller window means faster process time but it has to balance with risk to the blade.

10. Manually turn the microtome a full-turn, set the mode to SINGLE to test the cutting edge. Start the microtome by pressing START/STOP and ENABLE button together. If not happy with the cutting window, re-set it and test again until satisfied.
11. Now you are ready for sectioning. Set the mode to CONTINUOUS. Press START/STOP and ENABLE together to start the microtome. Pressing either button when microtome is running will make it stop *after completing* the current cycle.
    - When the microtome is stopped, always manually lock the turner by using the manual-lock bar above the manual turning handle; to avoid accidentally damaging the diamond blade.
    - The first cycles will be empty until the specimen comes in contact with the blade, and after that the initial slices made will just be trimming away on the extra resin. If there is a known damaged portion of the blade, move to that section of the blade for trimming.
12. After trimming and when ribbons begin to form, stop the microtome. If the slices are more or less rectangular in shape but no ribbons are formed, re-apply the glue by taking old layer off using forceps under microscope and putting a new layer on.
    - Always re-do the position adjustment if specimen has been removed from holder. There may have been slight changes in angle or position of the specimen and the blade may be damaged if this is the case.
13. Clean the diamond blade trough.
    - With a piece of tissue paper, gently go through surface of water. Most trimmed sections should attach to the wipe and be easily removed.
    - With the waste pipette, pipette away water of the trough until more or less empty. Then wipe down the trough with Kim-Wipe.
    - If the blade is dusty, clean by gently letting it slice through the pith.
14. As before, re-fill the trough with water and make sure the surface tension is at the blade. Move to a clean, undamaged position of the diamond blade for specimen sectioning.
15. Begin sectioning continuously by starting the microtome. The slices should glue together in ribbons and float on the surface of trough.

- Count the slices! It is very important to know exactly which slice number you are on for the reconstruction process.

16. When the ribbons are of a certain length (around 20~30 sections), stop the microtome. Gently lift the final slice (don't touch the blade) using eyelash brush and it should separate from the blade. Manipulate and float it to the bottom of trough.
17. Start microtome again and make more ribbons. When you have enough (3~4 ribbons for beginners) for a slide, mount them onto a slide glass. The slide glasses should be cleaned in the aforementioned steps and stored in distilled water.
18. Insert gently a clean slide glass from the side away from the blade. While inserting manipulate ribbons with eyelash brush so they all stay in correct order and position.
19. When half inserted, drop a few drops of distilled water along the slide glass using the CLEAN pipette. This gives enough surface tension to pull the ribbons up.
20. With the eyelash brush, pull the ribbons up to middle of the slide glass. The order of slices should be aligned left to right, lower to upper.
21. Lift the slide with all ribbons on, place on to a dark, flat surface. Suspend the ribbons with a couple more drops of distilled water with CLEAN pipette. Manipulate the ribbons so they are in neat and tidy order.
22. Place the slide glass onto the heat plate, which should already be on. The ribbons are likely to bend or move due to the temperature, but they cannot be manipulated as they will stick to the eyelash brush.
23. Repeat steps 15~22 to make more ribbons and slides.
    - If lose slices, take a note. Always count slices.
    - If ribbons not forming properly, re-apply the glue and then re-align the specimen.
    - If the trough gets dusty, replace water and clean again.
24. When you have sufficient slices for what you want to do, stop the microtome and lock it. Clean the trough and remove diamond blade, place it into the diamond blade holder box.
25. Remove the specimen.
26. The slides should be dry. When they are dry, remove them carefully from the hotplate and lable on the corner using a diamond-tip pen.
27. Store slides in a slide box.

Slide Staining Protocol

Ruthensteiner, 2008 Zoosymposia 1: 63-100.

1. Make "Richardson's Stain" = Methylene blue-azur II stain = Mallorys azur II-methylene blue stain by mixing:
   i. 1 gram of Methylene blue
   ii. 1 gram of Azur II
   iii. 1 gram of Sodium tetraborate ("borax")
   - And finally top up with distilled water to 100ml
2. This makes a stock solution. For use, dilute down 1:1 with distilled water to make 50% concentration. Sometimes 30%-40% gives a better result if 50% is too quick in staining.
3. Secure working area using cling film cover to prevent staining the bench.
4. Switch on hotplate.
5. Pour out some 50% concentration stain into glassware.
6. Place a slide glass to be stained on a flat surface.
7. With a syringe (covered with filter), squirt some stain over the slide glass. Spread with the needle.
8. Place slide glass with stain liquid on the hotplate for FIVE SECONDS.
9. Remove, pour stain back in the reservoir and rinse slide glass thoroughly with distilled water.
10. Dry the slide glass on hotplate or blott dry using Whatman Slideglass Blotter Paper.
11. Repeat steps 6-10 until all slides to be stained are done.

Cover-Slipping Protocol

Agar Scientific Araldite CY212 Embedding Kit R1030

- ✸ Coverslipping is required to achieve photographing of the slides with best possible quality.
- ✸ If the slides are of sufficient quality without coverslipping, this step is not necessary.
- ✸ All containers and equipments must be glass or silicone, and not plastic.

1. The standard embedding medium is obtained by mixing:
   - 20ml = 23.0g * Araldite CY212
   - 22ml = 22.0g * DDSA
   - 1.1ml = 1.2g * BDMA
     - Araldite CY212 may be replaced by Araldite M for the same effect.
     - For softer blocks, add 1.0ml of platiciser: dibutyl phthalate.
     - For harder blocks, replace 1.0ml of DDSA with 0.5ml of hardener: methyl nadic anhydride (MNA).
2. Wait for all solutions to warm up naturally to room temperature. This is to prevent water dew forming.
3. Warm up a graduated cylinder and a conical flask to 60 degrees Celcius in an oven. Care must be taken because it may be impossible to clean these post-mixing. A wider-
- The Araldite CY212 and DDSA may also be heated at 60 degrees before mixing to facilitate faster mixing.
4. Measure by volume Araldite CY212 and DDSA with the warmed measuring cylinder, and then immediately poured into the warmed conical flask.
5. Mix by swirling and using a glass stirrer. It is important that the two fluids are completely and thoroughly mixed for successful results.
6. Add BDMA and continue to mix until completely mixed.
7. With glass pipette, pipette a very small amount of mixed Araldite resin onto the slide mounted with histological sections.
8. Apply a glass coverslip carefully.
9. Repeat until all slides requiring cover slips are done. Place all slides into the oven set and preheated to 60 degrees Celcius.
10. The resin will set overnight, but for best effects leave for 24 to 48 hours in oven.
11. If there is any leftover mixed resin, label, seal with parafilm, and place into the freezer.
12. The sections are now ready to be digitised for importing to Amira v5.3.3.

Supplementary Material 2: Full Interactive 3D Model

(In hardcopy this material is provided on a CD supplemented to the thesis)

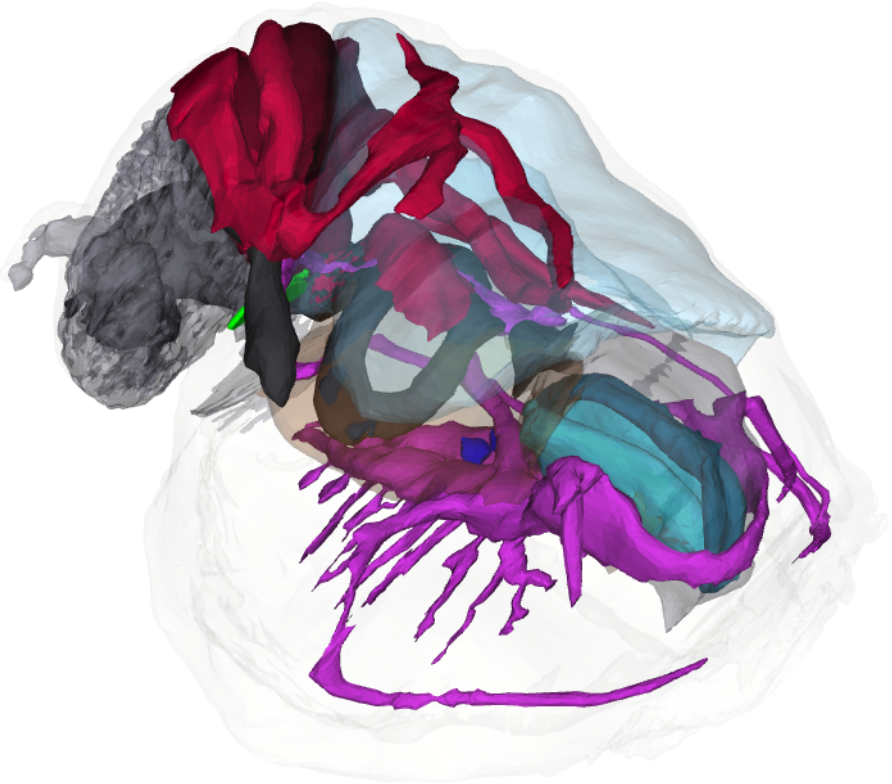

3D tomographic reconstruction of the 'scaly-foot gastropod', full interactive model. The interactive model can be accessed by clicking into the figure (Adobe Acrobat Reader v7 or higher). Hold left click and drag to rotate, hold down ctrl while doing so to move, and hold down shift while doing do to zoom (alternatively hold right click and drag or use mouse wheel). Switch between pre-saved views using the dropdown menu in the floating window or click on the view pane in the model tree. Components can also be activated or deactivated by toggling the checkbox in the model tree. The 3D PDF was generated using Adobe Acrobat Pro XI by importing .u3d files, converted from .obj exports of Amira v5.3.3 surface files.

Chapter 5

How the mollusc got its scales: convergent evolution of the molluscan scleritome

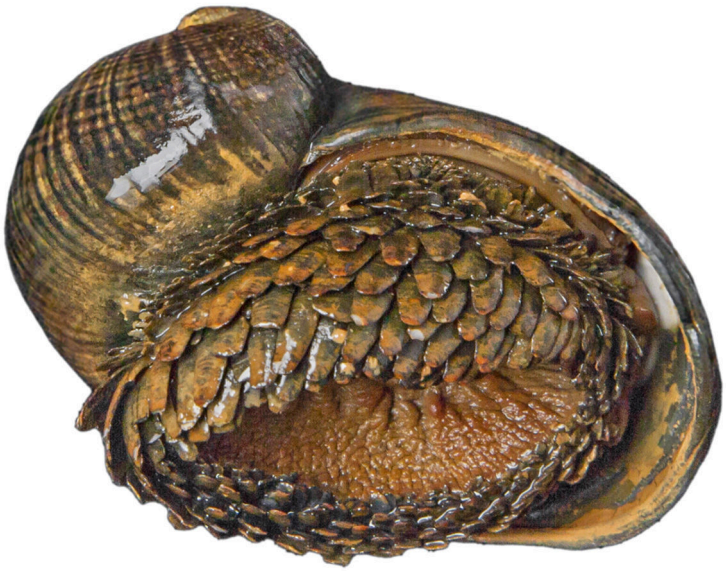

(*Biological Journal of the Linnean Society,* Published)

CHAPTER INTRODUCTION

The previous chapter dealt in detail the internal anatomy of the 'scaly-foot gastropod' *Chysomallon squamiferum*, and this chapter follows up to look at the most intriguing part of its external anatomy – the sclerites.

Chrysomallon squamiferum is unique among gastropods in having dermal sclerites. Though other gastropods, such as members of Acochlidea, have calcareous spicules these are very different from the 'scaly-foot gastropod' sclerites as they are subdermal (Schrödl & Neusser, 2010). The sclerites of *C. squamiferum* are superficially similar to structures known from the 'Aculifera' (i.e., molluscan classes Caudofoveata, Solenogastres, and Polyplacophora; Sigwart & Sutton, 2007) Polyplacophorans (chitons) especially, often produce large scales like *C. squamiferum*. In addition, Cambrian metazoans such as the clade Halwaxiida also carry similar scleritomes (Conway Morris & Caron, 2007). The similarity of these scleritomes with those of aculiferans has been used as a central evidence for their molluscan affinity especially as stem-group aculiferans (Vinther, 2009).

In this chapter, scleritomes of *Chrysomallon squamiferum* is investigated histologically to compare with those of chitons and halwaxiids. A possible origin of sclerites in *C. squamiferum* has been suggested to be multiplication of the operculum (Warén *et al*., 2003), and the likelihood of this hypothesis was also assessed histologically.

STATEMENT OF AUTHOR CONTRIBUTIONS

The main text of this chapter has been published in *Biological Journal of the Linnean Society*, as a Short Research Article (Manuscript ID BJLS-3698 / BIJ 12462; submitted October 2014, accepted November 2014, published January 2015). The authors (in this order) are Chong Chen (corresponding author), Jonathan T. Copley, Katrin Linse, Alex D. Rogers, and Julia D. Sigwart; the detailed author contributions are as follows.

The original idea for the project was conceived by JS and CC. Methodology and project plan were developed by JS. JTC and ADR provided funding for both sample collection on-board *RRS* James Cook research cruises JC66/67. On-board the cruises CC, JTC, and ADR participated in sample collection and tissue fixation of the specimens used in this study. JS secured polyplacophoran specimens for comparison. JS and CC were responsible for all laboratory work and data collection. CC wrote the original manuscript. All authors discussed the results and implications of the study in detail and edited the manuscript for improvement. JS, ADR, JTC, and KL supervised the work of CC during the length of this study.

Published Article:

Chen C, Copley JT, Linse K, Rogers AD, Sigwart J. 2015. How the mollusc got its scales: convergent evolution of the molluscan scleritome. *Biol J Linn Soc***:** doi: 10.1111/bij.12462.

How the mollusc got its scales: convergent evolution of the molluscan scleritome

Chong Chen[1*], Jonathan T. Copley[2], Katrin Linse[3], Alex D. Rogers[1], Julia Sigwart[4]

[1] Department of Zoology, University of Oxford, The Tinbergen Building, South Parks Road, Oxford OX1 3PS, United Kingdom

[2] Ocean and Earth Science, University of Southampton, European Way, Southampton SO14 3ZH, United Kingdom

[3] British Antarctic Survey, High Cross, Cambridge CB3 0ET, United Kingdom

[4] Queen's University Belfast, Marine Laboratory, Portaferry, Co. Down, N. Ireland BT22 1PF

** Corresponding author: chong.chen@zoo.ox.ac.uk*

Running Title

Convergent evolution of the molluscan scleritome

Abstract

Radiation of dramatically disparate forms among the phylum Mollusca remains a key question in metazoan evolution, and requires careful evaluation of homology of hard parts throughout the deep fossil record. Enigmatic early Cambrian taxa such as *Halkieria* and *Wiwaxia* (in the clade Halwaxiida) have been proposed to represent stem-group aculiferan molluscs (Caudofoveata + Solenogastres + Polyplacophora), as complex scleritomes were considered to be unique to aculiferans among extant molluscs. The scaly-foot gastropod (Neomphalina: Peltospiridae) from hydrothermal vents of the Indian Ocean, however, also carries dermal sclerites and thus challenges this inferred homology. Despite striking external similarities, the scaly-foot gastropod sclerites are secreted in layers covering outpockets of epithelium and are largely proteinaceous, while chiton (Polyplacophora: Chitonida) sclerites are secreted to fill an invaginated cuticular chamber and are largely calcareous. Marked differences in underlying epithelium of the scaly-foot gastropod sclerites and operculum suggest that the sclerites do not originate from multiplication of the operculum. This convergence between different classes highlights the ability of molluscs to adapt mineralised dermal structures, supported by extensive early fossil record of molluscs with scleritomes. Sclerites of halwaxiids are morphologically variable, undermining the assumed affinity of specific taxa with chitons, or the larger clade Aculifera. Comparisons with independently-derived similar structures in living molluscs are essential for determining homology among fossils and their position with respect to the enigmatic evolution of molluscan shell forms in deep time.

Keywords

Scaly-foot gastropod, Polyplacophora, Aculifera, *Wiwaxia*, *Halkieria*

Introduction

Extant classes of molluscs exhibit great disparity in body armour and shell forms, and this radiation within the phylum remains poorly understood. For example, Polyplacophora (chitons) have eight shell plates compared with two shells in Bivalvia, one in most other extant molluscan groups, and repeated reduction or loss across the phylum (Furuhashi *et al*., 2009). Central to solving this puzzle is evaluation of the homology of hard parts throughout the deep fossil record of molluscs as well as early mollusc-like animals. Scale-like structures are uncommon among extant Mollusca and were thought to be a distinctive characteristic uniting a total group of 'Aculifera', a proposed clade within Mollusca (Caudofoveata + Solenogastres + Polyplacophora; Scheltema, 1993; Sigwart & Sutton, 2007).

Many groups of Cambrian metazoans are also known for having dermal sclerites (e.g., halkieriids, tommotiids, sphogonuchitids; Bengtson, 1992). Halwaxiida, a clade of metazoans characterised by a body covered by sclerites and many having shell plates, is one representative group (Conway Morris & Caron, 2007). The most notable members are *Halkieria*, with two shells, one on the anterior end and one on the posterior end; *Wiwaxia*, with no shell (Fig. 1E); and *Orthrozanclus*, with only one anterior shell. The systematic position of halwaxiids has been extensively debated (e.g., Butterfield, 2006; Conway Morris & Caron, 2007); most recently they have been argued to be stem-group

aculiferans (Vinther & Nielsen, 2005; Vinther, 2009).

One important argument for halwaxiids' molluscan affinity has been the similarity of sclerites to those of the aculiferans, especially chitons. Vinther (2009) described a complex canal system in *Sinosachites delicatus* (Jell, 1981) and noted its resemblance to chiton aesthetes. Recently the idea of halwaxiids as early molluscs has been reinforced by similarities of *Wiwaxia* mouthparts to the radula of modern molluscs (Smith, 2012), yet sclerites continue to be a central piece of evidence tying halwaxiids to aculiferan molluscs (Smith, 2014).

An unusual gastropod discovered at hydrothermal vents in the Indian Ocean (Van Dover *et al*., 2001) challenges the idea that sclerites of halwaxiids reliably tie them to aculiferans. It has numerous dermal sclerites, imbricating like roof-tiles (Warén *et al*., 2003; Fig. 1A), covering the entire dorsal surface of the foot. These are often covered with a layer of iron sulfide (pyrite FeS_2 and greigite Fe_3S_4, Warén *et al*., 2003) although one population lacks it (Solitaire Field, Nakamura *et al*., 2012). This "scaly-foot gastropod" is the only known extant or extinct gastropod with dermal sclerites. Although the species is thus far not formally described, both genetic and morphological investigations reliably place scaly-foot gastropods within Peltospiridae (Warén et al., 2003), a family in the gastropod clade Neomphalina. The scaly-foot sclerites are superficially very similar to those of other molluscs, especially sclerites on chiton girdles (Fig. 1). Given the distant phylogenetic position of the two (a derived gastropod, and chitons) and that no other gastropods possess sclerites, these are unlikely to be homologous structures. The discovery of the scaly-foot gastropod implies that dermal

sclerites may be a rapidly evolving, derived structure, and brings the homology of halwaxiid and other molluscan sclerites to question, as mentioned briefly by Warén *et al*. (2003) and Smith (2014). Although it has been suggested in the past that the scaly-foot sclerites are homologous to an operculum and represent an operculum duplication event (Warén *et al*., 2003), the discovery of a true operculum in scaly-foot gastropods (Nakamura *et al*., 2012) casts doubt on this hypothesis. In this study, the anatomy of scaly-foot gastropods' sclerites was investigated to shed light on its anatomical origin via comparison with the gastropod operculum as well as dermal sclerite structures in aculiferans.

Materials & Methods

More than 300 specimens of the scaly-foot gastropod, ranging from juveniles of 5-10 mm shell length to adults of up to 45 mm shell length, from all three known localities were examined: Longqi vent field (Tao *et al*., 2014), Southwest Indian Ridge, 37°47.03'S 49°38.97'E ('Tiamat Chimney'), depth 2785 m, collected during RRS *James Cook* Voyage JC67 using the *Kiel6000* remotely operated vehicle (ROV), fixed and stored in 4% formalin (around 200 specimens); Solitaire vent field, Central Indian Ridge, 19°33.41'S, 65°50.89'E, depth 2606 m (approximately 100 specimens); Kairei vent field, Central Indian Ridge, 25°19.24'S, 70°02.43'E, depth 2415 m to 2460 m (20 specimens); Central Indian Ridge specimens are from the collections of the Japan Agency for Marine-Earth Science and Technology, fixed and stored either in 4% formalin or 99% ethanol.

For the scaly-foot gastropod, specimens from the three known localities were used to examine the ontogeny of vestigial operculum. For detailed morphological examination, the operculum and adjoining tissue, including sclerites, were dissected from the foot of adult and juvenile specimens from the Longqi vent field. For chiton specimens, a section of the girdle was removed from the right side of the body adjacent to valve II (first valve posterior of the head valve). The dissected tissues were decalcified in 2% EDTA for 48 hours and prepared for sectioning following the methods of Ruthensteiner (2008): implementing dehydration in an acetone series, embedding in Epon epoxy resin following the manufacturer's instructions (SIGMA 45359 Epoxy Embedding Kit), and serial sectioning at 1.5 μm using an automated rotary microtome (Leica RM2255) fitted with a diamond knife (DiaTome HistoJumbo 8 mm). Resulting sections were stained with the high contrast monochromatic Richardson's stain and examined with a compound microscope (Olympus BX41) with digital images captured via a SLR camera attached to the microscope trinocular (Olympus E-600).

Results and Discussion

The presence of sclerites has been a central theme in arguments about the placement of certain enigmatic Cambrian fossils, halwaxiids in particular, within Mollusca (Smith, 2014). Although the molluscan affinities of *Halkieria* and *Wiwaxia* among others are based on multiple lines of evidence (Vinther, 2009; Smith, 2012), the complex dorsal scleritomes of these taxa (Fig. 1) have been used to compare them directly with living representatives of Polyplacophora and spiculose aplacophorans (Vinther, 2009). Merged sclerites in halkierrids have been used to suggest sclerite fusion as the origin of

139 molluscan shell plates (Missarzhevsky, 1989; Bengtson, 1992).

140

141 Polyplacophoran sclerites are highly variable among chiton species (Eernisse &
142 Reynolds, 1994), with some taxa including prominent large aragonitic calcareous scales
143 (Fig. 1C). These scales do not form on any kind of stalk but sit on a compressed
144 secretory epithelium, at the bottom of a pocket within the cuticle, and the scales appear
145 to grow through secreting calcareous material to fill the cavity (Blumrich, 1891; Fig.
146 1D). These large scales are typical of the superfamily Chitonoidea; other species have
147 various structures, but all grow through the same mechanism of an infilled pocket of
148 epithelium underlying the girdle cuticle (Blumrich, 1891; Leise & Cloney, 1982).

149

150 Through the cross-section of a decalcified scaly-foot gastropod sclerite (Fig. 1B), clear
151 growth lines are visible. These sclerites do not contain calcareous material, but instead
152 are made almost entirely of conchiolin as previously reported (Warén *et al*., 2003). The
153 sclerite contains a projection of pedal tissue from the base to approximately 1/3 of the
154 length to the tip. The tissue is mainly pedal musculature penetrated by nerve fibres, and
155 a single layer of tall columnar epithelial cells is present on the contact surface with the
156 sclerite. The sclerite appears to be secreted in layers covering the epithelial layer, and
157 thus it grows by a new layer pushing older layers outwards. Other than the projection of
158 pedal musculature, sclerites of the scaly-foot gastropod have no internal structures.

159

160 A major question remains as to the anatomical origin of the gastropod scales. Early
161 suggestions that the scaly-foot sclerites represent an operculum duplication event
162 (Warén *et al*., 2003) were undermined by the discovery of a true operculum in

scaly-foot gastropods (Nakamura *et al*., 2012), and our examination of adults from all three populations confirm that all have an operculum. Clear differences in the underlying epithelium suggest that the sclerites do not represent multiplication of the operculum (Fig. 2). The adult operculum has a relaxed coiling and elongate shape, but in juveniles it is multi-spiral and circular (Nakamura *et al*., 2012; Fig. 2C). The scaly-foot gastropod operculum is attached to the foot by a small pad, and the anterior edge rests in a pocket surrounded by tall columnar epithelial cells, which are approximately double the height of those at the operculum attachment.

The secretory epithelium and structure of the sclerites clearly differ from the operculum, thus the scales apparently represent an independent mineralisation of other structures across the surface of the foot. Dermal tentacles are another notable feature of the plastic, multiplied out-pockets of epithelium widespread across the foot. Peltospirids, and the closely related gastropod clade Vetigastropoda (Aktipis & Giribet, 2012), are notable for repeated emergence of tentacles around the operculum and on the posterior part of the foot (McLean, 1989; Warén & Bouchet, 1989). These tentacles are entirely independent of the cuticular formation of sclerites in (for example) Polyplacophora, but similar structures cannot be excluded as a potential origin of scleritomes in fossil taxa.

Our examinations showed that the scaly-foot gastropod sclerites (Fig. 1B) are clearly constructed in very different manner to chiton scales (Fig. 1D), and are made of different materials. As might be expected from such phylogenetically distant clades as Polyplacophora and a single derived gastropod, the superficial similarity of these scleritomes is limited to a functional convergence, and not indicative of any apparent

187 anatomical homology. Importantly, the existence of convergent scales through different
188 growth mechanisms undermines comparisons of Halwaxiida to specific crown-group
189 taxa.
190
191 Halwaxiida (Conway Morris & Caron, 2007) represents a broad morphological diversity
192 of individual sclerites within and among taxa, similar to the structural diversity
193 observed within other classes of molluscs. *Halkieria* and sachtid sclerites have a central
194 spine that had a tissue-filled canal (Vinther, 2009), which are potentially more
195 analogous to the scales of the scaly-foot gastropod than cuticular elements in chitons or
196 aplacophorans.
197
198 The distinctive iron-mineralised scales of the scaly-foot gastropod inspired extensive
199 research into external structure, function, and potential animal-mediated precipitation of
200 minerals (Suzuki *et al*., 2006; Yao *et al*., 2010). These ongoing studies will provide a
201 sound basis to understand the anatomical origin of mineralised structures in the
202 scaly-foot gastropod and other molluscs, and inform the interpretation of such structures
203 in the deep molluscan fossil record. The presence of sclerite elements has multiple
204 independent evolutionary origins, possibly driven by myriad adaptations on the notably
205 plastic molluscan bauplan.
206
207 Molluscs *sensu lato* are capable of creating diverse mineralised dermal structures,
208 including two classes of aplacophoran molluscs (Solenogastres, Caudofoveata), chitons,
209 and many gastropods such as several heterobranch clades which produce subdermal
210 calcareous spicules for example Acochlidea (Schrödl & Neusser, 2010; Jörger *et al*.,

211 2010) and Rhodopemorpha (Brenzinger, Haszprunar & Schrödl, 2013). The
212 relationships among the living classes of molluscs remain contentious (e.g. Smith *et al.,*
213 2011; Stöger *et al*., 2013; Sigwart & Lindberg, in press). Fossils are an essential line of
214 evidence to establish the topology of molluscan phylogeny, which remains one of the
215 major questions in metazoan evolution (Telford & Budd, 2011; Telford, 2013; Sigwart
216 & Lindberg, in press). Claims of affinity of halwaxiids to any specific class within
217 Mollusca requires more than a 'just so' story, and calls for a detailed analysis of
218 morphological homology.
219

220 **Acknowledgements**

221

222 This research was supported by a Malacological Society of London Research Grant to
223 CC. The master and crew of the RRS *James Cook* as well as pilots and technical teams
224 of ROV *Kiel 6000* are acknowledged for their great support during the expedition JC67
225 funded by NERC Small Research Grant NE/H012087/1 to JTC. Enrico Schwabe
226 (Zoologische Staatsammlung, Munich) is thanked for providing specimens of
227 *Enoplochiton niger*. Dr Hiromi Watanabe and Dr Ken Takai (Japan Agency for
228 Marine-Earth Science and Technology) kindly allowed access to scaly-foot gastropod
229 specimens from the Central Indian Ridge. Finally, we would like to thank two
230 anonymous reviewers for their helpful comments.
231

References

Aktipis SW, Giribet G. 2012. Testing relationships among the vetigastropod taxa: a molecular approach. *Journal of Molluscan Studies* **78:** 12-27.

Bengtson S. 1992. The cap−shaped Cambrian fossil *Maikhanella* and the relationship between coelosclerítophorans and molluscs. *Lethaia* **25:** 401-420.

Blumrich J. 1891. Das Integument der Chitonen. *Zeitschrift für Wissenschaftliche Zoologie* **52:** 404-476.

Brenzinger B, Haszprunar G, Schrödl M. 2013. At the limits of a successful body plan – 3D microanatomy, histology and evolution of Helminthope (Mollusca: Heterobranchia: Rhodopemorpha), the most worm-like gastropod. *Frontiers in Zoology* **10**: 37

Butterfield NJ. 2006. Hooking some stem-group "worms": fossil lophotrochozoans in the Burgess Shale. *BioEssays* **28:** 1161-1166.

Conway Morris S, Caron J-B. 2007. Halwaxiids and the Early Evolution of the Lophotrochozoans. *Science* **315:** 1255-1258.

Eernisse D, Reynolds P, Harrison F, Kohn A. 1994. Polyplacophora. *Microscopic Anatomy of Invertebrates* **5**.

Fretter V. 1989. The anatomy of some new archaeogastropod limpets (Superfamily Peltospiracea) from hydrothermal vents. *Journal of Zoology* **218:** 123-169.

Furuhashi T, Schwarzinger C, Miksik I, Smrz M, Beran A. 2009. Molluscan shell evolution with review of shell calcification hypothesis. *Comparative Biochemistry and Physiology Part B: Biochemistry and Molecular Biology* **154:** 351-371.

Jörger KM, Stöger I, Kano Y, Fukuda H, Knebelsberger T, Schrödl M. 2010. On the origin of Acochlidia and other enigmatic euthyneuran gastropods, with implications for the systematics of Heterobranchia. *BMC Evolutionary Biology* **10:** 323.

Leise EM, Cloney RA. 1982. Chiton integument: ultrastructure of the sensory hairs of Mopalia muscosa (Mollusca: Polyplacophora). *Cell and Tissue Research* **223:** 43-59.

McLean JH. 1989. New archaeogastropod limpets from hydrothermal vents: new family Peltospiridae, new superfamily Peltospiracea. *Zoologica Scripta* **18:** 49-66.

Missarzhevsky V. 1989. Drevnejshie skeletnye okamenelosti i stratigrafiya pogranichnykh tolshch dokembriya i kembriya.[The oldest skeletal fossils and stratigraphy of the Precambrian–Cambrian boundary beds.]. *Trudy Geologicheskogo Instituta AN SSSR* **443:** 1-237.

Nakamura K, Watanabe H, Miyazaki J, Takai K, Kawagucci S, Noguchi T, Nemoto S, Watsuji T, Matsuzaki T, Shibuya T, Okamura K, Mochizuki M, Orihashi Y, Ura T, Asada A, Marie D, Koonjul M, Singh M, Beedessee G, Bhikajee M, Tamaki K. 2012. Discovery

of new hydrothermal activity and chemosynthetic fauna on the Central Indian Ridge at 18°–20°S. *PLoS ONE* **7:** e32965.

Ruthensteiner B. 2008. Soft part 3D visualization by serial sectioning and computer reconstruction. *Zoosymposia* **1**: 63-100.

Scheltema, AH. 1993. Aplacophora as progenetic aculiferans and the coelomate origin of mollusks as the sister taxon of Sipuncula. *Biological Bulletin* **184**: 57–78

Sigwart JD, Lindberg DR. *In press.* Concensus and confusion in molluscan trees. *Systematic Biology*.

Schrödl, M, Neusser TP. 2010. Towards a phylogeny and evolution of Acochlidia (Mollusca: Gastropoda: Opisthobranchia). *Zoological Journal of the Linnean Society* **158**: 124-154.

Sigwart JD, Sutton MD. 2007. Deep molluscan phylogeny: synthesis of palaeontological and neontological data. *Proceedings of the Royal Society B: Biological Sciences* **274:** 2413-2419.

Smith SA, Wilson NG, Goetz FE, Feehery C, Andrade SC, Rouse GW, Giribet G, Dunn CW. 2011. Resolving the evolutionary relationships of molluscs with phylogenomic tools. *Nature* **480:** 364-367.

Smith MR. 2012. Mouthparts of the Burgess Shale fossils Odontogriphus and Wiwaxia: implications for the ancestral molluscan radula. *Proceedings of the Royal Society B: Biological Sciences* **279:** 4287-4295.

Smith MR. 2014. Ontogeny, morphology and taxonomy of the soft-bodied Cambrian 'mollusc' Wiwaxia. *Palaeontology* **57:** 215-229.

Stöger I, Sigwart JD, Kano Y, Knebelsberger T, Marshall BA, Schwabe E, Schrödl M. 2013. The Continuing Debate on Deep Molluscan Phylogeny: Evidence for Serialia (Mollusca, Monoplacophora + Polyplacophora). *BioMed Research International* **2013:** 18.

Suzuki Y, Kopp RE, Kogure T, Suga A, Takai K, Tsuchida S, Ozaki N, Endo K, Hashimoto J, Kato Y, Mizota C, Hirata T, Chiba H, Nealson KH, Horikoshi K, Kirschvink JL. 2006. Sclerite formation in the hydrothermal-vent 'scaly-foot gastropod': possible control of iron sulfide biomineralization by the animal. *Earth and Planetary Science Letters* **242:** 39-50.

Tao C, Li H, Jin X, Zhou J, Wu T, He Y, Deng X, Gu C, Zhang G, Liu W. 2014. Seafloor hydrothermal activity and polymetallic sulfide exploration on the southwest Indian ridge. *Chinese Science Bulletin*: 1-11.

Telford MJ, Budd GE. 2011. Invertebrate evolution: bringing order to the molluscan chaos. *Current Biology* **21:** R964-R966.

Telford MJ. 2013. Mollusc Evolution: Seven Shells on the Sea Shore. *Current Biology* **23:** R952-R954.

Vinther J. 2009. The canal system in sclerites of lower Cambrian sinosachites (Halkieriidae:

Sachitida): significance for the molluscan affinities of the sachitids. *Palaeontology* **52:** 689-712.

Warén A, Bouchet P. 1989. New gastropods from East Pacific hydrothermal vents. *Zoologica Scripta* **18:** 67-102.

Warén A, Bengtson S, Goffredi SK, Van Dover CL. 2003. A hot-vent gastropod with iron sulfide dermal sclerites. *Science* **302:** 1007.

Yao H, Dao M, Imholt T, Huang J, Wheeler K, Bonilla A, Suresh S, Ortiz C. 2010. Protection mechanisms of the iron-plated armor of a deep-sea hydrothermal vent gastropod. *Proceedings of the National Academy of Sciences* **107:** 987-992.

Figures

Figure 1. (A) Apex view of a scaly-foot gastropod showing the shell and numerous sclerites, (B) Semithin central section through a fully grown scaly-foot gastropod sclerite showing dermal tissue canal penetrating the scale and layering of the scale conchiolin, (C) *Enoplochiton niger* showing sclerites on the girdle (ZSM Mol-20034094, La Herradura, Chile, coll. 17 Nov. 2003), (D) Semithin section of the same specimen (*E. niger*) girdle sclerite, (E) *Wiwaxia corrugata* Walcott, 1911 (ROM 61510), (F) Cross section of *W. corrugata* sclerites (ROM 62270). Scale bars: 10 mm (A, C), 5 mm (E), 1 mm (B, F), 0.5 mm (D). Labels indicate *analogous* structures, cu = cuticle, pm = pedal musculature, sc = sclerite, e = epithelium. Images (E) and (F) reproduced from Smith (2014) with kind permission from the Palaeontologial Association.

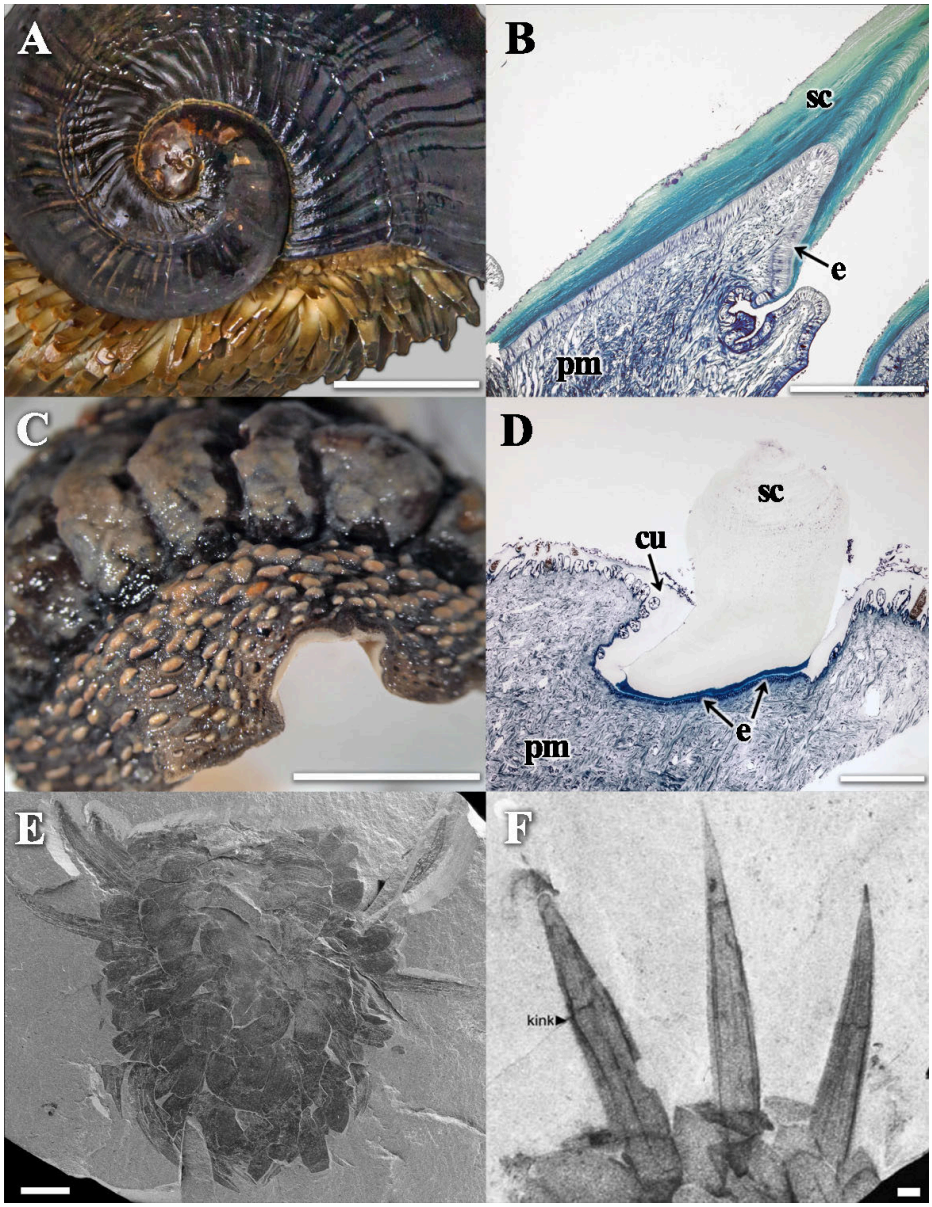

Figure 2. (A) Operculum of an adult scaly-foot gastropod seen *in situ*, with layers of sclerites above the operculum removed, (B) Semithin section through the scaly-foot gastropod operculum and scales with the white arrowhead indicating proximal end of operculum attachment, (C) Ontogeny of scaly-foot gastropod operculums: from top juvenile, sub-adult, adult specimens. Scale bars: 5 mm (A), 1 mm (B), 2 mm (C). Labels indicate *analogous* structures, pm = pedal musculature, sc = sclerite, e = epithelium.

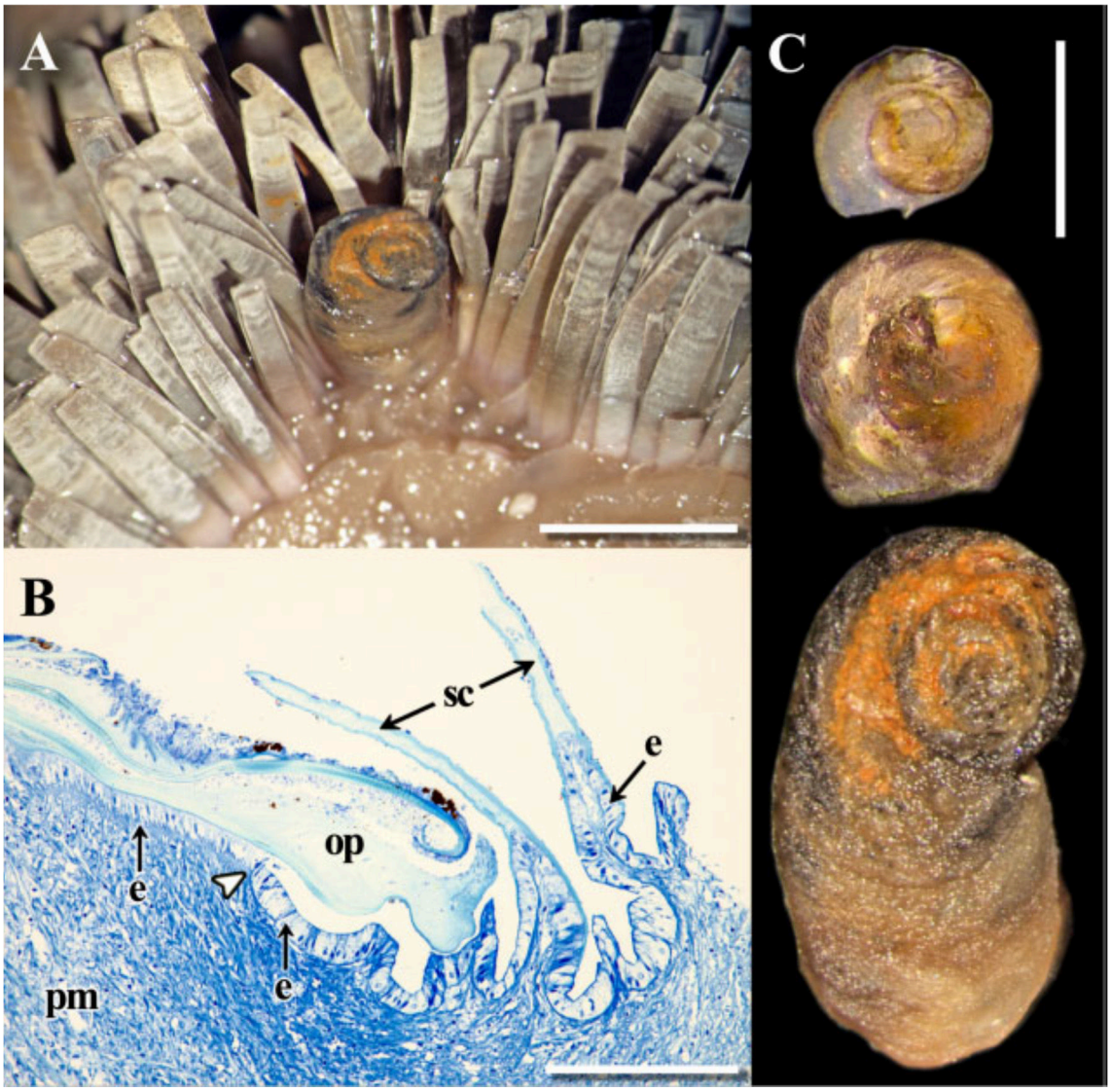

Chapter 6

A new genus of large hydrothermal vent-endemic gastropod (Neomphalina: Peltospiridae)

(*Zoological Journal of the Linnean Society,* In press)

Photo: Pete Bucktrout, British Antarctic Survey

CHAPTER INTRODUCTION

Expeditions to the first Antarctic hydrothermal vents on the East Scotia Ridge (ESR) yielded a very large peltospirid, up to 45 mm in shell length. Prior to this discovery *Chrysomallon squamiferum*, the 'scaly-foot gastropod', was by far the largest member of Peltospiridae (also up to 45 mm vs average of about 10 mm; Sasaki *et al*., 2010). The two share some similarities including large size, shell form, enlarged esophageal gland; but the ESR species does not have dermal sclerites and possesses a large concentric operculum. A later expedition to the Longqi vent field, Southwest Indian Ridge (SWIR) yielded a large peltospirid very similar to the one found in ESR.

This chapter investigates the relationship between the new ESR and SWIR large peltospirids using morphological and genetic methods, as well as formally describing them.

In the supplementary materials, their phylogenetic relationship with *Chrysomallon squamiferum* is explored and some information regarding the mineralogy are provided.

Disclaimer:

All nomenclatural relevant acts in this chapter are disclaimed for nomenclatural purposes according to Article 8.2-8.3 of the International Code of Zoological Nomenclature (Fourth Edition, incorporating amendments).

> **ICZN (International Commission on Zoological Nomenclature). 1999.** *International Code of Zoological Nomenclature, Fourth Edition*. London, UK: The International Trust for Zoological Nomenclature. 306 pp.

STATEMENT OF AUTHOR CONTRIBUTIONS

This chapter was written and formatted for submission in the *Zoological Journal of the Linnean Society* as a Research Article (ID ZOJ-01-2015-2058). It has been accepted for publication on March 25th, 2015 and is currently in press. The authors (in this order) are Chong Chen (corresponding author), Katrin Linse, Christopher N. Roterman, Jonathan T. Copley, and Alex D. Rogers; the detailed author contributions are as follows.

The original idea for the project was conceived by KL. Plan and methodology by KL, and modified by CC. JTC and ADR provided funding for both sample collection on-board *RRS* James Cook research cruises JC42 and JC66/67, as well as laboratory work afterwards. On-board the cruises all authors participated in sample collection and tissue fixation of the specimens used in this study. CC, KL, and CNR carried out all laboratory work. CC was responsible for all data analyses and wrote the original manuscript. All authors discussed the results and implications of the study in detail and edited the manuscript for improvement. ADR, JTC, and KL supervised the work of CC during the length of this study.

The supplementary materials included here were not part of the submitted manuscript but are included here for additional insights and discussion.

A new genus of large hydrothermal vent-endemic gastropod (Neomphalina: Peltospiridae)

Chong Chen*[1], Katrin Linse[2], Christopher N. Roterman[1],
Jonathan T. Copley[3], Alex D. Rogers[1]

[1] Department of Zoology, University of Oxford, Oxford, United Kingdom; [2] British Antarctic Survey, High Cross, Cambridge, United Kingdom; and [3] Ocean and Earth Science, National Oceanography Centre, University of Southampton, Southampton, United Kingdom

* Corresponding author: Chong Chen
University of Oxford
Department of Zoology
Tinbergen Building, South Parks Road
Oxford, OX1 3PS, United Kingdom
Tel: (+44) 01865 281329
E-mail: chong.chen@zoo.ox.ac.uk

Short running title

New genus of vent-endemic neomphalin gastropod

Abstract

Recently discovered hydrothermal vent fields on the East Scotia Ridge (ESR, 56-60°S 30°W), Southern Ocean and the Southwest Indian Ridge (SWIR, 37°S 49°E), Indian Ocean, host two closely related new species of peltospirid gastropods. Morphological and molecular (mitochondrial cytochrome c oxidase subunit I, COI) characterisation justify the erection of *Gigantopelta* gen. nov. within the Peltospiroidae with two new species *Gigantopelta chessoia* sp. nov. from ESR, and *Gigantopelta aegis* sp. nov. from SWIR. They attain an extremely large size for the clade Neomphalina, reaching 45.7 mm in shell diameter. The esophageal gland of both species is markedly enlarged. *G. aegis* has a thick sulphide coating on both the shell and the operculum of unknown function. The analysis of a 579bp fragment of the COI gene resulted in 19-28% pairwise distance between *Gigantopelta* and six other genera in Peltospiridae, while the range among those six genera was 12-28%. The COI divergence between the two newly described species of *Gigantopelta* was 4.43%. Population genetics analyses using COI (370 bp) of 30 individuals of each species confirms their genetic isolation and indicate recent rapid demographic expansion in both species.

Additional Keywords

Gigantopelta, East Scotia Ridge, Indian Ocean, Southern Ocean, population genetics

Introduction

Gastropods are an important component of the fauna of hydrothermal vents in terms of abundance and biomass. In some cases, they are amongst the dominant megafaunal groups that characterise vent biogeographic provinces (e.g., *Alviniconcha hessleri* Okutani & Ohta, 1988 and *Ifremeria nautilei* Bouchet & Warén, 1991 which dominate the west Pacific vents in the Manus, Fiji and Lau Basins). More than 218 gastropod species have been described from chemosynthetic ecosystems, of which more than 138 are believed to be endemic to these ecosystems (Sasaki *et al.*, 2010).

In 2010, the British expedition JC42 on board RRS *James Cook* sampled the hydrothermal vents at East Scotia Ridge (ESR) for the first time, discovering a hitherto unknown species of gastropod (Rogers *et al.,* 2012). This large gastropod was one of the dominant megafaunal taxa along with an undescribed species of yeti crab of the genus *Kiwa*, and the recently described eolepadid stalked barnacle *Vulcanolepis scotiaensis* Buckeridge, Linse & Jackson, 2013. These taxa occupied distinct zones around these vents, which were defined as specific assemblages (Marsh *et al*., 2012), with the peltospirid gastropods occurring in clusters just outside yeti crab assemblages around vent fluid sources (Fig. 2A, Marsh *et al.,* 2012). The gastropod species was identified to be a member of the superfamily Neomphaloidea (as Peltospirioidea) in the clade Neomphalina (Rogers *et al.,* 2012).

In 2011, another British expedition, RRS *James Cook* JC67, surveyed the first-known vent field on the Southwest Indian Ridge (SWIR), the Longqi (previously also known as

69 'Dragon'; Roterman *et al*., 2013) vent field (Tao *et al*., 2014). This expedition yielded
70 another peltospirid gastropod, morphologically closely resembling the species discovered
71 in ESR. This latter species was one of the dominant taxa, forming dense aggregations
72 mostly in areas of diffuse flow of vent fluids (Fig. 2B).
73
74 Neomphalina (Warén & Bouchet, 1993) is a clade of gastropods entirely endemic to
75 chemosynthetic environments (Sasaki *et al.,* 2010). The monophyly of this clade has been
76 well supported by molecular studies (McArthur & Koop 1999; Warén *et al.,* 2003; Aktipis
77 *et al.,* 2008; Aktipis & Giribet, 2010; 2012) but the morphology is very diverse between
78 members so that morphological characterisation is difficult (Sasaki *et al.,* 2010). The
79 Neomphalina comprise the superfamily Neomphaloidea which contains the families
80 Melanodrymiidae, Neomphalidae and Peltospiridae. The internal relationships between
81 these three families are unresolved even with molecular methods, as some studies support
82 monophyly of the families (e.g., Heβ *et al.,* 2008) while others do not (e.g., Aktipis &
83 Giribet, 2012). The position of this clade in the broader scheme of gastropod systematics
84 is still very much in debate, partly because of this morphological variability (Sasaki *et al.,*
85 2010). Most recent molecular phylogenies place Neomphalina basal to Vetigastropoda,
86 with Cocculinoidea as sister clade (Aktipis & Giribet, 2012).
87
88 The aim of the present study is to describe the morphology and genetic characterisation
89 of the two species and to assess their status within the clade Neomphalina. As the two
90 species are very closely related, population genetic methods are used to provide insights
91 into their diversification.
92

Materials & Methods

East Scotia Ridge

Following the initial discovery of hydrothermal vent sites on E2 (56°05.31'S 30°19.10'W) and E9 (60°03.00'S 29°58.60'W) segments of the ESR in 2009 on RRS *James Clark Ross* expedition JR224, vent fauna from these sites were collected during RRS *James Cook* expedition JC42 in the austral summer of 2011 using the remotely operated vehicle (ROV) *Isis* (Rogers *et al.,* 2012). Specimens of a large brown peltospiroid were collected using the suction sampler or scoop by the ROV *Isis* and either fixed in 96% pre-cooled ethanol or 4% buffered formaldehyde or frozen at -80ºC upon recovery. They were stored cooled or frozen until dissection or DNA extraction.

Southwest Indian Ridge

The Longqi vent field (37°47.03'S 49°38.96'E; Tao *et al*., 2014) was confirmed by the Chinese RV *Da Yang Yi Hao* expedition DY115-19 in 2007 (Tao *et al.,* 2012) and is the first visually-confirmed hydrothermal vent field on the Southwest Indian Ridge. This site was first sampled during the RRS *James Cook* expedition JC67 in 2011, and has previously been referred to as the Dragon vent field (Roterman *et al*., 2013). Specimens of another large peltospirid were collected using the suction sampler of ROV *Kiel 6000* and fixed in 10% buffered formalin for morphological examination and in 96% ethanol for genetic studies.

Morphology

External morphological investigation and dissection were carried out with a Leica 10x magnification dissection microscope. The radulae were dissected from specimens preserved in 100% ethanol or frozen and prepared for Scanning Electron Microscopy (SEM) using the following protocol. Tissues around the radula were dissolved with 10% KOH solution overnight. In large specimens, the area around the protoconch was dissected out to fit on SEM stubs, in small specimens, the entire shell was used. To clean before drying, samples underwent a hydration series in 75% - 60% - 40% - 20% - 0% ethanol solution, each step lasting 15 minutes and ending in a rinse in distilled water. Sonication in distilled water was carried out with a single drop of TWEEN 80 for 10 seconds followed by rinsing in distilled water for 15 minutes. The samples then underwent dehydration series in 0% - 20% - 40% - 60% - 75% ethanol solution, each step lasting 15 minutes. At the end of washing samples were rinsed in 100% ethanol for 15 minutes and then stored in fresh 100% ethanol. Washed specimens were dried completely using hexamethyldisilazane for 1-5 minutes and then air-dried overnight. After mounting on SEM stubs with carbon disks samples were coated with gold using a Quorum Technologies E5000 sputter coater. SEM imaging was undertaken using a Jeol JSM-5510 SEM (Department of Plant Sciences, University of Oxford). Specimens for protoconch investigation were dried and mounted in the same manner.

Soft parts were drawn using pencil with the aid of a Zeiss Stemi SV6 microscope mounted with a Zeiss camera lucida drawing tube, and then traced with a black pen. The image

was digitised by a HP Photosmart 2575 scanner at resolution of 600dpi and post-processed using Adobe Photoshop CS6.

Shell morphometric measurements were carried out using digital vernier callipers.

Genetics

For all genetic analyses, individuals collected from Segment E2, ESR and Longqi vent field, SWIR were used. Partial sequences of the mitochondrial cytochrome c oxidase subunit I (COI) gene, 579-bp in length, were used to check the sequence identity of the discovered peltospiroid species against other known species of Neomphalina. *Cocculina messingi* (Cocculinoidea) was used as an outgroup.

Genomic DNA was extracted from foot tissue using QIAGEN DNeasy Blood and Tissue Kit following the manufacturer's instructions (Crawley, West Sussex, United Kingdom), and extractions were stored in -20 ^{o}C freezers. Quality of the DNA was assessed using a Nanodrop 2000 spectrophotometer.

The COI region of the ESR peltospiroids was amplified with the primer pair LCO1490 and HCO2198 (Folmer *et al.,* 1994). Amplification of COI from the SWIR peltospirid required the design of the following primer pair from Peltospiridae COI sequences on GenBank using Primer3 (Rozen & Skaletsky, 2000) and resulted in a high success rate. These new primers are designated as: *SB1F* (5'- AGCCGTGTTGAAATTACGGTCAGT -3') and *SB1R* (5'- GTCTGCTTTACTGGGGACAGG -3'). This set of primers amplified

an approximately 480 bp fragment of COI.

The polymerase chain reaction was carried out in 12 µl reaction volumes, including 2 µl DNA template (100-200 ng/µl), 8 µl QIAGEN Master Mix, 0.4 µl double-distilled water, 1.6 µl primer mix containing 0.8 µl each of forward and reverse primers at concentrations of 4 pmol/µl. Thermocycling was performed using a Bio-Rad C1000 Thermal Cycler, with the following protocol: initial denaturation at 95 ºC for 15 minutes followed by 40 cycles of [denaturation at 94ºC for 45 seconds, annealing at 45ºC for 60 seconds, extension at 72ºC for 60 seconds], ending with final extension at 72ºC for 5 minutes. Amplification of the desired region was confirmed with 1% agarose gel electrophoresis with ethidium bromide. Successful PCR products were purified using either QIAGEN QIAquick PCR purification kit or Diffinity RapidTip, both using standard protocols.

Cycle sequencing reactions were carried out in 10 µl volumes, containing 0.5 µl BigDye Terminator v3.1 (Applied Biosystems), 2.5 µl 5x buffer, 2.5 µl PCR product, 2.5 µl primer (0.8 pmol/µl), 2 µl double-distilled water. The following protocol was used: initial denaturation at 96ºC for 1 minute followed by 25 cycles of [denaturation at 96ºC for 10 seconds, annealing at 50ºC for 5 seconds, extension at 60ºC for 4 minutes], ending with final extension at 60ºC for 4 minutes. Sequenced products were precipitated using the EDTA/ethanol method. Sequences were resolved from precipitated products using Applied Biosystems 3100 DNA sequencer (Sequencing Department, Department of Zoology, University of Oxford).

Alignment and editing of genetic sequences were carried out using the software Geneious

189 5.6 (Drummond *et al.,* 2011), and reads were manually quality-checked and corrected by
190 eye. Only sequences with both good quality matching forward and reverse reads were
191 used in downstream analyses. Pairwise distances of COI were calculated with software
192 MEGA 5.05 (Tamura *et al.,* 2011). Prior to phylogenetic analyses, the most suitable
193 evolutionary model was selected, using the Akaike Information Criterion in
194 PartitionFinder v1.0.1 (Lanfear *et al.,* 2012). This selected the GTR + I + G model for all
195 codon positions. Tree reconstruction was carried out with Bayesian inference using
196 program MrBayes 3.2 (Ronquist *et al.,* 2012). The total aligned sequence length used in
197 the analyses was 579bp. In the analysis, Metropolis-coupled Monte Carlo Markov Chains
198 were run for five million generations. Topologies were sampled every 100 generations,
199 and the first 25% were discarded as "burnin" to ensure chains had converged.
200
201 Population genetic inferences were made from the sequences of 30 specimens from each
202 species using the software Arlequin v3.5.1.3 (Excoffier & Lischer, 2010). The same
203 software was used for mismatch distribution analyses. The length of the COI sequences
204 used in the population genetic analyses was 370 bp as some specimens only had high-
205 quality readings of this length. Haplotype diversity (h), nucleotide diversity (π) and
206 pairwise F_{ST} were calculated, and the statistical significance of F_{ST} was calculated.
207 Departures from equilibrium as expected for neutral markers were tested statistically
208 using Tajima's D test (Tajima, 1989) and Fu's F_S test (Fu, 1997) in the same program,
209 using 10,000 permutations. Statistical parsimony networks were constructed using the
210 software TCS v1.21 (Clement *et al.,* 2000) with the connection probability set to 95%.
211

New COI sequences generated from this study and used for population genetics analyses are deposited in GenBank under accession numbers XXYYYYYY-XXYYYYYY (*Gigantopelta chessoia* sp. nov.) and XXYYYYYY-XXYYYYYY (*Gigantopelta aegis* sp. nov.) (Table 1).

Type specimens are deposited in the invertebrate collection at the Natural History Museum, London (NHMUK), the Zoological Collection of the Oxford University Museum of Natural History (OUMNH.ZC) and the Swedish Museum of Natural History (SMNH).

Results

Systematics

Clade NEOMPHALINA McLean, 1990

Superfamily NEOMPHALOIDEA McLean, 1981

Family PELTOSPIRIDAE McLean, 1989

***GIGANTOPELTA* gen. nov.**

Type species. *Gigantopelta chessoia* sp. nov., by original designation.

Etymology. Giganteus (Latin), gigantic; Pelta (Latin), shield. This refers to the extremely large adult shell size of the species in this genus for the family Peltospiridae. The genus name is feminine.

Diagnosis. Shell extremely large for family, reaching 45mm in adult shell length. Shell globose, rather loosely coiled with deep suture, 3-4 whorls. Spire depressed. Protoconch consisting of 0.5 whorls. Aperture very large, circular, expanding rapidly. Thick, dark olive periostracum enveloping edge of aperture. Shell milky white and thin, not nacreous. Columellar folds lacking. Concentric, multispiral operculum present. Foot large. Cephalic tentacles thick, broad, triangular, thinning towards tips. Eyes lacking. Snout tapering and thick. Esophageal gland hypertrophied. Single, bipectinate ctenidium. Sexes separate. Epipodial tentacles present surrounding operculum. Radula rhipidoglossate, formula ~ 50 + 4 + 1 + 4 + ~ 50. Central, lateral teeth strong, solid with smooth cusps. Marginal teeth long, slender, truncate, divided to about 20 toothlets to distal end.

Remarks. Adult *Gigantopelta* are easily distinguished from all other described peltospirids by their extremely large shell size. Furthermore, *Gigantopelta* can be distinguished from the limpet-like peltospirid genera *Ctenopelta* Warén & Bouchet, 1993*, Echinopelta* McLean, 1989*, Hirtopelta* McLean, 1989*, Nodopelta* McLean, 1989, and *Rhynchopelta* McLean, 1989 by having a coiled shell with 3-4 whorls. It can be distinguished from the three skeneiform genera, *Pachydermia* Warén & Bouchet, 1989, *Depressigyra* Warén & Bouchet, 1989 and *Lirapex* Warén & Bouchet, 1989, by its inflated form with a much more depressed spire and larger aperture. The shell surface is nearly smooth, which differs from all peltospirid genera except *Depressigyra*. The shell roughly resembles that of *Peltospira*, but has a more tightly coiled initial whorl, and lacks lamellar sculpture. Analysis of the soft parts shows an enlarged esophageal gland, a feature previously only known from the yet undescribed 'scaly-foot gastropod' (Warén *et*

al., 2003), which is also the only other known peltospirid to attain a similar size. In the 'scaly-foot gastropod' the esophageal gland houses symbiotic bacteria, but it is unclear whether this is also the case for *Gigantopelta*. *Gigantopelta* can be distinguished from the 'scaly-foot gastropod' easily as it does not possess dermal sclerites, has a large operculum, and a shell that is less vertically compressed, with a more circular aperture. The shell of *Gigantopelta* may be coated in a layer of sulphide, which is frequent among vent gastropods including the neomphalins (Hickmann, 1984; Warén and Bouchet 2001). *Gigantopelta* is also comparable to the Oligocene fossil genus *Elmira* Cooke, 1919 from a seep deposit near Bejucal, Cuba; whose possible affinity to Neomphalina based on resemblance to the 'scaly-foot gastropod' has been remarked by Kiel & Peckmann (2007). Although the type species *Elmira cornuarietis* Cooke, 1919 is approximately the same size as *Gigantopelta* (> 40mm in shell length), it carries broad revolving grooves which *Gigantopelta* lack. The true taxonomic affinity of *Elmira* is still unclear.

***Gigantopelta chessoia* sp. nov.**

(Figs. 2-7)

'Peltospiroidea n. sp.' – Rogers *et al.*, 2012: 7, Fig. 3D

'Undescribed species of peltospiroid gastropod' – Marsh *et al.*, 2012: 6, Fig. 5C, 5J.

Type material: Holotype. Shell diameter 36.30 mm, 99% ethanol, Fig. 3A-C. E2 segment, East Scotia Ridge, 56°05.31'S 30°19.10'W ('Cindy's Castle'), 2606 m deep, RRS *James Cook* expedition JC42, ROV *Isis* Dive 130, 20.01.2010, leg. A. D. Rogers (NHMUK

2015.XX). Paratypes. One dissected specimen, 99% ethanol (shell diameter 31.12mm, Fig. 4A-B; NHMUK 2015.XX), same data as for holotype; growth series of five specimens, 99% ethanol (NHMUK 2015.XX), same data as for holotype; growth series of five specimens, 99% ethanol (OUMNH.ZC.2013.02.002; SMNH Type Collection 8450), E2 segment, East Scotia Ridge, 56°05.34'S 30°19.07'W ('Cindy's Castle'), depth 2644 m, RRS *James Cook* expedition JC42, ROV *Isis* Dive 134, 24.01.2010, leg. A. D. Rogers; five specimens, 10% formaldehyde (NHM 2015.XX), same data as for the previous series.

Materials Examined: Approximately 200 specimens collected on RRS *James Cook* expedition JC42 with ROV *Isis*, on dives 130, 134 and 141. Collection data for dive 130: same as holotypes; dive 134: same as paratype series; dive 141: E9 Segment, East Scotia Ridge, 60°02.81'S 29°58.71'W ('Marsh Tower'), depth 2394 m, RRS *James Cook* expedition JC42, ROV *Isis* Dive 141, 30.01.2010, leg. A. D. Rogers.

Etymology: The species is named after the ChEsSO Consortium, under which ESR hydrothermal vents and this species were discovered.

Description / Diagnosis:

Shell: Shell (Fig. 4A-B) globose, 3-4 whorls, coiled tightly with a deep suture. Spire depressed. Aperture roughly circular, very large. Ratio of shell diameter to aperture length approximately 1:0.633 (average of 100 specimens). Shell trochiform to neritiform, holostomous. Protoconch (Fig. 5A) consists of 0.5 whorls, diameter about 210 μm. Irregular reticulate ornament present initially, becoming obsolete distally. Suture around

protoconch very deep. Teleoconch smooth, no distinct sculpture. Subtle growth lines, irregular protuberances present. Growth lines stronger on the body whorl, especially near the aperture. Periostracum thick, dark olive, enveloping the aperture. Ostracum and hypostracum milky white. Thin, fragile without periostracum. Columellar folds lacking. Callus extends to reach the columella. Area around callous concave. Maximum shell diameter 45.7mm.

Operculum: Operculum (Figs. 3C) with central nucleus present. Corneous, concentric, multispiral. Thin, flaky on fringe. Fringe often damaged. Juvenile operculum thin, semi-transparent, fringe not flaky (Fig. 5C).

Radula: Radula (Fig. 6A) rhipidoglossate. Ribbon approximately 0.5 mm wide and 4 mm long in adults. Formula ~ 50 + 4 + 1 + 4 + ~ 50. Central, lateral teeth cusp-like, pointed (Fig. 6C). Marginal teeth long, slender, bearing ~ 20 denticles at distal end (Fig. 6E). Central tooth triangular, very broad at base, tapering distally, smooth, no sculpture. Lateral teeth solid, bearing a clear protrusion at base.

Soft parts (Fig. 7A): Foot muscular, large. Fully retractable into shell, red when alive. Small epipodial tentacles present, surrounding posterior 2/3 of operculum. Cephalic tentacles thick, triangular, broad at base and thinning towards tips. Eyes lacking. Snout tapering, thick. Esophageal gland huge, approximately same size as aperture. Ctenidium bipectinate. Sexes separate. Shell muscle large, horse-shoe shaped. Intestine forms a simple loop.

Distribution: Only known from hydrothermal vents on segment E2 (56°05.2'S to 56°05.4S, 30°19.00'W to 30°19.35'W) and E9 (60°02.50'S to 60°03.00'S, 29°58.60'W to 29°59.00'W) of the East Scotia Ridge. This species forms dense aggregations rather close to vent effluents.

Remarks: The dispersal mechanism is inferred to be lecithotrophic from the protoconch, presumably with a planktonic dispersal stage. Table 2 shows the shell parameters of *G. chessoia*. The relationships between the six shell parameters measured were investigated and they were all linear across all life stages. Fig. 8 shows a scatterplot of shell diameter against shell height. See Rogers *et al.,* (2012) for details on location of hydrothermal vent sites. Marsh *et al.,* (2012) reports zonation patterns in E9 hydrothermal vents, where different animals dominate different zones according to distance from vent fluid exit. The area closest to fluid exit is dominated by three size classes of *Kiwa*, followed by multilayer assemblages of *Gigantopelta chessoia*, then *Vulcanolepis scotiaensis* Buckeridge, Linse & Jackson, 2013, and finally actinostolid anemones before the vent periphery zone.

Comparative remarks: Similar to *Gigantopelta aegis* sp. nov. described below. *G. chessoia* can be distinguished as it has a taller spire, less extensive callus, and area around callus being concave and not flattened as in *G. aegis*. Differences are seen in the structure of the radula. The central tooth of *G. chessoia* is much wider at base and triangular compared to that of *G. aegis* which is rectangular. Lateral teeth are sculptured in both species, but the marks occur nearer to the base of the teeth in *G. aegis*. *G. chessoia* can also be easily distinguished by the lack of sulphide deposits on shell and operculum, at

least from *G. aegis* found in Longqi Field, the only known habitat to date. Similarly, the operculum in *G. aegis* is much thicker than *G. chessoia* at all life stages.

***Gigantopelta aegis* sp. nov.**

(Figs. 2-7)

Type material: Holotype. Shell diameter 37.61mm, 99% ethanol, Fig. 3D-F. Longqi vent field, Southwest Indian Ridge, 37°47.03'S 49°38.97'E ('Tiamat'), 2785m deep, RRS *James Cook* expedition JC67, ROV *Kiel 6000* Dive 142, 29.11.2011, leg. J. T. Copley (NHMUK 2015.XX). Paratypes. One dissected specimen, 99% ethanol (shell diameter 35.24mm, Fig. 4C-D; NHMUK 2015.XX); growth series of five specimens, 99% ethanol (NHMUK 2015.XX; OUMNH.ZC.2013.02.003; SMNH Type Collection 8451). All paratypes above same collection data as for holotype. Five specimens, 10% formaldehyde (NHMUK 2015.XX): Longqi vent field, Southwest Indian Ridge, 37°47.03'S 49°38.96'E ('Tiamat' chimney), 2783m deep, RRS *James Cook* expedition JC67, ROV *Kiel 6000* Dive 140, 27.11.2011, leg. J. T. Copley (NHMUK 2015.XX).

Non-Type Materials Examined: Approximately 200 specimens, same collection data as the holotype.

Etymology: Aegis (Latin), the shield of Zeus and Athena. The specific name is an allusion of the thick and large sulphide-covered operculum to the mythical shield.

Description / Diagnosis:

Shell: Shell (Fig. 4B) globose, 3-4 whorls, trochiform to neritiform. Spire depressed.

Aperture holostomous. Tightly coilded. Suture deep. Aperture very large, circular, body whorl to aperture length ratio approximately 1:0.65 (average of 100 specimens). Protoconch (Fig. 5B) 0.5 whorls, about 210 μm in length. Sculpture unknown (surface layer of examined specimens affected by dissolution). Thick, orange to reddish sulphide layer covers periostracum. Periostracum dark olive with sulphides removed. Ostracum milky white. Ostracum thin, fragile without sulphide and periostracum. Periostracum slightly recurved at aperture. Columellar folds lacking. Callus extends extensively covering columellar region. Area around callus flattened (dark area in Fig. 3F). Shell smooth, lacking sculpture. Fine growth lines, subtle spiral cords present under sulphide layer. Maximum shell diameter 44.2mm.

Operculum: Operculum (Fig. 3E-F) present. Corneous, thin, flaky near the fringe. Concentric, multispiral. Covered by thick sulphide layer except outermost whorl, same material as those covering shell. Juvenile operculum lacking sulphide layer. Moderately thick, opaque, with concave shape (Fig. 5B).

Radula: Radula (Fig. 6B) rhipidoglossate. Ribbon in adults approximately 0.5 mm wide and 4 mm long. Formula ~ 50 + 4 + 1 + 4 + ~ 50. Central, lateral teeth (Fig. 6D) with sharp cusps. Central tooth rectangular. Lateral teeth bear a protrusion near the base. Marginal teeth (Fig. 6F) elongate with truncate distal ending, dividing into ~ 20 denticles.

Soft parts (Fig. 7B): Foot muscular, large. Fully retractable. Pale white when alive. Small epipodial tentacles present, surrounding posterior 2/3 of operculum. Cephalic tentacles thick, broad at base, tapering distally. Snout tapering, and thick. Esophageal gland huge

(see Fig. 7B). Intestines forming a simple loop. Ctenidium bipectinate. Sexes separate. Gonads rather displaced towards the head-foot. Shell muscle large, horse-shoe shaped.

Distribution: Only known from Longqi vent field, Southwest Indian Ridge (approx. 37°47.03' S 49°38.96' E), around 2700m depth. Found mostly on areas of diffuse flow but also on chimneys of active black smokers.

Remarks: Similar to *Gigantopelta chessoia* n. sp., see *Comparative Remarks* above for comparison. The sulphide covering of the shell and that forming the thick coating on the operculum is remarkable. The coating only covers the outer side, and can be removed from operculum intact by inserting a blade in between. The adult shells are completely covered with sulphide. Sulphide deposition appears to start very early in development, and from the protoconch; as in young specimens (~5mm maximum diameter) sulphide is only present as a tablet on the apex and not covering the whole shell. The shell parameters are given in Table 2. The relationships between the six parameters measured were investigated, and they were linear across all life stages. Fig. 8B shows a scatterplot of shell diameter against shell height.

Systematic Position

Based on the current characterisation, the morphological information places the new genus in Peltospiridae. *Gigantopelta* does not exhibit sexual dimorphism which is consistent with other peltospirids, whereas most neomphalid and melanodrymiid males

have a left cephalic tentacle modified to become a penis. Also notable is the truncated and comb-like ends of marginal teeth (Fig. 6E-F), which in Neomphalina is only present in Peltospiridae and Melanodrymiidae, with members of the Neomphalidae having claw-like ends. Irregular net-like protoconch sculpture seen in *G. chessoia* n. sp. is similar to those of some peltospirid genera such as *Depressigyra* and *Pachydermia*.

Genetic Support

Genetic analysis of five haplotypes from each of the two new species of *Gigantopelta* and all COI sequences for neomphaline gastropods available in GenBank confirms the placement of the new genus within the Neomphalina. Fig. 9 shows the Bayesian consensus tree resulting from the analysis of the partitioned COI dataset using each codon position as a partition. As COI sequences alone cannot provide adequate resolution to clarify the familial relationships within this clade, we refrain from making any phylogenetic conclusions here. The purpose of the analysis is only to show that *Gigantopelta* forms a discrete lineage within Neomphalina. The phylogenetic relationship of *Gigantopelta* and other neomphalines needs to be resolved in a multi-gene phylogenetic study in the future.

Table 3 shows a maximum-likelihood distance matrix constructed from COI sequences of seven Peltospiridae genera (the 'scaly-foot gastropod' is assumed to be a separate genus), including *Gigantopelta*. All species used are type species of the genus, except *Nodopelta* where COI sequences of the type species *N. heminoda* McLean, 1989 were not available so sequences for *N. subnoda* McLean, 1989 were used instead. Pairwise COI

452 divergence between the six non-*Gigantopelta* genera averaged 22.30% (range 12.78%-
453 28.49%), while their divergence from *Gigantopelta* averaged 22.80% (range 19.12%-
454 28.14%), supporting the generic status of the latter.
455
456 *Population Genetics*
457
458 The genetic diversity of *Gigantopelta chessoia* sp. nov. and *G. aegis* sp. nov. are
459 summarised in Table 4. From the COI sequence of 30 individual of each species
460 sequenced, 370 bp of overlapping fragment is used in the analyses here. From these, 10
461 haplotypes of *G. chessoia* and 12 haplotypes of *G. aegis* were found. In both species,
462 there is one dominant haplotype shared by 15 individuals in *G. chessoia* and 18 by *G.*
463 *aegis*. Three haplotypes, including the dominant haplotype, were shared by multiple
464 individuals in *G. chessoia* and two in *G. aegis*, other haplotypes were recovered as
465 singletons.
466
467 Statistical parsimony networks of the data were constructed to visualise the relationship
468 between the haplotypes of the two species, (Fig. 10). The non-dominant haplotypes
469 differed from the dominant haplotypes by only four mutations at most, with the majority
470 within one to two mutations. The COI networks of both species show a generally 'star-
471 burst' pattern, which is indicative of recent rapid demographic expansion. This is
472 supported by negative and significant Tajima's *D* for *G. aegis* and Fu's *Fs* values for both
473 species (Table 4), which reflects an excess of rare polymorphisms in the sample and
474 indicates either recent demographic expansion or evidence of a selective sweep (Fu, 1997).
475 Furthermore, the mismatch analysis (Table 4) returned non-significant sums of squared

476 deviation (SSD) and raggedness index, which signifies that both species do not deviate
477 from the model of demographic expansion. The haplotype diversity was very high but the
478 nucleotide diversity was low in both species, which may also be result of recent expansion.
479
480 The pairwise F_{ST} value shown in Table 5 is large and significant, revealing a very high
481 level of genetic divergence between the two species (F_{ST} = 0.8975, $p < 0.001$). This
482 strongly supports the morphological evidence which shows the two populations represent
483 separate species, and indicates there is currently no genetic connectivity and interbreeding
484 between the two species. This is also supported by the fact that there are no shared
485 haplotypes between the two species, and the most similar haplotype between the two is
486 separated by seven mutations (Fig. 10).
487
488 **Discussion**
489
490 The new genus *Gigantopelta* described herein is unusual among hydrothermal vent-
491 endemic gastropods. The members attain an extremely large size for the clade
492 Neomphalina, which are normally smaller than 15mm in shell diameter. The only other
493 known neomphaline to attain a similar size is the 'scaly-foot gastropod' from Indian
494 Ocean vents (Van Dover *et al.,* 2001; Warén *et al.,* 2003; Nakamura *et al.,* 2012). The
495 'scaly-foot gastropod' is also the only other known gastropod species to house
496 endosymbiotic bacteria in an enlarged esophageal gland (Goffredi *et al.,* 2004). It is not
497 clear whether this is a result of common ancestry or convergent evolution as the
498 phylogenetic relationship between *Gigantopelta* and the 'scaly-foot gastropod' is
499 currently unclear but is certainly of great interest for future studies.

Gigantopelta aegis is remarkable in the thick sulphide coating present on shell and operculum, though it is not clear whether the animal is responsible for controlling the deposit of sulphides. Future studies may reveal this to be an adaptation against predation or against hostile environmental conditions, in deep-sea hydrothermal vents where making the shell thicker with calcium carbonate is energetically costly because of the low pH of vent fluids. An example of such adaptation is seen in the 'scaly-foot gastropod' of the same family, which forms sclerites from sulphides and covers the shell with the same material (Yao *et al.,* 2010). Sulphides are abundant near hydrothermal vents and are perhaps the best available material to strengthen defensive structures in these extreme environments. However, as vents differ in their chemical and physical environment (Tivey, 2007) it is entirely possible that if *G. aegis* is found at another site in the future the specimens they may not have the sulphide overlay.

The population genetic analyses of the two *Gigantopelta* species show clearly that there is currently no gene flow between the two species in ESR and SWIR. However the two species are only 4.43% divergent in COI, and assuming the rate of the molecular clock is similar to the approximate rates in Vetigastropoda (substitution rate 1.2% per million years, Hellberg & Vacquier, 1999) this means the two species have been separated since approximately 1.85 million years ago (mya). Furthermore, a peltospirid substitution rate can be calculated from the COI divergence of 11.2% in *Pachydermia laevis* Warén & Bouchet, 1989 across the Easter Microplate (Matabos *et al*., 2011). The Easter Microplate formed about 3.88 mya (Plouviez *et al*., 2013), the substitution rate of *P. laevis* COI is thus 1.44% per million years. Estimating using this rate, the two *Gigantopelta* species

were separated approximately 1.54 mya. Both these estimates are very recent and suggests before then gene flow existed at that time between the hydrothermal vents on the two oceanic ridges, which was then cut off by a recent event. A similar scenario has been reported with the yeti crab *Kiwa* for which two closely related species are also present on ESR and SWIR for which the divergence was estimated at 1.5 mya with a 95% confidence range of 0.6–2.6 mya (Roterman *et al*., 2013). Separation of the ESR and SWIR *Kiwa* species was attributed to alterations in the intensity and latitude of the Antarctic Circumpolar Current fronts during the Mid-Pleistocene Transition (0.65 to 1.2 mya) or recent reduction in number of vent fields between the ESR and SWIR vents (Roterman *et al*., 2013). A similar close relationship is also suggested for two species of eolepadid barnacles and suggests historic dispersal from west to east of these taxa driven by the Antarctic Circumpolar current (Herrera *et al.*, 2015). The same events may have caused the separation of the two *Gigantopelta* species.

The diversification estimate given is recent but is very crude and subject to large error, leaving much room for a future refinement. This also assumes species at hydrothermal vents evolve at the same rate as the shallow water species, which remains to be evaluated. In fact the rates are likely to be very different for vent species. Using five vent-endemic invertebrate groups from the eastern Pacific including *Lepetodrilus* vent limpets Vrijenhoek (2013) established a mean rate of 0.234% per million years for COI. If rates for *Gigantopelta* are similar this will mean separation of the two species occurred approximately 9.47 million years ago. This mean rate is likely to be an underestimate of the true substitution rate however, as using an old vicariance event 28.5 mya to estimate COI substitution rates is problematic owing to saturation (Ho *et al*., 2011).

548 The ESR vents where *G. chessoia* occur are 6,000 km away from the Longqi vent field
549 where *G. aegis* occur, and the evidence that the two species are very closely related and
550 diverged only recently leads to the obvious question of the distribution of hydrothermal
551 vents in between the ESR and Longqi vent fields and what communities inhabit them. A
552 series of hydrothermal vents inferred to be active have been detected on SWIR near the
553 Bouvet Triple Junction (Bach *et al.,* 2002), and if survey of these vents in the future
554 uncovers another population of *Gigantopelta* it would certainly shed light on their
555 evolutionary history.
556
557 **Acknowledgements**
558
559 This work was funded by NERC Consortium Grant NE/D010470/1 2008-2012,
560 Chemosynthetically-driven ecosystems south of the Polar Front: Biogeography and
561 ecology (ChEsSO), and also NERC Small Research Grant NE/H012087/1, Biogeography
562 and ecology of the first known deep-sea hydrothermal vent site on the ultraslow-spreading
563 Southwest Indian Ridge. The funders had no role in research design, data analysis,
564 publication decisions and manuscript preparation. The authors would like to thank the
565 Masters and crews of the RRS *James Cook* expeditions JC42 and JC67 for their great
566 support of scientific activity during the cruises. The pilots and technical teams of ROV
567 *Isis* and ROV *Kiel 6000* are thanked for their sampling efforts. The authors also express
568 gratitude to staff of the UK National Marine Facilities at the National Oceanography
569 Centre for logistic and shipboard support. Special thanks to Dr Anders Warén (Swedish
570 Museum of Natural History) and Dr Sammy De Grave (Oxford University Museum of
571 Natural History) for providing valuable aid in taxonomy. Two anonymous reviewers are
572 thanked for their valuable suggestions and comments.

References

Aktipis SW, Giribet G. 2010. A phylogeny of Vetigastropoda and other "archaeogastropods": re-organizing old gastropod clades. *Invertebrate Biology* **129:** 220-240.

Aktipis SW, Giribet G. 2012. Testing relationships among the Vetigastropod taxa: a molecular approach. *Journal of Molluscan Studies* **78:** 12-27.

Aktipis SW, Giribet G, Lindberg DR, Ponder WF. 2008. Gastropod phylogeny: an overview and analysis. In: Lindberg DR and Ponder WF, eds. *Phylogeny and evolution of the Mollusca*. Berkeley, California: University of California Press. 201-237.

Bach W, Banerjee NR, Dick HJB, Baker ET. 2002. Discovery of ancient and active hydrothermal systems along the ultra-slow spreading Southwest Indian Ridge 10°–16°E. *Geochemistry, Geophysics, Geosystems* **3:** 1-14.

BODC (British Oceanographic Data Centre). 2010. *GEBCO Grid Display*. BODC.

Bouchet P, Rocroi JP. 2005. Classification and Nomenclator of Gastropod Families. *Malacologia* **47:** 397 pp.

Bouchet P, Warén A. 1991. *Ifremeria nautilei*, nouveau gastéropode d'évents hydrothermaux, probablement associé a des bactéries symbiotiques. *Comptes rendus de l'Académie des sciences, Ser. III* **312:** 495-501.

Buckeridge JS. 1983. The fossil barnacles (Cirripedia: Thoracica) of New Zealand and Australia. *New Zealand Geological Survey Paleontogical Bulletin* **50:** 1-51.

Buckeridge JS, Linse K, Jackson JA. 2013 *Vulcanolepas scotiaensis* sp. nov., a new deep-sea scalpelliform barnacle (Eolepadidae: Neolepadinae) from hydrothermal vents in the Scotia Sea, Antarctica. *Zootaxa* **3745:** 551-568.

Clement M, Posada D, Crandall KA. 2000. TCS: a computer program to estimate gene genealogies. *Molecular Ecology* **9:** 1657-1659.

Cooke CW. 1919. Contributions to the geology and paleontology of the West Indies. Prepared under the direction of Thomas Wayland Vaughan. *Carnegie Institution of Washington Publications* **291:** 103-156.

Drummond A, Ashton B, Cheung M, Heled J, Kearse M, Moir R, Stones-Havas S, Thierer T, Wilson A. 2011. Geneious v5.6. *Available from http://www.geneious.com*.

Esri. 2012. *ArcGIS Desktop: Release 10.1*. Environmental Systems Research Institute: Redlands, CA.

Excoffier L, Lischer HEL. 2010. Arlequin suite ver 3.5: a new series of programs to perform population genetics analyses under Linux and Windows. *Molecular Ecology Resources* **10:** 564-567.

Folmer O, Black M, Hoeh W, Lutz R, Vrijenhoek R. 1994. DNA primers for amplification of

mitochondrial cytochrome c oxidase subunit I from diverse metazoan invertebrates. *Molecular Marine Biology and Biotechnology* **3:** 294-299.

Fu Y. 1997. Statistical tests of neutrality of mutations against population growth, hitchhiking and background selection. *Genetics* **147:** 915-925.

Goffredi SK, Warén A, Orphan VJ, Van Dover CL, Vrijenhoek RC. 2004. Novel forms of structural integration between microbes and a hydrothermal vent gastropod from the Indian Ocean. *Applied and Environmental Microbiology* **70:** 3082-3090.

Hasegawa K. 1997. Sunken wood-associated gastropods collected from Suruga Bay, Pacific side of the Central Honshu, Japan, with descriptions of 12 new species. *National Science Museum monographs* **12:** 59-123.

Hellberg ME, Vacquier VD. 1999. Rapid evolution of fertilization selectivity and lysin cDNA sequences in teguline gastropods. *Molecular Biology and Evolution* **16:** 839-848.

Heβ M, Beck F, Gensler H, Kano Y, Kiel S, Haszprunar G. 2008. Microanatomy, shell structure and molecular phylogeny of *Leptogrya*, *Xyleptogyra* and *Leptogyropsis* (Gastropoda: Neomphalida: Melanodrymiidae) from sunken wood. *Journal of Molluscan Studies* **74:** 383-402.

Herrera S, Watanabe H, Shank TM. 2014 Evolutionary and biogeographical patterns from deep-sea hydrothermal vents. *Molecular Ecology.* In press. DOI: 10.1111/mec.13054

Hickman CS. 1984. A New Archaeogastropod (Rhipidoglossa, Trochacea) from Hydrothermal Vents on the East Pacific Rise. *Zoologica Scripta* **13:** 19-25.

Ho SYW, Lanfear R, Bromham L, Phillips MJ, Soubrier J, Rodrigo AG, Cooper A. 2011. Time-dependent rates of molecular evolution. *Molecular Ecology* **20:** 3087-3101.

Kano Y. 2008. Vetigastropod phylogeny and a new concept of Seguenzioidea: independent evolution of copulatory organs in the deep-sea habitats. *Zoologica Scripta* **37:** 1-21.

Kiel S, Peckmann J. 2007. Chemosymbiotic bivalves and stable carbon isotopes indicate hydrocarbon seepage at four unusual Cenozoic fossil localities. *Lethaia* **40:** 345-357.

Lanfear R, Calcott B, Ho SYW, Guindon S. 2012. Partitionfinder: Combined selection of partitioning schemes and substitution models for phylogenetic analyses. *Molecular Biology and Evolution* **29:** 1695-1701.

Macpherson E, Jones W, Segonzac M. 2005. A new squat lobster family of Galatheoidea (Crustacea, Decapoda, Anomura) from the hydrothermal vents of the Pacific-Antarctic Ridge. *Zoosystema* **27:** 709-723.

Marsh L, Copley JT, Huvenne VAI, Linse K, Reid WDK, Rogers AD, Sweeting CJ, Tyler PA. 2012. Microdistribution of faunal assemblages at deep-sea hydrothermal vents in the Southern Ocean. *PLoS ONE* **7:** e48348.

Matabos M, Plouviez S, Hourdez S, Desbruyères D, Legendre P, Warén A, Jollivet D, Thiébaut

E. 2011. Faunal changes and geographic crypticism indicate the occurrence of a biogeographic transition zone along the southern East Pacific Rise. *Journal of Biogeography* **38:** 575-594.

McArthur AG, Koop BF. 1999. Partial 28S rDNA sequences and the antiquity of hydrothermal vent endemic gastropods. *Molecular Phylogenetics and Evolution* **13:** 255-274.

McLean JH. 1989. New archaeogastropod limpets from hydrothermal vents: new family Peltospiridae, new superfamily Peltospiracea. *Zoologica Scripta* **18:** 49-66.

McLean JH. 1990. A new genus and species of neomphalid limpet from the Mariana vents : with a review of current understanding of relationships among Neomphalacea and Peltospiracea. *Nautilus : a monthly [then] quarterly journal devoted to the interests of conchologists* **104:** 77-86.

McLean JH. 1995. *Review of western Atlantic species of Cocculinid and Pseudococculinid limpets, with descriptions of new species (Gastropoda : Cocculiniformia)*. Natural History Museum of Los Angeles County: Los Angeles, CA.

Nakamura K, Watanabe H, Miyazaki J, Takai K, Kawagucci S, Noguchi T, Nemoto S, Watsuji T-o, Matsuzaki T, Shibuya T, Okamura K, Mochizuki M, Orihashi Y, Ura T, Asada A, Marie D, Koonjul M, Singh M, Beedessee G, Bhikajee M, Tamaki K. 2012. Discovery of new hydrothermal activity and chemosynthetic fauna on the Central Indian Ridge at 18°–20°S. *PLoS ONE* **7:** e32965.

Okutani T, Ohta S. 1988. A new gastropod mollusk associated with hydrothermal vents in the Mariana Back-Arc Basin, Western Pacific. *Venus : the Japanese journal of malacology* **47:** 1-9.

Pearse JS, Mcclintock JB, Bosch I. 1991. Reproduction of Antarctic benthic marine invertebrates: tempos, modes, and timing. *American Zoologist* **31:** 65-80.

Plouviez S, Faure B, Le Guen D, Lallier FH, Bierne N, Jollivet D. 2013. A new barrier to dispersal trapped old genetic clines that escaped the Easter Microplate tension zone of the Pacific vent mussels. *PLoS ONE* **8:** e81555.

Rogers AD, Tyler PA, Connelly DP, Copley JT, James R, Larter RD, Linse K, Mills RA, Garabato AN, Pancost RD, Pearce DA, Polunin NVC, German CR, Shank T, Boersch-Supan PH, Alker BJ, Aquilina A, Bennett SA, Clarke A, Dinley RJJ, Graham AGC, Green DRH, Hawkes JA, Hepburn L, Hilario A, Huvenne VAI, Marsh L, Ramirez-Llodra E, Reid WDK, Roterman CN, Sweeting CJ, Thatje S, Zwirglmaier K. 2012. The discovery of new deep-sea hydrothermal vent communities in the Southern Ocean and implications for biogeography. *PLoS Biology* **10:** e1001234.

Ronquist F, Teslenko M, van der Mark P, Ayres DL, Darling A, Höhna S, Larget B, Liu L, Suchard MA, Huelsenbeck JP. 2012. Mrbayes 3.2: Efficient bayesian phylogenetic

680 inference and model choice across a large model space. *Systematic Biology* **61:** 539-542.
681 **Roterman CN, Copley JT, Linse KT, Tyler PA, Rogers AD. 2013.** *The biogeography of the yeti*
682 *crabs (Kiwaidae) with notes on the phylogeny of the Chirostyloidea (Decapoda: Anomura)*.
683 **Rozen S, Skaletsky HJ. 2000.** Primer3 on the WWW for general users and for biologist programmers.
684 In: Krawetz S and Misener S, eds. *Bioinformatics Methods and Protocols: Methods in*
685 *Molecular Biology*. Totowa: Humana Press. 365-386.
686 **Sasaki T, Warén A, Kano Y, Okutani T, Fujikura K, Kiel S. 2010.** Gastropods from recent hot
687 vents and cold seeps: systematics, diversity and life strategies the vent and seep biota. *Topics*
688 *in Geobiology* **33:** 169-254.
689 **Tajima F. 1989.** Statistical method for testing the neutral mutation hypothesis by DNA polymorphism.
690 *Genetics* **123:** 585-595.
691 **Tamura K, Nei M, Kumar S. 2004.** Prospects for inferring very large phylogenies by using the
692 neighbor-joining method. *Proceedings of the National Academy of Sciences of the United*
693 *States of America* **101:** 11030-11035.
694 **Tamura K, Peterson D, Peterson N, Stecher G, Nei M, Kumar S. 2011.** MEGA5: Molecular
695 evolutionary genetics analysis using maximum likelihood, evolutionary distance, and
696 maximum parsimony methods. *Molecular Biology and Evolution* **28:** 2731-2739.
697 **Tao C, Li H, Jin X, Zhou J, Wu T, He Y, Deng X, Gu C, Zhang G, Liu W. 2014.** Seafloor
698 hydrothermal activity and polymetallic sulfide exploration on the Southwest Indian ridge.
699 *Chinese Science Bulletin***:** 1-11.
700 **Tao C, Lin J, Guo S, Chen YJ, Wu G, Han X, German CR, Yoerger DR, Zhou N, Li H, Su X,**
701 **Zhu J, the DY115-19 DY115-20 Science Parties. 2012.** First active hydrothermal vents on
702 an ultraslow-spreading center: Southwest Indian Ridge. *Geology* **40:** 47-50.
703 **Tivey MK. 2007.** Generation of seafloor hydrothermal vent fluids and associated mineral deposits.
704 *Oceanography* **20:** 50-65.
705 **Van Dover CL, Humphris SE, Fornari D, Cavanaugh CM, Collier R, Goffredi SK, Hashimoto**
706 **J, Lilley MD, Reysenbach AL, Shank TM, Von Damm KL, Banta A, Gallant RM, Götz**
707 **D, Green D, Hall J, Harmer TL, Hurtado LA, Johnson P, McKiness ZP, Meredith C,**
708 **Olson E, Pan IL, Turnipseed M, Won Y, Young CR, Vrijenhoek RC. 2001.** Biogeography
709 and ecological setting of Indian Ocean hydrothermal vents. *Science* **294:** 818-823.
710 **Vrijenhoek RC. 2013.** On the instability and evolutionary age of deep-sea chemosynthetic
711 communities. *Deep Sea Research Part II: Topical Studies in Oceanography* **92:** 189-200.
712 **Warén A, Bengtson S, Goffredi SK, Van Dover CL. 2003.** A hot-vent gastropod with iron sulfide
713 dermal sclerites. *Science* **302:** 1007-1007.
714 **Warén A, Bouchet P. 1989.** New gastropods from East Pacific hydrothermal vents. *Zoologica Scripta*
715 **18:** 67-102.

716 **Warén A, Bouchet P. 1993.** New records, species, genera, and a new family of gastropods from
717 hydrothermal vents and hydrocarbon seeps. *Zoologica Scripta* **22:** 1-90.
718 **Warén A, Bouchet P. 2001.** Gastropoda and Monoplacophora from hydrothermal vents and seeps;
719 new taxa and records. *Veliger* **44:** 116-231.
720 **Yao H, Dao M, Imholt T, Huang J, Wheeler K, Bonilla A, Suresh S, Ortiz C. 2010.** Protection
721 mechanisms of the iron-plated armor of a deep-sea hydrothermal vent gastropod. *Proceedings*
722 *of the National Academy of Sciences* **107:** 987-992.
723

Figures

Figure 1. Map of deep-sea hydrothermal vent fields where *Gigantopelta chessoia* sp. nov. and *G. aegis* sp. nov. are known to occur. This map was created using Esri ArcMap 10.1 (ESRI 2012) and General Bathymetric Chart of the Oceans (GEBCO) Grid Display Ver.2.13 (BODC 2010). Data source: Bathymetry, GEBCO; continents data. ArcWorld Supplement; oceanic ridges, United States Geologic Service (USGS). Abbreviations: SWIR = Southwest Indian Ridge, CIR = Central Indian Ridge, SEIR = South East Indian Ridge, A-AR = American-Antarctic Ridge, ESR = East Scotia Ridge, and MAR = Mid Atlantic Ridge.

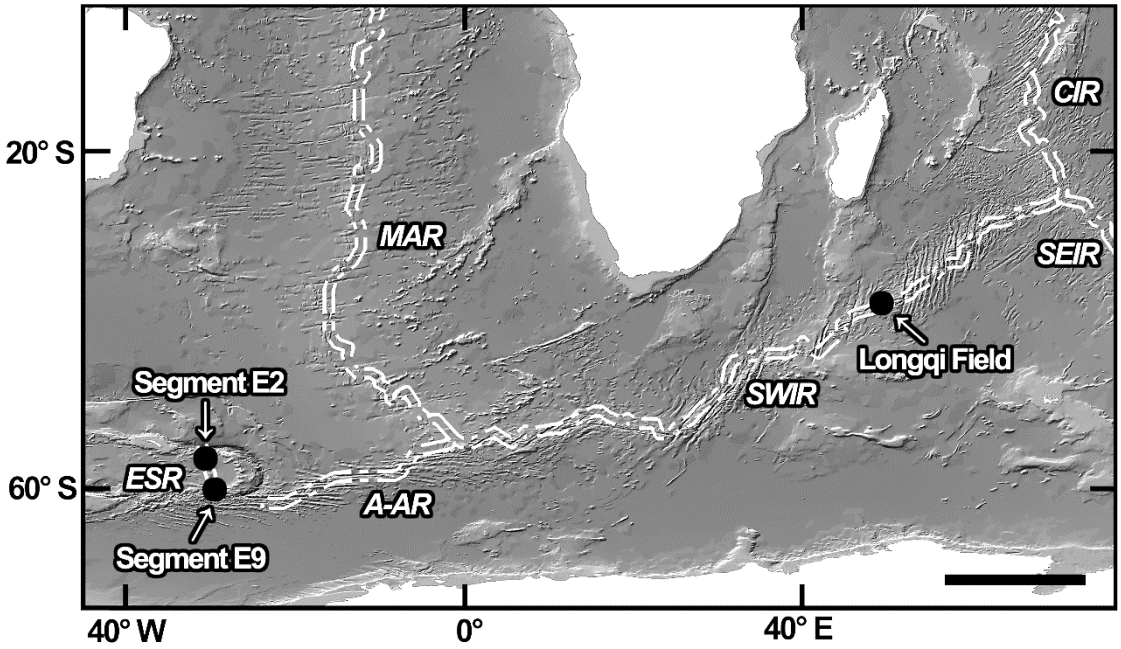

737 **Figure 2.** *In-situ* aggregations of the two new species of *Gigantopelta* gen. nov.: A, *G.*
738 *chessoia* at E2 segment, ESR; B, *G. aegis* at Longqi vent field, SWIR. Scale bars = 5cm.
739

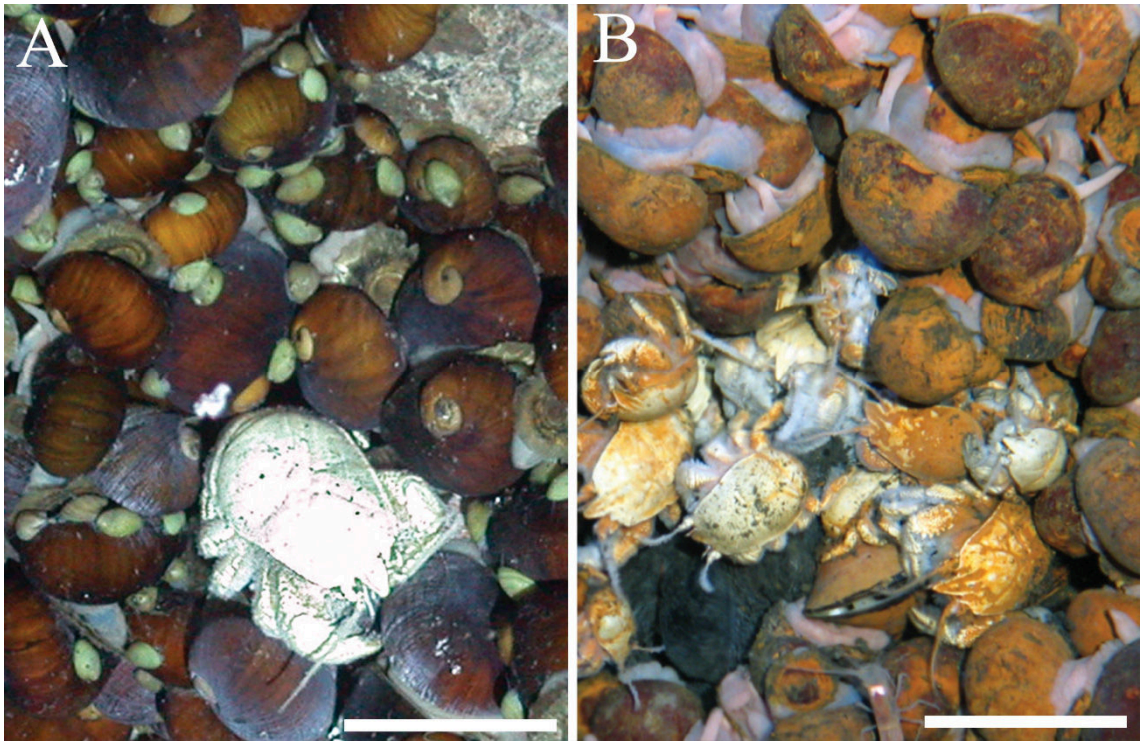

740
741

Figure 3. *Gigantopelta chessoia* sp. nov., holotype (NHM 2013-XX): A, aperture view; B, umbilical view; C. aperture view; scale bars = 1cm. *Gigantopelta aegis* sp. nov., holotype (NHM 2013-XX): D, aperture view; E, umbilical view; F, aperture view; scale bars = 1cm.

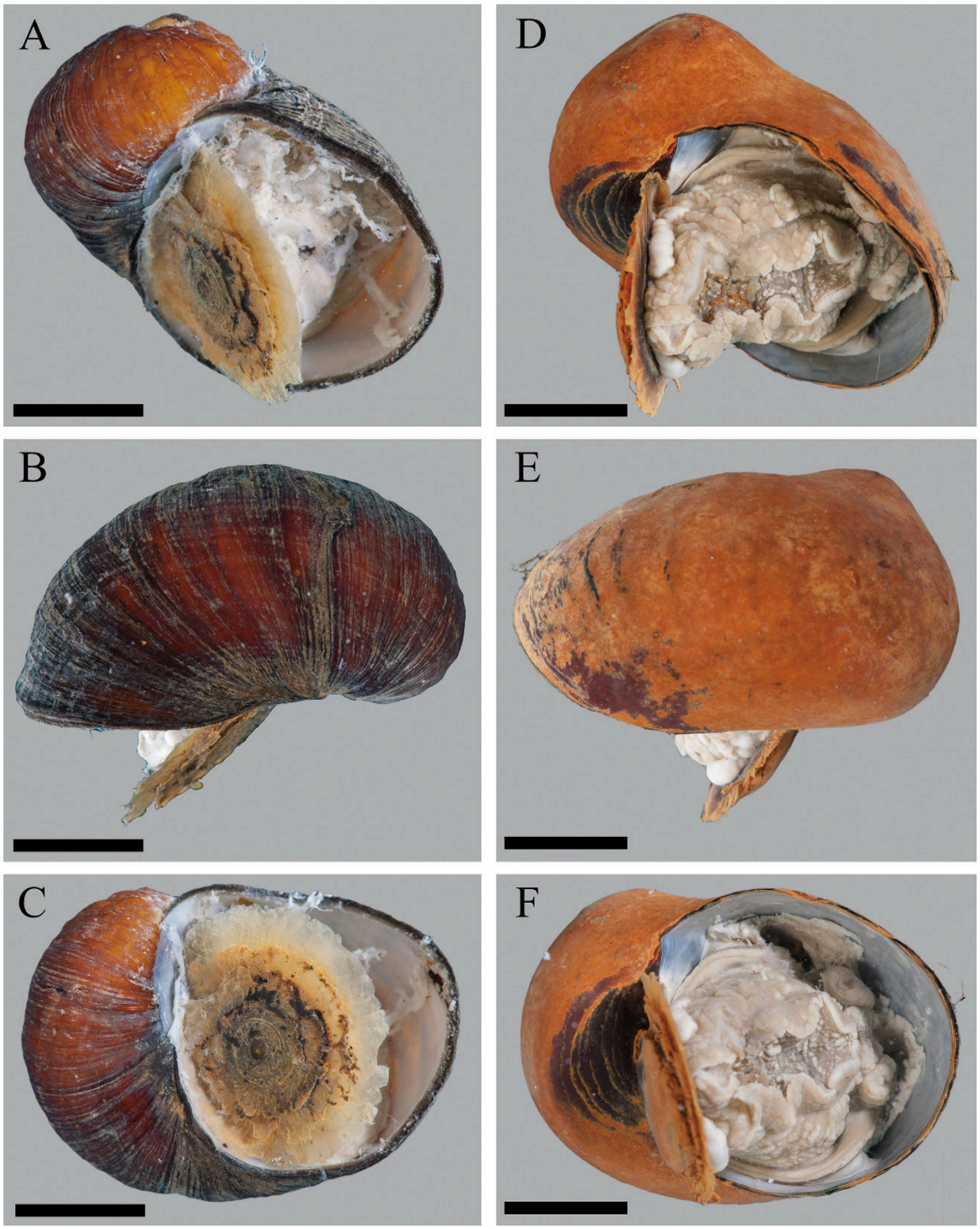

748 **Figure 4.** *Gigantopelta chessoia* sp. nov., paratype shell (NHM 2013-XX): A, aperture
749 view; B, abaperture view; scale bars = 1cm. *Gigantopelta aegis* sp. nov., paratype shell
750 (NHM 2013-XX): C, aperture view; D, abaperture view; scale bars = 1cm.
751

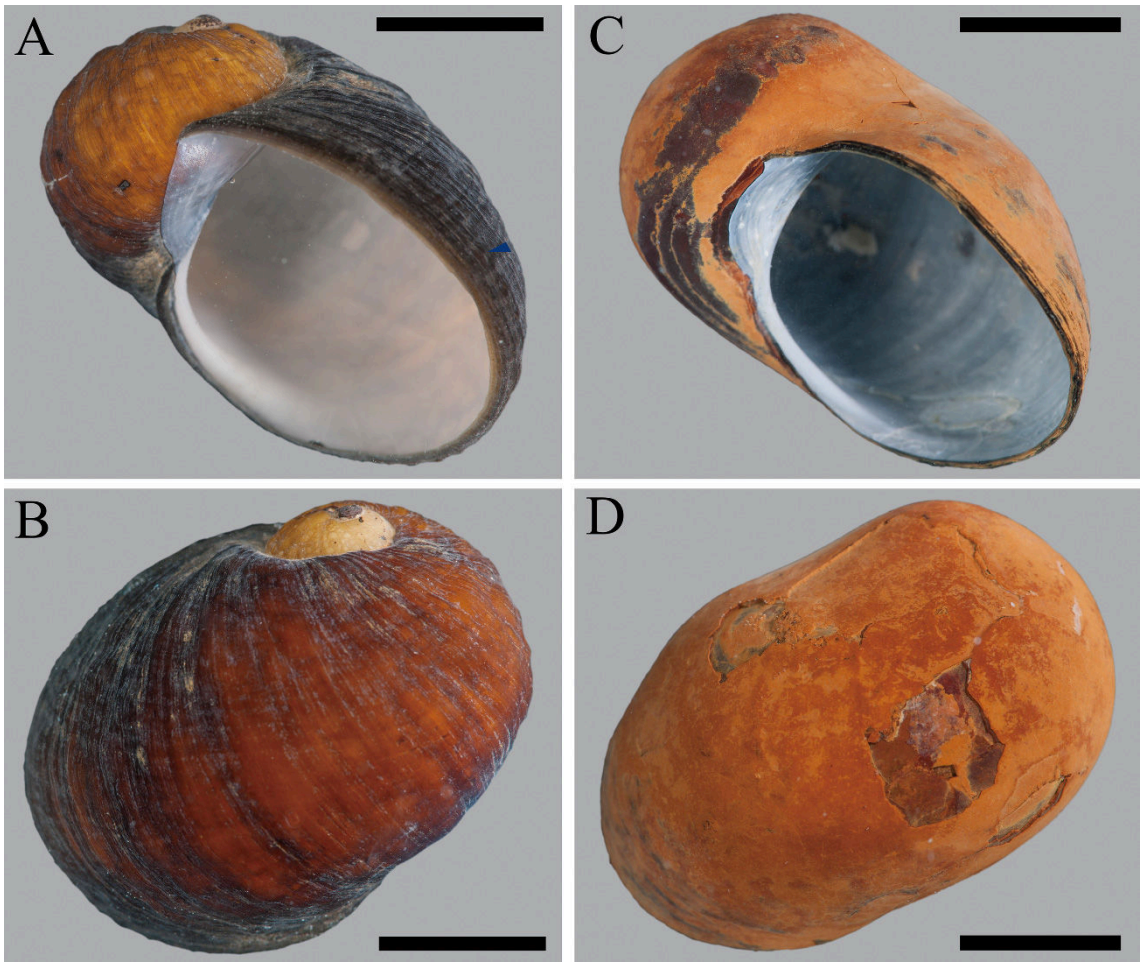

752
753

754 **Figure 5.** Protoconchs: A, *Gigantopelta chessoia* sp. nov., scale bar = 100μm; B,
755 *Gigantopelta aegis* sp. nov., scale bar = 100μm. Juvenile operculum: C, *G. chessoia* sp.
756 nov., scale bar = 500μm; D, *G. aegis* sp. nov., scale bar = 500μm.
757

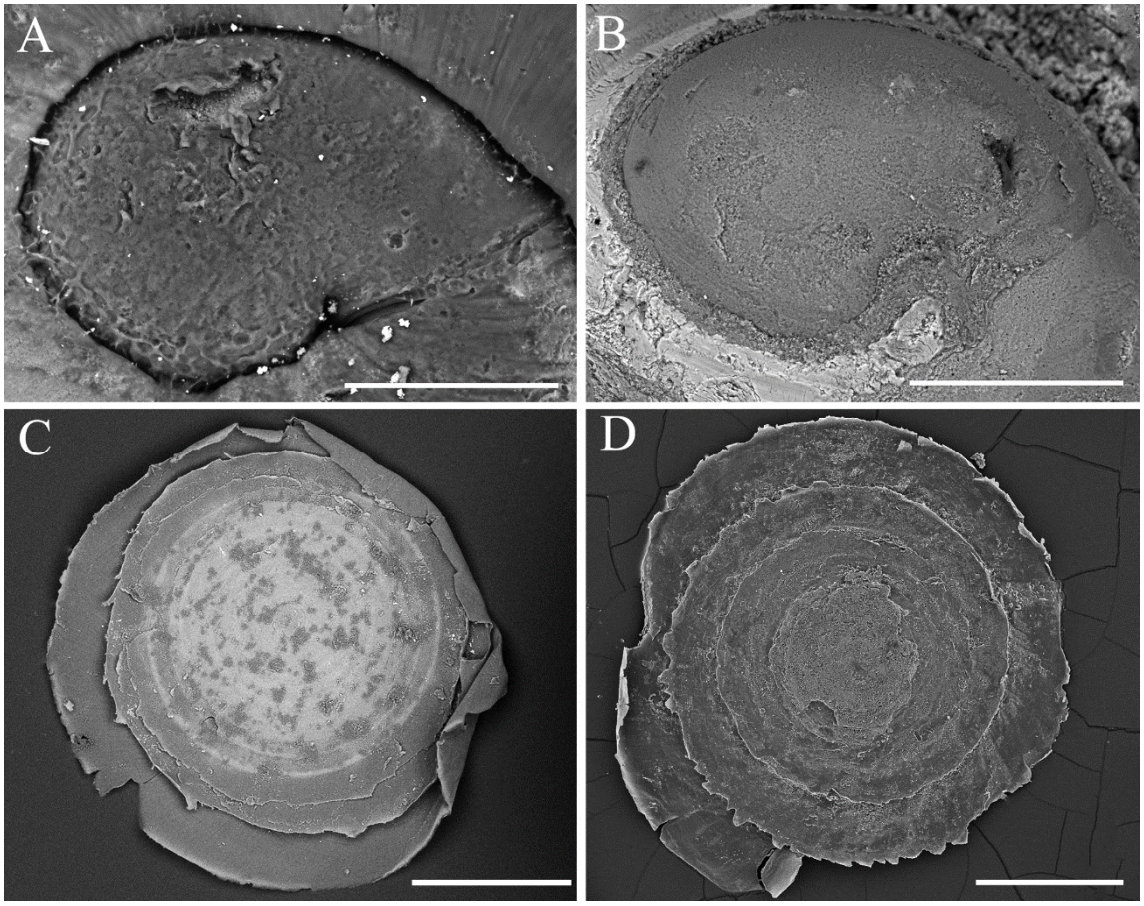

758
759

760 **Figure 6**. Radula. Overview: A, *Gigantopelta chessoia* sp. nov.; B. *Gigantopelta aegis*
761 sp. nov.; scale bars = 100μm. Central and lateral teeth close-up: C, *G. chessoia* sp. nov.;
762 D, *G. aegis* sp. nov.; scale bars = 20μm. Marginal teeth close-up: E, *G. chessoia* sp. nov.;
763 F. *G. aegis* sp. nov.; scale bars = 10μm.
764

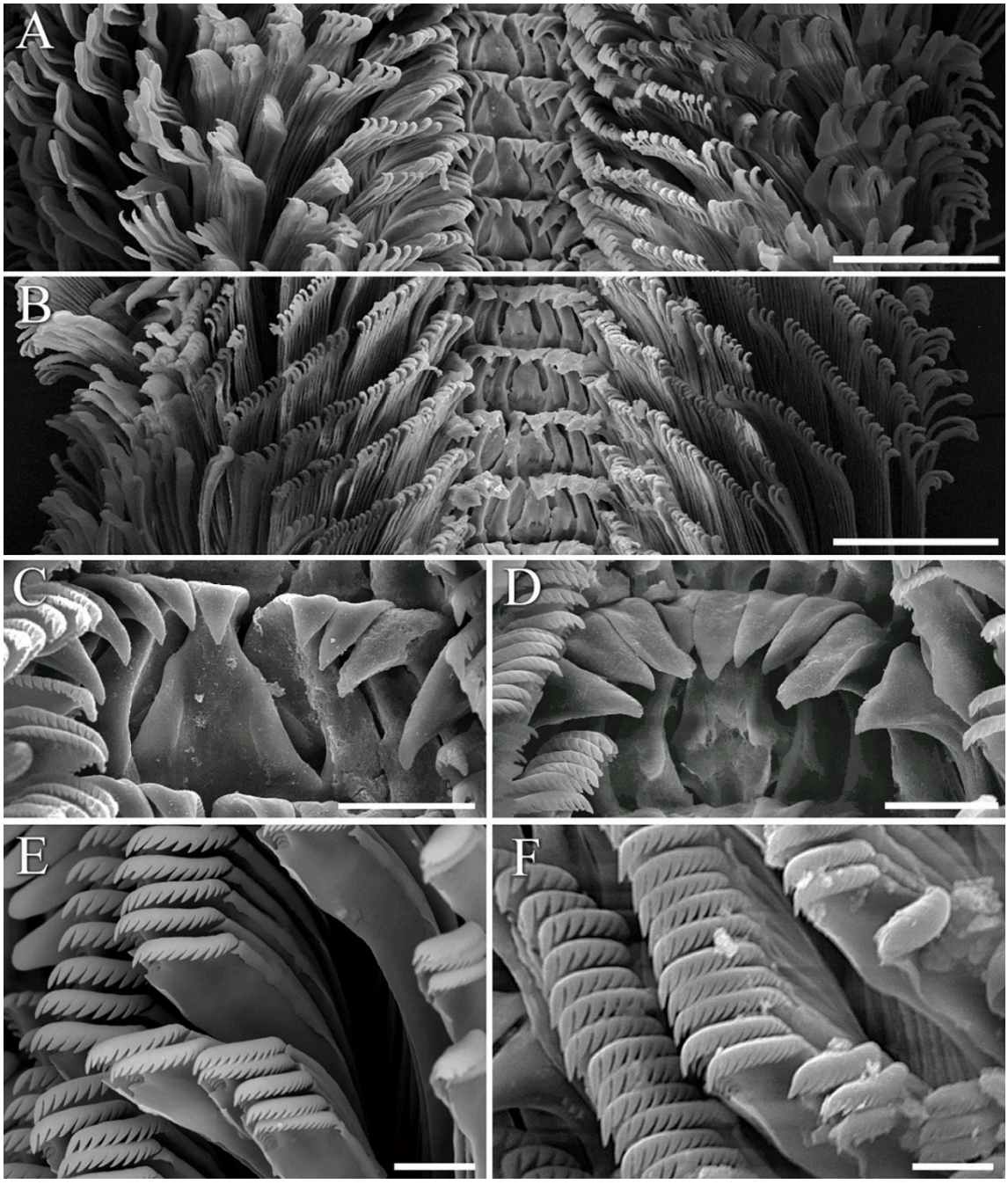

765
766

Figure 7. Illustration of soft parts with the mantle partially removed: A, *Gigantopelta chessoia* sp. nov.; scale bar = 1cm; B, *Gigantopelta aegis* sp. nov.; scale bar = 1cm. Abbreviations: ct = ctnidium, dg = digestive gland, eg = esophageal gland, et = epipodial tentacles, gd = gonad, pc = pericardium, ll = lateral lappet, o = operculum attachment, sn = snout, t = cephalic tentacles.

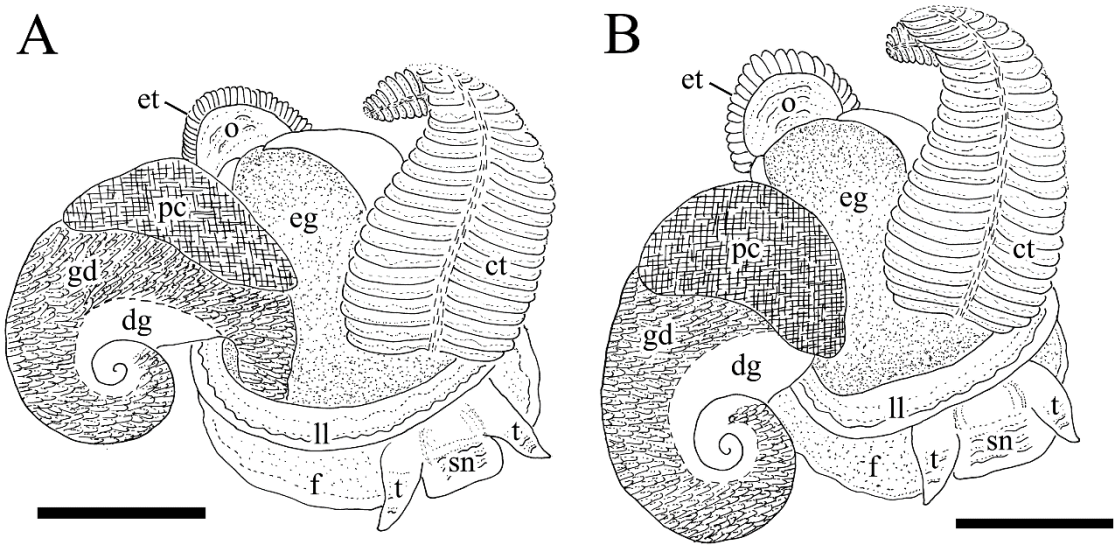

Figure 8. Scatterplot of shell diameter vs shell height across a size range of 100 specimens: A, *Gigantopelta chessoia* sp. nov. (line of best fit formula: y = 0.9045x - 0.6278, $R^2 = 0.99$); B, *Gigantopelta aegis* sp. nov. (line of best fit forumula: y = 0.8823x - 0.8362, $R^2 = 0.99$).

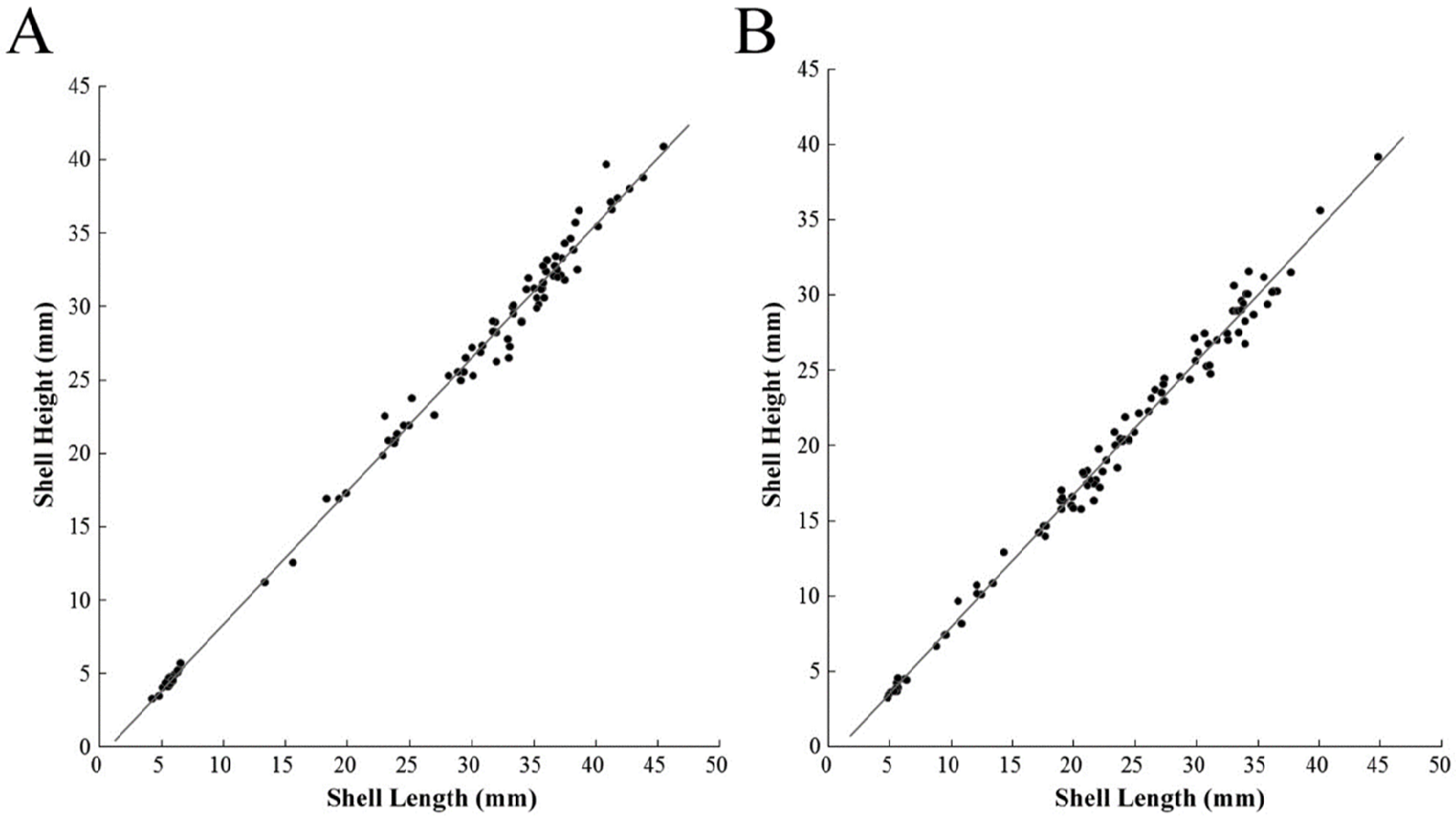

779
780
781

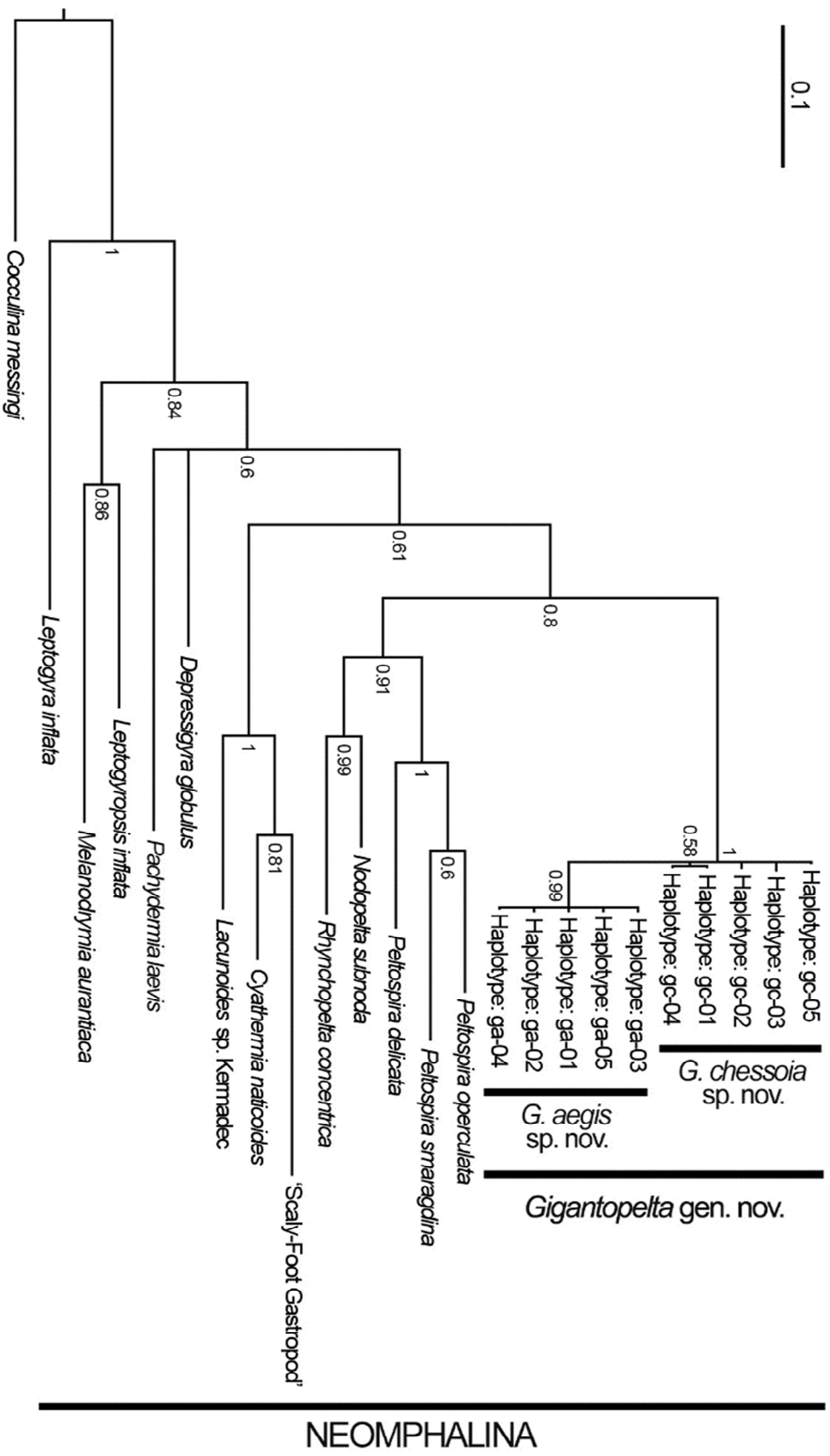

Figure 9. Consensus tree reconstructed from a 579bp fragment of COI gene using Bayesian inference. Metropolis-coupled Monte Carlo Markov Chains was run for five million generations, sampled every 100 generations with first 25% discarded as "burnin". Node values represent Bayesian posterior probability.

782 **Figure 10.** Haplotype parsimonious networks constructed from COI sequences of 30
783 specimens of: A, *Gigantopelta chessoia* sp. nov.; B, *Gigantopelta aegis* sp. nov. Open
784 circles are represented haplotypes, number inside the circles and sizes of the circles
785 corresponds to number of individuals sharing the haplotype. Closed circles are
786 hypothesised intermediate haplotypes that are not represented by sequences.
787

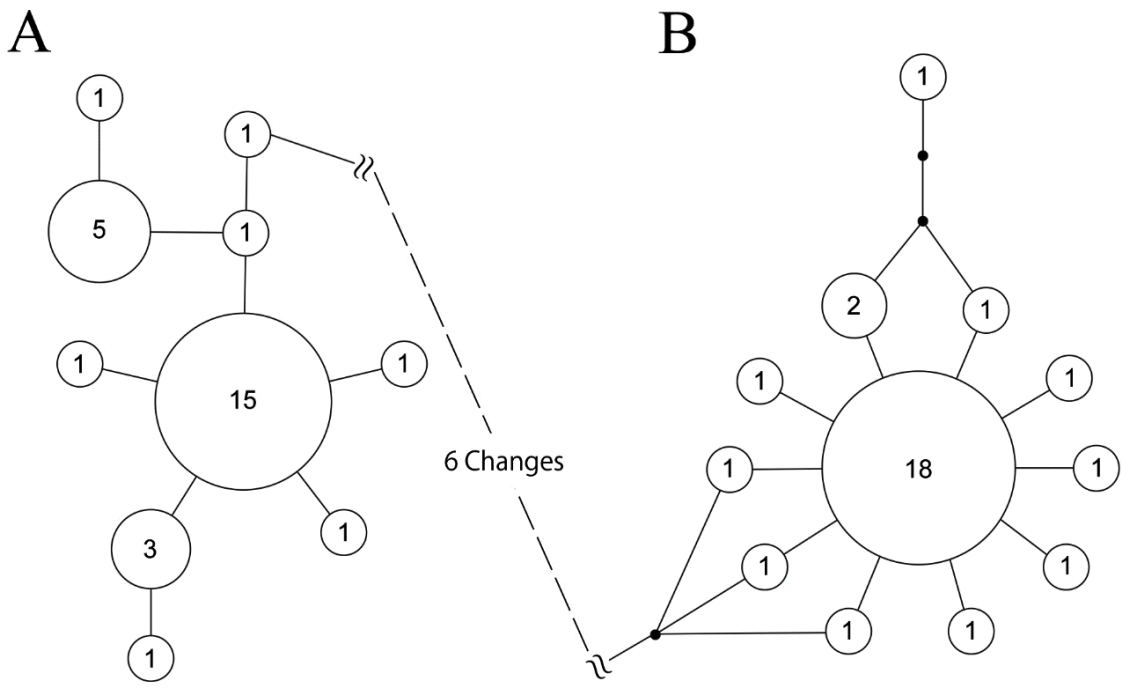

788

Tables

Table 1. List of taxa used in analyses with GenBank accession numbers.

Clade	Family	Taxa	COI
Neomphalina	Peltospiridae	*Nodopelta subnoda* McLean, 1989	GU984280
		Rhynchopelta concentrica McLean, 1989	GU984282
		Depressigyra globulus Warén & Bouchet, 1989	DQ093519
		Pachydermia laevis Warén & Bouchet, 1989	AB429222
		Peltospira delicata McLean, 1989	FJ977764
		Peltospira operculata McLean, 1989	GU984278
		Peltospira smaragdina Warén & Bouchet, 2001	GQ160764
		'Scaly-Foot Gastropod' (Undescribed, COI from Nakamura *et al.,* 2012)	AB540646
		Gigantopelta chessoia sp. nov. Haplotype: gc01-gc05	*This study*
		Gigantopelta aegis sp. nov. Haplotype: ga01-ga05	*This study*
	Neomphalidae	*Cyathermia naticoides* Warén & Bouchet, 1989	DQ093518
		Lacunoides sp. Kermadec (Undescribed, COI from Heβ *et al.,* 2008)	AB330999
	Melanodrymiidae	*Leptogyra inflata* Warén & Bouchet, 1993	AB330998
		Leptogyropsis inflata Hasegawa, 1997	AB365258
		Melanodrymia aurantiaca Hickman, 1984	GQ160763
Cocculiniformia	Cocculinidae	*Cocculina messingi* McLean & Harasewych, 1995	AY923910

795

796

797

Table 2. Shell parameters of *Gigantopelta chessoia* sp. nov. and *G. aegis* sp. nov. Range and proportion to shell diameter are calculated from 100 specimens across a size range in each species.

Parameters (mm)	**Shell**						**Aperture**				**Operculum**		
	Length			***Height***		***Dorsal-Ventral***		***Length***			***Height***		***Diameter***
***Gigantopelta chessoia* sp. nov.**													
Holotype (NHM 2013-XX)	36.30			31.74		26.27		24.94			27.22		21.73
Paratype (NHM 2013-XX)	31.12			26.50		22.25		21.24			23.91		17.87
Range	4.21	~	45.47	3.30	~	40.92	3.50	~	29.77	2.92	~	30.46	3.24	~	31.53	2.24	~	26.62
Proportion to Shell Length	1			0.865		0.727		0.633			0.719		0.566
SD of Proportion	-			0.050		0.035		0.034			0.040		0.048
***Gigantopelta aegis* sp. nov.**													
Holotype (NHM 2013-XX)	37.61			32.88		26.89		26.28			26.18		19.09
Paratype (NHM 2013-XX)	35.24			29.67		25.28		23.58			24.89		17.75
Range	4.87	~	44.83	3.42	~	39.21	3.33	~	32.63	2.60	~	31.05	3.20	~	30.66	1.92	~	23.79
Proportion to Shell Length	1			0.833		0.745		0.654			0.710		0.475
SD of Proportion	-			0.055		0.044		0.057			0.048		0.058

798

799

Table 3. Maximum-likelihood distance matrix of seven genera in Peltospiridae, including the two new species of *Gigantopelta* gen. nov., constructed from 579bp fragments of COI gene. Analyses were conducted using the Maximum Composite Likelihood model (Tamura *et al.* 2004).

		1	2	3	4	5	6	7	8
1	*Peltospira operculata*								
2	*Depressigyra globulus*	23.36%							
3	*Nodopelta subnoda*	15.99%	18.85%						
4	*Pachydermia laevis*	18.88%	23.16%	12.84%					
5	*Rhynchopelta concentrica*	22.34%	23.84%	19.99%	23.83%				
6	'Scaly-Foot Gastropod'	25.72%	28.78%	25.21%	27.43%	26.99%			
7	*Gigantopelta chessoia* sp. nov.	21.83%	21.83%	19.20%	19.25%	27.09%	28.35%		
8	*Gigantopelta aegis* sp. nov.	21.86%	25.25%	21.44%	21.05%	29.00%	28.63%	4.43%	

Table 4. Genetic diversity in COI (379 bp fragment) of the two new species of *Gigantopelta* gen. nov. Shown for each species are: sample size (*n*), number of haplotypes, number of polymorphic loci, haplotype diversity ($h \pm$ SD), nucleotide diversity ($\pi \pm$ SD), Tajima's *D* value, Fu's *Fs* value, sum of square deviations of the mismatch distribution (SSD) and raggedness index from the mismatch analyses.

Species	*n*	Haplotypes	Polymorphic Loci	$h \pm$ SD	$\pi \pm$ SD	Tajima's *D*	Fu's *F S*	SSD	Raggedness
Gigantopelta chessoia sp. nov.	30	10	9	0.7287 ± 0.0780	0.0037 ± 0.0026	-1.2271	-5.0511 **	0.0060	0.0147
Gigantopelta aegis sp. nov.	30	12	12	0.6460 ± 0.1014	0.0027 ± 0.0021	-2.2056 **	-10.6953 ***	0.0396	0.1356

* $p < .05$; ** $p < .01$; *** $p < .001$.

804

Table 5. F-statistics based on pairwise comparisons of COI haplotype frequencies of the two new species of *Gigantopelta* gen. nov. constructed from 370 bp fragments of COI gene of 30 individuals from each species.

	Gigantopelta chessoia sp. nov.	*Gigantopelta aegis* sp. nov.
	Pairwise *F ST*	
Gigantopelta chessoia sp. nov.	0.0000	-
Gigantopelta aegis sp. nov.	0.8975 ***	0.0000

Note. n = 30 for both species; Number of permutaions: 10000. * p < .05; ** p < .01; *** p < .001.

Supplementary Material 1: Five-gene phylogenetic reconstruction

Objective & Methods

To consolidate the familial placement of *Gigantopelta* gen. nov. and to investigate its phylogenetic relationship to the other known large-sized peltospirid – the 'scaly-foot gastropod' *Chrysomallon squamiferum*, a five-gene (COI, Histone 3, 16S rRNA, 18S rRNA, and 28S rRNA) phylogenetic reconstruction was carried out. All genes were newly sequenced for both, *Gigantopelta chessoia* sp. nov. and *G. aegis* sp. nov. For COI, H3, 16S, and 18S, the primers used are identical to those listed in Chapter 2. For 28S, however, different primers were used and these are listed in Table S1.1; for a number of difficult specimens two genus-specific primer pairs had to be designed (28S SB1F-SB1R and SB2F-SB2R). The specimens used were from Segment E2, East Scotia Ridge (*G. chessoia*; Rogers *et al*., 2012) and Longqi vent field, Southwest Indian Ridge (*G. aegis*; Copley, 2011).

Table S1.1. List of PCR (Polymerase Chain Reaction) primers used in the present study to obtain 28S sequence from *Gigantopelta chessoia* sp. nov. and *Gigantopelta aegis* sp. nov.

Name	Sequence 5'-3'	Citation
28Sa	GAC CCG TCT TGA AAC ACG GA	Whiting *et al.*, 1997
28Sb	TCG GAA GGA ACC AGC TAC	
D1F	GGG ACT ACC CCC TGA ATT TAA GCA T	Park & Ó Foighil, 2000
D1R	AAC TCT CTC MTT CAR AGT TC	
rd1a	CCC SCG TAA YTT AGG CAT AT	Edgecombe & Giribet, 2006
Rd5b	CCA CAG CGC CAG TTC TGC TTA	Schwendinger & Giribet, 2005
4.8a	ACC TAT TCT CAA ACT TTA AAT GG	
7b.1	GAC TTC CCT TAC CTA CAT	
SB1F	AGT AAC GGC GAG TGA AGC GGG	Newly designed
SB1R	CGG TTT CAC GTA CTC TTG AAC TCT CTC	
SB2F	AGT AAC GGC GAG TGA AGC GGG	
SB2R	CGG TTT CAC GTA CTC TTG AAC TCT CTC	

The newly obtained sequences were added to the dataset used in the five-gene phylogenetic reconstruction carried out in Chapter 2 of this thesis, and the analyses was repeated to include the two *Gigantopelta* species. The other data used and the genetic methodology is identical to those described in Chapter 2, details can be found in the Materials & Methods section. The evolutionary models selected by PartitionFinder v1.0.1 (Lanfear *et al*. 2012) were also the same. The total sequence length used was 2753-bp.

Phylogenetic reconstruction was carried out with Bayesian inference using MrBayes 3.2 (Ronquist *et al*., 2012). In the five-gene analyses, Metropolis-coupled Monte Carlo Markov Chains were run for five million generations. Convergence Topologies were sampled every 100 generations, and the first 25% were discarded as burn-in to ensure chains sampled a stationary position. The software Tracer v1.6 (Rambaut, Suchard & Drummond, 2013) was used to check for convergence, and calculate adequate burn-in values.

Results & Discussion

The resulting Bayesian phylogeny is shown in Figure S1.1. The topology generated is identical to the one presented in Chapter 2, with a well-supported (Bayesian Posterior Probability, BPP = 96%) monophyletic Peltospiridae within the also fully supported monophyletic clade Neomphalina (BPP = 100%). *Gigantopelta chessoia* sp. nov. and *Gigantopelta aegis* sp. nov. together form a fully supported genus *Gigantopelta* (BPP = 100%) that is placed within Peltospiridae, confirming its systematic position in the family.

Figure S1.1. Consensus tree reconstructed from a combined five-genes (H3, COI, 16S, 18S, 28S) 2753-bp dataset using Bayesian inference. In the analysis Metropolis-coupled Monte Carlo Markov Chains was run for five million generations, sampled every 100 generations with first 25% discarded as "burnin". Node values represent Bayesian posterior probability.

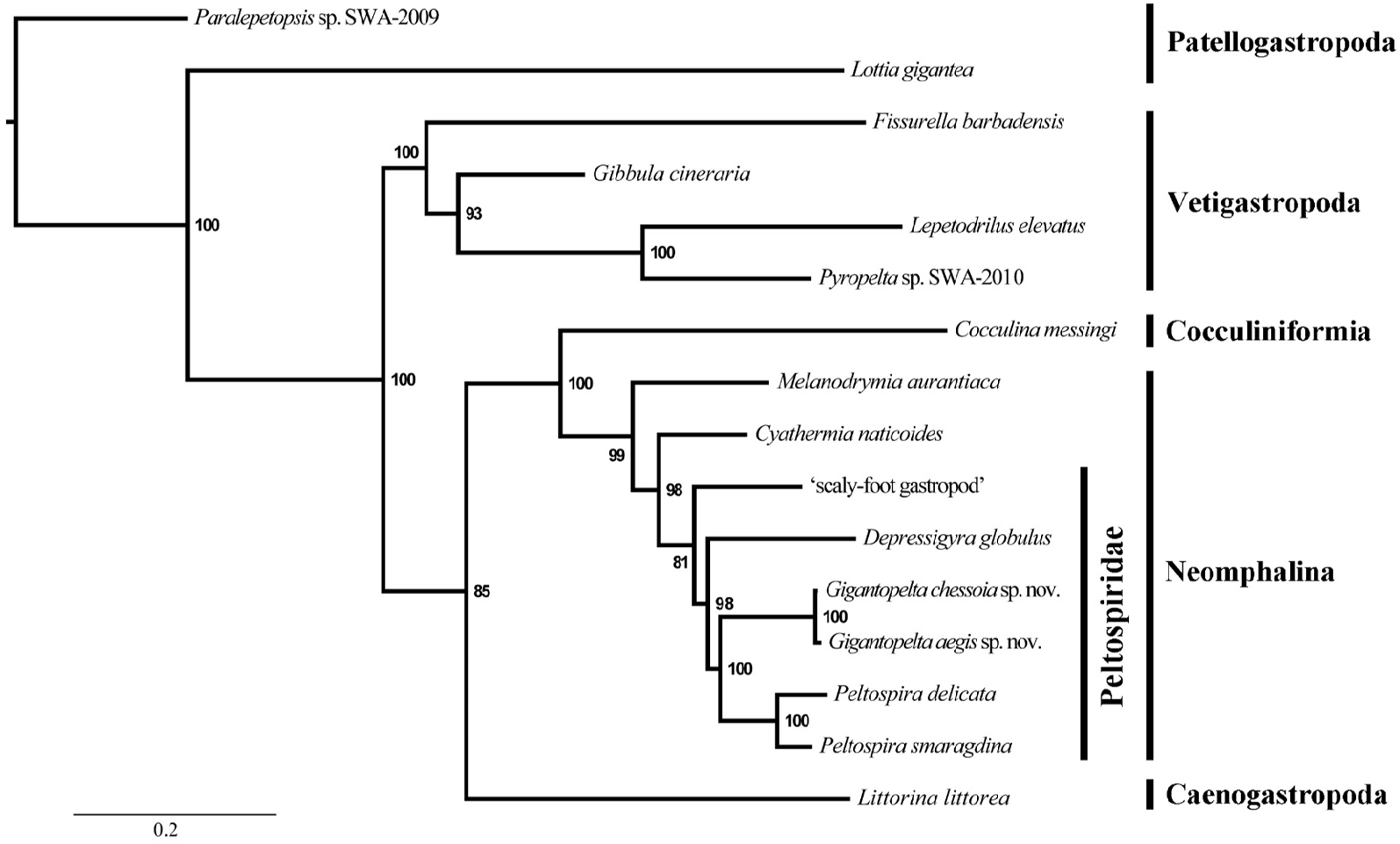

Most intriguingly however, according to this phylogeny within Peltospiridae *Gigantopelta* is not sister of the superficially similar 'scaly-foot gastropod' with which it shares characters such as gigantism and enlarged oesophageal gland (Figure S1.2). While the 'scaly-foot gastropod' was moderately well-supported to be basal in Peltospiridae (BPP = 81%) among the species included, *Gigantopelta* fell sister to *Peltospira* with full support (BPP = 100%). The *Gigantopelta-Peltospira* clade was sister to *Depressigyra* (BPP = 98%), these three genera together are sister to the basal 'scaly-foot gastropod'. These results suggest that despite the similarities between the two giant peltospirid genera, *Gigantopelta* and the 'scaly-foot gastropod', are actually not very closely related.

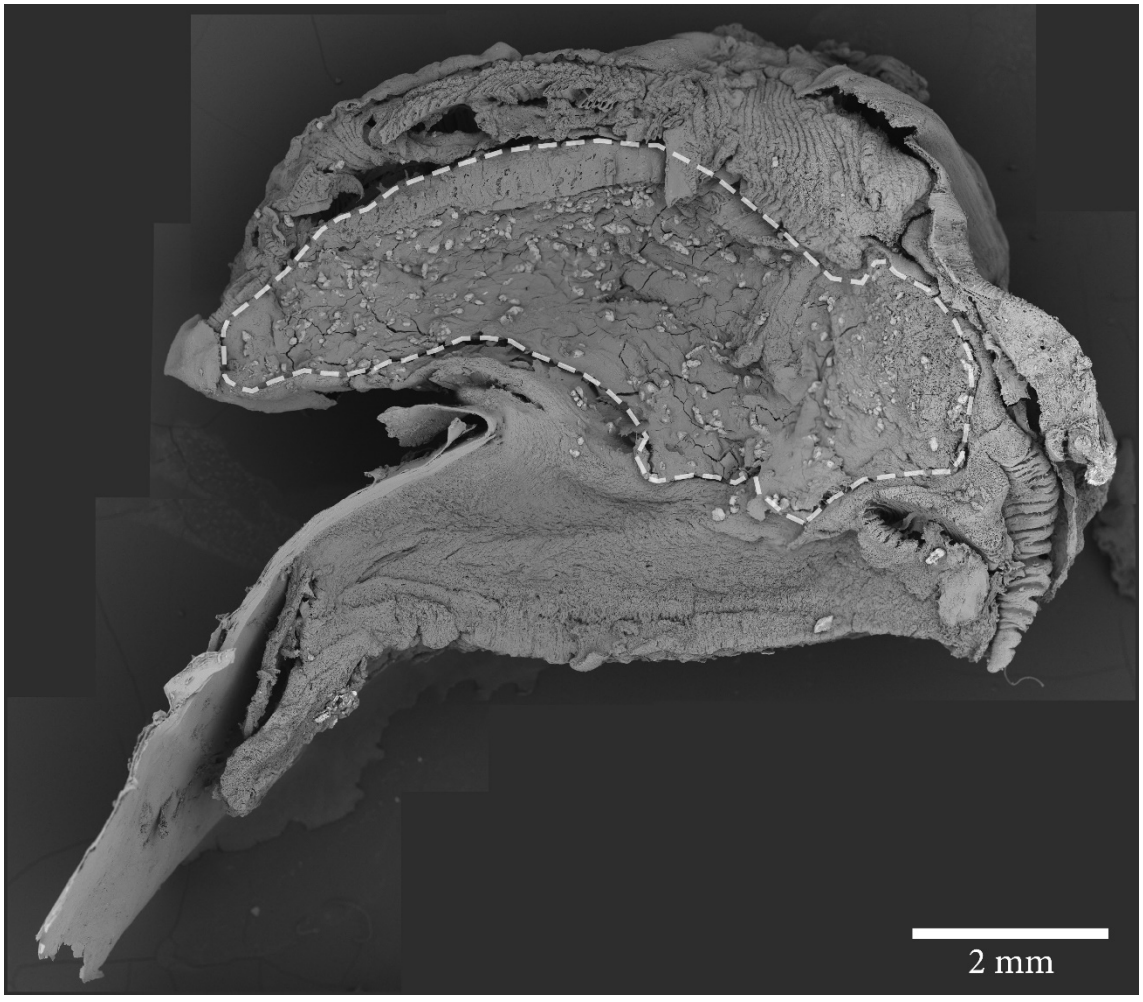

Figure S1.2. *Gigantopelta chessoia* sp. nov., sagittal section through a freeze-dried juvenile specimen to reveal the hypertrophied oesophageal gland (dotted line). Composite of 20 Scanning Electron Micrographs (Hitachi TM-3000, British Antarctic Survey, Cambridge, UK).

Gigantopelta chessoia sp. nov. has been inferred from stable isotope analyses to be reliant on endosymbiotic bacteria (Reid *et al*., 2013), which may be housed in the enlarged oesophageal gland like in the 'scaly-foot gastropod' (Goffredi *et al*., 2004). Although the oesophageal gland is a common structure among the plesiomorphic gastropod clades such as Vetigastropoda, Neomphalina, and Cocculiniformia (Sasaki, 1998); only in *Gigantopelta* gen. nov. and the 'scaly-foot gastropod' is the oesophageal gland known to be hypertrophied to fill the entire ventral side of mantle cavity (Warén *et al*., 2003). The results from the present analyses suggest that this similarity is likely to be a result of convergent evolution and that both gigantism and the greatly enlarged oesophageal gland have likely evolved independently twice within the family Peltospiridae. As vent gastropods, that have acquired endosymbionts, have a tendency towards gigantism (e.g., *Alviniconcha* and *Ifremeria* in Provannidae; Sasaki *et al*., 2010), the shared large size of *Gigantopelta* and the 'scaly-foot gastropod' may not be surprising if they both rely on endosymbiotic bacteria for nutrition. Whether this is in fact true for *Gigantopelta* however requires further histological investigation of the oesophageal gland using Transmission Electron Microscopy.

Another, less likely possibility is that the enlarged oesophageal gland and giant size are plesiomorphic characters among peltospirids and all other genera have lost these characters. Further, detailed examination of the internal anatomy of *Gigantopelta* spp. is likely to shed light on whether similarities between *Gigantopelta* and the 'scaly-foot gastropod' are due to sharing ancestral characters or convergent evolution.

References

Copley JT. 2011. Research cruise JC67, Dragon vent field, SW Indian Ocean, 27-30 November 2011 *RRS James Cook cruise report*: British Oceanographic Data Centre. Available from http://www.bodc.ac.uk/data/information_and_inventories/cruise_inventory/report/10593/.

Edgecombe GD, Giribet G. 2006. A century later – a total evidence re-evaluation of the phylogeny of scutigeromorph centipedes (Myriapoda : Chilopoda). *Invert Syst* **20:** 503-525.

Goffredi SK, Warén A, Orphan VJ, Van Dover CL, Vrijenhoek RC. 2004. Novel forms of structural integration between microbes and a hydrothermal vent gastropod from the Indian Ocean. *Appl Environ Microb* **70:** 3082-3090.

Lanfear R, Calcott B, Ho SYW, Guindon S. 2012. Partitionfinder: Combined selection of partitioning schemes and substitution models for phylogenetic analyses. *Mol Biol Evol* **29:** 1695-1701.

Park J-K, Ó Foighil D. 2000. Sphaeriid and corbiculid clams represent separate heterodont bivalve radiations into freshwater environments. *Mol Phylo Evol* **14:** 75-88.

Rambaut A, Drummond A. 2013. Tracer version 1.6. *Computer program and documentation distributed by the author, website http://beast.bio.ed.ac.uk/Tracer*.

Reid WDK, Sweeting CJ, Wigham BD, Zwirglmaier K, Hawkes JA, McGill RAR, Linse K, Polunin NVC. 2013. Spatial differences in East Scotia Ridge hydrothermal vent food webs: influences of chemistry, microbiology and predation on trophodynamics. *PLoS ONE* **8:** e65553.

Rogers AD, Tyler PA, Connelly DP, Copley JT, James R, Larter RD, Linse K, Mills RA, Garabato AN, Pancost RD, Pearce DA, Polunin NVC, German CR, Shank T, Boersch-Supan PH, Alker BJ, Aquilina A, Bennett SA, Clarke A, Dinley RJJ, Graham AGC, Green DRH, Hawkes JA, Hepburn L, Hilario A, Huvenne VAI, Marsh L, Ramirez-Llodra E, Reid WDK, Roterman CN, Sweeting CJ, Thatje S, Zwirglmaier K. 2012. The discovery of new deep-sea hydrothermal vent communities in the Southern Ocean and implications for biogeography. *PLoS Biol* **10:** e1001234.

Ronquist F, Teslenko M, van der Mark P, Ayres DL, Darling A, Höhna S, Larget B, Liu L, Suchard MA, Huelsenbeck JP. 2012. Mrbayes 3.2: Efficient bayesian phylogenetic inference and model choice across a large model space. *Syst Biol* **61:** 539-542.

Sasaki T. 1998. Comparative anatomy and phylogeny of the recent Archaeogastropoda (Mollusca: Gastropoda). *Univ Mus Tokyo Bull* **38:** 1-224.

Sasaki T, Warén A, Kano Y, Okutani T, Fujikura K, Kiel S. 2010. Gastropods from recent hot vents and cold seeps: systematics, diversity and life strategies. In: Kiel S, ed. *The Vent and Seep Biota*. Netherlands: Springer 169-254.

Schwendinger PJ, Giribet G. 2005. The systematics of the south-east Asian genus *Fangensis* Rambla (Opiliones : Cyphophthalmi : Stylocellidae). *Invert Syst* **19:** 297-323.

Warén A, Bengtson S, Goffredi SK, Van Dover CL. 2003. A hot-vent gastropod with iron sulfide dermal sclerites. *Science* **302:** 1007-1007.

Whiting MF. 2002. Mecoptera is paraphyletic: multiple genes and phylogeny of Mecoptera and Siphonaptera. *Zool Scr* **31:** 93-104.

Whiting MF, Carpenter JC, Wheeler QD, Wheeler WC. 1997. The Strepsiptera problem: phylogeny of the holometabolous insect orders inferred from 18S and 28S ribosomal DNA sequences and morphology. *Syst Biol* **46:** 1-68.

Zardoya R, Meyer A. 1996. Evolutionary relationships of the coelacanth, lungfishes, and tetrapods based on the 28S ribosomal RNA gene. *Proc Natl Acad Sci USA* **93:** 5449-5454.

Supplementary Material 2: Energy dispersive X-ray spectrometry results

Objective & Methods

To investigate the elemental composition of the thick deposit layer found on the shell and operculum (Figure S2.1) of *Gigantopelta aegis* sp. nov. (Longqi field, Southwest Indian Ridge; Copley, 2011; Tao *et al*., 2014) scanning electron microscopy with energy dispersive X-ray spectrometry (SEM-EDS) analyses was undertaken using a Hitachi TM-3000 SEM with added EDS system (British Antarctic Survey, Cambridge, UK). To produce fresh fractures, shell fragments of *G. aegis* sp. nov. were broken from the aperture and observed with the SEM-EDS without sputter-coating. The same was done with the shell of *G. chessoia* sp. nov. (Segment E2, East Scotia Ridge; Rogers *et al*., 2012) for comparison. EDS observation was carried out across a selected area of the fracture of *G. aegis* to observe the difference in elemental composition across different layers of the shell.

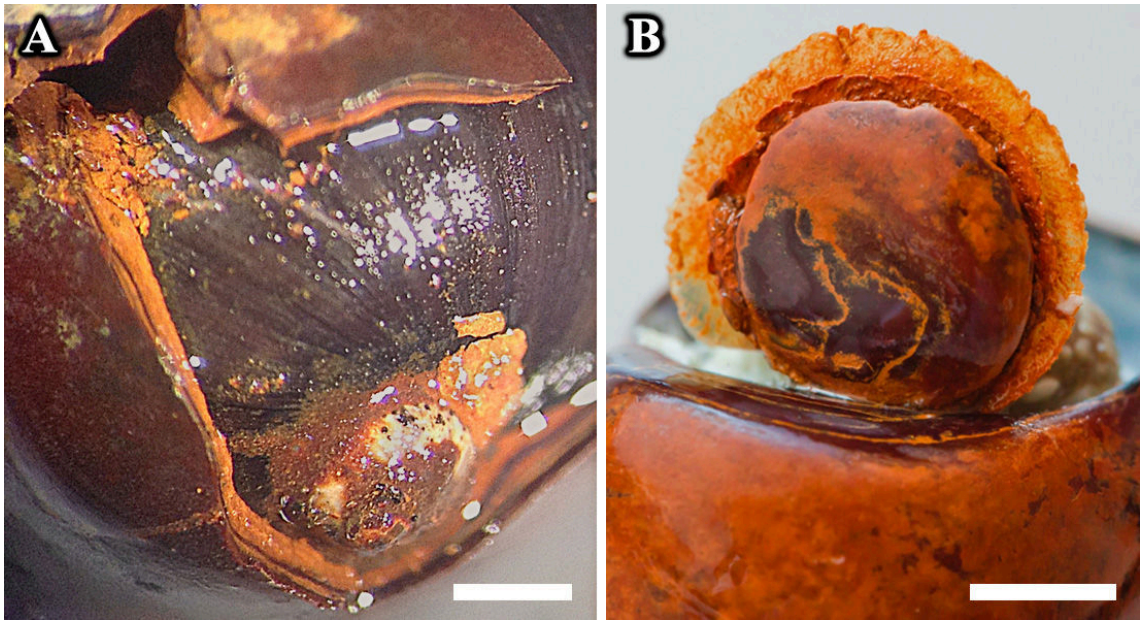

Figure S2.1. *Gigantopelta aegis* sp. nov. **A.** With the surface deposit layer cracked to show thickness and shell surface below. **B.** Sulfide deposit layer on the operculum. Scale bars = 5 mm.

Results and Discussion

SEM micrographs of the shell fracture surface (Figure S2.2) showed clearly the shell of *G. aegis* sp. nov. had three distinct layers (exterior deposit layer, periostracum, and shell) whereas the shell of *Gigantopelta chessoia* sp. nov. lacked the exterior deposit layer.

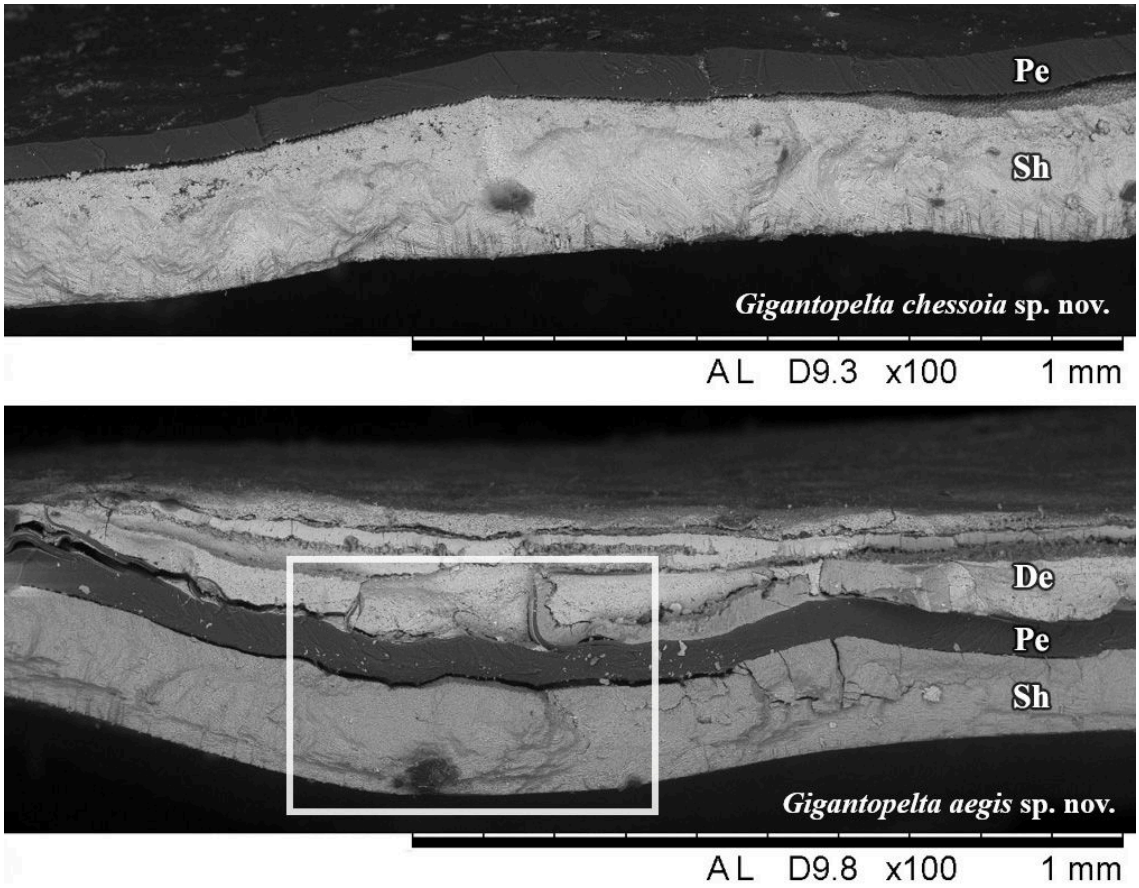

Figure S2.2. SEM micrographs of the shell fracture surface of *Gigantopelta chessoia* sp. nov. and *G. aegis* sp. nov, showing shell structure. White rectangle indicates area selected for EDS observation. Abbreviations. De = exterior deposit layer, Pe = periostracum, Sh = shell.

EDS analyses on the shell of *Gigantopelta aegis* sp. nov. showed that the exterior layer was not rich in sulfur, but instead quite rich in iron and oxygen (Figure S2.3). Iron was only rich on the external deposit and not in the calcium carbonate shell layer, which was clearly rich in calcium. This suggest that the thick deposit covering the shell of *G. aegis* is likely to consist of iron oxides. This differs from the 'scaly-foot gastropod' with which

it co-occurs (Copley, 2011), as the shell of the 'scaly-foot gastropod' is mineralised with iron sulfide (Yao *et al*., 2010; Chapter 2 Supplement Material, this thesis).

The fact that *Gigantopelta aegis* sp. nov. and the 'scaly-foot gastropod' co-occurs on the exact same locality but are apparently mineralised with different minerals is interesting and warrants further investigation. More detailed information on the nature of the deposits on *G. aegis* shell requires more analyses such as X-ray powder diffraction (XRD) analyses to elucidate, and more information is needed to understand the mechanism of mineralisation (whether through action of epibiont microbes, mediation by the gastropod, or abiotic depositing).

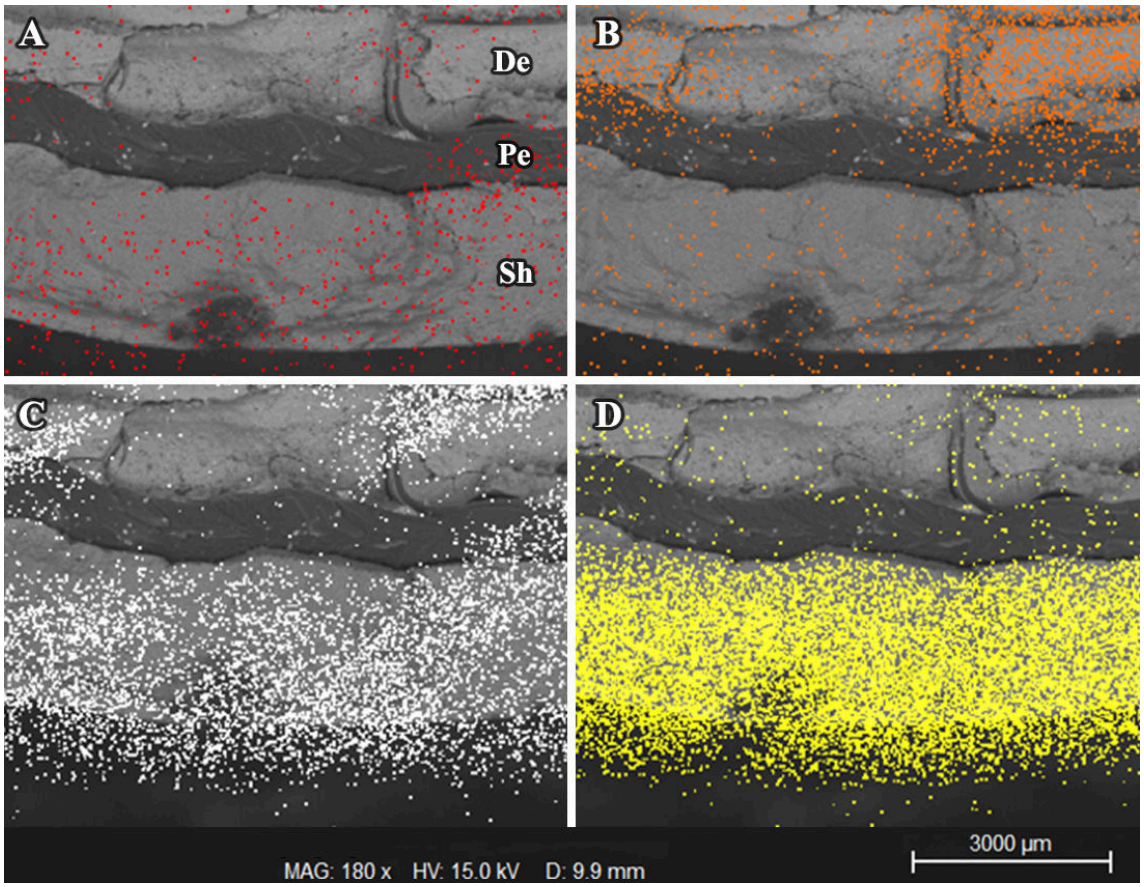

Figure S2.3. SEM-EDS observations of the fractured shell of *Gigantopelta chessoia* sp. nov. showing the distribution of four relevant elements. **A.** sulfur. **B.** iron. **C.** oxygen. **D.** calcium. Abbreviations. De = exterior deposit layer, Pe = periostracum, Sh = shell.

References

Copley JT. 2011. Research cruise JC67, Dragon vent field, SW Indian Ocean, 27-30 November 2011 *RRS James Cook cruise report*: British Oceanographic Data Centre. Available from http://www.bodc.ac.uk/data/information_and_inventories/cruise_inventory/report/10593/.

Rogers AD, Tyler PA, Connelly DP, Copley JT, James R, Larter RD, Linse K, Mills RA, Garabato AN, Pancost RD, Pearce DA, Polunin NVC, German CR, Shank T, Boersch-Supan PH, Alker BJ, Aquilina A, Bennett SA, Clarke A, Dinley RJJ, Graham AGC, Green DRH, Hawkes JA, Hepburn L, Hilario A, Huvenne VAI, Marsh L, Ramirez-Llodra E, Reid WDK, Roterman CN, Sweeting CJ, Thatje S, Zwirglmaier K. 2012. The discovery of new deep-sea hydrothermal vent communities in the Southern Ocean and implications for biogeography. *PLoS Biol* **10:** e1001234.

Tao C, Li H, Jin X, Zhou J, Wu T, He Y, Deng X, Gu C, Zhang G, Liu W. 2014. Seafloor hydrothermal activity and polymetallic sulfide exploration on the Southwest Indian Ridge. *Chinese Sci Bull***:** 1-11.

Yao H, Dao M, Imholt T, Huang J, Wheeler K, Bonilla A, Suresh S, Ortiz C. 2010. Protection mechanisms of the iron-plated armor of a deep-sea hydrothermal vent gastropod. *P Natl Acad Sci USA* **107:** 987-992.

Chapter 7

General discussion and concluding remarks

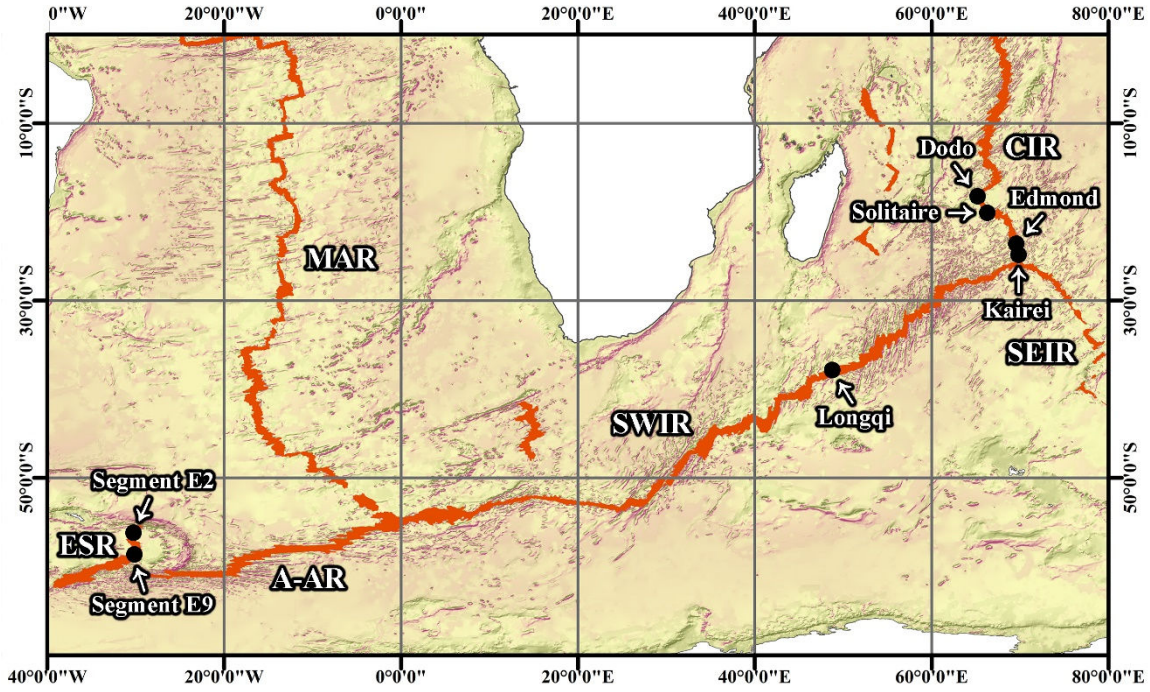

Introduction

This thesis centres around two groups of enigmatic deep-sea peltospirid gastropods endemic to hydrothermal vent ecosystems, from the Indian and Southern oceans. The new taxa were formally described and their systematic placements established by examining their taxonomy and systematics. Population genetics was used to assess the dispersal and connectivity across populations as well as demographic history. Their novel adaptations to the vent environment were uncovered through the characterisation of their internal anatomy. Sclerite evolution in the 'scaly-foot gastropod' was explored in comparison to other molluscs and Cambrian taxa.

Taxonomy and Systematics

The systematic portion of this thesis (Chapter 2, 6) consisted of formal descriptions of these giant peltospirids. The 'scaly-foot gastropod' from Longqi hydrothermal field, Southwest Indian Ridge (SWIR) was confirmed to be the same species as the populations known from Kairei field and Solitaire field on the Central Indian Ridge (CIR) using both genetic and morphology methods (Chapter 2). As this emblematic species remained unnamed until now and there has been considerable confusion in its nomenclature, a formal description in concordance with the International Code of Zoological Nomenclature (ICZN, 1999) has been long-overdue. The description is completed in this chapter designating Longqi, SWIR as the type locality to clarify the nomenclature. This would not have been possible without the kind permission and support of Dr Anders Warén (Swedish Museum of Natural History), whose pioneering

work (Warén *et al*., 2003) provided basis for much of the 'scaly-foot gastropod' research after its discovery. The manuscript name Dr Warén originally assigned to it, *Chrysomallon squamiferum*, is retained as the formal scientific name to avoid confusion with published literature.

The giant peltospirids with large operculum recently discovered from the Antarctic vents on the East Scotia Ridge (ESR; Rogers *et al*., 2012) and Longqi, SWIR (Copley, 2011) proved to be two separate but closely-related species from genetic and morphological analyses (Chapter 6). These could not be assigned to any established genera, and the new genus *Gigantopelta* was thus erected to house them. In addition to their large size, these two new species, *G. chessoia* from ESR and *G. aegis* from SWIR, have a much enlarged esophageal gland in common with *Chrysomallon squamiferum*, as well as a reduced intestinal loop. *C. squamiferum* house endosymbionts in the esophageal gland and rely on these for nutrition (Goffredi *et al*., 2004). The same may be true for these two operculated species of *Gigantopelta* (as suggested in Reid *et al*., 2013) but this requires further confirmation with Transmission Electron Microscopy. The thick rusty iron oxide deposit layer on the SWIR species of *Gigantopelta* may be the result of bacterial activity (as suggested for other peltospirid species; Warén & Bouchet, 2001) or biomineralisation.

The systematic position of both genera, *Chrysomallon* and *Gigantopelta,* were assessed genetically using a five-gene (COI, 16S, 18S, 28S, H3) phylogeny with other neomphaline species and non-neomphaline outgroups which supported their placement in Peltospiridae. Intriguingly, however, the well-resolved phylogeny does not place the

two giant genera together but separately, with the operculated genus *Gigantopelta* being sister to *Peltospira*. This indicates gigantism, as well as an enlarged esophageal gland (maybe also endosymbiosis) has most likely evolved separately twice within Peltospiridae; and that the superficial similarities between *Chrysomallon* and *Gigantopelta* is the result of convergent evolution. A less likely scenario is that gigantism with enlarged esophageal gland is an ancestral characteristic, and all other peltospirid genera have lost these subsequently.

Population Genetics

Chapter 3 of this thesis concerned population genetic analyses comparing all three known populations of *Chrysomallon squamiferum*, using partial sequences of the mitochondrial cytochrome oxidase *c* subunit I (COI) gene. Significant genetic differentiation between the SWIR population and CIR populations was detected for *C. squamiferum*. The CIR populations did not show any genetic differentiation, agreeing with previous studies (Nakamura *et al*., 2012; Beedessee *et al*., 2013). This has implications for the future management and environmental impact assessments for seafloor massive sulfide mining, such as in the case of Longqi as there is already plan to exploit seafloor massive sulfide deposits in this area (Tao *et al.*, 2014). COI population genetics of the two operculated giant peltospirids of the genus *Gigantopelta* were also investigated as part of Chapter 6, which confirmed and further demonstrated the status of the ESR and SWIR populations as isolated and discrete species.

For all populations of both genera, signals consistent with a scenario of recent

bottleneck followed by rapid demographic expansion was detected from results of neutrality tests, mismatch analyses, as well as generally star-shaped haplotype networks. This is commonplace among vent fauna (reviewed by Vrijenhoek, 2010), and most likely reflect instability in demography of vent organisms because of the relatively ephemeral and patchy nature of hydrothermal vent habitats. This means species endemic to the vent environment necessarily maintain a viable metapopulation network with extinction and new establishment of populations being commonplace (Vrijenhoek, 2010). Plouviez *et al*. (2009), for example, suggested similar bottleneck signatures seen in a number of species in the southern East Pacific Rise may be attributable to past eruptive events wiping out populations. Alternatively, a similar pattern of genetic bottlenecks may also represent a selective sweep (Bazin *et al*., 2006). Although this is less likely, it cannot be rejected without investigation using theoretically neutral markers such as microsatellites or neutral single nucleotide polymorphisms (SNPs). One piece of evidence supporting the recent bottleneck scenario, at least for ESR, is that similar patterns are recovered from *Kiwa* sp. in ESR, using neutral microsatellite markers (CN Roterman, unpublished data).

Directionality of gene flow was estimated for the three *Chrysomallon squamiferum* populations using Migrate-n. Between SWIR and CIR, the dominant inferred direction was from SWIR to CIR, likely driven by the prevailing eastward currents over SWIR including the Antarctic Circumpolar Current, Aghulas Current retroflection, and South Indian Current (Talley *et al*., 2011). Between the two CIR populations, the predominant direction was from the southerly Kairei to the northerly Solitaire, which is congruent with the direction of deep currents in the area resulting from circumpolar deep water

entering the Indian Ocean from south and flowing towards north (Talley *et al*., 2011). This is supported further by recent data on the hydrothermal plumes showing a north to northwest spread over Kairei field (Noguchi *et al*., 2015). These results highlight the overarching importance of ocean currents in driving larval transport of deep-sea hydrothermal vent animals.

Anatomy and Adaptation

Chrysomallon squamiferum has fascinated many with its external anatomy but its internal anatomy remained little-studied. To study its internal anatomy and look for possible adaptations to the extreme environment it inhabits, a juvenile specimen (3 mm shell length) was serially sectioned into semi-thin sections of 1.5 μm thickness and a 3D anatomical model was built using the specialist software Amira v5.3.3 in Chapter 4 of this thesis. This is the first such model to be built for the Peltospiridae, although not the whole Neomphalina as models for Melanodrymiidae exist (Heß *et al*., 2008). Further to the enlarged esophageal gland that houses endosymbionts, as known previously, a few more peculiarities were discovered for this species. It was revealed for the first time as a hermaphrodite, which is previously unknown among Peltospiridae and only paralleled by *Leptogyra* (which inhabits sunken wood and not hydrothermal vents) in the whole clade Neomphalina (Heß *et al*., 2008). Furthermore, its nervous system was found to be medullary in nature without discrete ganglia, which is unusually among Gastropoda (Fretter & Graham, 1994). Most significant however, *C. squamiferum* was newly discovered to have an extremely well-developed circulatory system characterised by a gigantic heart occupying more than 4% of body volume, with a very muscular ventricle.

The large gill occupies 15.5% of body volume, and there are blood sinuses around the body which are likely storage space for haemolymph.

Chrysomallon squamiferum only hosts one type of sulphur-oxidising gammaproteobacterial endosymbiont and they are almost clonal between host individuals (Nakagawa *et al*., 2014). *C. squamiferum* is considered to be reliant on the endosymbionts for nutrition (Goffredi *et al*., 2004) and the same endosymbionts are found in Kairei, Solitaire, and Longqi (J Howe, unpublished data; Nakagawa *et al*., in prep). One explanation for the large circulatory system is that it may be used by the gastropod to efficiently extract oxygen from its hypoxic or occasionally anoxic environment. The fact that the circulatory system primarily supplies the well vascularised esophageal gland, lead to the hypothesis that the enlarged circulatory system may also be used to supply resources to the endosymbionts. These may include either hydrogen sulfide (as in siboglinids; Arp *et al*., 1987; Goffredi *et al*., 1997) and/or oxygen (the genome of its endosymbiont contains all the genes necessary for aerobic respiration and it is considered to be able to switch between aerobic and anaerobic respiration; Nakagawa *et al*., 2014). *C. squamiferum* appears to have become a carrying vessel for its endosymbiont bacteria, like some other vent endemic holobionts such as the giant tubeworm *Riftia pachyptila* Jones, 1981.

Sclerite Evolution

Although many have been fascinated by the unique and strange sclerites produced by *Chrysomallon squamiferum*, unknown in any other gastropod, its origins remain

obscure. One widely quoted hypothesis is that the sclerites originated from multiplication of the operculum (Warén *et al*., 2003). The likelihood of this was tested through histological examination of the sclerites and operculum in Chapter 5, and was proved to be unlikely because of significant differences in the underlying secreting epithelium. This was underscored by the fact that a true operculum, which differs significantly from the sclerites, was found to be present in all three populations (Kairei, Solitaire, Longqi); it was only known from the Solitaire population previously (Nakagawa *et al*., 2012).

Furthermore, comparisons with polyplacophoran (Chitonida) scales revealed a completely different secretion mechanism and materal despite the superficial similarity. Sclerites of *C. squamiferum* are secreted in layers covering epithelial outpockets and are largely proteinaceous, while chiton scales are secreted to fill an invaginated cuticular chamber and are mostly calcareous. These results highlight the great capability of molluscs in producing diverse dermal and sub-dermal structures. Treating superficially similar molluscan sclerites as homologous structures without in-depth anatomical investigation can thus lead to erroneous conclusions. This has implications on the recent placement of Cambrian halwaxiids in the Mollusca as a stem-group ‘aculiferan’, as similarity between halwaxiid sclerite and polyplacophoran / aplacophoran sclerites is central to the argument (Vinther, 2009; Smith, 2014). The affinity of halwaxiids to molluscs is now supported by other evidence such as a radula-like structure (Smith, 2012) and they may really be molluscs. However, sclerite similarity should not be used as supporting evidence for analysis of this relationship without a detailed analyses of morphological homology. Indeed, in some aspects the halwaxiid sclerites are more like

those of *C. squamiferum* than chitons (e.g., tissue-filled internal canal; Vinther, 2009).

Limitations and Future Directions

Because of constraints in sample availability, time, and funding there have been a few limitations in the present study. It was not possible, for instance, to use higher resolution genetic markers such as microsatellites or SNPs to investigate the genetic connectivity between the three populations of *Chrysomallon squamiferum*. There was originally a plan to use SNPs markers to compare the three populations but the extracted genomic DNA was unfortunately fragmented and not suitable for genomic analyses. This was especially true for the Kairei population, for which very few specimens adequately preserved for molecular genetics were available (in Japan Agency for Marine-Earth Science and Technology, JAMSTEC). For genomic purposes specimens preserved in -80℃ freezer are required, and planned future cruises to CIR and SWIR should provide sufficient specimens to study population genetics with SNPs in the near future.

Another limitation was that only one site on the SWIR was sampled and studied. A number of further, potentially active vents have been detected on the SWIR (e.g., SWIR 63.9°E, Tao *et al.*, 2009; SWIR 58.9°E, German *et al.*, 1998; 53.25°E and 51.01ºE Tao *et al.,* 2014), with some such as the 51.0°E site and 53.25°E site confirmed to be active (Tao *et al.,* 2014). Figure 1 shows the currently confirmed and inferred vent fields on the SWIR. With only one site sampled on the SWIR, it is not currently possible to explore the dispersal and connectivity of *C. squamiferum* within the SWIR. Perhaps not all such vents have the same suitability for *Chrysomallon squamiferum* as it relies on

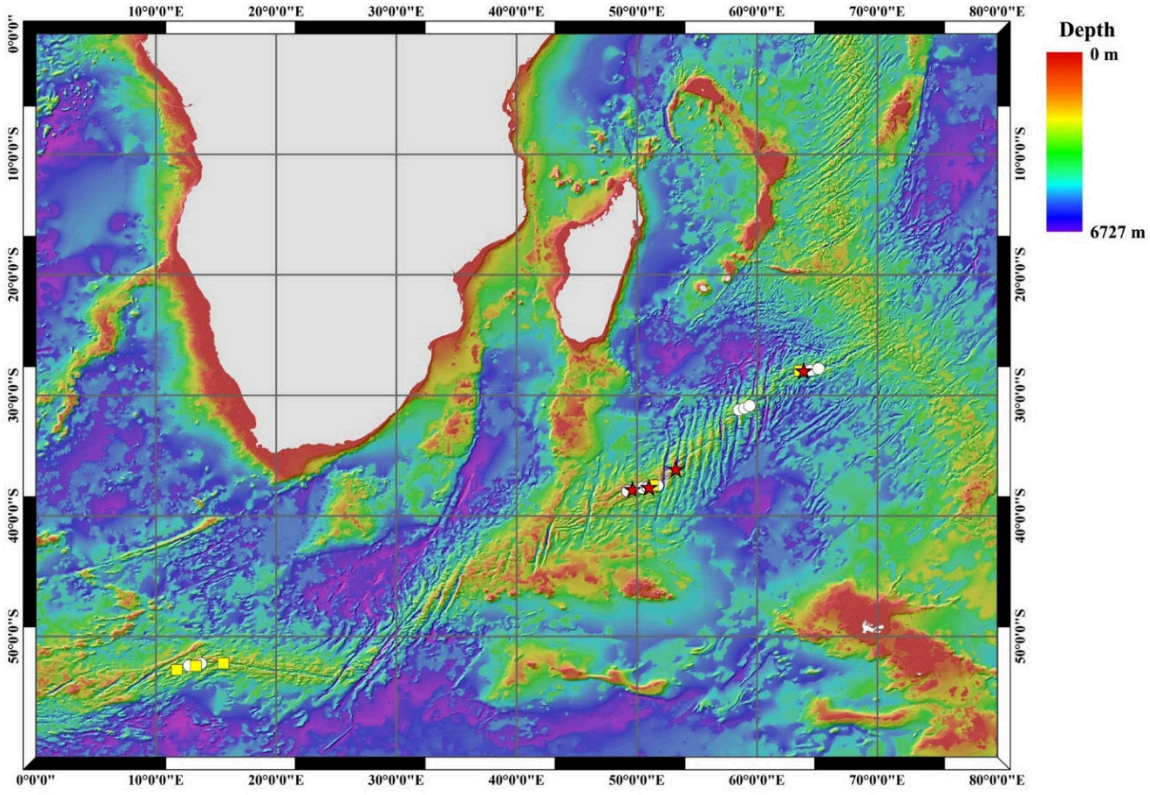

Figure 1. Map of the South West Indian Ocean showing positions of well constrained vent plumes (yellow boxes), poorly constrained plumes (white circles) and active hydrothermal vent fields (red stars) on the Southwest Indian Ridge. Map made using ArcMap 10.1 (Esri, 2012) with bathymetry data from GEBCO (BODC, 2010).

the presence of these endosymbionts for survival and may be present only at vents suitable for its symbionts which are nearly clonal across populations (Nakagawa *et al*., 2014). The suspected vents between Longqi and the CIR are thought to include sites in neovolcanic settings and sites hosted in ultramafic rocks. The expression of hydrothermalism (e.g. the occurrence of 'smoking craters' at Atlantic ultramafic sites; Petersen *et al.,* 2009) as well as chemistry of vent fluids (e.g. high concentrations of CH_4 and H_2 at ultramafic sites, high H_2S at basaltic; Douville *et al.*, 2002; Melchert *et al.,* 2008; Marbler *et al.*, 2010; Perner *et al.,* 2013) is known to differ between vents lying in ultramafic settings compared to those in volcanic settings. Future explorations of other SWIR vent fields will lead to more discoveries relating to the distribution of

this remarkable gastropod, undoubtedly providing key insights into its biogeography within SWIR.

Similarly, for both groups of giant peltospirids, future exploration of vent fields in yet-unexplored areas such as the Southeast Indian Ridge, Australian Antarctic Ridge, southern Mid-Atlantic Ridge, is likely to yield further populations of these gastropods or even further congeneric species and provide insights into their global biogeography. The Australian Antarctic Ridge, for example, has recently been a focus of international collaborative research led by the Korea Polar Research Institute (Park *et al*., 2011). Of course, sampling hydrothermal vent ecosystems located in high latitudes such as southern Indian Ocean and Southern Ocean is extremely difficult because of weather and sea conditions (Macpherson *et al*., 2005; Rogers *et al*., 2012). I have been very fortunate during the course towards my thesis to be able to collect and study valuable specimens from such remote areas.

The origin of *Chrysomallon squamiferum* sclerites remain unresolved. There is an ongoing collaboration project to attempt to answer this question using proteomics and transcriptomics, but this is still much in the development stage (Norio Miyamoto, JAMSTEC, pers. comm.). The basis for differences in iron sulfide coating between populations is also still unknown but likely to be a result of differences in fluid chemistry (Nakamura *et al*., 2012), although unfortunately the fluid chemistry of Longqi field is still unknown as no fluid was sampled during expedition JC67 (Copley, 2011).

The thick iron oxide sulfide layer found on *Gigantopelta aegis* in Longqi, SWIR is curious and warrants further investigation on its origin and mechanisms of precipitation (i.e., whether it is a result of epibiont activity, biomineralisation by gastropod, or abiotic depositing). There is also an ongoing collaboration to investigate this in further detail (Nishizawa Manabu and Ken Takai, JAMSTEC, pers. comm.).

Funding for a future research cruise to revisit Longqi, SWIR and Kairei, CIR, as well as exploring possible new vents in-between using the JAMSTEC R/V *Yokosuka* and DSV *Shinkai6500* has been secured with the cruise scheduled in February 2016 (Ken Takai, JAMSTEC, pers. comm.). It is hoped that this cruise will yield fresh, high-quality material of the SWIR giant peltospirids for a variety of future studies.

Concluding Remarks

Overall, the results from this thesis ascertained the placement of two enigmatic groups of giant vent-endemic gastropods, and lead to improved understanding of their ecology and evolution. The population genetics results highlight the important role of larval dispersal in maintaining metapopulations across the distribution of a vent-endemic taxon. The anatomical investigations emphasise the fact that adaptations of vent-endemic taxa remains little-known even in well-studied species, and that studying anatomy is a key aspect in understanding how these amazing animals have evolved to colonise and survive in such an extreme and volatile environment. There however remains many unresolved mysteries about these two genera of giant peltospirids such as

their global biogeography and origin of sclerites in the 'scaly-foot gastropod' *Chrysomallon squamiferum*, providing scope for more future studies on these species especially when opportunity comes for further sampling at relevant sites.

References

Arp AJ, Childress JJ, Vetter RD. 1987. The sulphide-binding protein in the blood of the vestimentiferan tube-worm, Riftia pachyptila, is the extracellular haemoglobin. *Journal of Experimental Biology* **128:** 139-158.

Bazin E, Glémin S, Galtier N. 2006. Population size does not influence mitochondrial genetic diversity in animals. *Science* **312:** 570-572.

Beedessee G, Watanabe H, Ogura T, Nemoto S, Yahagi T, Nakagawa S, Nakamura K, Takai K, Koonjul M, Marie DEP. 2013. High Connectivity of Animal Populations in Deep-Sea Hydrothermal Vent Fields in the Central Indian Ridge Relevant to Its Geological Setting. *PLoS ONE* **8:** e81570.

BODC (British Oceanographic Data Centre). 2010. *GEBCO Grid Display*. BODC.

Copley JT. 2011. Research cruise JC67, Dragon vent field, SW Indian Ocean, 27-30 November 2011 *RRS James Cook cruise report*: British Oceanographic Data Centre. Available from http://www.bodc.ac.uk/data/information_and_inventories/cruise_inventory/report/10593/.

Douville E, Charlou JL, Oelkers EH, Bienvenu P, Colon CFJ, Donval JP, Fouquet Y, Prieur D, Appriou P. 2002. The rainbow vent fluids (36°14′N, MAR): the influence of ultramafic rocks and phase separation on trace metal content in Mid-Atlantic Ridge hydrothermal fluids. *Chemical Geology* **184:** 37-48.

Esri. 2012. *ArcGIS Desktop: Release 10.1*. Environmental Systems Research Institute: Redlands, CA.

German CR, Baker ET, Mevel C, Tamaki K, the FST. 1998. Hydrothermal activity along the southwest Indian ridge. *Nature* **395:** 490-493.

Goffredi SK, Childress JJ, Desaulniers NT, Lallier FJ. 1997. Sulfide acquisition by the vent worm Riftia pachyptila appears to be via uptake of HS-, rather than H2S. *Journal of Experimental Biology* **200:** 2609-2616.

Goffredi SK, Warén A, Orphan VJ, Van Dover CL, Vrijenhoek RC. 2004. Novel forms of structural integration between microbes and a hydrothermal vent gastropod from the Indian Ocean. *Applied and Environmental Microbiology* **70:** 3082-3090.

Heß M, Beck F, Gensler H, Kano Y, Kiel S, Haszprunar G. 2008. Microanatomy, shell structre and molecular phylogeny of Leptogyra, Xyleptogyra and Leptogyropsis (Gastropoda: Neomphalida: Melanodrymiidae) from sunken wood. *Journal of Molluscan Studies* **74:** 383-401.

Marbler H, Koschinsky A, Pape T, Seifert R, Weber S, Baker ET, de Carvalho LM, Schmidt K. 2010. Geochemical and physical structure of the hydrothermal plume at the

ultramafic-hosted Logatchev hydrothermal field at 14°45′N on the Mid-Atlantic Ridge. *Marine Geology* **271:** 187-197.

Melchert B, Devey CW, German CR, Lackschewitz KS, Seifert R, Walter M, Mertens C, Yoerger DR, Baker ET, Paulick H, Nakamura K. 2008. First evidence for high-temperature off-axis venting of deep crustal/mantle heat: The Nibelungen hydrothermal field, southern Mid-Atlantic Ridge. *Earth and Planetary Science Letters* **275:** 61-69.

Nakagawa S, Shimamura S, Takaki Y, Suzuki Y, Murakami S-i, Watanabe T, Fujiyoshi S, Mino S, Sawabe T, Maeda T, Makita H, Nemoto S, Nishimura S-I, Watanabe H, Watsuji T-o, Takai K. 2014. Allying with armored snails: the complete genome of gammaproteobacterial endosymbiont. *The ISME Journal* **8:** 40-51.

Nakamura K, Watanabe H, Miyazaki J, Takai K, Kawagucci S, Noguchi T, Nemoto S, Watsuji T-o, Matsuzaki T, Shibuya T, Okamura K, Mochizuki M, Orihashi Y, Ura T, Asada A, Marie D, Koonjul M, Singh M, Beedessee G, Bhikajee M, Tamaki K. 2012. Discovery of New Hydrothermal Activity and Chemosynthetic Fauna on the Central Indian Ridge at 18°–20°S. *PLoS ONE* **7:** e32965.

Noguchi T, Fukuba T, Okamura K, Ijiri A, Yanagawa K, Ishitani Y, Fujii T, Sunamura M. 2015. Distribution and Biogeochemical Properties of Hydrothermal Plumes in the Rodriguez Triple Junction. In: Ishibashi J-i, Okino K and Sunamura M, eds. *Subseafloor Biosphere Linked to Hydrothermal Systems*: Springer. 195-204.

Park S-H, Langmuir C, Lin J, Hahm D, Kim S-S, Hong S-G, Lee YM, Michael P. 2011. Preliminary Results of a Recent Expedition to the Australian-Antarctic Ridge. *InterRidge International Workshop Report 'Circum-Antarctic Ridges' 28-30 September, 2011, Toulouse, France*.

Perner M, Hansen M, Seifert R, Strauss H, Koschinsky A, Petersen S. 2013. Linking geology, fluid chemistry, and microbial activity of basalt- and ultramafic-hosted deep-sea hydrothermal vent environments. *Geobiology* **11:** 340-355.

Petersen S, Kuhn K, Kuhn T, Augustin N, Hékinian R, Franz L, Borowski C. 2009. The geological setting of the ultramafic-hosted Logatchev hydrothermal field (14°45′N, Mid-Atlantic Ridge) and its influence on massive sulfide formation. *Lithos* **112:** 40-56.

Plouviez S, Shank TM, Faure B, Daguin-Thiebaut C, Viard F, Lallier FH, Jollivet D. 2009. Comparative phylogeography among hydrothermal vent species along the East Pacific Rise reveals vicariant processes and population expansion in the South. *Molecular Ecology* **18:** 3903-3917.

Reid WDK, Sweeting CJ, Wigham BD, Zwirglmaier K, Hawkes JA, McGill RAR, Linse K, Polunin NVC. 2013. Spatial differences in East Scotia Ridge hydrothermal vent food webs:

influences of chemistry, microbiology and predation on trophodynamics. *PLoS ONE* **8:** e65553.

Rogers AD, Tyler PA, Connelly DP, Copley JT, James R, Larter RD, Linse K, Mills RA, Garabato AN, Pancost RD, Pearce DA, Polunin NVC, German CR, Shank T, Boersch-Supan PH, Alker BJ, Aquilina A, Bennett SA, Clarke A, Dinley RJJ, Graham AGC, Green DRH, Hawkes JA, Hepburn L, Hilario A, Huvenne VAI, Marsh L, Ramirez-Llodra E, Reid WDK, Roterman CN, Sweeting CJ, Thatje S, Zwirglmaier K. 2012. The discovery of new deep-sea hydrothermal vent communities in the Southern Ocean and implications for biogeography. *PLoS Biol* **10:** e1001234.

Talley LD, Pickard GL, Emery WJ, Swift JH. 2011. Chapter 11 - Indian Ocean. In: Talley LD, Pickard GL, Emery WJ and Swift JH, eds. *Descriptive Physical Oceanography (Sixth Edition)*. 6th ed. Boston, MA: Academic Press. 363-399.

Tao C, Li H, Jin X, Zhou J, Wu T, He Y, Deng X, Gu C, Zhang G, Liu W. 2014. Seafloor hydrothermal activity and polymetallic sulfide exploration on the southwest Indian ridge. *Chinese Science Bulletin***:** 1-11.

Tao C, Wu G, Ni J, Zhao H, Su X, Zhou N, Li J, Chen YJ, Cui R, Deng X, Egorov I, Dobretsova IG, Sun G, Qiu Z, Deng X, Zhou J, Gu C, Li J, Yang J, Zhang K, Wu X, Chen Z, Lei J, Huang W, Zhou P, Ding T, Jin W, Li H, Lin J. 2009. New hydrothermal fields found along the SWIR during the Legs 5-7 of the Chinese DY115-20 Expedition (Abstract #OS21A-1150) *American Geophysical Union, Fall Meeting 2009*. San Francisco, California, USA: American Geophysical Union.

Vrijenhoek RC. 2010. Genetic diversity and connectivity of deep-sea hydrothermal vent metapopulations. *Molecular Ecology* **19:** 4391-4411.

Warén A, Bengtson S, Goffredi SK, Van Dover CL. 2003. A Hot-Vent Gastropod with Iron Sulfide Dermal Sclerites. *Science* **302:** 1007-1007.

Waren A, Bouchet P. 2001. Gastropoda and Monoplacophora from hydrothermal vents and seeps; new taxa and records. *The Veliger* **44:** 116-231.

Appendix

Research papers co-authored during the course of this DPhil, in reverse chronological order

Introduction to the Appendix

This appendix consists of five additional peer-reviewed research papers that I have contributed to and co-authored during the course of this DPhil. They are included in reverse chronological order. The detailed information and citation for each are as follows, in the same order:

Nakajima R, Yamamoto H, Kawagucci S, Takaya Y, Nozaki T, Chen C, Fujikura K, Miwa T, Takai K. *In press*. Post-drilling changes in seabed landscape and megabenthos in a deep-sea hydrothermal system, the Iheya North field, Okinawa Trough. *PLoS ONE*. (Manuscript ID: PONE-D-14-50157R1)

Nakamura M, Chen C, Mitarai S. 2015. Insights into life-history traits of *Munidopsis* spp. (Anomura: Munidopsidae) from hydrothermal vent fields in the Okinawa Trough, in comparison with the existing data. *Deep-Sea Research Part I: Oceanographic Research Papers*, **100**: 48-53.

Xu T, Sun J, Chen C, Qian P-Y, Qiu J-W. 2015. The mitochondrial genome of the deep-sea snail *Provanna* sp. (Gastropoda: Provannidae). *Mitochondrial DNA,* http://dx.doi.org/10.3109/19401736.2014.1003827.

Houart R, Moe CO, Chen C. 2015. Description of two new species of *Chicomurex* from the Philippine Islands (Gastropoda: Muricidae) with update of the Philippines species and rehabilitation of *Chicomurex gloriosus* (Shikama, 1977). *Venus: the Japanese Journal of Malacology,* **73**(1-2): 1-14

Houart R, Moe CO, Chen C. 2014. *Chicourex lani* sp. nov. (Gastropoda: Muricidae), a new species and its intricate history. *Bulletin of Malacology, Taiwan,* **37**: 1-14.

Post-drilling changes in seabed landscape and megabenthos in a deep-sea hydrothermal system, the Iheya North field, Okinawa Trough

Ryota Nakajima[1*], Hiroyuki Yamamoto[2], Shinsuke Kawagucci[2, 3, 4], Yutaro Takaya[2], Tatsuo Nozaki[2, 5], Chong Chen[6], Katsunori Fujikura[1], Tetsuya Miwa[2,7], Ken Takai[2, 3, 4]

[1] Department of Marine Biodiversity Research, Japan Agency for Marine-Earth Science and Technology (JAMSTEC), 2-15 Natsushima, Yokosuka, Kanagawa 237-0061, Japan

[2] Research and Development Center for Submarine Resources, Japan Agency for Marine-Earth Science and Technology (JAMSTEC), 2-15 Natsushima, Yokosuka, Kanagawa 237-0061, Japan

[3] Laboratory of Ocean-Earth Life Evolution Research (OELE), Japan Agency for Marine-Earth Science and Technology (JAMSTEC), 2-15 Natsushima, Yokosuka, Kanagawa 237-0061, Japan

[4] Department of Subsurface Geobiological Analysis and Research (D-SUGAR), Japan Agency for Marine-Earth Science and Technology (JAMSTEC), 2-15 Natsushima, Yokosuka, Kanagawa 237-0061, Japan

[5] Department of Systems Innovation, School of Engineering, The University of Tokyo, 7-3-1 Hongo, Bunkyo-ku, Tokyo 113-8656, Japan

[6] Department of Zoology, University of Oxford, South Parks Road, Oxford, OX1 3PS, United Kingdom

[7] Marine Technology and Engineering Center (MARITEC), Japan Agency for Marine-Earth Science and Technology (JAMSTEC), 2-15 Natsushima, Yokosuka, Kanagawa 237-0061, Japan

*Corresponding author

E-mail: nakajimar@jamstec.go.jp

Abstract

There has been an increasing interest in seafloor exploitation such as mineral mining in deep-sea hydrothermal fields, but the environmental impact of anthropogenic disturbance to the seafloor is poorly known. In this study, the effect of such anthropogenic disturbance by scientific drilling operations (IODP Expedition 331) on seabed landscape and megafaunal habitation was surveyed for over 3 years using remotely operated vehicle video observation in a deep-sea hydrothermal field, the Iheya North field, in the Okinawa Trough. We focused on observations from a particular drilling site (Site C0014) where the most dynamic change of landscape and megafaunal habitation was observed among the drilling sites of IODP Exp. 331. No visible hydrothermal fluid discharge had been observed at the sedimentary seafloor at Site C0014, where *Calyptogena* clam colonies were known for more than 10 years, before the drilling event. After drilling commenced, the original *Calyptogena* colonies were completely buried by the drilling deposits. Several months after the drilling, diffusing high-temperature hydrothermal fluid began to discharge from the sedimentary subseafloor in the area of over 20 m from the drill holes, 'artificially' creating a new hydrothermal vent habitat. Widespread microbial mats developed on the seafloor with the diffusing hydrothermal fluids and the galatheid crab *Shinkaia crosnieri* endemic to vents dominated the new vent community. The previously soft, sedimentary seafloor was hardened probably due to barite/gypsum mineralization or silicification, becoming rough and undulated with many fissures after the drilling operation. Although the effects of the drilling operation on seabed landscape and megafaunal composition are probably confined to an area of maximally 30 m from the drill holes, the newly established hydrothermal vent ecosystem has already lasted 2 years and is like to continue to exist until the fluid discharge ceases and thus the ecosystem in the area has been altered for long-term.

Introduction

In the last few decades, deep-sea hydrothermal ecosystems have been under increasing threat from various anthropogenic activities either underway or planned [1–3]. Recent technological developments have overcome the barrier of water depth and distance from shore, allowing the exploitation of previously inaccessible areas [4]. This has boosted the continuous expansion of anthropogenic activities in the hydrothermal vent ecosystems, including the exploitation of valuable mineral resources [5]. Hydrothermal vent sites produce seafloor massive sulfide (SMS) deposits with high-grade ores, giving them an attractive commercial prospect for mining [1,2].

Many potential impacts on the benthic community from mining activities are predicted: habitat loss and degradation, modification of fluid flux regimes, changes in diversity, and change of habitat conditions [1,3,6]. Although there is no case of commercial based seafloor mining on hydrothermal vent area so far, we can estimate the impacts or effects from mining activities from case studies of natural and artificial disturbances, such as volcanism and drilling [7]. Although disturbance caused by drilling may be different from proposed mining methods, including mechanical cutting, grabbing and dredging of vent chimney and hydrothermal deposits, impacts from drilling have the potential to serve as supporting evidence when assessing the risk of mining operation.

At present, the impact of drilling at hydrothermal systems is poorly understood (e.g. [8]). Most studies on the environmental impacts associated with deep-sea exploration (or commercial) drilling have been conducted in oil and gas field (e.g. [9–13]), focusing on how drilling deposits (cuttings and mud) affect mortality and survival rate of benthic animals (e.g. [12,11,10,14]). The drilling impact on seabed landscape and associated megabenthos in hydrothermal fields is likely to differ from these cases. Potential impacts that may be expected include the discharge of drilling deposits on to the seabed and subsequently high-temperature hydrothermal fluids from subseafloor. It is conceivable that the fluid discharges will attract

recruits from the surrounding vent communities, creating 'artificial' hydrothermal vent ecosystems [7]. Understanding how the benthic community responds to drill-induced disturbance will help shape future ecosystem conservation strategy in anticipation of upcoming SMS mining activities. It is therefore crucial to conduct monitoring and assessment of the effect of drilling on the benthic community of deep-sea hydrothermal fields.

In September 2010, Integrated Ocean Drilling Program (IODP) Expedition 331 was carried out at the Iheya North hydrothermal field in the Okinawa Trough, Japan using the deep-sea drilling vessel *Chikyu* to investigate active subseafloor microbial communities associated with the physical and chemical variation of hydrothermal fluid flow [15,16]. The expedition established several drilling-induced, 'artificial' hydrothermal vents [16,17]. These artificial vents provided unique research opportunities for estimating the influence of anthropogenic drilling to the benthic communities of deep-sea hydrothermal ecosystems. As a part of an environmental impact assessment, we surveyed the changes in the seabed landscape and habitat as well as the abundance and composition of the megafaunal benthic community around the drill holes for over 3 years. Our focuses in this study are to examine the extent and persistence of the effects of the drilling operations in the area and to elucidate how the habitat condition as well as the benthic megabenthos communities are altered by the drilling.

Materials and Methods

Ethics statement

The location for this study was not privately owned or protected in any way and no specific permits were required for the described field studies and sample collection. The field studies did not involve any endangered or protected species. No invertebrate megafaunal specimens were collected in this work, as it was carried out using video techniques.

Study location

Situated approximately 150 km off the Okinawa Island, Japan, the Iheya North field (27°45'-50'N; 126°53'-55'E) in the Okinawa Trough is a deep-sea hydrothermal field with a depth of ca. 1,000 m. Two decades of investigation since its discovery has revealed its geological background, fluid chemistry and microbiological characteristics [15,17–20]. Among the many active chimney sites, the 30 m high North Big Chimney (NBC) mound is the activity center of the field (Fig. 1b, [18]). The Iheya North field is characterized by thick soft sediments offering habitats for endobenthic invertebrates even around hydrothermal vent site, allowing both vent-type and seep-type communities to exist in the area [21,22]. Representative species of megabenthic vent animals in the Iheya North field are *Shinkaia crosnieri* galatheid crab, *Alvinocaris longirostris* shrimp, *Paralvinella* polychaetes, *Paralomis* lithodid crab, and *Bathymodiolus japonicus* and *B. platifrons* mussels. Representative species of the geofluid seepage zone of the Iheya North vent field is the endobenthic deep-sea clam, *Calyptogena* spp., which colonizes the sedimentary seafloor [23].

Of the several sites drilled during the IODP Expedition 331 (Fig. 1b, see also [16]), Site C0014 is located 450 m east of the NBC mound. Around Site C0014, both active and non-active chimneys as well as apparent hydrothermal fluid discharges were not identified through visual observations by previous submersible surveys [21]. This site was characterized by several *Calyptogena* clam colonies, which had been identified for more than 10 years before the drilling event, indicating the colonies were likely supported by seepage of hydrothermal fluid input [16,17]. In total, seven holes were drilled at Site C0014 (i.e., Holes A-G) in a narrow area within 10 m radius, overlapping with the *Calyptogena* colonies (see red stars in Figs. 1c, 2a). The holes were located at 1,060 m depth (Table 1). Hole G penetrated the deepest (136.7 m below the seafloor, mbsf), and the penetration depths of the other holes (Holes A-F) ranged from 4.2 to 44.5 mbsf (Table 1). Holes D and E were very closely located and they became one hole after the wall between them broke down (Hole D/E hereafter). At 11 months after the drilling operation only Holes D/E, B and G were visibly recognizable while the other holes had collapsed and filled up

due to their shallow penetration (~6.5 mbsf).

The multiple drilling operations penetrated the repeated hard layers that might have served as cap rocks, and high-temperature hydrothermal fluid were discharged from the holes as well as in the shallower sediments surrounding the holes [15–17]. A casing pipe was deployed down to ca. 120 mbsf at Hole G fixed with a corrosion cap (open outlet pipe) mounted on the gimballed guide base [15,16]. After casing and capping, diffusing hydrothermal fluid discharged not from the corrosion cap outlet but from the seafloor through the annulus, the space between the wall of the hole and the casing pipe at Hole G; the temperature of the diffusing fluids was found to be >240ºC [16]. Five months after the drilling, high-temperature hydrothermal fluid (304-311ºC) discharged from the casing pipe outlet at Hole G, and the fluid discharge from the pipe continued at 25 months after drilling [17]. Prior to the drilling (2 weeks before), a thermometer and an acrylic-glass sedimentation chamber with mounting stage were placed near Hole D/E (Fig. 3a). The thermometer recorded that the bottom surface temperature near Hole D/E had increased at 11 months and reached >50ºC at 14-15 months after drilling, which was the maximum temperature for the thermometer (the thermometer was broken at this time, see Fig. 4 in [17]).

Pre- and post-drilling video observations

Pre- and post-drilling seafloor video observations were carried out 2 weeks before drilling and 11, 16, 25, 38 and 40 months after drilling using JAMSTEC's remotely operating vehicles (ROVs) either *Hyper-Dolphin* or *Kaiko 7000 II* (Table 2). Video data were recorded with colour video cameras positioned in either vertical or oblique views by running the ROVs haphazardly around the drilling holes. At 2 weeks before and 11 months after drilling, a forward-facing video camera (Super HARP, Hamamatsu Photonic) recorded the seabed from the oblique view (the vertical distance of camera to vehicle bottom was 0.9 m). At 16, 25, 38 and 40 months after drilling, a downward-looking video camera (Handycam HDR-CX-700V, Sony) recorded the seabed vertically below the ROVs (the vertical distance of camera to vehicle bottom was 0.4 m).

The surveys were conducted at an altitude of 2.8 ± 0.3 m (the average distance of vehicle bottom to the bottom substrate during the imaging for each dive) and vehicle speed of ca. 0.25 m s^{-1}. The ROV angles during the video imagery were 5.1 ± 2.3º for pitch and 1.5 ± 0.6º for roll angles, thus causing some variation in subsequent measurements of seabed feature coverage and animal abundance. Positional data of ROVs from the Super-Short Baseline Navigation (SSBN) transponder were continuously recorded during the dives. The apparent outliers of the transponder were excluded before estimating the positional information of the vehicle. Position aberration of vehicles among the different survey periods were corrected based on the absolute positions of the gimballed guide base mounted on Hole G and the sedimentation chamber base placed near Hole D/E.

During the observation at 16 months post-drilling, in situ measurement of seawater pH was carried out using a submersible pH sensor for deep-sea (XR 420 CTD with AMP pH combined sensor, RBR Limited) which was installed on the ROV *Kaiko 7000 II*. Calibration of the pH sensor was performed pre- and post-dive operation of the ROV. In addition, hardness of the bottom sediment was examined by testing whether a push-core sampler can be inserted to the sediment (the concurrently collected sediment samples were used in other studies).

Video data analysis

The oblique and vertical video images were used for quantitative analysis of seabed features and megabenthic animals. Video clips were captured at 10-second intervals, using the software GOM Player (Gretech) in order to provide still image frames. Overlapping and unsuitable photographs (e.g., out of focus and high sediment re-suspension) were excluded from the analysis (excluded images constituted ~ 30% of the total generated images frames).

In order to derive % coverage of disturbed sediments indicated as white-colored clay-like substrate (drilling deposits) and microbial filamentous mats seen as either white or pink, the image frame sets collected by the video cameras were imported in the image analysis software CPCe (Coral Point Count with Excel extension, [24]). For each picture frame, 50-100 random

points were plotted and observed [25]. White-colored bacterial mats were impossible to distinguish from the white drilling deposits if the mat developed on or overlapped the deposits, and thus the coverage of white bacterial mats may be underestimated. The presence of fluid discharge observed as shimmering in each photograph was confirmed through cross-checking with original video clips, as it was difficult to determine if there was actually shimmering fluid from only still images. Distribution and coverage data of the discolored area and shimmering were plotted in a geographic information system using the software QGIS (version 2.2.0-Valmiera). In order to compare the seabed features (drilling deposits and microbial mats) between different sampling periods, we used the percentage cover within 10 m radius of Hole D/E as the hole was intensively visited by the ROVs.

The megabenthic invertebrate animals appeared in each image frame were identified to the lowest taxonomic levels possible and counted, and abundance of each animal was calculated from each image as number of individuals per m^2 (inds. m^{-2}). The seabed area of the image was estimated according to [26] for the perpendicular images and [27] for the oblique images using the underwater horizontal and vertical aperture angles of the camera and the camera-to-seafloor distance. We considered only animals with a minimum dimension ca. >30 mm. *Paralvinella* and polynoidea polychaetes were not counted as they were difficult to distinguish from the bottom substrate using our video observation from some distance. The distribution and abundance data of the megabenthic animals were plotted in geographical maps using QGIS. The abundances of observed animals between different sampling periods were compared within 10 m radius of Hole D/E. The statistical differences of these values were determined by multiple comparison Steel-Dwass test. Difference with $P<0.05$ was considered statistically significant.

At 16 and 40 months after drilling, carapace width length (mm) of the galatheid crab *Shinkaia crosnieri* that appeared in the perpendicular images recorded around Hole D/E was measured using the image analysis software Hakarundesu v0.7.1 (Natchan). The sedimentation chamber mount stage (base, 250 mm × 250 mm; height, 200 mm) that appeared in the images was used for length calibration. The statistical difference in the size of *S. crosnieri* between the

different sampling periods was determined by two-tailed Student's *t*-test. Difference with $P<0.05$ was considered statistically significant.

Results

Seabed landscapes before and after drilling

Prior to drilling, the sediment at Site C0014 was entirely dominated by fine-grained silty sediment (mud) (Figs. 2a, b, 3a). Pre-drilling video surveys revealed that there were no vent endemic animals within a 15 m radius of the center of the drill holes. The hydrothermal fluid seepage community characterized by live *Calyptogena* clam colonies was the most prominent feature in the soft sediment (Fig. 2b), though visual observation confirmed that more than 90% of the *Calyptogena* were dead shells. Rossellid sponges and laetmogonid holothrians were commonly observed around the clam colonies. The 15 m~ northwest of the drilling site was covered by hard substratum consisting of exposed bedrocks and boulders (Fig. 2a). Diffusing hydrothermal fluids were discharged from the fissures of the exposed bedrocks at some 20-30 m west-northwest of the drilling site, where vent endemic animals *Shinkaia crosnieri* galatheid crabs and *Bathymodiolus* mussel beds were observed (Figs. 2a, c). There was also a single small assemblage of *S. crosnieri* and *Bathymodiolus* mussels ca. 12 m northwest from Hole D/E (Fig. 2a).

After drilling commenced the drilling process deposited white-colored clay-like sediments (probably originating from drill cuttings and mud with clay mineral, barite and bentonite) on the seabed in the vicinity of the holes (Fig. 3b). This was visually confirmed at 11 months post-drilling. The multiple drilling operations drastically altered the seafloor landscape as the *Calyptogena* clam colonies were completely buried under the white-colored sediments. The white sediment extended 13-25 m from the center of drill holes at 16 months after drilling (Figs. 3g, 4). The mean coverage (%) of drilling deposits seen as clay-like white sediments within a 10 m radius of Hole D/E was 60.4 ± 31.2% at 16 months after drilling. The coverage of drill deposits

had decreased thereafter: 36.0 ± 21.5% at 25 months, and 20.3 ± 17.6% at 38-40 months post-drilling (Fig. 4). Although it was difficult to accurately assess the thickness of the newly deposited sediments, dead clam shells that appeared inside of Hole D/E suggest this was at least ca. 300 mm (Fig. 3i).

At 11 months after drilling, numerous tiny chimneys and drilling-induced hydrothermal fluid discharges seen as shimmering were observed on the white seafloor (Fig. 3b, see also Fig. 2l in [17]). The extent of shimmering fluid discharges induced by the drilling operations at 16 months after drilling was consistent with that of the white sediment, extending up to 24 m from the center of drill holes (Fig. 4). Naturally discharged shimmering water was also recognized from exposed bedrock areas at some 20 m west-northwest the drill site at this time (Fig. 4). The seawater pH showed lower values around the holes compared to the surrounding seafloor due to diffusive hydrothermal fluid discharges from the seafloor (Fig. 5). At 16 months after drilling the seawater pH increased with increasing distance from the holes; 7.09 ± 0.13 within 10 m from Hole D/E, 7.12 ± 0.12 at 10-20 m, 7.22 ± 0.06 at 20-30 m, and 7.39 ± 0.17 at 30-40 m.

Upon collection of the sedimentation chamber placed near Hole D/E at 16 months, bottom of the chamber was partially melted due to the increased bottom temperature (Fig. 3h). Considering the melting point of acrylic-glass [28], the seabed temperature likely have increased to at least 160ºC at 16 months. At 11 and 16 months after drilling, the bottom sediment around Hole D/E was soft enough for push core-samplers to penetrate into the sediment. However, the bottom had hardened after 25 months and the area which the core-samplers could penetrate into had become limited. At 38-40 months after drilling, the bottom was further hardened and it was impossible to insert the core-sampler into the sediment around Hole D/E and the bottom substratum was visually seen to be undulating with many fissures (Figs. 3f, l).

Unlike the drilling deposits, the coverage of bacterial mats around the holes increased over time (Fig. 6a, b). Two types of microbial mats, seen as white and pink colors, have developed after drilling commenced, extending 5-25 m from the center of holes. Before the drilling

commenced, white bacteria mats covered 10.3 ± 16.1% the seabed within 10 m radius from the point of Hole D/E, probably because the area hosted hydrothermal fluid seepage which also supported *Calyptogena* clam colonies. After drilling, the coverage of white bacterial mats had increased to 14.1 ± 18.4% at 16 months, 34.6 ± 19.7% at 25 months, and 46.5 ± 18.9% at 38-40 months (Fig. 6a). The pink-colored bacterial mats were not observed before drilling, but were first confirmed at 16 months post-drilling, covering 1.9 ± 3.6% within 10 m radius from Hole D/E, increasing thereafter: 7.7 ± 12.5% at 25 months and 12.5 ± 16.0% at 38-40 months post-drilling (Fig. 6b).

Changes in megafaunal assemblage composition after drilling

At 11 months after drilling, no benthic animals were observed 10 m radius around Hole D/E as the original *Calyptogena* clam colonies were buried under the drill deposits. At this time, however, a very low density (~0.27 inds. m^{-3}) of vent endemic galatheid crab *S. crosnieri* was found at 7.2-9.7 m northwest of Hole D/E (Fig. 7, geographical map not shown). At 16 months post-drilling the population of *S. crosnieri* has become widely distributed and dominated areas around the holes (Figs. 7, 8a). Another vent animal found at 16 months was *Alvinocaris longirostris* shrimp (Fig. 8b). We also confirmed the presence of other vent endemic animals such as *Paralvinella* polychaetes and polynoid polychaetes at this time, although their abundance was not counted.

The main distribution of *S. crosnieri* was restricted within a 10-15 m radius from the holes (Fig. 8a). The mean abundance of *S. crosnieri* within a 10 m radius of Hole D/E was 2.4 ± 7.2 inds. m^{-3} (max, 43 inds. m^{-3}) at 16 months after drilling (Fig. 7). Since the population of *S. crosnieri* was very patchily distributed, standard deviation (SD) was higher than the average. Although there were no significant differences among the different post-drilling periods (Steel-Dwass test; all test statistics, <0.6; 5% reference point, 2.57) probably due to the patchy distribution, mean abundance of *S. crosnieri* had increased by 4.5-fold at 25 months (mean, 10.5 ± 28.7 inds. m^{-3}; max, 110 inds. m^{-3}) compared to those at 16 months after drilling and became

relatively stable thereafter at 38 months (mean, 10.4 ± 20.4 inds. m^{-3}; max, 109 inds. m^{-3}) and 40 months (9.6 ± 20.1 inds. m^{-3}; max, 114 inds. m^{-3}). *S. crosnieri* was not found inside Hole D/E at 16 months but were found inside the holes at 25 months post-drilling and thereafter (Figs. 3i-k).

The mean carapace width length of *S. crosnieri* at 16 months (51 ± 11 mm) was significantly (*t*-test, $P = 0.0015\times10^{-6}$) higher than those at 40 months after drilling (43 ± 13 mm) (Fig. 10). At 16 months after drilling, larger individuals (60-70 mm width) dominated (35.1%), while at 40 months post-drilling smaller individuals (40-50 mm width) were the most predominant (25.8%) (Fig. 10). The proportion of individuals with 30-40 mm carapace width was only 3.0% at 16 months, but had increased to 15.6% at 40 months. There were no individuals with 20-30 mm carapace width at 16 months, but these appeared at 40 months (1.8%).

The mean abundance of *A. longirostris* shrimps at 16 months was 0.3 ± 0.8 inds. m^{-3} within 10 m radius of Hole D/E (max: 3.7 inds. m^{-3}). The abundance of *A. longirostris* at 25, 38 and 40 months after drilling was 0.2 ± 1.2 inds. m^{-3}, 1.1 ± 4.0 inds. m^{-3} and 0.4 ± 1.2 inds. m^{-3} with maximum abundance of 6.0, 21.6 and 10.0 inds. m^{-3}, respectively (Figs. 7, 8b). *Paralomis* sp. was not consistently observed within a 10 m radius of Hole D/E at 16 months, but appeared at 25, 38 and 40 months after drilling (Figs. 7, 9a), with a mean abundance of 0.07 ± 0.4 inds. m^{-3} at 25 months (max: 1.0 inds. m^{-3}), 0.004 ± 0.02 inds. m^{-3} at 38 months (max: 0.1 inds. m^{-3}) and 0.09 ± 0.2 inds. m^{-3} at 40 months (max: 0.7 inds. m^{-3}). However *Bathymodiolus* mussel, one of the typical sessile vent animals of the Okinawa Trough vents, has never been observed around the holes from our video investigations up to the most recent observation (i.e. 40 months post-drilling) (Fig. 9b).

Discussion

The results of this study revealed significant changes in the seabed landscape and megafaunal benthic community after an intensive drilling event in a deep-sea hydrothermal field. Although benthic animals that occupied the drilling site prior to drilling (such as live *Calyptogena*

clams in this case) were buried under drilling deposits as reported by previous studies (e.g., [17]), the amount of megabenthic animals lost in this drilling event was much greater than those at a normal, non-chemosynthetic deep-sea floor. This is due to deep-sea chemosynthetic habitats harboring a remarkably high abundance of benthic animals (e.g., 70-1,000 ind. m^{-2}, [29]) with a biomass of up to 500-1000 times greater [30,31], compared to the surrounding non-chemosynthetic sea floor (e.g., 0.2-6 inds. m^{-2}, [13]).

The extent of drilling impact on seabed landscape

The horizontal extent of the white drilling deposits in the present study was within 25 m of the drilling. This is similar to that reported from Orinoco Fan, Venezuela (10-25 m, [11]), while some other studies reported physical influence of exploitation drilling extended to approximately 100 m [9,12,13]. These differences may be due to the difference in the depths of drill holes and periods of time analyzed. Unlike any other reports though, the drilling event in the present study has subsequently caused hydrothermal fluid discharges seen as shimmering and lowering of seawater pH from the holes and the surrounding sediments, because Hole G penetrated into the subseafloor hydrothermal fluid reservoir [16]. The multiple drilling operations that disturbed the subseafloor hydrogeological structures may provide numerous vertical and lateral hydrothermal fluid pathway networks in the shallower sediments surrounding the holes [17].

During the study period, deposits from the drilling event have been gradually removed probably by lateral advection during high current events and from vertical redistribution in the sediments [12]. In contrast, bacterial mats have developed and become widespread. The newly emerged hydrothermal fluid discharges increased hydrothermal fluid inputs such as methane and hydrogen sulfide and increased the temperature of seafloor surface, promoting bacterial mat growth [32]. An increase in the areal extent of microbial mats up until 40 months post-drilling indicates a continuous supply of hydrothermal fluids from the subseafloor sources. This phenomenon differs from the microbial mat succession observed at the East Pacific Rise volcanic

eruption in 1991, which reported a marked reduction in the areal coverage of the microbial mats within one year (from >20 m^2 to <5 m^2) and no longer present 32 months after the eruption due to the reduction of hydrothermal flux [7]. Considering the horizontal extent of the shimmering fluid and white drilling deposits as well as newly developed bacterial mats, the horizontal impact distance by the scientific drilling was probably less than 30 m.

Seabed around the drill holes has been hardening throughout the post-drilling period, becoming rough and undulated with many fissures at 38-40 months after drilling. Unfortunately, we did not have sediment samples to characterize the hardening process in this study. However, the most likely process is barite/gypsum precipitation or silicification of the seafloor sediment. As mentioned earlier, high-temperature hydrothermal fluid (>160^{o}C) discharged through the seafloor sediment. If this hot fluid was mixed with ambient cold (4^{o}C) seawater, sulfate minerals such as anhydrite ($CaSO_4$), gypsum ($CaSO_4 \bullet 2H_2O$) and barite ($BaSO_4$) could be precipitated. The solubility of anhydrite in the ocean has a reverse relationship as a function of the temperature [33]. Thus, most of the anhydrite would be dissolved in the water when the seabed temperature decreased to ambient seawater temperature as previously observed at another IODP 331 drilling site (Site C0013, [17]), while some may remain as gypsum. Conversely, the solubility of barite is approximately three orders of magnitude lower than that of anhydrite [34], leading to survival of barite crystals. Indeed, a barite-rich chimney sample has been collected at the Iheya North field in the past, prior to the present study [35]. Barite also originated from drilling mud, which is used together with bentonite to adjust the density of circulative drilling mud water. Therefore, some fractions of barite crystal that harden the seabed may be of an artificial origin. Such barite/gypsum precipitation or silicification of the seafloor sediment might have sealed and plugged the hydrothermal paths within the sediment, which in turn converged the subseafloor hydrothermal flow. This process is a possible factor for the numerous fissures observed at 38-40 months, due to fluid pressure. Since bentonite is well known to produce low permeable layer that shut out the flow [36–38], artificially added bentonite in the drilling mud fluid may have also contributed to converge the subseafloor hydrothermal flow. Further investigation and additional sediment

sampling are necessary to elucidate the detailed mechanism of the seabed hardening after drilling.

Megafaunal assemblages at the artificial hydrothermal vents

Previous studies on the deep-sea drilling impacts in oil and gas fields showed that megafaunal density and diversity recovers partially from drilling disturbance after 3 years as there was significant removal of cuttings from those initially deposited [12]. Contrariwise, the disturbed ecosystems in the present study have not recovered to the pre-disturbed condition after 3 years, due to newly emerged hydrothermal fluid discharges from the subseafloor establishing new hydrothermal vent ecosystems. The 'artificial' vent ecosystem created has already lasted 2 years and is likely to be maintained as long as the hydrothermal fluid supply continues.

Originally, the drilling site was characterized by a chemosynthetic community sustained by hydrothermal fluid seepage (geofluid seep), where *Calyptogena* clams dominated. The clam colonies were however completely buried under the drilling deposits, and converted to a community consisting of typical vent-associated animals after several months. The galatheid crab *S. crosnieri* was predominant in the 'artificial' vent community, and their abundance around Hole D/E increased considerably from 11 months to 25 months, stablizing thereafter. We confirmed that a small number of *S. crosnieri* at 11 months within 10 m of Hole D/E and subsequent higher abundance at 16 months after drilling. This suggests the galatheid crabs started migrating to the drill site from 11 months when the bottom surface temperature around the holes started to increase, indicating hydrothermal fluid discharges [17]. Compared to the population at 40 months post-drilling, most individuals of *S. crosnieri* were larger in size in the 16 months post-drilling population, which also lacked small individuals (<3 cm carapace width). This strongly indicates that *S. crosnieri* migrated on foot to the drill site from existing nearby colonies by sensing the fluid discharge (chemistry and/or lowering of seawater pH), rather than through planktonic larvae dispersal. Although it may be possible for planktonic larvae of *S. crosnieri* to arrive at the drill site after 11 months, it is unlikely that individuals developed from planktonic larvae to adult in this short period (5 months, from 11 to 16 months) considering the general

crustacean growth rate [39]. Previous seabed observations confirmed several colonies of *S. crosnieri* outside of 20-40 m radius of the drill holes, implying their ability to migrate at least 20 m distance on foot.

Similarly, another typical vent animal *Alvinocaris* shrimp was confirmed at 16 months after drilling. *Paralomis* lithodid crabs have appeared at 25 months after drilling. *Paralomis* crabs are typical carnivores [23] and may have migrated into the drilling site following the migration of their potential preys, possibly *Shinkaia* galatheid crabs. Yet, another representative vent animal in the Iheya North field, *Bathymodiolus* mussels, has never been observed around Hole D/E throughout the study periods even when there are several mussel bed colonies at ca. 12-30 m distance around the drill holes. Although the sessile *Bathymodiolus* mussels can move short distances by depositing and releasing byssal threads [40,41], it is unlikely that they move such a long distance (20~ m) on foot. Consequently they can probably only migrate to the drill site through planktonic larvae dispersal. Assuming that the larvae had a steady growth of ca. 2 cm $year^{-1}$ [42], if they had settled after establishment of the 'artificial' vent community, these mussels must be visually recognizable from our ROV camera observation within 40 months after drilling. This strongly indicates that the drill site is unsuitable for mussel colonization. In the Okinawa Trough, *Shinkaia* crabs, *Alvinocaris* shrimps and *Paralvinella* polychaetes have been reported as being closely associated with active vents, while *Bathymodiolus* mussels occur distantly from active vents probably due to their lower tolerance levels of temperature and/or toxic substances such as hydrogen sulfide [43]. The high bottom temperature and/or high concentrations of hydrogen sulfide at the drill site may not provide suitable habitat for the mussels.

Conclusions

In conclusion, the intensive drilling campaign in the Iheya North hydrothermal field resulted in the complete collapse of the original hydrothermal-fluid-seepage community visually characterized by *Calyptogena* clams (some alive) due to drilling deposits. The subsequent

‘artificial’ hydrothermal fluid discharges from the holes and the surrounding seabed created ‘artificial’ hydrothermal vent ecosystems. The vent-endemic galatheid crab *S. crosnieri* quickly migrated to the newly created habitats and dominated the new vent community. Bottom substrate had hardened probably due to barite/gypsum mineralization or silicification, becoming rough and undulated with many fissures after drilling operation. Although the impacts of the drilling operation on seabed landscape and megafaual invertebrate composition were confined to an area of 30 m maximum from the drill holes, the newly established ‘artificial’ vent ecosystem from these drillings is likely to continue to exist until the fluid discharge ceases. Consequently, ecosystem in this area has been altered for long-term. It is indefinite how violent the disturbances to seabed will be, in the case of full-scale commercial mining. Such mining and their prerequisite feasibility studies of SMS deposits may require a large number of subseafloor drilling, for mineral deposit reserve assessment. Therefore, massive commercial mining anticipated in the near future will potentially create more ‘artificial’ hydrothermal vent ecosystems at a much greater scale.

Acknowledgements

We thank Center for Deep Earth Exploration (CDEX) for providing data for the IODP Expedition 331; the operation teams of ROVs (*Hyper-Dolphin* and *Kaiko 7000 II*) and the ship crews of R/V *Natsushima*, *Kairei* and *Kaiyo*; M. Morita and K. Yagasaki for their help in image analysis, and B. Thornton and A. Bodenmann (The University of Tokyo) for providing the altitude data of ROV.

References

1. Van Dover CL, Smith CR, Ardron J, Arnaud S, Beaudoin Y, Bezaury J, et al. Environmental management of deep-sea chemosynthetic ecosystems: justification of and considerations for a spatially based approach. ISA Technical Study: No.9. International Seabed Authority. 2011. Available at: http://www.isa.org.jm/files/documents/EN /Pubs/TS9/index.html#/30/.

2. Van Dover CL, Smith CR, Ardron J, Dunn D, Gjerde K, Levin L, et al. Designating networks of chemosynthetic ecosystem reserves in the deep sea. Mar Policy. 2012;36: 378–381.

3. Van Dover CL. Impacts of anthropogenic disturbances at deep-sea hydrothermal vent ecosystems: A review. Mar Environ Res. 2014;102: 59–72.

4. Glover AG, Smith CR. The deep-sea floor ecosystem: current status and prospects of anthropogenic change by the year 2025. Environ Conserv. 2003;30: 219–241.

5. Mengerink KJ, Van Dover CL, Ardron J, Baker M, Escobar-Briones E, Gjerde K, et al. A call for deep-ocean stewardship. Science. 2014;344: 696–698.

6. Boschen RE, Rowden AA, Clark MR, Gardner JPA. Mining of deep-sea seafloor massive sulfides: A review of the deposits, their benthic communities, impacts from mining, regulatory frameworks and management strategies. Ocean Coast Manag. 2013;84: 54–67.

7. Shank TM, Fornari DJ, Von Damm KL, Lilley MD, Haymon RM, Lutz RA. Temporal and spatial patterns of biological community development at nascent deep-sea hydrothermal vents (9°50′N, East Pacific Rise). Deep Sea Res Part II Top Stud Oceanogr. 1998;45: 465–515.

8. Copley JTP., Tyler PA, Van Dover CL, Schultz A, Dickson P, Singh S. Subannual temporal variation in faunal distributions at the TAG hydrothermal mound (26N, Mid-Atlantic Ridge). PSZN Mar Ecol. 1999;20: 291–306.

9. Currie DR, Isaacs LR. Impact of exploratory offshore drilling on benthic communities in the Minerva gas field, Port Campbell, Australia. Mar Environ Res. 2005;59: 217–233.

10. Jones DOB, Wigham BD, Hudson IR, Bett BJ. Anthropogenic disturbance of deep-sea megabenthic assemblages: a study with remotely operated vehicles in the Faroe-Shetland Channel, NE Atlantic. Mar Biol. 2007;151: 1731–1741.

11. Jones DOB, Cruz-Motta JJ, Bone D, Kaariainen JI. Effects of oil drilling activity on the deep water megabenthos of the Orinoco Fan, Venezuela. J Mar Biol Assoc UK. 2012;92: 245–253.

12. Jones D, Gates A, Lausen B. Recovery of deep-water megafaunal assemblages from hydrocarbon drilling disturbance in the Faroe−Shetland Channel. Mar Ecol Prog Ser. 2012;461: 71–82.

13. Gates AR, Jones DOB. Recovery of benthic megafauna from anthropogenic disturbance at a hydrocarbon drilling well (380 m depth in the Norwegian Sea). PLoS One. 2012;7: e44114.

14. Trannum HC, Nilsson HC, Schaanning MT, Øxnevad S. Effects of sedimentation from water-based drill cuttings and natural sediment on benthic macrofaunal community structure and ecosystem processes. J Exp Mar Bio Ecol. 2010;383: 111–121.

15. Takai K, Mottl MJ, Nielsen SH and the Expedition 331 Scientists. Proceedings of the Integrated Ocean Drilling Program vol. 331. Integr Ocean Drill Program Manage Int. Tokyo. 2011. doi:10.2204/iodp.proc.331.2011.

16. Takai K, Mottl MJ, Nielsen SH. IODP Expedition 331: Strong and Expansive Subseafloor Hydrothermal Activities in the Okinawa Trough. Sci Drill. 2012;13: 19–27.

17. Kawagucci S, Miyazaki J, Nakajima R, Nozaki T, Takaya Y, Kato Y, et al. Post-drilling changes in fluid discharge pattern, mineral deposition, and fluid chemistry in the Iheya North hydrothermal field, Okinawa Trough. Geochemistry, Geophys Geosystems. 2013;14: 4774–4790.

18. Kawagucci S, Chiba H, Ishibashi J. Hydrothermal fluid geochemistry at the Iheya North field in the mid-Okinawa Trough: Implication for origin of methane in subseafloor fluid circulation systems. Geochem J. 2011;45: 109–124.

19. Nakagawa S, Takai K, Inagaki F, Chiba H, Ishibashi J, Kataoka S, et al. Variability in microbial community and venting chemistry in a sediment-hosted backarc hydrothermal system: Impacts of subseafloor phase-separation. FEMS Microbiol Ecol. 2005;54: 141–155.

20. Tsuji T, Takai K, Oiwane H, Nakamura Y, Masaki Y, Kumagai H, et al. Hydrothermal fluid flow system around the Iheya North Knoll in the mid-Okinawa trough based on seismic reflection data. J Volcanol Geotherm Res. 2012;213-214: 41–50.

21. Watanabe H, Fujikura K, Kojima S. Japan: Vents and Seeps in Close Proximity. In: Kiel S, editor. The Vent and Seep Biota Aspects from Microbes to Ecosystems, Topics in Geobiolog, vol. 33. Topics in Geobiology. Dordrecht: Springer Netherlands; 2010. pp. 379–402.

22. Nakajima R, Yamakita T, Watanabe H, Fujikura K, Tanaka K, et al. Species richness and community structure of benthic macrofauna and megafauna in the deep-sea chemosynthetic

ecosystems around the Japanese archipelago: an attempt to identify priority areas for conservation. Divers Distrib. 2014;20: 1160–1172.

23. Fujikura K, Okutani T, Maruyama T. Deep-Sea Life –Biological Observations Using Research Submersibles. 1st ed. Kanagawa: Tokai University Press; 2008. (in Japanse with English abstract)

24. Kohler K, Gill S. Coral Point Count with Excel extensions (CPCe): A Visual Basic program for the determination of coral and substrate coverage using random point count methodology. Comput Geosci. 2006;32: 1259–1269.

25. Dumas P, Bertaud A, Peignon C, Léopold M, Pelletier D. A "quick and clean" photographic method for the description of coral reef habitats. J Exp Mar Bio Ecol. 2009;368: 161–168.

26. Jones DOB, Bett BJ, Tyler PA. Megabenthic ecology of the deep Faroe–Shetland channel: A photographic study. Deep Sea Res Part I. 2007;54: 1111–1128.

27. Nakajima R, Komuku T, Yamakita T, Lindsay DJ, Jintsu-uchifune Y, Watanabe H, et al. A new method for estimating the area of the seafloor from oblique images taken by deep-sea submersible survey platforms. JAMSTEC Rep Res Dve. 2014;19: 59–66.

28. Smith WF, Hashemi J. Foundations of Materials Science and Engineering. Boston: McGraw-Hill; 2006.

29. Rogers AD, Tyler PA, Connelly DP, Copley JT, James R, Larter RD, et al. The discovery of new deep-sea hydrothermal vent communities in the southern ocean and implications for biogeography. PLoS Biol. 2012;10: e1001234.

30. Tunnicliffe V. The biology of hydrothermal vents: ecology and evolution. Oceanogr Mar Biol An Annu Rev. 1991;29: 319–407.

31. Tunnicliffe V. Hydrothermal-vent communities of the deep sea. Am Sci. 1992;80: 336–349.

32. Jannasch HW. Microbial interactions with hydrothermal fluids. Seafloor Hydrothermal Systems: physical, chemical, biological and geological interactions. Geophys Monogr. 1995;91: 273–296.

33. Blount C, Dickson F. The solubility of anhydrite ($CaSO_4$) in NaCI-H2O from 100 to 450ºC and 1 to 1000 bars. Geochemica Cosmochim Acta. 1969;33: 227–245.

34. Blount C. Barite solubilities and thermodynamic quantities up to 300ºC and 1400 bars. Am Miner. 1997;62: 942–957.

35. Ueno H, Hamasaki H, Murakawa Y, Kitazon S, Takeda T. Ore and gangue minerals of sulfide chimneys from the North Knoll, Iheya Ridge, Okinawa Trough. JAMSTEC J Deep Res. 2003;22: 49–62.

36. Abeele WV. The influence of bentonite on the permeability of sandy silts. Nucl Chem Waste Manag. 1986;6: 81–88.

37. Kenney TC, Van Veen WA, Swallow MA, Sungaila MA. Hydraulic conductivity of compacted bentonite–sand mixtures. Can Geotech J. 1992;29: 364–374.

38. Sivapullaiah PV, Sridharan A, Stalin VK. Hydraulic conductivity of bentonite-sand mixtures. Can Geotech J. 2000;37: 406–413.

39. Mohamedeen H, Hartnoll R. Larval and postlarval growth of individually reared specimens of the common shore crab Carcinus maenas(L.). J Exp Mar Biol Ecol. 1990;134: 1–24.

40. Okoshi K, Sato-Okoshi W, Fujikura K. Significance for deep-sea bivalves of life-styles buried in the sediment or attached to objects. Japanese J Benthol. 2003;58: 77–83. (in Japanse with English abstract)

41. Arellano SM, Young CM. Pre- and post-settlement factors controlling spatial variation in recruitment across a cold-seep mussel bed. Mar Ecol Prog Ser. 2010;414: 131–144.

42. Dattagupta S, Bergquist DC, Szalai EB, Macko SA, Fisher CR. Tissue carbon, nitrogen, and sulfur stable isotope turnover in transplanted Bathymodiolus childressi mussels: Relation to growth and physiological condition. Limnol Oceanogr. 2004;49: 1144–1151.

43. Tokeshi M. Spatial structures of hydrothermal vents and vent-associated megafauna in the back-arc basin system of the Okinawa Trough, western Pacific. J Oceanogr. 2011;67: 651–665.

Figure Legends

Figure 1. Maps of the study area. (a) Location of the Iheya North hydrothermal field, Okinawa Trough. (b) An event map of the Iheya North field. Red stars and circles represent the IODP drilling sites (C0013, C0014 and C0016) and hydrothermal fluid venting sites, respectively. (c) Location of drill holes at Site C0014 (Holes A-G).

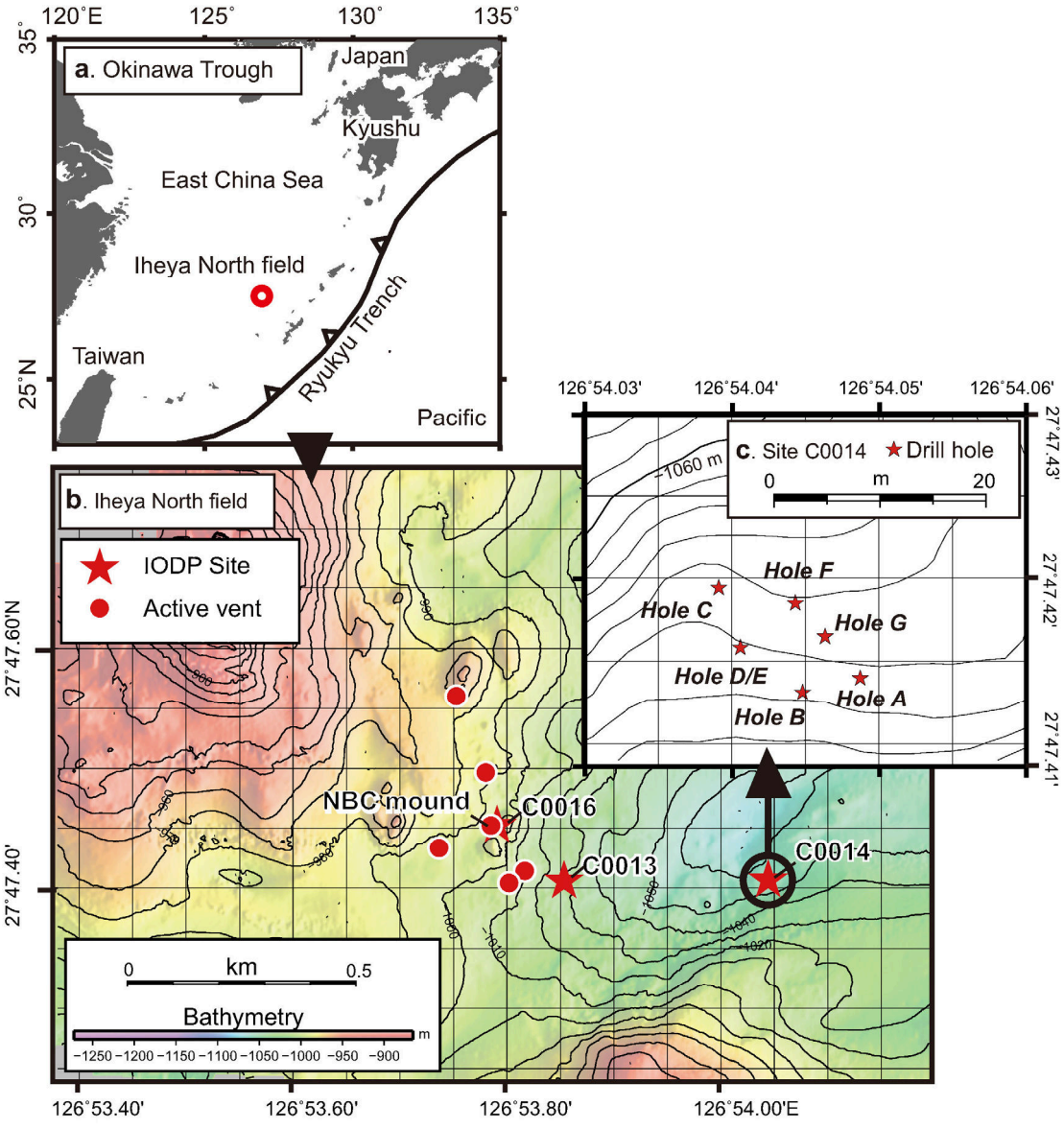

Figure 2. Habitat map around Site C0014. (a) Drill holes, % coverage of boulder and bedrock, and colonies of *Calyptogena* clams, *Bathymodiolus* mussels and both *Bathymodiolus* mussels and *Shinkaia crosnieri* galatheid crabs. (b) Pre-drilling seabed landscape near Hole D/E with *Calyptogena* clam colonies. (c) An example of *Bathymodiolus* mussels and *S. crosnieri* galatheid crabs colony.

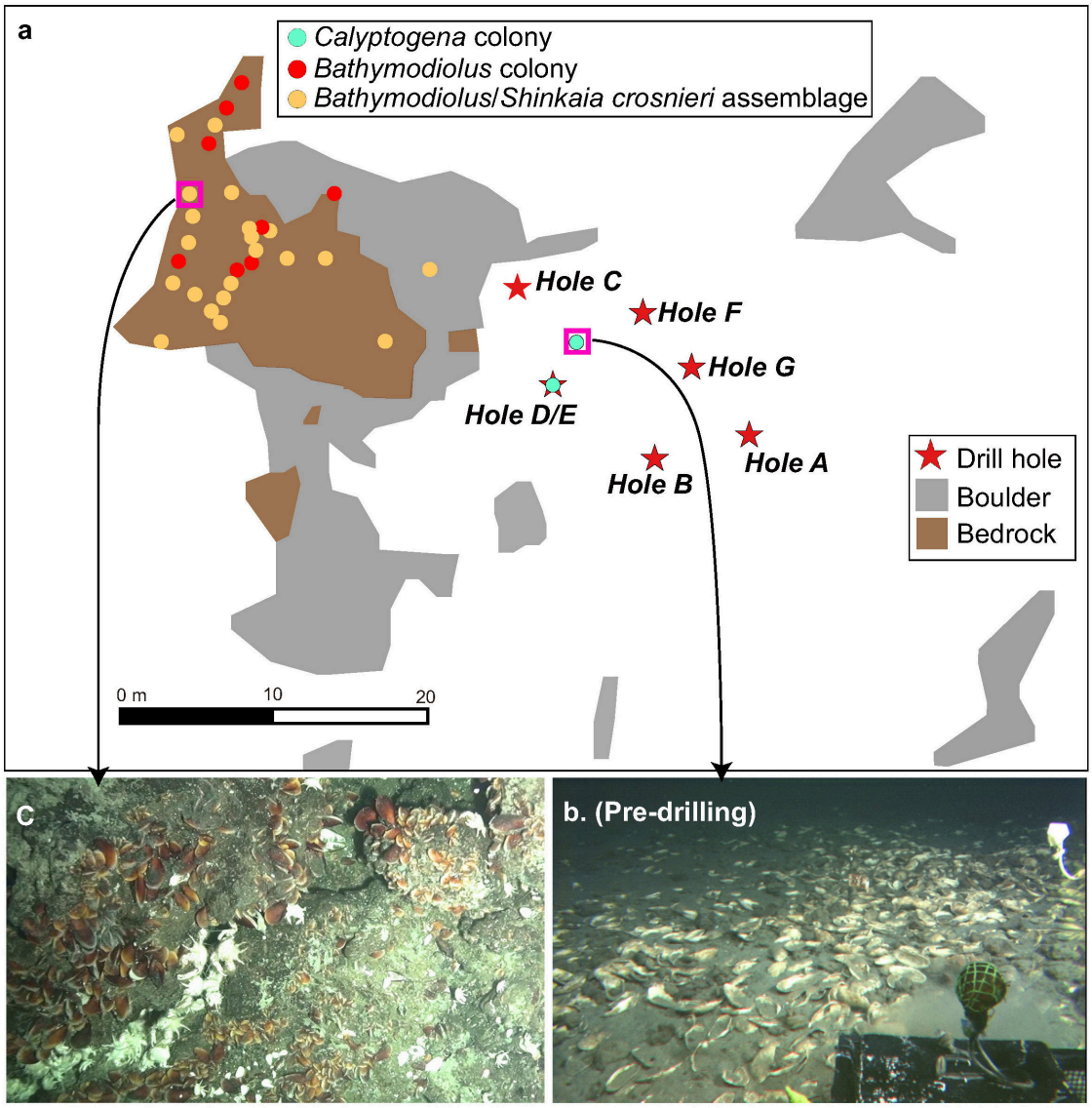

Figure 3. Temporal sequence of landscape at/around Hole D/E. Arrows in a-f indicate the sedimentation chamber base, which was placed at pre-drilling (a). Picture g indicates edge of cuttings and pictures i-k indicate perpendicular images of Hole D/E at 16, 25 and 38 months post-drilling, respectively.

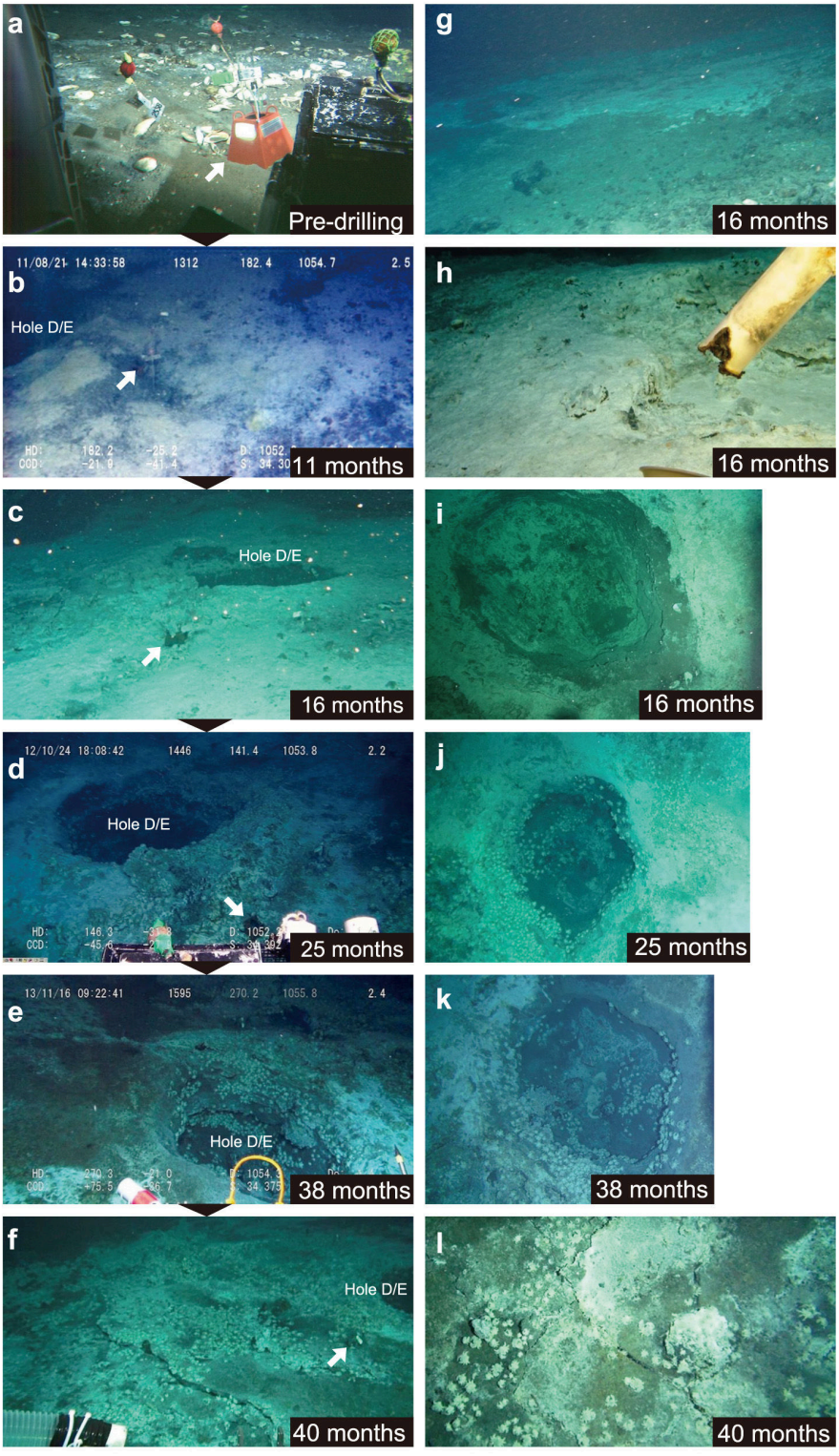

Figure 4. Temporal sequence of drilling deposits seen as white-color sediment as well as hydrothermal fluid discharges seen as shimmering at Site C0014. Dotted circles indicate the area within 10 m radius of Hole D/E.

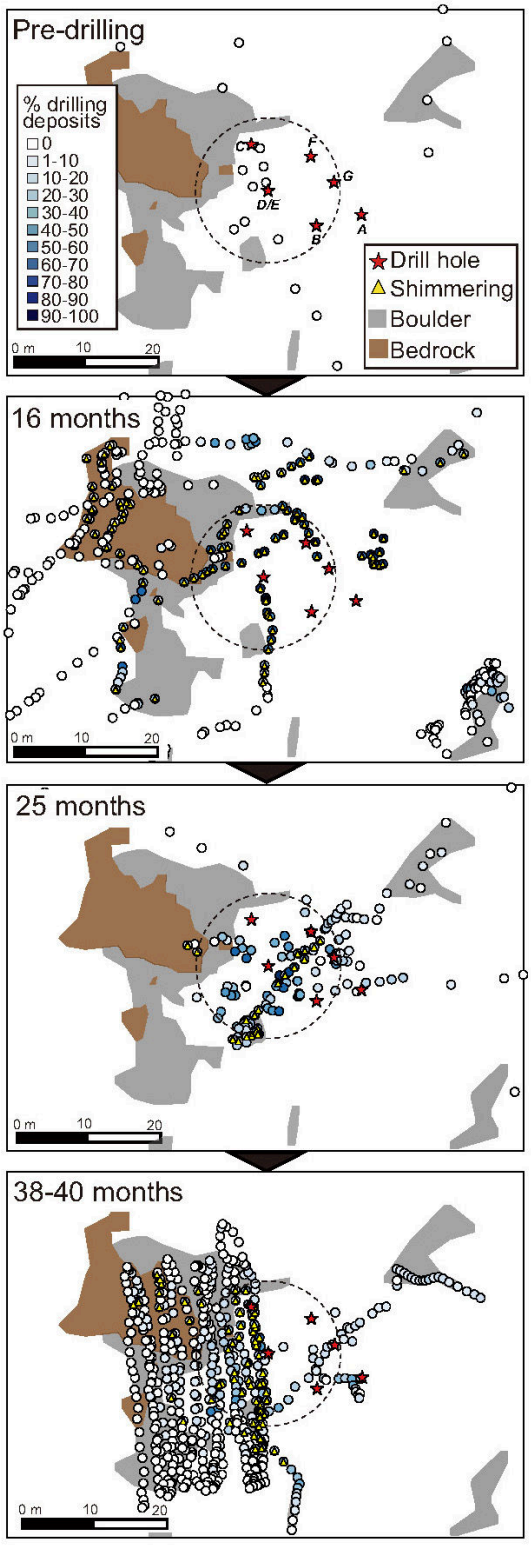

Figure 5. Distribution of seawater pH around drill holes at Site C0014 at16 months post-drilling. Dotted circles indicate the area within 10 m radios of Hole D/E.

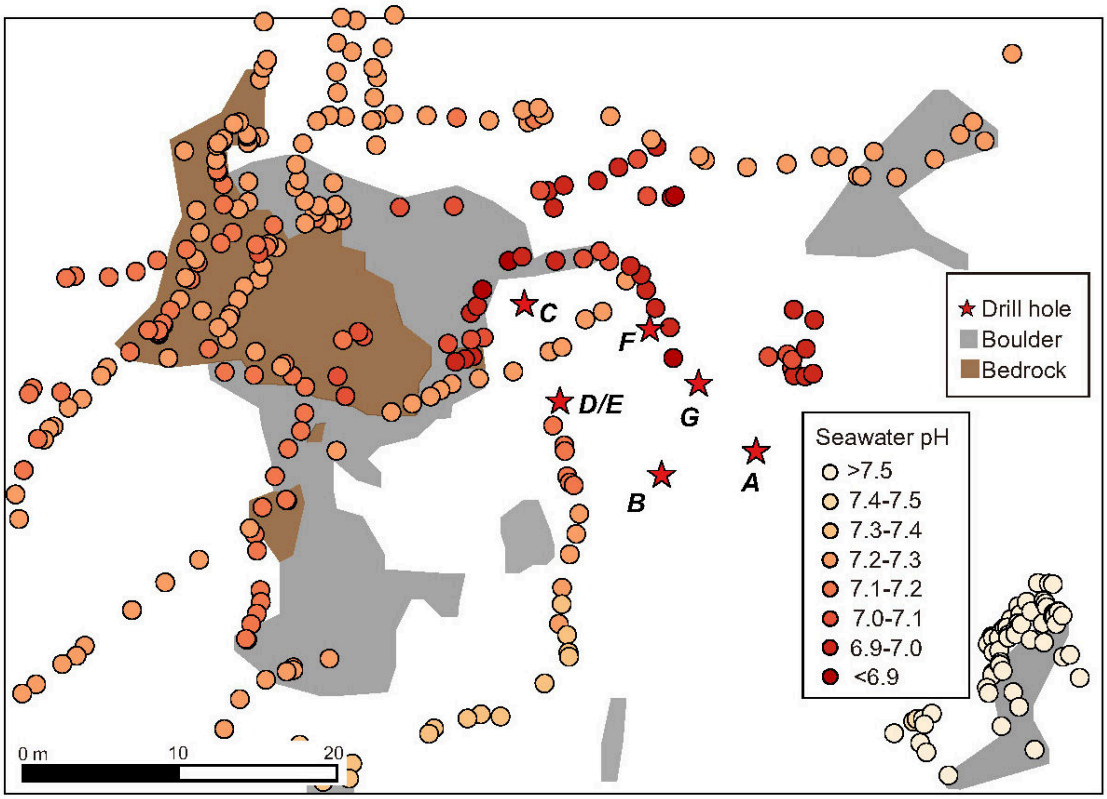

Figure 6. Temporal sequence of microbial mats at Site C0014. (a) white and (b) pink mats. Dotted circles indicate the area within 10 m radios of Hole D/E.

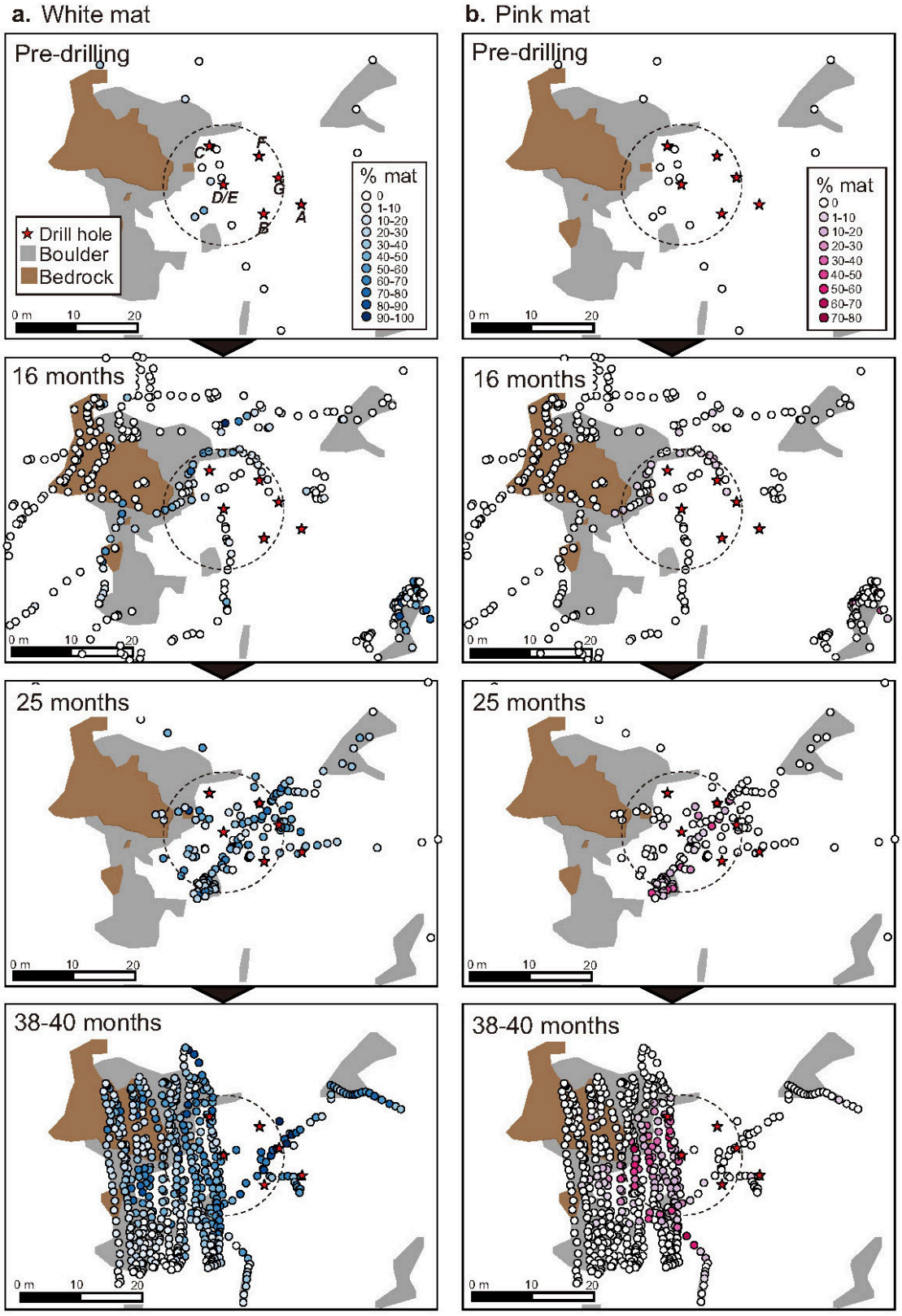

Figure 7. Temporal variations in the abundance of newly colonized megabenthos around Hole D/E. Abundance is average within 10 m radius from Hole D/E.

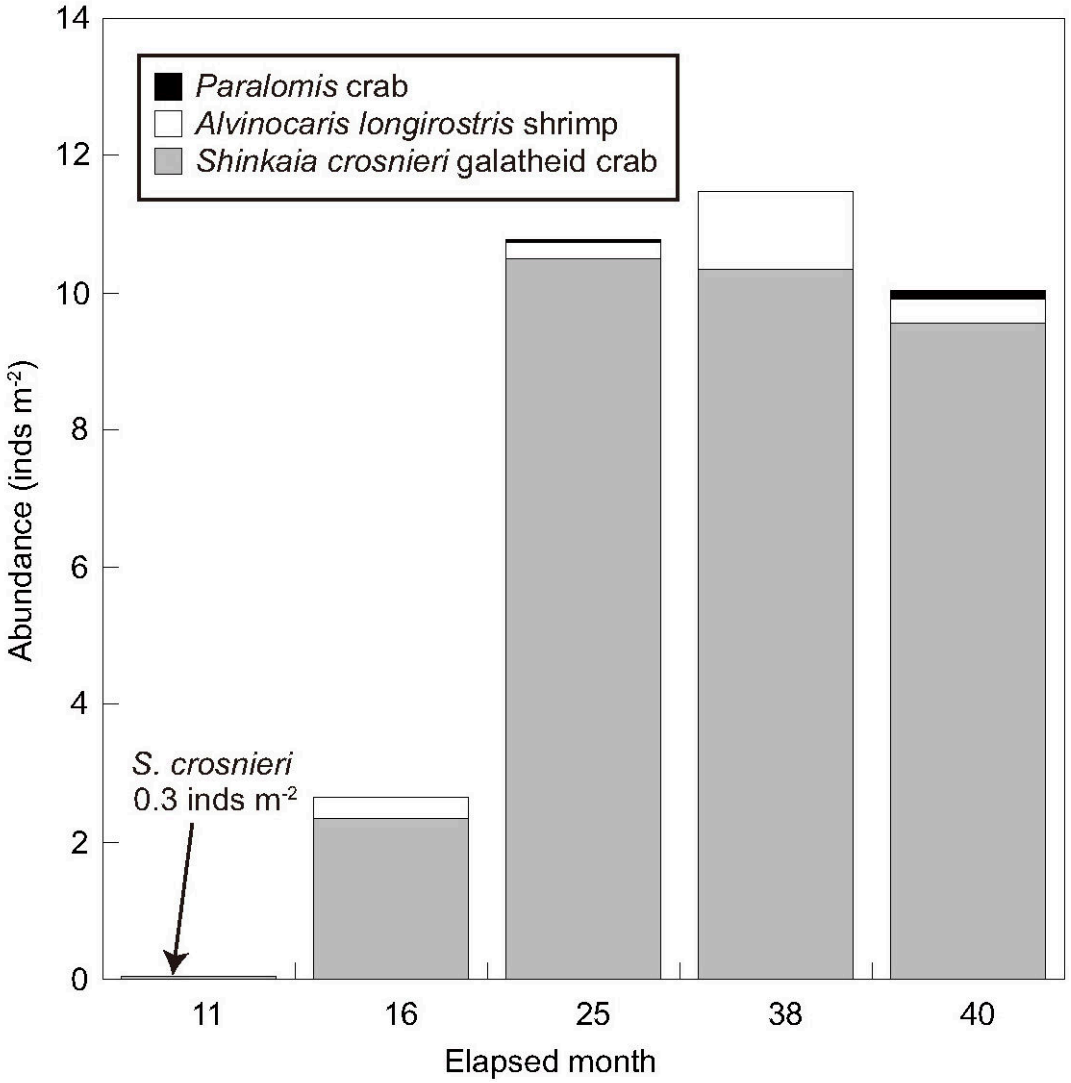

Figure 8. Temporal sequence in distribution and abundance of megabenthos at Site C0014. (a) *Shinkaia crosnieri* galatheid crabs and (b) *Alvinocaris longirostris* shrimps. Dotted circles indicate the area within 10 m radios of Hole D/E.

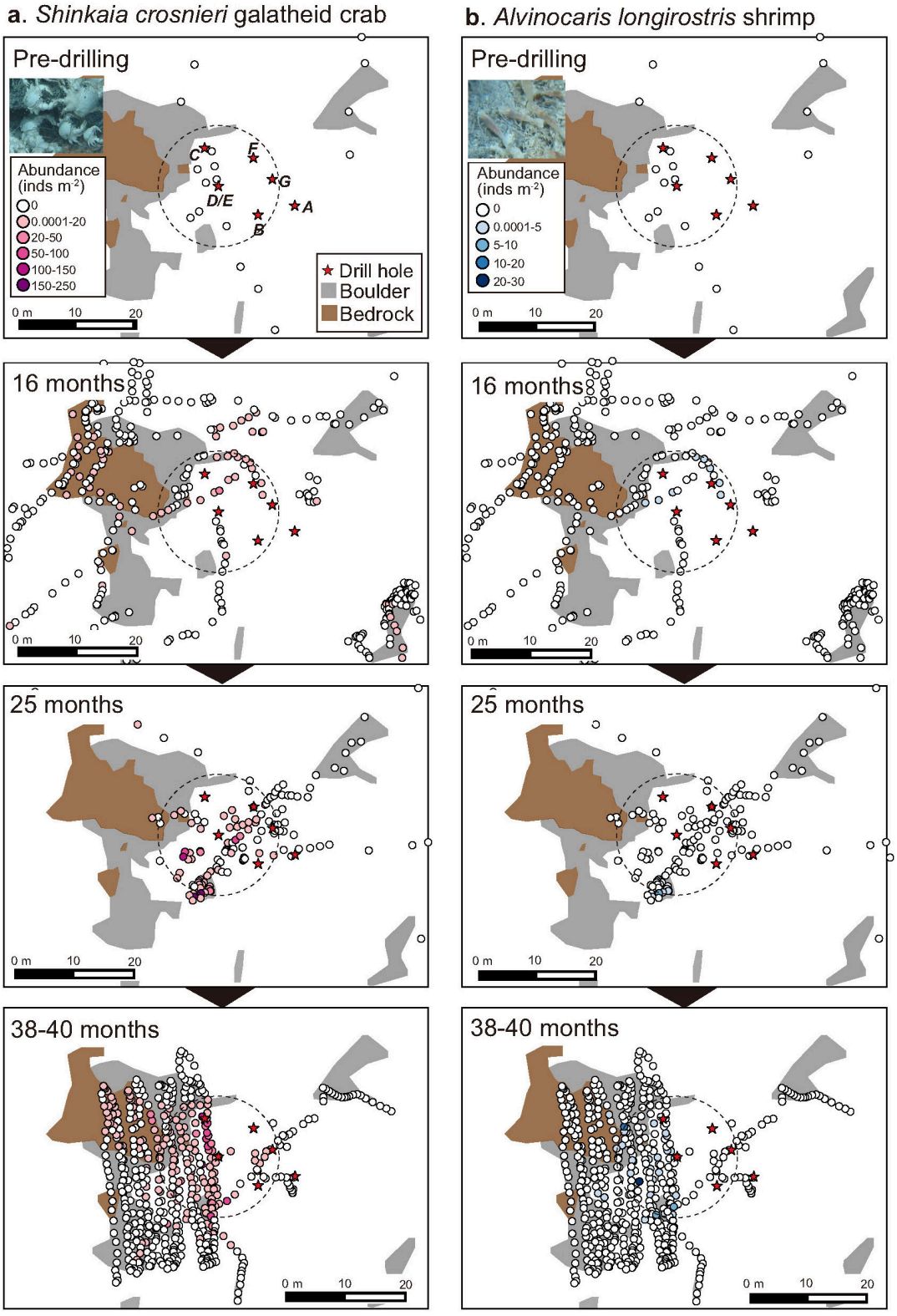

Figure 9. Temporal sequence in distribution and abundance of megabenthos at Site C0014. (a) *Paralomis* lithodid crabs and (b) *Bathymodiolus* mussels. Dotted circles indicate the area within 10 m radios of Hole D/E.

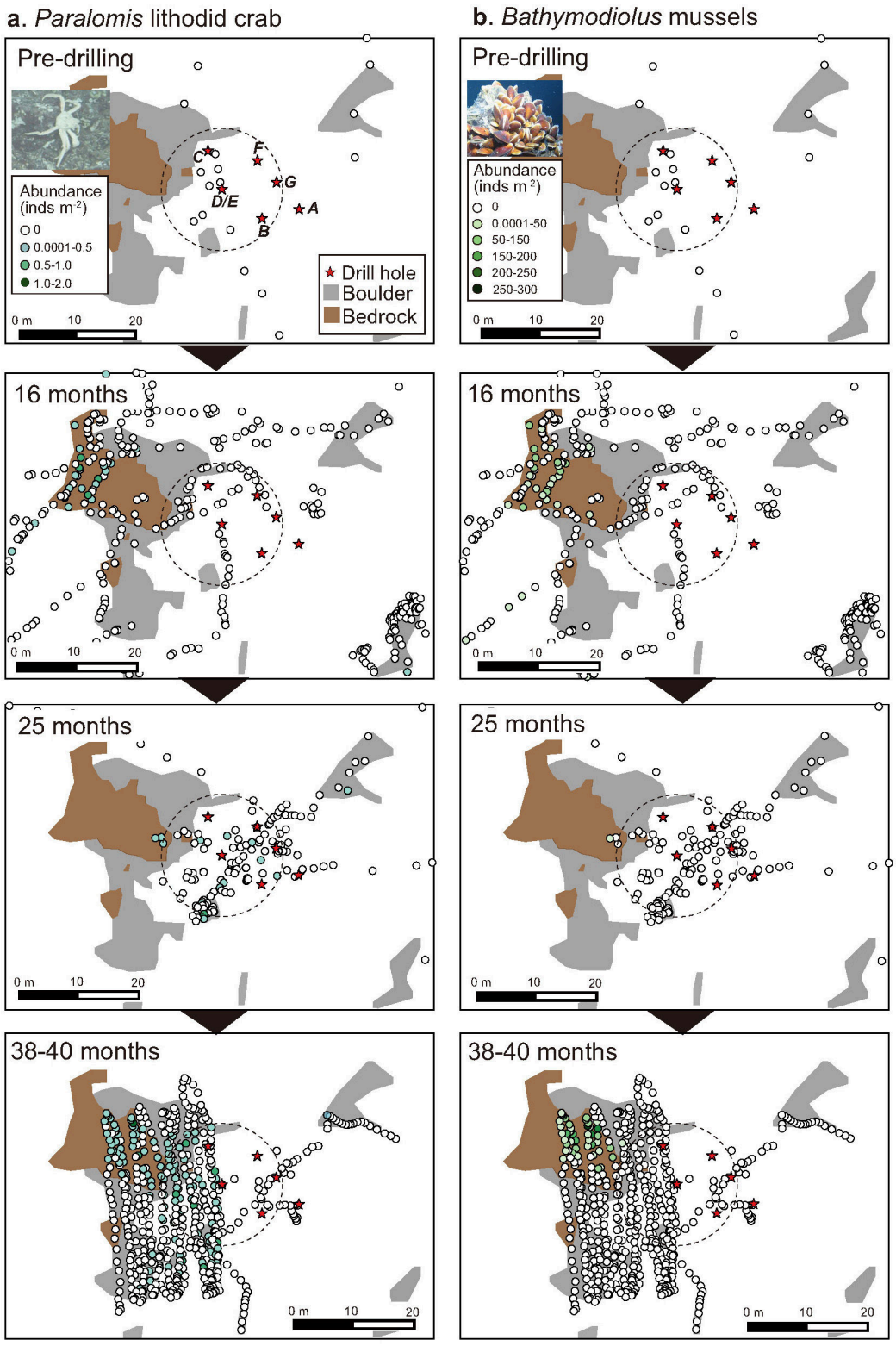

Figure 10. Size-frequency distribution of *Shinkaia crosnieri* galatheid crabs at (a) 16 months and (b) 40 months post-drilling. Each size-structure is based on galatheid crabs taken near Hole D/E.

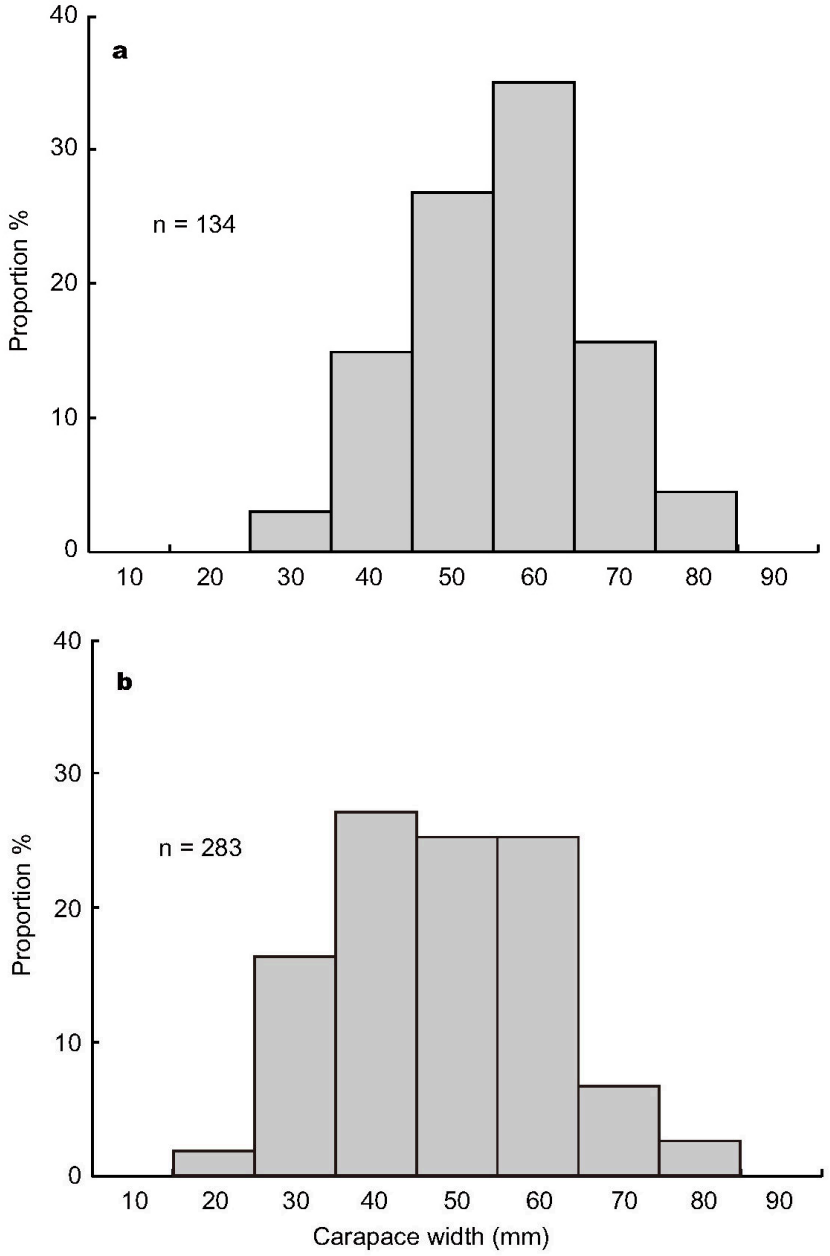

Tables

Table 1. Drill hole summary at Site C0014 in the Iheya North hydrothermal field, Okinawa Trough.

Hole	Latitude (N)	Longitude (E)	Water depth	Hole depth
			(m)	(mbsf)
A	27º47.4140'	126º54.0487'	1059.5	6.5
B	27º47.4131'	126º54.0448'	1059.0	44.5
C	27º47.4194'	126º54.0391'	1060.0	6.5
D	27º47.4158'	126º54.0406'	1060.0	16.0
E	27º47.4158'	126º54.0406'	1060.0	35.0
F	27º47.4185'	126º54.0443'	1060.8	4.2
G	27º47.4165'	126º54.0463'	1059.8	136.7

Table 2. Timing of investigations relative to the drilling event at Site C0014 in the Iheya North hydrothermal field, Okinawa Trough.

Date	Time elapsed	Cruise	ROV	Dive number
(mm/yy)				
Sep/2010	2 weeks before Drilling	NT10-E01	*Hyper-Dolphin*	1178
		IODP Exp331	ROV-C	
August/2011	11 months	NT11-15/16	*Hyper-Dolphin*	1312/1315
Jan/2012	16 months	KR12-02	*Kaiko 7000II*	537/538
Oct/2012	25 months	NT12-27	*Hyper-Dolphin*	1446/1447/1448/1450
Nov/2013	38 months	NT13-22	*Hyper-Dolphin*	1593/1595
Jan/2014	40 months	KY14-01	*Hyper-Dolphin*	1611

Deep-Sea Research I 100 (2015) 48–53

Contents lists available at ScienceDirect

Deep-Sea Research I

journal homepage: www.elsevier.com/locate/dsri

Note

Insights into life-history traits of *Munidopsis* spp. (Anomura: Munidopsidae) from hydrothermal vent fields in the Okinawa Trough, in comparison with the existing data

Masako Nakamura [a,*], Chong Chen [b], Satoshi Mitarai [a]

[a] Marine Biophysics Unit, Okinawa Institute of Science and Technology, Onna, Okinawa 904-0412, Japan
[b] Department of Zoology, University of Oxford, Oxford OX1 3PS, United Kingdom

ARTICLE INFO

Article history:
Received 17 March 2014
Received in revised form
29 January 2015
Accepted 3 February 2015
Available online 19 February 2015

Keywords:
Galatheidae
Sexual maturity
Egg volume
Hydrothermal vent

ABSTRACT

Squat lobsters in the genus *Munidopsis* are commonly found at, and near, hydrothermal vents. However, the reproductive traits of most *Munidopsis* spp. are unknown. This study examined the reproductive features of two *Munidopsis* species sampled from hydrothermal vent fields in the southern Okinawa Trough in February 2014. Three ovigerous females were collected: two *Munidopsis ryukyuensis* at Irabu Knoll (1661–1675 m depth) and one *M. longispinosa* at Hatoma Knoll (1482 m depth). Carapace sizes and egg volumes were measured and compared with those of other *Munidopsis* species. The ovigerous *M. ryukyuensis* specimens had postorbital carapace lengths of 10.3 and 11.8 mm, without the rostrum, and carapace widths of 8.6 and 9.7 mm. Mean egg volumes of *M. ryukyuensis* and *M. longispinosa* were ~4 mm^3. These results are consistent with early sexual maturity in *M. ryukyuensis* and lecithotrophic development in both species, as described in other species of the genus. These life-history traits may enable these vent species to maximize their reproductive and dispersive potential.

1. Introduction

Animals maximize their fitness in specific environments based on trade-offs among interconnected life traits (Stearns, 1992; Ramirez-Llodra, 2002; Reznick et al., 2002; Roff, 2002). Among such traits, age and size at maturity are important parameters because they reflect longevity and energy allocation strategies (Stearns, 1992). Early sexual maturation is advantageous for organisms living in unstable environments as it increases their probability of surviving long enough to reproduce (Stearns, 1992). Such species also tend to produce large numbers of relatively undeveloped offspring rather than investing in the care of relatively few offspring. Alternatively, they tend to have somewhat lower fecundity with multiple spawning events per year (Ramirez-Llodra, 2002). These strategies lead to high annual reproductive output, which reduces the risk of population extinction from unpredictable events.

Hydrothermal vents are inherently unstable and ephemeral, existing from several years to centuries (Macdonald, 1982; Converse et al., 1984; Grassle, 1985; Hessler et al., 1988; Lalou, 1991; Haymon et al., 1993). At fast-spreading ridges, vigorous venting activity causes abrupt changes in habitat and animal distribution (Perfit and Chadwick, 1998; Shank et al., 1998; Mullineaux et al., 2010, 2012). On the other hand, at slow-spreading ridges with greater temporal stability in vent activity (Copley et al., 2007), vent communities show some changes in species composition and abundance at the microhabitat level, reflecting changes in substrate (Gebruk et al., 2010) and temperature (Cuvelier et al., 2011). The reproductive traits of deep-sea species are believed to strongly reflect phylogenetic constraints and to exhibit the same degree of variation as those of sublittoral species (Gustafson and Lutz, 1994; Scheltema, 1994). In the case of animal species living near hydrothermal vents, variability in reproductive strategies may help to optimize their fitness in such environments (Van Dover, 2000; Young, 2003).

Among reproductive traits, early maturation is the most influential trait driving fitness (Ramirez-Llodra, 2002). Reproductive characteristics have been examined mainly for vent animals from the East Pacific Rise (EPR) and the Mid-Atlantic Ridge (MAR) (reviewed in Tyler and Young, 1999; Young, 2003; Adams et al., 2012), but little is known about reproductive traits of vent fauna in the western Pacific (Miyake et al., 2010; Nakamura et al., 2014). Evidence of early maturation has been observed in the vent shrimp *Rimicaris hybisae* (Nye et al., 2013) from the Mid-Cayman Spreading Centre and limpets in the genus *Lepetodrilus* from the EPR and MAR (Tyler et al., 2008) as well as the Okinawa Trough in the western Pacific (Nakamura et al., 2014).

Squat lobsters in the genus *Munidopsis* comprise 233 species worldwide, where they occur from shallow water to depths of

* Correspondence to: 1919-1 Tancha, Onna-son, Okinawa 904-0495, Japan. Tel.: +81 98 966 8694.
E-mail address: masako.nakamura@oist.jp (M. Nakamura).

http://dx.doi.org/10.1016/j.dsr.2015.02.007
0967-0637/

5000 m, but mainly on continental slopes and abyssal plains (Baba et al., 2008; Schnabel et al., 2011). In addition to cold seeps (Barry et al., 1996; Macpherson and Segonzac, 2005; Cubelio et al., 2007a) and whale falls (Bennett et al., 1994; Goffredi et al., 2004; Lundsten et al., 2010), they are commonly found in hydrothermal vent ecosystems (e.g., Williams and Van Dover, 1983; Baba, 2005; Martin and Haney, 2005; Cubelio et al., 2007b, 2008), and several *Munidopsis* species have been described from vent fields around Japan (Hashimoto et al., 1995; Ohta and Kim, 2001; Cubelio et al., 2007a, 2007c; Osawa and Takeda, 2007). Despite their diversity and wide distributions, their life-history characteristics remain virtually unknown (Baba et al., 2011; Kilgour and Shirley, 2014). The data that are available concern egg size in relation to body size and ocean depth (Van Dover and Williams, 1991). For ovigerous females, there are some additional data on body and egg sizes and depth of occurrence in the catalogues by Baba et al. (2008) and by Kilgour and Shirley (2014). In the laboratory, *Munidopsis serricornis* and *M. polymorpha* showed abbreviated larval development and their larvae were lecithotrophic (Samuelsen, 1972; Wilkens et al., 1990).

Here, we examine the reproductive attributes of two *Munidopsis* spp. from the Irabu Knowll and Hatoma Knoll hydrothermal vent fields in the southern Okinawa Trough, and compare them with those of other *Munidopsis* species.

2. Materials and methods

Munidopsis specimens were sampled at the Irabu Knoll (IR) and Hatoma Knoll (HA) hydrothermal fields in the Okinawa Trough using a suction sampler mounted on the Remotely Operated Vehicle (ROV) *Hyper-Dolphin* during the KY14-02 cruise of R/V *KAIYO* in February, 2014 (Fig. 1). Sampling was conducted at 1661–1675 m depth at IR and at 1482–1510 m depth at HA. Among the 11 individuals collected (2 at IR and 8 at HA), three were ovigerous (2 at IR and 1 at HA). Based on morphology, two individuals from IR were identified as *Munidopsis ryukyuensis* (Cubelio et al., 2007a), and the specimen from HA was identified as *M. longispinosa* (Cubelio et al., 2007a) (Fig. 2, Table 1). The other 8 individuals were one male and female *M. ryukyuensis*, 4 female *M. longispinosa*, and two juveniles (Table 2). The post-orbital carapace lengths (carapace lengths without the rostrum), carapace lengths with the rostrum, and carapace widths of all specimens were measured with digital calipers to the nearest 0.1 mm. Eggs were collected from the abdomen of each ovigerous specimen. Average egg radii were measured with Image-Pro Plus (ver. 7.0) from pictures taken under a binocular dissection microscope, and egg volumes were calculated from the average radius of each egg, assuming sphericity. These data were compared with data on the reproductive traits of *Munidopsis* spp.

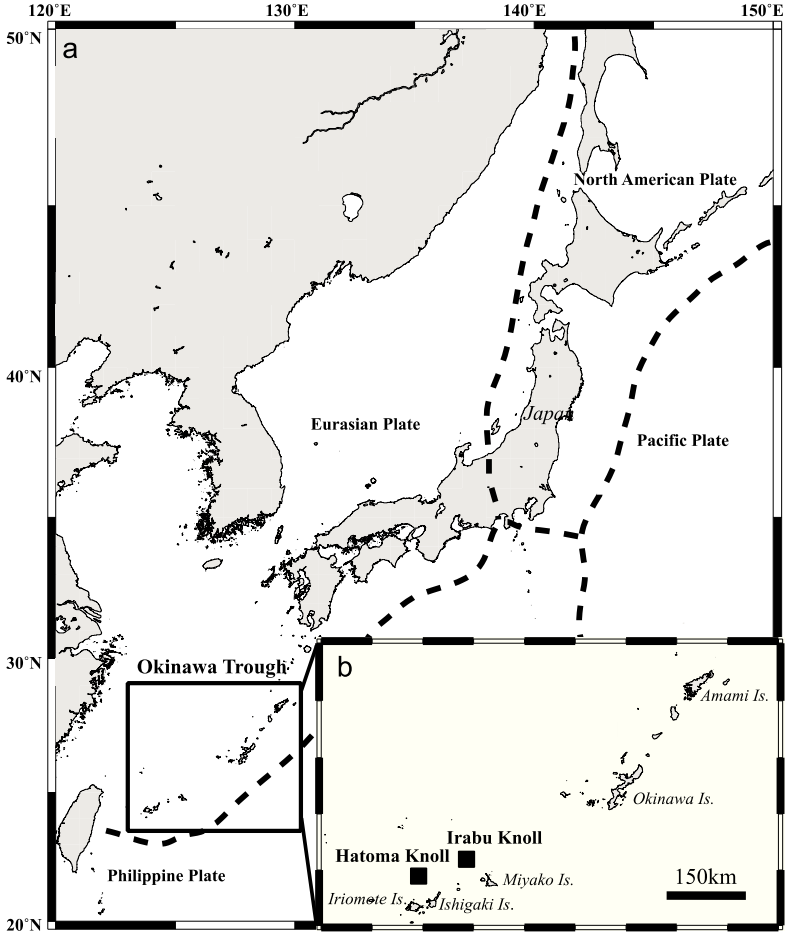

Fig. 1. Map of research sites where *Munidopsis* specimens were collected (black boxes): (a) the Okinawa Trough; (b) the two hydrothermal vent fields.

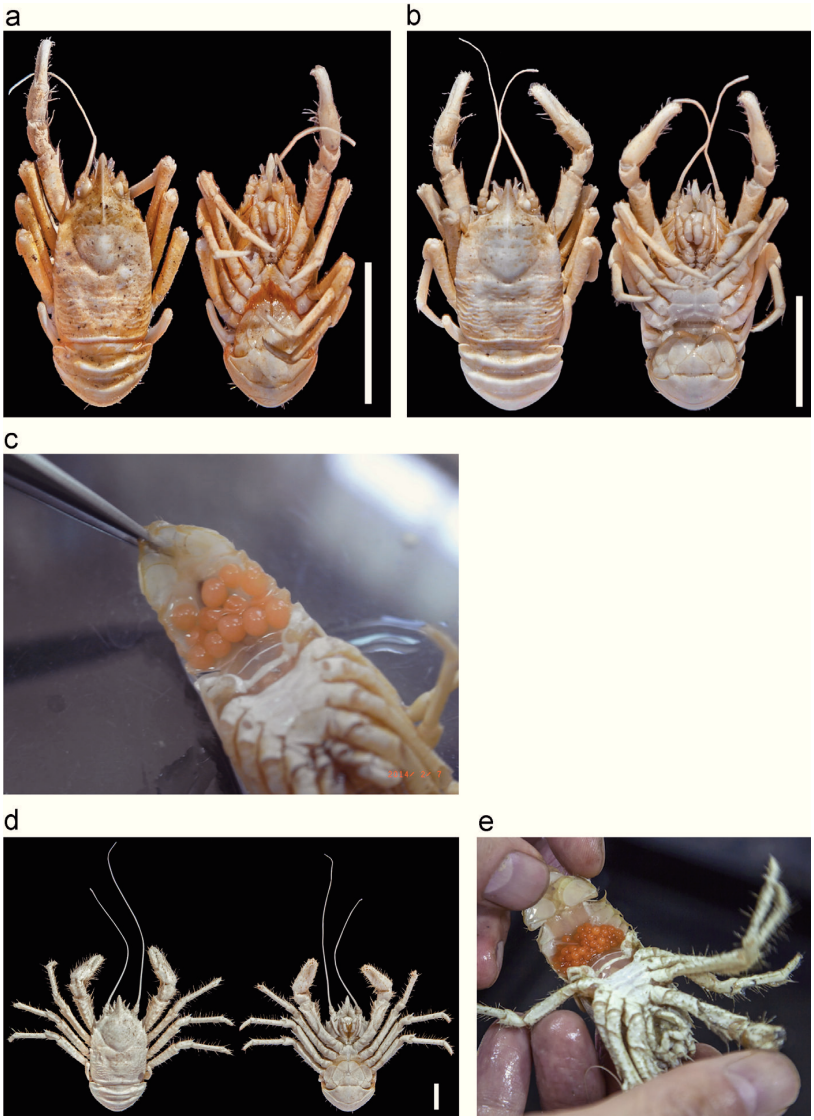

Fig. 2. Ovigerous *Munidopsis* specimens collected. (a) *M. ryukyuensis*-1 (1675 m deep, Irabu Knoll, 2014/ii/07), (b) *M. ryukyuensis*-2 (1661 m deep, Irabu Knoll, 2014/ii/07), (c) eggs held by *M. ryukyuenesis*-2, (d) *M. longispinosa* collected at (1482 m, Hatoma Knoll, 2014/ii/03), (e) eggs held by the same *M. longispinosa*. Size and other attributes are given in Table 1. Scale bars = 1 cm.

Table 1
Carapace sizes and egg properties of ovigerous *Munidopsis* specimens collected in hydrothermal vent fields in the Okinawa Trough.

Species name	Vent field	Sampling depth (m)	Carapace size (mm)			Number of eggs	Mean egg diameter (±SD) (mm)	Mean egg volume (±SD) (mm^3)
			Length with rostrum	Length without rostrum	Width			
M. ryukyuensis-1	Irabu Knoll	1675	13.4	10.3	8.6	6	1.93 ± 0.01	4.11 ± 0.01
M. ryukyuensis-2	Irabu Knoll	1661	15.0	11.8	9.7	13	2.01 ± 0.04	4.20 ± 0.04
M. longispinosa	Hatoma Knoll	1482	34.0	26.3	22.0	73	2.03 ± 0.04	4.22 ± 0.04

from three previous studies: Van Dover and Williams (1991), Baba et al. (2008) and Kilgour and Shirley (2014). Related data were taken from Baba (2005), Macpherson and Segonzac (2005), Macpherson (2007) and Macpherson et al. (2014). Although the data of Van Dover and Williams (1991) and Baba et al. (2008) were recorded as one datum point for each species, the data of Kilgour and Shirley (2014) were recorded as a range of observed depths, egg numbers, and egg sizes.

Table 2
Carapace sizes and sex of non-ovigerous *Munidopsis* specimens collected in hydrothermal vent fields in the Okinawa Trough.

Sample number	Species name	Vent field	Sampling depth (m)	Carapace size (mm)			Sex
				Length with rostrum	Length without rostrum	Width	
HPD1621-BC1-01	*Munidopsis ryukyuensis*	Hatoma Knoll	1482	11.3	8.4	6.9	Male
HPD1621-BC1-12	*Munidopsis* sp. JUVENILE	Hatoma Knoll	1482	4.4	3.6	2.8	Juvenile
HPD1621-BC1-12	*Munidopsis* sp. JUVENILE	Hatoma Knoll	1482	4.2	3.2	2.5	Juvenile
HPD1621-BC3-12	*Munidopsis longispinosa*	Hatoma Knoll	1482	18.5	14.1	11.7	Female
HPD1621-BC3-12	*Munidopsis longispinosa*	Hatoma Knoll	1482	19.9	15.3	12.0	Female
HPD1621-BOC-05	*Munidopsis longispinosa*	Hatoma Knoll	1482–1510	17.6	14.4	10.8	Female
HPD1621-BOC-05	*Munidopsis longispinosa*	Hatoma Knoll	1482–1510	12.8	9.9	7.9	Female
HPD1624-BC1-01	*Munidopsis ryukyuensis*	Irabu Knoll	1675	17.2	13.5	10.7	Female

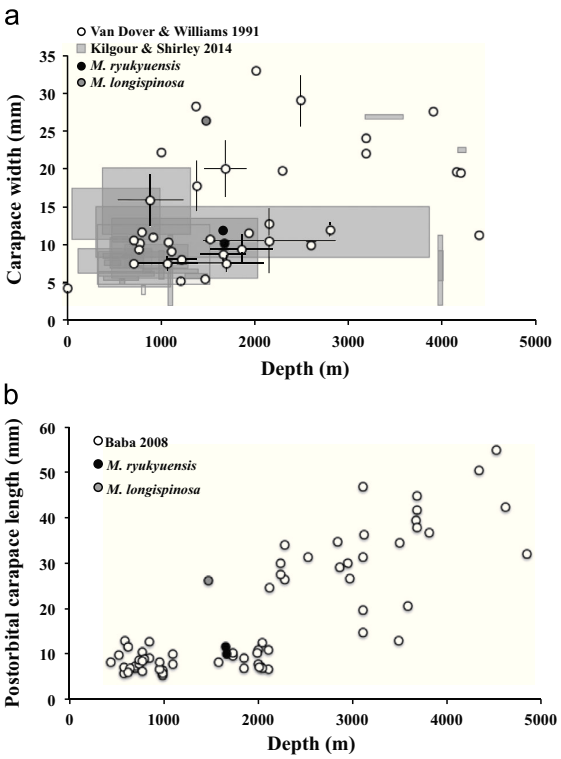

Fig. 3. The relationship between carapace size and water depth in *Munidopsis* species. (a) Comparison of carapace widths of *Munidopsis ryukyuensis* and *M. longispinosa* (present study) with those of ovigerous *Munidopsis* spp. from Van Dover and Williams (1991) and depth and width ranges from Kilgour and Shirley (2014). Standard deviations are indicated for some of the data of Van Dover and Williams. (b) Comparison of postorbital lengths of *M. ryukyuensis* and *M. longispinosa* (present study) with those of ovigerous *Munidopsis* spp. from Baba et al. (2008). For Van Dover and Williams (1991) and Baba et al. (2008), the widths and postorbital lengths were the measured values of material examined by these authors. The numbers of species considered were (a) 47 species and (b) 11 species.

3. Results and discussion

The present study showed that *Munidopsis ryukyuensis* can reach sexual maturity at carapace lengths of $\leq$15 mm, including the rostrum, and with a carapace width of $<$10 mm. This is smaller than the single ovigerous female *M. ryukyuensis* collected/sampled at Hatoma Knoll in April 2005, which had a carapace length of 17.4 mm, including the rostrum (Cubelio et al., 2007a). *Munidopsis ryukyuensis* specimens from the present study had some of the smallest carapace sizes recorded for ovigerous *Munidopsis* living in the deep sea at depths $>$1000 m (Fig. 3). The smallest carapace widths recorded at these depths were for *M. nitida* (2.5 mm; Kilgour and Shirley, 2014), while the smallest postorbital carapace lengths, without the rostrum, were reported for *M. curvirostra* (7.0 mm, Baba et al., 2008). In comparison, the ovigerous specimen of *M. longispinosa* had a carapace width of 22.0 mm and a postorbital carapace length of 26.3 mm. The non-ovigerous specimens of this species had a maximum width of 12 mm and a maximum length (without rostrum) of 15.3 mm (Table 2).

Our results imply early maturity in *Munidopsis ryukyuensis*, although its growth rate and average body size of adults must be examined to test this hypothesis. One interpretation of the potentially early maturity in *M. ryukyuensis* could be related to their habitat. They have often been observed at the periphery of vents, like many other galatheid species (Tsuchida et al., 2003). *Munidopsis* spp. are detritivores and usually congregate where dead animals are found (Galkin, 1997). However, their food sources are not always abundant and could be influenced by venting activity (Galkin, 1997). An environment with limited food resources could be unfavorable for growth and survival (Blicher et al., 2010). If *M. ryukyuensis* reaches maturity at an early stage in its life-history, it will have a higher probability of producing offspring and therefore surviving in the ephemeral and unstable vent environment (Ramirez-Llodra, 2002). Early maturity has already been observed in some vent animals, such as limpets (Kelly and Metaxas, 2007; Tyler et al., 2008; Nakamura et al., 2014) and shrimps (Nye et al., 2013).

The two *Munidopsis ryukyuensis* specimens studied had 6 and 13 eggs per individual whereas the specimen of *M. longispinosa* yielded 73 eggs (Table 1). Mean egg volumes were $\sim$4 mm^3 for both species. The similarity in egg volumes despite the difference in body size between *M. longispinosa* and *M. ryukyuenesis* could be related partly to maternal body size (Wilkens et al., 1990; Baba et al., 2011). Egg numbers may be higher in larger females of *M. ryukyuensis* (Baba et al., 2011). Increased clutch size as a function of body size was observed in *M. polymorpha* (Wilkens et al., 1990). It is also possible that *M. longispinosa* has delayed sexual maturity, producing a high number of eggs once adult size is reached. To determine which of these two scenarios is correct, a larger sample of ovigerous female specimens of both species must be examined.

Among decapods, species with fewer large, yolky eggs are most likely to have lecithotrophic larvae (Van Dover et al., 1985). Comparing the characteristics of the eggs observed in the present study with those of other *Munidopsis* spp. of similar body size ($\sim$10 mm and $\sim$20 mm, carapace width, data from Van Dover and Williams, 1991), the number of eggs per individual was relatively low for *M. ryukyuensis*, and relatively high for *M. longispinosa* (Fig. 4a). Mean egg volumes were relatively high for *M. ryukyuensis* and relatively low for *M. longispinosa* (Fig. 4b). However, in comparison with the egg volumes of other *Munidopsis* spp. with similar postorbital carapace lengths (data from Baba et al., 2008), the egg volumes of *M. ryukyuensis* and *M. longispinosa* were similar to those of other *Munidopsis* spp. (Fig. 4c). According to Van Dover et al. (1985),

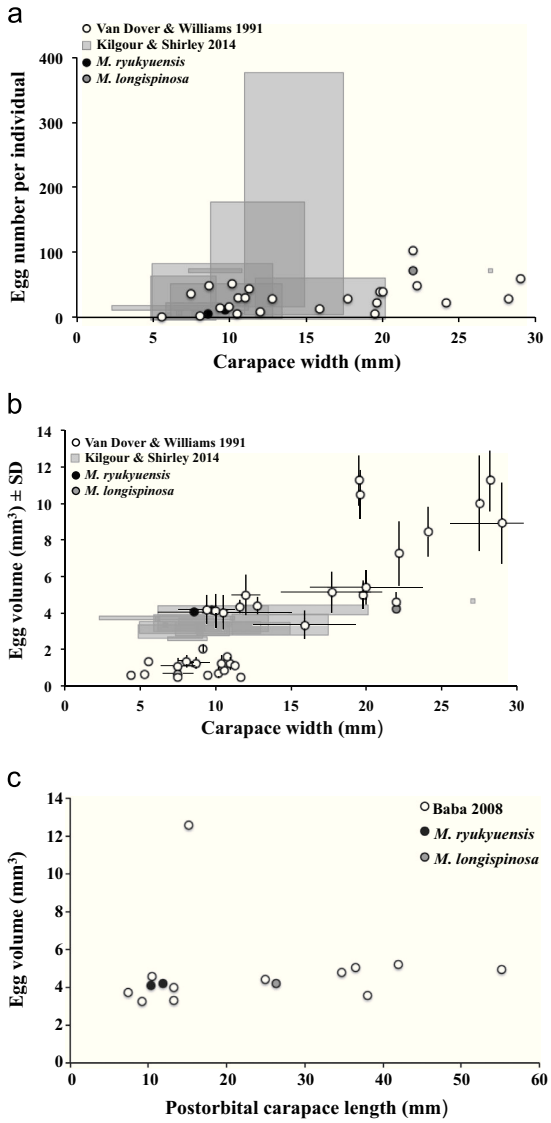

Fig. 4. The relationship between carapace size and egg properties in *Munidopsis* species. (a) Comparison of carapace width and egg number per individual of *Munidopsis ryukyuensis* and *M. longispinosa* (present study) with those of ovigerous *Munidopsis* spp. from Van Dover and Williams (1991) and egg number and width ranges from Kilgour and Shirley (2014). (b) Comparison of carapace width and egg volume (mm^3) of *M. ryukyuensis* and *M. longispinosa* (present study) with those of ovigerous *Munidopsis* spp. from Van Dover and Williams (1991) and egg number and width ranges from Kilgour and Shirley (2014). Standard deviations are indicated for some of the data of Van Dover and Williams. (c) Comparison of postorbital carapace length and egg volume (mm^3) of *M. ryukyuensis* and *M. longispinosa* (present study) with those of ovigerous *Munidopsis* spp. from Baba et al. (2008). The numbers of species considered were (a) 47 species, (b) 47 species, and (c) 11 species.

M. ryukyuensis could have lecithotrophic larvae. In addition, galatheid species with eggs $>0.5\ mm^3$ are predominantly lecithotrophic (Van Dover and Williams, 1991). Therefore, larvae of *M. ryukyuensis and M. longispinosa* are most likely also lecithotrophic.

Lecithotrophic larvae generally have limited lifespans due to their limited yolk reserves (Vrijenhoek, 1997; Levin, 2006). However, lecithotroph eggs should be large enough to support larval development without feeding during dispersal. In theory, the size and number of eggs are related to the fitness of offspring (Stearns, 1992) and for marine invertebrates, these traits are strongly related to the cost of larval dispersal (Burgess et al., 2013). Therefore, the relatively large eggs of *M. ryukyuensis* and *M. longispinosa* could potentially provide a food reserve sufficient to enable long-distance larval dispersal in the Okinawa Tough (Shanks et al., 2003; Siegel et al., 2003). Indeed, some vent animals with lecithotrophic larval stages are widely distributed in the Okinawa Trough, e.g., the barnacle *Neoverruca* sp. (Watanabe et al., 2005) and the limpet *Lepetodrilus nux* (Nakamura et al., 2014). The distributions of *M. ryukyuensis* and *M. longispinosa*, however, are not well known. Both species have been observed in the Hatoma Knoll (Cubelio et al., 2007a), and some other *Munidopsis* species have been reported from the Minami-Ensei Knoll (Hashimoto et al., 1995) and the Iheya Ridge (Ohta and Kim, 2001) in the Okinawa Trough. Moreover, it would be necessary to investigate how the larval biology of *M. ryukyuensis* and *M. longispinosa* (e.g., development time and vertical distribution in the water column) interact with ocean circulation and topography in order to determine their dispersal potential (Adams et al., 2012).

In summary, *Munidopsis ryukyuensis* reaches sexual maturity at a relatively small size. Large egg volume suggests lecithotrophic development, but also implies a food reserve that is optimal for their dispersal potential. As hydrothermal vents are patchily distributed, this species must have the potential for long-distance larval dispersal. Living in the same environment and having similar egg volume, *M. longispinosa* probably also has lecithotrophic development and the potential for long-distance larval dispersal. However, the timing of sexual maturity of *M. longispinosa* is unknown and its life-history traits cannot be determined from a single specimen. To understand the ecology of *M. ryukyuenesis* and *M. longispinosa*, further studies on early life-history characteristics, distribution patterns, and genetic population structure are required.

Acknowledgements

We are very grateful to the crew of the R/V *KAIYO*, the operational team of the ROV *Hyper-Dolphin*, and the research group of KY14-02. This research was supported by a Canon Foundation Grant-in-Aid for Scientific Research, no. 24570037 from the Japan Society for the Promotion of Science. We gratefully acknowledge the support of this work from Marine Biophysics Unit of the Okinawa Institute of Science and Technology Graduate University. We thank the anonymous reviewers for their very careful reviews and helpful comments, and OIST's technical editor, Dr. Steven D. Aird, for helping us to polish this manuscript.

References

Adams, D., Arellano, S., Gobenar, B., 2012. Larval dispersal: vent life in the water column. Oceanography 25, 256–268.
Baba, K., 2005. Deep-sea chirostylid and galatheid Crustaceans (Decapoda: Anomura) from the Indo-Pacific, with a list of species. Galathea Rep. 20, 317.
Baba, K., Macpherson, E, Poore, G.C.B., Ahyong, S.T., Bermudez, A., Cabezas, P., Lin, C.W., Nizinski, M., Rodrigues, C., Schnabel, K.E., 2008. Catalogue of squat lobsters of the world (Crustacea: Decapoda: Anomura—families Chirostylidae, Galatheidae and Kiwaidae). Zootaxa 1905, 1–220.
Baba, K., Fujita, Y., Wehrtmann, I.S., Scholtz, G., 2011. Developmental biology of squat lobsters. In: Poore, G.C.B., Ahyong, S.T., Taylor, J. (Eds.), The Biology of Squat Lobsters. CRC Press, USA, pp. 105–148.
Barry, J.P., Greene, H.G., Orange, D.L., Baxter, C.H., Robison, B.H., Kochevar, R.E., Nybakken, J.W., Reed, D.L., McHugh, C.M., 1996. Biological and geologic characteristics of cold seeps in Monterey Bay, California. Deep-Sea Res. 43, 1739–1762.
Bennett, B.A., Smith, C.R., Glaser, B., Maybaum, H.L., 1994. Faunal community structure of a chemoautotrophic assemblage on whale bones in the deep northeast Pacific Ocean. Mar. Ecol. Prog. Ser. 108, 205–223.
Blicher, M.E., Rysgaard, S., Sejr, M.K., 2010. Seasonal growth variation in *Chlamys islandica* (Bivalvia) from sub-Arctic Greenland is linked to food availability and temperature. Mar. Ecol. Prog. Ser. 407, 71–86.

Burgess, S.C., Bode, M., Marshall, D.J., 2013. Costs of dispersal alter optimal offspring size in patchy habitats: combining theory and data for a marine invertebrate. Funct. Ecol. 27, 757–765.
Converse, D.R., Holland, H.D., Edmond, J.M., 1984. Flow rates in the axial hot springs of the East Pacific Rise (21°N): implications for the heat budget and the formation of massive sulfide deposits. Earth Planet. Sci. Lett. 69, 159–175.
Copley, J.T.P., Jorgensen, P.B.K., Sohn, R.A., 2007. Assessment of decadal-scale ecological change at a deep Mid-Atlantic hydrothermal vent and reproductive time-series in the shrimp *Rimicaris exoculata*. J. Mar. Biol. Assoc. U.K. 87, 859–867.
Cubelio, S.S., Tsuchida, S., Watanabe, S., 2007a. New species of *Munidopsis* (Decapoda: Anomura: Galatheidae) from hydrothermal vent in Okinawa Trough and cold seep in Sagami Bay. Crustacean Res. 36, 1–14.
Cubelio, S.S., Tsuchida, S., Watanabe, S., 2007b. Vent associated *Munidopsis* (Decapoda: Anomura: Galatheidae) from Brothers Seamount, Lermadec Arc, Southwest Pacific, with description of one new species. J. Crustacean Biol. 27, 513–519.
Cubelio, S.S., Tsuchida, S., Hendrickx, M.E., Kado, R., Watanabe, S., 2007c. A new species of vent associated *Munidopsis* (Crustacea: Decapoda: Anomura: Galatheidae) from the Western Pacific, with notes on its genetic identification. Zootaxa 1435, 25–36.
Cubelio, S.S., Tsuchida, S., Watanabe, S., 2008. New species of *Munidopsis* (Decapoda: Anomura: Galatheidae) from hydrothermal vent areas of Indian and Pacific Oceans. J. Mar. Biol. Assoc. U.K. 88, 111–117.
Cuvelier, D., Sarradin, P., Sarrazin, J., Colaco, A., Copley, J.T., Desbruyeres, D., Glover, A.G., Santos, R.S., Tyler, P.A., 2011. Hydrothermal faunal assemblages and habitat characterisation at the Eiffel Tower edifice (Lucky Strike, Mid-Atlantic Ridge). Mar. Ecol. 32, 243–255.
Galkin, S.V., 1997. Megafauna associated with hydrothermal vents in the Manus Back-Arc Basin (Bismarck Sea). Mar. Geol. 142, 197–206.
Gebruk, A., Fabri, M., Briand, P., Desbruyere, D., 2010. Community dynamics over a decadal scale at Logatchev, 14°45′N, Mid-Atlantic Ridge. Cah. Biol. Mar. 51, 383–388.
Goffredi, S.K., Paull, C.K., Fulton-Bennett, K., Hurtado, L.A., Vrijenhoek, R.C., 2004. Unusual benthic fauna associated with a whale fall in Monterey Canyon, California. Deep-Sea Res. 51, 1295–1306.
Grassle, J.F., 1985. Hydrothermal vent animals: distribution and biology. Science 229, 713–717.
Gustafson, R.G., Lutz, R.A., 1994. Molluscan life history traits at deep-sea hydrothermal vents and cold methane/sulfide seeps. In: Young, C.M., Echelbarger, K.J. (Eds.), Reproduction, Larval Biology, and Recruitment of the Deep-Sea Benthos. Columbia University Press, New York, NY, pp. 76–97.
Hashimoto, J., Ohta, S., Fujikura, K., Miura, T., 1995. Microdistribution pattern and biogeography of the hydrothermal vent communities of the Minami-Ensei Knoll in the Mid-Okinawa Trough, Western Pacific. Deep-Sea Res. 42, 577–598.
Haymon, R.M., Fornari, D.J., Vondamm, K.L., Lilley, M.D., Perfit, M.R., Edmond, J.M., Shanks, W.C., Lutz, R.A., Grebmeier, J.M., Carbotte, S., Wright, D., Mclaughlin, E., Smith, M., Beedle, N., Olson, E., 1993. Volcanic-eruption of the Midocean Ridge along the East Pacific Rise Crest at 9-degrees-45–52′N—direct submersible observations of sea-floor phenomena associated with an eruption event in April, 1991. Earth Planet. Sci. Lett. 119, 85–101.
Hessler, R.R., Smithey, W.M., Boudrias, M.A., Keller, C.H., Lutz, R.A., Childress, J.J., 1988. Temporal change in megafauna at the Rose Garden hydrothermal vent (Galapagos Rift; eastern tropical Pacific). Deep-Sea Res. Part A 35, 1681–1709.
Kelly, N.E., Metaxas, A., 2007. Influence of habitat on the reproductive biology of the deep-sea hydrothermal vent limpet *Lepetodrilus fucensis* (Vetigastropoda: Molluscsa) from the Northeast Pacific. Mar. Biol. 151, 649–662.
Kilgour, M.J., Shirley, T.C., 2014. Reproductive biology of galatheoid and chirostyloid (Crustacea: Decapoda) squat lobsters from the Gulf of Mexico. Zootaxa 3754, 381–419.
Lalou, C., 1991. Deep-sea hydrothermal venting: a recently discovered marine system. J. Mar. Syst. 1, 403–440.
Levin, L.A., 2006. Recent progress in understanding larval dispersal: new directions and digressions. Integr. Comp. Biol. 46, 282–297.
Lundsten, L., Schlining, K.L., Frasier, K., Johnson, S.B., Kuhnz, L.A., Harvey, J.B.J., Clague, G., Vrijenhoek, R.C., 2010. Time-series analysis of six whale-fall communities in Monterey Canyon, California, USA. Deep-Sea Res. 57, 1573–1584.
Macdonald, K.C., 1982. Mid-ocean ridges: fine scale tectonic, volcanic and hydrothermal processes within the plate boundary zone. Annu. Rev. Earth Planet. Sci. 10, 155.
Macpherson, E., Segonzac, M., 2005. Species of the genus Munidopsis (Crustacea, Decapoda, Galatheidae) from the deep Atlantic Ocean, including cold-seep and hydrothermal vent areas. Zootaxa 1095, 1–60.
Macpherson, E., 2007. Species of the genus *Munidopsis* Whiteaves, 1784 from the Indian and Pacific Oceans and reestablishment of the genus *Galacantha* A. Milne-Edwards, 1880 (Crustacea, Decapoda, Galatheidae). Zootaxa 1417, 1–135.
Macpherson, E., Amon, D., Clark, P.F., 2014. A new species of *Munidopsis* from a seamount of the Southwest Indian Ocean Ridge (Decapoda: Munidopsidae). Zootaxa 3753, 291–296.
Martin, J.W., Haney, T.A., 2005. Decapod crustaceans from hydrothermal vent and cold seeps: a review through 2005. Zool. J. Linn. Soc.—Lond. 145, 445–522.
Miyake, H., Kitada, M., Itoh, T., Nemoto, S., Okuyama, Y., Watanabe, H., Tsuchida, S., Inoue, K., Kado, R., Ikeda, S., Nakamura, K., Omata, T., 2010. Larvae of deep-sea chemosynthetic ecosystem animals in captivity. Cah. Biol. Mar. 51, 441–450.
Mullineaux, L.S., Adams, D.K., Mills, S.W., Beaulieu, S.E., 2010. Larvae from afar colonize deep-sea hydrothermal vents after a catastrophic eruption. Proc. Natl. Acad. Sci. U.S.A. 107, 7829–7834.
Mullineaux, L.S., Le Bris, N., Mills, S.W., Henri, P., Bayer, S.R., Secrist, R.G., Siu, N., 2012. Detecting the influence of initial pioneers on succession at deep-sea vents. PLoS One 7, e50015.
Nakamura, M., Watanabe, H., Sasaki, T., Ishibashi, J., Fujikura, K., Mitarai, S., 2014. Life history traits of *Lepetodrilus nux* in the Okinawa Trough, based upon gametogenesis, shell size, and genetic variability. Mar. Ecol. Prog. Ser. 505, 119–130.
Nye, V., Copley, J.T., Tyler, P.A., 2013. Spatial variation in the population structure and reproductive biology of *Rimicaris hybiae* (Caridea: Alvinocarididae) at hydrothermal vents on the Mid-Cayman spreading centre. PLoS One 8, e60319.
Ohta, S., Kim, D., 2001. Submersible observations of the hydrothermal vent communities on the Iheya Ridge, Mid Okinawa Trough, Japan. J. Oceanogr. 57, 663–677.
Osawa, M., Takeda, M., 2007. Deep-sea Galatheidae (Crustacea, Decapoda, Anomura) from Tosa Bay and Okinawa Trough, southern Japan. Bull. Natl. Mus. Nat. Sci., Ser. A 33, 133–146.
Perfit, M.R., Chadwick, W.W., 1998. Magmatism at Mid-ocean Ridges: Constraints from Volcanological and Geochemical Investigations. Faulting Magmatism at Mid-ocean Ridges, 59–115.
Ramirez-Llodra, E., 2002. Fecundity and life-history strategies in marine invertebrates. Adv. Mar. Biol. 43, 87–170.
Reznick, D., Bryant, M.J., Bashey, F., 2002. *r*- and *k*-selection revisited: the role of population regulation in life-history evolution. Ecology 83, 1509–1520.
Roff, Derek A., 2002. Life History Evolution. 7. Sinauer Associates, Sunderland.
Samuelsen, T.J., 1972. Larave of *Munidopsis tridentate* (Esmark) (Decapoda, Anomura) reared in the laboratory. Sarsia 48, 91–98.
Scheltema, R.S., 1994. Adaptations for Reproduction Among Deep-Sea Benthic Molluscs: An Appraisal. Reproduction, Larval Biology, and Recruitment of the Deep-Sea Benthos, 44.
Schnabel, K.E., Cabezas, P., McCallum, A., Macpherson, E., Ahyong, S.T., Baba, K., 2011. Worldwide distribution patterns of squat lobsters. In: Poore, G.C.B., Ahyong, J., Taylor, J. (Eds.), The Biology of Squat Lobsters. CRC Press, USA, pp. 149–182.
Shank, T.M., Fornari, D.J., Von Damm, K.L., Lilley, M.D., Haymon, R.M., Richard, A.L., 1998. Temporal and spatial patterns of biological community development at nascent deep-sea hydrothermal vents (9°50′N, East Pacific Rise). Deep-Sea Res. Pt. 45, 465–515.
Shanks, A.L., Grantham, B.A., Carr, M.H., 2003. Propagule dispersal distance and the size and spacing of marine reserves. Ecol. Appl. 13, S159–S169.
Siegel, D.A., Kinlan, B.P., Gaylord, B., Gaines, S.D., 2003. Lagrangian descriptions of marine larval dispersion. Mar. Ecol. Prog. Ser. 260, 83–96.
Stearns, S.C., 1992. The Evolution of Life Histories. Oxford University Press, Oxford; New York.
Tsuchida, S., Fujiwara, Y., Fujikura, K., 2003. Distribution and population structure of the galatheid crab *Shinkaia crosnieri* (Decapoda: Anomura: Galatheidae) in the southern Okinawa Trough. JPN. J. Benthol. 58, 84–88.
Tyler, P.A., Young, C.M., 1999. Reproduction and dispersal at vents and cold seeps. J. Mar. Biol. Assoc. U.K. 79, 193–208.
Tyler, P.A., Pendlebury, S., Mills, S.W., Mullineaux, L., Eckelbarger, K.J., Baker, M., Young, C.M., 2008. Reproduction of gastropods from vents on the East Pacific Rise and the Mid-Atlantic Ridge. J. Shellfish Res. 27 (1), 107–118.
Van Dover, C.L., Factor, J.R., Williams, A.B., Berg Jr., C.J, 1985. Reproductive patterns of decapod crustaceans from hydrothermal vents. Biol. Soc. Wash. Bull. 6, 223–227.
Van Dover, C.L., 2000. The Ecology of Deep-Sea Hydrothermal Vents. Princeton University Press, Princeton, UK.
Van Dover, C.L., Williams, A.B., 1991. Egg size in squat lobsters (Galatheoidea): constraint and freedom. Crustacean Egg Prod. 7, 143–156.
Vrijenhoek, R.C., 1997. Gene flow and genetic diversity in naturally fragmented metapopulations of deep-sea hydrothermal vent animals. J. Hered. 88, 285–293.
Watanabe, H., Tsuchida, S., Fujikura, K., Yamamoto, H., Inagaki, F., Kyo, M., Kojima, S., 2005. Population history associated with hydrothermal vent activity inferred from genetic structure of neoverrucid barnacles around Japan. Mar. Ecol. Prog. Ser. 288, 233–240.
Wilkens, H., Parzefall, J., Ribowski, A., 1990. Population biology and larvae of the anchialine crab *Munidopsis polymorpha* (Galatheidae) from Lanzarote (Canary Islands). J. Crustacean Biol. 10, 667–675.
Williams, A.B., Van Dover, C.L., 1983. A new species of *Munidopsis* from submarine hydrothermal vents of the East Pacific Rise at 21°N (Anomura-Galatheidae). Proc. Biol. Soc. Wash. 96, 481–488.
Young, C.M., 2003. Reproduction, development and life-history traits. Ecosyst. World, 381–426.

Mitochondrial DNA

http://informahealthcare.com/mdn
ISSN: 1940-1736 (print), 1940-1744 (electronic)

Mitochondrial DNA, Early Online: 1–2
 DOI: 10.3109/19401736.2014.1003827

informa
healthcare

MITOGENOME ANNOUNCEMENT

The mitochondrial genome of the deep-sea snail *Provanna* sp. (Gastropoda: Provannidae)

Ting Xu[1], Jin Sun[1], Chong Chen[2], Pei-Yuan Qian[3], and Jian-Wen Qiu[1]

[1]*Department of Biology, Hong Kong Baptist University, Hong Kong, China,* [2]*Department of Zoology, University of Oxford, Oxford, UK, and* [3]*Division of Life Science, the Hong Kong University of Science and Technology, Hong Kong, China*

Abstract

The genomic DNA of two *Provanna* sp. individuals was extracted, sequenced using an Illumina HiSeq1500, and the mitogenome was assembled. The nearly complete metogenome was 16,183 bp in length, consisting of 37 typical metazoan mitochondrial genes with the typical caenogastropod mitochondrial gene order. All mitochondrial genes were encoded on the heavy strand with the exception of eight transfer RNA genes. To reconstruct the phylogenetic position of the deep-sea Provannidae, we used amino acid sequences of all the 13 mitochondrial protein-coding genes in Bayesian inference, maximum likelihood, and maximum parsimony analyses with sequences of selected gastropods. The resultant phylogenetic trees supported the placement of Provannidae in the superfamily Abyssochrysoidea of the clade Littorinimorpha of Gastropoda, providing new data for understanding the phylogeny of these deep-sea snails.

Keywords

Deep-sea, gastropoda, mitogenome, *Provanna*, Provannidae

History

Received 10 November 2014
Revised 17 November 2014
Accepted 5 December 2014
Published online 28 January 2015

Provannidae is a family of snails inhabiting chemosynthesis based communities such as hydrothermal vents, hydrocarbon seeps, sunken wood, and whale-falls (Bouchet & Rocroi, 2005; Colgan et al., 2007; Warén & Bouchet, 2001). It belongs to the superfamily Abyssochrysoidea nested within Littorinimorpha (Osca et al., 2014), but the family is paraphyletic (Johnson et al., 2010). In the present study, we described the mitogenome of *Provanna* sp., the second representative of the family Provannidae and the first of the genus *Provanna*, to enrich the taxon sampling of mitogenomes in Provannidae and to better understand the phylogenetic position of this family of deep-sea gastropods.

Snails were collected from a methane seep on the continental slope of the South China Sea (22°06.921′N, 119°17.131′E; 1122 m depth) during the manned submersible Jiaolong's 55th dive on 19 June 2013 and were identified as closely related to *Provanna* sp. OL1 based on the morphology of the shell and

Table 1. Characteristics of *Provanna* sp. mitochondrial genome.

Gene	Start	Stop	Length (bp)	Intergenic nucleotides[a]	Start codon	Stop codon	Strand[b]
cox3	443	1222	780	41	ATG	TAA	+
trnK(ttt)	1264	1334	71	9			+
trnA(tgc)	1344	1413	70	7			+
trnR(tcg)	1421	1489	69	6			+
trnN(gtt)	1496	1564	69	8			+
trnI(gat)	1573	1640	68	5			+
nad3	1646	1999	354	1	ATG	TAA	+
trnS1(gct)	2001	2068	68	0			+
nad2	2069	3130	1062	4	ATG	TAA	+
cox1	3135	4670	1536	22	ATG	TAA	+
cox2	4693	5379	687	8	ATG	TAA	+
trnD(gtc)	5388	5455	68	0			+
atp8	5456	5614	159	2	ATG	TAA	+
atp6	5617	6312	696	35	ATG	TAA	+
trnM(cat)	6348	6414	67	5			–
trnY(gta)	6420	6485	66	4			–
trnC(gca)	6490	6554	65	1			–
trnW(tca)	6556	6621	66	1			–
trnQ(ttg)	6623	6684	62	7			–

(*continued*)

Correspondence: Jian-Wen Qiu, Department of Biology, Hong Kong Baptist University, Hong Kong, China. Tel: +852 34117055. Fax: +852 34115995. E-mail: qiujw@hkbu.edu.hk

Table 1. Continued.

Gene	Start	Stop	Length (bp)	Intergenic nucleotides[a]	Start codon	Stop codon	Strand[b]
trnG(tcc)	6692	6758	67	0			–
trnE(ttc)	6759	6829	71	0			–
rrnS	6830	7784	955	−5			+
trnV(tac)	7780	7846	67	−18			+
rrnL	7829	9230	1402	17			+
trnL2(taa)	9248	9314	67	37			+
trnL1(tag)	9352	9418	67	0			+
nad1	9419	10,360	942	0	ATG	TAA	+
trnP(tgg)	10,361	10,427	67	3			+
nad6	10,431	10,931	501	8	ATG	TAA	+
cytb	10,940	12,079	1140	13	ATG	TAA	+
trnS2(tga)	12,093	12,160	68	0			+
trnT(tgt)	12,161	12,228	68	13			–
nad4L	12,242	12,538	297	23	ATG	TAG	+
nad4	12,544	13,905	1362	4	ATC	TAA	+
trnH(gtg)	13,910	13,975	66	0			+
nad5	13,976	15,697	1722	3	ATG	TAA	+
trnF(gaa)	15,701	15,768	68	856			+

[a]Negative numbers indicate overlapping nucleotides between adjacent genes.
[b]+ and – represent the heavy and light strands, respectively.

radula, and the partial *COI* sequence (Supplementary Figure S1 and S2, Supplementary methods, and Table S1). Genomic DNA was extracted from two individuals, pooled for library construction and sequenced by the Illumina HiSeq1500 platform. In total, 5.6 Gb paired-end reads of 100 bp length were generated. After removing adapters, unpaired, short and low quality reads, 4.9 Gb (~88%) high-quality reads were used in *de novo* assembly using ABySS v1.3.6 (Library of Medicine, Bethesda, MD) with a *k*-mer size of 57. Among the assembled sequences, a contig with a length of 16,183 bp was considered the mitogenome (NCBI accession number: KM675481), based on the sequence similarity with protein-coding genes (PCGs) of *Ifremeria nautilei,* the other member of this family with a sequenced mitogenome. Annotation of the PCGs, ribosomal RNA (*rRNA*) and transfer RNA (*tRNA*) genes followed Zhang et al. (2014). Briefly, PCGs and rRNA genes were annotated by MITOS. *tRNA* genes were determined by both MITOS and tRNAscan-SE v1.21 (Library of Medicine, Bethesda, MD). The boundary of each gene was identified and manually checked by alignment with other published gastropod mitogenomes.

The mitogenome of *Provanna* sp. was nearly complete, containing 13 PCGs, two rRNA genes, and 22 tRNA genes (Table 1 and Supplementary Figure S3). With the exception of eight tRNA genes, all mitochondrial genes were encoded on the heavy strand. ATG was the start codon for most of the protein-coding genes with the exception of *nad4* whose start codon was ATC. TAA was the stop codon for all genes except for *nad4L* whose stop codon was TAG. The *Provanna* sp. mitogenome had 26 small non-coding regions ranging from 1 to 41 bp. The only large non-coding region was 856 bp in length, which is likely the control region. The mitogenome gene order of *Provanna* sp. was identical to that of other caeogastropods (Grande et al., 2008; Williams et al., 2014).

Concatenated amino-acid sequences of all 13 PCGs were used in Bayesian inference (BI), maximum likelihood (ML), and maximum parsimony (MP) analyses (Supplementary methods). The reconstructed phylogeny supported the placement of *Provanna* sp. and *I. nautilei* in Provannidae, and Provannidae in Abyssochrysoidea of the Littorinimorpha clade (Supplementary Figure S4 and Table S2).

Acknowledgements

The authors thank Chinese Ocean Mineral Resources Research and Development Association (COMAR) and National Deep Sea Center of China for inviting J. -W. Qiu to participate in the cruise, the pilots and operation team of the Jiaolong's, and the captain and crew of R/V Xiangyanghong 9 for their hospitality and support, and Dr. Hiromi Watanabe for helpful discussion.

Declaration of interest

Financial support for the sequencing and laboratory analysis was provided by Hong Kong Baptist University (FRG2/13–14/009) and the Strategic Priority Research Program of Chinese Academy of Sciences (XDB06010102). The authors alone are responsible for the content and writing of the paper.

References

Bouchet P, Rocroi JP. (2005). Classification and nomenclature of gastropod families. Malacologia 47:1–397.

Colgan DJ, Ponder WF, Beacham E, Macaranas J. (2007). Molecular phylogenetics of Caenogastropoda (Gastropoda: Mollusca). Mol Phylogenet Evol 42:717–37.

Grande C, Templado J, Zardoya R. (2008). Evolution of gastropod mitochondrial genome arrangements. BMC Evol Biol 8:61.

Johnson SB, Warén A, Lee RW, Kano Y, Kaim A, Davis A, Strong EE, et al. (2010). *Rubyspira*, new genus and two new species of bone-eating deep-sea snails with ancient habits. Biol Bull 219:166–77.

Osca D, Templado J, Zardoya R. (2014). The mitochondrial genome of *Ifremeria nautilei* and the phylogenetic position of the enigmatic deep-sea Abyssochrysoidea (Mollusca: Gastropoda). Gene 547:257–66.

Warén A, Bouchet P. (2001). Gastropoda and Monoplacophora from hydrothermal vents and seeps; new taxa and records. Veliger 44: 116–231.

Williams ST, Foster PG, Littlewood DT. (2014). The complete mitochondrial genome of a turbinid vetigastropod from MiSeq Illumina sequencing of genomic DNA and steps towards a resolved gastropod phylogeny. Gene 533:38–47.

Zhang Y, Sun J, Li X, Qiu JW. (2014). The mitochondrial genome of the deep-sea glass sponge *Lophophysema eversa* (Porifera, Hexacinellida, Hyalonematidae). Mitochondrial DNA Aug 1:1–2.

Supplementary material available online at http://biol.hkbu.edu.hk/?page_id=823
Supplementary Figures S1–4, Tables S1–2, and Methods with References.

Supplementary Fig. S1. *Provanna* sp. (A) Shell, scale bar = 1 mm. (B) Radula detail, scale bar = 20 µm.

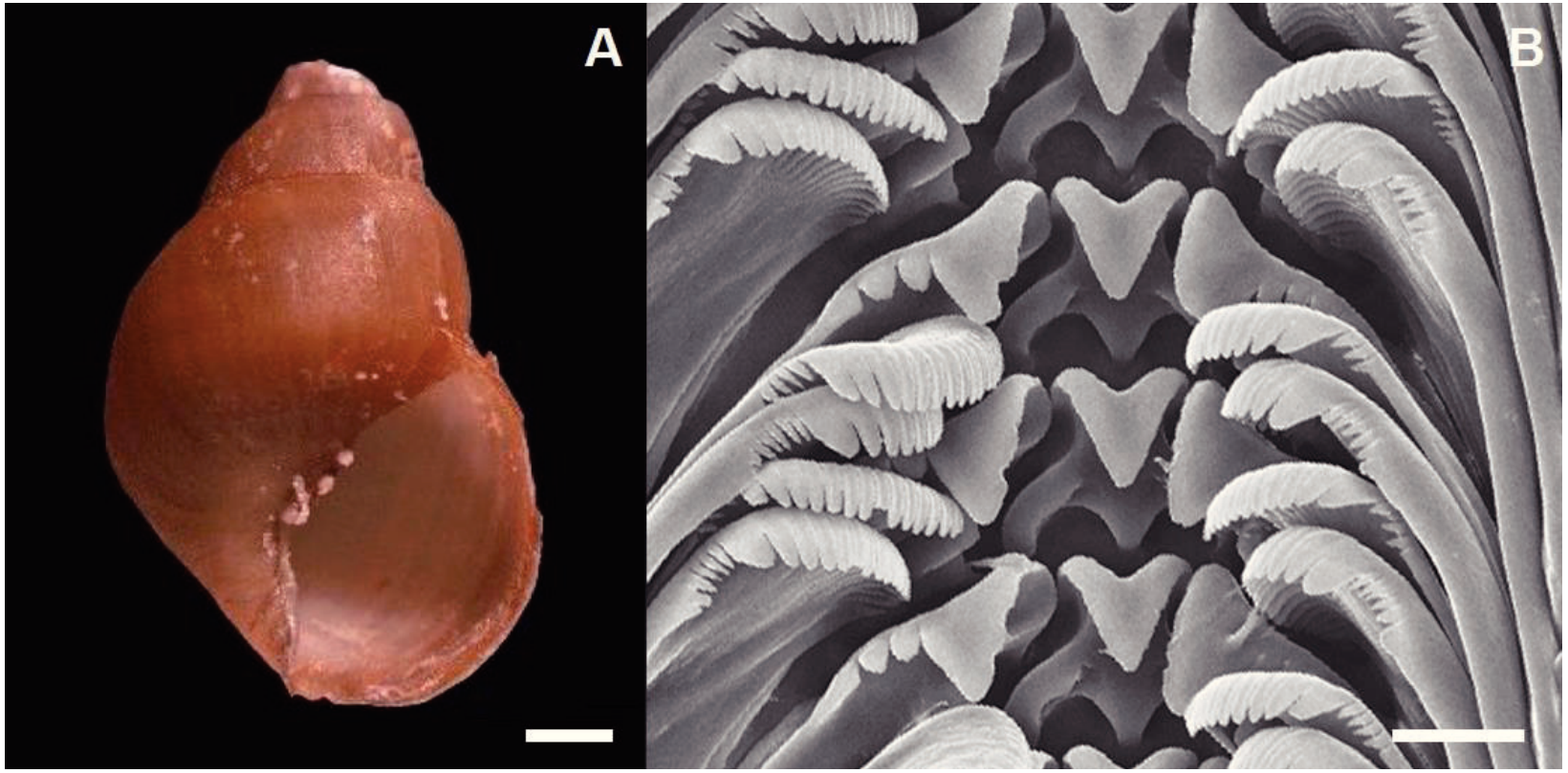

Supplementary Fig. S2. Phylogenetic analysis (ML topology) of Abyssochrysoidea based on partial *COI* sequences (347 bp). Numbers at each node represent the bootstrap value for ML analysis, bootstrap value for MP analysis, and posterior probability for Bayesian analysis. Dashes (-) indicate Bayesian posterior probabilities below 0.90 or bootstrap supports below 70. Two species of Abyssochrysidae were used as the outgroups.

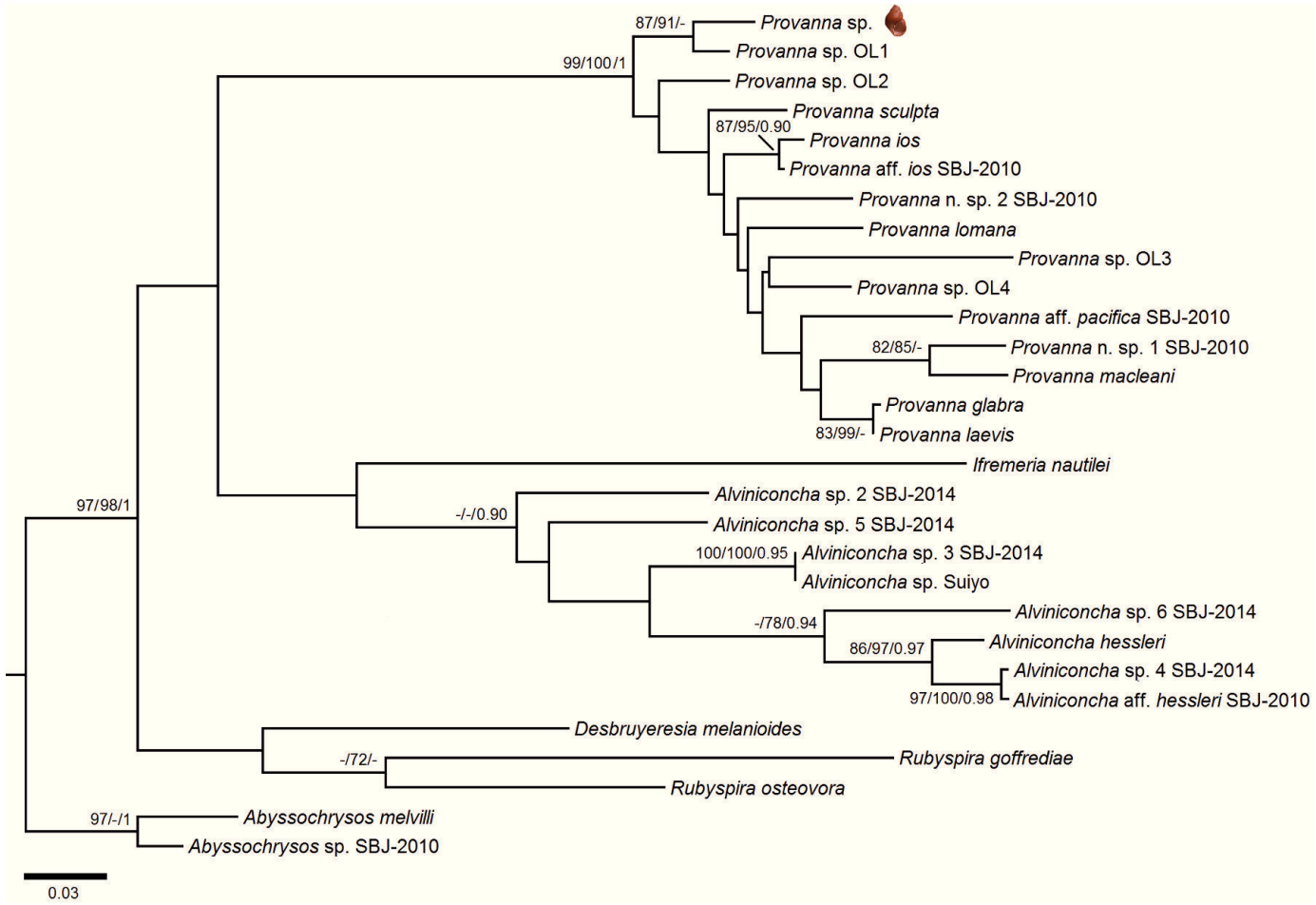

Supplementary Fig. S3. Mitochondrial gene map of *Provanna* sp.. Purple, pink, and red indicates the locations of PCGs, rRNA and tRNA genes, respectively. Arrows denote the directions of transcription. Genes located on the heavy strand are shown on the outer circle and those on the light strand are shown on the inner circle. A gap on the outer circle indicates the location of the possibly missing base pairs.

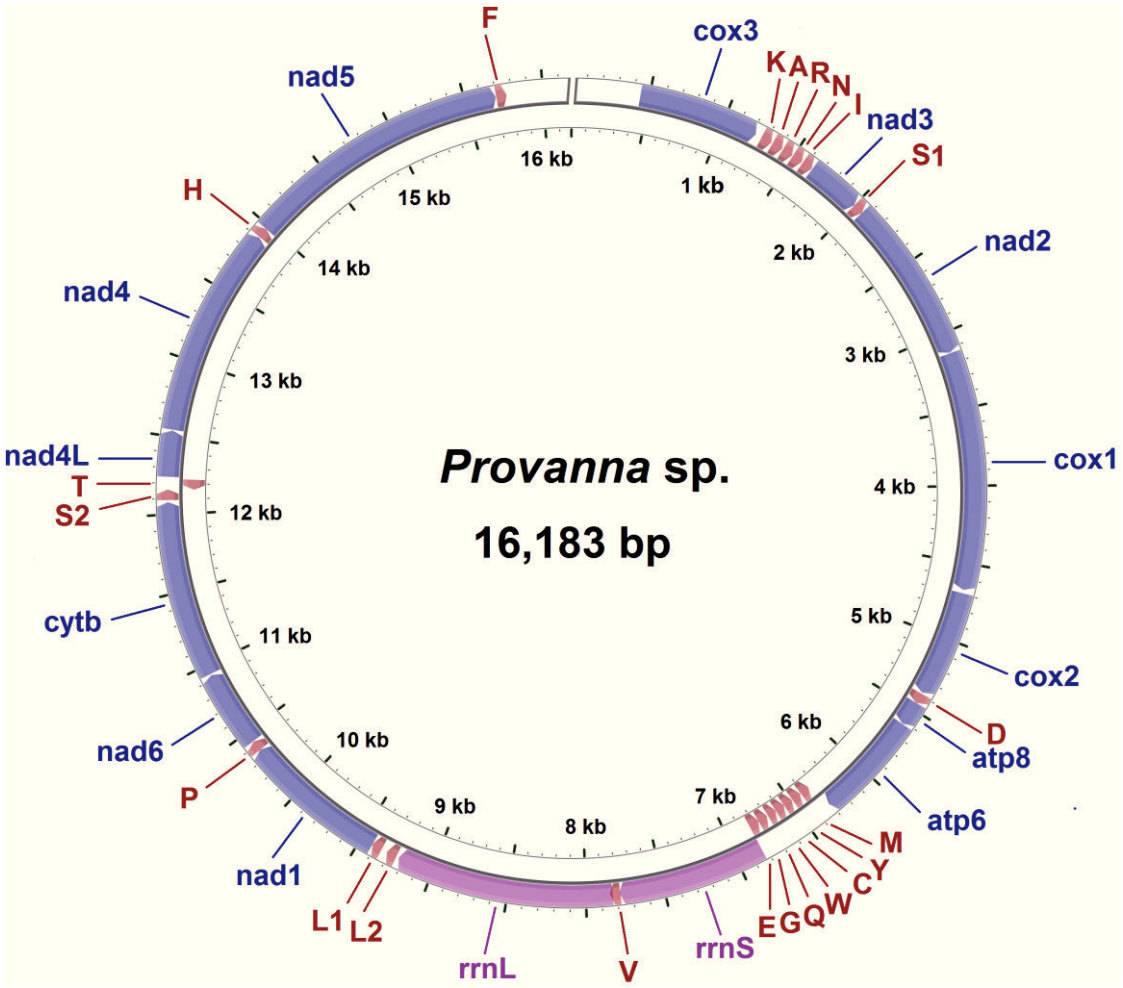

Supplementary Fig. S4. Phylogenetic tree inferred from the concatenated amino acid (AA) sequences of 13 PCGs (3,021 AAs) based on the BI topology with BI posterior probability, and ML and MP bootstrap value at each node. Dashes (-) indicate Bayesian posterior probabilities below 0.90 or bootstrap supports below 70. Taxon groups are indicated by vertical lines. A species of Cephalopoda (*Octopus vulgaris*) was used as the outgroup.

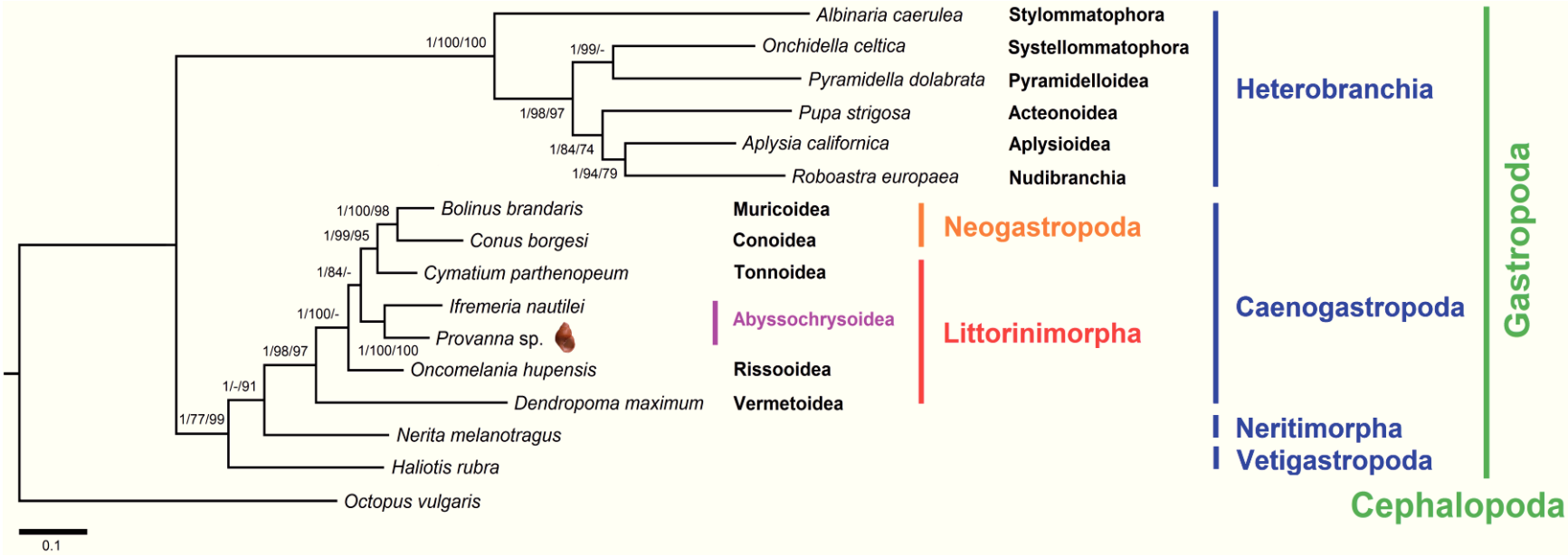

Supplementary Table S1. List of Abyssochrysoidea snails used for phylogenetic analysis in this study with accession numbers.

Species	Accession No.
Outgroup (Abyssochrysidae)	
Abyssochrysos melvilli	GQ290611
Abyssochrysos sp. SBJ-2010	GQ290609
Ingroup (Provannidae)	
Alviniconcha aff. *hessleri* SBJ-2010	GQ290602
Alviniconcha hessleri	KF467955
Alviniconcha sp. 2 SBJ-2014	KF467874
Alviniconcha sp. 3 SBJ-2014	KF467675
Alviniconcha sp. 4 SBJ-2014	KF467741
Alviniconcha sp. 5 SBJ-2014	KF467921
Alviniconcha sp. 6 SBJ-2014	KF467896
Alviniconcha sp. Suiyo	AB856040
Desbruyeresia melanioides	GQ290596
Ifremeria nautilei	AB235217
Provanna aff. *ios* SBJ-2010	GQ290587
Provanna aff. *pacifica* SBJ-2010	GQ290593
Provanna glabra	AB810174
Provanna ios	GQ290585
Provanna laevis	GQ290594
Provanna lomana	KF467665
Provanna macleani	GQ290583
Provanna n. sp. 1 SBJ-2010	GQ290577
Provanna n. sp. 2 SBJ-2010	GQ290578
Provanna sculpta	GQ290595
Provanna sp. OL1	AB810148
Provanna sp. OL2	AB810216
Provanna sp. OL3	AB810184
Provanna sp. OL4	AB810199
Rubyspira goffrediae	GQ290575
Rubyspira osteovora	GQ290573

Supplementary Table S2. List of molluscan taxa used for phylogenetic analysis in this study with accession numbers.

Species	Accession No.	Systematic position
Outgroup (Cephalopoda)		
Octopus vulgaris	NC_006353	Coleoidea; Neocoleoidea; Octopodiformes; Octopoda; Incirrata; Octopodidae; *Octopus*
Ingroup (Gastropoda)		
Albinaria caerulea	NC_001761	Heterobranchia; Euthyneura; Panpulmonata; Eupulmonata; Stylommatophora; Sigmurethra; Clausilioidea; Clausiliidae; Alopiinae; *Albinaria*
Aplysia californica	NC_005827	Heterobranchia; Euthyneura; Euopisthobranchia; Aplysiomorpha; Aplysioidea; Aplysiidae; *Aplysia*
Bolinus brandaris	NC_013250	Caenogastropoda; Hypsogastropoda; Neogastropoda; Muricoidea; Muricidae; *Bolinus*
Conus borgesi	NC_013243	Caenogastropoda; Hypsogastropoda; Neogastropoda; Conoidea; Conidae; *Conus*
Cymatium parthenopeum	NC_013247	Caenogastropoda; Hypsogastropoda; Littorinimorpha; Tonnoidea; Ranellidae; *Cymatium*
Dendropoma maximum	NC_014583	Caenogastropoda; Hypsogastropoda; Littorinimorpha; Vermetoidea; Vermetidae; *Dendropoma*
Haliotis rubra	NC_005940	Vetigastropoda; Haliotoidea; Haliotidae; *Haliotis*
Ifremeria nautilei	KC757644	Abyssochrysoidea; Provannidae; *Ifremeria*
Nerita melanotragus	GU810158*	Neritimorpha; Cycloneritimorpha; Neritoidea; Neritidae; *Nerita*
Onchidella celtica	NC_012376	Heterobranchia; Euthyneura; Panpulmonata; Eupulmonata; Systellommatophora; Onchidioidea; Onchidiidae; *Onchidella*
Oncomelania hupensis	NC_013073	Caenogastropoda; Hypsogastropoda; Littorinimorpha; Rissooidea; Pomatiopsidae; *Oncomelania*
Pupa strigosa	NC_002176	Heterobranchia; Lower Heterobranchia; Acteonoidea; Acteonidae; *Pupa*
Pyramidella dolabrata	NC_012435	Heterobranchia; Euthyneura; Panpulmonata; Pyramidelloidea; Pyramidellidae; *Pyramidella*
Roboastra europaea	NC_004321	Heterobranchia; Euthyneura; Nudipleura; Nudibranchia; Doridina; Anadoridoidea; Polyceridae; *Roboastra*

* Nearly complete mitochondrial genome.

Supplementary Methods with References

The *COI* sequence of *Provanna* sp. was aligned to the orthologous sequences of 26 provannids and two abyssochrysids on GenBank with MUSCLE v3.8.31 (Edgar, 2004). The conserved regions of aligned sequences were identified using Gblocks v0.91b (Castresana, 2000; Talavera & Castresana, 2007) under default settings, yielding 347 bp positions for the phylogenetic analysis.

Based on Osca et al. (2014), the complete mitochondrial genomes of 14 representatives of main gastropod orders (*Lottia digitalis* belonging to Patellogastropoda was removed due to high divergence) and one cephalopod were used here. Amino-acid sequences for all 13 PCGs were extracted from GenBank. MUSCLE v3.8.31 (Edgar, 2004) was used for alignment. The aligned sequences were trimmed by Gblocks v0.91b (Castresana, 2000; Talavera & Castresana, 2007) with the 5th parameter set to h (only positions where half or more of the sequences have a gap are treated as a gap position), and concatenated by Mesquite v2.75 (Maddisn & Maddison, 2011). A total of 3,021 concatenated amino acids remained after discarding the ambiguously aligned sites, corresponding to ~78% of the 3,895 amino acids in the initial alignment.

Trees were constructed with the partial *COI* sequences for 29 abyssochrysoid snails, and the concatenated amino-acid sequences for all PCGs of one cephalopod and 15 gastropods including two provannids. BI analysis was conducted with MrBayes v3.2.0 (Ronquist & Huelsenbeck, 2003) using the GTR+G+I and WAG model, respectively. Four Markov chains were applied for one million generations and sampled every 100 generations, with the first 25% as the burn-in. ML analysis was performed in raxmlGUI v1.3 (Silvestro & Michalak, 2012), running with the thorough bootstrap (10 runs; 500 pseudoreplicates). The GTR+G model was used for the *COI* dataset, whereas the PROTGAMMA+GTR model was used for the amino-acid dataset. BP analysis was conducted with PAUP* v4.0 (Swofford, 2002) using heuristic searches for 100 replicates, with random taxon addition and tree-bisection-reconnection (TBR) branch swapping.

Castresana J. (2000). Selection of conserved blocks from multiple alignments for their use in phylogenetic analysis. Mol Biol Evol 17: 540–552.

Edgar RC. (2004). MUSCLE: multiple sequence alignment with high accuracy and high throughput. Nucleic Acids Res 32: 1792–1797.

Maddison WP, Maddison DR. (2011). Mesquite: a modular system for evolutionary analysis.

Version 2.75. Available at: http://mesquiteproject.org.

Ronquist F, Huelsenbeck JP. (2003). MrBayes 3: Bayesian phylogenetic inference under mixed models. Bioinformatics 19: 1572–1574.

Silvestro D, Michalak I. (2012). raxmlGUI: A graphical front-end for RAxML. Org Divers Evol 12: 335–337.

Swofford, DL. (2002). PAUP*. Phylogenetic analysis using parsimony (*and other methods). Version 4. Sinauer Associates, Sunderland, Massachusetts.

Talavera G, Castresana J. (2007). Improvement of phylogenies after removing divergent and ambiguously aligned blocks from protein sequence alignments. Syst Biol 56: 564–577.

VENUS 73 (1–2): 1–14, 2015

Description of Two New Species of *Chicomurex* from the Philippine Islands (Gastropoda: Muricidae) with Update of the Philippines Species and Rehabilitation of *Chicomurex gloriosus* (Shikama, 1977)

Roland Houart[1]*, Christopher Owen Moe[2] and Chong Chen[3]

[1]*Institut royal des Sciences naturelles de Belgique, rue Vautier, 29, B-1000 Bruxelles, Belgium*
[2]*98-080 Uao Place #B2 Aiea, Hawaii 96701, USA*
[3]*Department of Zoology, University of Oxford, Oxford OX1 3PS, United Kingdom*

Abstract: Four species of *Chicomurex* are discussed and illustrated. Two new species are described from the Philippines, with geographical distribution extending to New Caledonia for one. *Chicomurex gloriosus* (Shikama, 1977) is reinstated as a valid name and *C. venustulus* (Rehder & Wilson, 1975) is restricted to the Marquesas Islands. Seven species are listed from the Philippines.

Keywords: Muricidae, *Chicomurex*, rehabilitation, new species, Indo-West Pacific

Introduction

Radwin & D'Attilio (1976) considered *Chicomurex* Arakawa, 1964 a synonym of *Phyllonotus* Swainson, 1833 and only *Chicomurex laciniatus* (Sowerby, 1841) was then included, as *Phyllonotus laciniatus*, from the Philippines. However this was not later widely accepted as the two genera differ in both shell and radula characters, and *Chicomurex* has been recognised as a valid genus by subsequent authors (Houart, 1992; Merle *et al.*, 2011).

Springsteen & Leobrera (1986) illustrated four species from the Philippines as *Chicoreus superbus* (Sowerby, 1889), *C. laciniatus* and *C. venustulus* Rehder & Wilson, 1975 and *C. superbus problematicus* (Lan, 1981). Houart (1992) illustrated five species of *Chicomurex* from the Philippines as *C. laciniatus*, *C. problematicus*, *C. superbus*, *C. turschi* (Houart, 1981) and *C. venustulus*; he also considered *Chicoreus gloriosus* Shikama, 1977 a synonym of *C. venustulus*. These species were confirmed by Houart (2008) with the exception of *C. turschi* which was no longer included in the Philippines malacological fauna. The illustration of *C. turschi* in Houart (1992, fig. 432) is correct but it has not been recorded from the Philippines since then and its presence needs to be confirmed. Merle *et al*. (2011) reinserted *C. turschi* but their illustrated specimens from the Philippines (Merle *et al*., 2011: pl. 78, figs. 11–12) are probably specimens of *Naquetia vokesae* (Houart, 1986) or a related species. See discussion and Table 2 for a summary of these and other misidentifications. Recently also, Houart (2013) described two new species from north of Mindanao, south of Leyte and off Bohol. Houart *et al*. (2014) proved *C. problematicus* to be a junior subjective synonym of *C. superbus*. The species illustrated as *C. superbus*, mostly occurring in Taiwan and Japan, was misidentified in all recent publications and remained without any valid name; it was then described as *C. lani* Houart, Moe & Chen, 2014.

* Corresponding author: roland.houart@skynet.be

In the present paper we describe two additional *Chicomurex* species from the Philippines, reinstate the name *C. gloriosus* (Shikama, 1977) and confine *C. venustulus* to the Marquesas. At present seven *Chicomurex* species are known to occur with certainty in the Philippines: *C. globus* n. sp., *C. gloriosus* (= *C. venustulus* auct.), *C. laciniatus*, *C. ritae* Houart, 2013, *C. pseudosuperbus* n. sp., *C. superbus* (= *C. problematicus*) and *C. tagaroae* Houart, 2013.

Materials and Methods

This report deals with species collected and gathered during several years in the Philippines and in some other localities from the Indo-West Pacific. The material originates from the collections of the authors. Other material belongs to MNHN and was collected during three expeditions organized by MNHN and IRD. Three of the species reviewed or described here were collected in New Caledonia during the LAGON expedition in 1985, 1988 and 1989, during the MUSORSTOM 9 expedition in the Marquesas in 1997 and during the SANTO 2006 expedition in Vanuatu.

Over 300 specimens of all related species within the genus *Chicomurex* were studied. Specimens were carefully compared to type material, written description, and to each other.

The two new species described here were taken alive, by tangle nets in 80–300 m, in the central Philippines. Other material was obtained from the South China Sea, Guam, Papua New Guinea, Vanuatu and New Caledonia, living at 18–124 m. Their description is based on all the examined specimens.

The chresonymy is cited only for misidentified figures in recent books or monographs.

The bathymetric distribution is calculated by taking the lowest measure of the maximum depth and the highest measure of the minimum depth for live-collected specimens.

Repositories: CC, collection of Chong Chen; CM, collection of Christopher Moe; IRSNB, Institut royal des Sciences naturelles de Belgique, Bruxelles, Belgium; KPM, Kanagawa Prefectural Museum, Yokohama, Japan; MNHN, Muséum national d'Histoire naturelle, Paris, France; NHMUK, Natural History Museum London; NSMT, National Museum of Nature and Science, Tokyo, Japan; RH, collection of Roland Houart; USNM, National Museum of Natural History, Washington, D.C., USA.

Abbreviations: CP, Chalut à perche (beam trawl); DR, Drague à roches (rocks dredge); DW, Drague Warén (Warén dredge); IRD, Institut de Recherche pour le Développement (Formerly ORSTOM); ORSTOM, Office de la Recherche Scientifique et Technique d'Outre Mer (now IRD); lv, live-collected specimen; dd, empty shell.

Terminology used to describe the spiral cords and the apertural denticles (after Merle, 2001 and 2005) (Figs. 1, 2) (terminology in parentheses: erratic feature). *Spiral cords*: ab, abapical (or abapertural); abis, abapical infrasutural secondary cord (on subsutural ramp); ABP, abapertural primary cord on the siphonal canal; abs, abapertural secondary cord on the siphonal canal; ad, adapical (or adapertural); adis, adapical infrasutural secondary cord (on subsutural ramp); ADP, adapertural primary cord on the siphonal canal; ads, adapertural secondary cord on the siphonal canal; IP, infrasutural primary cord (primary cord on subsutural ramp); MP, median primary cord on the siphonal canal; ms, median secondary cord on the siphonal canal; P, primary cord; P1, shoulder cord; P2-P6, primary cords of the convex part of the teleoconch whorl; s, secondary cord; s1-s6, secondary cords of the convex part of the teleoconch whorl (example: s1 = secondary cord between P1 and P2; s2 = secondary cord between P2 and P3, etc.); t, tertiary cord. *Aperture*: D1 to D6, Abapical denticles; ID, Infrasutural denticle.

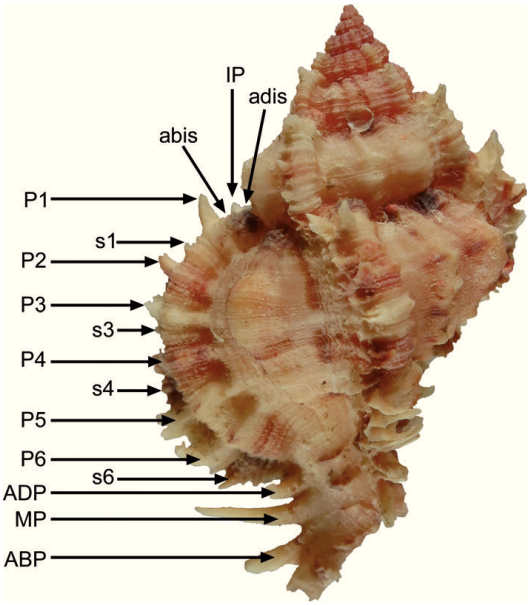

Fig. 1. Spiral cords morphology of *Chicomurex globus* n. sp. (holotype), as an example to indicate positions of morphological characters and terminologies used.

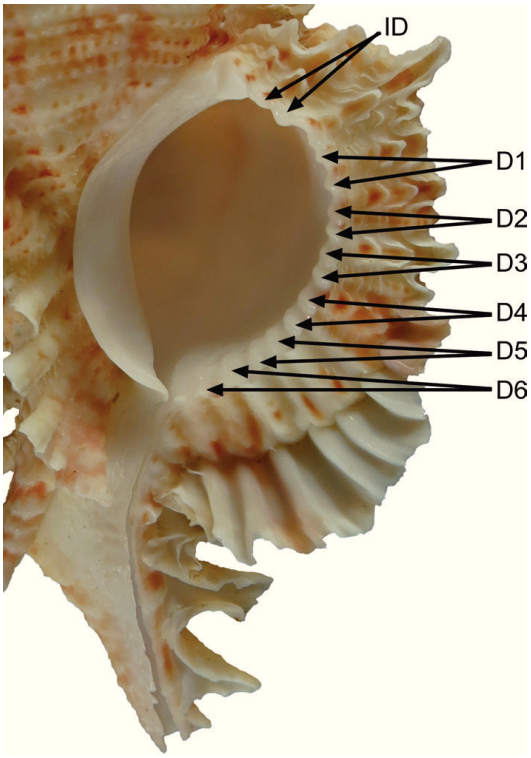

Fig. 2. Apertural denticles of *Chicomurex pseudosuperbus* n. sp. (holotype), as an example to indicate positions of morphological characters and terminologies used.

Systematic Account

Family Muricidae Rafinesque, 1815
Genus *Chicomurex* Arakawa, 1964

Type species by original designation: *Murex superbus* G. B. Sowerby III, 1889, Recent, Philippines.

Chicomurex globus n. sp.

(Figs. 1, 3E–F, 4A–L)

Chicoreus superbus – Kaicher, 1973: card 139 [non *Murex superbus* G. B. Sowerby III, 1889].
Chicomurex superbus – Kubo & Kurozumi, 1995: pl. 94, fig. 2 [non *Murex superbus* G. B. Sowerby III, 1889].
Phyllonotus species – Hinton, 1977: 27, fig. 4a (only) (subfossil).
Chicomurex venustulus – Houart, 1992: 124 (in part), figs. 118–119 (radula), 425–426, 429; Houart, 2008: 146, pl. 368, fig. 1 (only); Merle *et al.*, 2011: pl. 77, fig. 14 (only) [non *Chicoreus* (*Chicomurex*) *venustulus* Rehder & Wilson, 1975].

Type material: Holotype MNHN IM 2000-27394, 1 paratype IRSNB IG 32625/MT.3011, 1 paratype NSMT-Mo 78794, 1 paratype NHMUK 20140022, 2 paratypes CM (all from the type locality); 1 paratype USNM1231368, Lipata, Surigao, Philippines, by tangle nets, in 150 m; 1 paratype CC, 2 paratypes CM, 1 paratype RH (all from Surigao Straits, Mindanao, Philippines, by tangle nets, in 200 m, all lv).

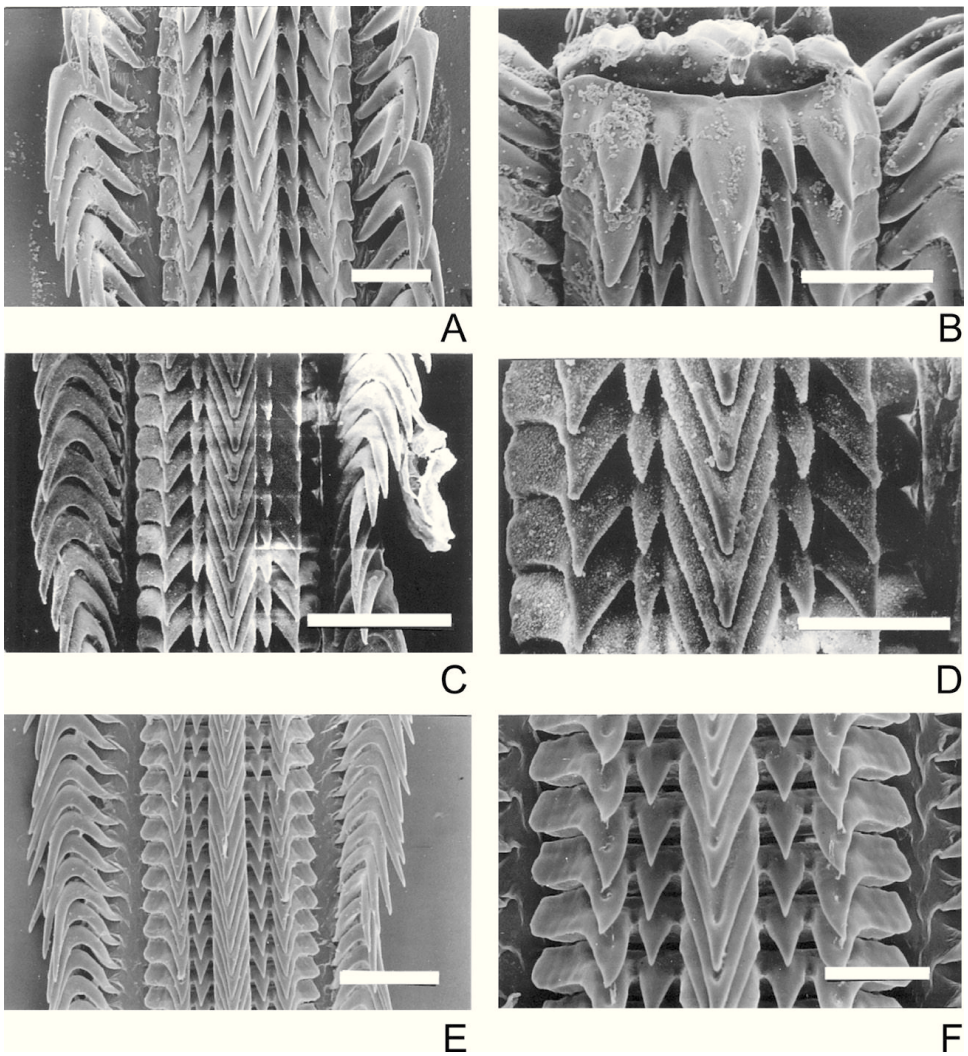

Fig. 3. Radulae. **A–B**. *Chicomurex laciniatus* (Sowerby, 1841), Papua New Guinea. **C–D**. *Chicomurex gloriosus* (Shikama, 1977), Taiwan (Fig. 5I). **E–F**. *Chicomurex globus* n. sp., New Caledonia. Scale bars: A–B, D, F = 50 µm; C–E = 100 µm.

Type locality: Davao Bay, Mindanao, off eastern Samal Island, Philippines, by tangle nets, in 200–300 m.

Other material examined: *South China Sea*: Macclesfield Bank, sand and shell debris, 75 m, 1988 (RH, 1 lv). *Philippines*: Davao Bay, Mindanao, off eastern Samal Island, by tangle nets, in 200 m (CM, 6 lv); Lipata, Surigao, trawled in 150 m (CC, 1 lv); Surigao, northeastern Mindanao, trawled in 80–100 m (RH, 31 lv & dd, mostly juveniles); Surigao, trawled in 150 m (RH, 3 lv) (CM 7 lv). *Guam*: dredged from Agana Bay, 108–124 m (RH, 1 lv). *Papua New Guinea*: Durangit (Madang Province), Hansa Bay, 45 m, 1978 (RH, 1 lv). *New Caledonia*: Lagon Nord, LAGON, n.o."Vauban" stn. DW542, 6 March 1985, 49–50 m (MNHN, 1 lv); Secteur de Poum, abords de l'Ile de Neba, n.o."Alis", stn. DW1009, 2 May 1988, 18–20 m (MNHN, 2 lv); secteur des Belep, n.o."Alis", stn. DW1134, 26 October 1989, 40 m (MNHN, 1 lv). *Vanuatu*: Segong Channel, SANTO 2006, stn. DR03, 10 September 2006, 2–30 m (MNHN, 1 dd).

Distribution: Okinawa, South China Sea, southern Philippines, Guam, Papua New Guinea, Vanuatu and New Caledonia, living in 18–200 m. *Chicomurex globus* n. sp. is also known from subfossil beds, off Matupit, near Rabaul, Papua New Guinea (Fig. 4J).

Etymology: *globus* (L), ball, sphere, named after its rounded outline, like a ball.

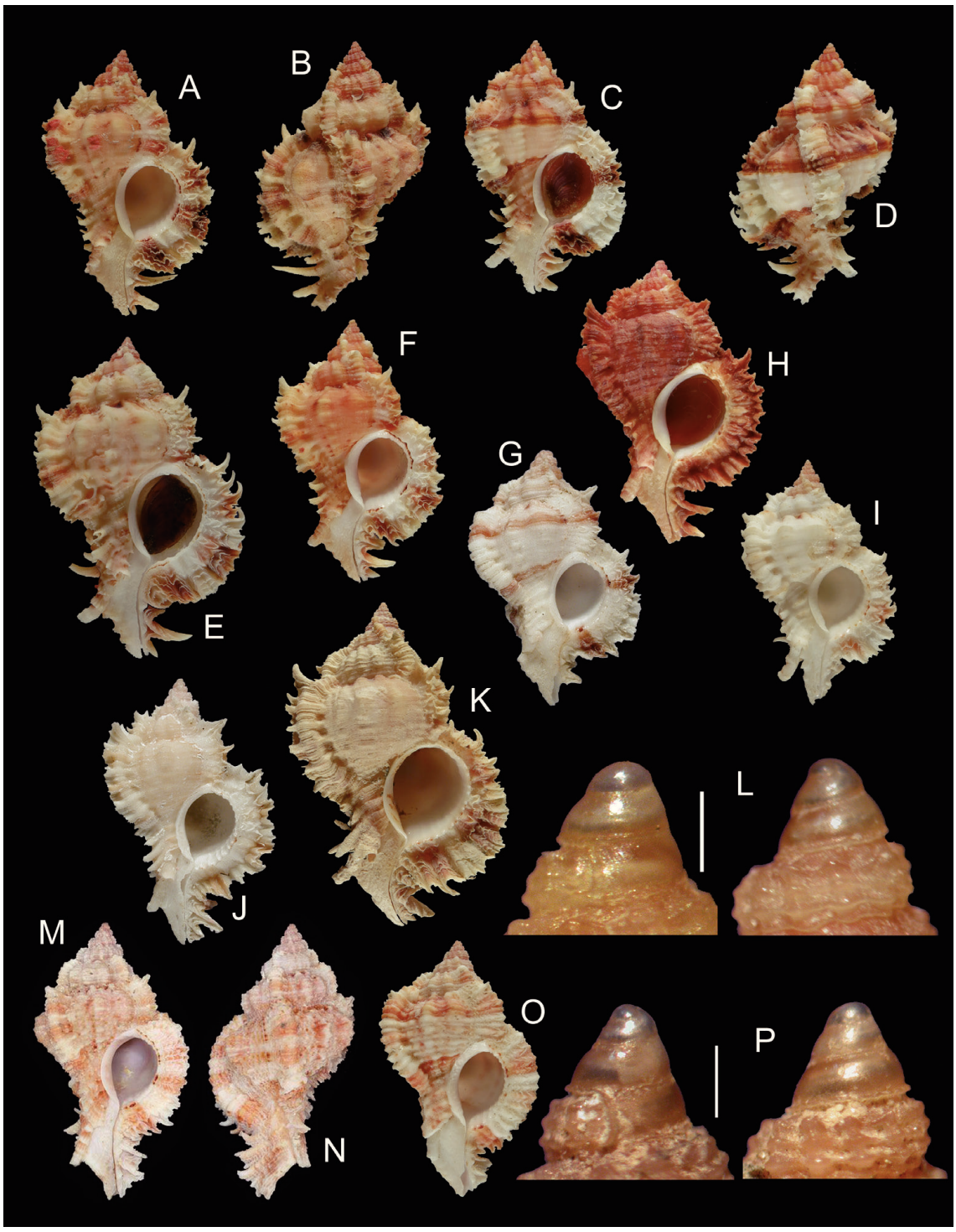

Fig. 4. A–L. *Chicomurex globus* n. sp.; A–B, Davao Bay, Mindanao, off eastern Samal Is., tangle nets, 200–300 m, Philippines, holotype MNHN IM 2000-27394, 39.7 mm; C–F, Surigao straits, Mindanao, 200 m, in tangle nets, Philippines (C–D, CM, 35 mm; E, paratype CM, 49.9 mm; F, paratype CC, 35.7 mm); G, Durangit (Madang Province), Hansa Bay, 45 m, 1978, Papua New Guinea, RH, 34.7 mm; H, South China Sea, Macclesfield Bank, 75 m, 1988, RH, 36.5 mm; I, dredged from Agana Bay, 108–124 m, March 1990, Guam, RH, 33.5 mm; J, subfossil beds, off Matupit, near Rabaul, Papua New Guinea, RH, 35.9 mm; K, New Caledonia, Secteur de Poum, near Neba Is., LAGON, stn. DW1009, 18–20 m, May 1988, MNHN, 53.3 mm; L, protoconch, Surigao, Basul Is., Philippines, RH (scale bar = 500 μm). **M–P**. *Chicomurex venustulus* (Rehder & Wilson, 1975); M–N, off Southwest coasts of Tahuata, Marquesas Islands, 66–71 m, holotype USNM 707241, 40.5 mm; O, Hiva Oa Is., Marquesas Islands, MUSORSTOM 9, stn. CP1227, 84–85 m, August 1997, MNHN, 34.9 mm; P, protoconch, Nuku Hiva, Marquesas Islands, RH (scale bar = 500 μm).

Description: Shell medium sized for the genus, up to 53 mm in length at maturity (MNHN). Average length/width ratio 1.56–1.62, extremes 1.54 and 1.87. Shell globose, broad, lightly built, spinose and nodose. Subsutural ramp narrow, weakly sloping, convex. Creamy white, light tan, tan or chestnut brown, darker coloured below the suture or occasionally on entire subsutural area. Occasionally with two darker coloured spiral bands on P2-s2 and on P6-s6. Other darker spiral band, when present, only obvious on axial varices, covering P3-s3. Tan or brown blotches on axial nodes, on base of varices and on dorsal side of siphonal canal. Shell occasionally entirely white or brown. Aperture glossy white with more or less obvious fine dark brown line along edge of outer apertural lip.

Spire high with 2.45 protoconch whorls and teleoconch of up to 8 broadly convex, weakly shouldered, spinose and nodose whorls. Suture weakly adpressed.

Protoconch (Fig. 4L) small, conical, acute, whorls smooth, with a narrow, single keel abapically. Width 750–800 μm, height 800 μm. Terminal lip erect, of sinusigera type.

Axial sculpture of teleoconch whorls consisting of high, narrow, nodose ribs on two first teleoconch whorls; other whorls with 3 varices, each varix with short, acute, adapically curved, open, primary and secondary spines. Shoulder spine shortest, narrowest, other primary spines increasing in length and breadth abapically. Other axial sculpture of 2 or 3 intervarical ribs or nodes. First and second teleoconch whorls with 11 or 12 ribs, third with 4 or 5 ribs and starting varices, from third or fourth whorl 3 varices per whorl with 2 or 3 intervarical ribs. Intervarical ribs or nodes more strongly developed on penultimate and last whorls. Last whorl usually with a strong and high node followed by a weakly lower one.

Spiral sculpture of low, narrow, nodose, primary, secondary and tertiary cords and numerous narrow threads. First and second teleoconch whorls with visible P1-P4, third with (IP), P1, s1, P2-P4, fourth with IP, P1, s1, P2, s2, P3, s3, P4, fifth whorl starting adis and abis, sixth whorl of a juvenile shell with adis, IP, abis, P1, s1, P2, s2, P3, s3, P4, s4, P5, s5, P6, s6 and two additional tertiary cords below s6, followed by ADP, MP, ABP. Adult shell with similar morphology. Varices with short, strongly abaxially and adapically curved spines extending from primary cords and few spinelets from secondary cords. Spines increasing in length abapically, P4, P5, P6 and ADP very strongly curved, webbed, MP slightly straighter and longer, ABP short, narrow, weakly or strongly abapically bent.

Aperture moderately small, roundly ovate. Columellar lip narrow, smooth or covered with small folds or rugae, more obvious abapically; low parietal tooth at adapical extremity; rim partially erect, adherent at adapical extremity. Anal notch shallow, broad. Outer lip erect, crenulated, with weak, elongate denticles within, usually ID split and D1-D6 split. Siphonal canal short, moderately narrow, strongly dorsally recurved at tip, narrowly open.

Operculum dark brown, ovate with subapical nucleus and numerous concentric ridges; attached surface with broad callused rim.

Radula (Fig. 3E–F) typical for *Chicomurex* with numerous crowded rows of teeth and a rachidian with large, broad, triangular central cusp, a smaller, broad, triangular lateral denticle and a slightly larger, triangular lateral cusp. Lateral tooth narrow, sickle shaped.

Remarks: *Chicomurex globus* n. sp. was misidentified as *C. venustulus* auct. (= *C. gloriosus*) by Hinton (1977), Houart (1992, 2008) and Merle *et al.* (2011) (see also Table 2). *C. globus* n. sp. differs from *C. gloriosus* in having a comparatively smaller shell for a same number of teleoconch whorls, it is also comparatively broader and rounder and the siphonal canal is shorter (see Table 1) compared to the more elongate *C. gloriosus* which has a quite longer siphonal canal and a more strongly shouldered shell. *C. globus* n. sp. also has a very strongly dorsally recurved ADP spine on the siphonal canal *vs* only weakly recurved in *C. gloriosus*. The varical spines are also more strongly dorsally recurved in *C. globus* n. sp., in particular the P5 and P6 spines, while straight or almost straight in *C. gloriosus*.

Table 1. Main shell characters and colour variation.

Characters	*C. gloriosus*	*C. venustulus*	*C. globus* n. sp.	*C. pseudosuperbus* n. sp.
Maximum length	60 mm	40.5 mm	53 mm	85 mm
Maximum width	34 mm	22 mm	30.9 mm	39.3 mm
Average ratio	2.01	1.8	1.65	2.07
Average length of Siphonal canal *vs* length of shell	41%	34%	32%	39%
Average height of aperture *vs* length of shell	27%	31%	31%	29%
Average width of aperture *vs* width of shell	42%	40%	40%	45%
Shape of shell	Shouldered	Shouldered	Rounded	Shouldered
Spiral cords covered by colour spiral band	s2-P5	(s1) P2-s2	P2-s2	P2-s2
	s2-s5	(P4-s4)	P3-s3 (on varices only)	s6-t6
	P3-s4	S6-tt	P6-s6	

The intervarical ribs or nodes of the last teleoconch whorl are generally lower in *C. globus* n. sp. and the suture of whorls are less adpressed. The banded form of *C. globus* n. sp. has the band covering P2-s2, P6, s6, and, less obvious, on P3-s3. In *C. gloriosus* the colour band is broader, generally covering s2-P5, or s2-S5, or P3-s4.

Chicomurex globus n. sp. was also confused with *C. superbus* auct. by Kaicher (1973). The shell illustrated as *C. superbus* by many authors was recently described as *C. lani*. It differs markedly from *C. globus* n. sp. and does not need to be compared here.

Chicomurex globus n. sp. differs from *C. venustulus* from the Marquesas in having a larger shell relative to the number of teleoconch whorls, in being more globose with a less strongly adpressed suture, a broader aperture and also in having comparatively narrower varices. The position of the coloured spiral bands is also different (see Table 1).

Chicomurex pseudosuperbus **n. sp.**

(Figs. 2, 5K–O)

Chicoreus (*Chicomurex*) *superbus* – Springsteen & Leobrera, 1986: 132, pl. 36, fig. 1 [non *Murex superbus* G. B. Sowerby III, 1889].

Chicomurex venustulus – Houart, 1992: 124 (in part), fig. 430 (only); Merle *et al*., 2011: pl. 77, figs. 8–9 (only) [non *Chicoreus* (*Chicomurex*) *venustulus* Rehder & Wilson, 1975].

Chicomurex superbus – Houart, 2008: 144, pl. 367, fig. 6 (only); 146, pl. 368, figs. 5 and 7 (only) [non *Murex superbus* G. B. Sowerby III, 1889].

Type material: Holotype MNHN IM 2000-27395, 1 paratype IRSNB IG 32626/MT.3012, 1 paratype NSMT-Mo 78795 (all from the type locality); 1 paratype CC (200 m, off Balut Island, Philippines), 2 paratypes CM (off Cebu, Philippines), 3 paratypes RH (off Cebu, Philippines) (all lv).

Type locality: Off Mactan Island, Cebu, Philippines.

Other material examined: *Japan*: Okinawa, Zanpa Misaki, scuba in 60 m (CM, 2 lv). *Taiwan*: no other data (RH, 1 dd). *Philippines*: Bohol, Kalituban Island, by tangle nets in *ca*. 90 m (RH, 1 lv); Balicasag Island, by tangle nets (RH, 1 lv) (CM, 7 lv) (CC, 1 lv); Davao (RH, 1 lv) (CM, 2

Table 2. Summary of misidentified species with their original and their correct identification.

Authors	Figures	Original identification	Correct identification
Kaicher (1973)	Card 139	*Chicoreus superbus*	*Chicomurex globus* n. sp.
Hinton (1977)	p. 27, fig. 4a	*Phyllonotus* species	*C. globus* n. sp.
	p. 27, fig. 4	*Phyllonotus* species	*C. gloriosus*
Houart (1981)	p. 10, text fig. p. 7	*Chicoreus venustulus*	*C. gloriosus*
Springsteen & Leobrera (1986)	Pl. 36, fig. 1	*Chicoreus superbus*	*C. pseudosuperbus* n. sp.
	Pl. 36, fig. 3	*Chicoreus venustulus*	*C. gloriosus*
Lai (1987)	Pl. 30, fig. 1	*Chicoreus superbus*	*C. gloriosus*
Dharma (1988)	Pl. 25, fig. 9	*Chicomurex venustulus*	*C. gloriosus*
Drivas & Jay (1988)	Pl. 20, fig. 3	*Chicoreus superbus*	*C. gloriosus*
Houart (1992)	265, 428	*Chicomurex venustulus*	*C. gloriosus*
	425, 426, 429	*Chicomurex venustulus*	*C. globus* n. sp.
	430	*Chicomurex venustulus*	*C. pseudosuperbus* n. sp.
Kubo & Kurozumi (1995)	Pl. 94, fig. 2	*Chicomurex superbus*	*C. globus* n. sp.
Tsuchiya (2000)	Pl. 184, fig. 31	*Chicomurex venustulus*	*C. gloriosus*
Thach (2005)	Pl. 36, fig. 3	*Chicomurex venustulus*	*C. gloriosus*
Houart (2010)	Pl. 367, fig. 6	*Chicomurex superbus*	*C. pseudosuperbus* n. sp.
	Pl. 368, fig. 1	*Chicomurex venustulus*	*C. globus* n. sp.
	Pl. 368, figs. 2–4	*Chicomurex venustulus*	*C. gloriosus*
	Pl. 368, figs. 5, 7	*Chicomurex superbus*	*C. pseudosuperbus* n. sp.
Robin (2008)	p. 249, fig. 2	*Chicomurex venustulus*	*C. gloriosus*
Merle *et al.* (2011)	Pl. 77, figs. 8–9	*Chicomurex venustulus*	*C. pseudosuperbus* n. sp.
	Pl. 77, figs. 10–13, 15, 17–18	*Chicomurex venustulus*	*C. gloriosus*
	Pl. 77, fig. 14	*Chicomurex venustulus*	*C. globus* n. sp.
Thach (2012)	Pl. 53, fig. 621 (left)	*Chicomurex venustulus*	*C. gloriosus*

lv); South Mindanao, Samal Island, Davao Bay, by tangle nets in 100–150 m, January 2004 (RH, 1 lv) (CM, 3 lv); no other data (RH, 2 lv, juveniles). *Australia*: Queensland (CM, 1 lv).

Distribution: Japan, Taiwan, Philippine Islands, New Caledonia (CM, in litt.) and Queensland, Australia (CM), living in 60–200 m.

Etymology: Named *pseudosuperbus* because it was misidentified as *Chicomurex superbus* in recent literature.

Description: Shell large for the genus, up to 85 mm in length at maturity. Average length/width ratio 1.98–2.13, extremes 1.97 and 2.27. Shell lanceolate, broadly ovate, heavy, weakly spinose, squamous and nodose. Subsutural ramp narrow, weakly sloping, convex.

Creamy white or light tan with numerous dark brown spots on spiral cords, occasionally with

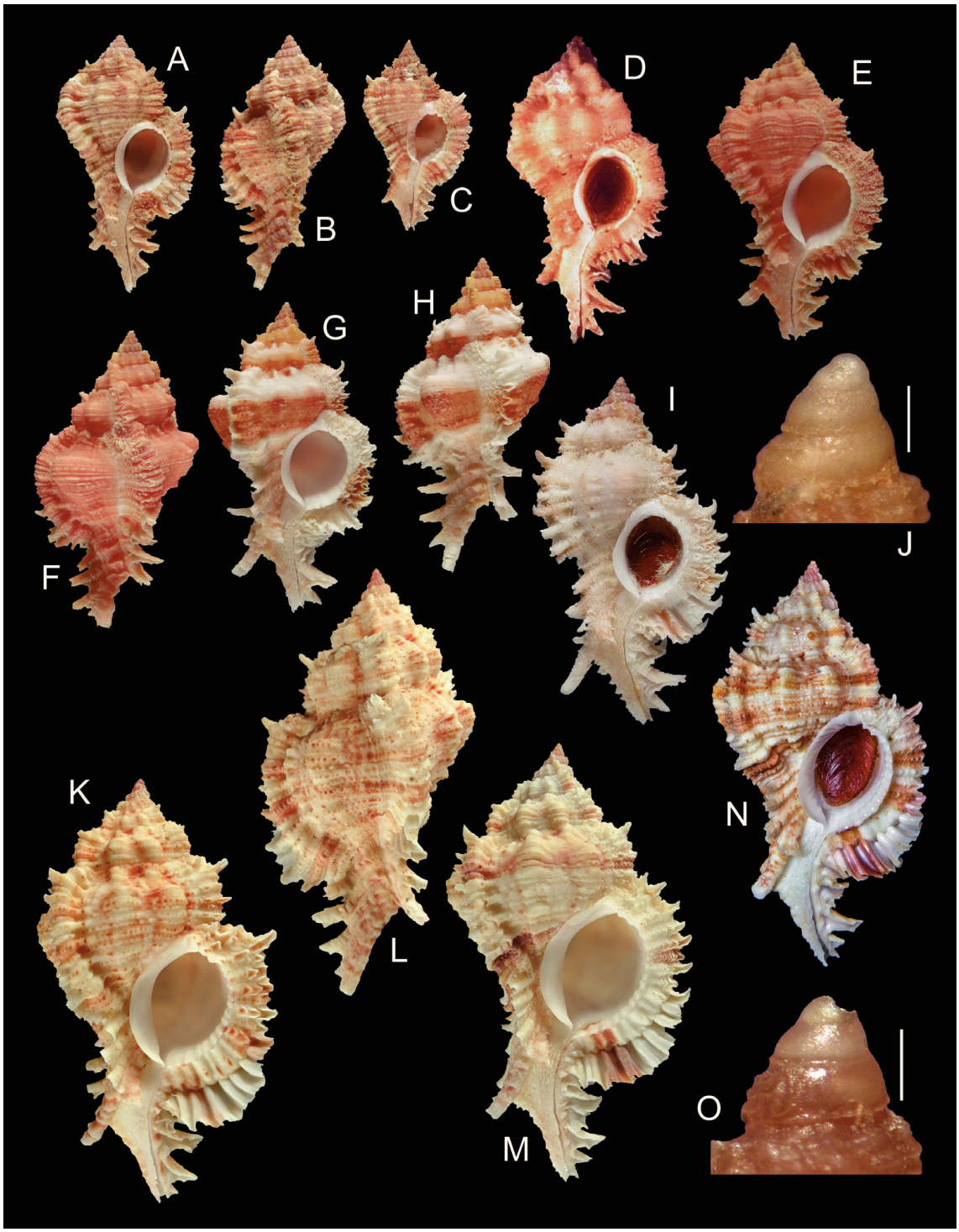

Fig. 5. A–C. *Chicomurex venustulus* (Rehder & Wilson, 1975); A–B, Nuku Hiva, Marquesas Islands, MUSORSTOM 9, stn. DR1183, 86–120 m, August 1997, MNHN, 38.4 mm; C, Hiva Oa Is., Marquesas Islands, MUSORSTOM 9, stn. DW1203, 60–61 m, August 1997, MNHN, 24.2 mm. **D–J**. *Chicomurex gloriosus* (Shikama, 1977); D, off Cebu Is., Philippines, holotype KPM 3275, 49.5 mm (from a colour slide); E–F, Balut Is., Philippines, RH, 49.1 mm; G–H, Balut Is., Philippines, RH, 50.9 mm; I, South Taiwan Strait, RH, 54 mm; J, protoconch, Surigao, Basul Is., Philippines, RH (scale bar = 500 µm). **K–O**. *Chicomurex pseudosuperbus* n. sp.; K–L, Cebu, Philippines, holotype MNHN IM 2000-27395, 74.5 mm; M, Cebu, Philippines, paratype RH, 74.6 mm; N, Balut Is., Philippines, 200 m, paratype CC, 64.5 mm; O, protoconch, Philippines (no other data), RH (scale bar = 500 µm).

brown band covering P2, s2 and s6, t6 and space between these cords. Aperture glossy white, occasionally with fine dark brown, continuous or interrupted, line along outer edge.

Spire high with 2+ protoconch whorls (partially broken in examined specimens). Teleoconch of up to 7 or 8 broad, weakly convex, shouldered, spinose and nodose whorls. Suture slightly adpressed. Protoconch (Fig. 5O) small, conical. Whorls smooth, with a narrow, single keel abapically. Terminal lip erect, of sinusigera type.

Axial sculpture of teleoconch whorls consisting of low, narrow, nodose ribs on 2 or 3 first whorls and high, narrow, rounded varices and intervarical ribs on other whorls, each varix with short, narrow, open primary and secondary spinelets. Other axial sculpture of 2 low, broad intervarical ribs, broader and higher on penultimate and last whorls. First and second whorl with 11 or 12 ribs, third whorl starting varices, fourth with 3 varices and 3 or 4 narrow intervarical ribs, fifth whorl with 3 varices and 3 intervarical ribs, sixth whorl with 3 varices and 2 or 3 intervarical ribs. Penultimate and last whorls with 3 varices and 2 strong intervarical ribs or nodes; last whorl usually with a stronger and a weaker node. Spiral sculpture of high, rounded, narrow, squamous, primary, secondary and tertiary cords and weak threads. First whorl with visible P1-P4, second with P1-P4 or starting s1, third with IP, P1, s1, P2, s2, P3, s3, P4, fourth starting adis and abis, fifth with adis, IP, abis, P1, s1, P2, s2, P3, s3, P4. Subsutural area of sixth whorl of a juvenile with adis, IP adis and additional threads, followed abapically by P1, s1, P2, s2, P3, s3, P4, s4, P5, s5, P6, s6, ADP, MP and ABP; s6 almost similar in strength and height to P6, followed by 2 or 3 strong tertiary cords. Morphology of adult shells similar. Spiral cords ending as short spines on varices. IP-P4 extending as very short, open, slightly adapically curved spines; P4-s6 somewhat longer, increasing in length and width abapically, webbed; ADP strongly dorsally recurved, MP longer, straight or weakly curved, ABP shorter; secondary cords forming short spinelets between primary spines.

Aperture large, broadly ovate. Columellar lip moderately broad, flaring, smooth, with 2 or 3 elongate, weak knobs abapically or covered with small rugae; low parietal tooth at adapical extremity. Anal notch broad, moderately deep. Outer lip erect, crenulated, with weak elongate denticles within: ID split and D1-D6 split. Siphonal canal long, broad, weakly dorsally recurved, narrowly open, with 3 frondose, broad, short spines: ADP, MP, ABP and occasional ads.

Operculum dark brown, ovate with subapical nucleus and numerous concentric ridges. Attached surface with broad, callused rim.

Radula unknown.

Remarks: *Chicomurex pseudosuperbus* n. sp. was confused with *C. superbus* auct. (= *C. lani*) by Springsteen & Leobrera (1986) and Houart (2008), and with *C. venustulus* auct. (= *C. gloriosus*) by Merle *et al.* (2011). *Chicomurex pseudosuperbus* n. sp. differs from *C. gloriosus* in having a larger shell relative to the number of teleoconch whorls and a comparatively narrower aperture. Like in *C. globus* n. sp. the colour bands are situated differently on the last teleoconch whorl. In *C. gloriosus* they cover s2-P5 or s2-s5 or P3-s4 (see Table 1). In *C. pseudosuperbus* n. sp. they cover P2-s2 and s6 plus one or two tertiary cords below s6. *C. pseudosuperbus* n. sp. differs from *C. superbus* in having a narrower shell with a comparatively higher spire, less coloured spiral cords and often, less obvious secondary spiral cords. In *C. superbus* the secondary cords are almost as broad and high than the primary cords or weakly smaller, in *C. pseudosuperbus* n. sp. they are half the size of the primary cords or even more. *C. pseudosuperbus* n. sp. differs from *C. lani* in having a larger shell relative to the number of teleoconch whorl, a more adpressed suture, a comparatively longer siphonal canal, more obvious axial nodes on the last teleoconch whorl and a more scabrous shell. Also, *C. lani* is not currently confirmed from the Philippines (Houart *et al.*, 2014). *C. pseudosuperbus* n. sp. differs strongly from the two other species with conical protoconch, *C. globus* n. sp. and *C. venustulus* which do not need to be compared here.

Chicomurex gloriosus (Shikama, 1977)

(Figs. 5D–J)

Chicoreus gloriosus Shikama, 1977: 14, pl. 2, fig. 8.
Phyllonotus species – Hinton, 1977: 27, fig. 4 (only) (subfossil).
Chicoreus (*Chicomurex*) *venustulus* – Houart, 1981: 10, text-fig. p. 7; Springsteen & Leobrera, 1986: 132, pl. 36, fig. 3 [non *Chicoreus* (*Chicomurex*) *venustulus* Rehder & Wilson, 1975].
Chicoreus superbus – Lai, 1987: 63, pl. 30, fig. 1; Drivas & Jay, 1988: pl. 20, fig. 3 [non *Murex superbus* G. B. Sowerby III, 1889].
Chicomurex venustulus – Houart, 1992: 124 (in part), figs. 265, 268 (holotype of *C. gloriosus*), 428; Tsuchiya, 2000: 371, pl. 184, fig. 31; Thach, 2005: 113, pl. 36, fig. 3; Houart, 2008: 146, pl. 368, figs. 2–4; Robin, 2008: 249, fig. 2; Thach, 2012: pl. 53, fig. 621 (left); Merle *et al.*, 2011: pl. 77, figs. 10–13, 15, 17–18 (only) [non *Chicoreus* (*Chicomurex*) *venustulus* Rehder & Wilson, 1975].

Type material: Holotype KPM 3275.

Type locality: Off Cebu Island, Philippines.

Material examined: Holotype and more than 100 specimens (lv and dd) from throughout the geographical range.

Distribution: Japan, Taiwan, Vietnam, the Philippines, Papua New Guinea, in the Pacific; Madagascar (MNHN), Indonesia, Reunion and Mauritius (Drivas & Jay, 1988) in the Indian Ocean.

Remarks: *Chicomurex gloriosus* was first illustrated as *C. venustulus* by Houart (1981) then followed by Springsteen & Leobrera (1986). Houart (1992) classified *C. gloriosus* as subjective junior synonym.

However, after a careful comparison with new material from the Philippines (*C. gloriosus*) and from the Marquesas (*C. venustulus*) it appears that both species have some, permanent, different shell characters. *C. gloriosus* is larger relative to the number of teleoconch whorls, reaching 60 mm in length *vs* 40.5 mm for *C. venustulus*, it is not as stocky as *C. venustulus* and the siphonal canal is comparatively longer, while the intervarical nodes are generally higher, forming a stronger node on the last whorl. The coloured spiral bands, when present, also differs in being placed on different parts of the last whorl (see Table 1).

We here reinstate the name *C. gloriosus* as a valid name.

Chicomurex venustulus (Rehder & Wilson, 1975)

(Figs. 4M–P, 5A–C)

Chicoreus (*Chicomurex*) *venustulus* Rehder & Wilson, 1975: 7, figs. 4, 5, frontispiece figs. 2, 3.
Chicoreus venustulus – Cernohorsky, 1978: 65, pl. 18, fig. 5 (holotype); Kaicher, 1978: card 1596 (holotype).
Siratus venustulus – Abbott & Dance, 1982: 133, text-fig. (holotype).
Chicomurex venustulus – Houart, 1992: 124 (in part), fig. 225 (only) (holotype).
NOT *Chicoreus* (*Chicomurex*) *venustulus* – Houart, 1981: 10, text-fig. p. 7; Springsteen & Leobrera, 1986: 132, pl. 36, fig. 3 [= *Chicomurex gloriosus* (Shikama, 1977)].
NOT *Chicomurex venustulus* – Houart, 1992: 124 (in part), figs. 265, 268 (holotype of *C. gloriosus*), 428; Tsuchiya, 2000: 371, pl. 184, fig. 31; Thach, 2005. 113, pl. 36, fig. 3; Houart, 2008: 146, pl. 368, figs. 2–4; Robin, 2008: 249, fig. 2; Thach, 2012: pl. 53, fig. 621 (left); Merle *et al*., 2001: pl. 77, figs. 10–13, 15, 17–18 (only) [= *Chicomurex gloriosus* (Shikama, 1977)].

Type material: Holotype USNM 707241.

Type locality: Off south-western coasts of Tahuata, Marquesas Islands, 66–71 m.

Material examined: Holotype USNM 707241 (photos). MUSORSTOM 9, stn. DW1144, 85–95 m (1 dd); stn. DR1151, 70–77 m (1 dd); stn. DW1152, 85–150 m (2 dd); stn. CP1156, 80 m (1 dd); stn. CP1158, 109–110 m (1 lv); stn. DW1170, 104–109 m (11 lv and dd); stn. CP1177, 108–112 m (2 lv); stn. CP1178, 74–75 m (1 lv); stn. DR1181, 102–130 m (2 dd); stn. DR1183, 86–120 m (2 dd); stn. CP1189, 70 m (1 lv); stn. DW1203, 60–61 m (3 lv); stn. DW1217, 85–87 m (3 dd); stn. CP1227, 84–85 m (1 lv); stn. CP1228, 107–108 m (2 lv and dd); stn. DR1245, 85–130 m (1 dd); stn. DW1256, 70–72 m (1 dd); stn. DR1257, 85–127 m (2 dd); stn. DW1260, 49–100 m (1 dd); stn. CP1265, 90–92 m (2 lv and dd); stn. DR1292, 95–100 m (2 lv, 3 dd); stn. DR1293, 50 m (3 lv); stn. CP1294, 100 m (1 lv); stn. CP1295, 50–54 m (1 lv); stn. DR1297, 90–150 m (4 dd); stn. CP1304, 50–58 m (1 dd); stn. DR1305, 90–155 m (2 dd) (all MNHN). Nuku Hiva, 60 m, 1993 (RH, 4 lv & dd); Hago Fupa, Nuku Hiva, 40–60 m, 1993 (RH, 1 dd); Nuku Hiva, 108–112 m, 1997 (RH, 1 lv); Nuku Hiva, 104–109 m, 1997 (RH, 1 lv).

Distribution: The Marquesas, living at 54–109 m.

Remarks: See under *Chicomurex gloriosus*.

Acknowledgements

We are very grateful to Guido T. Poppe (Philippines) for the gift of material with many juvenile and subadult specimens which allowed us to observe the ontogeny of a few species. We are also very thankful to Nicolas Puillandre (MNHN) who sent us the sequences of some *Chicomurex* species from New Caledonia and to Andrea Barco (Universita di Roma "La Sapienza", Dipartimento di Biologia Animale e dell'Uomo, Roma) who did the same for the sequence of *Chicomurex gloriosus* from Madagascar; to Virginie Héros and Barbara Buge (MNHN) for searching for specimens of *Chicomurex* in the collections of the museum and for sending them in loan; to Kensaku Muraoka (then in KPM) for having sent the holotype of *C. gloriosus* in loan in 1985 and to Ellen E. Strong (NMNH) for the permission to illustrate the holotype of *Chicomurex venustulus*.

References

Abbott, R. T. & Dance, S. P. 1982. *Compendium of Seashells*. ix + 410 pp. E. P. Dutton, Inc., New York.

Cernohorsky, W. O. 1978. *Tropical Pacific Marine Shells*. 352 pp. Pacific Publications, Sydney.

Dharma, B. 1988. *Siput Dan Kerang Indonesia* (*Indonesian Shells*). xvi + 111 pp. Pennerbit, Jakarta.

Drivas, J. & Jay, M. 1988. *Coquillages de la Réunion et de l'Ile Maurice*. 159 pp. Delachaux & Niestlé, Neuchâtel-Paris.

Hinton, A. G. 1977. *Guide to Shells of Papua New Guinea*. 74 pp. R. Brown & Assoc., Port Moresby.

Houart, R. 1981. New Muricidae named after 1971. *Conchiglia* (144–145): 6–10.

Houart, R. 1992. The genus *Chicoreus* and related genera (Gastropoda: Muricidae) in the Indo-West Pacific. *Mémoires du Muséum national d'Histoire naturelle* (A) 154: 1–188.

Houart, R. 2008. Muricidae. *In*: Poppe, G. (ed.), *Philippine Marine Mollusks*, pp. 132–221. Conchbooks, Hackenheim.

Houart, R. 2013. Description of two new *Chicomurex* species (Gastropoda: Muricidae) from the Philippine Islands. *Novapex* 14: 69–75.

Houart, R., Moe, C. & Chong, C. 2014. *Chicomurex lani* n. sp. (Gastropoda: Muricidae), a new species from Taiwan and its intricate history. *Bulletin of Malacology, Taiwan* 37: 1–14.

Kaicher, S. D. 1973, 1978. *Card Catalogue of World-wide Shells*, *Muricidae I*. Privately published, St. Petersburg, Florida.

Kubo, H. & Kurozumi, T. 1995. *Molluscs of Okinawa.* 263 pp. Okinawa Shuppan Co. Ltd, Urazoe.

Lai, K. Y. 1987. *Marine Gastropods of Taiwan* (2). 116 pp. Taiwan Museum, Taipei.

Merle, D. 2001. The spiral cords and the internal denticles of the outer lip in the Muricidae: terminology and methodological comments. *Novapex* 2: 69–91.

Merle, D. 2005. The spiral cords of the Muricidae (Gastropoda, Neogastropoda): importance of ontogenetic and topological correspondences for delineating structural homologies. *Lethaia* 38: 367–379.

Merle, D., Garrigues, B. & Pointier, J. P. 2011. *Fossil and Recent Muricidae of the World. Part Muricinae*. 648 pp. Conchbooks, Hackenheim.
Radwin, G. & D'Attilio, A. 1976. *Murex Shells of the World. An Illustrated Guide to the Muricidae*. 284 pp. Stanford University Press, Stanford.
Rehder, H. A. & Wilson, B. R. 1975. New species of marine mollusks from Pitcairn Island and the Marquesas. *Smithsonian Contributions to Zoololy* (203): i–iv, 1–16.
Robin, A. 2008. *Encyclopedia of Marine Gastropods*. 480 pp. AFC and Conchbooks, Hackenheim.
Shikama, T. 1977. Descriptions of new and noteworthy Gastropoda from Western Pacific and Indian Ocean. *Science Reports of the Yokohama National University*, *Section II*, *Biology-Geology* 24: 9–23.
Springsteen, F. J. & Leobrera, F. M. 1986. *Shells of the Philippines*. 377 pp. Carfel Seashells Museum, Manila.
Thach, N. N. 2005. *Shells of Vietnam*. 337 pp. + 91 pls. Conchbooks, Hackenheim.
Thach, N. N. 2012. *New Records of Molluscs from Vietnam*. 276 pp., 151 pls. 48HrBooks Co. Akron, Ohio.
Tsuchiya, K. 2000. Muricidae. *In*: Okutani, T. (ed.), *Marine Mollusks in Japan*, pp. 364–421. Tokai University Press, Tokyo.

(Received February 10, 2014 / Accepted August 16, 2014)

フィリピン産オガサワラガンゼキ属 2 新種の記載およびウタヒメセンジュの復権を含むフィリピン産種群の見直し

Roland Houart・Christopher Owen Moe・陳　　充

要　約

オガサワラガンゼキ属 *Chicomurex*（下に述べるようにタイプ種 *C. superbus* は最近クマドリガンゼキに修正された）は，*Chicoreus* 属の亜属や *Phyllonotus* 属の異名とされることもあったが，歯舌の形態の違いなどから，現在では独立の属と認められている。フィリピンにおける本属の分布記録を整理すると，まず Springsteen & Leobrera（1986）は *Chicoreus* 属として *C. superbus*（G. B. Sowerby III, 1889），*C. laciniatus*，*C. venustulus* Rehder & Wilson, 1975 と *C. superbus problematicus* (Lan, 1982) の 4 種を図示している。Houart（1992）は *C. turschi*（Houart, 1981）を加えるとともに，*Chicoreus gloriosus* Shikama, 1977 を *C. venustulus* の異名とみなしたが，後に Houart（2008）は *C. turschi* の分布からフィリピンを除外した。さらに，Houart（2013）は *C. tagaroae* と *C. ritae* の 2 新種を記載し，Houart *et al*.（2014）は *C. problematicus* が *C. superbus* の異名であることを示した。従来日本や台湾などの文献で *C. superbus* として知られていた種（カザリガンゼキ）はこれとは別種であり，*C. lani* Houart, Moe & Chen, 2014 として新種記載された。

このような状況の下で，本論文においては，さらにフィリピンから従来クマドリガンゼキやウタヒメセンジュなどに混同されていた 2 種 *C. globus* n. sp. と *C. pseudosuperbus* n. sp. を新種として記載した。また，*C. venustulus* はマルキーズ（マルケサス）諸島に固有な種であることを示すとともに，従来その異名とされてきた *C. gloriosus* は独立した種であり，従来フィリピンから *C. venustulus* として報告されていたものはこれに当たることを明らかにした。これにより，フィリピンに分布するオガサワラガンゼキ属は下記の 7 種となる：*C. globus* n. sp.，ウタヒメセンジュ*C. gloriosus*，オトヒメガンゼキ *C. laciniatus*，*C. ritae* Houart, 2013，*C. pseudosuperbus* n. sp.，クマドリガンゼキ C. *superbus*（= *C. problematicus*），*C. tagaroae* Houart, 2013。

Chicomurex globus n. sp. オドリコセンジュ（新種・新称）

本種は従来様々な文献で主にウタヒメセンジュ“*C. venustulus*”（現在の *C. gloriosus*）に誤同定されてき

た。また，久保・黒住（1995）が沖縄からオガサワラガンゼキ “*C. superbus*” として図示している個体もこの種に当たる。本種は，ウタヒメセンジュに最も近似するが，それよりも小型で，殻幅が広く，水管溝が短い。また，水管溝状の棘が強く背面に反り返ることや，細い褐色帯が肩と殻底に現れることでも区別される。

タイプ産地：フィリピン，ミンダナオ島，ダバオ湾，水深 200 m（タングルネット）。

分布：日本（沖縄），南シナ海，フィリピン南部，グアム，パプア・ニューギニア，ヴァヌアツ，ニューカレドニア，水深 18〜200 m。

Chicomurex pseudosuperbus n. sp. ニセクマドリガンゼキ（新種・新称）

本種も従来 “*C. venustulus*” や “*C. superbus*” に誤同定されてきた。Springsteen & Leobrera（1986）が “*C. superbus*” として図示している個体は本種である。本種は，クマドリガンゼキ C. *superbus* からは，殻がより細長く螺塔が高いこと，螺肋が顕著に彩色されないこと，螺肋間の二次肋が弱いことにより区別される。また，ウタヒメセンジュとは，殻がやや大型であること，殻口が狭いこと，色帯の位置が *C. globus* n. sp. と同様であることなどで異なる。オガサワラガンゼキ *C. lani* にも近似するが，大型であること，縫合が浅いこと，水管溝が長いこと，体層で縦肋が太く，節状になること，表面がざらざらしていることで区別される。なお，オガサワラガンゼキは現在のところフィリピンからは記録されていない。

タイプ産地：フィリピン，セブ，マクタン島沖。

分布：日本（沖縄島残波岬，SCUBA 60 m），台湾，フィリピン，ニューカレドニア，オーストラリア（クイーンズランド），水深 60〜200 m。

Chicomurex lani sp. nov. (Gastropoda: Muricidae), a new species from Taiwan and its intricate history

Roland Houart*[1] Christopher Owen Moe[2] Chong Chen[3]

[1*] Research associate, Institut royal des Sciences naturelles de Belgique, rue Vautier, 29, B-1000 Bruxelles, Belgium

[2] 98-080 Uao Place #B2 Aiea, Hawaii 96701, USA

[3] Department of Zoology, University of Oxford, Oxford OX1 3PS, United Kingdom

Correspondence author Email: roland.houart@skynet.be

Abstract

A new species of *Chicomurex* that was confused with *C. superbus* (Sowerby, 1889) in several publications is described from Taiwan and *C. problematicus* (Lan, 1981) is considered a junior subjective synonym of *C. superbus*. The holotypes of both *C. superbus* and *C. problematicus* are illustrated and *C. superbus is* redescribed.

Keywords: *Chicomurex superbus*, *Chicomurex lani* sp. nov., Muricidae, history, new species, Taiwan.

臺灣產新種骨螺：藍氏千手螺 (*Chicomurex lani*) 之記載及其錯綜複雜的歷史

Roland Houart*[1] Christopher Owen Moe[2] 陳充[3]

[1*] Research associate, Institut royal des Sciences naturelles de Belgique, rue Vautier, 29, B-1000 Bruxelles, Belgium

[2] 98-080 Uao Place #B2 Aiea, Hawaii 96701, USA

[3] Department of Zoology, University of Oxford, Oxford OX1 3PS, United Kingdom

Correspondence author Email: roland.houart@skynet.be

本文記載骨螺科*Chicomurex*屬中一種在多處文獻中被混淆為華麗千手螺 *C. superbus* (Sowerby, 1889)的新種骨螺並將其命名為藍氏千手螺 (*Chicomurex lani*)，模式標本產地為臺灣。華麗千手螺與疑問骨螺 *C. problematicus* (Lan, 1981)實為同種，疑問骨螺則為華麗千手螺的同種異名。本文亦圖解華麗千手螺及疑問骨螺之模式標本，並重新描述華麗千手螺。

關鍵字：華麗千手螺、藍氏千手螺、骨螺科、歷史、新種、台灣

Introduction

Chicomurex superbus (Sowerby, 1889) was described from a single specimen collected in Hong Kong by Dr. Hungerford (Sowerby, 1889: 565). The original figure illustrates a shell with a high spire, a long, broad siphonal canal and a relatively broad, shouldered shell (Fig. 20).

One of us (CM) recently noted that the holotype of *C. superbus* figured by the National Museum of Wales on its website: http://naturalhistory.museumwales.ac.uk/, was probably the same species recently described by T.C. Lan (1981) as *Phyllonotus superbus problematicum*, currently known as *C. problematicus*. It differs obviously from other specimens illustrated afterwards by several authors as *C. superbus*. The shell in the National Museum of Wales when compared to Sowerby (1889: pl. 38, figs 10, 11) has a seemingly lower spire and the siphonal canal is badly broken.

The holotype of *C. superbus* was also illustrated by Abbott & Dance (1982: 133) but it was not specified as holotype in their publication, nor in some corrections published afterwards by Dance (1986).

After a correspondence with the National Museum of Wales it became certain that the specimen in their collection was indeed the holotype of *C. superbus* and that the siphonal canal was broken afterwards. The spire is also slightly lower than the original drawing but this kind of exaggeration in drawings is often seen in older publications.

After examination of the holotype it became obvious to us that the shell described afterwards by Lan (1981) was in fact the true *Chicomurex superbus* and that the species illustrated by several authors, including Lan (1981) as *C. superbus* remained unnamed.

Material and methods

Over 100 mixed specimens of all related species within the genus *Chicomurex* were studied. Most material was from the collections of the authors or borrowed type material from museums. Specimens were carefully compared to type material, written description, and to each other. Included were shells from most known locations for those species.

The chresonymy is only cited for the specimens illustrated as *Chicomurex superbus* or *C. problematicus*, whatever the genus used in the publication, and which represent indeed these species. Other species illustrated as *C. superbus* or *C. problematicus* but which represent different species are the subject of a forthcoming paper and are not cited in this paper.

Abbreviations

Repositories

AMS: Australian, Museum, Sydney, Australia.
CC: collection of Chong Chen.
CM: collection of Christopher Moe.
IRSNB: Institut royal des Sciences naturelles de Belgique, Bruxelles, Belgium.
MNHN: Muséum national d'Histoire naturelle, Paris, France.
NMW: National Museum of Wales, Cardiff, U.K.
NTM: National Taiwan Museum, Taipei, Taiwan.
RH: collection of Roland Houart.

Terminology used to describe the spiral cords and the apertural denticles (after Merle 1999 and 2001)

Terminology in parentheses: erratic feature (Figs 1-2).

Spiral cords

ab abapical (or abapertural); **abis** abapical infrasutural secondary cord (on subsutural ramp); **ABP** abapertural primary cord on the siphonal canal; **abs** abapertural secondary cord on the siphonal canal; **ad** adapical (or adapertural); **adis** adapical infrasutural secondary cord (on subsutural ramp); **ADP** adapertural primary cord on the siphonal canal; **ads** adapertural secondary cord on the siphonal canal; **IP** infrasutural primary cord (primary cord on subsutural ramp); **MP** median primary cord on the siphonal canal; **ms** median secondary cord on the siphonal canal; **P** primary cord; **P1** shoulder cord; **P2-P6** primary cords of the convex part of the teleoconch whorl; **s** secondary cord; **s1-s6** secondary cords of the convex part of the teleoconch whorl (example: s1 = secondary cord between P1 and P2; s2 = secondary cord between P2 and P3, etc.); **t** tertiary cord.

Aperture

D1 to D6 abapical denticles; **ID** Infrasutural denticle.

Results

Systematics

Order Neogastropoda

Family Muricidae

Genus *Chicomurex* Arakawa, 1964

Type species: *Murex superbus* Sowerby, 1889

***Chicomurex lani* sp. nov. (Figures 2, 4-6, 7-13)**

Chicoreus superbus – Habe, 1961: 50, pl. 25, fig. 14 [not *Chicomurex superbus* (Sowerby, 1889)].
Murex superbus – Lan, 1981: 12, fig. 6 [not *Chicomurex superbus* (Sowerby, 1889)].
Chicomurex superbus – Houart, 1992: 121, figs 67, 124-125, 227, 231, 424; Tsuchiya, 2000: 371, pl. 184, fig. 30; Robin, 2008: 249, fig. 1; Zang, 2008: 170; Merle et al. 2011: 42, 106, 109-110, pl. 77, figs 1-5 [not *Chicomurex superbus* (Sowerby, 1889)].
Murex (*Chicoreus*) *supersus* (sic) Shikama, 1963: 70, pl. 54, fig. 8 [not *Chicomurex superbus* (Sowerby, 1889)].
Naquetia superbus – Fair, 1976: 79, pl. 14, fig. 174 [not *Chicomurex superbus* (Sowerby, 1889)].
Phyllonotus superbus – Radwin & D'Attilio, 1976: 92, pl. 6, fig. 2 (only) [not *Chicomurex superbus* (Sowerby, 1889)].

Type material examined: Type specimen: Holotype: TMMT 201401, from the type locality, dry shell. Paratypes: IRSNB (1): IG 32538/MT.2989, NMW.Z. 2013.066.00001 (1), MNHN -IM-2012-2700 (1), RH (2), CC (1), CM (1) (all from the type locality);

Other material: Northeast Taiwan (RH, 3); Taiwan (RH, 1) (CM, 4); Japan, Nada, Gobō (RH, 1); Wakayama Prefecture (CM, 1; RH, 1) (CM, 3); Okinawa Japan (CM, 3); Vanuatu, New Caledonia, Chesterfields (MNHN, many specimens); Queensland, Australia, trawled in 150m (CM, 1)

Type locality: Southwest Taiwan, 200 m, October 2008.

Etymology: L. *lani*: the name is dedicated to the late Mr. T.C. (Tsu Chiao) Lan (1931-2004), Taiwan, a shell dealer and author~~s~~ of several publications.

Description: Shell (Figs 2, 4, 6, 7-13) large sized for the genus, up to 90 mm in length at maturity. Length/width ratio 1.95-2.03 (extremes 1.81-2.09). lanceolate, broadly ovate, weakly spinose, nodose. Subsutural ramp broad, weakly sloping, lightly convex, almost straight, extending to P2.

Pinkish white or creamy white with numerous light orange to dark brown blotches on and between spiral cords and on axial varices. Aperture glossy white.

Spire high with 3 protoconch whorls (partially broken in examined specimens) and teleoconch of up to 8 broad, convex, weakly shouldered, spinose and nodose whorls. Suture impressed.

Protoconch (Fig. 4) small, conical, smooth, glossy, with a narrow, single keel abapically. Maximum width 1100 µm. Terminal lip thin, raised, of sinusigra type.

Axial sculpture of teleoconch whorls consisting of strong, broad, nodose ribs and high, strong, narrow, nodose varices; each varix of last teleoconch whorl with 8 or 9 short, broad, broadly open, blunt, primary and secondary spines; shoulder spine short or moderately long, second short, spines increasing in length abapically. IP spine short. Most abapical spines P5 and P6 longest, s6 weakly shorter, P2-P4 short. First teleoconch whorl with 11 axial ribs, second with 13, third with 12 or 13, fourth with 8 or 9 ribs, starting varices at end of whorl, fifth to last whorl with 3 varices and 2, occasionally 3 intervariceal, nodose ribs, more conspicuous on shoulder.

Spiral sculpture of low, strong, narrow, squamous and nodose primary, secondary and tertiary cords. First whorl with visible P1-P3, second with P1-P3, starting s1, occasionally with P4 covered by next whorl, third starting IP, fourth with IP, P1-P3 (P4) and secondary cords s1-s3, fifth whorl with adis, IP, abis, starting tertiary cords, sixth whorl of a juvenile specimen with adis, IP, abis, P1, s1, P2, s2, P3, s3, P4, s4, P5, s5, P6, s6 and some tertiary cords. Last teleoconch whorl of adults similar, secondary cord s6 broad, almost as broad as primary cords, followed abapically by a strong tertiary cord.

Aperture very large, broad, roundly ovate. Columellar lip broad, smooth or with 2 or 3 very weak knobs abapically; weak, elongate parietal tooth at adapical extremity. Rim partially erect, adherent at adapical extremity, strongly flaring abapically. Anal notch shallow or moderately deep, broad. Outer lip weakly erect, crenulate, with weak, low denticles within: ID, D1, D2 split, D3 split, D4 split, D5 split and D6.

Siphonal canal long, broad, tapering abapically, weakly dorsally recurved, narrowly open, with 3 or 4 weakly frondose, long spines extending from ADP, MP, ABP and abs. ADP spine weakly dorsally bent.

Operculum light or dark brown, ovate with subapical nucleus and strong concentric ridges.

Radula (Fig. 5) with crowded rows of teeth. Rachidian with broad, long, triangular central cusp flanked by a short, triangular, lateral denticle, lateral cusp moderately long and comparatively narrow. Lateral teeth sickle-shaped, moderately narrow, weakly broader at base.

Distribution: Southern Japan, Taiwan, Vanuatu, Coral Sea, New Caledonia, Northeast Australia, southern Great Barrier Reef, Lady Elliot Is., bathymetric range approximately 40 to 300 m for living specimens.

Remarks: See under *Chicomurex superbus* (Sowerby, 1889).

***Chicomurex superbus* (Sowerby, 1889)** (Figures 1, 3, 14-24)

Murex superbus Sowerby, 1889: 565, pl. 28, figs 10, 11.
Phyllonotus superbus problematicum Lan, 1981: 11, Figs 1-4 (*Murex problematicum* on the plate).
Chicomurex superbus – Wilson, 1994: 27, pl. 2, fig. 17a-b; Houart, 2008: 144, pl. 367, fig. 5 (only); 146, pl. 368, fig. 6 (only).
Siratus superbus – Abbott & Dance, 1982: 133, text fig. (holotype illustrated); Okutani, 1983: 24, fig. 10; 1991: pl. 62, fig. 6.
Chicoreus superbus problematicus – Lai, 1987: 63, pl. 30, fig. 2.
Chicomurex problematicus – Houart, 1992: 119, figs 229, 266; 1994: 81, pl. 11, fig. 75; Tsuchiya, 2000: 371, pl. 184, fig. 32; Thach, 2005: 113, pl. 34, fig. 16; Robin, 2008: 248, fig. 8; Merle et al., 2011: 108, 110, pl. 77, figs 6, 7.
Chicomurex problematica – Houart, 2008: 144, pl. 367, fig. 4.

Type material examined: *Murex superbus*: holotype NMW 1955.158.00016 (Figs 14-17); *Phyllonotus superbus problematicum*: holotype, copyright National Taiwan Museum, TMMT 8113 (digital images) (Figs 18-20).

Other material examined: Japan, Okinawa (CM, 2); Wakayama (CM, 2); Taiwan, 1984 (RH, 1); Northeast Taiwan, trawled on deep coral base, 1979 (RH, 1); Philippines, Balut Is., in tangle nets (RH, 3) (CM, 2); off Punta Engano, in shell nets, 1983 (RH, 2); north Mindanao, by tangle nets, 120 m (RH, 1); Mactan Is, Cebu, 1980 (RH, 2); Mactan, Cebu (CM 3); Zamboanga (CM, 1); Bohol, Panglao, (RH, 1); Northeast Australia, Queensland, east of Townsville, 172-178 m, (AMS C.156450, 1).

Type locality: *Murex superbus*: Hong Kong; *Phyllonotus superbus problematicum*: Philippines, Cebu, Bohol, 300 m.

Description: Shell (Figures 1, 3, 14-24) medium sized for the genus, up to 82 mm in length at maturity. Length/width ratio 1.83-2.00 (extremes 1.79-2.02). biconical, broadly ovate, heavy, spinose, nodose. Subsutural ramp broad, weakly sloping, lightly convex, extending to P2.

White or greyish white with primary and secondary cords topped with light or dark brown blotches or lines; some dark brown blotches between axial ribs on subsutural area and light brown or tan between some spiral cords, more obvious on varices. Area between P4 and P6 occasionally lighter colored giving the appearance of a broad, lighter colored spiral band. Aperture white.

Spire high with 3 protoconch whorls and teleoconch of up to 8 broad, convex, strongly shouldered, spinose and nodose whorls. Suture impressed.

Protoconch (Fig. 3) small, conical, last whorl minutely punctate, with a narrow, single keel abapically. Maximum width 900 µm, height 900 µm. Terminal lip thin, raised, of sinusigra type.

Axial sculpture of teleoconch whorls consisting of high, broad, rounded ribs and high, strong, narrow, rounded varices; each varix of last teleoconch whorl with 16 or 17 short, frondose, narrow, open, primary and secondary spines and spinelets; subsutural area spinelets short, webbed, shoulder spine weakly longer, followed by small, not webbed, short spines, extending from s1 to s3; P4 spine short, connected to narrow s4; P5 to s6 longest spines, increasing in length and strength abapically, strongly webbed.

Spiral sculpture of low, rounded, narrow, squamous, primary, secondary and tertiary cords. First and second whorls with visible P1-P3, occasionally with P4 covered by next whorl; third and fourth whorls with IP, P1, s1, P2, s2, P3, s3, P4; fifth whorl with adis, IP, abis, P1, s1, P2, s2, P3, s4, P4 and a few threads between primary and secondary cords; sixth whorl of a juvenile specimen with adis, IP, abis, P1, s1, P2, s2, P3, s3, P4, s4, P5, s5, P6, s6 and two or three additional, broad, tertiary cords. Primary cords flanked by tertiary cords; P1-P4 cords narrow, P5 and P6 broader and higher, s6 broadest and highest cord. Last teleoconch whorl of adult shells similar.

Aperture large, narrow, ovate. Columellar lip broad, with 3 or 4 elongate, weak knobs abapically and a strong parietal tooth at adapical extremity. Rim partially erect, adherent at adapical extremity, strongly flaring abapically. Anal notch shallow or moderately deep, broad. Outer lip weakly erect, crenulate, with very weak, low, elongate denticles within: ID, D1 split, D2 split, D3 split, D4 split, D5 split and D6 or D6 split.

Siphonal canal moderately long, broad adaperturally, strongly tapering abapically, weakly dorsally recurved, narrowly open, with 5 or 6 short, webbed spines or spinelets extending from ADP, ads, MP, ms, ABP, and occasionally abs. ADP spine weakly dorsally bent.

Operculum dark brown, ovate with subapical nucleus and strong concentric ridges.

Radula unknown.

Distribution: Southern Japan, Taiwan, Hong Kong, Vietnam, Philippines, northeast Australia, Coral sea in 40 to 300 m for living specimens.

Remarks: *Chicomurex lani* sp. nov. and *C. superbus* were very often confused in the past as seen above. This confusion is mainly due to the misinterpretation of the original figure of *C. superbus* because both species are easily distinguishable. *Chicomurex lani* is more rounded, less shouldered, with a comparatively higher spire and a broader aperture with broader columellar lip abapically. The primary spiral cords are broader, the secondary spiral cords are comparatively lower and narrower and the axial varices are narrower. The shell of *C. lani* is also less spinose with less or absent spinelets and less webbed spines; this is more obvious on the abapical part of the varices and on the siphonal canal.

The color is also different; the spiral cords are obviously less colorful in *C. lani* while they are regularly and strongly topped with brown in *C. superbus*.

Acknowledgements

We are very grateful to Harriet Wood (National Museum of Wales) for useful information and for the loan of the holotype of *Murex superbus*, to Ying-Tzung Shie and Ming Chen National Taiwan Museum for providing the digital images of the holotype of *Phyllonotus problematicum*, to Thierry Backeljau, Yves Samyn and Yves Barette (Institut royal des sciences naturelles de Belgique) for their help and collaboration, to Anders Warén (Natural History Museum, Stockholm) for radula preparation and SEM work of the radula of *Chicomurex lani* nov. sp., and to Yu-Hsiu Yen (Taiwan) for her most useful help and collaboration in writing different reports and applications to the National Taiwan Museum for the copyright of digital photographs and for depositing the holotype, and for transporting the holotype to the Museum.

References

Abbott, R.T. & S.P. Dance 1982. *Compendium of seashells*, E.P. Dutton, Inc. New York: i-ix, 1-410.

Dance, S.P., 1986. Corrections to the first printing of the Compendium of Seashells by R. T. Abbott and S. P. Dance. *Pallidula* 17(1): 3-10.

Fair, R.H., 1976. *The Murex Book, an illustrated catalogue of Recent Muricidae* (Muricinae, Muricopsinae, Ocenebrinae), Sturgis Printing Co., Honolulu, Hawaii: 138 pp.

Habe, T. 1961. *Coloured illustrations of the shells of Japan* (II). Hoikusha, Osaka. ix + 183 pp.

Houart, R., 1992. The genus *Chicoreus* and related genera (Gastropoda: Muricidae) in the Indo-West Pacific. *Mémoires du Muséum national d'Histoire naturelle*, (A), 154: 1-188.

Houart, R., 1994. Illustrated catalogue of Recent species of Muricidae named since 1971. Wiesbaden: 179 pp.

Houart, R. 2008. Muricidae. *In*: Poppe G. (ed.), *Philippine Marine Mollusks*, Conchbooks, Hackenheim, Germany: 132-220.

Lai, K.Y. 1987. *Marine Gastropods of Taiwan* (2), Taipei, National Taiwan Museum: 116 pp.

Lan, T.C., 1981. Description of a new sub-species of Muricidae from the Philippines and Taiwan. *Bulletin of Malacology Republic of China* 8: 11-13.

Merle, D. 1999. *La radiation des Muricidae (Gastropoda : Neogastropoda) au Paléogène: approche phylogénétique et évolutive.* Paris. Unpublished thesis, Muséum national d'Histoire naturelle : i-vi, 499 pp.

Merle, D. 2001. The spiral cords and the internal denticles of the outer lip in the Muricidae: terminology and methodological comments. *Novapex* 2(3): 69-91.

Merle, D., B. Garrigues, & J.P. Pointier 2011. *Fossil and Recent Muricidae of the World -Part Muricinae-* . Conchbooks, D-55546 Hackenheim, 648 pp.

Okutani, T. 1981. *World Seashells of Rarity and Beauty*. Tokyo, National Science Museum: i-iii, 1-12, 48 pls.

Okutani, T. 1983. *World Seashells of Rarity and Beauty*. *Revised and Enlarged Edition* Tokyo, National Science Museum: i-viii, 1-206.

Okutani, T. 1991. *World Seashells of Rarity and Beauty* (*Kawamurai Collection*). Tokyo, National Science Museum: i-viii, 1-206.

Radwin G. & A. D'Attilio, 1976. *Murex shells of the world. An illustrated guide to the Muricidae.* Stanford University Press, Stanford: 284 pp.

Robin, A. 2008. *Encyclopedia of Marine Gastropods*. AFC and Conchbooks, D-55546 Hackenheim, 480 pp.

Shikama, T., 1963. *Selected shells of the world illustrated in colours* (I). Hokuryu-Kan: 154 pp.

Sowerby, G.B. 1889. Descriptions of fourteen new species of shells from China, Japan and the Andaman Islands. *Proceedings of the Zoological Society of London* 56:565-570.

Thach, N. N. 2005. Shells of Vietnam. Conchbooks, D-55546 Hackenheim, 337 pp, 91 pls.

Tsuchiya, K. 2000. Muricidae. *In*: Okutani, T. (ed.), *Marine Mollusks in Japan*, Tokai University Press, Tokyo: 364-421.

Wilson, B. 1994. *Australian Marine Shells*. Vol. 2. Odyssey Publishing, Kallaroo: 370 pp.

Zhang, S. 2008. Atlas of Marine Mollusks in China (in Chinese), Ocean Press, China, 383 pp.

Figures 1-6

1. *Chicomurex superbus* (Sowerby, 1889). Terminology of the apertural denticles; 2. *Chicomurex lani* sp. nov., holotype, terminology of the spiral cords morphology; 3. Protoconch of *Chicomurex superbus* (scale bar 500 µm); 4. Protoconch of *Chicomurex lani* sp. nov. (scale bar 500 µm); Radula of *C. lani* sp. nov. Coral Sea (illustrated Fig. 6) (scale bar 100 µm); 6. *Chicomurex lani* sp. nov., Coral Sea, 24°02' S, 159°38' E, 83.5 mm.

Figures 7-16. *Chicomurex lani* sp. nov.

7-9. Holotype TMMT 201401, Southwest Taiwan, 200 m, 66.8 mm (photo copyright National Taiwan Museum); 10. Paratype RH, Southwest Taiwan, 200 m, 63.5 mm; 11-13. Paratype MNHN -IM-2012-2700, Southwest Taiwan, 200 m, 64.1 mm; 14-15. Taiwan, 80 mm, RH; 16. Queensland, Australia, 77 mm, CM.

Figures18-24. *Chicomurex superbus* (Sowerby, 1889)

17-19. Holotype of *Murex superbus* Sowerby, 1889, NMW 1955.158.00016, Hong Kong, 63.7 mm; 20. Original illustration (Fig. 11) of Sowerby, 1889; 21-23. Holotype of *Phyllonotus superbus problematicum* Lan, 1981, TMMT 8113, Philippines, Cebu, Bohol, 300 m, 77.8 mm (photo copyright National Taiwan Museum); 24. Northeast Taiwan, trawled on deep coral base, 1979, 55.3 mm (RH); 25-26. Philippines, North Mindanao, tangle nets, ca 120 m, 82.4 mm (RH).

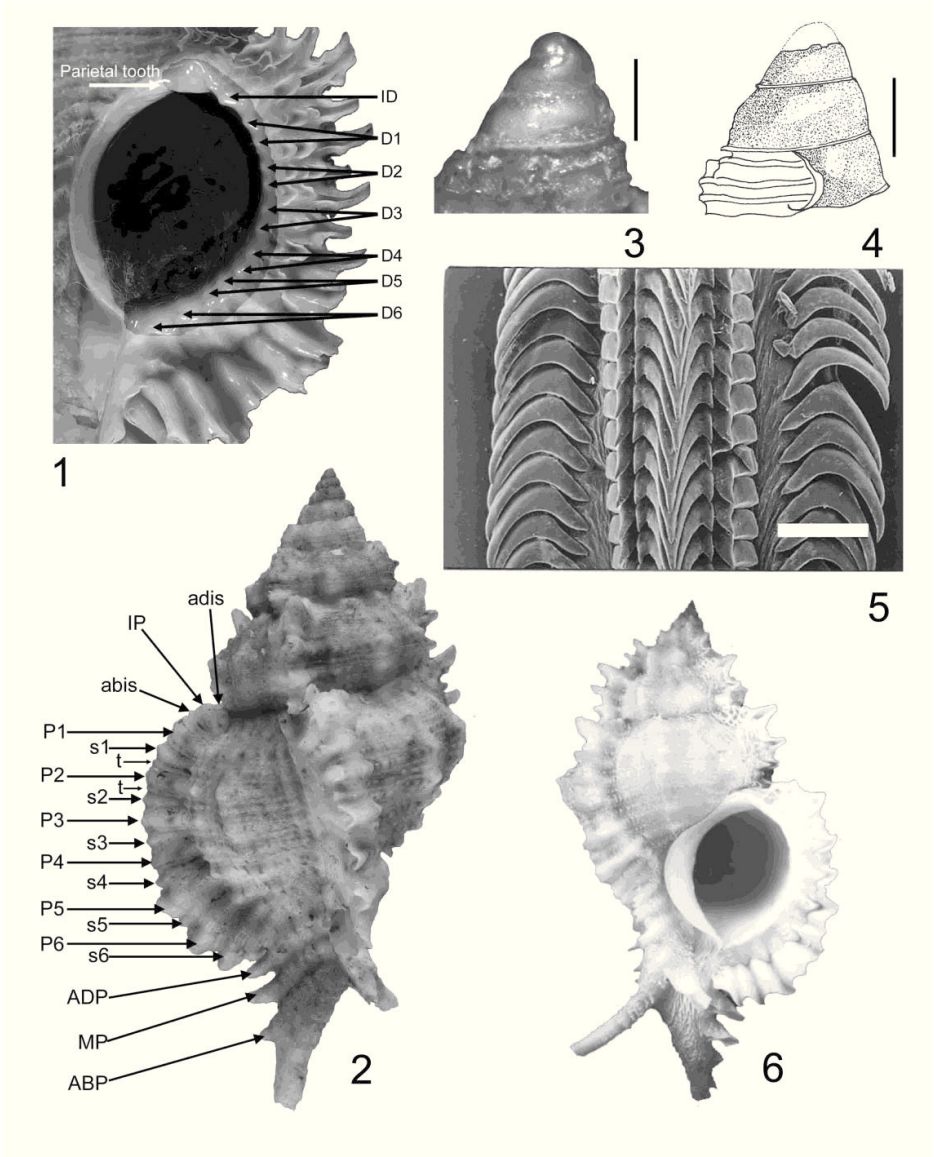
Parietal tooth
ID
D1
D2
D3
D4
D5
D6
1
3
4
5
adis
IP
abis
P1
s1
t
P2
t
s2
P3
s3
P4
s4
P5
s5
P6
s6
ADP
MP
ABP
2
6

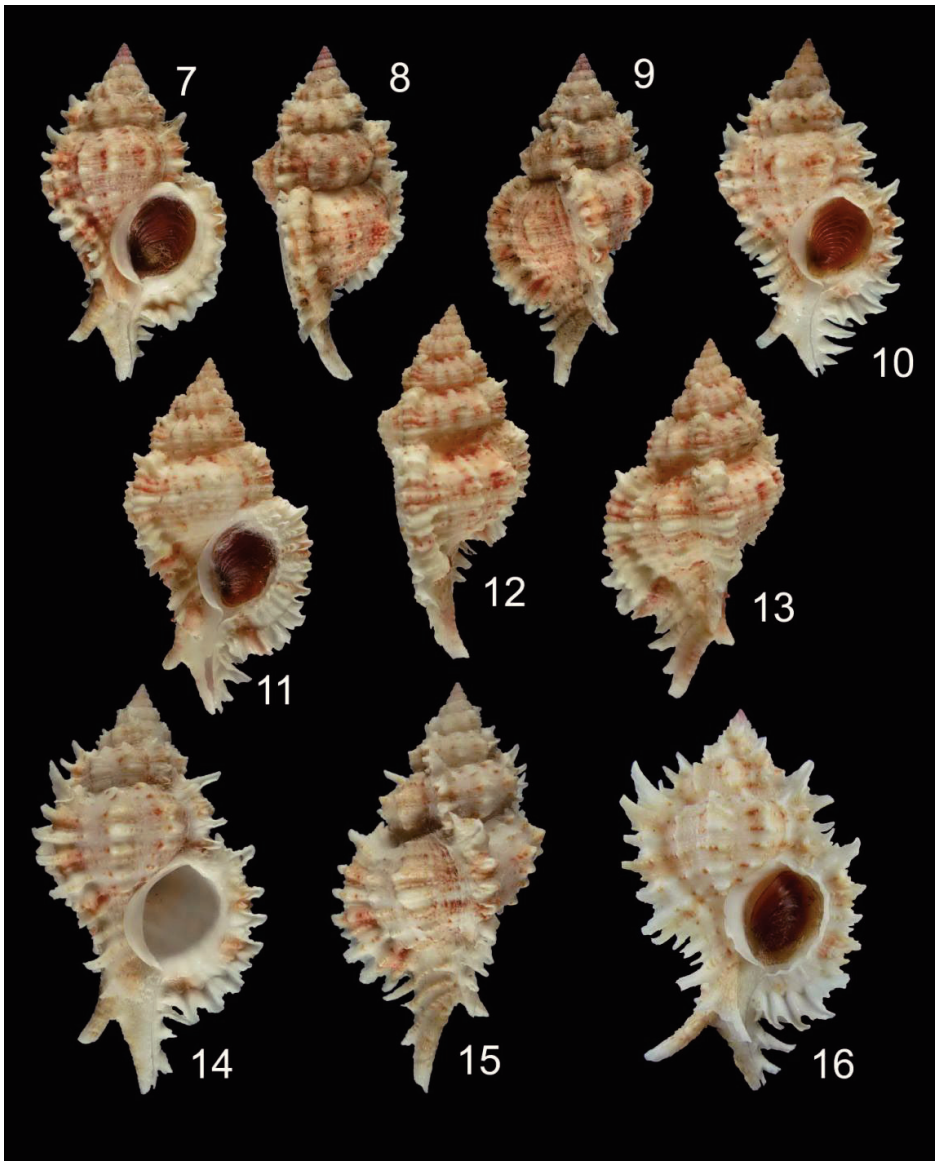
7
8
9
10
11
12
13
14
15
16

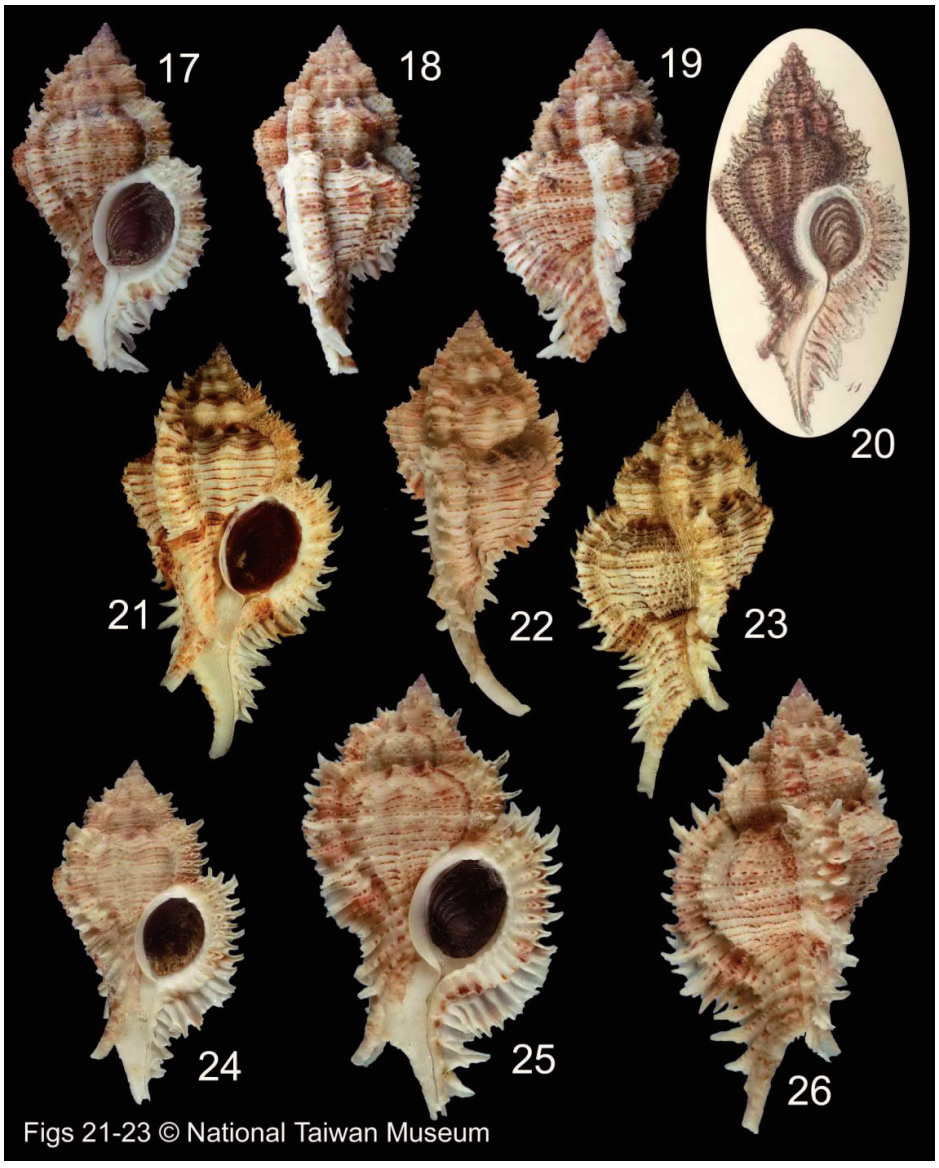
17
18
19
20
21
22
23
24
25
26
Figs 21-23 © National Taiwan Museum